UNITED STATES
DEPARTMENT OF THE INTERIOR
GEOLOGICAL SURVEY

NATIONAL EARTHQUAKE HAZARDS REDUCTION PROGRAM, SUMMARIES OF TECHNICAL REPORTS VOLUME XXXI

Prepared by Participants in

NATIONAL EARTHQUAKE HAZARDS REDUCTION PROGRAM

Compiled by

Muriel L. Jacobson

The research results described in the following summaries were submitted by the investigators on October 31, 1990 and cover the period from April 1, 1990 through October 1, 1990. These reports include both work performed under contracts administered by the Geological Survey and work by members of the Geological Survey. The report summaries are grouped into the five major elements of the National Earthquake Hazards Reduction Program.

Open File Report No. 90-680

The data and interpretations in these progress reports may be reevaluated by the investigators upon completion of the research. Readers who wish to cite findings described herein should confirm their accuracy with the author.

CONTENTS

Earthquake Hazards Reduction Program

Page

ELEMENT I - Recent Tectonics and Earthquake Potential

Determine the tectonic framework and earthquake potential of U.S. seismogenic zones with significant hazard potential

Objective (I-2): Source zone characteristics

Identify and map active crustal faults, using geophysical and geological data to interpret the structure and geometry of seismogenic zones.

Objective (I-3): Earthquake potential

Estimate fault slip rates, earthquake magnitudes, and recurrence intervals for seismogenic zones and faults disclosed by research under Objectives T-1 and T-2, using geological and geophysical data.

Page

ELEMENT II. Earthquake Prediction Research

Collect observational data and develop the instrumentation, methodologies, and physical understanding needed to predict damaging earthquakes.

Objective (II-1): Prediction Methodology and Evaluation

Develop methods to provide a rational basis for estimates of increased earthquake potential. Evaluate the relevance of various geophysical, geochemical, and hydrological data for earthquake prediction.

1. Develop, operate and evaluate instrumentation for monitoring potential earthquake precursors.
2. Analyze and evaluate seismicity data collected prior to medium and large earthquakes.
3. Obtain and analyze data from seismically active regions of foreign countries through cooperative projects with the host countries.
4. Systematically evaluate data and develop statistics that relate observations of specific phenomena to earthquake occurrence.
5. Develop, study and test prediction methods that can be used to proceed from estimates of long-range earthquake potential to specific short-term predictions..174

Objective (II-2): Earthquake Prediction Experiments

Conduct data collection and analysis experiments in areas of California capable of great earthquakes, where large populations are at risk. The experiments will emphasize improved coordination of data collection, data reporting, review and analysis according to set schedules and standards.

1. Collect and analyze data for an earthquake prediction experiment in southern California, concentrating on the southern San Andreas fault from Parkfield, California to the Salton Sea.
2. Collect and analyze data for an earthquake prediction experiment in central California, concentrating on the San Andreas fault north of Parkfield, California..249

Page

Objective (II-3): Theoretical, Laboratory and Fault Zone Studies

Improve our understanding of the physics of earthquake processes through theoretical and laboratory studies to guide and test earthquake prediction observations and data analysis. Measure physical properties of those zones selected for earthquake experiments, including stress, temperature, elastic and anelastic characteristics, pore pressure, and material properties.

1. Conduct theoretical investigations of failure and pre-failure processes and the nature of large-scale earthquake instability.

2. Conduct experimental studies of the dynamics of faulting and the constitutive properties of fault zone materials.

3. Through the use of drilled holes and appropriate down hole instruments, determine the physical state of the fault zone in regions of earthquake prediction experiments..............................325

Objective (II-4): Induced Seismicity Studies

Determine the physical mechanism responsible for reservoir-induced seismicity and develop techniques for predicting and mitigating this phenomena.

1. Develop, test, and evaluate theories on the physics of induced seismicity.

2. Develop techniques for predicting the character and severity of induced seismicity.

3. Devise hazard assessment and mitigation strategies at sites of induced seismicity.....................

ELEMENT III Evaluation of Regional and Urban Earthquake Hazards

Delineate, evaluate, and document earthquake hazards and risk in urban regions at seismic risk. Regions of interest, in order of priority, are:

1) The Wasatch Front

2) Southern California

3) Northern California

ELEMENT IV Earthquake Data and Information Services

ELEMENT V: Engineering Seismology

LOMA PRIETA

Seismic Monitoring of the Shumagin Seismic Gap, Alaska

14-08-0001-A0616

Geoffrey A. Abers
Lamont-Doherty Geological Observatory of Columbia University
Palisades, New York 10964
(914) 359-2900

Investigations

Seismic data from the Shumagin seismic network were collected and processed to obtain digital waveforms, origin times, hypocenters, and magnitudes for local and regional earthquakes. The data are used for earthquake source characterization, determination of earth structure, studies of regional tectonics, analysis of possible earthquake precursors, and seismic hazard evaluation. Yearly bulletins are available starting in 1984 through 1989.

Results

Shumagin network data were used to locate 137 earthquakes from January 1 to June 30, 1990, bringing the total number of digitally recorded events in Shumagin network catalog to 5662 since 1982. The seismicity for the first half of 1990 is shown in map view on Figure 1 and in cross section on Figure 2. Events shown by solid symbols are those events that meet the following quality criteria: located by 8 or more P or S arrivals, vertical error from *Hypoinverse* less than 10 km, and horizontal error less than 5 km. Other events are shown by open symbols. These criteria provide a rough indication of the location quality, and show that epicenters more than 100 km from the nearest station are rarely well determined. Additional numerical tests of hypocenter stability show that when the entire network is operating, shallow events west of 166°W, east of 156°W, or seaward of the trench can not be reliably located. Also, depths of shallow earthquakes are only well-determined beneath the Shumagin Islands (e.g., Figure 3). No events with $m_b \geq 5.0$ have been recorded within the network since July, 1988. A shallow $m_b = 4.9$ event beneath the Sanak Basin (54.3°N, 161.5°W) was felt in Sand Point on June 19. This cluster has persisted throughout the 17 years of newtork operation.

The overall pattern in Figures 1-2 resembles the long term seismicity (e.g., Figure 3). Seismicity is concentrated near the base of the main thrust zone between 35 and 50 km depth, and immediately above it within the overriding plate. Seismicity contours below 30 km depth parallel the volcanic arc, rather than the trench, and become closer to the trench west of the network (Figure 1). Seismicity appears to be sparse where the main thrust zone is shallower than 35 km, between the Shumagin Islands and the trench. Deeper seismicity extends to depths of 200 km. Some locations near 100 km depth on Figure 2 correlate with the lower plane of the double seismic zone seen in long-term seismicity. The entire catalog since 1982 was relocated in a joint inversion with 2D velocity variations, and stable locations were extracted (Figure 3). These relocations show many details of the fine structure of seismicity and place tight (<5 km) bounds on the thickness of the seismogenic zone.

The major activity during the last six months was the summer field season, July 3-28, 1990. Because of the termination of DOE support for seismic monitoring, previously 2/3 of our monitoring budget, we were forced to drastically scale back our processing operations and to remove ~1/3 of our stations. A total of 5 stations (FPS, SNK, BLH, PN6, and IVF) and 3 telemetry repeaters were removed this summer; one of the vertical sensors was temporarily re-installed at a repeater site on Unga Is. that previously had no seismometer (ZKB). The other major network change was completion of the previously-planned installation of a 3-component Guralp CMG-4 broad-band sensor (high-pass corner at 0.05 Hz) at our central site in Sand Point. The instrument is currently recording velocity continuously at 20 s.p.s. and triggered at 100 s.p.s.

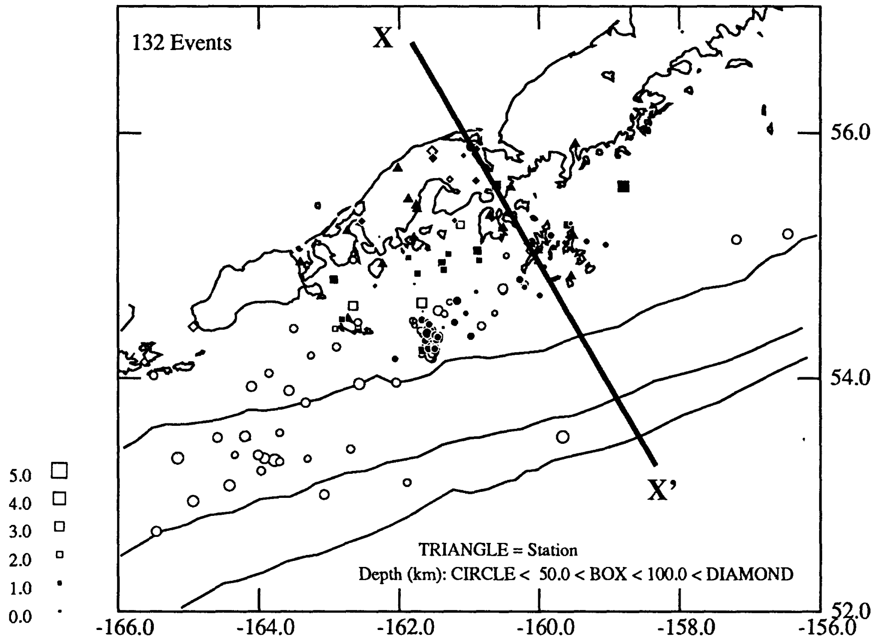

Figure 1. Map of seismicity located by the Shumagin seismic network from January to June, 1990. Symbol shapes show depths, sizes show magnitudes. Filled symbols meet criteria for well-located events, described in text.

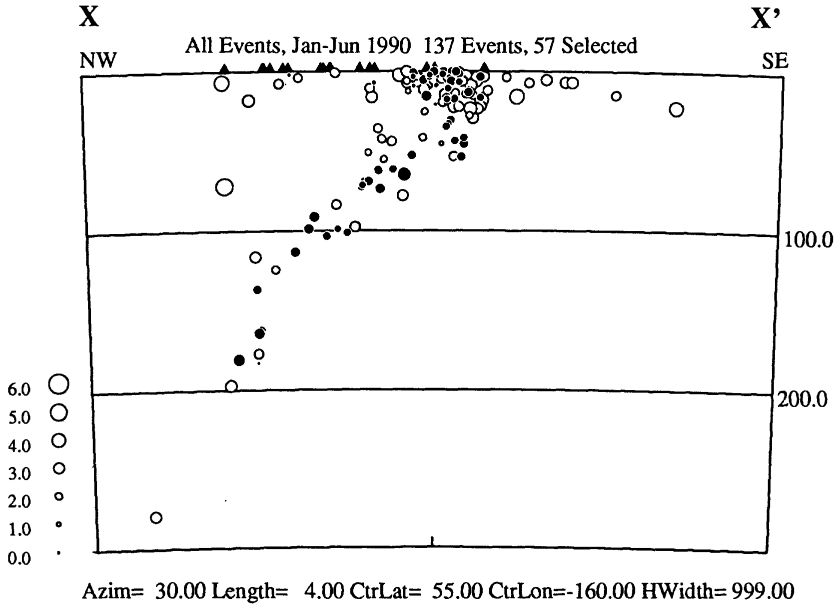

Figure 2. Cross-section of all Shumagin Network seismicity January-June 1990, located in Figure 1.

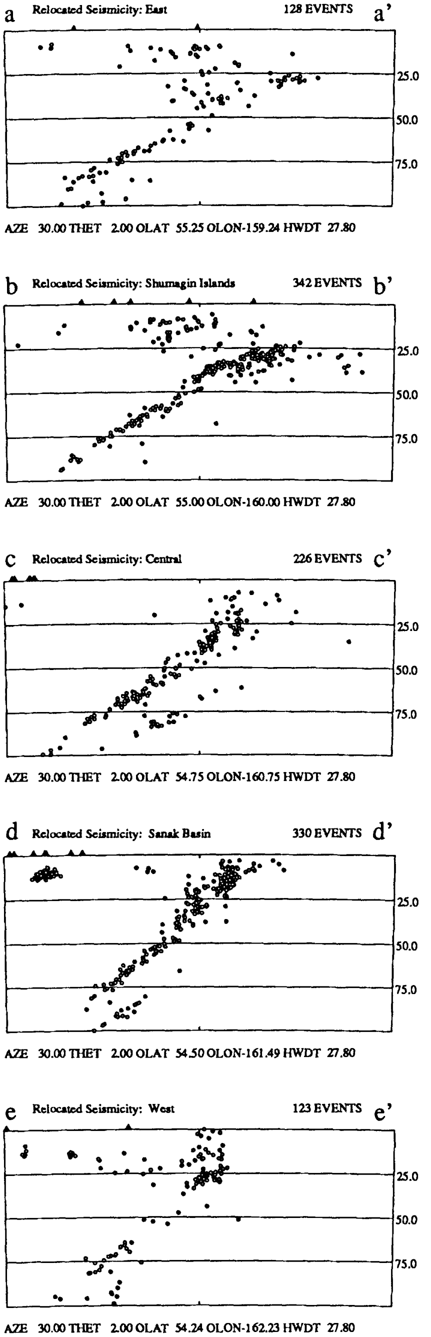

Figure 3. Relocated shallow earthquakes in the Shumagin region, 1982-1989. Earthquakes are subset of events, relocated in a joint inversion with 2D velocity. Events are selected on the basis of stability of the hypocenter inversion and the number of picked arrivals (minimum of 15). Five shallow cross-sections (left) are shown for the upper 100 km (scale on right of cross-sections), showing fine-scale structure of the seismic zone. Locations of cross-sections are shown on map, below. Triangles on top of sections are the network stations. A well-defined plate boundary above 50 km is only seen on section b-b', where stations are located immediately over the shallow plate contact. Most shallow earthquakes on b-b' define a zone less than 5 km wide, roughly the accuracy of the locations. Similarly, deeper events form a narrow zone or plane. Upper-plate earthquakes are found in a wide zone overlying the plate contact, and suggest possibly significant deformation in the forearc away from the trench. Depths of earthquakes on other cross-sections vary with the velocity structure because no stations overlie the events, and are probably less reliable.

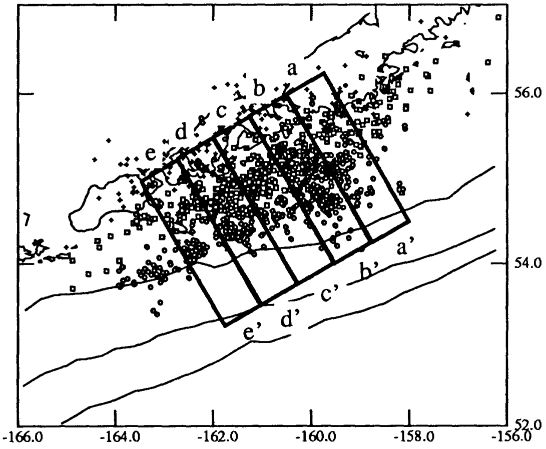

Partial Support of Joint USGS-CALTECH Southern California Seismographic Network

#14-08-0001-A0613

Clarence R. Allen
Robert W. Clayton
Egill Hauksson

Seismological Laboratory,
California Institute of Technology
Pasadena, CA 91125 (818-356-6912)

INVESTIGATIONS

This Cooperative Agreement provides partial support for the joint USGS-Caltech Southern California Seismic Network. The purpose is to record and analyze data from local earthquakes and generate a data base of phase data and digital seismograms. The primary product derived from the data base is a joint USGS-Caltech catalog of earthquakes in the southern California region.

RESULTS

Seismicity

The Southern California Seismographic Network (SCSN) recorded 4426 earthquakes during the six months from April through September 1990, an average of 738 per month, making it a relatively quiet reporting period (Figure 1). The prominent areas of microseismicity were the usual ones: the Coso and Kern River areas, the San Jacinto fault, the southern Elsinore fault, the Imperial Valley and the San Bernardino and Little San Bernardino Mountain areas.

There were only two events of M_L4.0 or larger. One was a M_L4.6 Upland aftershock at 2232 GMT on April 17. The Upland earthquake occurred on February 28, 1990 just south of the San Gabriel mountain front, and had an M_L of 5.2. The second largest earthquake this reporting period was an M_L4.2 that took place in the Salton City area, near the Clark fault on the western edge of Imperial Valley, at 0338 GMT on August 31. This event was followed by numerous aftershocks.

Aftershocks continued at a rate clearly higher than background in the Oceanside sequence (M_L5.3 on July 13, 1986) and the Coalinga sequence (M_L6.3 on May 3, 1983).

Focal Mechanisms

The focal mechanism for earthquakes of $M \geq 3.5$ are shown in Figure 2. A total of 18 events of $M \geq 3.5$ were recorded from 1 January to 30 September and reliable focal mechanisms could be determined for 13 events. The six events for which focal mechanisms were not determined were either aftershocks or located near the edge or outside of the network. Two events showing strike-slip faulting occurred near the Garlock fault in January. Six events occurred along the San Jacinto fault zone. Two of these occurred near the southern end of the Clark fault and showed right-lateral strike-slip faulting on a northwest trending plane. The 1990 Upland ($M_L=5.2$) mainshock was followed by a $M_L=4.6$ aftershock on April 17, which showed similar left-lateral strike-slip motion. Three events showing strike-slip and normal faulting were recorded adjacent to the San Andreas fault.

Weekly Seismicity Report

In January 1990, the Seismographic Network initiated a weekly seismicity report, patterned after a similar report issued by the U.S. Geological Survey in Menlo Park. The language of the "earthquake report" is aimed at the general public. So far, the report has been enthusiastically received. A few members of the local media have started basing regular news features on it.

TABLE . Locations and Focal Mechanisms of $M \geq 3.5$ Earthquakes that Occurred During January - September 1990

Origin	Time	Latitude	Longitude	Depth	Mag	Focal Mechanisms		
Day	UT	N	W	km	M_L	Ddir	Dip	Rake
900111	0122 10.27	35-13.34	118-13.22	1.6	3.5	115	65	20
900119	1239 17.92	35-13.42	118-13.48	1.5	3.6	110	75	-10
900205	0051 01.93	33-29.83	116-27.29	10.8	3.5	115	75	30
900218	1552 59.97	33-30.26	116-27.22	10.4	4.2	110	75	20
900228	2343 36.71	34-08.27	117-42.16	4.1	5.2	310	70	0
900404	0213 39.78	34-19.28	117-05.64	2.9	3.7	125	85	0
900407	0107 05.26	33-51.63	116-09.29	4.3	3.8	105	4	-80
900417	2232 27.32	34-06.26	117-43.20	3.6	4.6	045	90	-160
900418	1432 49.36	33-51.62	116-09.52	9.5	3.6	155	75	30
900617	0608 05.43	34-02.65	117-15.28	13.6	3.7	345	80	-10
900805	2127 03.70	33-19.35	116-24.59	10.8	3.6	315	85	0
900831	0105 48.92	33-14.02	116-01.97	13.3	3.9	45	80	-150
900831	0337 59.89	33-14.11	116-02.47	13.3	4.2	310	75	-20

Publications Using Network Data (Abstracts excepted).

Jones, Lucile, Kerry E. Sieh, Egill Hauksson, and L. Katherine Hutton, The 3 December 1988 Pasadena, California, earthquake: evidence for strike-slip motion on the Raymond fault, *Bull. Seismo. Soc. Am., 80,* No. 2, 474-482, 1990.

Magistrale, Harold, Part I: Superstition Hills California earthquakes of 24 November 1989.Part II: Three-dimensional velocity structure of southern California, Ph.D. thesis, California Institute of Technology, 1990.

Hauksson, E. Earthquakes, faulting and stress in the Los Angeles Basin, *J. Geophys. Res.*, 95, 15365-15394, 1990.

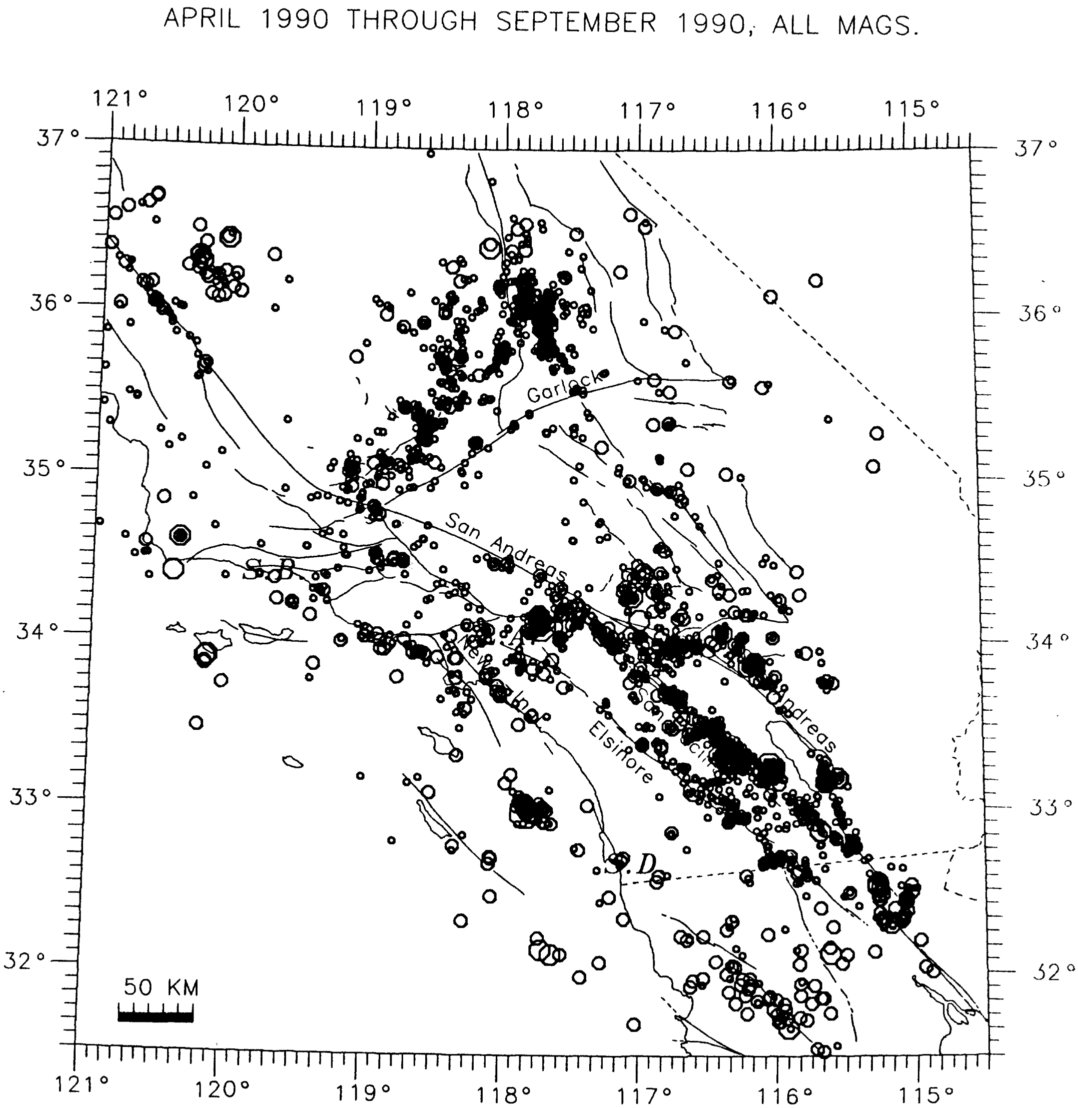

Figure 1. Map of epicenters of earthquakes in the southern California region, 1 April to 30 September 1990.

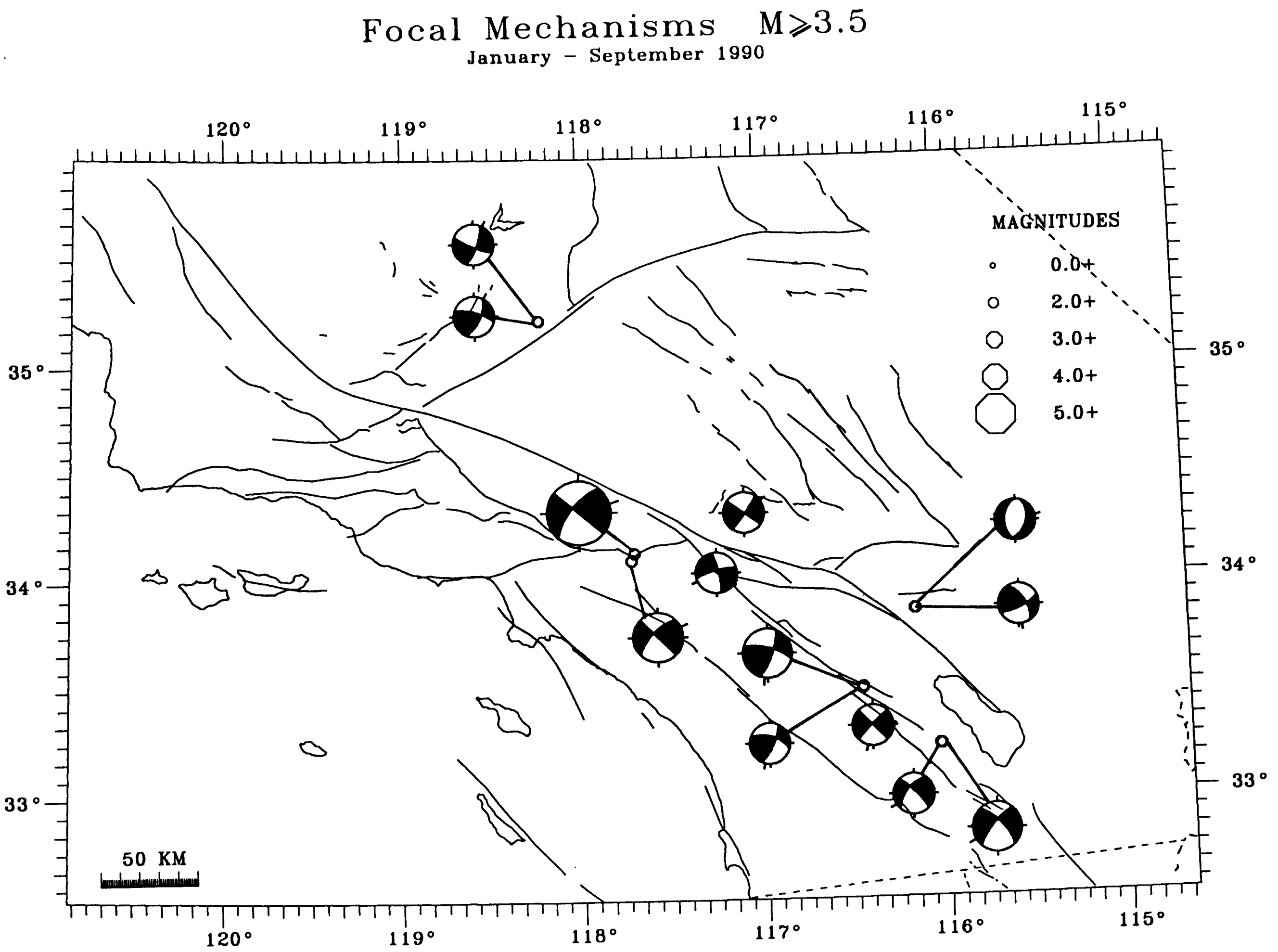

Figure 2. Focal mechanisms of earthquakes of M≥3.5 that occurred in southern California from 1 January to 30 September 1990. (See also enclosed table).

Regional Seismic Monitoring Along The Wasatch Front Urban Corridor And Adjacent Intermountain Seismic Belt

14-08-0001-A0621

W. J. Arabasz, R. B. Smith, J. C. Pechmann, and S. J. Nava
Department of Geology and Geophysics
University of Utah
Salt Lake City, Utah 84112
(801) 581-6274

Investigations

This cooperative agreement supports "network operations" associated with the University of Utah's 83-station regional seismic telemetry network. USGS support focuses on the seismically hazardous Wasatch Front urban corridor of north-central Utah, but also encompasses neighboring areas of the Intermountain seismic belt. Primary products for this USGS support are quarterly bulletins and biennial earthquake catalogs.

Results (April 1-September 30, 1990)

General accomplishments. During the report period, significant efforts related to: (1) adding redundancy to our capabilities for earthquake surveillance and response—including use of a color-display terminal for rapid visual display of epicenters and development of software for use with a battery-powered laptop computer for backup earthquake-location capability; (2) siting and installing two new three-component telemetry stations in the Salt Lake Valley (one located on deep alluvium and the other on bedrock) to examine site-amplification effects from diverse seismic sources; (3) promoting, for the second time, a major initiative to the Utah state legislature for modernizing seismic-network instrumentation in Utah; and (4) developing a detailed proposal to the USGS for funding a first stage of our network modernization (PC-based network recording, workstations for data analysis, and four digital seismographs) with matching funds from the University of Utah.

Network Seismicity. Figure 1 shows the epicenters of 696 earthquakes ($M_L \leq 3.9$) located in part of the University of Utah study area designated the "Utah region" (lat. 36.75°-42.5°N, long. 108.75°-114.25°W) during the six-month period April 1, 1990 to September 30, 1990. The seismicity sample includes twelve shocks of magnitude 3.0 or greater (labeled in Fig. 1) and five felt earthquakes (M_L = 3.9, 3.4, 2.8, 2.7, 2.6).

The largest earthquake during the six-month report period was a felt shock of M_L3.9 on June 28, 1990 (00:05 UTC), located 27 km southeast of Snowville. The earthquake was preceded by shocks of M_L3.1 on June 24 (01:27 UTC) and M_L3.4 (felt) on June 25 (22:06 UTC). Other significant seismicity during the report period included: (i) continuing earthquakes in the Blue Springs Hills area of north-central Utah (clustered epicenters 45 km west of Logan), the location of an M_L 4.8 earthquake on July 3, 1989; and (ii) a cluster of 57 earthquakes (20 events of magnitude 2.0-2.8) 38 km southeast of Salina (see clustered epicenters east of Richfield). The latter cluster is about 14 km southeast of the location of an M_L5.4 earthquake on January 30, 1989.

Reports and Publications

Arabasz, W. J., Pechmann, J. C., Smith, R. B., Nava, S. J., and McPherson, E., *University of Utah Regional Seismic Network, Report for USGS Network Review*, August 1990, 51 pp.

Nava, S. J., Earthquake Activity in the Utah Region, October 1 - December 31, 1989, *Survey Notes (Utah Geological and Mineral Survey)*, v. 23, no. 4, p. 11, 1989; January 1 - March 31, 1990, *Survey Notes (Utah Geological and Mineral Survey)*, v. 24, no. 1, p. 13, 1990.

Nava, S. J., Earthquake Activity in Utah, October 1 - December 31, 1989, January 1 - March 31, 1990, *Wasatch Front Forum (Utah Geological and Mineral Survey)*, v. 6, no. 1-2, pp. 8-9, 1990.

Nava, S. J., Pechmann, J. C., Arabasz, W. J., Brown, E. D., Hall, L. L., Oehmich, P. J., McPherson, E., and Whipp, J. K., *Earthquake Catalog for the Utah Region, January 1, 1986 to December 31, 1988*, University of Utah Seismograph Stations Special Publication, 1990, 96 pp.

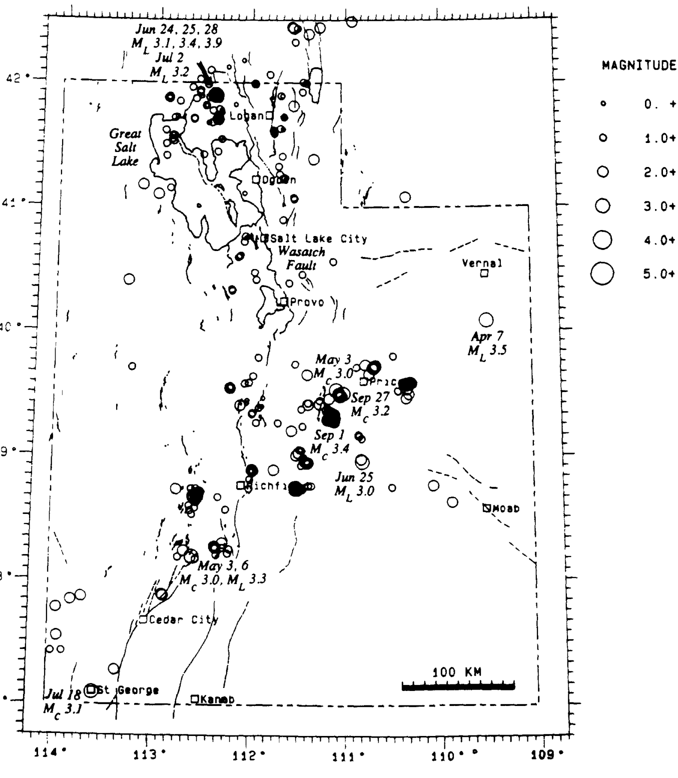

Figure 1. Earthquake Activity in the Utah Region, April 1, 1990, through September 30, 1990.

1. Regional Seismic Monitoring in Western Washington
and
2. Seismic Monitoring of Volcanic and Subduction Processes in Washington and Oregon

1. 14-08-0001-A0622
2. 14-08-0001-A0623

R.S. Crosson, S.D. Malone, A.I. Qamar and R.S. Ludwin
Geophysics Program
University of Washington
Seattle, WA 98195
(206) 543-8020
April 1, 1990 - Sept. 30, 1990

Investigations

Operation of the Washington Regional Seismograph Network (WRSN) and routine preliminary analysis of earthquakes in Washington and Northern Oregon are carried out under these contracts. Quarterly bulletins which provide operational details and descriptions of seismic activity in Washington and Northern Oregon are available from 1984 through the second quarter of 1990. Final catalogs are available from 1970, when the network began operation, though 1986. The University of Washington operates approximately 80 stations west of 120.5°W, 28 of which are supported under A0622, and 40 under A0623. This report includes a brief summary of significant seismic activity. Additional details are included in our Quarterly bulletins.

During this reporting period we installed four new stations in central Oregon. These stations had been planned for several years, but problems relating to telemetry routes made installation impossible until this year, when the Oregon Department of Transportation (DOT) gave us access to their microwave network. The new stations are telemetered via the DOT network to Portland, via the BPA (Bonneville Power Administration) microwave net to Seattle, and then by phone line to the UW.

Excluding blasts, probable blasts, and earthquakes outside the U. W. network, 1083 earthquakes west of 120.5°W were located between April 1, 1990 and September 30, 1990. Of these, 534 were located near Mount St. Helens, which has not erupted since October of 1986. Fifteen earthquakes were reported felt in western Washington during the period covered by this report. East of 120.5°W, 83 earthquakes were located, and none felt.

The largest earthquake during this reporting period was a M_L 5.2 earthquake (PDE M_b 4.4) on April 14 at the edge of the North Cascades near the town of Deming. This was part of a sequence of shallow earthquakes (less than 3 km deep) which began with a M_C 4.3 earthquake on April 2, and included 91 events of magnitude 1.5 or greater. Thirteen of these earthquakes were large enough to be reported felt to the UW. Investigators deploying portable equipment in the area reported that many additional earthquakes were felt. Activity decreased through the summer, and ceased about the end of August. Anthony Qamar of the University of Washington and James Zollweg of Boise State University are preparing a paper on this sequence.

An unusual earthquake of magnitude 3.2 occurred near Tillamook, Oregon at ~ 45 km depth on April 6, and was felt in northwestern Oregon. Earthquakes at this depth as far south as Oregon are quite rare, although not unknown.

Publications

Barker, S.E. and S.D. Malone, 1990 (submitted), Magmatic system geometry at Mount St. Helens modeled from the stress field associated with post-eruptive earthquakes, JGR.

Ludwin, R. S., S.D. Malone, R.S. Crosson, A.I. Qamar, 1990 (in press), Washington Earthquakes 1985, in U.S. Earthquakes, National Earthquake Information Service.

Ludwin, R. S., S.D. Malone, R.S. Crosson, A.I. Qamar, 1990 (in press), Washington Earthquakes 1986, in U.S. Earthquakes, National Earthquake Information Service.

Ludwin, R. S., S.D. Malone, R.S. Crosson, A.I. Qamar, 1990 (in press), Washington Earthquakes 1987, in U.S. Earthquakes, National Earthquake Information Service.

Ludwin, R. S., S.D. Malone, R.S. Crosson, A.I. Qamar, 1990 (in preparation), Washington Earthquakes 1988, in U.S. Earthquakes, National Earthquake Information Service.

Ludwin, R. S., S.D. Malone, R.S. Crosson, A.I. Qamar, 1990 (in preparation), Washington Earthquakes 1989, in U.S. Earthquakes, National Earthquake Information Service.

Ludwin, R. S., C.S. Weaver, and R.S. Crosson, 1990 (in press), Seismicity of Washington and Oregon, in: Slemmons, D.B., E.R. Engdahl, D. Blackwell and D. Schwartz, editors, Decade of North American Geology associated volume CSMV-1; Neotectonics of North America.

Neri, G. and S.D. Malone, 1989, An analysis of the earthquake time series at Mt. St. Helens, Washington, in the framework of recent volcanic activity, Jour. Volcan. Geother. Res., Vol. 38, pp. 257-267.

Thompson, K.I., 1990 (in preparation), Seismicity of Mt. Rainier - a detailed study of events to the west of the mountain and their tectonic significance, BSSA.

Univ. of Wash. Geophysics Program, 1990, Quarterly Network Report 90-A on Seismicity of Washington and Northern Oregon

Univ. of Wash. Geophysics Program, 1990, Quarterly Network Report 90-B on Seismicity of Washington and Northern Oregon

Univ. of Wash. Geophysics Program, 1990 (in preparation), Quarterly Network Report 90-C on Seismicity of Washington and Northern Oregon

Abstracts

Jonientz-Trisler, C., C. Driedger, and A. Qamar, 1990, Seismic signatures of debris flows on Mt. Rainier, WA, EOS, Vol. 71, No. 36, p. 1068

Jonientz-Trisler, C., and C. Driedger, 1990 (in press), Seismic evidence of historic debris flows and dry season floods on Mount Rainier, Washington, 1961-1990, EOS, Fall 1990 PNAGU

Moran, S. C., and S.D. Malone, 1990, Pre-1980 seismicity at Mt. St. Helens: is the past the key to the present, EOS, Vol. 71, No. 36 p. 1067

Moran, S. C., and S.D. Malone, 1990 (in press), Focal mechanism solutions from recent earthquakes in the deeper magmatic system at Mt. St. Helens, EOS, Fall 1990 PNAGU

Qamar, A. and J. Zollweg, 1990 (in press), The 1990 Deming Washington earthquakes: a sequence of shallow thrust earthquakes in the Pacific Northwest, EOS, Fall 1990 PNAGU

Nabelek, J., K. Werner, R. Yeats, and S. Malone, 1990 (in press), The August, 1990, Woodburn, Oregon earthquake sequence: constraints from broadband regional recording and geological implications, EOS, Fall 1990 PNAGU.

Seismological Data Processing Project

9930-03354

John Evans, Greg Allen, Moses Smith
U.S. Geological Survey
Branch of Seismology
345 Middlefield Road, Mail Stop 977
Menlo Park, California 94025
(415) 329-4753

This Project provides UNIX computer support to the Branch of Seismology. "Investigations, results and reports" are not part of our duties. We supply network management, systems management, installation, backups, maintenance, and trouble shooting to Branch UNIX computers. There are currently 18 UNIX computers in the Branch of Seismology: an Integrated Solutions Inc., multi-user system; a SUN 4/280 file server; 6 SUN SPARCstation 1s; 6 SUN 3/60 workstations; 2 SUN 3/50 workstations; 1 SUN 3/80 workstation; 1 SUN SPARCstation SLC.

During the last 6 months of FY90 we provided the following services for the Branch:

1. Maintained RTP data system buffer service to Branch UNIX and VAX computers.
2. Supported the Branch Administrative Office's PC network, by installing hardware and software.
3. Started the upgrades of the SUN computers to the latest version of the SUN operating system.
4. Upgraded the Alaska project's SUN 3/60 computers to SPARCstation 1s.
5. Installed 2, Branch of Seismology, Apple MacIntosh computers, on the Branch of Tectonophysics Appletalk computer network.
6. Purchased a SUN SPARCstation SLC in order to provide a "public Branch workstation.
7. Continued supplying backups for the UNIX computers.
8. Arranged for various hardware repairs for the UNIX computers.
9. Started planning for the retirement of the ISI UNIX computer, and subsequent move of users to the SUN 4/280 computer.

Central California Network Operations

9930-01891

Wes Hall
Branch of Seismology
U.S Geological Survey
345 Middlefield Road-Mail Stop 977
Menlo Park, California 94025
(415)329-4730

Investigations

Maintenance and recording of 342 seismograph stations (446 components) located in Northern and Central California. Also recording 68 components from other agencies. The area covered is from the Oregon border south to Santa Maria.

Results

1. Bench Maintenance Repair

A. seismic VCO units	169
B. summing amplifiers	24
C. Seismic test units	4
D. V02H / V02L VCO units	45
E. DC-DC converters	10

2. Production/Fabrication

A. J512A VCO units	10
B. J512B VCO units	12
C. dc-dc converter/regulators	8
D. summing amplifiers	17
E. V02H / V02L VCO units	8

3. Completed Open File report: "J312, J412H, J512a Field Note Summary"

4. Connected additional 128 channel input to Willie Lee's portable IBM based monitor.

5. Shortened and rerouted cables from telemetry frame to PI tape recorders.

6. Completed RFP and technical evaluation for two additional field technicians.

7. Order parts for the fabrication of 100ea J512 VCO's

8. Updated documentation of wiring list from discriminator out to CUSP and RTP

9. New seismic stations:
   CSV (Stone Valley), MPRV, MPRZ (Pilot Ridge), PRP (Reason Peak), LSR (Sweetbrier).

10. New seismic components
    MHDZ (Hidden Dam), CBRN (Bollinger Canyon Road), KCPZ (Cahto Peak), LSFZ (South Fork), LRDZ (Redding Peak).

11. Stations deleted:
    LRSZ, LRSV, LHH, LMDN, LMDE, LSS, LGH (Medicine Lake); CDUN (Duarte Ranch), LCA, (Castella), JLPI, JLPJ, JLPK, JLPF, JLPZ (Loma Prieta)

Central Aleutians Islands Seismic Network

Agreement No. 14-08-0001-A0259

Carl Kisslinger, Sharon Kubichek, Bruce Kindel, and Julie Hill
Cooperative Institute for Research in Environmental Sciences
Campus Box 216, University of Colorado
Boulder, Colorado 80309

(303) 492-6089

Brief Description of Instrumentation and Data Reduction Methods

The Adak seismic network consists of 13 high-gain, high-frequency, two-component seismic stations and one six-component station (ADK) located at the Adak Naval Base. Station ADK has been in operation since the mid-1960s; nine of the additional stations were installed in 1974, three in 1975, and one each in 1976 and 1977.

Data from the stations are FM-telemetered to receiving sites near the Naval Base, and are then transferred by cable to the Observatory on the Base. Data were originally recorded by Develocorder on 16 mm film; since 1980 the film recordings are back-up and the primary form of data recording has been on analog magnetic tape. The tapes are mailed to CIRES once a week.

At CIRES, the analog tapes are played back through an analog-to-digital (a-to-d) converter into a computer at four-times the speed at which they were recorded. This computer then digitizes the data, automatically detects events, demultiplexes each event, and writes them to disk. These events are edited to eliminate spurious triggers, and a tape containing only seismic events is created. All subsequent processing is done from this tape. Times of arrival and wave amplitudes are read from an interactive graphics display terminal. The earthquakes are located using a program originally developed for this project by E. R. Engdahl, which has been modified several times since.

Data Annotations

The scheduled maintenance trip for summer 1990 has not been conducted yet, due to medical problems of contract personnel. Currently, the only major unit not working on Adak is the satellite link with the GOES time clock. This does not present a problem as the network has a second functioning clock. Three stations are down as a result of a lightning strike at the end of the 1988 summer maintenance trip.

Current Observations

Since August 1989, we have been digitizing and locating all of our data on a SUN workstation with a Cutler Digital Design a-to-d converter. In January 1990, this workstation was upgraded to a SUN 3/60 level CPU with 8 megabytes of internal memory (RAM). This has helped somewhat with our system hang problems; however, we still have a system hang an average of two times a day when digitizing. Discussion with SUN hardware personnel revealed that this level of workstation can adequately support no more than three peripherals on the SCSI bus. With our disk drives, cartridge tape unit, and the a-to-d converter, we have 4 peripherals on the SCSI bus. SUN personnel expressed some surprise that we were functioning at all with this load. This situation cannot be improved without purchase of a second workstation for which we do not have funding. Despite this problem, we are now up-to-date on digitizing 1990 data and have begun to digitize older data (early 1989 and 1988). We are, however, about three months behind in locating current data and still have a backlog of 1988 and 1989 data to locate. In May, 1990, version 4.1 of the UNIX operating system was installed. No major problems resulting from the system upgrade have been encountered and version 4.1 seems to better handle the digitizing process.

The location work for this report includes: (1) 75 earthquakes located for September, 1989; (2) 260 earthquakes located for March, April, and May, 1990; and, (3) 51 earthquakes located for a special study of events that occurred during January 8 - 10, 1989. Included in the March, 1990 results is a subset of data, consisting of the M_b 6.3 earthquake that occurred on March 12 and forty-nine of its aftershocks. This subset, as well as the January 8 - 10, 1989 data, are part of a continuing study of seismicity patterns in the Andreanof Islands region.

The total of events located for all time periods is 386. Twenty-five of the 1989 events and twenty-two of the 1990 events, which were located with data from the Adak network, were also large enough to be located teleseismically (U.S.G.S. PDEs). The epicenters of the March, April, and May, 1990 events are shown in Figure 1 and a vertical cross-section of the data is given in Figure 2. It should be briefly noted that the level of seismic activity for May, 1990 (Figure 1) is similar to the pre-1982 level. This suggests that the interpreted period of quiescence, from 1982 until the M_s 7.7 earthquake in May 1986, has ended (Kisslinger, 1988).

More detailed information about the network status, maps and cross-sections for the 1989 data, and a catalog of all hypocenters determined for the time period reported are included in our Semi-Annual Data Report to the U.S.G.S. Recent research using these data is reported in the Technical Summary for U.S.G.S. Grant No. G1368.

References

Kisslinger, C. (1988). An experiment in earthquake prediction and the 7 May 1986 Andreanof Islands earthquake, *Bull. Seism. Soc. Am.* **78,** 218-229.

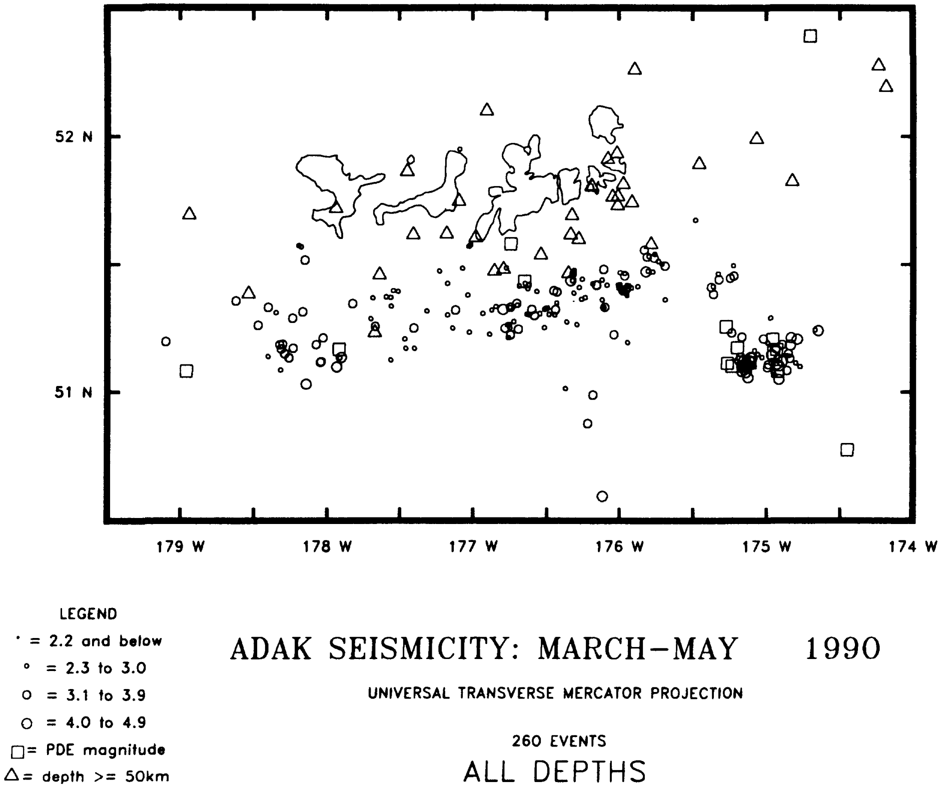

Figure 1: Map of seismicity located for March, April, and May, 1990. All epicenters were determined from Adak network data. Events marked with squares are those for which a teleseismic body-wave magnitude has been determined by the U.S.G.S.; all other events are shown by symbols which indicate the duration magnitude determined from Adak network data. The islands mapped (from Tanaga on the west to Great Sitkin on the east) indicate the geographic extent of the Adak seismic network.

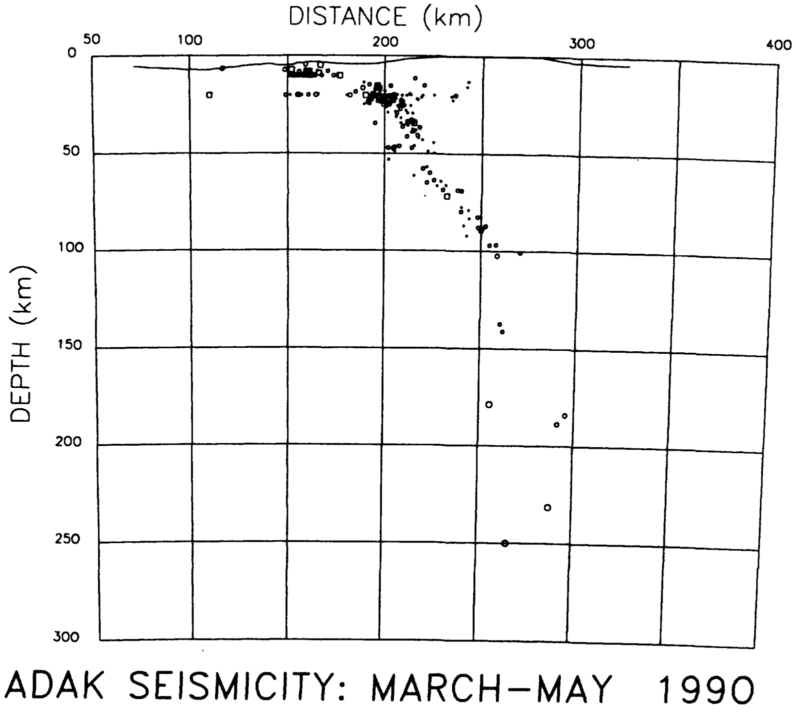

Figure 2: Vertical cross section of seismicity located for March, April, and May, 1990. Events are projected according to their depth (corresponding roughly to vertical on the plot) and distance from the pole of the Aleutian volcanic line. The zero-point for the distance scale marked on the horizontal axis of the plot is arbitrary. Events marked with squares are those for which a teleseismic body-wave magnitude has been determined by the U.S.G.S.; all other events are shown by symbols which indicate the duration magnitude determined from Adak network data. The irregular curve near the top of the section is bathymetry.

Alaska Seismic Studies

9930-01162

John C. Lahr, Christopher D. Stephens,
Robert A. Page, Kent A. Fogleman
Branch of Seismology
U. S. Geological Survey
345 Middelfield Road
Menlo Park, California 94025
(415) 329-4744

Investigations

1) Continued collection and analysis of data from the high-gain short-period seismograph network extending across southern Alaska from the volcanic arc west of Cook Inlet to Yakutat Bay, and inland across the Chugach Mountains. This region spans the Yakataga seismic gap, and special effort is made to monitor for changes in seismicity that might alter our assessment of the imminence of a gap-filling rupture.

2) Cooperated with the USGS Branch of Alaskan Geology, the Geophysical Institute of the University of Alaska (UAGI), and the Alaska Division of Geological and Geophysical Surveys in operating the Alaska Volcano Observatory (AVO). Under this program, our project monitors the seismicity of the active volcanoes flanking Cook Inlet and operates six- and an ten-station arrays of seismographs near Mt. Spurr and Mt. Redoubt, respectively.

3) Cooperated with the Branch of Engineering Seismology and Geology and the UAGI in operating 15 strong-motion accelerographs in southern Alaska, including 11 between Icy Bay and Cordova in the area of the Yakataga seismic gap.

Results

1) Preliminary hypocenters determined using data from the regional network for the period January-June 1990 are shown in Figures 1 and 2. Shallow seismicity (Figure 1) tends to be concentrated in many of the same areas that have been active for at least the last few years. Apparent decreases in the rate of shallow seismicity in an around the Yakataga seismic gap and Prince William Sound are most likely a systematic effect caused by station outages and by the less reliable nature of current event detection and recording procedures in these areas. For the area extending from west of Prince William Sound to the volcanic arc, a sharp increase in the magnitude level for completeness of both crustal and subcrustal shocks that occurred after April 1990 also appears to be a systematic effect caused by a change in event detection procedures.

Notable earthquakes that occurred within this time period include: 1) a magnitude 4.5 M_a (4.2 m_b) shock on May 21, located 42 km deep near latitude 61.3° N, longitude 145.0° W. This event, at the northwest corner of the Yakataga seismic gap, is one of the largest shocks known to occur within the northeastward-dipping Wrangell Wadati-Benioff seismic zone (WBZ). A prelimiary focal mechanism determined using initial P-wave polarities indicates that the least-compressive stress axis dips westward at a shallow angle, normal to the dip direction of the subducted plate. In contrast, events within the northwestward-dipping Aleutian WBZ to the west have least-compressive stress axes that are oriented predominantly downdip. 2) a crustal shock of magnitude 5.2 (4.9 m_b) on January 7 located near latitude 65.1° N, longitude 149.3° W. This event had at least one foreshock, a magnitude 2.4 event that occurred 15 s before the mainshock, and 17 aftershocks with magnitudes ranging from 1.1 to 2.2 that occurred within 24 h; the largest aftershock was a magnitude 3.1 event that occurred on January 14. 3) An unusual earthquake doublet within the Aleutian WBZ about 30 km southeast of Redoubt volcano on March 9-10. These shocks both had magnitudes of about 5 (the second one being slightly smaller), were located about 2 km apart, and were separated in time by about 13.5 h. On June 7, another shock of about magnitude 5 occurred within about 15 km of the earlier pair, and 4) A tight cluster of crustal shocks related to the recent eruptive sequence at Redoubt volcano.

2) The eruption sequence at Redoubt volcano, which began on December 14, 1989 (Alaska Volcano Observatory Staff, 1990), continued until April 21, 1990. Of eight major eruptions that occurred between March 5 and April 21, five were preceded by detectable swarms of long-period (0.3-0.5 s) events. Although weak compared to the dramatic swarms that presaged the largest eruptions, which occurred on December 14 and January 2, these swarms were the basis for warnings issued before the eruptions on March 23 and April 6. Near the end of the sequence, eruptions occurred at remarkably uniform intervals, averaging 4.5 ± 0.9 days for February 15-March 14 and 8.0 ± 1.2 days for March 14-April 15 (Page and others, 1990). Times of eruptions were predicted by linear extrapolation of previous eruptions. On this basis, advance warning was provided for the April 15 eruptions, which occurred within the 3½-day, 70-percent prediction window on April 12. No detectable swarm preceded this eruption, hence is could not have been forecast on the basis of seismicity.

Two new vertical-component seismographs were installed on Redoubt volcano in close proximity (within about 340 m) to the existing site RSO, located 2 km south of the summit, in order to investigate in more detail the slowness and coherence of seismic waves generated by volcano-related earthquakes. The site RED, located 7 km south-southwest of the summit of Mt. Redoubt, was upgraded to a three-component station.

3. Upgrades to the regional network of high-gain seismographs during routine maintenance included convertion of the station CRQ

to solar power. Operation of many of the remote sites using solar power has proved to be reliable and cost effective. For example, the station SKN operated for 5 years on solar power without interruption or field visits.

No strong-motion recorders were triggered by earthquakes in southern Alaska during the last year. The strong-motion recorder at Whittier was moved to Portage.

4. Throughout the eruption sequence at Redoubt volcano, AVO has relied on a PC-based data acquisition program (MDETECT; Tottingham and others, 1989) that was modified to also generate spectral data using a digial-signal-processing board (Rogers, 1989). Recently this software was further modified to write the spectral data to disk files in SUDS format (Ward, 1989) and to send the data to the parallel port for communication with another PC.

Modifications to correct a timing problem on the 128-channel multiplexer board designed by Ellis (1989) were completed. Two modified boards have been operating successfully on PC-based data acquisition systems in Menlo Park for several months. The installation of one or more boards in Fairbanks is awaiting the porting of software that includes spectral analysis of seismic signals.

A menu-driven dBase (Aston-Tate Corp., Torrence, CA) application program was written to manage three data bases that cover purchases, field operations and inventory.

References

Alaska Volcano Observatory Staff, 1990, The 1989-1990 eruption of Redoubt Volcano, EOS, Trans. Amer. Geophys. Union, v. 71, p. 265-275.

Ellis, J. O., 1989, Expanding the input multiplexer for the Data Translation, Inc. Model DT2821 analog-to-digital converter, U. S. Geological Survey Open-File Report 89-191, 6 p.

Page, R. A., J. N. Davies, J. A. Power, J. C. Lahr, and C. D. Stephens, 1990, Forecasting the March and April 1990 eruptions at Redoubt volcano, Alaska, EOS, Trans. Amer. Geophys. Union (Dir. Approv. 08/28/90).

Rogers, J. A., 1989, Frequency-domain detection of signals using a DSP coprocessor board, in, Lee, W. H. K., ed., IASPEI Software Library, V. 1: Toolbox for Seismic Data Acquisition, Processing, and Analysis, Seismological Society of America, El Cerrito, CA, pp. 151-172,.

Tottingham, D. M., Lee, W. H. K., and Rogers, J. A., 1989, User manual for MDETECT, in, Lee, W. H. K., ed., IASPEI Software Library, V. 1: Toolbox for Seismic Data Acquisition, Processing, and Analysis, Seismological Society of America, El Cerrito, CA, p. 45-84.

Ward, P. L. , 1989, SUDS: Seismic Unified Data System, U. S. Geological Survey Open-File Report 89-188, 122 pp.

Reports

Chouet, B. A., R. A. Page, J. N. Davies, J. A. Power, J. C. Lahr, D. H. Harlow, and C. D. Stephens, 1990, Forecasting the December 14, 1989 and January 2, 1990 eruptions at Redoubt volcano, Alaska, EOS, Trans. Amer. Geophys. Union (abs., in press).

Grantz, Arthur, A. R. Green, D. G. Smith, J. C. Lahr, and Kazuya Fujita, 1989, Major Phanerozoic tectonic features of the Arctic Ocean region, Plate 11, in: Volume L, The Geology of North America, The Geological Society of America, Boulder, CO.

Harlow, D. H., J. A. Power, B. A. Chouet, J. C. Lahr, and R. A. Page, 1990, Earthquake families and their implications for the eruption dynamics of Redoubt volcano, Alaska; December 13, 1989 to January 3, 1990, EOS, Trans. Amer. Geophys. Union (abs., in press).

Lahr, J. C., and W. H. K. Lee, 1990, Preparing data files for AcroSpin, in: IASPEI Software Library, v. 2., pp. 165-184, Seismological Society of America, El Cerrito, CA.

Lahr, J. C., J. A. Power, D. H. Harlow, and R. A. Page, 1990, Spatial and temporal distribution of seismicity associated with the recent eruptions of Redoubt volcano, Alaska, EOS, Trans. Amer. Geophys. Union (abs., in press).

March, G. D., J. A. Power, D. H. Harlow, and J. C. Lahr, 1990, Acquisition, processing, storage, and display of seismic data during the 1989-1990 eruption of Redoubt volcano, Alaska, EOS, Trans. Amer. Geophys. Union (abs., in press).

Page, R. A., J. N. Davies, J. A. Power, J. C. Lahr, and C. D. Stephens, 1990, Forecasting the March and April 1990 eruptions at Redoubt volcano, Alaska, EOS, Trans. Amer. Geophys. Union (Dir. Approv. 08/28/90).

Power, John, J. N. Davies, R. A. Page, J. C. Lahr, D. H. Harlow, B. A. Chouet, G. D. March, and T. L. Murray, 1990, Seismic evolution of the 1989-1990 eruption of Redoubt volcano, Alaska, EOS, Trans. Amer. Geophys. Union (abs., in press).

Stephens, C. D., J. N. Marso, J. C. Lahr, and J. A. Rogers, 1990, Realtime seismic spectral amplitude monitoring during the 1989-1990 eruptions of Redoubt volcano, Alaska, EOS, Trans. Amer. Geophys. Union (abs., in press).

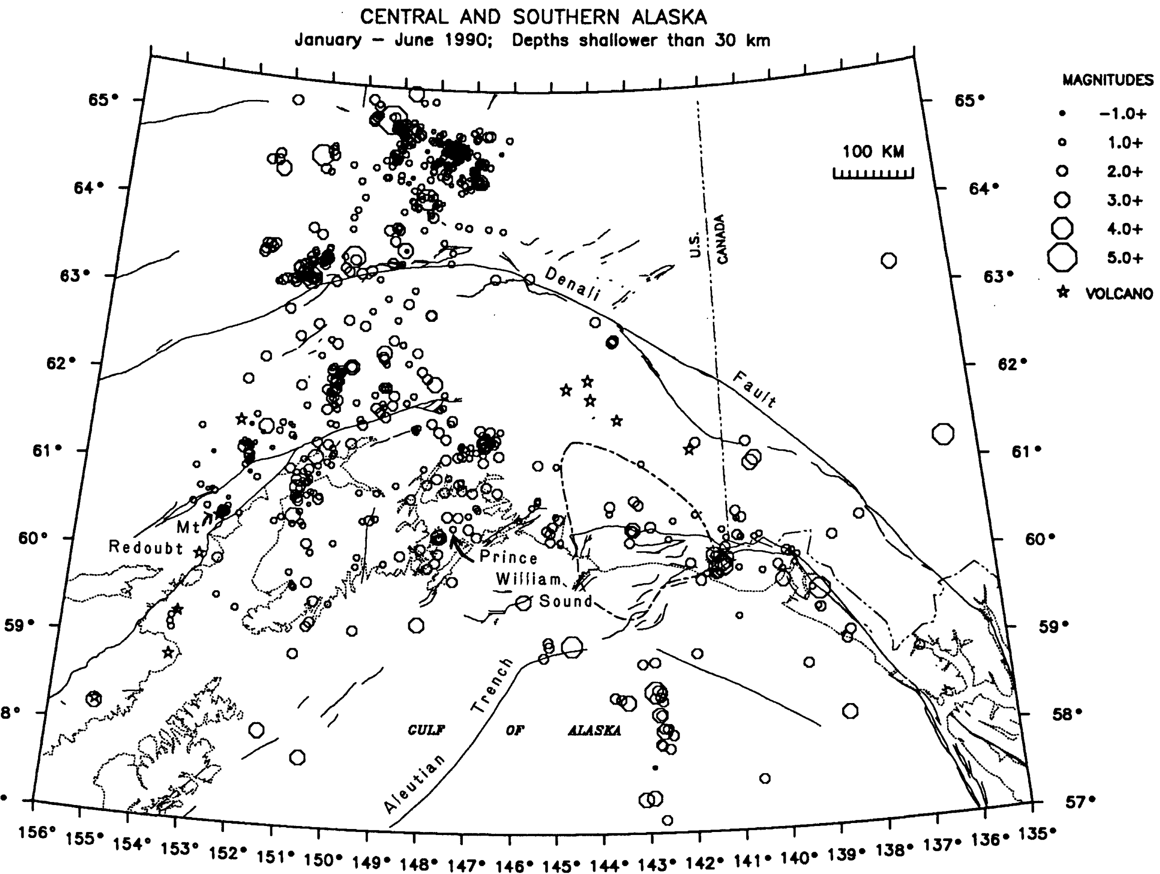

Figure 1. Epicenters of 959 shallow earthquakes that occurred between January and June 1990 (processing for this time period is not yet completed). Magnitudes are determined from amplitudes of seismic signals; the magnitude threshold for completeness varies across the network. Contour with alternating long and short dashes outlines inferred extent of Yakataga seismic gap. Neogene and younger faults (George Plafker, personal communication, 1988) are shown as solid lines.

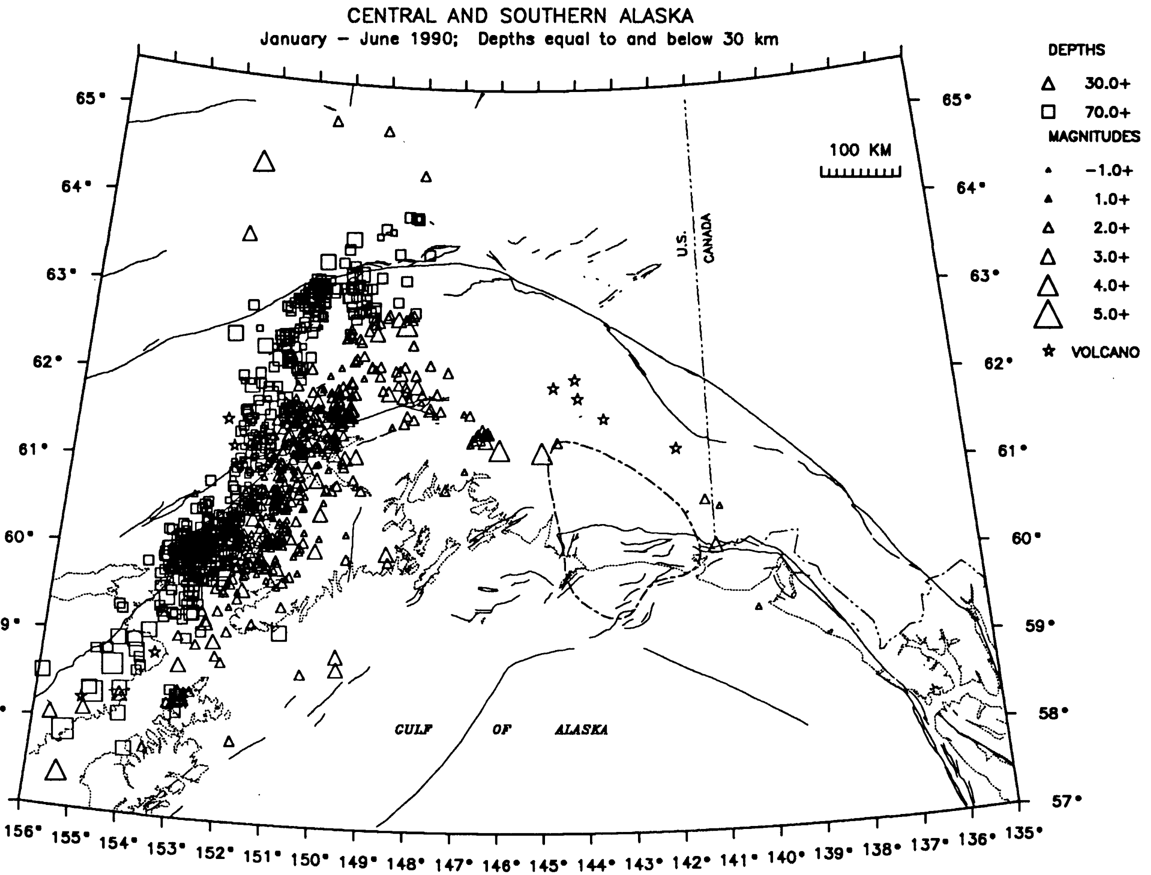

Figure 2. Epicenters of 1066 intermediate and deep shocks that occurred between January and June 1990. See Figure 1 for details about magnitudes and identification of map features.

Northern and Central California Seismic Network Processing

9930-01160

Fredrick W. Lester
Branch of Seismology
U.S. Geological Survey
345 Middlefield, MS 977
Menlo Park, CA 94025
(415) 329-4747

Investigations

1. In 1966 a seismographic network was established by the USGS to monitor earthquakes in central California. In the following years the network was expanded to monitor earthquakes in most of northern and central California, particularly along the San Andreas Fault, from the Oregon border to Santa Maria. In its present configuration there are over 500 single and multiple component stations in the network. The primary responsibility of this project is to monitor, process, analyze, and publish data recorded from this network.

2. This project continues to maintain the primary seismic data base for the years 1969 to the present on both computers and magnetic tapes for those interested in doing research using the network data. As soon as older data are complete and final the preliminary data base is updated with the final phases and locations.

3. Lately video has become increasingly useful in documenting research activities being conducted by the USGS, especially activities related to the Parkfield Prediction Experiment. In addition, computer animation of geophysical data sets have allowed researchers to study the data in time series and in 3-dimensions. The two technologies work well in communicating the research being done here to a wide audience that includes other geoscientists as well as untrained but interested laymen who are able to understand the material when it is presented in a visually appealing way.

4. As time permits some research projects are underway on some of the more interesting or unusual events or sequences of earthquakes that have occurred within the network.

Results

1. Figure 1 illustrates 11345 earthquakes located in northern and central California and vicinity during the time period April through September 1990. This level of seismicity is higher than normal for a six month period. The increase is due primarily to the most important earthquake sequence in California in many years, the aftershocks of the Loma Prieta Earthquake of October 1989. That earthquake occurred on October 17, 1989 in the Santa Cruz Mountains, approximately 16 kilometers northeast of Santa Cruz. To date we have located more than 7000 aftershocks and they are continuing at a rate of about 3 to 4 per day of all magnitudes. The largest aftershocks recorded include a magnitude 5.2 aftershock 37 minutes after the mainshock, a magnitude 5.0 aftershock on October 19, 1989, a magnitude 5.4 aftershock on April 27, 1990, and a magnitude 5.0 on April 27. The aftershocks are occurring in a 55 kilometer long zone from south of Los Gatos at the north end to east of Watsonville at the south end (Figure 1).

Some of the increase in seismicity during this time was also due to a sequence of earthquakes in the Alamo area of central California, mostly during the month of April. The sequence included three magnitude 4 or larger quakes and a few hundred smaller ones. The largest, magnitude 4.6, occurred on April 27.

Seismic data recorded by the network are being processed using the CUSP (Caltech USGS Seismic Processing) system. CUSP was designed by Carl Johnson in the early 1980's and has since undergone some revisions for the Menlo Park operation. On September 1, 1989 we began using revised CUSP software in a generic format. This new format makes CUSP more universally acceptable to groups that are using or plan to use it in the future because the commands are relatively non-specific to any particular group operation.

In the future we plan to begin publishing, probably on a monthly basis, a preliminary catalog of earthquakes for northern and central California. The format is not yet established but it will probably be some type of listing of events accompanied by a text explaining the processing and what is in the catalog, and a map showing the epicenters. The catalog will be approximately complete at the magnitude 1.5 in the central core of the network and something approaching M2.0 in the more remote portions of the net.

2. The current catalog is relatively complete and correct through July 1990. The data from August and September are incomplete and some errors still remain to be identified and corrected. Some additional data need to be added to all months from outside sources and quarry blasts need to be identified for July through September.

3. New hardware was purchased for the new Geologic Division video editing room by Steve Walter. He is currently aiding in setting up the new facility which will greatly enhance our ability to produce high quality videos.

4. Steve Walter continues to investigate the seismicity in the Medicine Lake region following a magnitude 4.0 earthquake occurred in that area on September 30, 1988 followed by many aftershocks. The seismicity has subsided to a very low level at the present time but there has been renewed interest in this region because of this activity and it's possible relationship to associated volcanic activity. Steve is currently co-authoring a paper in progress that will describe the historical seismicity and crustal deformation in the Medicine Lake region.

   Nan Macgregor and Dave Oppenheimer are currently analyzing data from the April 1990 Alamo earthquake sequence. Plans are to underway to relocate historical earthquakes in the region and compare those with the April activity. Focal mechanisms will be determined for some of the more important earthquakes and used to define the regional stress pattern in this area that lies between the southern end of the Concord fault and the northern end of the Calaveras fault. Results of this investigation will be published later this Fall or Winter.

Reports

None

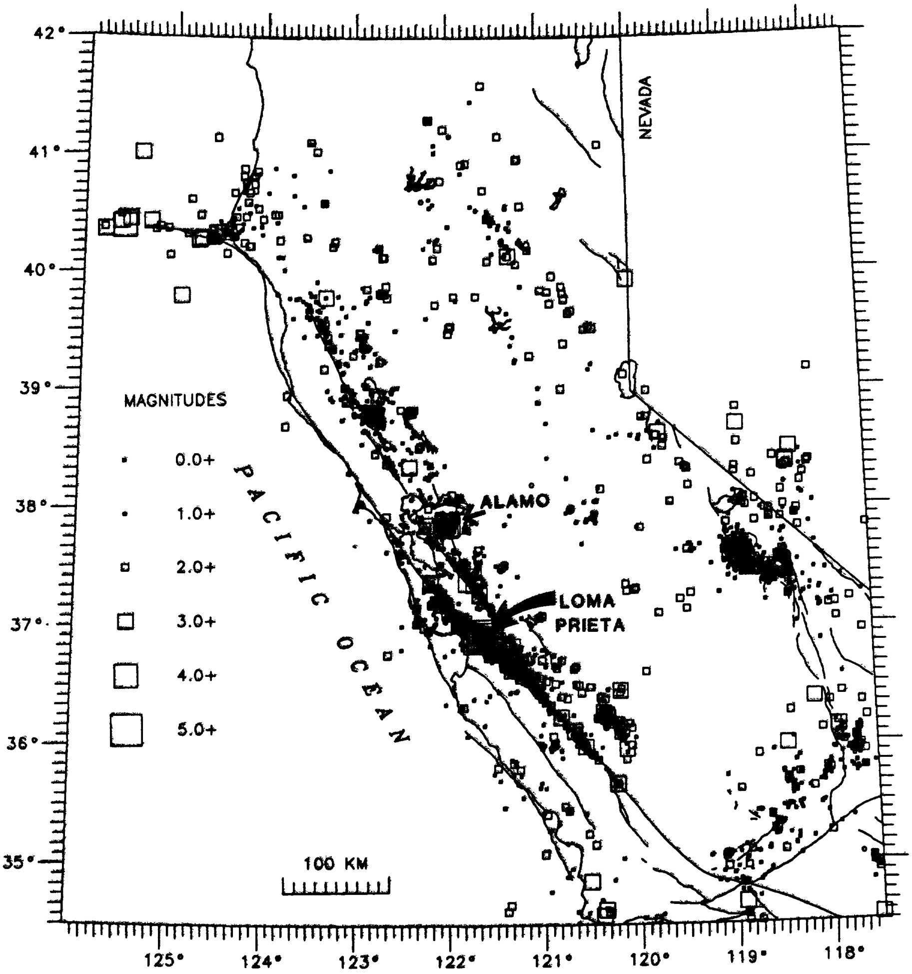

FIGURE 1. Seismicity for northern and central California and vicinity during April - September 1990

Western Great Basin - Eastern Sierra Nevada Seismic Network

Cooperative Agreement 14-08-0001-A00
1 April 1990 - 1 September 1990

W.A. Peppin
Seismological Laboratory, MS 168
University of Nevada
Reno, NV 89557
(702) 784-4315

Investigation

This contract supported continued operation of a seismic network in the western Great Basin of Nevada and eastern California, with the purpose of recording and locating earthquakes occurring in the western Great Basin, and acquiring a data base of phase times and analog and digital seismograms form these earthquakes. Research using the data base was performed under USGS contract 14-08-0001-G1524 and is reported elsewhere in this volume.

Results

During the time period 1 April 1990 to 31 September 1990 2,080 earthquakes were registered by the University of Nevada within the University of Nevada seismic network, which monitors the eastern Sierra Nevada - Western Great Basin area with special emphasis on the regions west of Reno, Nevada, within the Excelsior Mountains, and near Long Valley caldera (Figure 1). Of these, 17 were magnitude 3 and greater, but none in the Nevada region reached 4.0 in magnitude. Most of the earthquakes are located near Long Valley caldera or Chalfant Valley, showing a reduction in activity from the previous six months. The swarm in the south moat of the caldera continues, but with reduced levels of activity.

Seismicity in the vicinity of the caldera is shown in Figure 2. The south moat activity is the concentration just east of the town of Mammoth Lakes. The activity north of Bishop is the continuing aftershocks of the 1986 Chalfant Valley sequence. Activity in the mountain block south of the caldera continues to occur in a diffuse region of NNE lineations, as it has for many years. Earthquakes continue to show under Mammoth Mountain, just west of Mammoth Lakes, but at a far reduced rate.

Catalogs covering the seismicity are in review, and will shortly to be published for the time period through 31 December 1989 The previous network computer system, consisting of a PDP11/70 and a PDP11/34 was replaced by the Microvax/CUSP system on 7 November 1989. The completion of a bulletin through 1989 will put, in a single place, all of the information taken from the PDP11/70 system. Every effort has been made to maintain consistent procedures in making the transfer to the CUSP system, so that the completeness of the catalog, the computation of magnitudes, and the location procedures will be comparable. However, researchers should note that some inconsistency is bound to creep in, and so use of UNR catalog data through 1989 must be made with caution through the transition period to CUSP. Before 7 November 1989 all of the catalog locations were obtained from the PDP11/70 system; after 1 January 1990 all come from the CUSP system; for the two months November and December 1989 the catalog contains a mix of events. Because of considerable computer down time in December 1989, quite a bit of data was lost. We are now working on merging data with the USGS CUSP system in Menlo Park to recover this lost data, and plan to include this in our bulletin as well.

With the onset of the CUSP system, the network data stream now includes calibrated digital waveforms from ten wideband (0.05 to 20 Hz) three-component digital stations located around this region (Figure 3, showing UNR network stations as triangles with the digitals named). Therefore, the MEM/GRM file pairs after 7 November 1989 also contain this information together with the uncalibrated vertical waveforms used for earthquake timing. Also operating on the Microvax system is an Exabyte data logger, which continuously records the incoming digital data on tape, and is being kept as an ongoing data library, providing access to data for distant teleseisms and large events. Calibration pulses for the digital stations (not complete at this writing) are found on the UNR Microvax system in ROOT$DUA0:[CALPULSES]. The UNR computer can be reached either by 1200-baud remote modem (numbers 702-784-1592 or 702-784-4270): please call Bill Peppin at 702-784-4975 for information how to log onto the computer (KERMIT is available). The microvax cluster can also be accessed through the TELNET addresses 134.197.33.248 and 134.197.33.249 and supports TCP/IP communications through the FTP file transfer package from Wollongong and Associates.

Figure 1

Nevada – Western Great Basin Seismicity
1 Apr 1990 through 31 Sept 1990

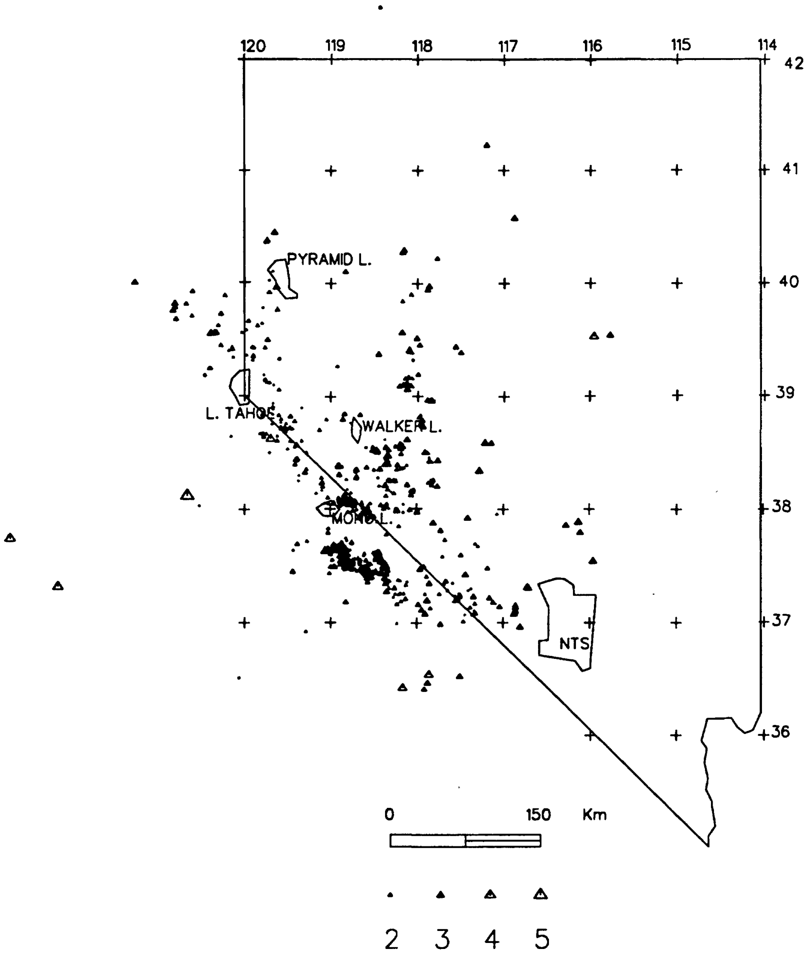

Figure 2

Mammoth – White Mountains Seismicity
1 Apr 1990 – 30 Sept 1990

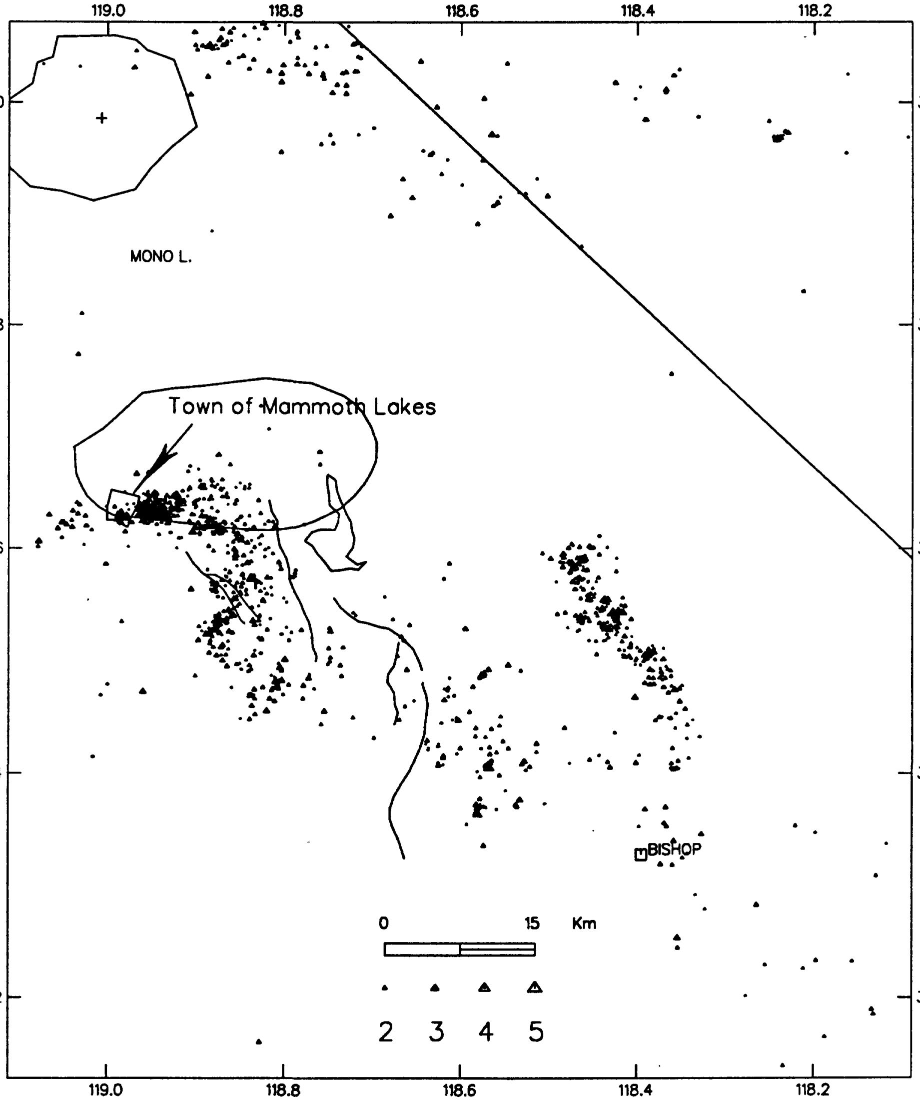

Figure 3

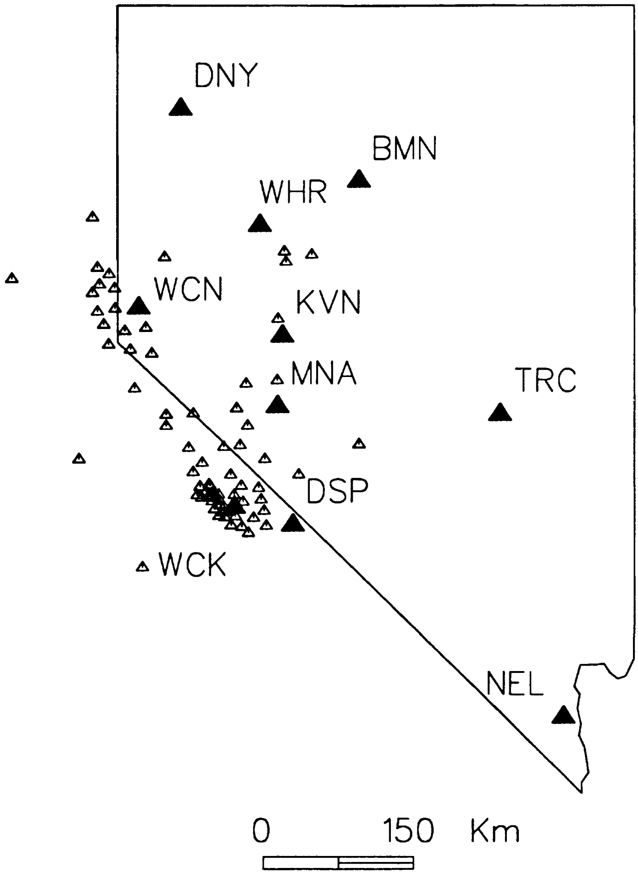

Regional Microearthquake Network in the Central Mississippi Valley

14-08-0001-A0619

William V. Stauder and Robert B. Herrmann
Department of Earth and Atmospheric Sciences
Saint Louis University
3507 Laclede
St. Louis, MO 63103
(314) 658-3131

Investigations

The purpose of the network is to monitor seismic activity in the Central Mississippi Valley Seismic zone, in which the large 1811-1812 New Madrid earthquakes occurred. The following section gives a summary of network observations during the first six months of the year 1990, as reported in Network Quarterly Bulletins No. 63 and 64.

Results

In the first six months of 1990, 102 earthquakes were located by the 42 station regional telemetered microearthquake network operated by Saint Louis University for the U.S. Geological Survey and the Nuclear Regulatory Commission. Figure 1 shows 98 earthquakes located within a 4° x 5° region centered on 36.5°N and 89.5°W. The magnitudes are indicated by the size of the open symbols. Figure 2 shows the locations and magnitudes of 90 earthquakes located within a 1.5° x 1.5° region centered at 36.25°N and 89.75°W.

In the first six months of 1990, 53 teleseisms were recorded by the PDP 11/34 microcomputer. Epicentral coordinates were determined by assuming a plane wave front propagating across the network and using travel-time curves to determine back azimuth and slowness, and by assuming a focal depth of 15 kilometers using spherical geometry. Arrival time information for teleseismic P and PKP phases has been published in the quarterly earthquake bulletin.

The significant earthquakes occurring in the first six months of 1990 include the following:

1. January 24 (1820 UTC). Southern Indiana. mbLg 3.9 (FVM), 3.8 (NEIS), 4.0 (BLA). Felt (V) at Leavenworth, Ind. and Rhodelia, Ky. Felt (IV) at Indiana cities of Branchville, Corydon, Derby, Grantsburg, Mauckport, Magnet, Rome and Saint Croix. Also felt (IV) at Kentucky cities of Battletown, Brandenburg, Ekron, Guston, Hawesville, Lewisport, Payneville, Sample, Stephensport, Union Star, Webster and West Point.
2. January 27 (1405 UTC). Southern Indiana. mbLg 3.6 (FVM), 3.5 (NEIS). Felt (IV) at Indiana cities of Derby, Grantsburg, Magnet, Rome and St. Croix. Also felt (IV) at Battletown, Ky.

3. March 2 (0701 UTC). Southern Illinois. mbLg 3.7 (FVM), 3.6 (NEIS). Felt (V) at Greenville, Hagarstown, Saint Peter, Smithboro and Vernon. Felt (IV) at Alma, Keyesport, Odin and Shobonier.
4. March 12 (1648 UTC). Missouri-Arkansas Border Region. mbLg 3.0 (SLU), CL 2.8 (CERI). Felt (IV) at Arkansas cities of Clarkridge, Henderson, Lakeview, and Mountain Home. Also felt (IV) at Howards Ridge, Missouri.
5. March 18 (1622 UTC). Missouri-Arkansas Border Region. mbLg 3.3 (FVM), MD 3.0 (CERI). Felt (IV) at Alton, Missouri.
6. April 24 (0942 UTC). Southern Illinois. mbLg 3.2 (FVM), mbLg 3.0 (NEIS). Felt (III) at Martinsville, Illinois.

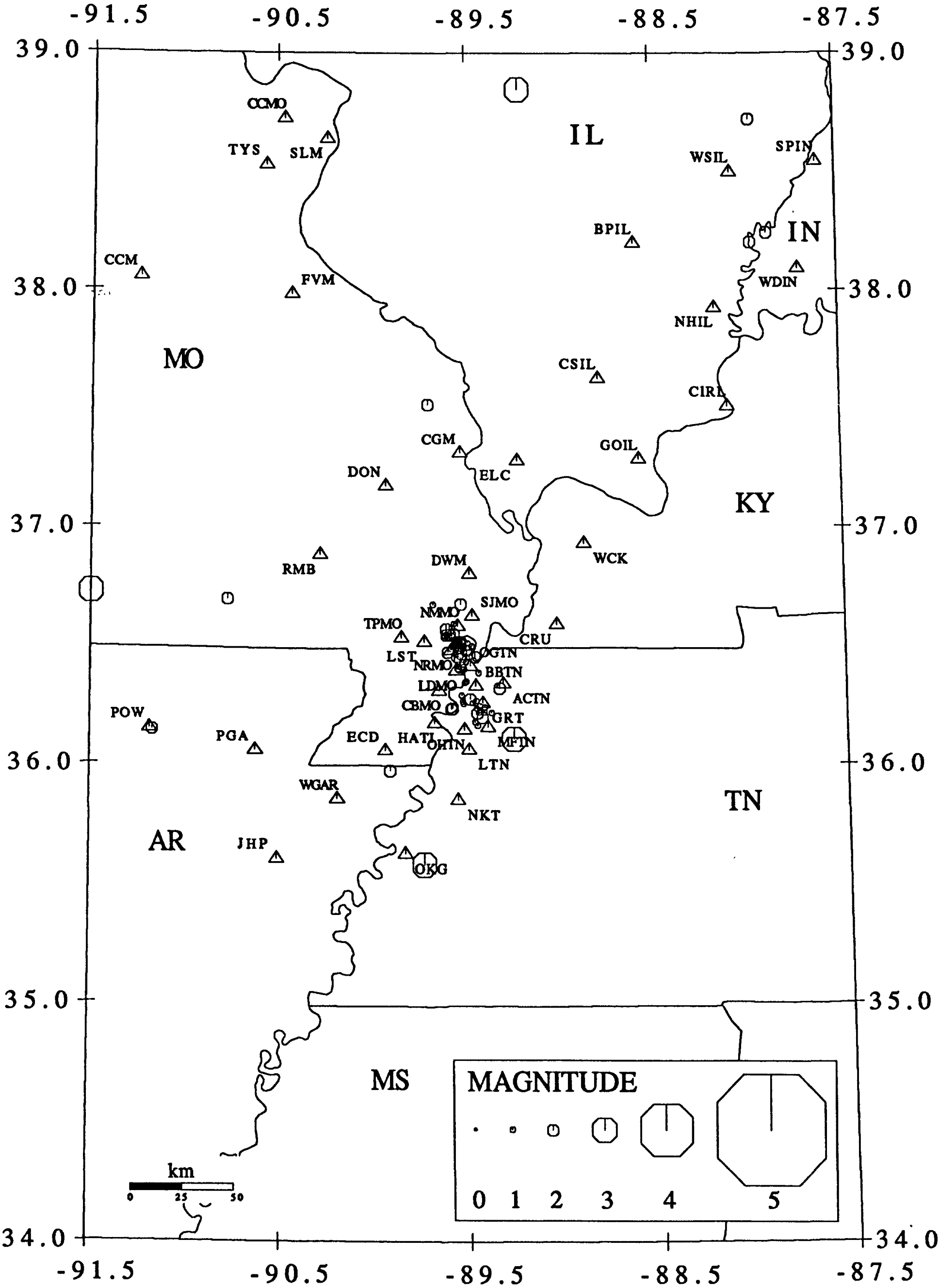

FIGURE 1

CUMULATIVE EVENTS 01 JAN 1990 TO 30 JUN 1990

LEGEND : △ STATION ○ EPICENTER

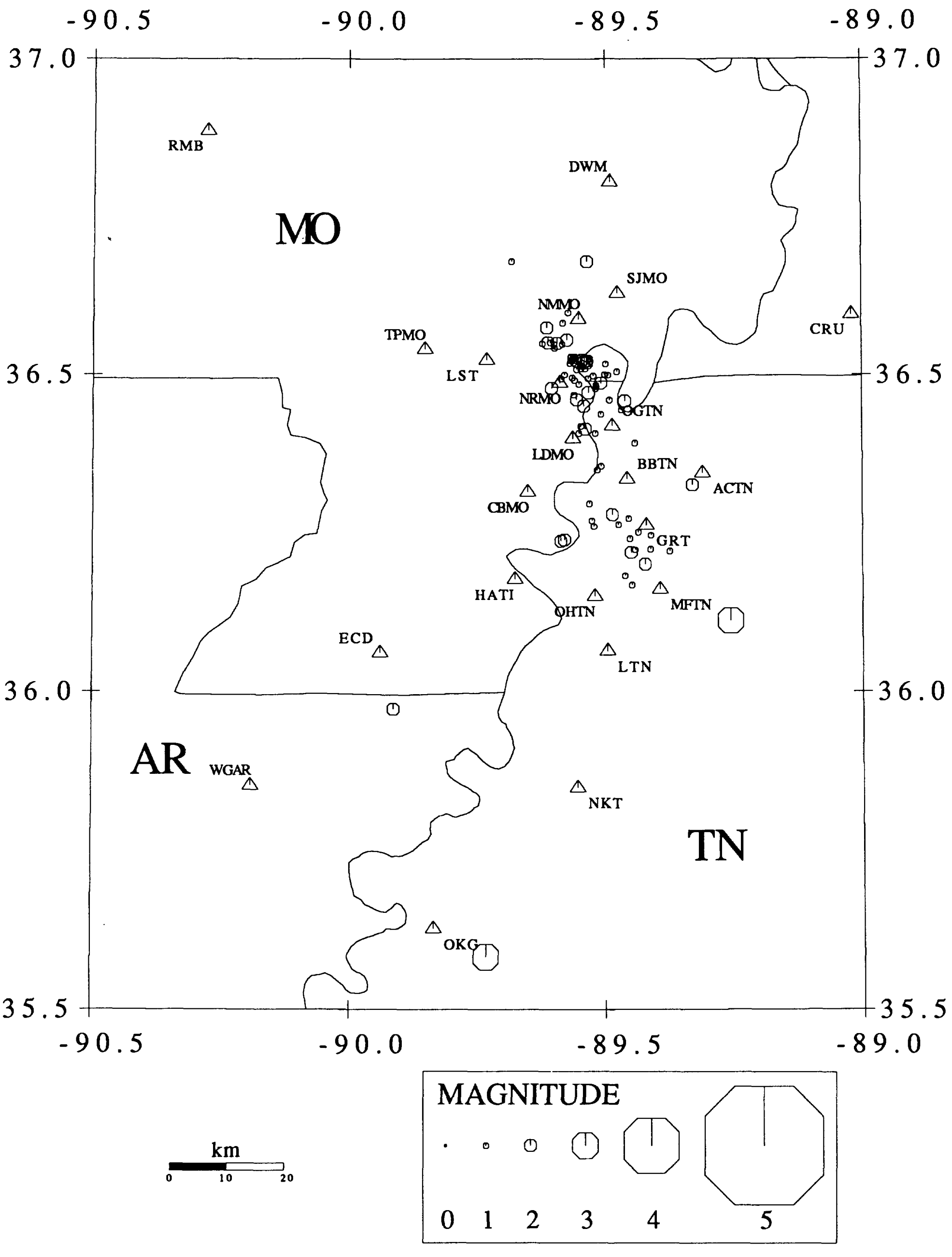

FIGURE 2
CUMULATIVE EVENTS 01 JAN 1990 TO 30 JUN 1990
LEGEND : △ STATION ○ EPICENTER

Consolidated Digital Recording and Analysis

9930-03412

Sam Stewart
Branch of Seismology
U. S. Geological Survey
345 Middlefield Road Mail Stop 977
Menlo Park, California 94025

Investigations.

The "Consolidated Recording and Analysis " project has as its primary goal the design, development and support of computer-based systems for processing earthquake data recorded by large, telemetered seismic networks. This includes (1) realtime systems capable of monitoring up to 1000 stations and detecting and saving waveforms from earthquakes registering just slightly above background noise level to very large ones, (2) near-realtime and offline systems to analyze, catalog and archive the detected waveforms, (3) support and documentation for the users of the system.

Hardware for these systems is based upon Digital Equipment Corporation (DEC) VAX series of micro-computers. Currently, this includes the VAX 750, microVAX II, and VAXstations 2000, 3100 and 3200.

Software is based upon the DEC/VMS operating system, the CUSP database system, and the GKS graphics system. VMS is a major operating system, well documented and developed, and has a rich variety of system services that facilitate our own system development. CUSP is a state-driven data base system designed for systematically processing large numbers of earthquakes recorded by large local seismic networks. It was developed by Carl Johnson of the USGS. GKS is an international-standard graphics analysis package that provides interactive input facilities as well as graphical output to a workstation. We use the DEC implementation of GKS.

The main goal for the last year has been to complete development of the "Generic" version of CUSP. This is a more modular, more generalized, more integrated version of CUSP than the one we have used since 1984. The Generic CUSP consists of a realtime earthquake event detection and processing module, the earthquake (offline) processing module (QED, Quake EDitor) a new interactive graphics module known as "TIMIT", a new interactive station display program known as "STNMAP", and extensive online documentation in the form of "help" files. Generic CUSP retains the use of the Tektronix 4014 graphics terminals with the high-speed graphics interface, and adds the ability to use the DEC VS2000 and VS3xxx series of workstations for interactive graphic analysis of earthquakes.

Results.

1. The various modules of Generic CUSP are essentialy finished, in the sense that they can be used for routine network processing operations. Practically, Generic CUSP will never be "finished"; there will always be changes to make.

2. The CALNET processing project (see F.W. Lester, project 9930-01160, this volume) is ready to change to all new CUSP processing modules. As reported earlier, that project started using the generic CUSP database commands on Sept.1,1989.

   During this report period, we added three new DEC 3100 workstations to the VAXCluster environment, to be used with the interactive timing program "TIMIT". CALNET analysts are using these workstations routinely to time and process earthquakes on the VAX/750 computer. The new realtime earthquake data acquisition system, referred to as the RT system, started serious operation for CALNET on Sept. 1, 1990. We are running it in parallel with the PDP 11/44 realtime system, to compare the results of the two systems. Our goal is to have a smooth transition from the 11/44 system to the Generic CUSP RT system.

3. Digitizing of the daily FM-telemetry tapes has resumed. This essential process came to a stop in February 1990 when the old Data General computer finally broke down. We bought a used MicroVAX computer and installed our standard Generic CUSP software on it.

4. Documentation was written for the TIMIT module.

5. We continue to provide CUSP software support, VMS operating system support, and VAX hardware support to various seismic networks in the western U.S. During this report period the INEL seismic network came online using VAX/VMS, CUSP and CAMAC technology, and the University of Nevada (Reno) brought a third CUSP RT system online to to support high-frequency data acquisition from foam-block fault slip experiments.

6. We continue to provide hardware and software support for the two Parkfield seismic networks (Varian and Haliburton).

7. During this report period we assumed responsibility for providing VAX/VMS services to the Branch of Seismology in Menlo Park.

Reports:

None.

Earthquake Hazard Research in the Greater Los Angeles Basin and Its Offshore Area

#14-08-0001-A0620

Ta-liang Teng and Thomas L. Henyey

Center of Earth Sciences
University of Southern California
Los Angeles, CA 90089-0740
(213) 740-5838

INVESTIGATIONS

This Contract provides partial support to monitor earthquake activity in the Los Angeles Basin and the adjacent offshore area. Upgrade of network instrumentation is accomplished by installing Optimum Telemetry System (OTS) for onscale waveform recording of local earthquakes, and installation of more downhole seismometers has improved network coverage and sensitivity necessary for an adequate seismic monitoring in a large metropolitan area. An in-house funding is made available to install six 3-component short-period stations on the USC campus. This tight array of stations is used primarily for strong motion site effect studies.

RESULTS

The 1 July 1989 - 30 June 1990 Los Angeles Basin Seismicity

During this 12 month period, the seismicity in the Los Angeles Basin and its adjacent area (Figure 1A) remains quite active; it is dominated by a strong cluster of events centered around 34° 08' N 117° 42'. The main shock of this cluster of events is the February 28, 1990 Upland earthquake of magnitude $M_L5.2$ (revised from $M_L5.5$ given in last report). The cluster is shown on the top right of Figure 1A. The origin of this group of events can be traced back to a smaller cluster taken place at the same location with the $M_L4.6$ mainshock occurred on 26 June 1988. The activity in the Santa Monica bay remains high; this can be related to two earlier larger events: a $M_L5.0$ event on January 19, 1989 some 25 km south of Malibu, followed by a $M_L4.0$ event 10 km offshore southwest of Point Dume on February 2, 1989. Except for the Long Beach to Seal Beach segment, the Newport-Inglewood fault is very active from Beverly Hills to Newport. Along this trend, events can be found as far south as Dana Point. Many events group around the Whittier fault trend, some of them are Whittier Narrows aftershocks. A few sizable events are located in the epicentral regions of the earlier 1988 Pasadena earthquake and the 1971 San Fernando earthquake.

The 1 April - 30 September 1990 Los Angeles Basin Seismicity

Figure 1B give the seismicity of the last six month period. There is no significant change in the general pattern of event occurrence. The overall activity level appears to have reduced somewhat. The four minor aftershock clusters noted above -- in Santa Monica bay, Whittier Narrows, Pasadena, and San Fernando -- have reduced to background levels. But the Upland aftershocks are still going strong.

A plot of cumulative number of earthquakes in the monitoring area during 1 July, 1989 to 30 June, 1990 is given in Figure 2A. Clearly, the largest jump of this curve occurs on 28 February, 1990 when the M_L5.2 Upland earthquake and many of its aftershocks took place.

Focal mechanisms of three largest Upland aftershocks are given in Figure 2B. They are very consistent among themselves, giving a NE-striking left-lateral strike-slip fault, which is essentially the same as the mechanism reported for the main shock.

The OTS waveform data from many Los Angeles basin earthquakes are used in a study of earthquake sources, as well as a study of deep crustal reflections. Network data are used for study of site effect. Strong motion data are used for source inversion and for a calibration of the magnitude scale.

REFERENCES

Hauksson, E. and L. M. Jones, The 1987 Whittier Narrows earthquake sequence in Los Angeles, southern California: Seismological and tectonic analysis, J. Geophys. Res., 94, 9569-9590, 1989.

Hauksson, E. and G. V. Saldivar, Seismicity (1973-1986) and active compressional tectonics in the Santa Monica Bay, southern California, J. Geophys. Res., 94, 9591-9606, 1989.

Hauksson, E. and R. S. Stein, The 1987 Whittier Narrows earthquake: a metropolitan shock, J. Geophys. Res., 94, 9545-9547, 1989.

Hauksson, E., Earthquakes, faulting, and stress in the Los Angeles Basin, J. Geophys. Res., 95, 15365-15394, 1990.

Hauksson, E., T. L. Teng, T. L. Henyey, M. Robertson, J. K. McRaney and L. Hsu, Earthquake hazard research in the Los Angeles Basin and its offshore area, Annual Technical Report, submitted to the U.S. Geological Survey, December 1988, 90 pp.

Robertson, M. C. and E. Hauksson, Three-dimensional fine velocity structure of the Los Angeles Basin, Fall AGU meeting, 1989.

Li, S.B. and T.L. Teng, Dependence of Richter magnitude scale on site conditions and local geology, Fall AGU meeting, 1990.

Teng, T.L. and J. Wang, Analysis of short-period waveform in the Los Angeles basin, Fall AGU meeting, 1990.

Su, F., S. Koyanagi, Y. Zeng, K. Mayeda, T.L. Teng, and K. Aki, A recursive stochastic inversion of site effect using coda waves, Fall AGU meeting, 1990.

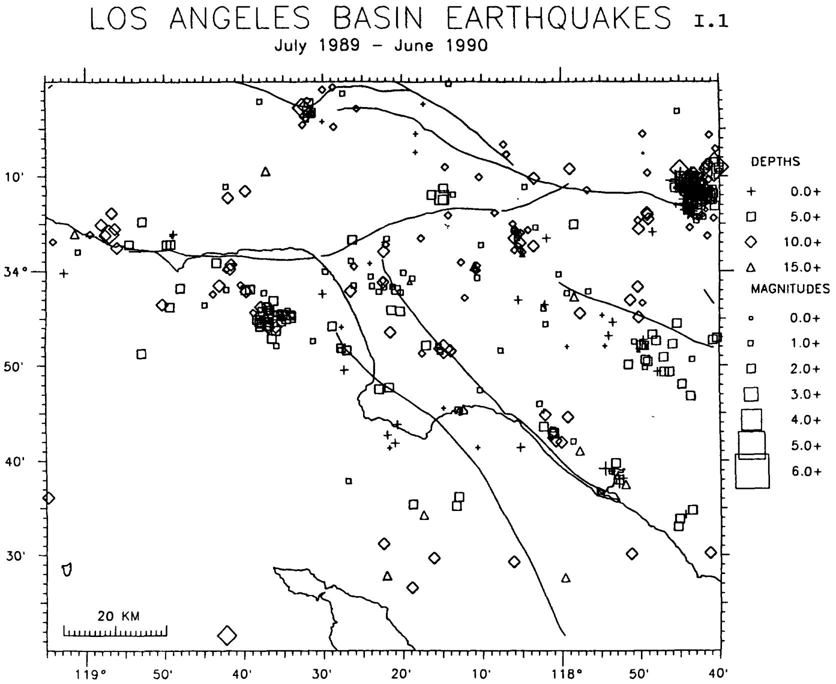

Figure 1A. Seismicity recorded between July 1989 and June 1990 by the USC network.

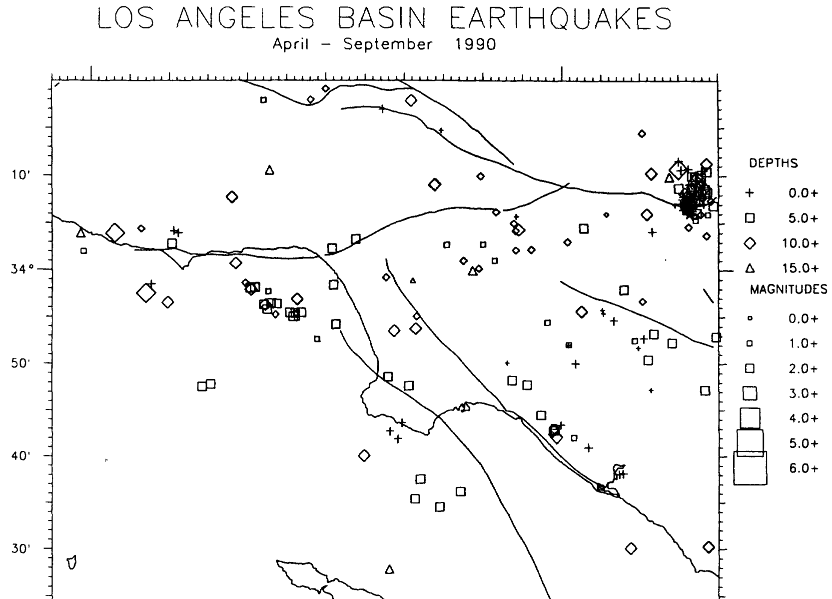

Figure 1B. Seismicity recorded between April 1, 1990 and September 30, 1990 by the USC Los Angeles basin seismic network.

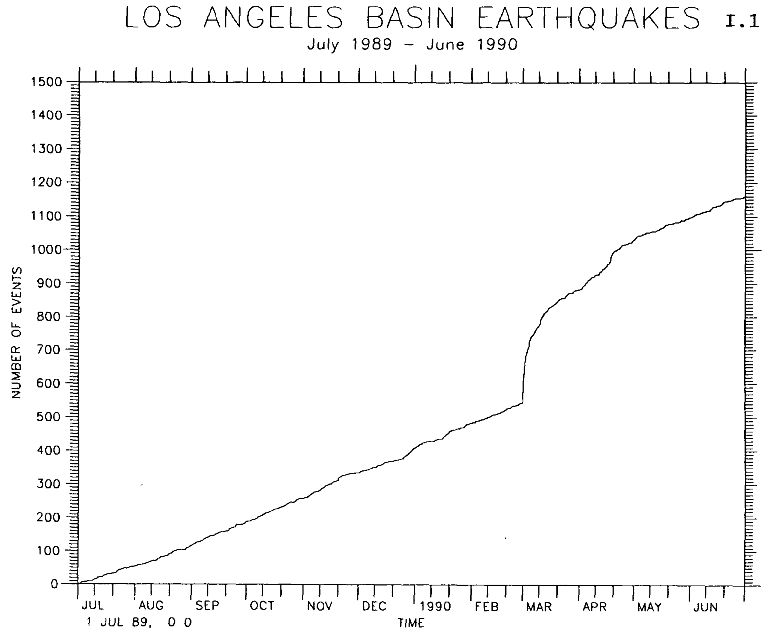

Figure 2A. Cumulative number of earthquakes in the Los Angeles basin recorded by the USC Los Angeles basin seismic network between July 1, 1989 and June 30, 1990.

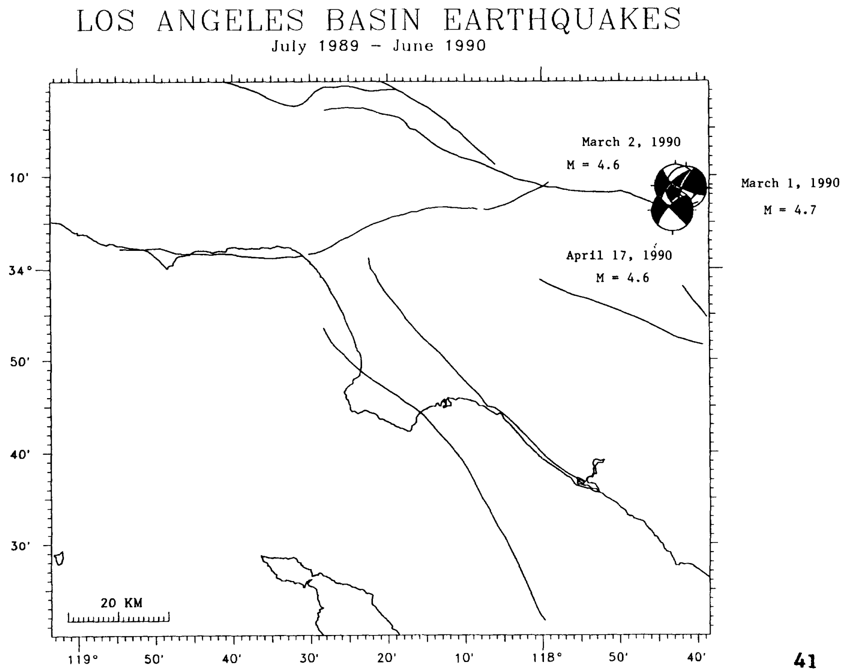

Figure 2B. Focal mechanisms of M ≥ 4.0 earthquakes recorded in the Los Angeles basin between July 1, 1989 and June 30, 1990.

Field, Experiment Operations

9930-01170

John Van Schaack
Branch of Seismology
U. S. Geological Survey
345 Middlefield Road MS-977
Menlo Park, California 94025
(415) 329-4780

Investigations

This project performs a broad range of management, maintenance. field operation, and record keeping tasks in support of seismology and tectonophysics networks and field experiments. Seismic field systems that it maintains in a state of readiness and deploiys and operates in the field (in cooperation with user projects) include:

a. 5-day recorder portable seismic systems.
b. "Cassette" seismic refraction systems.
c. Portable digital event recorders.

This project is responsible for obtaining the required permits from private landowners and public agencies for installation and operation of network sensors and for the conduct of a variety of field experiments including seismic refraction profiling, aftershock recording, teleseism P-delay studies, volcano monitoring, etc.

This project also has the responsibility for managing all radio telemetry frequency authorizations for the Office of Earthquakes. Volcanoes, and Engineering and its contractors.

Personnel of this project are responsible for maintaining the seismic networks data tape library. Tasks includes processing daily telemetry tapes to dub the appropriate seismic events and making playbacks of requested network events and events recorded on the 5-day recorders.

Results

Seismic Refraction

Personnel from this project were responsible for the logistics and contracts for the TACT experiment in Alaska. The experiment consisted of about 700 instruments being deployed at 100 meter spacing for a three hundred kilometer profile across the Brooks Range. Approximately 67 shots were fired at 47 different locations along the profile. A method was developed to fire charges as large as 4.000 lbs in lakes with depths of 10 feet or less with effeciencies approaching that of drilled shotholes.

Portable Networks

Seventeen 5-day magnetic tape recorders, along with 5 digital recorders and 8 telemetered sensors are being used in a tomographic study of the Loma Prieta earthquake rupture area. The experiment started in July 1990 and will end in November 1990. Stations from the Central California Seismic network are also being included in the experiment.

Tape Dubbing

Magnetic tapes of all stations in the Central Cal. Net. are now being dubbed at the M4 level for earthquakes, as a consequence the dubbing effort has been reduced by 60%. All smaller events to M2.5 are digitized only and added to the quarterly catalog and data library.

Geothermal Seismotectonic Studies

9930-02097

Craig S. Weaver
Branch of Seismology
U. S. Geological Survey
at Geophysics Program AK-50
University of Washington
Seattle, Washington 98195
(206) 442-0627

Investigations

1. Continued analysis of the seismicity and volcanism patterns of the Pacific Northwest in an effort to develop an improved tectonic model that will be useful in updating earthquake hazards in the region. (Weaver, Yelin)

2. Continued acquisition of seismicity data along the Washington coast, directly above the interface between the North American plate and the subducting Juan de Fuca plate. (Weaver, Yelin, Norris, UW contract)

3. Continued seismic monitoring of the Mount St. Helens area, including Spirit Lake (where the stability of the debris dam formed on May 18, 1980 is an issue), Elk Lake, and the southern Washington-Oregon Cascade Range (north of Newberry Volcano). The data from this monitoring is being used in the development of seismotectonic models for southwestern Washington and the interaction of the Basin and Range with the Oregon Cascades. (Weaver, Grant, Norris, Yelin, UW contract)

4. Study of Washington and northern Oregon seismicity, 1960-1989. Earthquakes with magnitudes greater than 4.5 are being re-read from original records and will be re-located using master event techniques. Focal mechanism studies are being attempted for all events above magnitude 5.0, with particular emphasis on the 1962 Portland, Oregon event. (Yelin, Weaver)

5. Study of earthquake catalogs for the greater Parkfield, California region for the period 1932-1969. Catalogs from the University of California (UCB) and CalTech (CIT) are being compared, duplicate entries noted, and the phase data used by each reporting institution are being collected. The study is emphasizing events greater than 3.5, and most events will be relocated using station corrections determined from a set of master events located by the modern networks. (Meagher, Weaver)

6. Study of estuaries along the northern Oregon coast in an effort to document probable subsidence features associated with paleosubduction earthquakes (Grant).

7. Study of seismically recorded rockslides and avalanches on Cascade volcanoes (Norris).

Results

1. Within the last few years the local seismic network around Mount Rainier has increased to 5 stations. The network was originally intended to provide increased hypocentral resolution of the shallow earthquakes occurring beneath the summit, but recently it has allowed rockfalls and debris flows to be detected as well. On August 16, 1989, a rockfall with an estimated volume of 1-2 X 10^6 m^3 fell from the 3400m level on Russell Cliff on the north side of Mount Rainier. The rockfall was not visually observed due to poor weather, but it generated

four discrete seismic signals that were widely recorded across the seismic network in Washington and northern Oregon. The signals showed characteristics of rockfall seismograms, and computer analysis of one event showed it originated high on the north face of Mt. Rainier. U.S. Geological Survey and University of Washington personnel advised officials at Mount Rainier National Park of the rockfall, who searched their records for any climbers from that area that had not reported in; fortunately, there were none. The seismic network allowed detection of this rockfall in real-time nearly a full day before it was visually observed.

The success in detecting the Russell Cliff rockfall has prompted a search of archived seismic records for a seismogram from the December 1963 Little Tahoma rockfall sequence on the eastern flank of Mount Rainier. This rockfall left a combined deposit an order of magnitude larger in volume (approximately 11×10^6 m^3) than that in 1989. Two rockfall-like seismic signals probably associated with the Little Tahoma sequence have been found on the December 6 records from the seismograph station at Longmire, suggesting this as the date of the main portion of the slide as opposed to December 14 given by previous USGS investigators.

The ability to detect mass movements demonstrates the duel usefulness of seismic monitoring for both volcano hazard mitigation as well as earthquake monitoring. The success with these small to moderate rockfalls and debris flows indicates that larger, more hazardous such events can be detected as well. At present, however, real-time identification requires continuous visual recording of seismograms from stations within a few km of likely source areas, and the presence of experienced personnel who can quickly discern between such signals and others such as large local earthquakes. This is particularly true of active volcanoes, as small eruptions may generate seismograms of similar appearance to those from rockfalls and debris flows.

2. Based on the agreement between the dip of the Juan de Fuca plate as inferred from earthquake hypocenters determined from the modern seismographic network and the dip of the T-axes calculated for the larger magnitude historical earthquakes, we believe that we can confidently predict the intraplate earthquake source region for the entire plate (Figure 1). We expect that future large magnitude (~7) interplate events will occur within the Juan de Fuca plate (and the Gorda plate beneath southernmost Oregon and northern California) in the depth range of the 1949 and 1965 events (54 and 60 km respectively). Although the depths of these events are considered to be well-known, we have chosen to bracket our source region at a shallower depth. An examination of the University of Washington seismic catalog for the years 1970 through 1989 shows that all of the intraplate earthquakes greater than magnitude 4 are below 45 km and that none have been located deeper than the 1976 event. Therefore, we have used the depth range of 45 to 60 km for our estimate of the probable source region for intraplate events (Figure 2).

We emphasize that this probable source region represents the likely areal extent within which an event may occur; the actual dimensions of the fault area associated with an earthquake of approximate magnitude 7 would be expected to be similar to the 40 km long-fault estimated for the 1949 south Puget Sound earthquake. The querried area in southern Oregon represents the region of unknown plate geometry where no intraplate earthquakes have been located either because any events that did occur were not large enough to be detected by the existing seismic network or no events have occurred. In northern California Benioff zone earthquakes again allow the plate depth to be estimated from the trench eastward to the western edge of the Cascade Range so we have shown the probable source area here between the same depth limits as in Washington and northern Oregon.

Reports

Grant, W. C. and Weaver, C. S., 199?, Seismicity of the Spirit Lake area: Estimates of possible earthquake magnitudes for engineering design, in *The formation and significance of major lakes impounded during the 1980 eruption of Mount St. Helens, Washington, U. S. Geological Survey Professional Paper,* edited by R. L Shuster and W. Meyer, (forever in press). Funded by Earthquake, Geothermal, and Volcano Hazards.

Zollweg, J. E., 1990, High frequency earthquakes following the 1985 eruption of Nevada del Ruiz, Columbia, *J. Volcan. and Geotherm. Res., 41,* 355-367. Funded by Volcano Hazards.

Ludwin, R., C. S. Weaver, and R. S. Crosson, 1990, Seismicity of Washington and Oregon, *GSA Decade of North American Geology Associated Volume, Neotectonics,* (in press). Funded by Geothermal, Volcano Hazards and Earthquake Programs.

Weaver, C. S., Norris, R. D., and C. Jonientz-Trisler, 1990, Seismological monitoring in the Cascade Range, 1960-1989: Earthquakes, eruptions, avalanches, and other curiosities, in *Geoscience Canada, 17,* (in press). Funded by Volcano, Geothermal, and Earthquake Hazards Programs.

Yelin, T. S. and H. J. Patton, (in journal review), Seismotectonics of the Portland, Oregon region, *Bull. Seis. Soc. Am.,* (38 pages, 11 figures, submitted). Funded by Earthquake and Geothermal Programs.

Norris, R. D., (in revision), The Holocene Cascade volcanoes: A history of monitoring and current land managment, for *U. S. Geol. Surv. Open-File Report, xx-xxx,* (80 pages). Funded by Volcano Hazards.

Shedlock, K. M., and Weaver, (in review), Program for earthquake hazards assessment in the Pacific Northwest, *U. S. Geol. Surv. Circular xxxx,* (51 pages, 18 figures). Funded by Earthquake Hazards.

Weaver, C. S. and K. M. Shedlock, (in review), Estimates of seismic source regions from considerations of the earthquake distribution and regional tectonics, for *U.S. Geol. Surv. Prof. Paper, Earthquake Hazards in the Pacific Northwest,* A. Rogers, W. Kockelman, G. Priest, and T. Walsh, eds., (34 pages, 10 figures). Funded by Geothermal and Earthquake Programs.

Yelin, T. S., (in review), A revised catalog of earthquakes in Washington state and northern Oregon: 1960-1969 with comments on spatial and temporal seismicity patterns, 1960-1989, for *U.S. Geol. Surv. Prof. Paper, Earthquake Hazards in the Pacific Northwest,* A. Rogers, W. Kockelman, G. Priest, and T. Walsh, eds., (24 pages, 4 figures). Funded by Geothermal and Earthquake Programs.

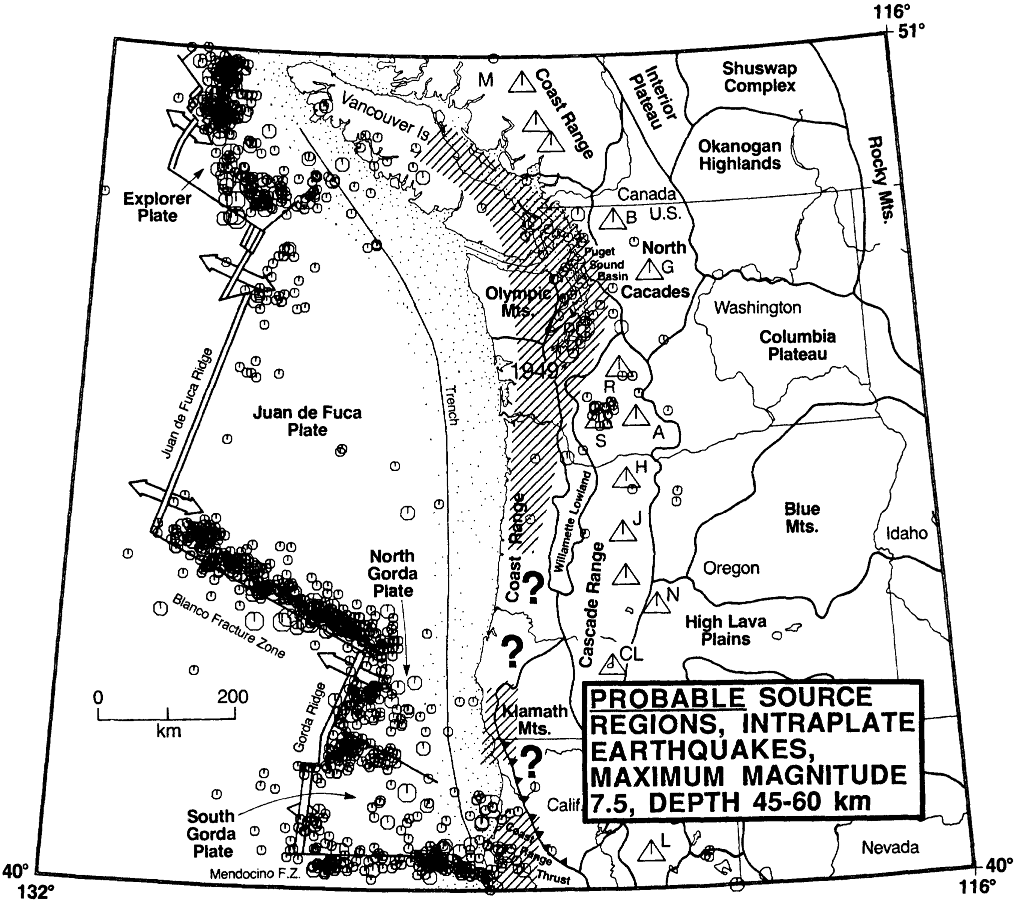

Figure 1. Schematic of the probable source region for intraplate, down-dip tensional earthquakes. Large magnitude earthquakes (~7-7.5) are expected anywhere within the shaded region. Question marks indicate areas where there are no earthquakes located within the Juan de Fuca plate and the plate geometry is uncertain. Large triangles are major Quaternary stratovolcanoes in the Cascade Range. The 1949 earthquake (M_S=7.1) is the largest known earthquake within the subducting Juan de Fuca plate system.

RUPTURE HISTORIES OF THE 1934 AND 1966 PARKFIELD, CALIFORNIA, EARTHQUAKES: A TEST OF THE CHARACTERISTIC EARTHQUAKE HYPOTHESIS

14-08-0001-G1784

Gregory C. Beroza
Department of Geophysics, Stanford University,
Stanford, CA, 94305-2215 (415)723-4958

Thomas H. Jordan
Rm. 54-518, Massachusetts Institute of Technology,
Dept. of EAPS,Cambridge, MA, 02139 (617) 253-3382

The 1966 Parkfield Earthquake

We have carried out an analysis of the near-source records for the 1966 Parkfield earthquake to determine the rupture history. We have found it difficult to distinguish effects due to changes in the rupture time from effects due to changes in the slip amplitude. Instead of trying to solve for both rupture time and slip amplitude, we assume a range of rupture velocities parameterized by the fraction of the shear wave velocity β, and solve for the slip amplitude. Consequently our results could be biased if rupture velocity varied greatly during the earthquake. On the other hand, we can place constraints on the extent of coseismic rupture and the average rupture velocity.

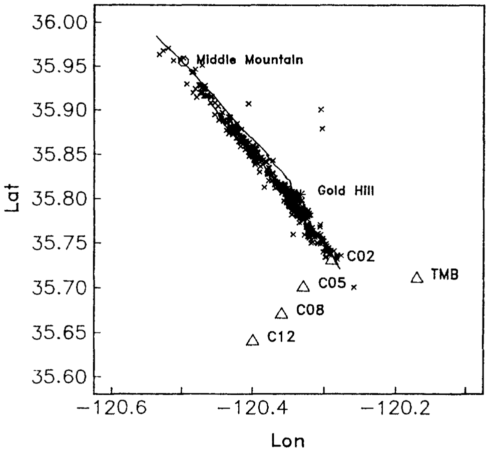

Figure 1. The location of strong-motion stations that recorded the 1966 Parkfield earthquake are shown as triangles. Well located aftershocks [*Eaton et al.*, 1970] are shown together with the surface trace of the San Andreas Fault. The right-step near Gold Hill is apparent in the aftershock distribution.

We performed a least-squares fit to the horizontal components of the Cholame-Shandon array: C05, C08, C12, and Temblor (Figure 1). C02 was excluded from the analysis due to the possibility that the data were affected by propagation effects and because the high-frequency, near-source approximation would be invalid if shallow coseismic rupture extended beyond Gold Hill. We found that rupture velocities greater than 0.80β or less than 0.65β either fit the data very poorly with very little slip over most of the rupture surface or resulted in unreasonable models with a large amount of slip on a very short fault, inconsistent with the geodetic data and teleseismic estimates of the seismic moment [*Tsai and Aki*, 1969].

Our best-fitting slip model assumes a rupture velocity of 0.70β, has a small region of high slip near the hypocenter, a region of high slip about 10 km southeast of the hypocenter, and a larger region of high slip from 25-30 km to the southeast. This model would suggest that rupture propagated well past the right-step at Gold Hill and very near to station C02. However, a troublesome aspect of this rupture model is that there is very little slip on a large part of the fault over which the geodetic data indicate that the slip was highest—about 15-25 km to the southeast of the hypocenter [*Segall and Harris*, 1987]. Unless a great deal of post-seismic slip occurred over that entire area, this model is inconsistent with the geodetic data.

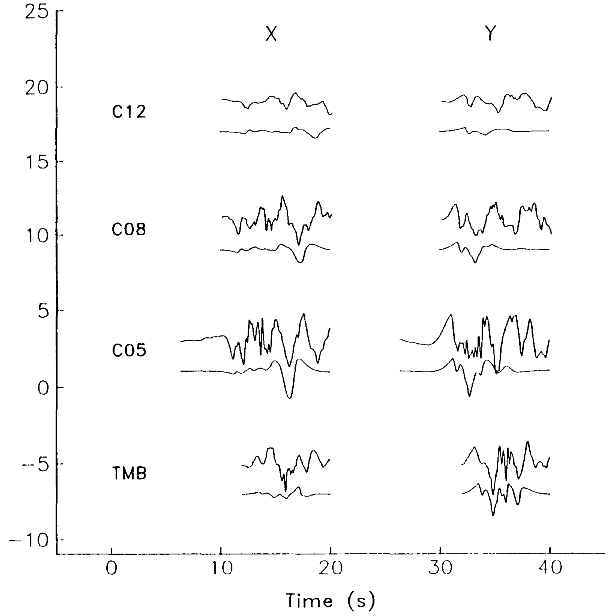

Figure 2. The fit to the strong-motion data for the 1966 Parkfield earthquake for our preferred rupture model. Synthetic waveforms are shown below the data for each of the horizontal components. The offset on the y axis corresponds to the distance of the station from the surface trace of the San Andreas fault.

Our preferred model assumes a slightly higher rupture velocity of 0.75β and fits the strong-motion data nearly as well. The fit to the data is shown in figure 2 and the rupture model is shown in Figure 3. In this model slip extends to about 24 km to the southeast of the hypocenter, near the offset in the fault at Gold Hill. There is a small region of high slip 33 km along-strike, but this is not significant. The majority of slip occurs from 10-23 km along-strike and at depths ranging from 2-12 km. The region of high slip is located at the same distance along the fault as in the geodetic model of *Segall and Harris* [1987]. This model is also supported by independent estimates of the rupture velocity [e.g. *Trifunac and Udwadia*, 1974; *Lindh and Boore*, 1981].

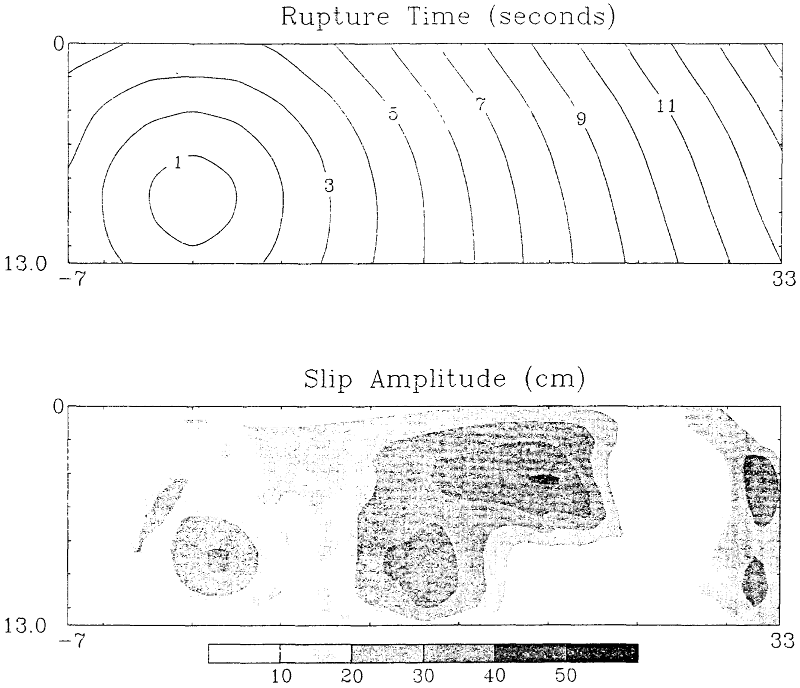

Figure 3. The constant rupture velocity model for the Parkfield earthquake assuming a rupture velocity of 0.75β. The3 fit to the data is shown in Figure 2. This model is consistent with geodetic models of slip in the 1966 sequence. The sensitivity of our rupture models for this earthquake to the rupture velocity is a consequence of the poor source-station distribution. The regional-distance data have a much better azimuthal distribution with respect to the source and will not be nearly as sensitive to the assumed rupture velocity.

To summarize, the results from the near-source data indicate that the rupture velocity was fairly low in this earthquake, $0.65\beta < v < 0.80\beta$. We also obtain lower values for the shear fracture energy $\sim 5 \times 10^5$ J/m^2 for the Parkfield earthquake relative to that found for the Morgan Hill and Imperial Valley earthquakes $\sim 2 \times 10^6$ J/m^2 [*Beroza and Spudich*, 1988; *Beroza*, 1989]. The extent of coseismic slip is not well determined by the near-source data alone. However, taken together with models derived from the geodetic data our results suggest a model in which coseismic rupture terminates near the offset in the San Andreas fault at Gold Hill with post-seismic slip occurring farther to the southeast. These conclusions could change; however, if there are strong variations in the rupture velocity during the earthquake. A more definitive determination of the extent of rupture in the 1966 earthquake and in the 1934 earthquake from seismic data is being undertaken using the regional-distance, Wood-Anderson data.

Analysis of the 1934 and 1966 Parkfield Earthquakes Using Wood-Anderson Data

We have collected Wood-Anderson seismograms from the Archives of the University of California at Berkeley and the California Institute of Technology for earthquakes dating from 1931 to 1975 in the Parkfield region. The seismograms have all been reproduced and enlarged for digitization with funding and support from the U.S. Geological Survey. We are currently working on the digitization of the dataset.

The digitized Wood-Anderson data will be used to infer the rupture history of the 1934 and 1966 events and to test the characteristic earthquake hypothesis. Records of the foreshocks to the two earthquakes indicate a remarkable degree of similarity in the foreshocks suggesting that the foreshocks are quite similar in the frequency band of the Wood-Anderson instruments and that the response of the Wood-Anderson seismographs is quite stable over the 32-year period 1934-1966.

The Wood-Anderson data should substantially increase our resolution of the rupture history of the 1966 earthquake. This is especially true given the poor distribution of strong motion stations relative to the 1966 earthquake with the associated pitfalls. How well we will be able to recover the rupture history of the 1934 earthquake will depend on the accuracy of the regional-distance Green's functions calculated using the proposed techniques. We are encouraged by the apparent stability of the instrument response over the long time interval between the two Parkfield earthquakes.

Analysis of geodetic measurements at the southern end of the rupture zone bracketing the 1934 earthquake indicate that there were substantial differences in the 1934 and 1966 sequences [*Segall et al.*, 1990]. Inversions for three-dimensional velocity structure in the Parkfield region indicates considerable along-fault heterogeneity [*Michael and Eberhart-Phillips*, 1990]. It has been suggested that such anomalies may correspond to changes in material properties that strongly influence rupture propagation.

References

Beroza, G. C., Near-source imaging of seismic rupture, Ph.D. Thesis, 198 pp., Mass. Inst. of Technol., Cambridge, 1989.

Beroza, G. C., and P. Spudich, Linearized inversion for fault rupture behavior: application to the 1984, Morgan Hill, California, earthquake, *J. Geophys. Res.*, *93*, 6275-6296, 1988.

Eaton, J. P., M. E. O'Neill, and J. N. Murdock, Aftershocks of the 1966 Parkfield - Cholame, California earthquake: a detailed study, *Bull. Seismol. Soc. Am.*, *60*, 1151-1197, 1970.

Lindh, A. G., and D. M. Boore, Control of rupture by fault geometry during the 1966 Parkfield earthquake, *Bull. Seismol. Soc. Am.*, *71*, 95-116, 1981.

Michael, A. J., and D. Eberhart-Phillips, Correlation of heterogeneity in seismic behavior and seismic velocities, *Seismol. Res. Lett.*, *61*, 34, 1990.

Segall, P., Y. Du, and W. Thatcher, Were the 1934 & 1966 Parkfield earthquakes similar?, *Seismological Research Letters*, *61*, 22, 1990.

Segall, P., and R. Harris, Earthquake deformation cycle on the San Andreas fault near Parkfield, California, *J. Geophys. Res.*, *92*, 10,511-10,525, 1987.

Trifunac, M. D., and F. E. Udwadia, Parkfield, California, earthquake of June 27, 1966: a three-dimensional moving dislocation, *Bull. Seismol. Soc. Am.*, *64*, 511-533, 1974.

Publications

Beroza, G. C., Near-Source Imaging of seismic Rupture, Ph.D. Thesis, 198 pp., Mass. Inst. of Technol., Cambridge, 1989.

Beroza, G. C., Observations of heterogeneous rupture from strong-motion data: examples from California earthquakes, *Seismological Research Letters*, *61*, 47, 1990.

Seismic Source Analysis Using Empirical Green's Functions

9910-02676

J. Boatwright, and L. Wennerberg
Branch of Engineering Seismology and Geology
345 Middlefield Road, MS 977
Menlo Park, California 94025
(415) 329-5609, 329-5607, 329-5659

Investigations

1. Inversion for the distribution of stress release in an earthquake rupture process.
2. Recording and analysis of aftershocks of the 1989 Loma Prieta earthquake.
3. Analysis of accelerograms written by the mainshock and aftershocks of the 1983 Coalinga earthquake.

Results

1. Boatwright, DiBona, Cocco (1989) have designed, programmed, and applied an iterative inversion scheme which uses positivity constraints to deconvolve recordings of small earthquakes from recordings of larger earthquakes, and which minimizes the number of sub-events necessary by using an F-test to check the statistical significance of each added subevent. The inversion determines the space-time distribution of the stress release comprising the earthquake. It has been applied to a set of 9 unfiltered accelerograms of body-waves radiated by a $M_L = 5.3$ Coalinga aftershock; the error reduction from the inversion was 75%. Different methods of constraining the solution were tested: the most physical solution was obtained by constraining the rupture velocity of the process to be less than the S-wave velocity.

2. GEOS digital event recorders were deployed at 21 sites in San Francisco and 14 sites extending from Woodside to Fremont across the Southern San Francisco Bay. These instruments recorded some 85 aftershocks of the Loma Prieta earthquake over a period of two months following the earthquake. The set of recordings represents one of the most extensive data sets ever obtained in an urban or suburban environment, and can be expected to yield significant information for the evaluation of seismic hazard in these areas. In particular, these recordings can be used to complement the strong motion recordings of the mainshock in the Bay Area. Boatwright, Seekins, and Mueller (1990) have completed an analysis of the recordings obtained in the Marina District which yielded estimates of the ground amplification throughout the Marina, as well as upper bounds for the main shock ground motion in the Marina. Boatwright, Fletcher, Mueller, and Fumal (1990) derives and tests a new technique for separating source and site terms in sets of multiply recorded earthquakes, and applies this technique to a set of 28 Loma Prieta aftershocks recorded at 5 stations located within 30 km of the epicenter. The aftershocks range in size from $M = 2.1$ to $M = 4.6$; the derived at not affected by f_{max}.

3. Wennerberg (1990a) has derived a variant of Boatwright's (1988) filtering strategy in which the recordings of small earthquakes are amplified a long periods using a zero-phase-shift filter to simulate the recordings of large simple earthquakes or of large subevents within a complex rupture process. Wennerberg (1990b) applies this technique to synthesize the accelerograph recording of the $M_L = 6.7$ Coalinga mainshock, using the recording of a $M_L = 5.3$ aftershock. A sum of filtered accelerograms corresponding to eleven subevents gives a credible match to the main shock accelerogram. Corresponding stress parameters for the sub-events vary over a factor of five, and the sum of the subevent moments is consistent with independent estimates of the seismic moment of the main shock.

References

Boatwright, J., 1988, The seismic radiation from composite models of faulting, *Bulletin of the Seismological Society of America*, v. 78, p. 489-508.

Wennerberg, L., 1990a, Stochastic summation of empirical Green's functions, Bulletin of the Seismological Society of America, in press.

Publications

Boatwright, J., M. DiBona, and M. Cocco, 1989, The dynamic decomposition of the earthquake rupture process, EOS, p. 243.

Boatwright, J., L.C. Seekins, and C.S. Mueller, 1990, Ground motion amplification in the Marina District, U.S. Geological Survey Open-File Report 90-253., p. F1-F18.

Boatwright, J., J.B. Fletcher, C.S. Mueller, and T. Fumal, 1990, A general inversion scheme for source, site, and propagation cvharacteristics using multiply recorded sets of moderate-sized earthquakes, submitted to BSSA.

Wennerberg, L., 1990b, Observing source complexity in locally recorded accelerograms from Coalinga, California, Earthquake Notes, in press.

Analysis of the 1957 Andreanof Islands Earthquake
14-08-0001-G1766

Thomas M. Boyd
Colorado School of Mines
Department of Geophysics
Golden, CO 80401
(303) 273-3522

Project Summary and Goals

Recent studies have indicated that the spatial distribution of moment release can be quite heterogeneous along any particular rupture zone. The most common explanation for this heterogeneity has been the rupture of strong patches, or asperities, along the fault plane [e.g., Ruff and Kanamori, 1983]. These strong patches could possibly arise from spatial variations in the frictional characteristics of the fault surface or from geometrical barriers inherent to the fault's shape. Alternatively, the spatial distribution of moment release could have little to do with the physical characteristics of the fault's surface and may be related to the dynamics of slip and how regions of a fault interact with neighboring regions [e.g., Rundle and Kanamori, 1987; Horowitz and Ruina, 1989].

Distinctions between these two models can not be made by the analysis of single events [e.g., Thatcher, 1990]. Conclusive observations can only be drawn from a study of the moment-release distribution generated by several great earthquakes, all of which rupture the same fault segment. If this distribution is controlled by the physical characteristics of the fault's surface, then one might expect the moment distributions to be similar for each of the earthquakes. One might also expect to be able to identify the sites of large moment release during the next great earthquake from the spatial distribution of the smaller interseismic events. If, however, the distribution of moment release is controlled by fault interactions, then one might expect the moment distributions to differ, particularly if the events have different, but overlapping rupture bounds.

In this context, an excellent region of study is the central Aleutian Arc. In 1986, a magnitude 8.0 (M_w) earthquake occurred along the Aleutian Arc near the Andreanof Islands. The slip distribution, aftershock, and preshock sequence of this earthquake have been described in a number of recent studies. Prior to 1986, the central Aleutian Arc was ruptured by another great earthquake in 1957 ($M_w > 8.5$). The 1957 Andreanof Islands earthquake remains poorly understood. Its seismic moment, slip distribution, and even rupture area have not been well constrained. The short time span between the 1957 and 1986 earthquakes provides us with a unique opportunity to study a complete seismic cycle bounded by two instrumentally recorded great earthquakes. In fact, it represents the only complete seismic cycle along the Alaska-Aleutian Arc which has been instrumentally observed. Currently published and ongoing research efforts have focused mainly on the final two-thirds of the rupture cycle. To help supplement our picture of the seismic processes involved during the entire rupture cycle, verify the recently proposed set of seismic hazard estimates, and shed light on the possible mechanical consequences of the seismically observed moment distribution, a more fundamental understanding of the rupture characteristics of the 1957 event, including more robust estimates of its rupture bounds, seismic moment, and slip distribution are needed.

Determination of the Rupture Length of the 1957 earthquake by modeling surface-wave directivities

A Ph.D. student working under this project (D. F. Lane) has spent the past few months developing and testing a technique to constrain several source parameters for poorly recorded events. His technique is based on the directivity function originally described by

Ben-Menahem [1961]. The advantage to using this function over other waveform modeling techniques is that it is independent of receiver characteristics, propagation medium, source mechanism, and source-time function. From the directivity function we can estimate the direction and velocity of propagation of the rupture front and the rupture length. Its nonlinear nature, however, makes it extremely ill-suited for use with most conventional inversion procedures. Thus, previous investigators have only forward modeled the directivity function.

Simulated annealing is a stochastic technique ideally suited to problems in which the function being optimized is nonlinear with numerous local minima. Based upon a Monte Carlo scheme developed by Metropolis et al. [1953] each component of a model M_i is given a random perturbation and a change in an objective function, ΔE, is computed. If ΔE is less than zero (i.e., the change reduced the variation between the simulated and observed data) the perturbation is accepted. If ΔE is positive, the perturbation is accepted with probability

$$P(\Delta E) = e^{\frac{-\Delta E}{T}} \tag{1}$$

where T represents a control parameter analogous to temperature. By repeating this basic step a number of times, one simulates the thermal motion of atoms in contact with a heat bath at temperature T.

A simulated annealing procedure has been developed and initially tested using data from the May 7, 1986 Andreanof Islands earthquake recorded at BCAO. Using this procedure the rupture velocity was determined to be 1 km/s, and the eastern and western portions of the fault to have lengths of 98 and 134 km respectively. The estimated rupture velocity agrees well with that of 1.5±0.5 km/s determined by Boyd and Nábělek, [1989] from body-wave modeling. The rupture length, although larger than the 145 km determined from body-wave modeling is remarkably consistent with the size of the aftershock zone. The results of the simulated annealing procedure along with the observed data are shown in Figure 1.

Records from Pietermaritzburg, South Africa were employed to extract the fault parameters of the 1957 Aleutian Island earthquake. Our findings, Figure 1, indicate that the observed directivity is best modeled by a bilateral source with eastern and western fault segments of 612 and 151 km respectively, and a rupture propagation velocity of 2.9 km/s. A second solution, described by Ruff et al. [1985], was also located. This solution consists of eastern and western fault lengths of 235 and 387 km respectively, and a rupture propagation velocity of 1.7 km/s. Because the first solution is consistent with the tsunami source area and the spatio-temporal distribution of the aftershock sequence described below, and because the misfit between the observed and calculated directivities are marginally better we contend that it provides a more accurate description of the rupture bounds of the 1957 earthquake.

Aftershock Relocations and Source Mechanisms

Using the slab geometry described by Boyd and Creager [1990] and Creager and Boyd [1990] we have calculated *P-wave* travel-time perturbations to approximately 550 stations as a function of epicentral position. We are only relocating shallow earthquakes. As such, residuals are calculated assuming a source depth of 33 km. Differences in an event's actual source depth should not greatly affect the residual pattern since variations in source depth tradeoff with origin time, but do not greatly affect epicentral estimates. The calculated residuals are used directly as epicentrally varying station corrections to generate relocated epicenters without additional ray tracing.

Figure 2 shows the relative relocation vectors and the final locations for all of the events listed in the *ISS* bulletin for the year 1957. Our locations differ from those produced using a spherically symmetric earth model from about 30 km in the central Aleutians to about 10 km in the eastern Aleutians. For any given relocation, the standard error in latitude is typically less than 10 km while that in longitude is less than 4 km. We find that activity is not uniformly distributed along the fault zone, but occurs within distinct clusters. Aftershock activity along the length of the rupture zone (shaded) defined by the surface-wave modeling described below initiated within 6 hours of the mainshock (Figure 3). The initiation of activity along the western 225 km of the aftershock zone was delayed by 23 hours. Although one event occurred within the eastern 150 km of the aftershock zone almost immediately after the mainshock, activity was sparse and did not intensify until 3 days after the mainshock. The timing of the aftershock sequence, therefore, appears to be consistent with the rupture model proposed in the previous section.

We are currently adding to this analysis events listed in the *BCIS*. These data are being optically scanned and reformatted by an undergraduate research assistant. At present, an additional 150 events which occurred from January 1957 through April 1957 have been scanned, and are currently being relocated. By the 1990 fall AGU meeting, we will have relocated all of the events listed in the *ISS* and *BCIS* bulletins for the year 1957.

We have also begun to constrain the source mechanisms for as many of the aftershocks of the 1957 event as possible. Initially we are analyzing events for which Stauder and Udias [1963] determined *S-wave* polarizations. We use Stauder and Udias's *S-wave* polarizations and the *P-wave* first motions listed in the ISS to determine the type of faulting (i.e., thrust, normal or strike slip). Figure 4 shows the *P-wave* first motions and *S-wave* polarizations for three aftershocks. The source mechanisms on the left are those which would be expected for shallow-angle thrust faults. For the first two events minor adjustments to the source mechanisms can explain most of the *P* and *S-wave* observations (source mechanisms on the right). The third event, however, does not to be a simple thrust earthquake. Although the mechanism on the right is a possible solution, the data are not consistent enough to constrain these anomalous mechanisms. We are modeling waveform data collected from several stations to help constrain these anomalous mechanisms.

References

Ben-Menahem, A., Radiation of seismic surface-waves from finite moving sources, *Bull. Seismol. Soc. Am.*, *51*, 401-435, 1961.

Boyd, T. M., and K. C. Creager, The Geometry of Aleutian Subduction: Three-Dimensional Seismic Imaging, in press, *J. Geophys. Res.*, 1990.

Boyd, T. M., and J. L. Nábělek, Rupture process of the Andreanof Islands earthquake of May 7, 1986, *Bull. Seism. Soc. Am.*, *78*, 1653-1673, 1988.

Creager, K. C., and T. M. Boyd, The Geometry of Aleutian Subduction: Three-Dimensional Kinematic Flow Model , in press, *J. Geophys. Res.*, 1990.

Horowitz, F. G., and A. Ruina, Slip patterns in a spatially homogeneous fault model, *J. Geophys. Res.*, *94*, 10,279-10,298, 1989.

Metropolis, N., A. Rosenbluth, M. Rosenbluth, A. Teller, and E. Teller, Equation of state calcuations by fast computing machines, *J. Chem. Phy.*, *21*, 1087-1092, 1953.

Ruff, L., and H. Kanamori, The rupture process and asperity distribution of three great earthquake from long-period diffracted P-waves, *Phys. Earth and Planet. Inter.*, *31*, 202-230, 1983.

Ruff, L., H. Kanamori, and L. R. Sykes, The 1957 great Aleutian earthquake (abstract), *EOS*, *66*, 298, 1985.

Rundle, J. B., and H. Kanamori, Application of an inhomogeneous stress (patch) model to complex subduction zone earthquakes: A discrete interaction matrix approach, *J. Geophys. Res.*, *92*, 2606-2616, 1987.

Stauder, W. and A. Udias, S-wave studies of earthquake of the North Pacific, Part II: Aleutian Islands, *Bull. Seismol. Soc. Am.*, *53*, 59-77, 1963.

Thachter, W., Oreder and diversity in the modes of Circum-Pacific earthquake recurrence, *J. Geophys. Res.*, *95*, 2609-2624, 1990.

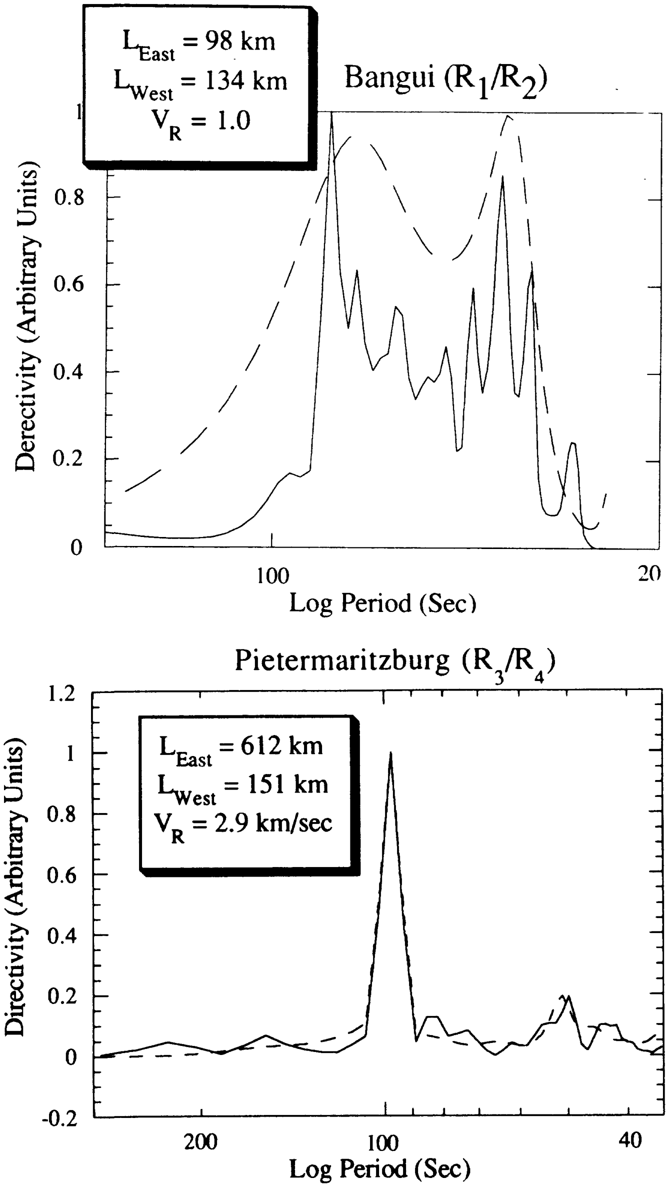

Figure 1: Normalized surface-wave directivity functions for the 1986 Anderanof Islands earthquake (top) and the 1957 Aleutian Islands earthquake (bottom). Both are recorded at African stations: Bangui, 1986; Pietermaritzburg, 1957. Solid lines are the observed directivities, dashed are the directivities calculated using the source parameters indicated in the boxes.

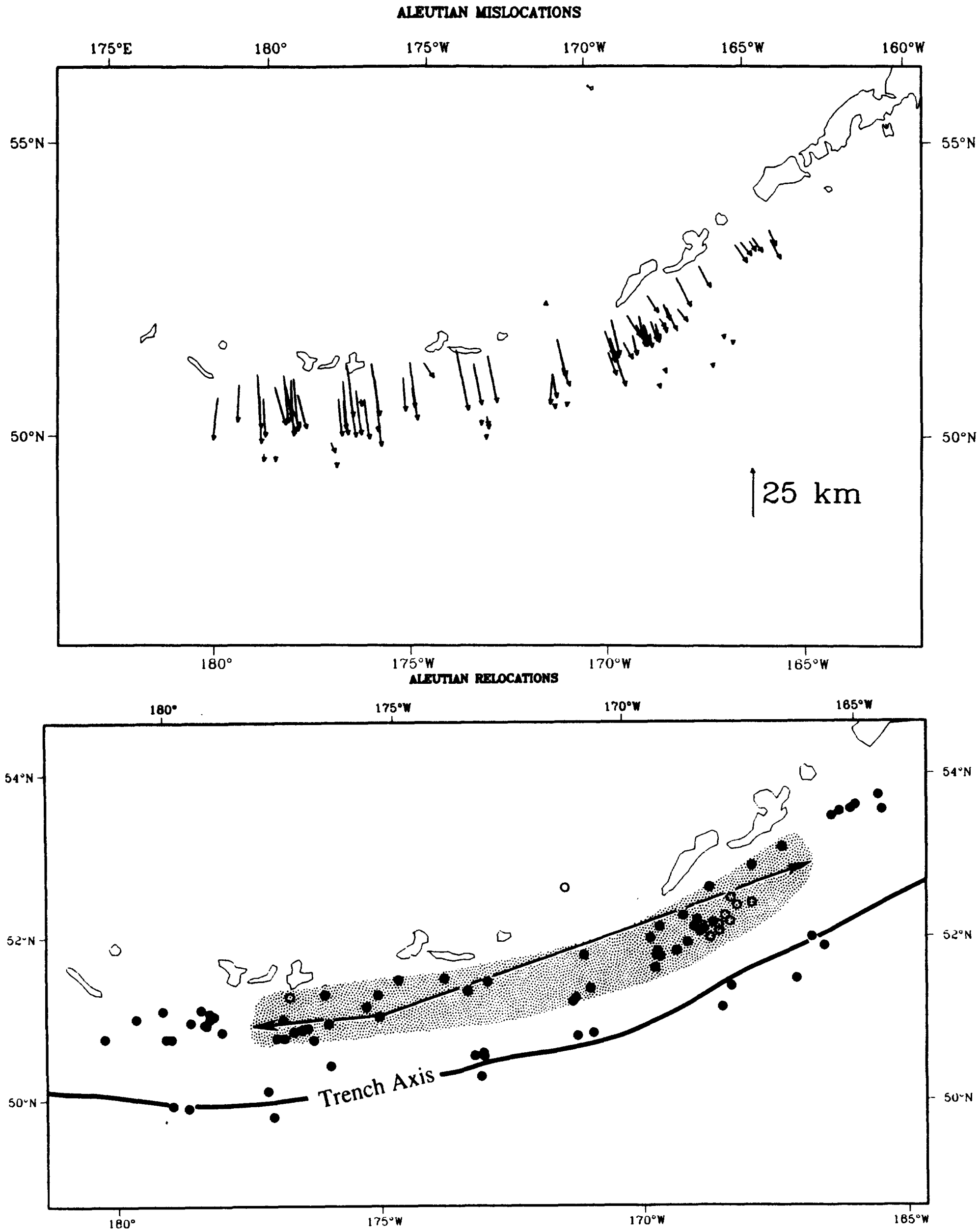

Figure 2: Top figure shows the relocation vectors computed for all events listed in the *ISC* that occurred in 1957. Tail of each arrow is located at the spherically symetric earth model location. Each arrow points in the direction of the slab corrected location. Bottom figure shows the final relocations for each of these events. Closed circles are aftershocks, open circles preshocks. Shaded region indicates the rupture area derived from the analysis of surface-wave directivities.

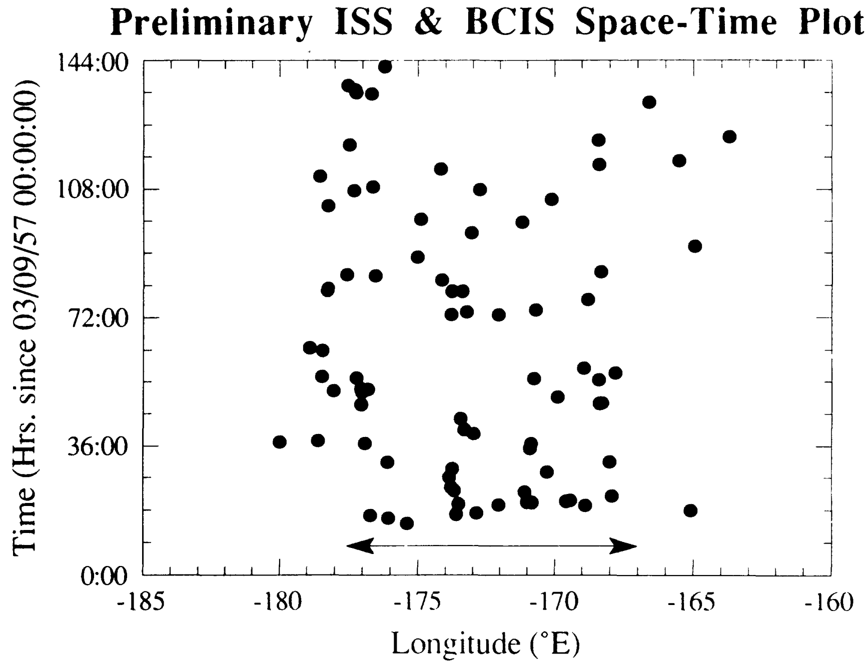

Figure 3: Space-time plot of the first 4 days of aftershock activity. Preliminary relocations for events listed in both the *ISS* and *BCIS* are shown. Arrows indicate the rupture bounds derived from the analysis of surface-wave directivities.

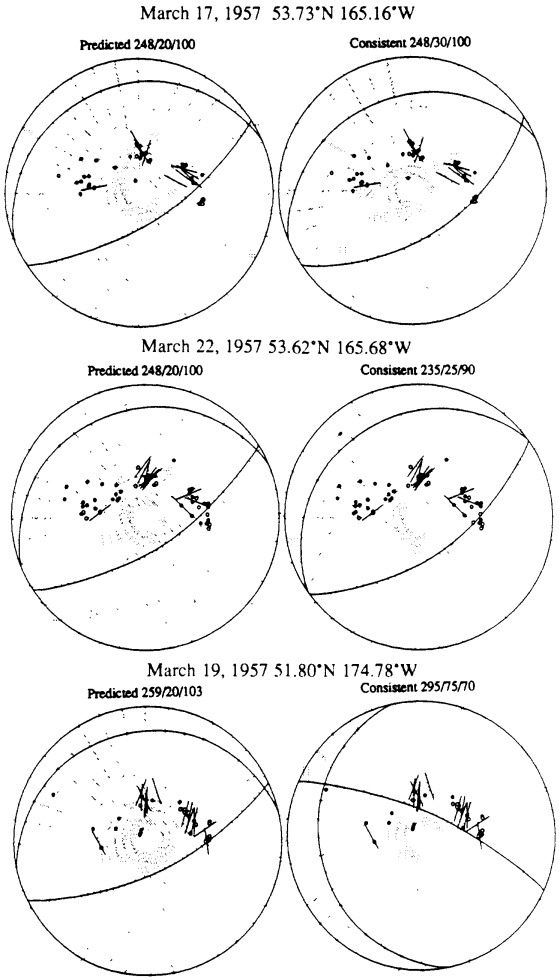

March 17, 1957 53.73°N 165.16°W

Predicted 248/20/100

Consistent 248/30/100

March 22, 1957 53.62°N 165.68°W

Predicted 248/20/100

Consistent 235/25/90

March 19, 1957 51.80°N 174.78°W

Predicted 259/20/103

Consistent 295/75/70

Figure 4: Sample *P-wave* first motion and *S-wave* polarization observations. Focal spheres to the left show the predicted *P-wave* nodal planes and *S-wave* polarization angles for shallow-angle thrust events. To the right are shown focal mechanisms that best fit the observations. The top two events are consistent with thrust earthquakes. The bottom event does not appear to be a normal, shallow-angle thrust earthquake.

Earthquake Hazard Investigations in the Pacific Northwest

14-08-0001-G1803

R.S. Crosson and K.C. Creager
Geophysics Program
University of Washington
Seattle, WA 98195
(206) 543-8020

April 1, 1990 - Sept. 30, 1990

Investigations

The objective of this research is to investigate earthquake hazards in western Washington, including the possibility of a large subduction-style earthquake between the North American and Juan de Fuca plates. Improvement in our understanding of earthquake hazards is based on better understanding of the regional structure and tectonics. Current investigations by our research group focus on the configuration of the subducting Juan de Fuca plate, differences in characteristics of seismicity between the overlying North American and the subducting Juan de Fuca plates, and kinematic modeling of deformation of the Juan de Fuca slab,

We have found anomalous P phases from intraslab earthquakes that are characterized by energetic arrivals, low apparent velocity of 5.8 -6.0 km/sec. and appearance at a restricted set of stations located at updip azimuths with respect to the subducted Juan de Fuca slab. We interpret these phases to represent P-phase energy trapped within the subducted oceanic crust. They may ultimately prove to be of value in refining our knowledge of slab structure. This work was carried out by Ivar Mundal, and a manuscript is presently near completion on our preliminary interpretation.

Deep three-dimensional velocity structure of the Cascadia subduction zone

Teleseismic arrivals recorded on the Washington Regional Seismograph Network (WRSN) are the only data set that has been found to resolve the upper mantle structure of the subducting JDF plate and of the regional structure of the Cascadia Subduction Zone as a whole. Previous velocity models obtained from studies of teleseismic arrival residual times has low resolution, due in part to the use of (1) small and incomplete data sets, (2) inaccurate, visually chosen arrival times without dependable error estimates and (3) inappropriate linear inversion techniques. In order to obtain a high resolution, well constrained CSZ structure we have made improvements in each of these three areas.

The large digital data set that has been accumulating at the WRSN over the past ten years is of high quality and spans ranges of azimuth and distance heretofore unexploited by teleseismic studies.

Earlier, we developed a novel technique for efficiently extracting from the data both highly accurate relative arrival times and quantitative uncertainty estimates (for use in weighting data in inversion). These times are used with a conjugate gradient inversion technique to obtain an estimate of the least squares solution to a set of overdetermined equations with an additional constraint on the roughness of the model.

Our preliminary results image a high-velocity arched structure dipping to the east at an approximately 60 degree angle below the Puget Sound region and slightly steeper both to the North and South of this area. This structure we interpret to be the subducting Juan de Fuca tectonic plate. This work is being carried out by John VanDecar as part of his Ph.D. research.

Lateral velocity variations within the shallow crust

We have concluded our preliminary tomographic study of lateral velocity variations in the shallow crust with the publication of an article "Tomographic imaging of local earthquake delay times for 3-D velocity variation in western Washington" by Lees and Crosson in JGR.

Kinematic Modeling

Ling-Yun Chiao, as part of his Ph.D. research, is continuing to work on the theoretical formulation and numerical implementation of the kinematic modeling of the subducted slab. Due to the oceanward concave shape of the trench, the Cascadia slab has to deform laterally to accommodate the change of geometric configuration while subducting. We have developed a numerical scheme to calculate the minimum amount of membrane deformation, and its spatial distribution, for a slab to accommodate a given geometry. For the Cascadia subduction zone, our modeling indicates that the concentration of seismic activity beneath the Puget Sound region, and the observed arching structure each are caused by the along-strike compression that is forced by the bend in the trench.

We have been calculating the flow field within a thin sheet given the geometry of that sheet. This approach has the disadvantage that the results are sensitive to second derivatives of the chosen geometry. We are currently working on a scheme to simultaneously invert for the flow field and geometry, with soft constraints on the slab geometry.

Articles

Boyd, T.M., and K.C. Creager, 1990 (in press), The geometry of Aleutian subduction: Three-dimensional seismic imaging, JGR.

Creager, K.C. and T.M. Boyd, 1990 (in press), The geometry of Aleutian subduction: Three-dimensional kinematic flow modeling, JGR.

Lees, J.M. and R.S. Crosson, (in press), Bayesian ART versus conjugate gradient methods in tomographic seismic imaging: An application at Mount St. Helens, Washington, AMS-SIAM: Conference on spatial statistics and imaging - June, 1988.

Mundal, I., M. Ukawa, and R.S. Crosson, 1990 (in preparation), Normal and anomalous P phases from local earthquakes, and slab structure of the Cascadia Subduction zone, BSSA

Lees, J.M. and R.S. Crosson, 1990, Tomographic imaging of local earthquake delay times for 3-D velocity variation in western Washington, JGR, Vol. 95, pp. 4763-4776.

Lees, J.M. and J.C. VanDecar, (submitted to PAGeophys.), Seismic tomography constrained by Bouguer gravity anomalies, with application to western Washington, U.S.A..

Reports

Final Technical Report: 1989, 1990 (in preparation), Earthquake Hazard Research in the Pacific Northwest, USGS Grant # 14-08-0001-G1390.

Abstracts

Chiao, L.Y., and K.C. Creager, 1990, Geometric Constraints of Cascadia Subduction, EOS, Fall 1990 AGU.

Mundal, I., M. Ukawa, and R.S. Crosson, 1990, Evidence of subducting Juan de Fuca plate in apparent velocities observed from subcrustal earthquakes, EOS, Vol. 71, No. 36, p. 1067.

VanDecar, J.C., R.S. Crosson, and K.C. Creager, 1990 (in press), Deep three-dimensional velocity structure of the Cascadia subduction zone, EOS, Fall 1990 AGU

VanDecar, J.C., R.S. Crosson, and K.C. Creager, 1990 (in press), Deep three-dimensional velocity structure of the Cascadia subduction zone, EOS, Fall 1990 PNAGU

VanDecar, J.C., R.S. Crosson, and K.C. Creager, 1990 (in press), Teleseismic travel-time inversion for Cascadia subduction zone structure employing three-dimensional ray tracing, presented at the XXII General Assembly, European Seismological Commission, Barcelona, Spain, Fall, 1990.

Seismotectonics in the Northeastern United States

14-08-001-G1796

John E. Ebel
James W. Skehan, S.J.
David C. Roy
Weston Observatory
Dept. of Geology and Geophysics
Boston College
Weston, MA 02193
(617) 899-0950

Objective: The primary objective of this research is to improve the calculated locations of earthquake hypocenters in New England (particularly to better constrain the event focal depths) by relocating earthquakes using new network station travel-time residuals. These residuals are to be found from a time-term tomographic analysis of the P wave arrivals on the New England Seismic Network (NESN) stations from the 1984 Maine Seismic Refraction Profile (MSRP) and from the 1988 New York-New England Seismic Refraction Experiment (NY-NEX). The relocated earthquake hypocenters will be used to reexamine the present seismotectonics of the northeastern United States in an effort to identify seismically active structures in the region.

Data Preparation and Analysis: Since the last report, the primary effort has been aimed at developing a reliable computer code to perform the tomographic time-term analysis. The code development and testing has taken longer than expected, although recent tests on synthetic data show that code is working properly. All of the P-wave first arrival times from the 1988 NY-NEX experiment have been read for the New England Seismic Network stations, and those data are being merged with the P-wave arrival times from the 1984 Maine Seismic Refraction Experiment for a data set of travel times covering much of New England. This merged data set will be analyzed shortly.

Preliminary Results: An initial tomographic time-term analysis of the 1988 NY-NEX data starting from the refraction model for northern New England determined by the U.S.G.S. was run, but subsequently the station elevations were found to have been incorrectly input, invalidating the results obtained. Thus, while no results are available at the present time, we anticipate that all the of the time-term tomographic analyses will be completed by the end of October, 1990. Using the stations time-term residuals which will be found, selected earthquakes from central and northern New England will be relocated in an effort to improve their hypocenters, particularly their focal depths.

Seismicity and Crustal Structure in an Active Collisional Orogen, Soviet Central Asia

14-08-0001-G1802

Michael W. Hamburger, Gary L. Pavlis
Department of Geological Sciences, Indiana University
Bloomington, Indiana 47405
(812) 855-2934

Terry L. Pavlis
Department of Geology and Geophysics
University of New Orleans
New Orleans, Louisiana 70148
(504) 286-6797

Investigations

This program focuses on the highly active seismic zone between the Pamir and Tien Shan mountain belts in Soviet Central Asia. The Garm region is located directly atop the collisional boundary between the Indian and Eurasian plates, and is associated with a dense concentration of both shallow and intermediate-depth earthquakes. Since the early 1950's, Garm has been the home of the Complex Seismological Expedition (CSE), whose primary mission is the prediction of earthquakes in the USSR (Nersesov *et al.*, 1979). Beginning in 1975, the USGS, in cooperation with the CSE, has operated a telemetered seismic network nested within a stable CSE network that has operated in the area for over thirty years. The fundamental aims of the present research project are: (1) to elucidate the structures and processes involved in active deformation of a complex collisional plate boundary, and (2) to examine the temporal variations in seismicity near Garm, in the form of changing spatial, depth, and stress distribution of microearthquakes that precede larger events. The seismological data base for this study includes the combined resources of the global, regional, and local seismic networks. Geological structures in the Garm region have been studied using compilation of published geological information, analysis of satellite imagery, and geological field work in the Peter the First, Gissar, and Darvaz mountain ranges near Garm.

Results

Teleseismic Travel Time Inversion. In collaboration with Alek Lukk (Institute of Physics of the Earth, Moscow), we have compiled traveltime data from 218 teleseismic earthquakes recorded at the Garm network stations, in order to obtain information on mid- to lower crustal velocities. These data have been augmented by arrival time data from fourteen regional seismic stations operating in the Pamir, in the Tadjik Depression, and in Afghanistan. We have begun work with a new teleseismic inversion routine based on the work of Al-Shukri and Mitchell (1987). The first stage of data reduction involved calculation of travel time residuals from the raw arrival time data, removal of clearly unreliable readings, and examination of azimuthal characteristics of the traveltime residuals. Based on unexpectedly high station residuals, we were led to reexamining the original seismograms for teleseismic arrival times. This work was completed during the summer of 1990. We anticipate using the revised arrival time data to obtain a three-dimensional velocity model for the crust and upper mantle of the Garm region by early next year.

Geologic Structure. Much of our work during this period has focused on analysis of geologic data from the Garm region. We have just completed a review of the seismicity and geologic structure for the region (Hamburger *et al.*, 1990), and a preliminary report on field investigations in the central Peter the First Range and Darvaz Range during June-July 1990 (Pavlis and

Hamburger, 1990). Since returning from the field in July the primary efforts on this project have been twofold: (1) analysis of the pre-orogenic geologic history of the Darvaz-Peter First ranges of Soviet Central Asia; and (2) evaluation of the active geologic structures associated with crustal seismicity beneath the Peter the First Range.

Our work on geologic history of the Garm region has included compilation of published stratigraphic data to supplement our field 1990 observations. These observations indicate that the Jura-Cretaceous stratigraphy of the Tadjik depression (Figure 1) is inconsistent with previously published tectonic models (e.g., Leith, 1985), which called for a Jura-Cretaceous rifting of the southern margin of Asia. The stratigraphic and field observations made in a transect through the Darvaz Range, south of the Garm region, indicate that Jurassic and Early Cretaceous clastic sedimentary rocks were derived largely from uplifted sources to the south. These data suggest that the hypothesis of an open Cretaceous ocean to the south of the Tadjik depression is unworkable because the major sediment source for this period was located at the site of the proposed Cretaceous ocean basin. These observations are suggestive of clastic sedimentation in a basin located landward of an active Andean or collisional margin within the Pamir Range to the south of Garm.

In order to examine active tectonic structures within the seismically active Garm region, we have completed two structural cross sections across the core of the Peter the First Range (PFR)--one from Garm to the Darvaz Range and a second from Khait to the Darvaz Range (see Figure 2). The PFR is an actively deforming fold-thrust belt marked by intense seismicity as well as Quaternary deformation. The core of the PFR is structurally complex, with a record of both out-of-sequence thrusting and back-thrusting above a decollement in Upper Jurassic evaporites. The details of the deep structure beneath the uppermost thrust system are largely unconstrained from surface geology, although seismicity data may ultimately allow further constraints on the deep structure beneath the Peter the First Range. Nonetheless, two critical observations can be made based on these structural sections (Figure 3):

(1) The Darvaz Range exposes markedly deeper structural levels than adjacent regions. Combined with observed steep monoclinal dips and stratigraphic continuity with Tadjik Depression sediments, this relationship is interpreted as a major hanging-wall ramp anticline-syncline pair exposed along the Obi-Khingou River (upper left portion of sections) where Permian-age rocks are exposed. To the north (right) of this fault-bend fold the decollement is localized in upper Jurassic evaporites and only Cretaceous and Cenozoic rocks are exposed in the Peter the First Range.

(2) One of the most significant structural features of the Peter the First Range is clear evidence for a major back-tilting event within the fold-thrust system. This structural feature is recognized by a group of tight, nearly isoclinal folds in the core of the Peter the First Range with axial surfaces that dip to the north at moderate angles (approximately 45°). These structures project westward into normal fold-thrust belt structures with upright to south-dipping folds, consistent with the predominant northward vergence of the fold-thrust belt (see Figure 6 in Hamburger *et al.*, 1990). In some fold-thrust belts, reverse-vergence folding can be ascribed to box folding or "pop-up" folds. This mechanism is precluded for this region, however, because the back-folds are less than 15 km from the structural front and there is insufficient volume in the subsurface to produce the back-folding and still maintain an approximate cross-section balance through a box-folding or pop-up folding mechanism. Our preliminary conclusion from this analysis is that back-tilting requires active duplexing at depth (section A, Figure 3) or back-rotation above a deeper thrust system within the basement (section B, Figure 3), or both. In either case, these deep structures are relevant to evaluation of earthquake hazards in the Garm region because this section crosses the area most strongly affected by the largest historical earthquake in the region, the 1949 M=7.5 Khait earthquake. These observations imply a possible connection between the Khait earthquake and a more deep-seated thrust system beneath the Peter the First Range.

References

Al-Shukri, H. J. and B. J. Mitchell, 1987, Three-dimensional velocity variations and the relation to the structure and tectonic evolution of the New Madrid seismic zone, *J. Geophys. Res., 92,* 6377-6390.

Hamburger, M. W., D. R. Sarewitz and G. A. Popandopulo, 1990, Structural and seismic evidence for intracontinental subduction beneath the Peter the First Range, Soviet Central Asia, *Geol. Soc. Am. Bull.,* in review.

Leith, W., 1985, A mid-Mesozoic extension across Central Asia?, *Nature, 313,* 567-570.

Pavlis, T. L., and M. W. Hamburger, 1990, The Jura-Cretaceous Tadjik Depression, Soviet Central Asia: Rifted margin of Asia vs. foreland basin, *Geol. Soc. Am. Abs. w/ Prog.,* in press.

Nersesov. I.L., Yu, P. Skovorodkin, and T.V. Guseva, 1979, Results of complex studies in the Garm geodynamic polygon, *Izvestiya, Physics of the Solid Earth, 15:4,* 47-55.

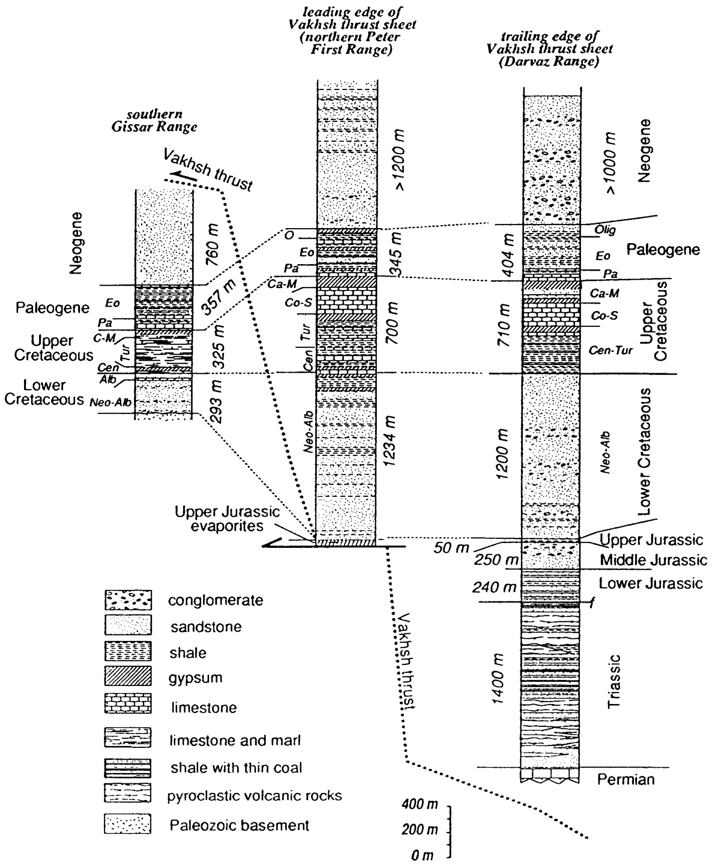

Figure 1. Stratigraphic sections of the Gissar, Peter the First, and Darvaz ranges in the Garm region. Note the appearance of a coarse clastic component in the Jura-Cretaceous section of the Darvaz Range, suggesting an uplifted source area in the Pamir (south of the Darvaz Range) during this period.

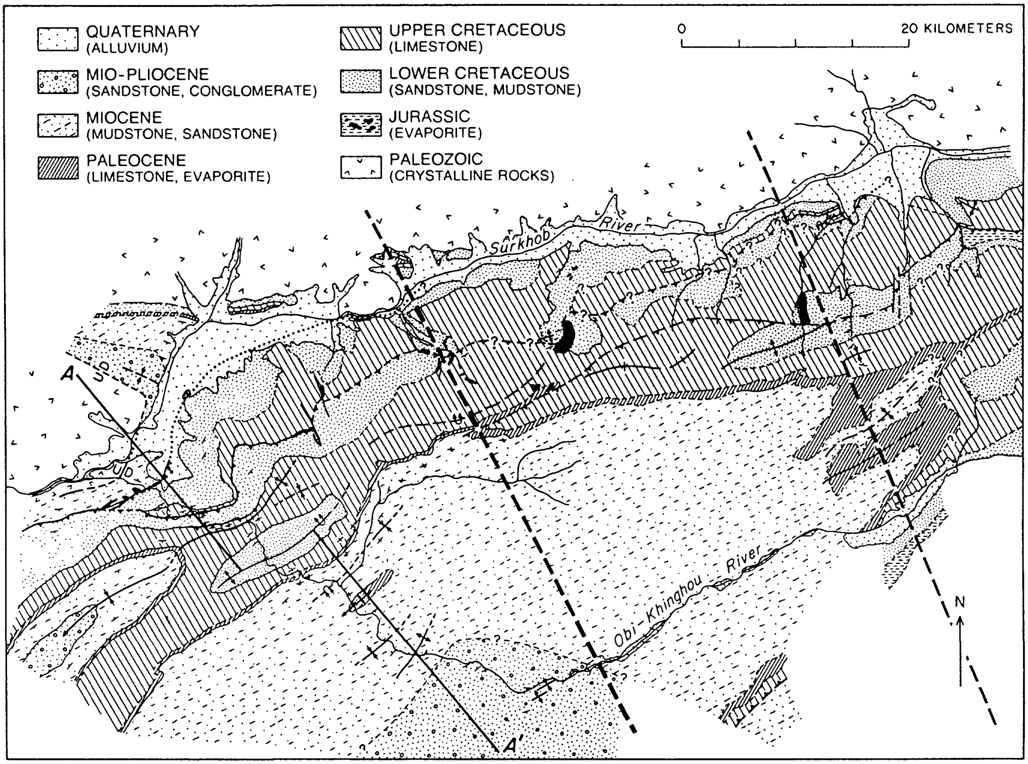

Figure 2. Reconnaissance geological map of the Garm region, based on field mapping, analysis of satellite imagery, and field data collected by V.I. Shevchenko (pers. comm., 1989]. Contacts and structures are shown in solid symbols where well constrained by field observation or imagery interpretation, dashed where approximate, queried where uncertain, and dotted where inferred. Heavy dot-dash line indicates drainage network of the Surkhob and Obi-Khingou rivers. Black areas indicate exposures of Jurassic evaporites, primarily gypsum. Heavy solid line labelled AA' indicates position of geological cross section shown in Hamburger et al. (1990). Heavy dashed lines indicate locations of sections completed during 1990 field season. The easternmost section is shown in Figure 3.

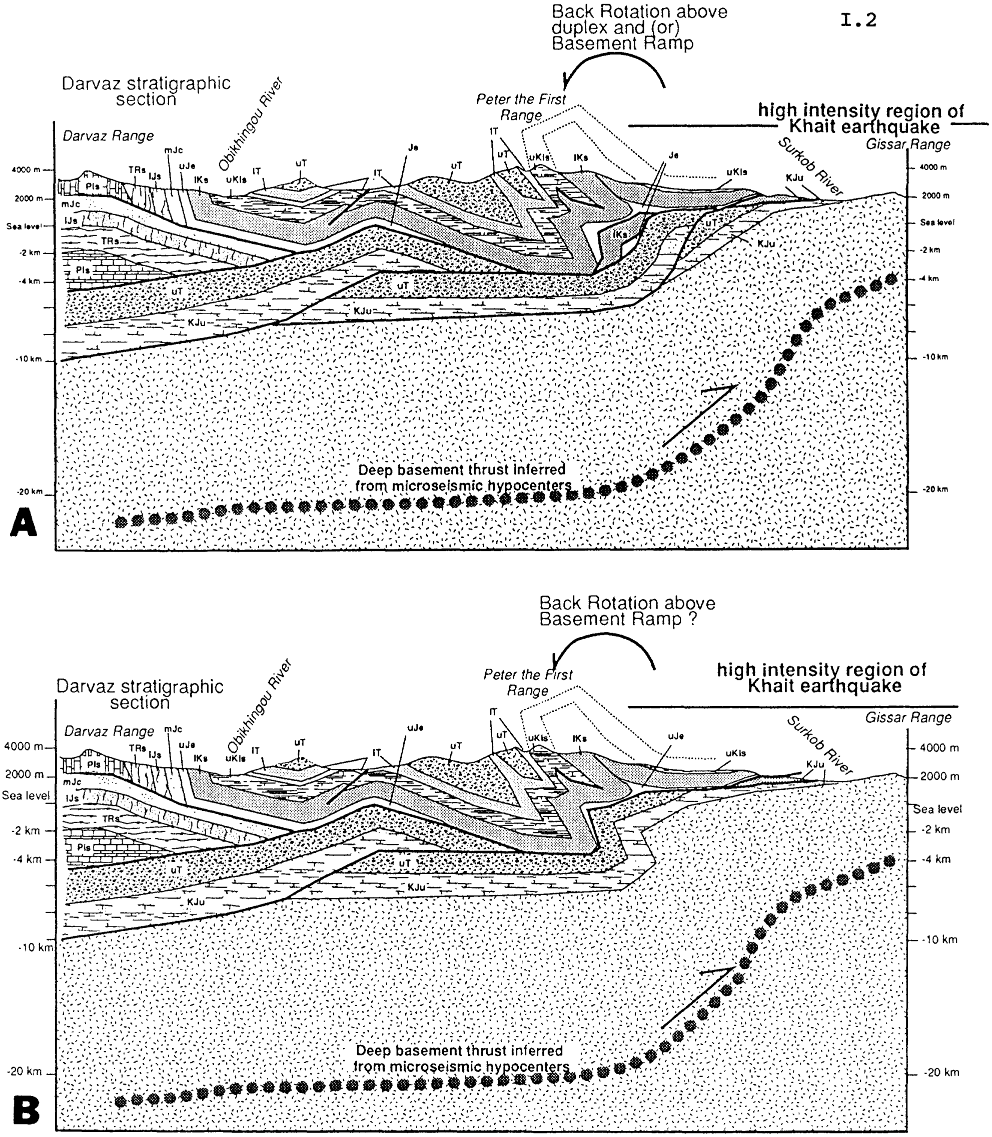

Figure 3. Two preliminary cross sections showing the major structures along a transect from the Darvaz Range to the Gissar Range. Sections are essentially end members in a family of cross-sections and differ primarily in the subsurface interpretation of the structure beneath the Vakhsh thrust sheet to account for the major backfolding in the core of the Peter the First Range. Section A shows at least part of the back-rotation as a consequence of duplexing beneath the leading edge of the thrust sheet. Section B, however, ascribes all back-rotation to a ramp within a deep-seated basement thrust. Cross-sections have not yet been restored to test for section balance.

Symbols: Pls=Permian limestone, TRs=Triassic sedimentary and volcanic rocks; lJs=Lower Jurassic sedimentary rocks; mJc=Middle Jurassic conglomerate and sandstone; uJe=Upper Jurassic evaporites and shale; lKs=lower Cretaceous sandstone, siltstone, conglomerate and shale; uKls=Upper Cretaceous limestone and marl; lT=lower Tertiary limestone, shale, and marl; uT=upper Tertiary (Neogene) sandstone and conglomerate.

Analysis of Earthquake Data from the Greater Los Angeles Basin and Adjacent Offshore Area, Southern California

#14-08-0001-G1761

Egill Hauksson

Seismological Laboratory,
California Institute of Technology,
Pasadena, CA 91125
818-356 6954

INVESTIGATIONS

Seismotectonic analysis of earthquake data recorded by the CIT/USGS and USC networks during the last 15 years in the greater Los Angeles basin. Improve models of the velocity structure to obtain more accurate earthquake locations including depth and to determine focal mechanisms. Studies of the earthquake potential and the detailed patterns of faulting along major faults in the metropolitan area and adjacent regions.

A comprehensive study entitled: *Source Parameters of the 1933 Long Beach Earthquake*, has been accepted for publication in Bull. Seismol. Soc. Amer.

RESULTS

Source Parameters of the 1933 Long Beach Earthquake.

Regional seismographic network and teleseismic data for the 1933 (M_L=6.3) Long Beach earthquake sequence have been analyzed. Both the teleseismic focal mechanism of the mainshock and the distribution of the aftershocks are consistent with the event having occurred on the Newport-Inglewood fault (Figure 1). The focal mechanism had a strike of 315°, dip of 80° to the northeast and rake of -170° (Figure 2). Relocation of the foreshock-mainshock-aftershock sequence using modern events as fixed reference events, shows that the rupture initiated near the Huntington Beach-Newport Beach City boundary and extended unilaterally to the northwest to a distance of 13-16 km. The centroidal depth was 10 ± 2 km. The total source duration was 5 s and the seismic moment was $5*10^{25}$ dyne-cm, which corresponds to an energy magnitude of M_W=6.4. The source radius is estimated to have been 6.6-7.9 km, which corresponds to a Brune stress drop of 44-76 bars. Both the spatial distribution of aftershocks and inversion for the source time function suggest that the earthquake may have consisted of at least two subevents. When the slip estimate from the seismic moment of 85-120 cm is compared with the long term geological slip rate of 0.1-1.0 mm/yr along the Newport-Inglewood fault, the 1933 earthquake has a repeat time on the order of a few thousand years.

The 1933 (M_W=6.4) Long Beach earthquake showed right-lateral motion along the NIF with a small normal component. Slip along the NIF thus contributes to the relative plate motion between the Pacific and North-American plates. The normal component indicates continued subsidence of the southwest corner of the Los Angeles basin. The absence of a thrust component is consistent with the slip partitioning model of the seismotectonics of the Los Angeles basin by Hauksson (1990). The mainshock was a factor of two smaller in seismic moment than the 1971 (M_W=6.6) San Fernando earthquake, not a factor of 5 smaller as previously thought. The distribution of aftershocks and the source time function suggest that the mainshock may have consisted of two subevents. It released strain along a 13-16 km long segment of the NIF from Newport Beach to the southern edge of Long Beach. Accumulated strain along the section of the

NIF within the City of Long Beach thus may not have been released, even though this segment of the fault experienced a relatively high level of aftershock activity.

PUBLICATIONS and REPORTS

Hauksson, E. The 1993 Long Beach earthquake and its aftershocks, (Abstract), *Seis. Res. Letters*, 61, 42, 1990.

Hauksson, E., Earthquakes, faulting,and stress in the Los Angeles Basin, *J. Geophys. Res.*, 95, 15365-15394, 1990.

Hauksson, E. and S. Gross, Source Parameters of the 1933 Long Beach Earthquake, *Bull. Seismol. Soc. Amer.*, in press, 1991.

Hauksson, E. and L. M. Jones, The 1988 and 1990 Upland earthquakes: Left-lateral faulting adjacent to the central Transverse Ranges, submitted to the AGU fall meeting, 1990.

Hauksson, E. and L. M. Jones, The 1988 and 1990 Upland earthquakes: Left-lateral faulting adjacent to the central Transverse Ranges, submitted to *J. Geophys. Res.* 1990.

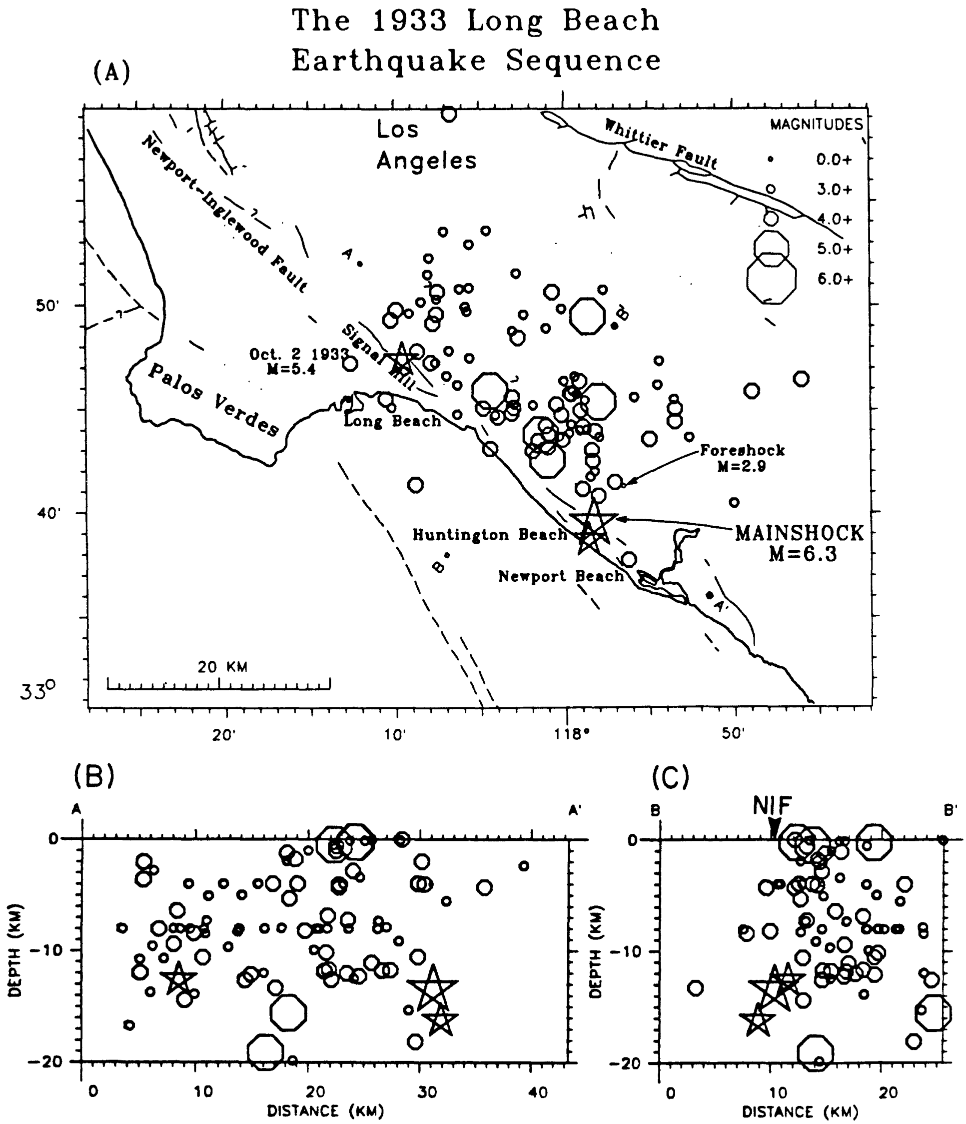

Figure 1 (A) Map showing the final locations of the 1933 foreshock-mainshock-aftershock sequence recorded during the first 6 days of aftershock activity. (B) A cross section A-A' along strike of the Newport-Inglewood fault. (C) A cross section B-B' normal to the strike of the Newport-Inglewood fault.

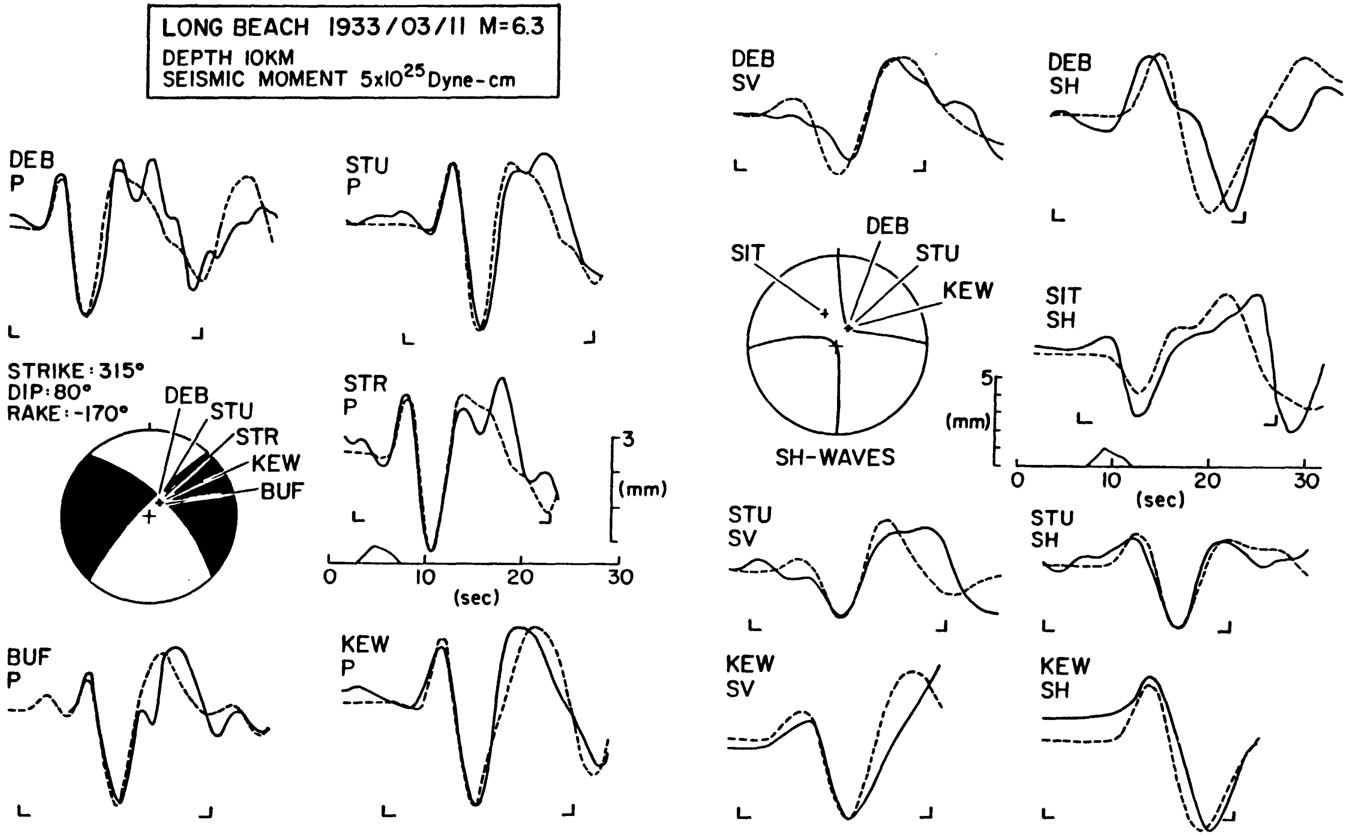

Figure 2 (Left) The lower-hemisphere P-wave focal mechanism of the mainshock that is based on modeling of teleseismic waveforms shows strike-slip faulting. P-, SH- and SV-waveforms are drawn with solid lines and calculated synthetic seismograms are drawn with dashed lines. The brackets indicate the part of the waveform used in the inversion. (Right) The corresponding SH-wave focal mechanism. The best fitting average source time function is also shown.

Source Characteristics of California Earthquakes and Attenuation Effects

14-08-001-G1872

Donald V. Helmberger
Seismological Laboratory
California Institute of Technology
Pasadena, CA 91125
(818)356-6998

Investigations

Our long term objective is to determine the characteristics of earthquakes occurring in Southern California. The basic strategy has been to study the larger modern events since they are well-recorded and then to compare the records from these events (Masters) to interpret historic events or recent ones to obtain quick preliminary results. The primary data sets for these studies are the PAS (low gain recording), long term running teleseismic stations such as De Bilt, starting in 1917, and some of the older Caltech stations. Essentially we think better locations can be obtained using a combination of waveform data and travel time constraints.

Results

This summary will concentrate on the location and source parameters at the Lompoc, California Earthquake of Nov. 4, 1927, see reference. We will address the problems associated with relocating, and determining the style of faulting of the Lompoc earthquake from an assortment of teleseismic and regional seismograms. Since the response of most early instruments is poorly known we have concentrated on a few well calibrated stations, namely those at Berkeley, Tucson, and Pasadena for regional constraints and the teleseismic station at De Bilt (Netherlands). The latter station which remains in operation, also recorded the recent Loma Prieta event and numerous modern events in the general vicinity of Lompoc; the 1969 Santa Lucia Banks, 1983 Coalinga, and 1978 Santa Barbara earthquakes. Location constraints for the Lompoc event were established from the De Bilt recording by comparing S-P and SSS-S waveform matches against the above master events to avoid the effect of unknown clock errors on locations using absolute times. These same seismograms were modeled synthetically to obtain estimates of depth, faulting parameters, and source strength. A similar approach was applied using the regional seismograms.

The 1927 Lompoc earthquake (November 4, 5.51 PST, M_S=7.0) occurred before the deployment of regional seismic arrays in California, with the result that the location and mechanism of the earthquake have been subject to considerable uncertainty. Byerly (1930) located the event offshore Point Arguello at 34°32'N, 121°24'W (figure 1). Gawthrop (1978; 1981) located it at 34.9°N, 120.7°W, much closer to the coast, using teleseismic data, and suggested that this earthquake occurred on the Hosgri fault. Hanks (1979; 1981) located it at an intermediate position of 34.6°N, 120.9°W using regional seismic data. This uncertainty in location has resulted in corresponding uncertainty in the tectonic nature of the event and its association with offshore faults. However, the development of synthetic seismogram techniques in recent years in conjunction with a set of recent earthquakes has provided an opportunity to obtain more accurate estimates of the location, focal depth, focal mechanism and seismic moment of the earthquake using the sparse azimuthal distribution of seismograms that were recorded.

The master events selected for comparison with the 1972 Lompoc earthquakes are the November 5, 1969 magnitude M_S 6.0 Santa Lucia Bank earthquake and the 1983 magnitude M_S 6.4 Coalinga earthquake. Portions of the De Bilt seismograms for the 1927 Lompoc earthquake and these two more recent events are shown in figure 2 along with associated synthetics. The similar P to S amplitude relationships of these seismograms suggest that the three events all have similar focal mechanisms. The large P amplitude relative to S is consistent with the reverse-slip mechanisms previously obtained for the 1969 and 1983 events.

Figure 2 shows the Lompoc and Coalinga S-wave recordings at De Bilt, with the horizontal components digitized and rotated to the radial and transverse components. The ratio of SV to SH has proven useful in determining focal mechanisms, and was used by Choy (1985) in determining the focal mechanism of the Coalinga earthquake displayed in the lower panel. Forward computations were performed using this source model for the Coalinga event, the model of Bent and Helmberger (1990) for the Santa Lucia Banks event, and the model of Bent (1990) for a well-constrained Coalinga aftershock to generate synthetic seismograms for comparison with the De Bilt recordings. Since De Bilt is located near an SH node of the Coalinga event, we find a very small S arrival on the transverse component as predicted. The Lompoc seismogram shows a stronger SH arrival, and the lower panel indicates the rotation in strike from 300 degrees to 340 degrees necessary to move the SH node away from De Bilt and match the recorded SH amplitude. If the mechanism of the Lompoc earthquake is purely dip slip, then the strike is constrained with 5^o. Allowing some component of strike-slip would allow the strike to be more nearly north-south. This mechanism is compatible with nearly all of the polarity measurements available for the Lompoc earthquake.

The true azimuth from the event to BKS is uncertain by about 10^o because of the location uncertainty and therefore the nodal position is equally uncertain. Synthetic seismograms covering this range of azimuths are shown in the upper panel of figure 3 using the focal mechanism at the bottom of figure 2 and a seismic moment of $1.0x10^{26}$ dyne-cm. The sharpness of the nodal crossing in the synthetic seismograms is more subdued in the Berkeley and Lick seismograms than in the data. The close agreement between the recorded and synthetic seismograms for a strike direction of 340 degrees, further confirms the nearly pure reverse mechanism of the 1927 Lompoc earthquake.

Hanks (1979) used S-P time of 12.8 seconds to draw an arc from Santa Barbara to locate the 1927 earthquake, using the travel time curve of Richter (1958) for the southern California region. To evaluate this travel-time curve we read the S-P times at Santa Barbara of more recent earthquakes that are located in the vicinity of the 1927 earthquake, specifically those larger than magnitude 3 between 1980 and 1989. Our results agree with his and we have adopted his arc from Santa Barbara, see figure 1.

We have used SSS-S and S-P time differences to estimate the location of the Lompoc earthquake with respect to the Santa Lucia Banks and Coalinga earthquakes. The S-P results produce the location given in figure 1. The difference in SSS-S interval between the Lompoc and Santa Lucia Banks earthquakes was measured by aligning the two S waves using cross-correlation, and then finding the time difference between the two SSS waves using cross-correlation, as shown in the lower panel of figure 3. The SSS-S time of the Lompoc event is 0.5 second greater than that of the Santa Lucia Banks event, placing the Lompoc earthquake about 12 km south of the location derived from S-P. The proximity of the Lompoc and Santa Lucia Banks earthquakes in distance is reflected in the similarity of their waveforms; this is particularly evident when the Santa Lucia Banks record is lowpass filtered to provide a better comparison with the larger Lompoc earthquake.

Given the uncertainties, we conclude that the distance of the Lompoc earthquake from De Bilt is not significantly different from the distance of the Santa Lucia Banks earthquake from De Bilt. Together with the Santa Barbara arc, the De Bilt arc through the Santa Lucia Banks epicenter gives a location of 34.35°N, 120.9°W, see figure 1. This location lies about 25 km south of Hanks' (1979) location, but within the uncertainty of that location

In summary, our results indicate a north-northwesterly striking thrust event located about 40 km west of Point conception which is in excellent agreement with the recent tsunami modeling results by Satake and Somerville (1990). This location is 20 km southwest of that proposed by Hanks and well within his error bars. We obtain a moment of 1×10^{26} dyne-cm, a trapezoidal time history of (2,2,2) sec. and a source depth of 10 km. The weak beginning of the P_{nl} wavetrain at Berkeley indicates some source complexity, which is characteristic of large events. The fault parameters are strike = N20°W, dip = 66NE, and rake = 95°. These results are in agreement with the geodetic study by Savage and Prescott but disagree in magnitude with estimates made by Hanks. The worksheets for the Lompoc earthquake prepared by Gutenberg and Richter show an M_s of 7.0 and an m_β (long-period body wave magnitude) of 7.3, compared with the moment magnitude of 6.6 derived from the seismic moment of 1×10^{26} dyne-cm obtained in this paper. The body waves of the Loma Prieta event (M_s= 7.1) appear distinctly larger than the Lompoc event at De Bilt, in agreement with our lower estimate of source strength.

REFERENCES

Bent, A. and D. V. Helmberger (1990). Source characteristics of five moderate earthquakes occurring off the California coast, submitted to *BSSA*.

Byerly, P. (1930). The California earthquake of November 4, 1927. *BSSA 68*, 53-66.

Choy, G. (1985). Source parameters of the Coalinga California earthquake of May 2, 1983 inferred from broad-band waves, *USGS Open File Report* 85-44, 83-105.

Gawthrop, W. (1978). The 1927 Lompoc, California earthquake. *BSSA 68*, 1705-1716.

Hanks, T. (1979). The 1927 Lompoc, California earthquake (November 4, 1927; m=7.3) and its aftershocks. *BSSA 69*, 451-462.

Helmberger, D. V., and G. R. Engen (1980). Modeling the long period body waves from shallow earthquakes at regional distances. *BSSA 70*, 1699-1714.

Helmberger, D., P. G. Sommerville, J.T. McLaren, L. J. Burdick, E. Garnero, A. Bent and L. S. Zhao (1990). The location and source parameters of the Lompoc, California Earthquake of Nov. 4, 1927, (submitted, *BSSA*).

Satake, K. and P. G. Sommerville (1990). Location and size of the 1927 Lompoc, California earthquake from tsunami data, submitted to *BSSA*.

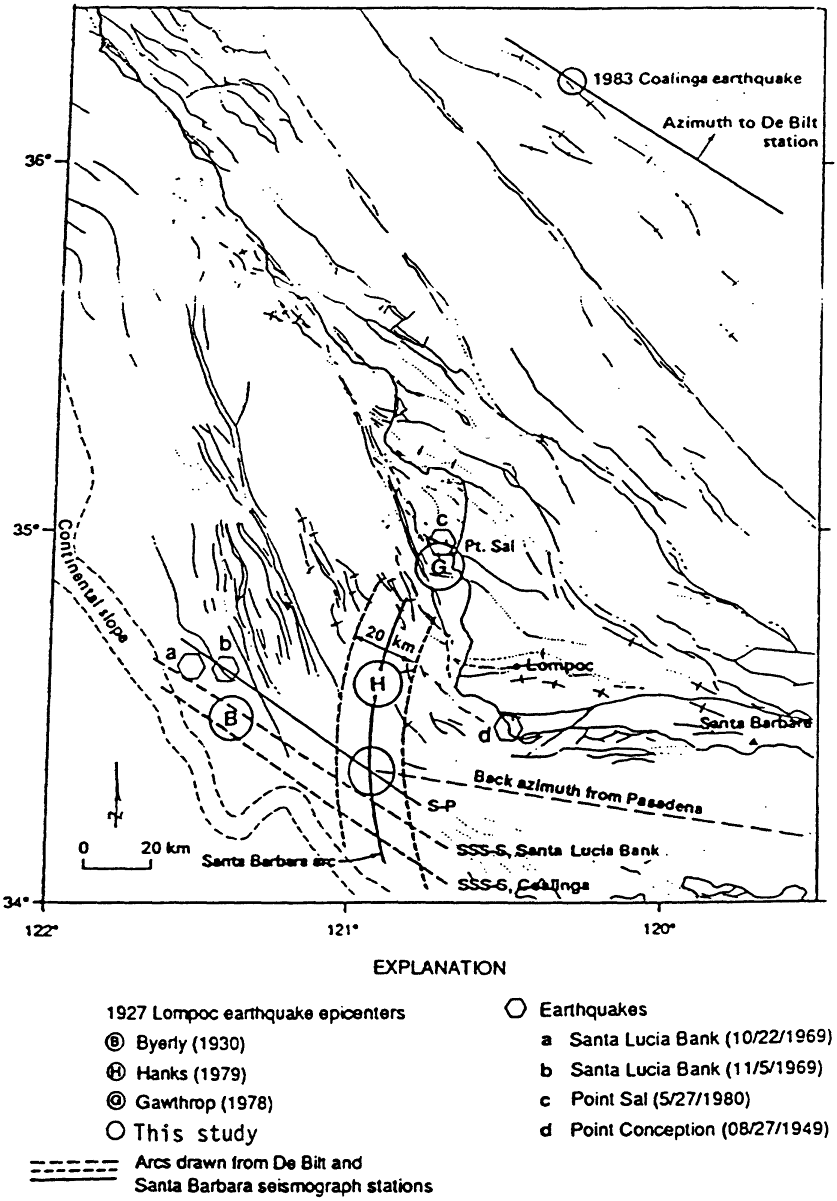

Figure 1. Constraints on the location of the 1927 Lompoc earthquake from differential travel times of P, S, and SSS phases at De Bilt with respect to the 1969 Santa Lucia Banks and 1983 Coalinga earthquakes, from S-P times of aftershocks recorded at Santa Barbara, and from the back azimuth of P-waves recorded at Pasadena.

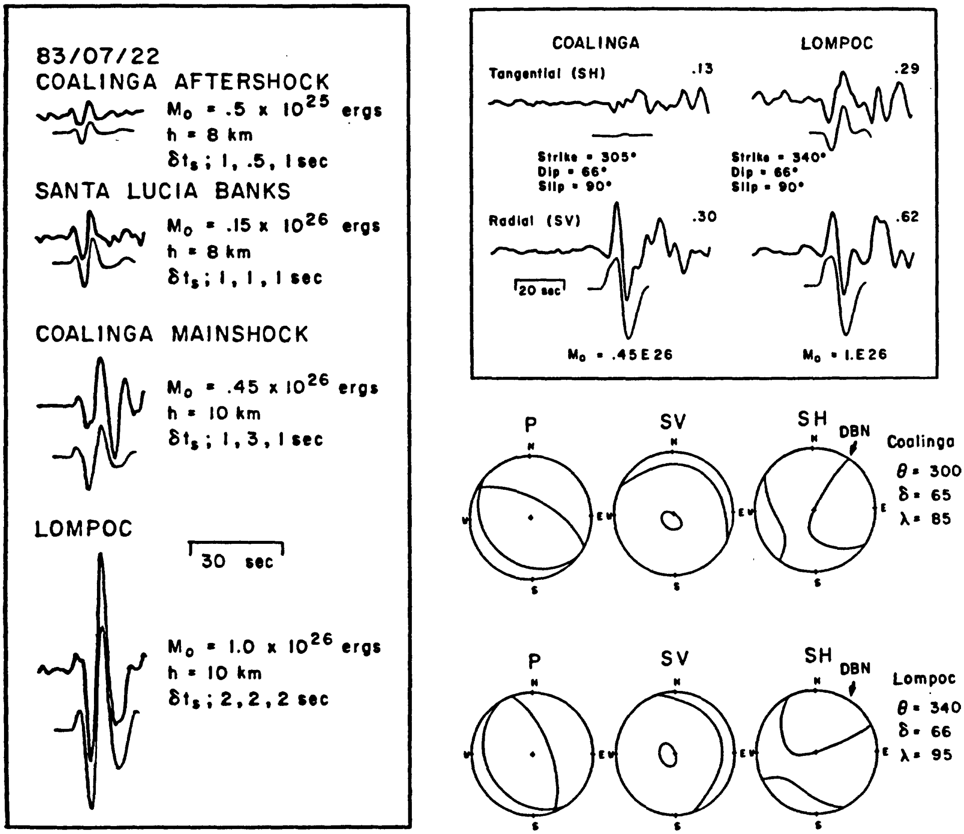

Figure 2. The column on the left displays the P-waves observed at De Bilt and corresponding synthetics predicted for known solutions except for Lompoc which was determined by forward modeling. The best fitting mechanism is given on the right, along with SV & SH comparisons with Coalinga.

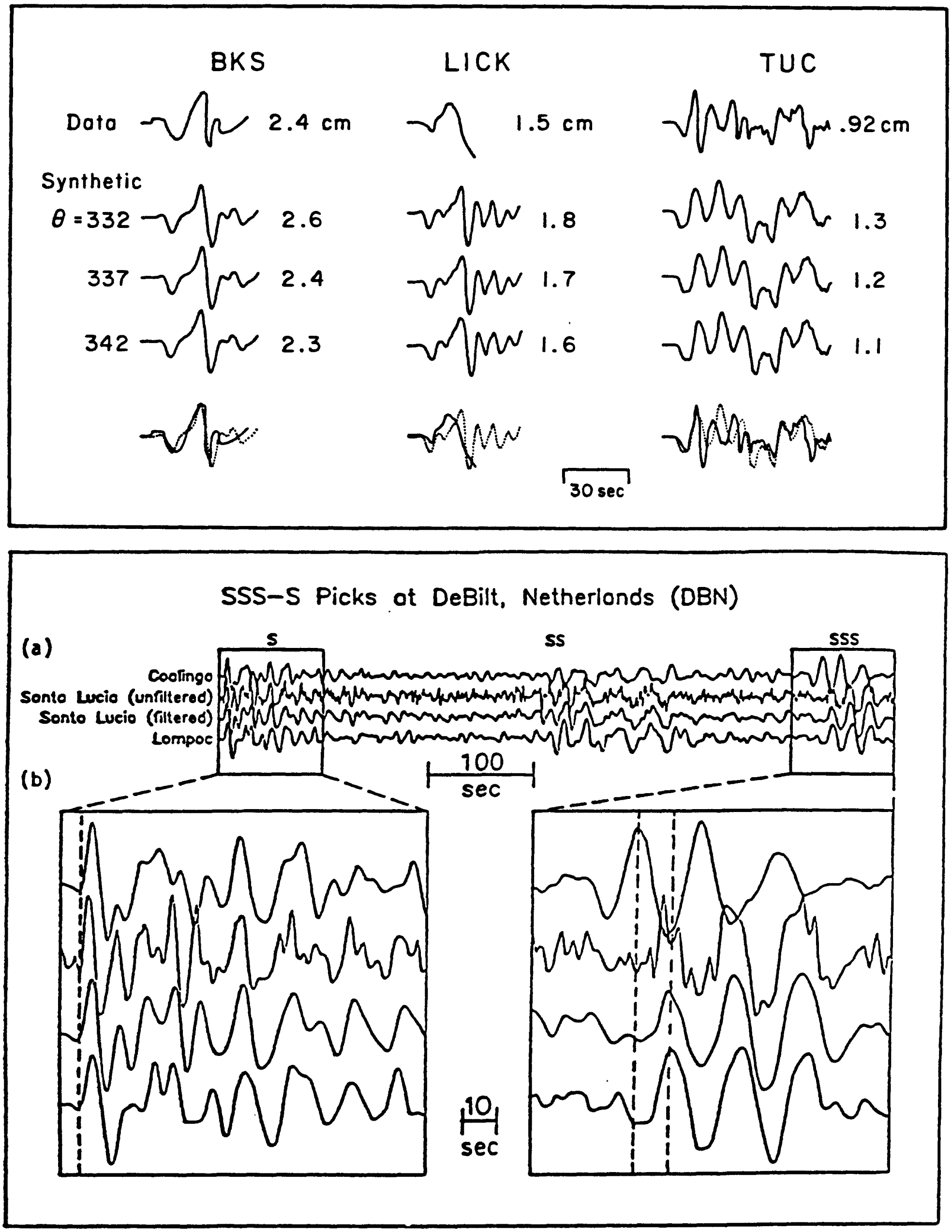

Figure 3. Synthetics and observed regional waveform data is given in the top panel following the technique and models used in matching these stations for the above master events, Santa Lucia Banks, etc., after Bent and Helmberger (1990). The lower panel displays the De Bilt seismograms for Lompoc and master events displaying the similarity between Lompoc and the Santa Lucia Banks events in (SSS-SS) waveshape and timing.

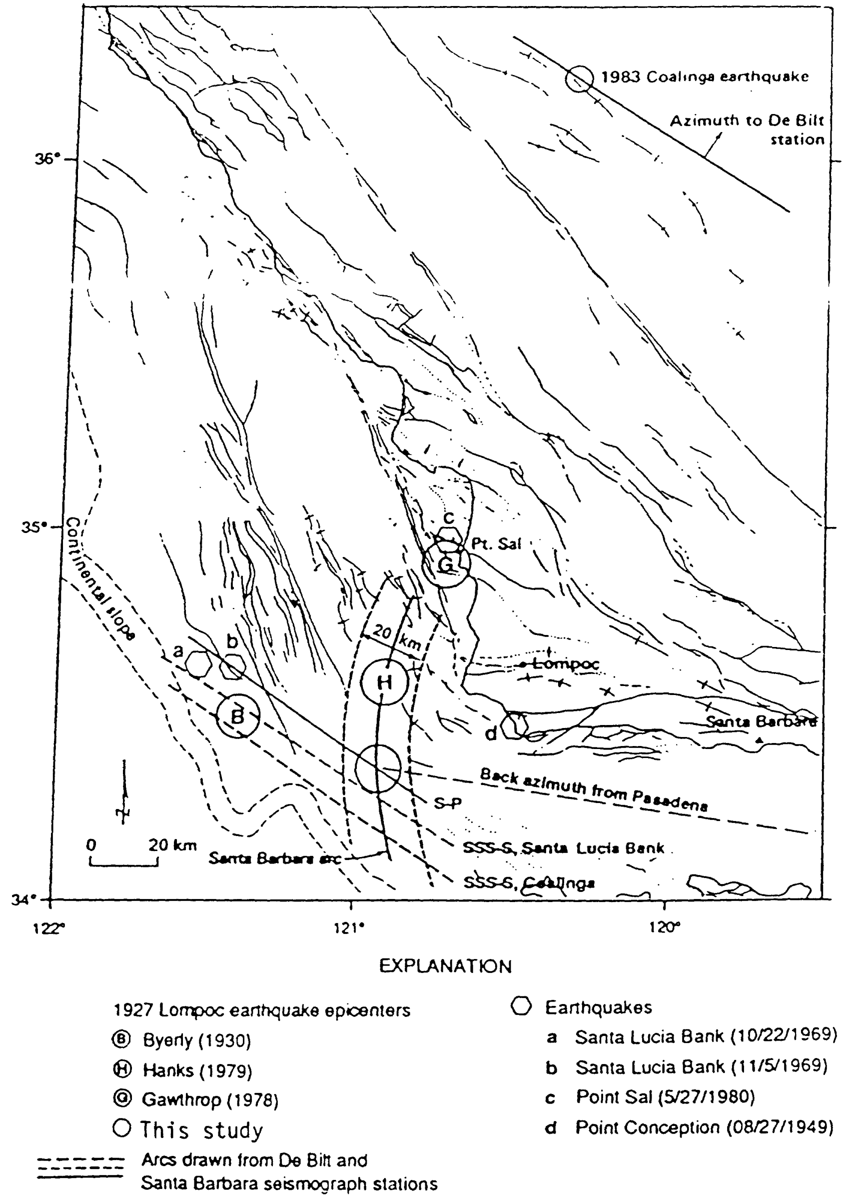

Figure 1. Constraints on the location of the 1927 Lompoc earthquake from differential travel times of P, S, and SSS phases at De Bilt with respect to the 1969 Santa Lucia Banks and 1983 Coalinga earthquakes, from S-P times of aftershocks recorded at Santa Barbara, and from the back azimuth of P-waves recorded at Pasadena.

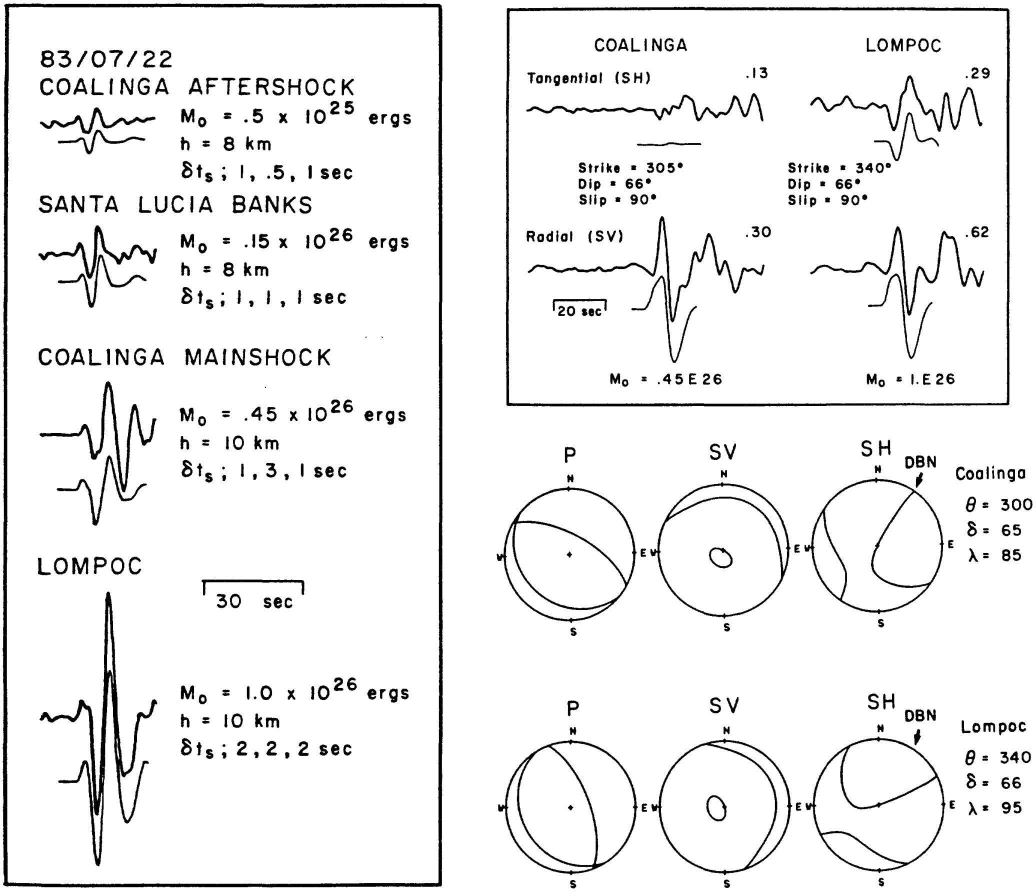

Figure 2. The column on the left displays the P-waves observed at De Bilt and corresponding synthetics predicted for known solutions except for Lompoc which was determined by forward modeling. The best fitting mechanism is given on the right, along with SV & SH comparisons with Coalinga.

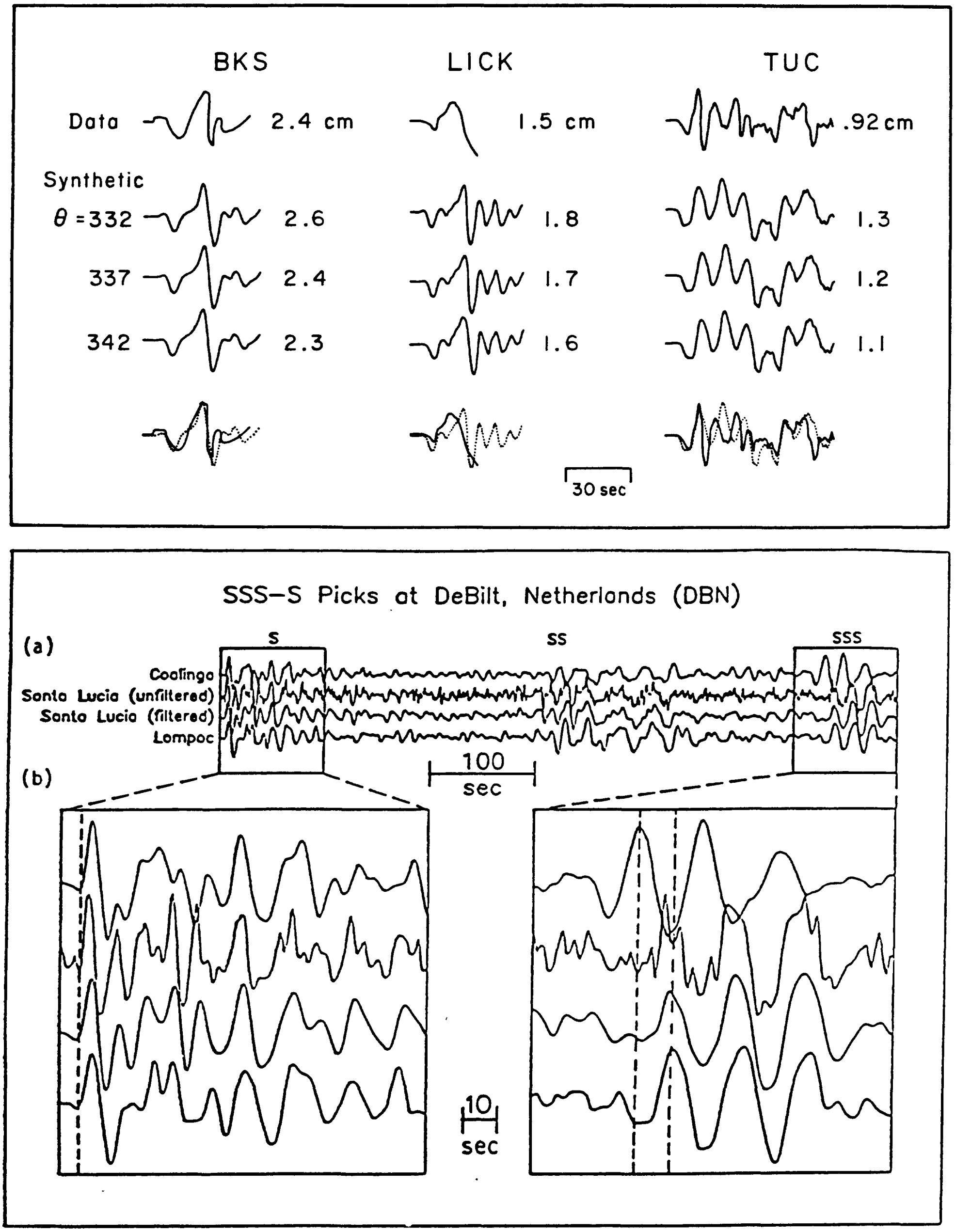

Figure 3. Synthetics and observed regional waveform data is given in the top panel following the technique and models used in matching these stations for the above master events, Santa Lucia Banks, etc., after Bent and Helmberger (1990). The lower panel displays the De Bilt seismograms for Lompoc and master events displaying the similarity between Lompoc and the Santa Lucia Banks events in (SSS-SS) waveshape and timing.

Geologic Mapping of the Island of Hawaii - Kaoiki Fault Zone

Program Task No. I.2

Marie D. Jackson
Branch of Igneous and Geothermal Processes
U. S. Geological Survey
2255 North Gemini Drive
Flagstaff, Arizona, 86001
FTS 765-7186

Investigations

1. Field and mechanical study of ground cracks associated with the 1974 $M_L=5.5$ and 1983 and $M_L=6.6$ Kaoiki, Hawaii, earthquakes.

Results

1. *Importance of the Kaoiki Fault Zone.* The Kaoiki seismic zone, a young tectonic feature of Mauna Loa volcano, Hawaii (Fig. 1), is the site of recurrent moderate- and large-magnitude earthquakes that cause serious damage. The Kaoiki is the subject of a forecast for a $M_L=6$ earthquake before the turn of the century (Wyss, 1986). The relation between volcano-seismic processes and faulting within the Kaoiki zone is being studied so as to increase our ability to assess earthquake hazards and test Wyss's prediction in this area.

   The November 30, 1974 $M_L=5.5$ and November 16, 1983 $M_L=6.6$ earthquakes generated zones of left-stepping, en echelon ground cracks that extend for several kilometers on the lower SE flank of Mauna Loa. Most large magnitude earthquakes occur along pre-existing faults; in contrast, these major Kaoiki earthquakes propagated new ruptures, at least in their surface expression. The Kaoiki seismic zone is unique because its ground ruptures record the initial stages of development of a strike-slip fault zone: future ground ruptures should be expected to merge into a mature fault zone. Geologic mapping by this project and by Endo (1985) shows that at least four ground-rupture zones are concentrated within an area of 30 km^2.

   The 1983 M=6.6 earthquake caused damage to the Island of Hawaii and preceded an eruption on the NE-rift zone of Mauna Loa volcano in March 1984. Similiarly, the November 1974 Kaoiki earthquake preceded the July 1975 Mauna Loa summit eruption. Many aftershocks of the 1983 event are strike-slip but an equal number are low-angle thrust events. Based on aftershock data and body-wave modelling, Thurber et al. (1989) suggested that the 1983 mainshock initiated as a strike-slip event of moderate magnitude, which preceded the main moment release on a low-angle thrust fault. I have used geologic field data collected along the zone of ground breakage and mechanical analysis to evaluate the importance of strike-slip faulting in the 1983 earthquake.

2. *General Objectives.* This project examines the history and mechanisms of faulting within the Kaoiki zone that will form the basis for seismic hazard evaluations for the Island of Hawaii. This study investigates: 1) the faulting and earthquake mechanisms involved in the 1974 and 1983 Kaoiki events and 2) the deformation of the Mauna Loa and Kilauea volcanic edifices

resulting from the mutual inflation of their summit magma chambers and the seaward migration of Mauna Loa's SE flank. Field work undertaken by this study includes 1) the preparation of a 1:10,000 scale geologic map of the rupture zone generated by the 1983 earthquakes, and another, much older, undated earthquake; and 2) detailed outcrop-scale mapping (<1:1000 scale) of three critical exposures of the 1983 ground cracks and one excellent exposure of the oldest crack zone. Endo (1985) mapped the 1974 ground cracks at 1:1360 scale, and these data are included in this study. Analytical work includes mechanical analysis of the nature and depth of faulting underlying the 1974 and 1983 cracks.

3. *Summary of Data Collected.* In the past six months, Jackson completed a manuscript, to be submitted to Journal of Geophysical Research, that describes the structure and propagation path of the 1974 and 1983 Kaoiki ground ruptures, and their relation to the long-term geologic history and recent seismicity of Mauna Loa's SE flank. The manuscript received Branch Chief approval on 8/14/90, and Jackson is currently making revisions to the paper, which should be ready to be submitted next month.

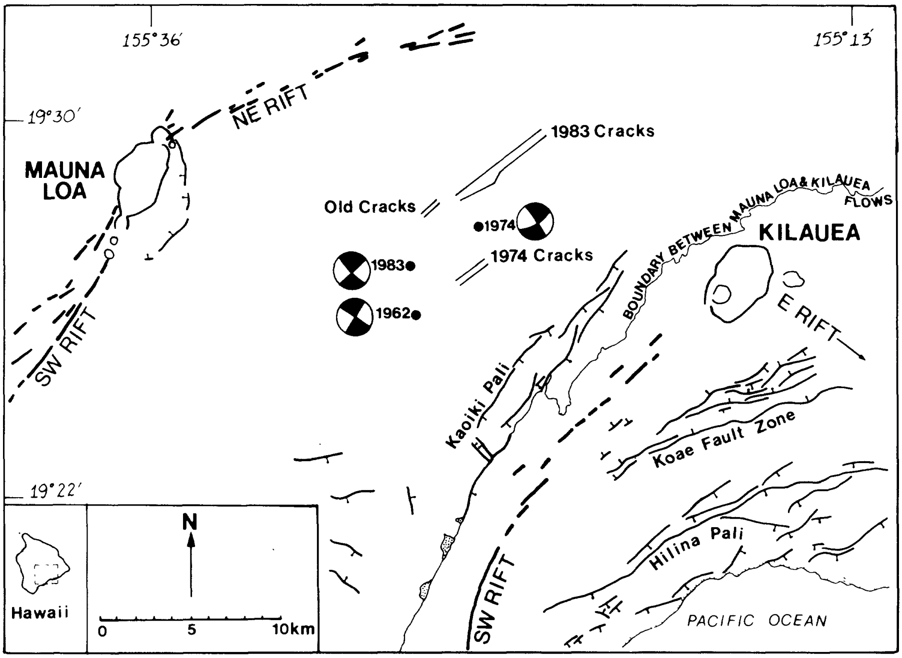

Figure 1. Generalized map showing locations of ground ruptures, focal mechanisms and locations of important strike-slip Kaoiki earthquakes, and major fault and rift systems within the southeast flank of Mauna Loa volcano and the southwest part of Kilauea volcano.

4. *Analysis of Field data.* Ground ruptures from the 1983 M_L=6.6 earthquake, the 1974 M_L=5.5 earthquake, and an older undated earthquake trend N48°-N55°E, a direction nearly parallel to nodal planes of the 1983 and 1974 main shocks' focal mechanisms (Fig. 1). Individual ruptures consist of arrays of left-stepping, en echelon cracks, with predominantly opening displacements, which strike roughly EW, about 30°-50° clockwise from the overall trend of the zones. Some of the cracks are linked by secondary fractures to form left-stepping, 25- to 150-m-long cracks arrays that accomodated small right-lateral shear displacements. Geologic mapping of the 1983 rupture (Fig. 2) shows that the 25- to 150-m-long arrays coalesce at shallow depths to form left-stepping, 300- to 900-m-long cracks arrays that nearly parallel the overall trend of the rupture. In the 1974 rupture, linkage of these longer arrays takes place at the earth's surface. Detailed descriptions of the morphology and linkages of the cracks, and their displacement patterns are presented in previous EQHRP reports.

Field observations of the Kaoiki earthquake ground cracks and fracture analysis of the 1983 event give important insights about how the Kaoiki earthquakes create new ruptures. We hypothesize that the propagating ruptures induced tensile failure of the near-surface rocks. As the coseismic deformation progressed, the opening-mode cracks created in the crack tip region of the parent strike-slip fault coalesced, and crack segments linked to form progressively longer, left-stepping crack arrays that became sub-parallel to the overall trend of the rupture zone and coalesced themselves at shallow depths. Figure 3 shows map-view sketches of stages in the propagation of the parent strike-slip fault into the host rocks just ahead of its tip.

A. The first stage in the process is the formation of a cloud of tensile cracks ahead of the tip of the parent fault as it begins to slip. The cracks strike about EW, normal to the seismically-determined least compressive stress (Endo, 1985). As strain increases certain cracks are in opportune positions to link, creating 25- to 150-m-long cracks arrays that transfer small right-lateral shear displacements.

B. With continuing coseismic increase in strain and displacement in the host rocks, certain of the 25- to 150-m-long cracks link to form 300- to 600-m-long cracks arrays. We suggest that these longer arrays have greater heights, and they are more efficient at transmitting shear displacements

C. The 300- to 900-m-long arrays make a much smaller angle, 10° to 15°, with the trend of the parent fault. As the strain continues to increase, these cracks link to form 2- to 4-km-long crack arrays that parallel the parent fault. Linkage is made easier by the presence of numerous short cracks, 25- to 150-m-long crack arrays and brecciated zones between these structures.

D. Finally, the 2- to 4-km-long crack arrays rupture through the host rocks and form a through-going zone of strike-slip ground breakage. This process repeats itself again and again as the parent fault propagates through the host rocks.

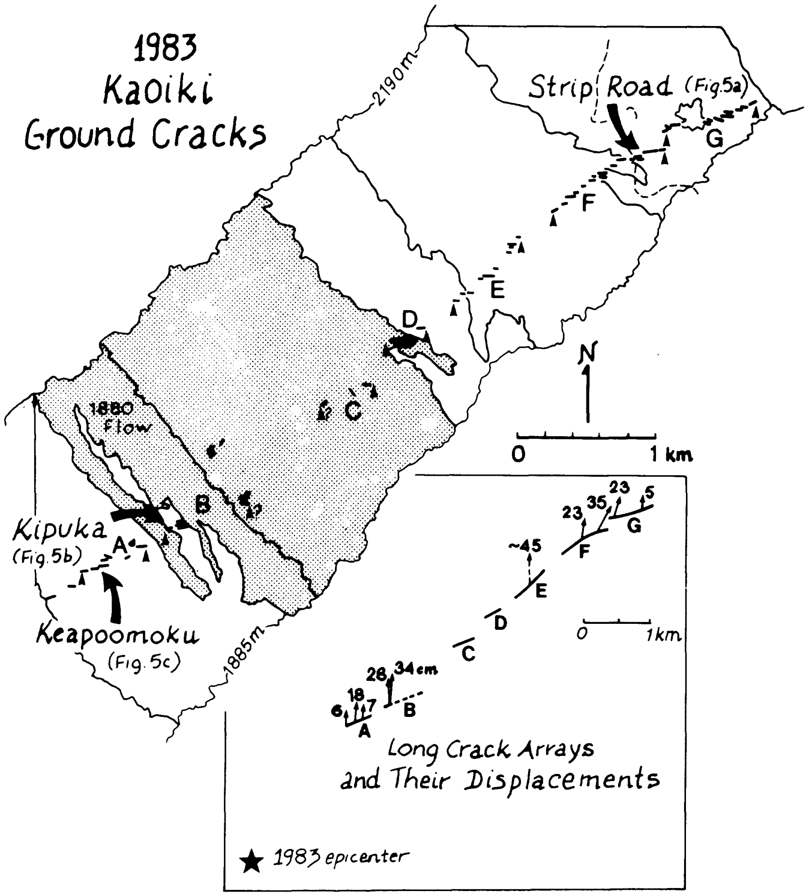

Figure 2. Geologic map of the 1983 Kaoiki ground rupture (1:10,000) scale. Large aa fields (stippled pattern) make detection of some of the cracks impossible. Arrows shows the tips and terminations of left-stepping 300- to 900-m-long arrays. Inset shows the mainshock epicenter (star), the distribution of the longer arrays, and cumulative displacements across the zone.

The ground cracks are part of a "fracture-process zone" ahead of the parent fault that, during propagation, stressed the rocks above its tip (Pollard et al., 1982). An approximate calculation that uses an estimated fault size and the observed seismic moment, and treats the 1983 Kaoiki earthquake as a Mode-III crack, demonstrates that motion along a parent fault that extends to a height of somewhat less than a kilometer below the earth's surface generates sufficient tensile stress above its tip to induce tensile failure parallel to the mapped cracks (Jackson et al., 1988). The analysis suggests that if the 300- to 900-m-long en echelon arrays (Fig. 2) have heights equal to their lengths, then they may connect directly with the parent fault.

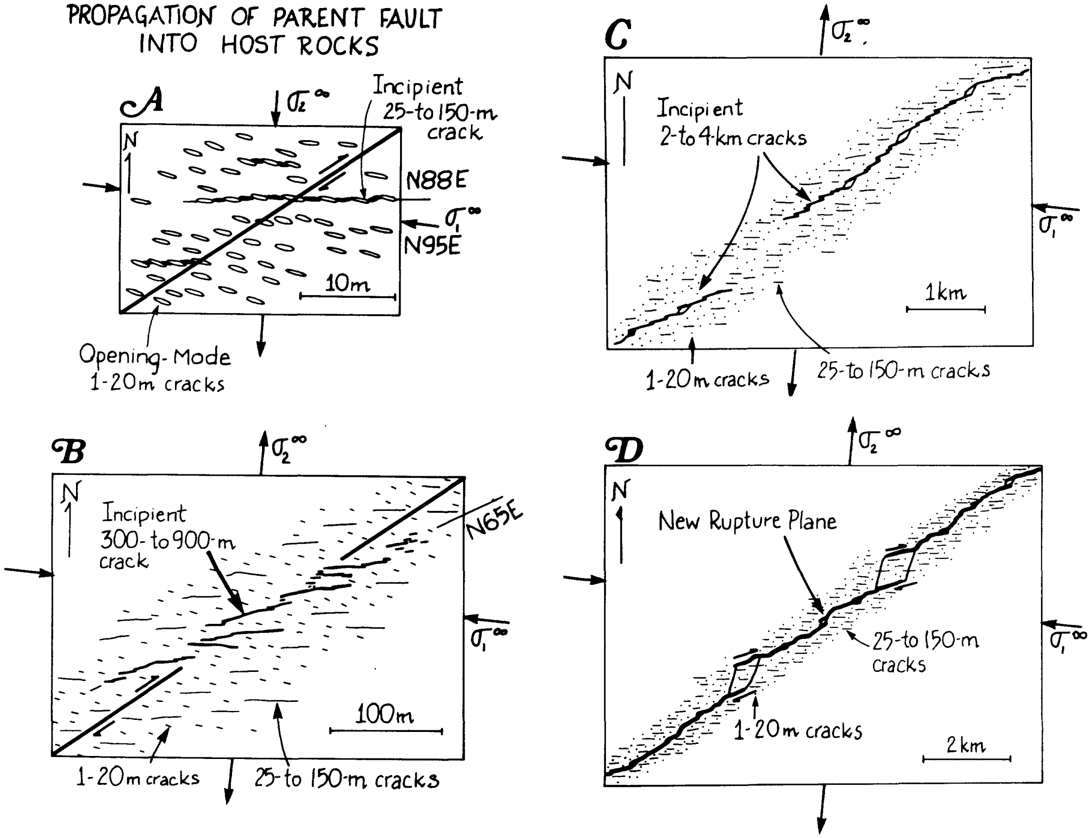

Figure 3. Sketches showing stages in the propagation of a Kaoiki strike-slip rupture. See text for explanation.

5. *Conclusions.* Recent papers describing the seismicity and tectonics of Mauna Loa and Kilauea volcanoes (Swanson et al., 1976; Lipman et al., 1985; Thurber et al., 1989) have established the importance of low-angle seaward thrusting of these volcanoes' south flanks along a layer of old ocean floor sediments that lies at about 8 to 11 km depth. This process is responsible for the M=7.2 and M=6.1 earthquakes that occurred within Kilauea volcano in 1975 and 1989 and, perhaps, the Great Ka'u earthquake of 1868 (Wyss, 1988).

In the Kaoiki seismic zone, located between the summits of Mauna Loa and Kilauea volcanoes (Fig. 1), both low-angle thrusting events and NE-striking strike-slip earthquakes coexist. Although strike-slip earthquakes are absent within the Hilea area, located SW of the Kaoiki zone, low-angle thrust earthquakes occur extensively in this region. It is possible that the Kilauea edifice and its root into the mantle form a centrally-pinned buttress and barrier to southward displacement of the south flank of Mauna Loa in the Kaoiki area. This part of Mauna Loa is therefore forced to move laterally along strike-slip zones.

We confirm the importance of right-lateral strike-slip faulting in the Kaoiki seismic zone. A M=6 earthquake is predicted for the Kaoiki before the end of the century (Wyss, 1986). We now have an excellent set of base maps and field observations with which to measure ongoing deformation in this fascinating area.

References cited

Endo, E. T., 1985, Seismotectonic framework for the southeast flank of Mauna Loa volcano, Hawaii: Ph.D. Thesis, Univ. of Wash., Seattle.

Jackson, M. D., E. T. Endo, P. T. Delaney, 1988, Ground rupture from the 1983 Kaoiki earthquake, Mauna Loa volcano, Hawaii (abs.): Seismological Research Letters, v. 59, p.35.

Jackson, M. D., and E. T. Endo, in press, Genesis of a strike-slip fault zone: he 1974 and 1983 Kaoiki ground ruptures, Mauna Loa Volcano, Hawaii (abs): Transactions of the American Geophysical Union, Fall Meeting. To BWTR 8/89.

Lipman,P. W., J. P. Lockwood, R. T. Okamura, D. A. Swanson, and K. M. Yamashita, 1985, Ground deformation associated with the 1975 magnitude-7.2 earthquake and resulting changes in the activity of Kilauea volcano; U. S. G. S. Prof. Pap., 1276, 45 pp.

Pollard, D. D., P. Segall, P. T. Delaney, 1982, Formation and interpretation of dilatant echelon cracks: Geological Society of America Bulletin, v. 93, p. 1291-1303.

Swanson, D. A., W. A. Duffield, and R. S. Fiske, 1976, Displacement of the south flank of Kilauea volcano: the result of forceful intrusion of magma into the rift zones: U. S. G. S. Prof. Pap., 963, 30 pp.

Thurber, C. H., Y. Li, and C. Johnson, 1989, Seismic detection of a low-velocity layer beneath the southeast flank of Mauna Loa, Hawaii: Geophys. Res. Let., v. 16, p. 649-652.

Wyss, M., 1986, Regular intervals between Hawaiian earthquakes: Implications for predicting the next event: Science, v. 234, p. 726-728.

Wyss, M., 1988, A proposed source model for the Great Ka'u, Hawaii, earthquake of 1868: Bull. Seis. Soc. Amer., v. 78, p. 1450-1462.

Earthquake and Seismicity Research Using SCARLET and CEDAR

Grant No. 14-08-0001-G1774

Hiroo Kanamori, Clarence R. Allen and Robert W. Clayton
Seismological Laboratory, California Institute of Technology
Pasadena, California (818) 356-6914

Investigations

1. Broadband Study of the December 3, 1988, Pasadena Earthquake Sequence
by Ma, Kuo-Fong and Hiroo Kanamori

2. Seismic Strain Rates in Southern California
by Weishi Huang, H. Kanamori and L. T. Silver

3. Three-Diomensional Attenuation Structure of Kilauea-East Rift Zone, Hawaii
by Phyllis Ho-Liu, Carl Johnson, Jean-Paul Montagner, Hiroo Kanamori and Robert Clayton

Results

1. Broadband Study of the December 3, 1988, Pasadena Earthquake Sequence

The Pasadena earthquake (M_L=4.9) of 3 December, 1988, occurred at a depth of 16 km, probably on the Santa Monica-Raymond fault which is recognized as one of the most important faults in the Los Angeles basin in terms of its seismic potential. Prior to this event, no earthquake larger than magnitude 4 had been recorded since 1930 in this area. High-quality seismograms were recorded with the Pasadena very broadband (VBB) system (IRIS-TERRAscope station) for not only the main shock but also the aftershocks at an epicental distance at 3 to 4 km. We determined the focal mechanisms of 9 aftershocks using these data. The first motion data for most of the aftershocks are too incomplete to determine the mechanism using the conventional method. We approximated the moment rate function by a triangle and inverted the amplitudes and polarities of P, SV and SH waves to determine the seismic moment and the three fault parameters (dip, rake and strike). Our results show that the mechanisms of the aftershocks are essentially similar to the mechanism of the main shock with some variation. The average orientations of the P and T axes of the aftershocks are consistent with the strike of Raymond fault. The ratio of the logarithm of the cumulative seismic moment of aftershocks to that of the seismic moment of the main shock is significantly smaller than commonly observed. It suggests that most moment release of the earthquake resulted from a strong region of the fault plane. The lack of aftershocks of the Pasadena earthquake is consistent with the failure of strong asperities.

2. Seismic Strain Rates in Southern California

We determined the focal mechanisms of 271 Quality-A earthquake with M_L=3 which occurred in southern California during the period 1981-1988. We divided the geographic distribution of seismicity into 10 domains and estimated seismic strain rates in each by tensorially summing the seismic moment tensors for individual events. We interpreted the summed moment tensor in each domain in terms of both seismic slip and convergence rates. The deformation pattern for the entire region can be represented as a sum of the San Andreas fault (SAF) type strike-slip motion and the NS convergence. Of the 271 analyzed events, 28% are thrust events, but they released 44% of the total seismic energy. The NS seismic convergence rate in the central Transverse Ranges is about 8mm/yr for this period, which is comparable to the regional convergence rate estimated from geological and geodetic data. Except for the San Jacinto fault domain, which has a seismic slip rate of 13.6mm/yr, the seismic strain rates are much smaller than the geologically determined slip rates. For instance, summation of all the events in the 250Km-wide zone along the SAF yields only 11.2mm/yr right-lateral slip. The result is shown in Figure 1.

3. Three-Diomensional Attenuation Structure of Kilauea-East Rift Zone, Hawaii

The three-dimensional attenuation structure in the crust underneath Kilauea, the East Rift Zone and Maua Loa is imaged using both an iterative back-projection inversion method and a generalized no block inversion method. The Kilauea shallow magma chamber, East Riftr Zone and the Mauna Loa magma chamber are delineated as attenuating anomalies. Detailed inversion suggests the existence of shallow magma reservoirs at Maua Uli and Pu'u O'o, the present sites of magma eruptions. The Hilina Fault zone is highly attenuating, dominating the attenuating anomalies at shallow depths. The "pipeline" system between Kilauea and the East Rift Zone shows up as a continuous supply channel extending down to a depth of approximately 6 km. The southwest Rift Zone, on the other hand, is not delineated by attenuating anomalies, except at a depth of 8-12 km where an attenuating anomaly is imaged west of Pu'u Kou. The Mauna Loa chamber is seated at a deeper level (about 6-10 km) than the Kilauea magma chamber. A highly attenuating anomaly extending from Kilauea to the Northest rift of Mauna Loa seems to indicate an apparent linkage between the two volcanoes. Resolution in the Mauna Loa area is not as good as in the Kilauea are due to poor ray coverage. There is a trade-off between the imaged depth extent of the magma chamber under Mauna Loa and the error. Kilauea magma chamber, on the other hand, is well resolved according to resolution test done at the location of the magma chamber.

References

Ma, Kuo-Fong and H. Kanamori, Broadband study of the December 3, 1988, Pasadena earthquake sequence, to be submitted to Bull.Seismol. Soc. Am., 1990.

Huang, W., H. Kanamori, and H. Kanamori, Seismic strain rates in Southern California, abstract, 1990 Fall Agu meeting, 1990.

Ho-Liu, Phyllis, Carl Johnson, Jean-Paul Montagner, Hiroo Kanamori, and Robert Clayton, Three-diomensional attenuation structure of Kilauea-East Rift zone, Hawaii, submitted to Bull. Volcanology, 1990.

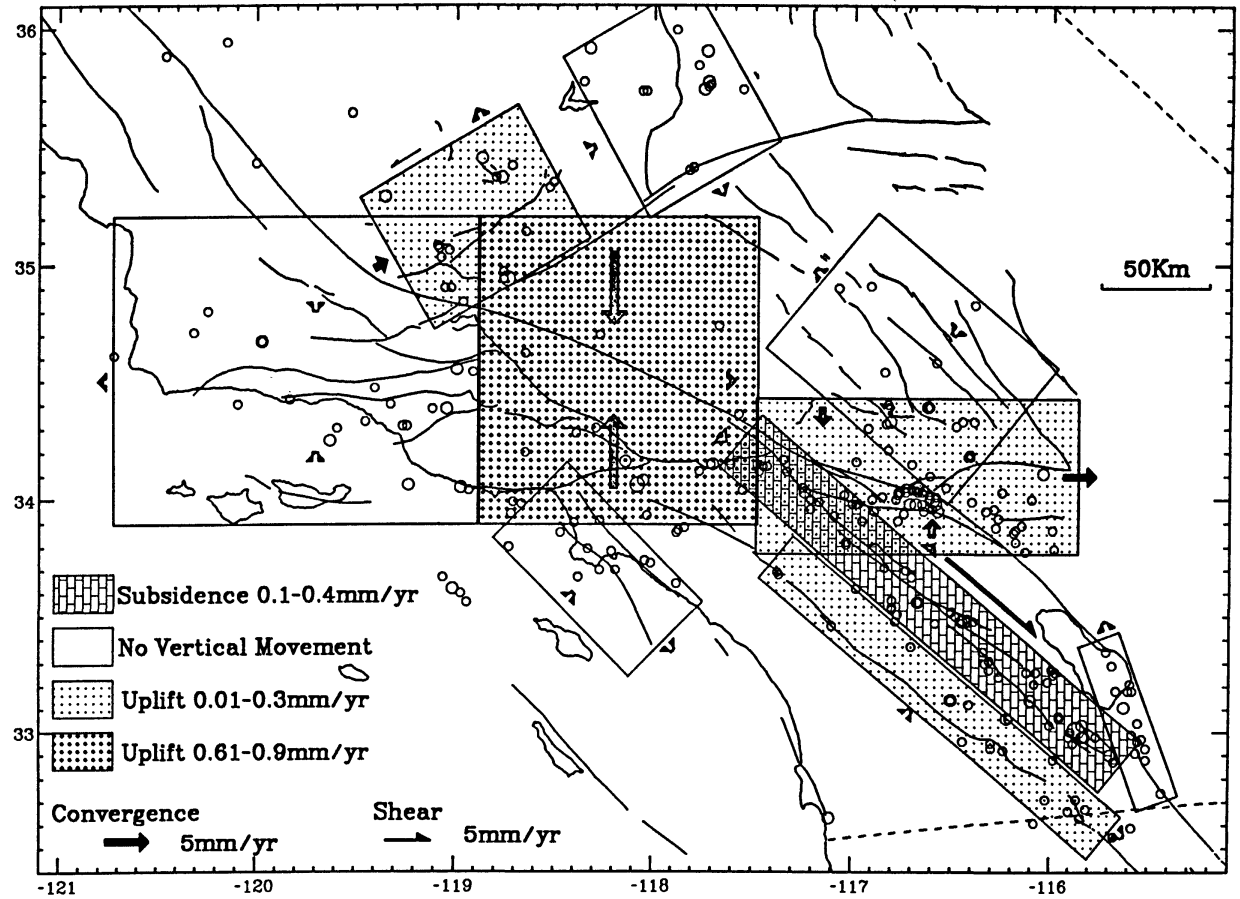

Figure 1. Seismic strain rates in southern California for the period 1981-1988.

Seismicity Patterns and the Stress State in Subduction-Type Seismogenic Zones

Grant Number 14-08-0001-G1810

Carl Kisslinger
Cooperative Institute for Research in Environmental Sciences
Campus Box 216, University of Colorado
Boulder, Colorado 80309-0216
(303) 492-6089

Research during May through September, 1990 was directed to the following efforts: (1) completion of the earthquake doublet analysis for detection of changes in material properties related to the preparation for and occurrence of a strong earthquake; (2) modeling the changes in the stress state in the main thrust zone due to the occurrence of moderate earthquakes and the relation of stress changes to subsequent seismicity; (3) analysis of an event that filled a gap in the distribution of aftershocks of the May 7, 1986 great earthquake; and (4) completion of the study of aftershock sequences in southern California.

Doublet Analysis

The project on the detection of velocity changes in the main thrust zone associated with the occurrence of a major earthquake by the analysis of earthquake doublets has been completed. Twelve doublets, selected to yield sampling of the material in the neighborhood of the rupture in the May 7, 1986 Andreanof Islands earthquake, were analyzed by the cross-spectral method. The individual events were relocated and members of a doublet were almost all within 100-200 meters of each other. Shear velocity changes with time along doublet-to-station paths were found to have a strong azimuthal variation, from 0.7% to the north-northwest of the source to no change at 50° to 60° east or west of north.

The velocity changes observed depended on both the segment of the thrust zone sampled and the time interval spanned by the doublet. The eastern segment (176.0° to 176.7° W) showed little to no change during 1981-1985, but a large negative change (-0.6%) during the interval spanning the 1986 mainshock. The central segment (176.7° to 177.2° W) showed a large negative change (-0.5%) during 1981-1983, little to no change during 1983-1985, and a large negative change (-0.7%) during the interval spanning the 1986 mainshock. The region to the west of 177.2° W, the western end of the 1986 break, showed only a slight positive change (0 to 0.2%) during 1985-1986. A summary of velocity changes for the interval spanning the 1986 mainshock is shown in Figure 1.

The observed velocity changes have been interpreted as due to anisotropic effects of changing stress associated with the preparation for the mainshock and its occurrence. During the time interval of pronounced quiescence, on which the intermediate-term prediction of the 1986 earthquake was based, the velocity changed little or not at all. This implies, in our interpretation, that the stresses in the active volume were changing little during the quiescence.

Publications. The results of this study are the basis of the Ph.D. dissertation: W.M. Kazi, *Velocity changes in the Central Aleutian Islands determined from the analysis of earthquake doublets using cross spectral analysis method,* University of Colorado, August, 1990. A summary was presented to the Spring, 1990, Annual meeting of the American Geophysical Union: W.M. Kazi and C. Kisslinger, "Doublet Analysis in Central Aleutian Subduction Zone," *EOS, 71:* 568, 1990.

Effect of earthquake occurrence on stress distribution in a subduction zone

The objective of this project is to determine whether the contribution to the stress field at specific points within the active seismic zone is large enough to be useful in predicting future earthquakes. The redistribution of stress due to event occurrence within the part of the Aleutian subduction zone monitored by the Central Aleutians Seismic Network is modeled. The changes due to the static stress pulse associated with larger earthquakes are calculated at selected points, based on a point source dislocation model. The relation of the computed stresses to the distribution of subsequent seismicity is then examined. Because the stress field is constructed from seismicity information only, significant contributions to the variability of stress due to other processes, especially aseismic deformations, may be missed.

The model assumes that all of the earthquakes occur on faults with the same orientation, with the same slip direction. This assumption is reasonable, at least for the larger events, for a seismic zone characterized by a dominant focal mechanism, such as the thrust mechanism in the main thrust zone of the study area.

In the work so far, the traction field due to larger events, magnitude 4 and above, was calculated. The seismicity distribution in the surrounding area was examined for evidence of an increase in activity where the traction component parallel to the slip vector was positive and a decrease where that component was negative. A "seismicity spatial distribution function", which represents quantitatively how the spatial distribution changed from before to after the larger earthquake, was defined. The computed traction field is cross-correlated with the seismicity spatial distribution function, to obtain a measure of the similarity of the change in seismicity and the traction distribution. The traction-seismicity measure is the difference between the traction field averaged over the events after the large earthquake and the same traction field averaged over the preceding events. A positive value indicates that the seismicity distribution resembles the traction field, because the seismicity increased in areas in which the traction was positive and/or decreased where it was negative.

First results are:

(1) An assumed mechanism for the larger earthquakes resulted in a fraction of large earthquakes with a positive measure that would be expected to occur in 4.6 of 100 random trials.

(2) The same assumed mechanism showed the strongest influence of the stress pulse on the seismicity closest to the larger earthquakes.

(3) When the mechanism was varied systematically through a range of orientations, one of the two geometries with the largest number of increased values of the traction-seismicity measure is low-angle thrust, typical of central Aleutian earthquakes.

(4) First motions predicted for the mechanism with the highest value of the traction-seismicity measure agreed with observed first motions to an extent that has only a 15% probability of arising by chance.

Although each of these points is only modestly significant, together they provide substantial support for the hypothesis that the occurrence of small earthquakes with the observed spatial distribution is being influenced by the stress pulses of larger events.

Earthquake of March 12,1990

An earthquake with m_b 6.1 occurred 30 km south-southwest of the epicenter of the May 7, 1986 mainshock epicenter, on March 12, 1990. This event is of special interest because its aftershock sequence filled in a "gap" in the aftershock zone of the 1986 earthquake where no aftershocks of that event occurred. One of the questions left by the investigation of the 1986 aftershocks has been whether the patches without aftershocks, and, in most cases little premainshock activity, were weak zones, in which no strain accumulates, or strong patches at which the stress pulse applied by the strong mainshock was not sufficient to trigger aftershocks.

The eastern half of the March 12 sequence, including the mainshock epicenter, overlapped a swarm of earthquakes that occurred on January 9-10, 1989 and partially filled in the "gap" left by the 1986 earthquake. A tight cluster of aftershocks in the western part of the zone filled a spot devoid of previous activity. Eight foreshocks preceded the March 12 event, starting with an m_b 4.8 on February 27. The three early foreshocks were close to each other, on the western edge of the gap; the last three were close to the mainshock, and their locations converged on the mainshock epicenter, eight days before.

The approximate stress drop for the mainshock was 3 bars, calculated from the seismic moment computed by Harvard and the rupture area estimated from the aftershock distribution. The p-value (Omori decay rate) of the aftershocks was 1.07 ± 0.06 (normal), with a b-value of 0.68 (low).

The tentative conclusion, pending completion of the study, is that this particular "gap" in the 1986 aftershocks marked a strong patch on the thrust zone, not a weak one. The stress pulse applied to this site by the 1986 mainshock was only slightly greater than the static shear strength, and four years passed before failure occurred to produce a late, strong aftershock. However, the stress drop in the event was quite normal and does not indicate unusually high stresses at this site.

Southern California Aftershocks

As part of the general study of aftershocks as indicators of fault zone properties and tectonic influences on earthquake generation, a study of 39 southern California aftershock sequences, 1933-1988, has been completed. The principal conclusions are:

(1) the mean p-value in southern California is 1.10, with many sequences on the principal faults exhibiting values close to this.

(2) Values of p significantly higher and lower than this mean value do occur, from 0.69 to 1.81.

(3) The p-values are not correlated with mainshock magnitude, the b-values of the sequences, or the difference between the magnitudes of the mainshock and the strongest aftershock. The data are insufficient to test a dependence of p on depth.

(4) Crustal temperature, as indicated by surface heat flow, is a dominant factor in controlling aftershock decay rate. High p-values (fast decay rate) occurs at places with high surface heat flow, and conversely. This correspondence, which was noted in a general way for Japan by Mogi in 1967, is the first physical cause found that puts order into the geographic distribution of p-values. The physical explanation is that high temperature causes shortened stress relaxation times in the fault zone materials, so the aftershocks die out more rapidly. Temperature is not the sole governing factor, and the properties of individual faults, such as heterogeneity, play a role.

This work was done in collaboration with L. M. Jones, U.S.G.S., Pasadena.

Presentation and Publication A paper summarizing this work was presented at the Western Pacific Geophysics Meeting, Kanazawa, Japan, August, 1990: C. Kisslinger and L. M. Jones, Properties of Aftershock Sequences in Southern California, *EOS, 71:* 895, 1990.

A version with more recent findings will be presented at the Fall Annual Meeting of the American Geophysical Union: C. Kisslinger and L. M. Jones, Aftershock Sequence Decay Rates in Southern California are Controlled by Crustal Temperature.

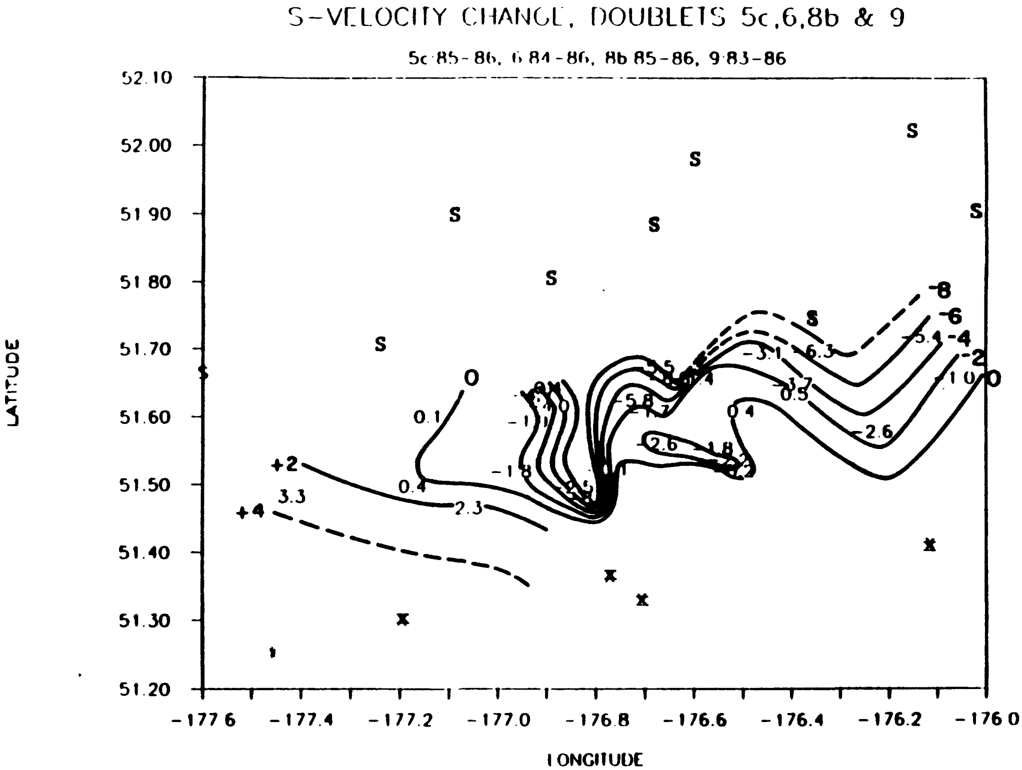

Figure 1. Spatial distribution of combined S-velocity change for selected doublets spanning the occurrence of the May 7, 1986 Andreanof Islands earthquake. The first event in each doublet occurred in 1983, 1984, or 1985, the second in 1986, after the major earthquake. X marks the sources; S, the stations used. The contour values are fractional change in S-wave velocity X 1000.

Slip History of San Andreas and Hayward faults

9910-04192

J. J. Lienkaemper
Branch of Engineering Seismology and Geology
U.S. Geological Survey
345 Middlefield Road, MS 977
Menlo Park, California 94025
(415) 329-5642

Investigations

Determine slip rates and earthquake recurrence times on San Andreas and Hayward faults. Compare rates of geologically determined surface slip to rates of historic creep and geodetically determined deep slip. Analyze effects of structural complexity and fault segmentation upon inferring recurrence from slip rate.

Results

1. Earlier Work. Along most of the Hayward fault, offset features yield creep rates of 3.5-6.5 mm/yr over decades, but a 4-km-long segment in south Fremont has crept at 8-10 mm/yr [*Lienkaemper and Borchardt, 1990; Lienkaemper et al., in review*]

USGS/CDMG trenching in central Fremont 1986-1987 [*Borchardt et al.*, in review] showed a Holocene slip rate of 5 mm/yr which may be too low because it excludes much of the 200-m-wide fault zone. Thus the 8 to 10 mm/yr creep rate in south Fremont may better represent the full long-term slip rate on the fault. Testing this possibility, in 1989 we trenched the Masonic site in Union City where the fault seems narrower.

2. Quaternary Slip Rates, Masonic Site. We identified six buried fan units offset by the fault, yielding slip of: C) 0-20 m, E) 46 ± 5 m, G) 66 ± 5 m, I) 88 ± 5 m, K) 131 ± 6 m, and M) 167 ± 6 m. Radiocarbon dates constrain slip rate well for two apexes: 8.0 ± 0.6 mm/yr (8.3 ka) on G, and ≤9.2 mm/yr (14.2 ka) on K. Dates on apex E bracket the rate between ≥7.4 and ≤9.9 mm/yr. The trench in 1990 should improve both stratigraphic control and accuracy of slip. We are now logging it. Thus far the slip on apex G is confirmed but work on the other units continues.

The Masonic slip rate is only 8 mm/yr, but such geologic rates are often minima because faults are wide compared to lengths of slip markers. Our goal at Masonic is to see if the 9 mm/yr creep in south Fremont reflects long-term slip rate for the entire Hayward fault. Masonic data support this conclusion, but we may still underestimate the full slip rate of the Hayward fault because the 9-mm/yr creep segment showed surface rupture in 1868.

Reports

Borchardt, G., J. J. Lienkaemper, and K. Budding, Holocene slip rate of the Hayward fault at Fremont, California: in review.

Lienkaemper, J. J., and G. Borchardt, Holocene slip rate, historic creep, and the potential for large earthquakes on the Hayward fault, California (abstr.): EOS, 1990.

Lienkaemper, J. J., G. Borchardt, and M. Lisowski, Historic creep rate and potential for seismic slip along the Hayward fault, northern California: submitted to JGR.

Earthquake Research in the Eastern Sierra Nevada Western Great Basin Region

Contract 14-08-0001-C1524, 1 April - 30 Sept 1990

W.A. Peppin
Seismological Laboratory
University of Nevada
Reno, NV 89557
(702) 784-4218

Investigations

This contract supports continued research focused on the eastern Sierra Nevada and western Great Basin region. We have investigated: (1) seismicity near the south moat of the caldera using an array of portable event recorders and waveform inversion of these for the seismic moment tensor, (2) pulse-width studies for estimates of stress drops, and (3) mantle anisotropy under the western U.S. Some of these results are described below.

Results

(1) Waveform Inversion

Steve Horton has produced a program for doing waveform inversion. The program is comparable to ones written by Brian Stump and Andres Mendez, but is made to take the general source input from program PROSE. As yet, the new code has not been applied to the waveform data collected in spring 1990 near the south moat of the Long Valley caldera pending work on the Loma Prieta earthquake. Application should begin within the next two months.

(2). Pulse-Width Studies

Smith and Priestley have presented estimates of stress drops as obtained by the pulse-width method of Frankel and Kanamori (1983). Their results are significant for use in arrays such as ours where most of the signals are uncalibrated vertical waveforms. Their results show low stress drop in the region believed to have ruptured in the main event of the 1984 Round Valley sequence and higher stresses around the edges of this zone. During this contract period, we are making a comparison between stress drops computed from the pulse-width method with those obtained by spectral analysis from the new three-component wideband (0.05 to 20 Hz) data at station WCK, located just west of the Round Valley aftershock zone in the mountain block south of Long Valley caldera, using events quite close to this site so as to minimize path effects. Data accumulated to date includes only a few events with magnitude greater than 3. There is considerable lack of correlation between pulse widths and the S-wave spectral corner frequencies at this site. However, WCK has a significant site response, even though it was chosen to be a "rock" recording site. The gain at WCK is now reduced so that larger events can be recorded at this site for such analysis.

(3). Anisotropy Studies.

We have recently (Silver and Savage, 1990) made a study of anisotropy in the mantle under western North America using teleseismic records from 27 stations in the Nevada - California region. S-wave splitting is azimuthally dependent along the San Andreas fault (based on 18 stations) and one station in the Sierran Block (CMB) shows the largest time separation yet seen on this continent (2.1 +- 0.2 seconds), with the fast direction N78W. The results are summarized in Figure 1.

In the northwest Basin and Range province, four stations give an average fast direction of anisotropy of N74E, while station ELK gave N78W, in general agreement with the present-day direction of extension. Note in the figure that fast directions in the southern Great Basin are markedly different from those in the northern Great Basin, indicating differences in the mantle to accompany differences in magnetic signature, gravity, and topography in the two regions.

these observations are interpreted in terms of strain-induced, lattice-preferred orientation of olivine in the upper mantle. For several nearby geologic regions, the anisotropic signatures are consistent within each region, but vary greatly between regions. Along the San Andreas fault, results are dependent upon the back-azimuth of the teleseismic event. These observations suggest that rapid changes occur in the perferred orientation of olivine in the upper mantle, and that the boundaries within the upper mantle correspond to geologic boundaries at the surface. The changes in olivine orientation probably represent changes in the present rheology or applied stress, or in the pre-existing fabric.

The large anisotropy under the Sierran block, if confirmed at more stations, implies an unusually deep-seated (> 200 km) anisotropic feature within ghe upper mantle. This E-W fast feature cannot be caused by past compressional episodes, which should yield N-S fast.

Written Submittals, This Contract Period

Johnson, P.A., dePolo, C.M. and W.A. Peppin, 1990. The M 4.6 Fish Lake Valley, Nevada earthquake of 15 January 1990 and the White Mountains Seismic Gap, Seis. Res. Lett., 61, 41.

Peppin, W.A., 1990. Real-time analog and digital data acquisition through CUSP, Seis. Res. Lett., 61 51.

Savage, M.K., Peppin, W.A. and U.R. Vetter, 1990. Shear-wave anisotropy and stress direction in and near Long Valley caldera, California, 1979-1988, Jour. Geophys. Res., 95,11,165-11,177.

Silver, P.G. and M.K. Savage, 1990. Mantle anisotropy beneath western North America from teleseismic shear-wave splitting, 1990 fall AGU meeting, submitted.

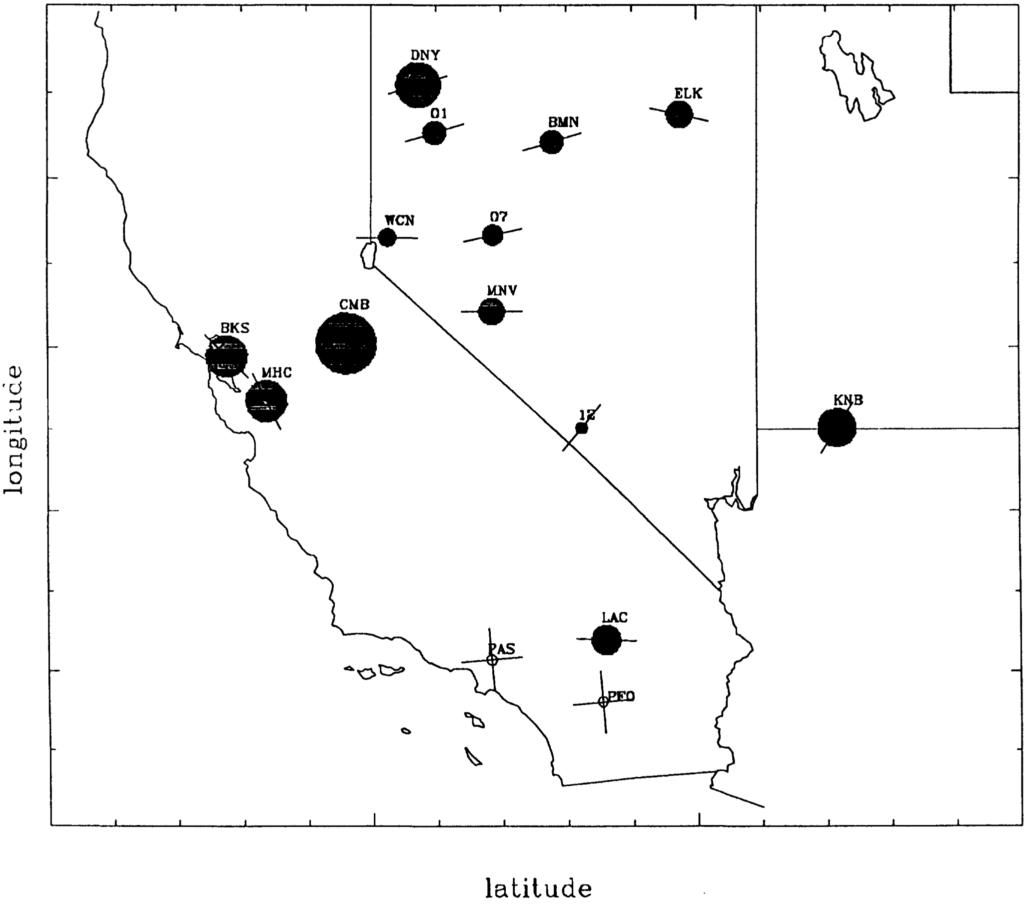

Figure 1. Shear-wave splitting measurements from the California - Nevada region. Lines designate average fast polarization direction Φ from the best measurements at each station, including only events with westerly back azimuths for the stations in California. Size of circles is proportional to Δt, the anisotropic S splitting time. Open symbols are those for which no anisotropy was measured using SKS phases: in these cases, the anisotropy may be either nonexistent, or the fast or slow direction may be parallel to the back azimuth of the event, designated by the sets of orthogonal lines.

Salton Trough Tectonics and Quaternary Faulting

9910-01292

Robert V. Sharp
Branch of Engineering Seismology and Geology
345 Middlefield Road, MS 977
Menlo Park, California 94025
(415) 329-5652

Investigations

1. Post-seismic near-field deformation, 1989 Loma Prieta earthquake.

2. Surface faulting associated with the M_s 7.8 Nueva Ecija earthquake, Philippines, 16 July 1990 (with C. Newhall, USGS; R. Punongbayan, and J. Umbal (Philippine Institute of Volcanology and Seismology).

Results

1. On the 226th post-earthquake day, the relative horizontal positions of the three reference marks were remeasured with a theodolite and EDM across the "Pink House" fractures, which displayed rather impressive coseismic left-lateral offset of Summit Road (on the mountain ridge SW of the San Andreas fault, SE of State Highway 17). The data indicate continuing small-scale, ENE-directed extension over a 270-m interval spanning the surface fracture. The 13 mm extension is interesting principally because its orientation is about normal to the fracture trace and about 70 degrees clockwise from the coseismic left-lateral displacement vector measured adjacent to Summit Road. Thus, the post-seismic changes are not only small in magnitude but also directed at a high angle to the coseismic slip at this site.

   One of the objectives of this monitoring was to see if post-seismic deformation might reveal clues to the origin of these fractures--that is, whether they were primary tectonic breaks. The post-seismic data do have implications regarding this question, but they take a curious form. Three kinds of forces may be relevant to the creation of the coseismic fractures along Summit Road--*i.e.*, tectonic forces due to the tractions of the underlying coseismic displacement, transient inertial forces due to the strong ground shaking, and the gravitational force that acts continuously. At the time of the mainshock, all of these forces are present, but in post-seismic time only residual tectonic forces and gravity exist. If the coseismic fracture displacement were gravitationally driven, why is the post-seismic deformation so unlike it, particularly in the direction of motion? This dissimilarity suggests that the gravitational force played a minor role in producing the coseismic slip there. If the crack were a primary tectonic feature, then the observed post-seismic deformation is unlike continuing afterslip that has been described in conjunction with other surface faulting events. By discounting the likelihood of dominance of both tectonic and gravitational forces, inertial force due to strong ground motion remains as the prime suspect. It is unfortunate that there were no strong motion recordings made along this mountain ridge.

The ratio of the left-lateral to dipslip components of coseismic movement on the "Pink House" fracture, about 1.24, is exceedingly difficult to explain by a recently proposed mechanism of conversion of pure bedding-plane dipslip upward to oblique slip on a clockwise rotated fracture. There are severe geometric constraints that allow for a small amount of this kind of conversion, but to obtain a dominant strike-slip component would require rotations so large that they are inconsistent with the orientations of bedding planes that have been recorded along the mountain ridge.

2. Left-lateral surface rupture broke along parts of both the northwest-trending Philippine fault and its northward splay in the Cordillera Central, the Digdig fault, over a distance exceeding 110 km. The main shock location, near the Philippine fault at Bongabon about 30 km from the southeast end of the surface rupture, implies that most of the rupture spread unilaterally toward the northwest. Not only did aftershocks extend northward more than 100 km beyond the observed length of the surface breaks, but also their complex pattern suggests the possibility that additional faults may have ruptured at the surface. Although no breaks were observed along the Philippine fault strand where it bounds the Cordillera Central to the west of the Digdig branch, aftershocks occurred near this trend as far as the west coast near Lingayen Gulf.

   The maximum horizontal component of surface slip, more than 6 m, was observed on the Digdig fault near Capintalan, about 160 km north of Manila, at the northern extremity of the surface investigation. Even larger displacements are possible in the as-yet-unchecked northern sections of the fault. Although this maximum is one of the largest strike-slip surface movements on the earth in this century, the 3-4 m average slip is expectable for earthquakes of this magnitude. The largest displacement found on the Philippine fault, near Kamuning and the mainshock epicenter, was about 5. m. Vertical components of slip were consistently subordinate but reversing in sense at several places along the rupture; the largest measured vertical offsets were about 2 m.

   Post-seismic creep was monitored at Rizal near the midpoint of known surface rupture; between the 13th and 20th post-earthquake days creep was negligible at that site. A possible 2 cm lateral displacement occurred by the 21st day, perhaps at the time of a strong nearby aftershock.

Reports

Sharp, Robert V., and Umbal, J. 1990, Surface displacement on the Philippine-Digdig fault associated with the M_s 7.8 Nueva Ecija earthquake of 16 July 1990: Eos (Abstract, in press).

CAPTION FOR FIGURE 1 -- 9910-01292

Map of surface faulting associated with the 1990 Nueva Ecija earthquake. Heavy lines indicate left-lateral fault ruptures that were observed and measured on the ground. Dotted lines represent other fault traces within the region of aftershock activity; surface displacement on these is either absent or unknown (locations from geologic map of Philippines, 1963 edition of PBM). Heavy dots are NEIC-located epicenters of aftershocks ($4.4 \leq M \leq 6.5$) within 27 days of the mainshock (circled dot). Open circle near Bongabon shows approximate epicenter of aftershock associated with small creep displacement observed at Rizal. All epicentral locations are approximate. Labels PFZ and DF indicate Philippine fault zone and Digdig fault, respectively.

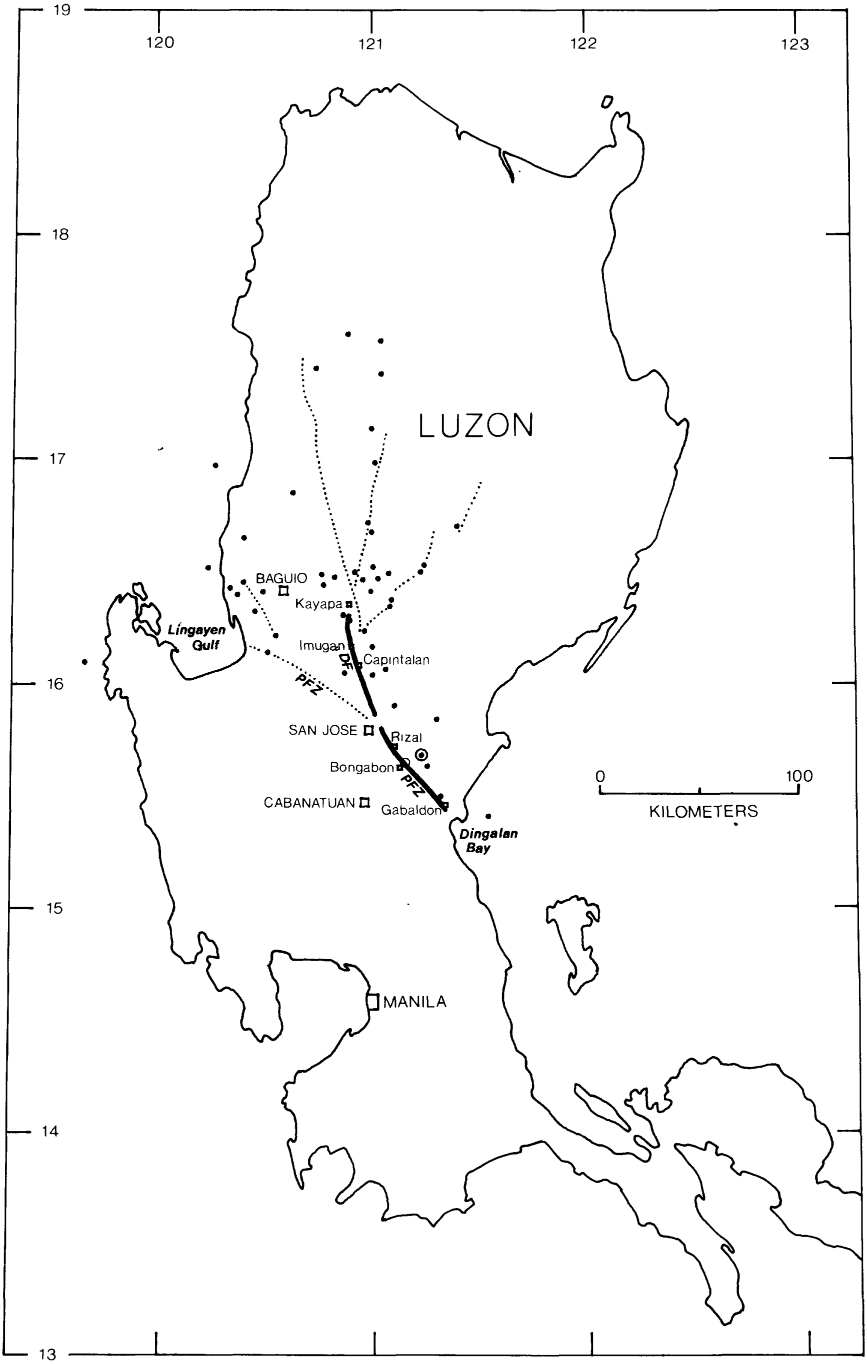
19
18
17
16
15
14
13
120
121
122
123
LUZON
BAGUIO
Kayapa
Lingayen Gulf
Imugan
DF
Capintalan
PFZ
SAN JOSE
Rizal
Bongabon
PFZ
CABANATUAN
Gabaldon
Dingalan Bay
0
100
KILOMETERS
MANILA

Figure 1

Seismotectonic Framework and Earthquake Source Characterization (FY90) Wasatch Front, Utah, and Adjacent Intermountain Seismic Belt

14-08-0001-G1762

R.B. Smith, W.J Arabasz, and J.C. Pechmann*
Department of Geology and Geophysics
University of Utah
Salt Lake City, Utah 84112-1183
(801) 581-6274

Investigations: April 1, 1990 - September 30, 1990

1. Magnitudes of prehistoric Intermountain seismic belt earthquakes from surface rupture lengths and displacements.
2. Paleoseismicity and contemporary deformation of the Teton fault, Wyoming.
3. Rate of decay of aftershocks in the Utah region.
4. Estimation of seismic moments of Intermountain seismic belt earthquakes from Wood-Anderson seismograms.

Results

1. We have calculated surface wave magnitudes for the most recent prehistoric scarp-forming earthquakes associated with Quaternary normal faults of the Intermountain seismic belt (ISB). The magnitude estimates are based on unweighted least squares linear regressions of M_S on both surface rupture lengths and maximum surface displacements of instrumentally-recorded normal-faulting events in intraplate extensional regimes of the western U.S. and other parts of the world. The earthquakes used in the regressions (16 total) have a magnitude range of $6.4 \leq M_S \leq 7.6$ and are limited to those with the following characteristics: 1) either purely normal or oblique-normal surface offset, 2) measured scarp heights and rupture lengths, and 3) calculated surface wave magnitudes. These data yield the following relations:

$$M_S = 0.85 \text{ Log } L + 5.7$$

$$M_S = 0.66 \text{ Log } D + 6.8$$

where L = length (km) and D = maximum measured surface displacement (m). Standard deviations and correlation coefficients are ± 0.24 M_S units and 0.76, respectively, for the first equation and ± 0.22 and 0.82 for the second.

---

*J.O.D. Byrd, C. Li, D.B. Mason, and D. Wu also contributed significantly to the work reported here.

These scaling relations were applied to a new compilation of fault parameters and ages determined by trenching and morphologic studies of 25 of the most prominent Late Quaternary faults in the ISB. Many of the faults that have been quiescent during historical time show notable Quaternary activity. Maximum magnitudes (M_S) range from 6.3 to 7.3 along the primary seismogenic structures: Wasatch, Lost River, Lemhi, Beaverhead, Madison, Teton, Star Valley, East Cache, and Bear Lake faults. The ~370-km-long Wasatch fault dominates the ISB paleoseismicity with magnitudes consistently greater than 6.5 and averaging 6.9 for its 12 mapped segments.

2. The Teton fault extends for ~55 km along the east side of the Teton Range at the northeastern edge of the Basin-Range province. In a project funded jointly by the National Park Service and the U.S. Geological Survey, we have identified two to three Quaternary segments for the fault, 13 to 42 km in length, that are marked by 3 to 50 m high fault scarps in Pinedale (~14,000 yr) moraines and younger fluvial/alluvial deposits. In contrast, the Teton fault occupies a prominent gap at the M 3+ level in the historical seismicity of the Intermountain seismic belt. A trench across the 20-km-long southern segment exposed a 4.1 m normal fault displacement on a fault dipping 85° E that is associated with one, and possibly two, prehistoric slip events. Conventional radiocarbon dates averaged from two samples recovered from a paleosol indicate an age of faulting of 7,175 ± 100 radiocarbon years. If a younger event has contributed to the total offset, the displacements associated with the 7,175 yrs b.p. and younger events are on the order of 1.3 m and 2.8 m, respectively. Comparison of the 4.1 m offset with offsets produced by historical normal faulting earthquakes suggests that it was the product of a single $M_S = 7.2 \pm 0.3$ event, or possibly two $M_S = 7.0 \pm 0.3$ events. For the single-event scenario, comparison with the historical normal fault data suggests that the entire length of the Teton fault would have ruptured. In the two-event case, the southern segment and all, or part, of the middle segment of the fault would have ruptured. Extrapolation of the "single event" 4.1 m offset onto the 13 m high, multiple event scarps in the vicinity of the trench site suggests that the Teton fault is characterized by post glacial slip-rates of 0.5 mm/yr, assuming a conservative estimate of 30,000 yr for glacial cessation, or 1.6 mm/yr using the commonly accepted 14,000 yr Pinedale age.

In a cooperative project with Art Sylvester of the University of California, Santa Barbara, we have conducted two leveling surveys of an east-west profile across the middle segment of the Teton fault. The 22-km-long leveling line was established in 1988 to first order surveying standards. The results of the initial 1989 re-observation of this line indicate that the footwall block, the Teton Range, *subsided* up to 7.8 mm ± 0.7 mm relative to the valley floor over the one-year period. On geological grounds, we expected the mountain block to rise rather than subside. This observation of mountain block subsidence is considered very anomalous and reflects unknown processes that may be related to the current quiescence of the Teton fault. There are several possible explanations for this unusual aseismic behavior, such as interseismic energy accumulation, seismic energy release in the Gros Ventre block to the east that is locking the Teton fault, or footwall subsidence due to lateral deviatoric compression on a uniform upper-crustal block, including the fault. Nonetheless, the measured deformation occurred as *aseismic creep*, i.e., without accompanying earthquakes. These observations notably represent the first well-documented evidence of aseismic creep across a major normal fault in the western U.S.

3. As a follow-up to observations by Veneziano and others (1987; *Eos* 68, 1368-69) of suppressed earthquake clustering in the vicinity of the Wasatch fault, compared to neighboring regions, we have undertaken a systematic study of aftershocks in the Utah region. In particular, we are interested in the variability of the parameters K, c, and p in the modified Omori law, which describes the time-dependent decay in numbers of aftershocks: $N(t) = K / (t+c)^{p}$, where t is time after the main shock and N(t) is the number of events per unit time. For preliminary calibration, well-recorded earthquake sequences associated with seven main shocks, $4.7 \leq M_L \leq 6.0$, 1975-1989, were analyzed in detail. The Omori decay parameter, p, ranges from 0.7 to 1.2. For one relatively deep sequence, 20-25 km deep in Precambrian basement, $p = 0.95 \pm 0.12$, close to the mean value for the seven sequences. Faced with the persistent obstacle of having many individual sequences with too few events for appropriate statistical processing, we have begun collaborative work with P. A. Reasenberg, USGS, to apply his composite-cluster methodology (Reasenberg, 1990; *Seism. Res. Lett. 61*, 40). We are proceeding to analyze and group secondary events in our catalog in such a way that the Omori parameters can be compared to results in California—as well as allow testing for space-time differences within the Utah region. For the latter purpose, original seismograms have been extensively re-examined to document the time-size distribution of aftershocks associated with seven main shocks, $4.0 \leq M_L \leq 5.7$, that occurred in the Wasatch Front region during 1962-1972, before the start of modern network monitoring in 1974.

4. We are analyzing data from 58 aftershocks of the 1983 Borah Peak, Idaho, earthquake to test and calibrate for the Intermountain seismic belt a simplified method for estimating seismic moments from Wood-Anderson seismograms. The method is similar to that proposed by Bolt and Herraiz (1983; *Bull. Seism. Soc. Am. 73*, 735-748) and assumes a relation of the following form:

$$\log M_O = a + b \times \log (C \times D \times R^P)$$

where R is the hypocentral distance of the station, C is the maximum peak-to-peak amplitude, D is the duration between the S arrival and the onset with amplitude C/d, and a, b, p, and d are constants to be determined empirically. Our measurements of C and D come primarily from synthetic Wood-Anderson seismograms made from horizontal-component digital recordings obtained by the USGS at 12 stations located at epicentral distances of less than 50 km. Additional measurements come from analog Wood-Anderson seismographs located in Utah at epicentral distances of 400 to 480 km. Seismic moments for the 58 calibration events have been previously determined from pulse areas of SH-waves recorded on the USGS digital stations or from long-period data recorded at regional and teleseismic distances. To complete this investigation, we are currently making direct comparisons of SH-wave pulse areas and the quantity $C \times D \times R^P$ to test the theoretical basis of the Bolt and Herraiz technique, and are evaluating whether or not this technique provides better estimates of M_O than the empirical M_O - M_L relation determined from the same data.

Reports and Publications

Arabasz, W.J. and G. Atwood (1990). Seismic instrumentation—A five-element, $3 M state initiative for Utah's earthquake program, *Seism. Res. Lett. 61*, 37.

Byrd, J.O.D. and R.B. Smith (1990). Dating recent faulting and estimates of slip rates for the southern segment of the Teton fault, Wyoming, *Geol. Soc. Am. Abstracts with Programs 22 [6]*, 4-5.

Johnston, A., W. Arabasz, G. Bollinger, J. Filson, R. Herrmann, L. Jones, and W. Benson (1990). The future of seismic networks in the United States, *Seism. Res. Lett. 61*, 36.

Pechmann, J.C., S.J. Nava, and W.J. Arabasz (1990). Left-lateral shear beneath the NW Colorado Plateau: The 1988 San Rafael swell and 1989 So. Wasatch Plateau earthquakes, *Seism. Res. Lett. 61*, 44.

Pechmann, J.C. and B.S. Thorbjarnardottir (1990). Waveform analysis of two preshock-main shock-aftershock sequences in Utah, *Bull. Seism. Soc. Am. 80*, 519-550.

Smith, R.B., J.O.D. Byrd, and D.D. Susong (1990). Field trip no. 6: Neotectonics and structural evolution of the Teton fault, in *Geologic Field Tours of Western Wyoming and Parts of Adjacent Idaho, Montana, and Utah*, S. Roberts, Editor, *Geol. Surv. Wyoming Public Info. Circ. 29*, 126-138.

Smith, R.B., J.O.D. Byrd, A.G. Sylvester, and D.D. Susong (1990). Neotectonics and earthquake hazards of the Teton fault, *Geol. Soc. Am. Abstracts with Programs 22 [6]*, 45.

Sylvester, A.G., J.O.D. Byrd, and R.B. Smith (1990). Aseismic (?) reverse creep across the Teton fault, Wyoming, with implications for interseismic strain, *Geol. Soc. Am. Abstracts with Programs 22 [7]*, 88.

Identification of Active Faults and Source Characteristics in the New Madrid Seismic Zone

14-08-0001-G1870

William V. Stauder
Department of Earth and Atmospheric Sciences
Saint Louis University
3507 Laclede
St. Louis, MO 63103
(314) 658-3131

Investigations

The purpose of this research is to investigate the spatial distribution of earthquake foci a) in the middle or off-set portion of the New Madrid Seismic Zone (NMSZ) between New Madrid, Missouri and Gratio, Tennessee, and b) along the southern portion of the zone, especially in the neighborhood of the Blytheville Arch. The hypothesis is that the spatial distribution, together with focal mechanisms, will identify the orientation of fault surfaces and the motion on the faults in these ambiguous portions of the zone.

Hypocenters determined by SLU in the NMSZ using data from seven or more stations from 1979 to the present form the basic data set. There are more than 1138 such events (see Figure 1).

Advantage is taken of the presence of elements of the 40-station, three-component PANDA array deployed in the central part of the NMSZ during the last quarter of 1989 through the first two quarters of 1990. Digital trace and phase data, which were picked by the Center for Earthquake Research and Information (CERI) have been received for the first seven array tapes covering the period 18 November 1989 through 13 July 1990. There are 94 events recorded by both PANDA and SLU networks, out of a total of 107 events recorded for the entire period by SLU. During the next report period, these events will be used as set of master events in the relocation of all SLU network events in the NMSZ noted above.

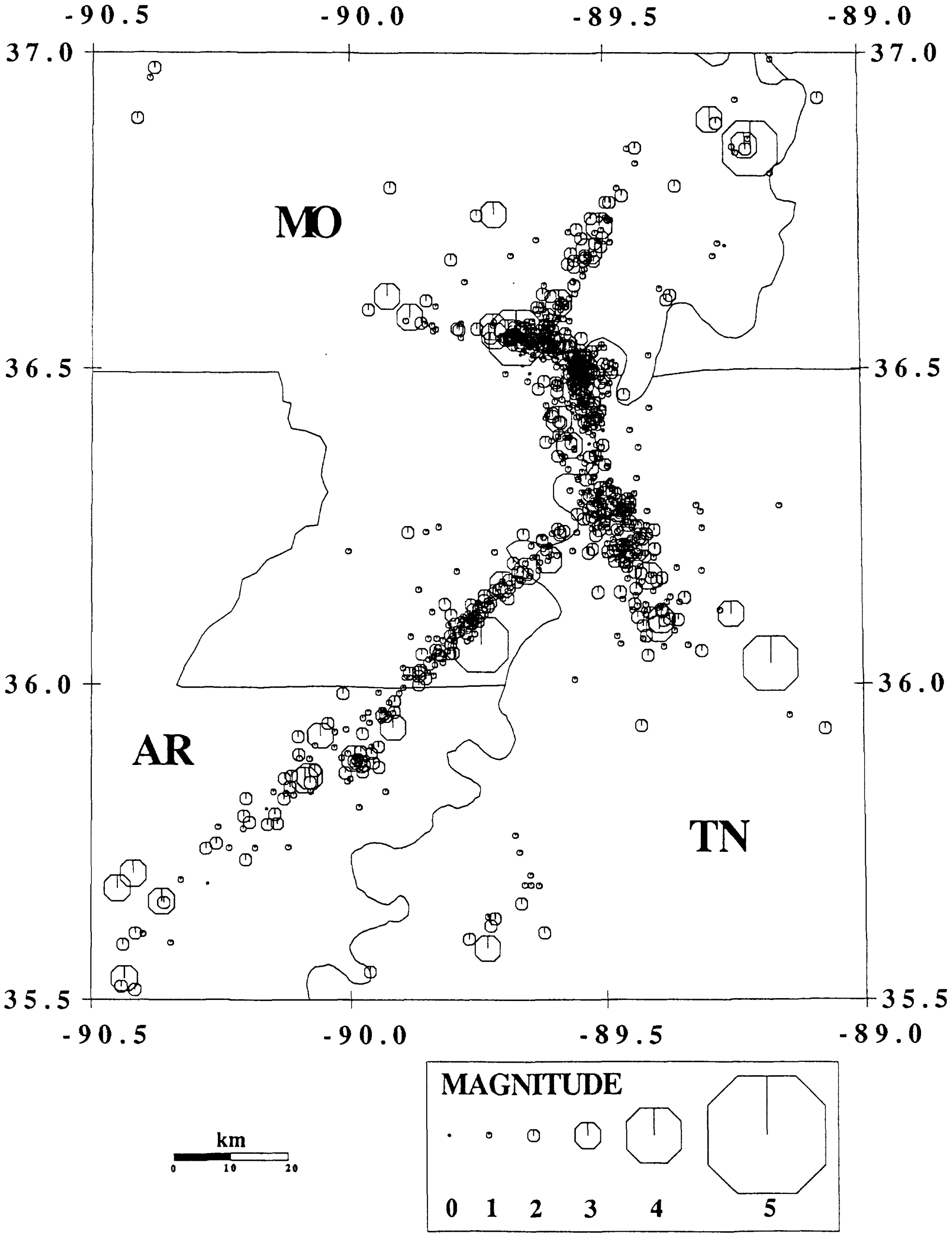

FIGURE 1 -- All events 1 January 1979 through 31 March 1990 (135 months) recorded by SLU network with seven or more stations (1138 events). These events will all be reprocessed in a JVHD relocation procedure.

Use of Short-Period Waveforms in Seismotectonic Studies

#14-08-0001-G1795

Ta-liang Teng

Center of Earth Sciences
University of Southern California
Los Angeles, CA 90089-0740
(213) 740-5838

INVESTIGATIONS

This research makes use of the waveforms and spectrums of the short-period seismic data to investigate properties on wave propagation beyond the conventional travel-time and polarity studies. Through particle motion analysis using on-scale waveform data, we investigate the crustal anisotropy. Identifying the lower crust reflections and converted waves, we study the structure of the Los Angeles Basin and its surrounding basement rocks. An analysis of the spectrums provides information on attenuation and source properties.

RESULTS

Seven seismic stations in the Los Angeles basin are equipped with Optimum Telemetry System(OTS) which is a front-end microprocessor-controlled gain-ranging device that upgrades the recording of the conventional telemetrered seismic signals to achieve a 120 dB effective dynamic range. With OTS operating in the past several years, we have obtained a large volume of on-scale, 3-component recordings of local earthquakes. We have completed the scanning and sorting of all digital waveforms recorded on the OTS in the Los Angeles Basin during the past two years. Amplitude calibrations are done based on the decoded gain codes associated with the OTS data. The results are well calibrated, on-scale, 3-component waveforms. An examination on these waveforms show that many arrivals between P and S, as well as those clear after S cannot be explained by normal coda decay as a result of the scattering process. We have constructed seismic sections using data from many earthquakes recorded at a single station. From these seismic sections we try to identify arrivals that can be modelled as reflections or converted waves using a ray-tracing technique. Many phases arrived later than the P and S are identified and are used to study the crustal reflectors and boundaries such as the basement boundary, the lower crust reflector, and the Moho. At the same time, waveform analysis is applied to isolated body wave signals for information concerning the source characteristics and the Q structure of the southern California crust.

REFERENCES

Li, S.B. and T.L. Teng, Dependence of Richter magnitude scale on site conditions and local geology, Fall AGU meeting, 1990.

Teng, T.L. and J. Wang, Analysis of short-period waveform in the Los Angeles basin, Fall AGU meeting, 1990.

Su, F., S. Koyanagi, Y. Zeng, K. Mayeda, T.L. Teng, and K. Aki, A recursive stochastic inversion of site effect using coda waves, Fall AGU meeting, 1990.

Hisada, Y, S. Yamamoto, S. Tani, and T.L. Teng, Broadband seismograms on the Los Angeles Basin during the 1990 Upland earthquake, Japan seismological Society Fall meeting, 1990.

Late Quaternary Recurrence Intervals on the Owens Valley Fault Zone, Lone Pine, California

14-08-0001-G1783

Paul Bierman and Alan Gillespie
Department of Geological Sciences, Mail Stop AJ-20
Seattle, WA 98195

Objectives: Our investigation has two main objectives: to constrain more tightly current estimates of recurrence intervals and fault slip rates for the Lone Pine fault, a subsidiary strand of the Owens Valley Fault Zone and to evaluate rigorously the accuracy, precision, and utility of rock varnish dating methods.

Results: Since the preparation of the last report we have done the following:

Continued processing thermoluminesence samples with Dr. G. Berger, Western Washington University. We are dating 12 samples from the two trenches opened across the colluvial wedge shed from the Lone Pine fault. We anticipate that initial age data will be available in early 1991.

Collected 44 varnished cores from a granodiorite boulder sequentially exposed on the fault scarp at Lone Pine. We have analyzed varnish on the cores using an SEM and are presently reducing the data. Data gathered from this boulder will constrain the spatial variance of rock varnish chemistry and indicate whether cation ratio dating will be useful for constraining faulting rates at Lone Pine.

Prepared and analyzed three synthetic rock varnish standards. We have conducted a blind interlaboratory comparison which suggests that many if not all previously published cation ratios may be inaccurate. We are using these standards to control the quality of our SEM analyses.

Collected rock varnish samples from features of known age for the purpose of testing sample preparation methods for ^{14}C analyses of rock varnish.

Dissemination of Results: We have presented and will continue to present our data and findings at meeting of professional societies and in refereed publications. We are presenting three poster sessions at the Geological Society of America, Penrose conference on Methods of Exposure Age Determination, October 1990.

Publications Resulting from NEHRP funding:

Bierman, P. and Gillespie, A., *in review*, Range Fires: A significant factor in exposure-age determination and geomorphic surface evolution: *Geology*.

Bierman, P. and Kuehner, A., *in revision*, Analysis of synthetic rock varnish standards by SEM/EDS, SEM/WDS, XRF, and ICP: Implications for the accurate measurement of Ba, Ti, and rock varnish cation ratios: *Scanning Electron Microscopy International*, accepted for publication pending revision.

Bierman, P. and Gillespie, A., *in press*, Accuracy of rock varnish chemical analyses: implications for cation ratio dating: *Geology*.

Bierman, P., Kuehner, S., and Gillespie, A., *in press*, Precision of rock varnish chemical analyses and cation-ratio ages: *Geology*.

Bierman, P. and Gillespie, A., 1990, Range Fire: A dramatic and significant factor in the dating and evolution of Geomorphic Surfaces: Geological Society of America Abstracts with Programs.

Bierman, P. and Gillespie, A., 1990, An independent evaluation of the potential precision and accuracy of rock-varnish cation ratio dates:Geological Society of America Abstracts with Programs.

Bierman, P. and Gillespie, A., 1990, Varnish cation-ratio ages - How precise can they be? Geological Society of America Abstracts with Programs, Vol. 22, No. 3, p. A8.

Bierman, P. and Gillespie, A., 1989, Rock varnish, alluvial fans,and tectonism in the southern Owens Valley, CA: Geological Society of America Abstracts with Programs, Vol. 21, No. 6, p. A343.

Surface Faulting Studies

9910-02677

M.G.Bonilla
Branch of Engineering Seismology and Geology
U.S. Geological Survey
345 Middlefield Road, MS 977
Menlo Park, CA 94025
(415) 329-5615

Investigations

1. Geology of Marina District
2. Visibility of faults cut by exploratory trenches

Results

1. The geology of the Marina District of San Francisco is under study to better understand the pattern of earthquake damage there. Maps dating back to 1851, archival materials including photographs, published reports, and logs of borings made from 1912 to 1990 were used to decipher the geology, including the artificial fills. Preliminary results given in an open-file report are being revised on the basis of newly-compiled borings, old maps, and old photographs.
2. Revisions were made on a manuscript on factors affecting the visibililty of faults cut by exploratory trenches.

Reports

Bonilla, M. G., 1990, Natural and artificial deposits in the Marina District, *in* Effects of the Loma Prieta earthquake on the Marina District San Francisco, California: U. S. Geological Survey Open-File Report 90-253, p. A-1-A-24.

Bennett, M.J., Bonilla, M.G., and Holzer, T.L., in press, Liquefaction in the Marina District, San Francisco, California, during the Loma Prieta earthquake [abs.]: Geological Society of America Abstracts with Programs

Bonilla, M. G., and Lienkaemper, J. J., in press, Factors affecting the recognition of faults exposed in exploratory trenches: U. S. Geological Survey Bulletin 1947.

Bonilla, M. G., in press, Historical faulting, *in* Moore, G.W., Chairman, Geodynamic Map of the Circum-Pacific Region, Arctic Sheet: U.S. Geological Survey Map CP-38, scale 1:10,000,000.

10/90

Northern San Andreas Fault System

9910-03831

Robert D. Brown
Branch of Engineering Seismology and Geology
U.S. Geological Survey
345 Middlefield Road, MS 977
Menlo Park, California 94025
(415) 329-5620

Investigations

1. Research and review of work by others on the tectonic setting and earthquake potential of Diablo Canyon power plant (DCPP), near San Luis Obispo, California. Activities are in an advisory capacity to the Nuclear Regulatory Commission (NRC) staff and are chiefly to review and evaluate data and interpretations obtained by Pacific Gas and Electric Company (PG&E) through its long-term seismic program.

2. Advisory activities for Bay Area Regional Earthquake Preparedness Project (BAREPP) and San Francisco Bay Conservation and Development Commission (BCDC), both of which are state agencies.

3. Synthesis studies of the geology, seismology, and tectonics of the San Andreas fault system, especially in northern California.

Results

1. Completed review of geologic data and interpretations regarding the tectonic setting and earthquake potential near Diablo Canyon power plant. Prepared a draft report summarizing USGS review comments regarding PG&E's interpretation of earthquake hazard at Diablo Canyon, circulated the draft internally for peer comments, and began revision for final document.

2. Completed final reviews of an assembled mock-up of Professional Paper 1515 on the San Andreas fault system, which now awaits printing.

3. Prepared draft chapter, with R. E. Wallace and D. H. Hill, on the San Andreas fault system for a book, *The Geological Character of Active Fault Zones*, edited by R. Bucknam and P. Hancock, and sponsored by the International Geological Correlation Program.

Reports

1. Brown, Robert D., 1990, Geology and land use: Networks, earthquake preparedness news, Bay Area Regional Earthquake Preparedness Project, v. 5, no. 2, p. 11.

Seismic Hazards of the Hilo 7 1/2' Quadrangle, Hawaii

9950-02430

Jane M. Buchanan-Banks
Branch of Geologic Risk Assessment
U.S. Geological Survey
David A. Johnston Cascades Volcano Observatory
5400 MacArthur Boulevard
Vancouver, Washington 98661
(206) 696-7996

Investigations

Revised manuscript on the geology of the Hilo 7 1/2' Quadrangle, Island of Hawaii, based on BWTR review.

Results

Manuscript returned from BWTR in April and next few months were devoted to incorporating suggested changes into text and description of map units; tables required extensive revision to make them more readable and improve clarity of depiction of sampling sites on map sheet. Revisions completed and manuscript forwarded to BWTR at end of September for final check on consistency before it receives Director's approval.

Tables of chemical analyses for open-file report on the chemistry of the Hilo quadrangle rock samples were also revised as a result of this review.

Stream Responses to Uplift and Climatic Change, North Canterbury, New Zealand

NSF-USGS Joint Project
Progress Report October 1990

William B. Bull
Department of Geosciences
University of Arizona
Tucson, Arizona 85721
(602) 621-6024

INVESTIGATIONS

Introduction and Objectives

The Charwell River in the northeastern part of the South Island of New Zealand is a superb fluvial system in which to investigate responses of streams to vertical and horizontal earth deformation and climatic changes during the late Quaternary. The moderately small watershed is underlain by fractured greywacke sandstone and extends to the crest of the Seaward Kaikoura Range. Streamflow from the 30 km^2 main branch joins flow from the 10 km^2 right branch a short distance downstream from the highly active Hope fault. My work has been concentrated in the piedmont reach for the purposes of 1) describing stratigraphy, sedimentology, and soil profiles of valley fills, 2) dating aggradation events and flights of degradation terraces, and 3) estimating late Quaternary displacement rates along the faults of the Hope fault system. These data will form the basis for understanding the tectonic and geomorphic responses of streams in this humid region to climatic changes. The Charwell River site has proved to be an excellent model for differentiating between tectonic, climatic, and complex response stream terraces (Bull, 1990, 1991), and has the potential for being one of the world's best dated flights of stream terraces. Dating is proceeding in several stages. This report summarizes the results of radiocarbon dating and provides brief descriptions of dated stratigraphic units.

Tectonic Setting

The 220 km long Hope fault is the most active splay of the Alpine shear system in the Marlborough region. The fault bounds the south side of the Seaward Kaikoura Range and thus separates the watershed and piedmont reaches of the Charwell River. It strikes at about 073° across the South Island from the Alpine fault on the northwest side of the Southern Alps to the southwestern end of the Hikurangi Trench. It is part of a diffuse transpressional transform boundary between the Australian and Pacific plates that links the Tonga-Kermadec, Hikurangi, and Puysegur trenches. Oblique plate convergence is large (about 47 m/ky at 264° ± 2°) for the Hope fault with a compressional component of as much as 22 m/ky that tends to raise the Southern Alps at 5-8 m/ky and thicken their crustal root (Walcott, 1984; Allis, 1981; Bull and Cooper, 1986). My work (Bull, in preparation, a, b, c) shows that this fault has a slip rate that is similar to that of the San Andreas fault of California (33 ±3 m/ky during the past 40 ka) but also has a large component of vertical movement (2 to 6 m/ky [Bull, 1985; Bull and Cooper, 1986]).

A tectonic setting of rapid horizontal and vertical displacement is largely responsible for the Charwell River being a most unusual and valuable study area (Bull and Knuepfer, 1987). The watershed reach has been shifted progressively to the northeast relative to the piedmont reach. Former piedmont valleys of the Charwell River are preserved because of the rapid right-lateral tectonic translocation. Each valley records a major shift in stream-channel position to the east. The river is confined in a 50-65 m deep valley during times of maximum degradation such as the present. Avulsion cannot occur during times of stream-channel entrenchment, but continued lateral movements between the drainage basin and piedmont reaches set the stage for abrupt changes in channel position. Optimal conditions for the piedmont reach to adjust its position relative to the tectonically translocated drainage basin occurred during times of maximum aggradation when streamflows issuing from the Seaward Kaikoura Range spread out on unentrenched alluvial fans, which have completely filled piedmont valleys. At these times streams in the piedmont reach are free to seek new courses farther to the east in order to correct for the amount of tectonic translocation that had occurred since the preceding avulsion. The subsequent episode of degradation creates a new piedmont valley that tends to be separated from the prior valley by a distance equal to the amount of tectonic offset between the watershed and piedmont reaches since the preceding time of piedmont valley formation. Along most streams, aggradation and degradation episodes generally are stacked on top of each other in a bewildering complex of partial stratigraphic and geomorphic records. The tectonic setting of the Charwell River tends to preserve complete records of both aggradation and degradation in tectonically translocated valleys through which the river no longer flows. The Charwell River flows due south from the Seaward Kaikoura Range and then turns to the southwest, cutting across and exposing the stratigraphic record contained in its ancestral valleys, which have been tectonically translocated as much as 3-4 km. This tectonic setting is ideal for geomorphic, stratigraphic, pedogenic, paleoclimatic, neotectonic, and paleobotanical studies of the past 100 ka because separate chapters in the history of the river have been set aside and largely preserved as former river valleys.

RESULTS

Climatically-Controlled Deposition of Late Quaternary Alluvium

Times of full-glacial climatic conditions were characterized by backfilling of valleys and local deposition of alluvial fans downstream from the range-bounding Hope fault. About 20-50 m of aggradation occurred along the Charwell River. Times of aggradation and degradation reflect global climatic changes (Bull, 1990, Chapter 5) that locally caused large variations in rates of bedload and water yield from hillslopes. Such climate-change induced increases in bedload transport rate resulted in distinctive episodes of deposition of fluvial gravels. From oldest to youngest, these are named Quail Downs, Dillondale, Flax Hills, Stone Jug, and Dog Hills aggradation events. Their deposition is summarized below with an emphasis on the Flax Hills and Stone Jug aggradation events.

Two stages of Flax Hills aggradation were preceded by extensive strath beveling as the valley floor was widened by lateral erosion into soft bedrock. Aggradation began with 2 m of alternating sand and gravel. Peaty silt and fine-grained sand beds with fossil reeds and leaves are common. Transported fossil wood is common in silt, sand, and gravel, and locally fossil tree trunks in growth position are encased by sequences of 2-20 mm thick beds. Each bed typically grades upward from sand to silt to clayey or peaty silt, but some beds have reversed particle-size grading. Each graded bed appears to be a low-energy slackwater deposit that records a flood event on a forested flood plain. The second stage comprises the overlying aggradation facies and consists of 35-50 m of massive silty water-laid gravels, with indistinct beds that are 20-100 cm thick. Rare pieces of transported carbonized wood occur in the lower half of the massive facies of braided-stream deposits. Silty sand lenses are not common but they occur at any position in the aggradation gravels.

Stone Jug aggradation was preceded by less extensive strath beveling than before the Flax Hills aggradation event. Stone Jug aggradation began abruptly with deposition of 15-30 m of thick, poorly bedded yellowish-brown water-laid silty gravels on underlying straths or surfaces cut into Flax Hills gravels. This uniform oxidized, massive lithology is the only depositional facies.

Dog Hills aggradation is defined as diachronous, small alluvial fans, and valley fills that were deposited on bedrock or older alluvium immediately downstream from the range-bounding Hope fault. Brief episodes of aggradation characterize the small watersheds draining the crush zone of the Hope fault. The typical section consists of oxidized interbedded water-laid and debris-flow deposits; depositional hiatuses include incipient buried soil profiles, cut-and-fill structures, and possibly abrupt transitions to either water-laid or debris-flow modes of deposition.

Radiocarbon Dating of Late Quaternary Deposits and Terraces

The Charwell River study area provides a most valuable opportunity to use several types of age control to learn more about active tectonics and about geomorphic responses to late Quaternary climatic changes. Samples for radiocarbon are mainly from the lower stage of Flax Hills deposits (49 to 43 ka) and from the Dog Hills alluvium. Apparently full glacial climates during the later half of Flax Hills time (38 to 31 ka) and during Stone Jug time (26 to 14 ka) were too cold, dry, and windy to allow trees to grow. Samples collected immediately above strath surfaces will help constrain the times of strath formation. Some strath surfaces may be regarded as time lines that pass through a tectonically deforming landscape (Bull, 1990, 1991). Radiocarbon ages less than 20 ka can be valuable for calibration of weathering rinds on surficial greywacke cobbles (Whitehouse and others, 1986; Knuepfer, 1988).

The table appended to this report summarizes the results of the radiocarbon dating for the stratigraphic units noted above. The next dating methodology to be employed is thermoluminescence dating of 15 samples selected from a suite of 63 samples collected from the Charwell River study area. The dating will be done by Steve Forman of the University of Colorado.

References Cited

Allis, R. G., 1981, Continental underthrusting beneath the Southern Alps of New Zealand: Geology, v.9, p. 303-307.

Bull, W.B., 1985, Correlation of flights of global marine terraces: in Tectonic Geomorphology, M. Morisawa and J. Hack, editors, Proceedings 15th Annual Geomorphology Symposium, State University of New York at Binghamton, Boston, George Allen and Unwin.

Bull, W.B., 1990, Stream-terrace genesis—implications for soil development, in P.L.K. Knuepfer and L.D. McFadden (editors), Soils and Landscape Evolution, 1990 Binghamton Geomorphology Symposium: Geomorphology, v. 3, pp. 351–368.

Bull, W. B., 1991, Geomorphic responses to climatic change: New York, Oxford University Press.

Bull, W.B., in preparation (a), Precision lichenometry defined by coseismic rockfalls: submitted to Arctic and Alpine Research

Bull, W.B., in preparation (b), Offset asymmetric alluvial fans along the Hope fault, New Zealand, to be submitted to Geology in Dec, 1990

Bull, W.B., and Cooper, A.F., 1986, Uplifted marine terraces along the Alpine fault, New Zealand: Science, v. 234, p. 1225-1228.

Bull, W.B., and Knuepfer, P.L.K., 1987, Adjustments by the Charwell River, New Zealand to uplift and climatic changes: Geomorphology, v. 1, pp. 15–32.

Bull, W.B., Cowan H. A., Pettinga J. R., in preparation (c), Segmentation of the Hope fault, New Zealand

Knuepfer, P.L.K., 1988, Estimating ages of late Quaternary stream terraces from analysis of weathering rinds and soils: Geological Society of America Bulletin, v. 100, p. 1224-1236.

Walcott, R.I., 1984, The major structural elements of New Zealand: in Walcott, R.I., editor; An Introduction to the Recent Crustal Movements of New Zealand, Royal Society of New Zealand Miscellaneous Series Publication 7, p. 1-6.

Whitehouse, I. E., McSaveney, M. J., Knuepfer, P. L. K., and Chinn T. J., 1986, Growth of weathering rinds on Torlesse sandstone, Southern Alps, New Zealand: in Rates of chemical weathering of rocks and minerals, Academic Press, p. 419-435.

Summary of radiocarbon analyses from sites along the south side of the Seaward Kaikoura Range, New Zealand.

Laboratory sample number	Latitude	Longitude	Material	Conventional date (ka)^{a}	$\delta^{13}C$ (‰)	Calendric age ^{b}
NZ^{c}-R11694/4	42°23.83'S	173°23.59'E	Driftwood in bedded gravel of Dog Hills alluvium	0.582 ±0.036^{d}	-25.4	0.638 ±0.024 ka. 51% probability that date is between 1376 and 1432 A.D. 44% probability that date is between 1302 and 1363 A.D.
NZ-R11694/6	42°25.53'S	173°21.63'E	Charcoal in colluvial wedge on top of soil profile; Stone Jug degradation terrace	0.678 ±0.048^{d}	-24.9	0.667 ±0.022 ka. 95% probability that date is between 1275 and 1398 A.D.
NZ-R11694/1	42°24.33'S	173°21.90'E	Charcoal in debris-flow bed in small fan of Dog Hills alluvium cut by the Hope fault	0.733 ±0.043^{d}	-25.4	0.691 ±0.015 ka. 72% probability that date is between 1229 and 1322 A.D.
A^{e}-3536	42°24.33'S	173°21.90'E	Charcoal in debris flow bed in small fan of Dog Hills alluvium cut by the Hope fault	0.840 ±0.060	-26.2	0.738 ±0.054 ka. 88% probability that date is between 1154 and 1261 A.D.
NZ-R11694/3	42°23.84'S	173°23.60'E	Driftwood in peat lens beneath paleosol in Dog Hills alluvium	3.370 ±0.043^{d}	-26.3	3.59 ±0.029 ka. 52% probability that date is between 1676 and 1619 B.C. 48% probability that date is between 1736 and 1678 B.C.
A-5703	42°25.10S	173°19.39'E	Charcoal in debris-flow bed in alluvial-fan deposits of Dog Hills alluvium	4.400±0.120	-24.7	4.98 ±0.115 ka. 73% probability that age is between 3140 and 2910 B.C.
NZ-R11752/3	42°26.34'S	173°22.31'E	Peat layer in clayey silt, basal Flax Hills deposits	20.000 ±1.0^{d}	-30.1	21.85 B.C.^{f}
NZ-R11752/1	42°27.69'S	173°21.62'E	Driftwood branches in sand lens basal Flax Hills deposits	>34.300^{d}	-26.9	

A-5697	42°27.50'S	173°21.79'E	Carbonized driftwood in oxidized sand lens of basal Flax Hills deposits on strath 17.5 m above Charwell River	35.92 +1.25/-1.08	-28.6
NZ-R11752/2	42°27.42'S	173°20.99'E	Branch of driftwood in gravel lens of upper Flax Hills deposits	>38.500[d]	-28.0
A-5219	42°15.30'S	173°43.35'E	Trunk in debris flow of upper Flax Hills deposits	39.620 +3.320/-2.340	-28.0
NZ-(R2)[g]	42°15.30'S	143°43.35'E	Trunk in debris flow of upper Flax Hills deposits	>41.500[d]	
A-5700	42°28.47'S	173°19.40'E	Tree trunk in growth position buried by slackwater beds of basal Flax Hills deposits; about 20 m above strath, 21.6 m above Goat Hills Creek	43.73 +3.62/-2.49	-26.3
A-5705	42°27.60'S	173°21.69'E	Tree trunk in growth position buried by slackwater beds of basal Flax Hills deposits; 5.6 m above of old Charwell River strath	44.32 +4.78/-2.98	-26.8
A-5702	42°28.41'S	173°19.40'E	Driftwood trunk or branch in gravel bed of basal Flax Hills deposits 3.1 m above strath	46.87 +5.78/-3.33	-27.3
A-5699	42°26.03'S	173°21.99'E	Driftwood below deformed lake beds of basal Flax Hills deposits upstream from the now inactive Charwell fault	46.29 +5.31/-3.17	-26.2
A-5695	42°25.75'S	173°21.85'E	Driftwood mat in pond of basal Flax Hills deposits upstream from fault crossing Charwell River	>47.4	-26.8

A-5698	42°27.50'S	173°21.79'E	Fresh driftwood in reduced sand lens of basal Flax Hills deposits on strath 15 m above Charwell River	47.60 +5.64/-3.28	-28.6
A-5704	42°26.03'S	173°19.40'E	Driftwood trunk or branch in gravel bed of basal Flax Hills deposits 1.8 m above strath	>47.94[h]	-29.4
A 5701	42°28.47'S	173°19.40'E	Twigs buried by slackwater beds; about 20 m above strath and 18.2 m above Goat Hills Creek	49.19[i]	-27.2

---

[a] Half-life of 5568 years is used; 1 sigma counting errors are shown. Age before 1950 A.D. has been corrected for carbon isotope fractionation using the $\delta^{13}C$ value normalized to -25‰.

[b] Calibrated ^{14}C age to account for variations in the specific activity of ^{14}C in atmospheric CO_2, using the program of Stuiver and Reimer (1986). A. D. Calendric age = 1950 - A.D. calibrated age. B.C. Calendric age = 1949 + B.C. calibrated age.

[c] Radiocarbon laboratory at the New Zealand Institute of Nuclear Sciences.

[d] The author greatly appreciates the assistance of the New Zealand Geological survey in dating this sample.

[e] Radiocarbon laboratory at the University of Arizona.

[f] Calibrated ^{14}C age to account for variations in the specific activity of ^{14}C in atmospheric CO_2, using the comparisons of uranium-thorium ages and radiocarbon ages of Barbados corals (Bard et al., 1990). 1949 A.D. - (20,000 + 3,800) years = 21.85 ka.

[g] R2 is a field sample number.

[h] This sample had a ^{14}C activity between 1σ and 1σ above the background activity, and therefore is reported as an "apparent age".

[i] This sample had a ^{14}C activity of less than 1σ and 2σ above the background activity.

Characterization of Quaternary Deformation Associated with Concealed Thrust Faulting

14-08-0001-G1875

Thomas F. Bullard
Geomatrix Consultants, Inc.
One Market Plaza
Spear Street Tower, Suite 717
San Francisco, California 94105
(415) 957-9557

William R. Lettis
William Lettis & Associates
936 Dewing Avenue, Suite G
Lafayette, California 94549
(415) 284-5789

Recent moderate-to-large earthquakes in the southwestern and southern San Joaquin Valley (Coalinga, 1983, M_L 5.5; Arvin-Tehachapi, 1952, M_L 7.3) and the Los Angeles Basin (Whittier Narrows, 1987, M_L 5.9) have focused attention on the presence of previously unidentified active thrust faults that are postulated to underlie areas of late Quaternary fold deformation. Analyses of focal mechanisms and distributions of aftershocks indicate that these earthquakes occurred at mid-to-lower crustal depths (6 to 12 km) (Eaton, 1985; Hauksson and Jones, 1989). General spatial coincidence of the earthquake epicenters with anticlinal fold axes (Coalinga earthquake with Anticline Ridge; Avenal earthquake with Kettleman Hills; Arvin-Tehachapi earthquake with Wheeler Ridge; and Whittier Narrows earthquake with Elysian Park Anticline) and geodetic data that document coseismic fold growth (Stein, 1985; Lin and Stein, 1989) suggest a genetic association between these active thrust faults and shallow-crustal anticlinal fold growth.

Two primary concerns associated with blind faults are our ability (or inability) to : 1) identify the presence of these faults beneath surface folds and to evaluate whether or not they are active; and 2) characterize the behavior of these faults as seismic sources (e.g., maximum magnitude, recurrence, etc.). Conventional geomorphic, paleoseismic, and geodetic techniques and criteria, which are aimed at identifying and characterizing active surface faults (e.g., geologic mapping, trenching, geomorphic analyses), may not lead to the recognition of these blind earthquake sources. Geologists in private industry and with state and federal agencies are confronted with the task of evaluating seismic hazards in areas of potential blind seismogenic sources without the benefit of industry standards, regulatory criteria, or conventional methodologies for characterizing these sources.

OBJECTIVES

The goal of this study is to conduct a detailed Quaternary geological evaluation in the immediate vicinity of the epicentral region of the 1987 M_L 5.9 Whittier Narrows Earthquake in order to detect tectonic deformation associated with blind thrust faults by characterizing Quaternary surface deformation. Geodetic observations indicate that coseismic uplift of the anticline occurred during and/or immediately following the 1987 Whittier Narrows earthquake (Lin and Stein, 1989). Quantification of the Quaternary physical and behavioral characteristics of this anticline, therefore, will provide data necessary to assess the kinematic and geometric relationship of the fold to the underlying fault and to assess the Quaternary rate of activity on this fault.

This project is divided into two phases: 1) initial investigations (1989) were designed to develop a Quaternary stratigraphy for the Whittier Narrows region from which to evaluate Quaternary deformation; and 2) the collection of soils and age data for determination of rates of deformation. The goal of our current study is to gather soils data, date surficial deposits, and integrate the Quaternary deformational data into predictive kinematic models of surface deformation derived from carefully constructed and controlled, balanced retrodeformable cross sections in the study area.

PRELIMINARY RESULTS

Our 1989 investigations involved Quaternary mapping from early and recent aerial photographs (including the 1928 Fairchild Collection), and morphometric analyses of landscape elements from modern and turn of the century topographic maps (to provide information on the study region prior to widespread urbanization in the Los Angeles area) and from field data. Field studies were conducted in order to: confirm mapping from aerial photographs; obtain additional information on Quaternary and bedrock deposits and structures; provide a basis for morphometric analyses; and identify locations for future soil studies. The field studies confirmed the existence of fluvial terraces (Q1 oldest, Q5 youngest) preserved in major wind gaps cut through the 250+ m-high hills associated with the Elysian Park Anticline. A southwest-trending gravel body >50 m thick cuts through the windgap between the Montebello Hills and Monterey Park Hills. We interpret this to indicate a pre-late Pleistocene phase of cutting and filling by an ancestral San Gabriel River.

A variety of morphometric techniques were used to evaluate the tectonic geomorphology of the study area. These included: construction of generalized topographic maps to depict regional slope; construction of subenvelope, envelope, and residual maps to quantify areas of maximum relief; analysis of drainage net maps and drainage basin asymmetry to detect tectonic tilting; construction of longitudinal profiles of streams and terraces; and analysis of the morphology and morphometry of streams.

The field investigations, air photo interpretation, and morphometric analyses define at least two en echelon Quaternary anticlines in the region, one centered beneath the Monterey Park Hills and one below the Montebello Hills (Fig. 1). The anticlines appear to be asymmetric with steep, linear south flanks and more gentle, deeply dissected northern flanks. The Montebello Hills anticline is about 7 km long and 1.5 km wide; the Monterey Park anticline is about 11 km long and 3 km wide. Late Cenozoic uplift occurs within the Montebello Hills

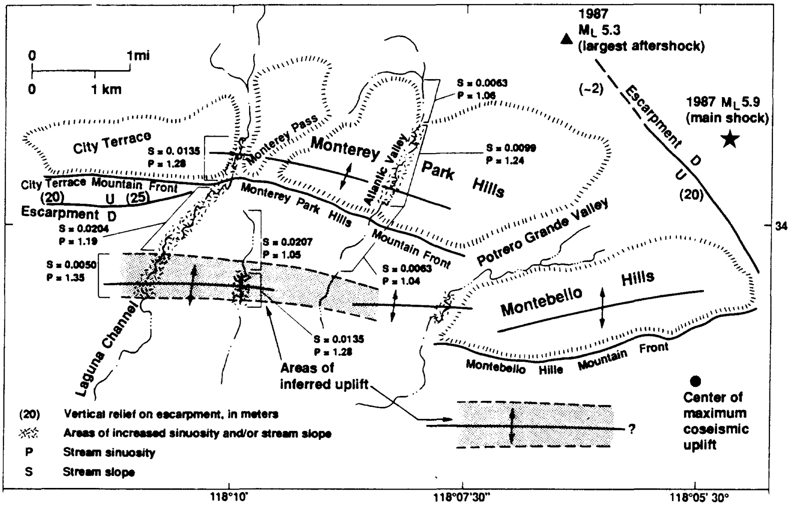

Figure 1. Map showing linear structural features, loci of piedmont incision, mountain front, stream slope, and stream sinuosity showing loci of increased sinuosity in the study area.

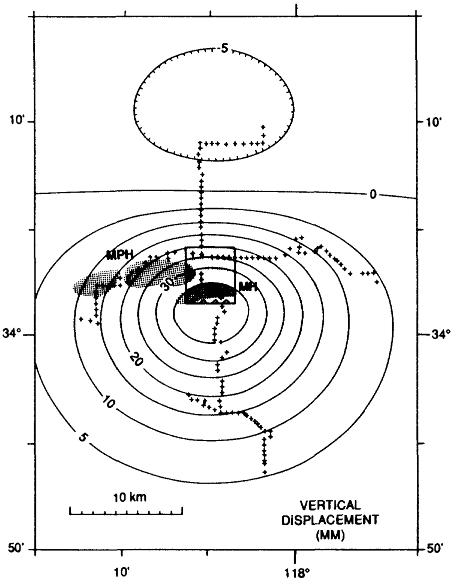

Figure 2. Map showing predicted coseismic uplift associated with the 1987 Whittier Narrows earthquake. Predicted uplift is based on pre- and post-event geodetic surveys along lines indicated by crosses and on elastic deformation associated with the earthquake on the blind thrust (shaded rectangle). Study area is shaded and labelled MPH (Monterey Park Hills [maximum long-term uplift]) and MH (Montebello Hills). Adapted from Lin and Stein (1989).

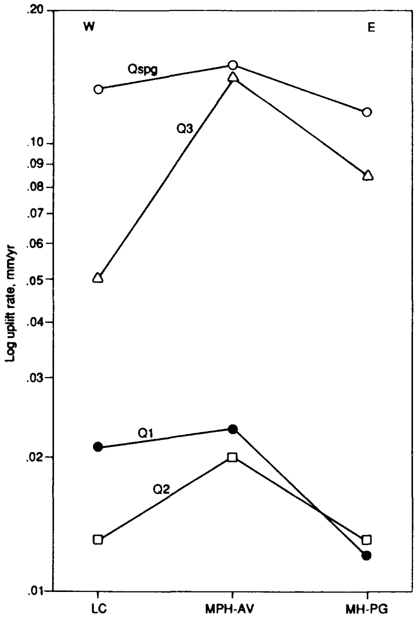

Figure 3. Graph showing preliminary uplift rates from west to east in the study area. Qspg is pediment surface cut across the Montebello Hills. Refer to Figure 1 for locations: LC = Laguna Channel; MPH-AV = Monterey Park Hills-Atlantic Valley; MH-PG = Montebello Hills-Potrero Grande Valley.

several km west of the point of maximum coseismic uplift of the 1987 Whittier Narrows earthquake and west of the surface projection of the fault plane associated with the 1987 event as reported by Lin and Stein (1989) (Fig. 2). The residual maps suggest that maximum uplift has been at least 80 m during an, as yet, undefined period of Quaternary time. Very preliminary uplift rates, based on correlation of soil development of the Quaternary units with existing soils-based chronologies in the Los Angeles Basin region are ≤0.15 mm/yr (long term). Long term uplift rates also indicate spatial variation with the greatest rates in the Monterey Park Hills and decreasing to the west and east (Fig. 3).

Variation in the amount of uplift along the hills and the apparent right en echelon step in the anticlinal axis and front of the Monterey Park-Montebello Hills may reflect possible segmentation of the underlying thrust fault. North-trending lineaments are evident on the residual maps and aerial photography and may represent the surface expression of one or more tear faults that segment the underlying thrust fault.

Two, somewhat anomalous escarpments are found north and south of the Monterey Park-Montebello Hills area (Fig. 1). The escarpment south of City Terrace is 20 to 25 m high and is associated with anomalous drainage development on the upper side of the escarpment. The escarpment north of Montebello Hills ranges in height from 20 m on the south to <2 m in the north. This linear feature cuts across interfluves and is not related to stream incision from ancestral channels of the Rio Hondo or other rivers in the region. The escarpment is aligned along trend with the largest aftershock of the 1987 Whittier Narrows earthquake, a northwest-trending, high-angle southwest dipping strike-slip fault. We postulate that the escarpment may be the surface expression of a strike-slip fault, possibly a northwestern continuation of the Whittier fault system, or a lateral tear fault in the underlying blind thrust fault that produced the 1987 event. Placed in context of the regional tectonic framework, the Monterey Park Hills and Montebello Hills may represent restraining bend folds related to a left step in the right lateral Elsinore-Whittier Fault Zone near the intersection with the Santa Monica-Raymond Fault Zones.

Due to the late starting date (August 1, 1990) of the most recent phase of the project, little additional work is completed. Preliminary field investigations indicate that it will be possible to correlate soils in the study area with established soil chronosequences in the region (McFadden, 1982; Rockwell, 1983). Where surface exposures are available, basic soil characteristics observed are: Unit Q1 soils have a partially preserved profile with at least a 2.5 YR Bt horizon; Unit Q2 soils have 2.5 YR Bt horizons with strong subangular blocky structure and thick, continuous clay films; Unit Q3 soils have 5 YR Bt horizons, with strong subangular blocky structure, and moderately thick to thick continuous clay films; Unit Q4 soils have 7.5 YR Bt horizons; and Unit Q5 soils are minimally developed with an A-Cox profile. We are seeking permission to trench on selected sites that will provide us with the opportunity to obtain complete, detailed soils data for each Quaternary unit. Samples for numerical dating will be collected from trenches; horse bones from the Q3 deposit will soon be dated. Preliminary rates of deformation and spatial patterns of deformation are currently being incorporated into balanced retrodeformable geologic cross sections across the Monterey Park Hills and Montebello Hills. These sections will aid the development of predictive, spatial and temporal kinematic models for the progressive surface deformation associated with fault bend and fault propagation folding that accompanies active, blind thrust faulting.

REFERENCES

Davis, T.L., Namson, J., and Yerkes, R.F., 1989, A cross section of the Los Angeles area: seismically active fold and thrust belt, the 1987 Whittier Narrows earthquake, and earthquake hazard: Journal of Geophysical Research, v. 94, no. B7, p. 9644-9664.

Eaton, J.P., 1985, The May 2, 1983 Coalinga earthquake and its aftershocks: a detailed study of the hypocenter distribution and of the focal mechanisms of the larger aftershocks, in M.J. Rymer and W.L. Ellsworth, (eds.), Mechanics of the May 2, 1983 Coalinga, California earthquake: USGS Open-File Report 85-44, p. 132-201.

Hauksson, E. and Jones, L.M., 1989, The 1987 Whittier earthquake sequence in Los Angeles, southern California: seismological and tectonic analysis: Journal of Geophysical Research, v. 94, no. B7, p. 9569-9589.

Lin, J., and Stein, R.S., 1989, Coseismic folding, earthquake recurrence, and the 1987 source mechanism at Whittier Narrows, Los Angeles Basin, California: Journal of Geophysical Research, v. 94, no. B7, p. 9614-9632.

McFadden, L.D., 1982, The impacts of temporal and spatial climatic changes on alluvial soils genesis in southern California [Ph.D. thesis]: Tucson, Arizona, University of Arizona, 430 p.

Rockwell, T.K., 1983, Soil chronology, geology and neotectonics of the north central Ventura Basin [Ph.D. thesis]: Santa Barbara, California, University of California, 425 p.

Stein, R.S., 1985, Evidence of surface folding and subsurface fault slip from geodetic elevation changes associated with the 1983 Coalinga, California earthquake, in M.J. Rymer and W.L. Ellsworth, (eds.), Mechanics of the May 2, 1983 Coalinga, California Earthquake: USGS Open-File Report 85-44, p. 225-253.

Late Quaternary Slip Rates on Active Faults of California

9910-03554

Malcolm M. Clark
Branch of Engineering Seismology and Geology
345 Middlefield Road, MS 977
Menlo Park, California 94025
(415) 329-5624, FTS 459-5624

Investigations

1. Recently active traces of Calaveras fault zone at Tres Pinos Creek and San Felipe Creek, California (K.J. [Kendrick) Harms, J.W. Harden, M.M. Clark).
2. Recently active traces of Owens Valley fault zone, California (Sarah Beanland [NZGS], Clark).
3. Degradation of fluvial terrace risers along Lone Pine Creek, San Bernardino County. (Harms, in conjunction with J.B.J. Harrison, L.D. McFadden (UNM), and R.J. Weldon [University of Oregon]).
4. Revision of slip-rate table and map of late-Quaternary faults of California (Clark, Kendrick, J.J. Lienkaemper, K.R. Lajoie, C. Prentice, M.J. Rymer, D.P. Schwartz, R.V. Sharp, J.D. Sims, J.C. Tinsley, R.J. Weldon).
5. Late-Quaternary evolution of the San Timoteo Badlands region, southern California (Kendrick, in conjunction with D.M. Morton and L.D. McFadden).

Results

4. We are in the process of revising, updating, and publishing (as a USGS Bulletin) the slip-rate table and map of late-Quaternary faults of California (USGS OFR 84-106). Our aim is to review all entries in OFR 84-106 and add all new data generated since its release. We welcome any relevant unpublished data from workers in this field.

5. A minimum of three surfaces have been recognized through the mapping of the Quaternary units in San Timoteo and Reche Canyons, San Bernardino and Riverside Counties. In San Timoteo Canyon nine soils have been described on three surfaces and two associated paleosurfaces. An additional soil has been described in Reche Canyon. Preliminary analysis indicates that development of these soils is similar to that of soils in Cajon Canyon, 40 km to the northwest, although eolian input is less than in the San Timoteo area.

Reports

None in this reporting period.

Investigation of coastal neotectonics and paleoseismicity of the southern Cascadia margin as recorded in coastal marsh systems

Agreement No. 14-08-0001-G1799

Mark Darienzo and Curt Peterson
Department of Geology
Portland State University
Portland, Oregon 97207

(503)-725-3022

Wetlands in four northern Oregon estuaries (Neawanna Creek (46°), Nestucca Bay (45.2°), Siletz Bay (44.9°) and Yaquina Bay (44.6°)) were investigated for evidence of coseismically buried peats, both in cores and cutbanks (figure 1). These wetlands are gaps in the paleoseismological record of the northern Oregon coast north of 44° latitude. Findings from this study, when combined with prior work in Netarts Bay (45.4°) and Alsea Bay (44.4°) (Darienzo and Peterson, 1990; Peterson and Darienzo, 1990) and in Nehalem Bay (45.7°) and Salmon River (45.0°) (Grant and McLaren, 1987; Grant, 1989), should provide a unifying paleoseismological document for the northern Oregon coast.

Preliminary results from selected cores of three of these bays are as follows: A) The subsurface of the Necanicum/Neawanna Creek marshes contain at least six buried peats to a depth of three meters (figures 2 and 3). Associated with one of the buried peats, approximately one meter below the surface, are in situ tree roots protruding from the cutbanks nearby. Protruding roots can be seen for several hundred meters along the creek. Sand caps a few of the buried peats, especially in cutbanks and at those core sites near the creek, and in one location, sand drapes a tree root. B) Cores from Nestucca Bay (figures 4 and 5 (top 6 meters)), in contrast, contain at least ten buried peats to a depth of eight meters at core sites 2 and 5. In addition, several buried peats were identified between 8 and 13 meters depth at core site 2, providing the longest record of peat burial on the Oregon coast. At a depth of approximately 2.25 meters in core 2, there is an abrupt transition between a muddy peat containing freshwater diatoms and overlying *Triglochin* rhizomes, frequently a tidal flat colonizer. This suggests rapid submergence and a change of environment from a very high marsh to a tidal flat. C) Siletz Bay (figures 6 and 7) cores contain up to six burial events to a depth of four meters. The buried peats of the spit have thick sand capping layers. Sand also caps buried peats at similar depths below the surface in cores E and F, almost 3 kilometers from the spit.

Further work, which includes radiocarbon dating of the burial events and laboratory analyses of core samples, is required to answer the following questions. Are the buried peats a result of coseismic subsidence? If coseismic, are the burial events in the marshes of northern Oregon synchronous? Finally, if synchronous, what are the magnitudes of these paleoearthquakes?

References

Darienzo, M.E. and C.D. Peterson, 1990. Episodic tectonic subsidence of late Holocene salt marshes, northern Oregon, central Cascadia margin. Tectonics, 9: 1-22.

Grant, W.C. and D.D. McLaren, 1987. Evidence for Holocene subduction earthquakes along the northern Oregon coast (abstract). EOS, 68: 1496.

Grant, W.C., 1989. More evidence from tidal-marsh stratigraphy for multiple late Holocene subduction earthquakes along the northern Oregon coast (abstract). Geological Society of America Abstracts with Programs, 21: 86.

Peterson, C.D. and M.E. Darienzo, 1990. Discrimination of climatic, oceanic and tectonic forcing of marsh burial events from Alsea Bay, Oregon, U.S.A. (U.S. Geological Survey Professional Paper, submitted).

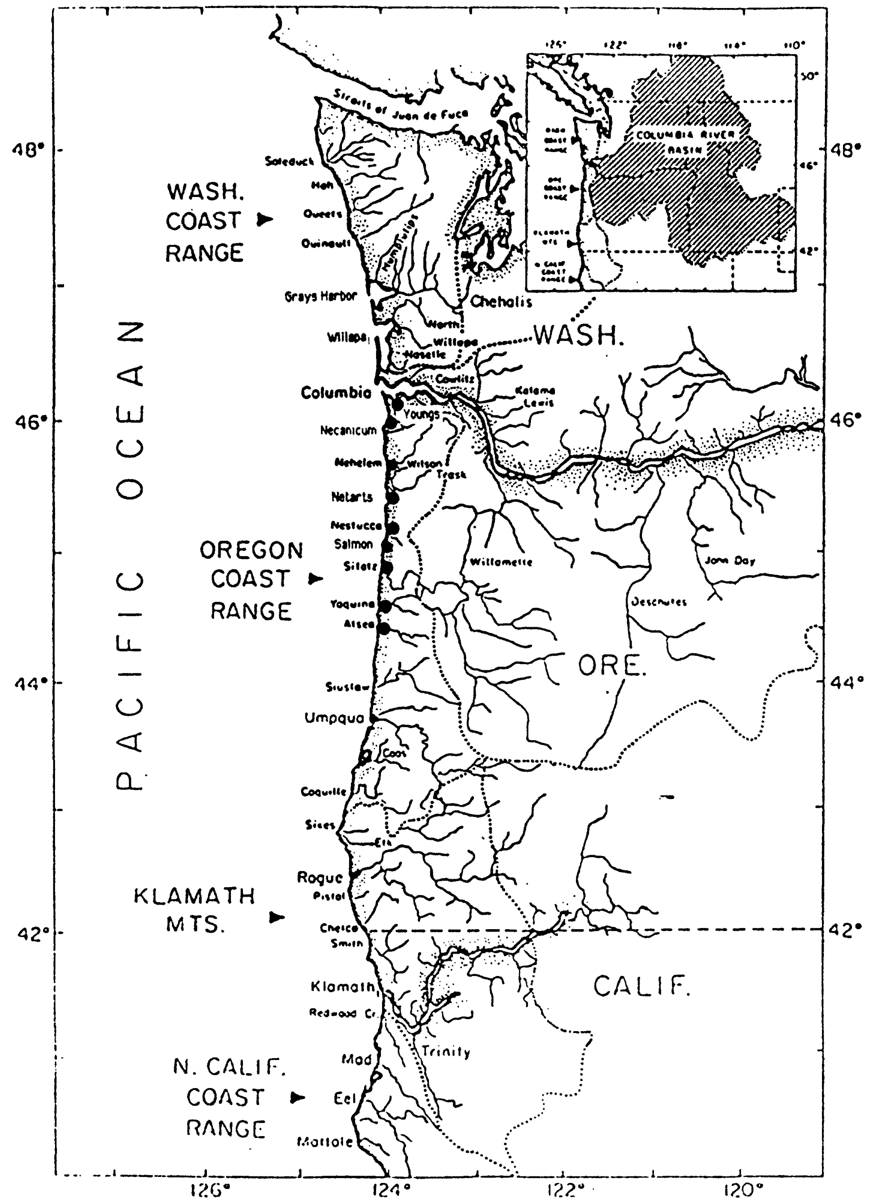

Figure 1. General location map of the northern Oregon estuaries (indicated by ●).

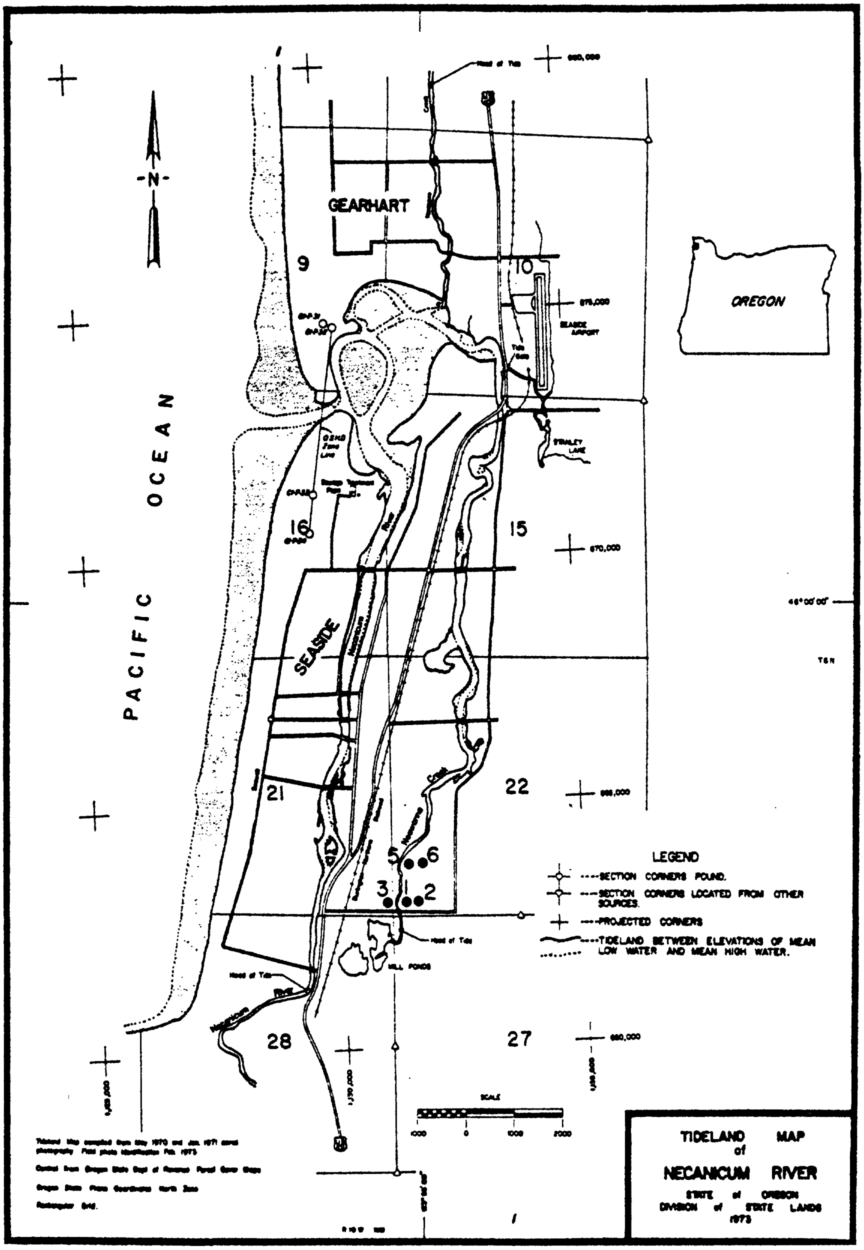

Figure 2. Map of the Necanicum/Neawanna showing the location of selected marsh core sites (●) near Neawanna Creek.

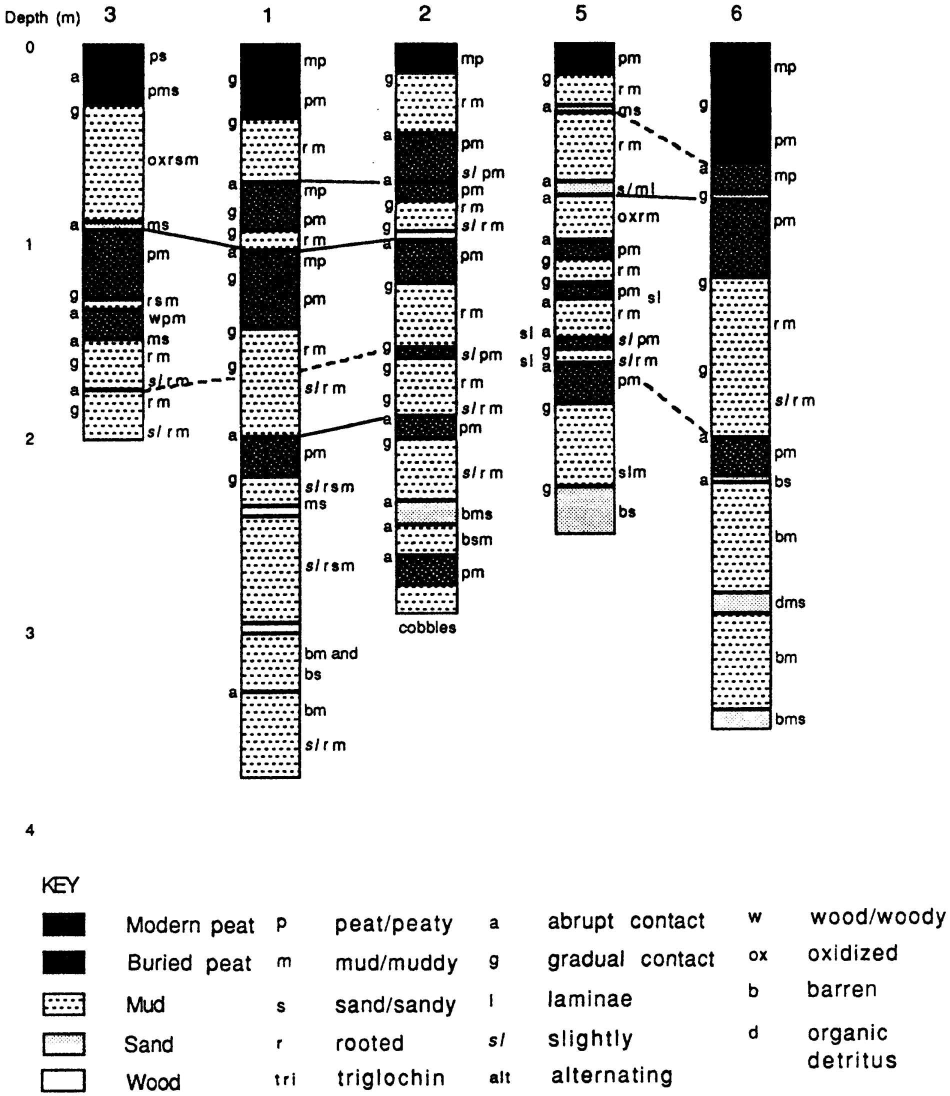

Figure 3. Preliminary stratigraphy of cores from the Neawanna marshes (see figure 2).

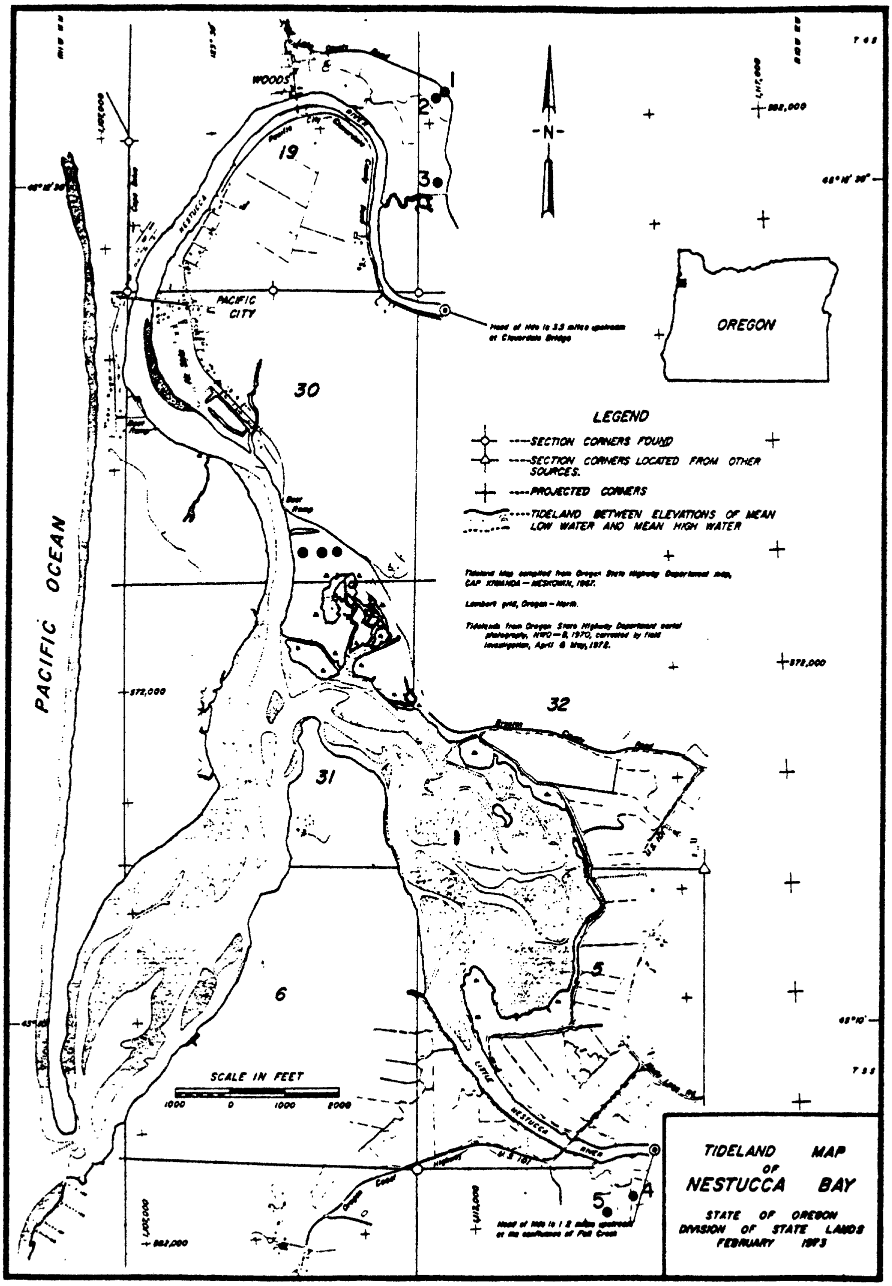

Figure 4. Map of Nestucca Bay showing the location of selected core sites (●) in wetlands near the Nestucca and Little Nestucca Rivers.

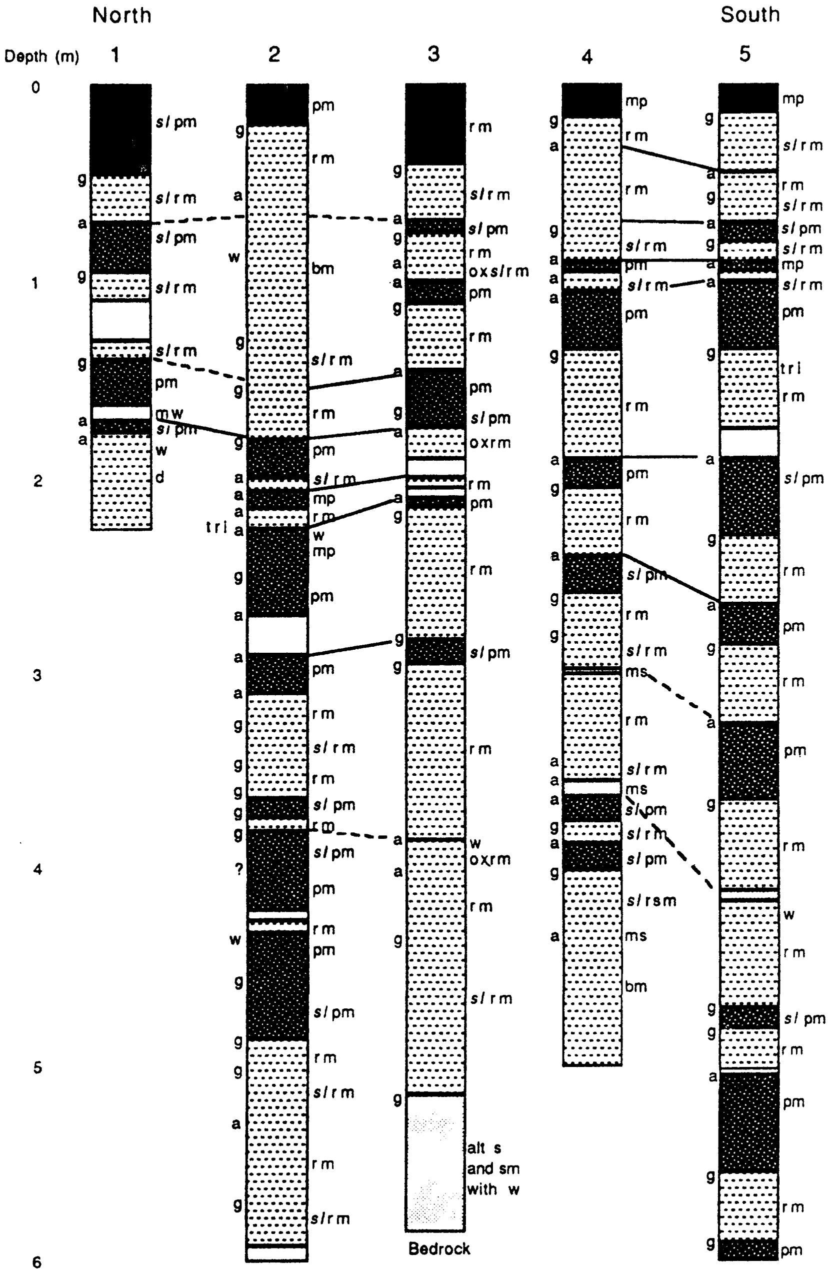

Figure 5. Preliminary stratigraphy of cores from the Nestucca wetlands (see figure 4).

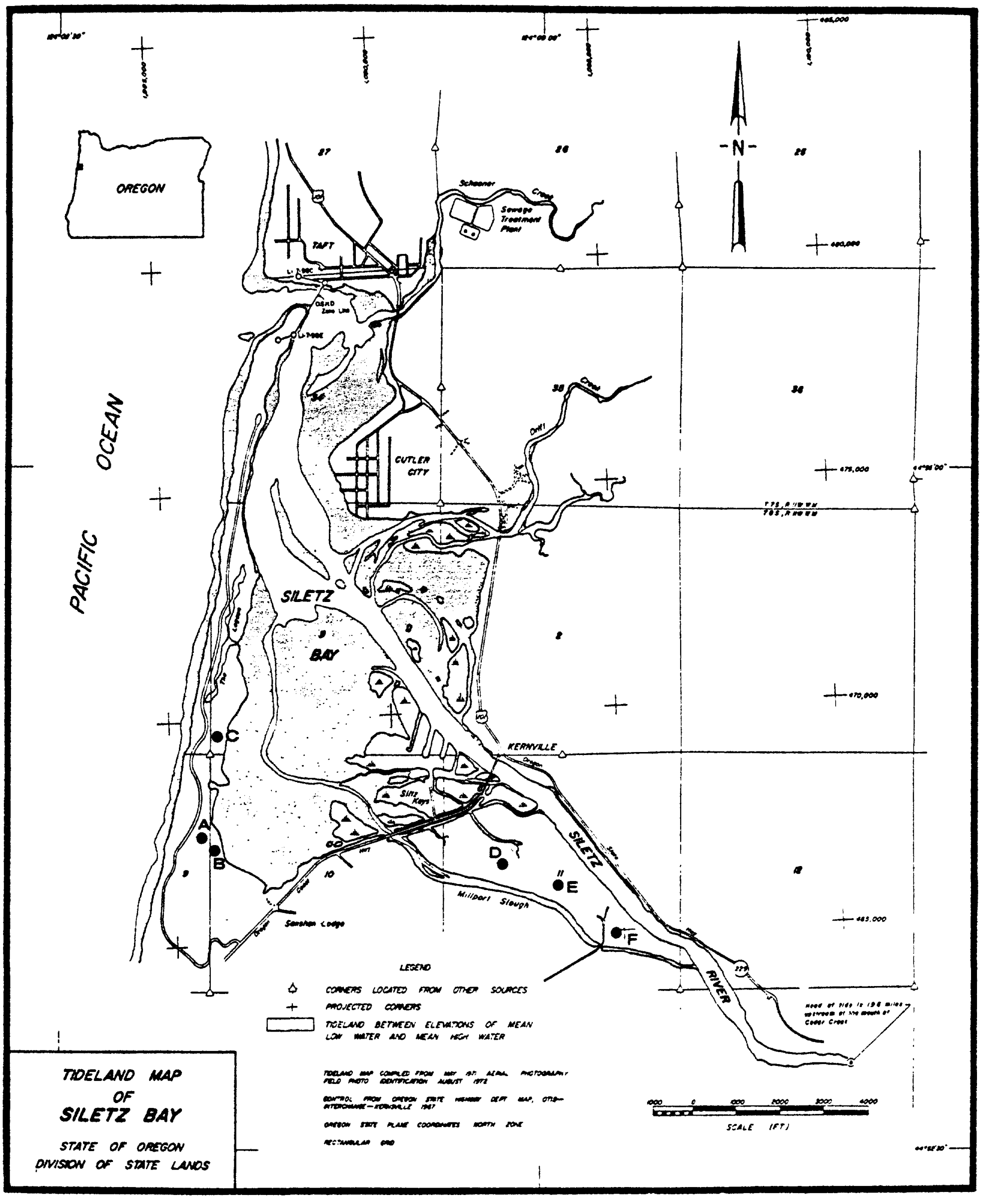

Figure 6. Map of Siletz Bay showing the location of selected marsh core sites (●) on the spit and between the Siletz River and Millport Slough.

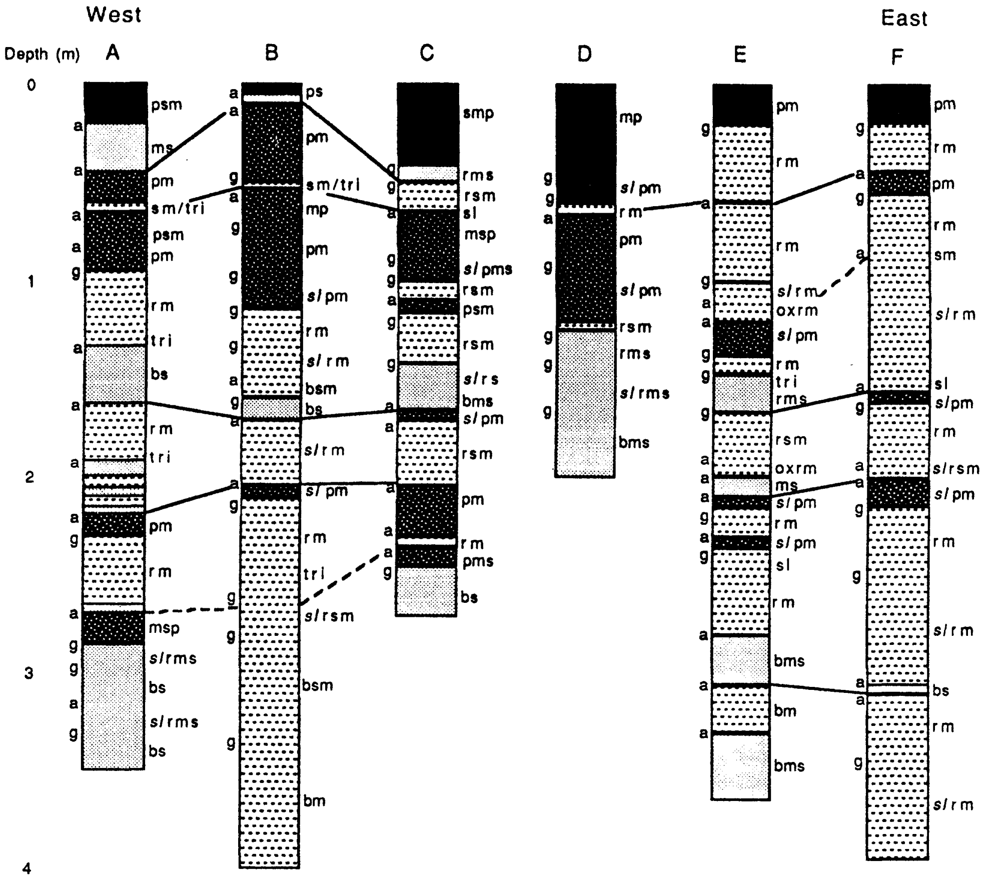

Figure 7. Preliminary stratigraphy of cores from the Siletz marshes (see figure 6).

Assessing the Temporal and Stratigraphic Limitations in Paleoseismic Studies in Normal Faulted Terrain

Agreement No. 14-08-0001-G1813

Steven L. Forman[1] and James McCalpin[2]
[1]Center for Geochronological Research and Dept of Geological Sciences,
University of Colorado, Boulder CO 80309;
[2]Dept. of Geology, Utah State University
Logan, Utah 84322

This research will evaluate and provide a basis for improving the temporal and stratigraphic limits for recognizing paleoearthquakes in normal faulted terrain. Two outstanding problems are the accurate dating of paleoseismic events and the recognition of moderate magnitude events (M5.5 to 7.0) in the stratigraphic record. Specifically, we are assessing the resolution of the thermoluminescence (TL) and ^{14}C methods to date Holocene displacements on the Weber segment, Wasatch fault zone, Utah. TL analysis will concentrate on samples from the same stratigraphic level and from close stratigraphic intervals. The effects of pedogenesis on TL age estimates of soils will also be investigated. We hope to improve the resolution and precision of radiocarbon dating of buried soils by dating separate organic fractions by AMS. The stratigraphic recognition of paleoseismic events will be extended by studying colluvial sediments shed post historic displacements of < 1m.

Data Collection

Sediment samples for TL and ^{14}C studies have been collected from numerous stratigraphic levels from the re-excavated Kaysville Trench and the Garner Canyon natural exposure, both on the Weber segment, Wasatch fault zone. Procedures have been developed to isolate organic fractions (humics and humins) for ^{14}C dating, which will be used on buried A horizon samples from Garner Canyon. These samples will be analyzed in Boulder, Co.

We have also collected a suite of samples from colluvium shed post the 1983 Borah Peak, Idaho earthquake. Colluvial wedge structure was determined by the following factors: 1) Parent material, 2) Style of surface rupture, 3) Scarp height, 4) Ambient geomorphic gradient, and 5) Scarp aspect. Eleven in-situ colluvial wedges were sampled by cementing the wedge onto plywood with foam insulation and will be analyzed in detail at Logan, Ut.

Results

The TL age estimates for sediment samples collected from the re-excavation of the Kaysville Trench, indicate that sedimentary environment strongly controls the accuracy of the TL method. Buried A horizons yield TL ages in agreement with radiocarbon ages on disseminated organics from the same horizons. However, overlying colluvial and fluvial sediments yield TL age estimates 2 to 4 times greater than the underlying TL and ^{14}C age estimates.

Preliminary observations of the sampled colluvial wedges indicate: 1)The strength of the clast fabirc for a colluvial wedge varies inversely with the percentage of fine-grained matrix in the colluvium, and 2) Small free faces (<0.5m high) expose only the finer-grained loess cap found on many early Holocene-late Pleistocene deposits. Thus small colluvial wedges are difficult to recognize is because the parent material is finer grained that exposed in larger free faces.

Publications

Forman, S.L. (editor), 1989, Dating Methods Applicable to Quaternary Geologic Studies in the Western United States. Utah Geologic and Mineral Survey, Miscl. Publication, 89-7; 80p.

Forman, S.L. and Machette, M.N. (in press), Thermoluminescence dating of sediment. in: Chapter 17: Dating Methods Applicable to the Quaternary; Quaternary Non-glacial Geology of the conterminous United States. Decade of North American Geology (DNAG) Volume 21.

Forman, S.L., Nelson, A.R. and McCalpin, J. (in press), Thermoluminescence dating of fault-scarp derived colluvium: deciphering the timing of paleoearthquakes on the Weber segment of the Wasatch fault zone, north-central Utah. J. Geophysical Research.

McCalpin, J. and Forman, S.L. (in press), History of Quaternary faulting on the east Cache Fault zone, north-central Utah. Bull. of Seismological Society of America.

Holocence and Recent Drainage Disruption of Packwood Creek and Slip Rates along the Calaveras Fault near Anderson Reservoir

Project Number 14-08-0001-G1877

Deborah R. Harden and Alexander Gallego
Department of Geology
San Jose State University
1 Washington Square
San Jose, CA 95192

(408) 924-5021

Packwood Creek is a 17-km^2 drainage basin that is presently tributary to Anderson Reservoir (Mt. Sizer 7.5' quadrangle). The basin shows strong geomorphic evidence of disruption by motion on the Calaveras Fault. Packwood Creek appears to have been at least partly defeated by slip along the Fault, causing it to undergo extensive alluviation in Packwood Valley above Dairy Flat.At least 7 meters of alluvial fill are present beneath the extensive terrace surface that marks the Valley floor. At the upstream end of the valley, the surface of Packwood Valley lies approximately 7.5 meters above the present channel of Packwood Creek, converging downstream to about 3.5 meters above the channel below Dairy Flat.

Following this period of alluviation, upper Packwood Creek was captured by a headward-eroding stream, creating its present channel configuration and triggering incision of Packwood Valley. Field mapping and hand leveling of the terraces at 1':50' scale have led to recognition of at least 4 terraces inset into the Valley surface, recording the progressive incision of upper Packwood Creek, presumably after its capture. A preliminary C^{14} date of 8900 +/- 260 yr BP was obtained from charcoal in alluvium at the downstream end of Packwood Valley in a unit correlative with one of the older inset terraces. Four additional samples from older alluvial units are currently being analyzed at the Radiocarbon Laboratory at Washington State University, Pullman. Correlation and dating of the alluvial deposits in Packwood Valley will establish the timing of partial ponding and subsequent capture and incision of Packwood Creek. On the basis of the preliminary date, the fill in Packwood Valley appears to be correlative with the younger terraces mapped by Kendrick and others in San Felipe Creek, the probable former outlet of Packwood Valley before its capture. Detailed stratigraphic interpretation and soil descriptions of the valley fill are in progress.

Hand-auguring in Dairy Flat, located at the downstream end of Packwood Valley, revealed the presence of at least 5 meters of fine-grained alluvium, confirming that it is an abandoned alluvial surface of Packwood Creek; we plan to excavate 2 backhoe test pits in Dairy Flats during November, 1990.

TECTONICS OF CENTRAL AND NORTHERN CALIFORNIA

9910-01290

William P. Irwin
Branch of Engineering Seismology and Geology
U.S. Geological Survey
345 Middlefield Road, MS 977
Menlo Park, California 94025
415/329-5639 or 415/329-5639

Investigations

1. Study of the paleotectonic significance of the distribution of thin-bedded chert in various terranes of the California Coast Ranges and Klamath Mountains.

2. Preparation and revision of manuscripts pertaining to the geology and tectonics of northern California and southwestern Oregon.

Results

1. Radiolarian chert was sampled in several different terranes of the Coast Ranges and Klamath Mountains, in a collaborative effort with E.A. Mankinen, C.D. Blome, and M.J. Rymer, to determine the paleolatitudes of the original depositional sites of the various chert bodies and the magnitude of their possible post-depositional tectonic transport. The sample localities are of Early Jurassic and Permian ages. The Early Jurassic localities are of Franciscan chert in terranes on both sides of the San Andreas fault, from the San Rafael Mountains at the south end of the Coast Ranges to Zenia in the northern Coast Ranges near the latitude of Cape Mendocino. The Permian chert is in the North Fork terrane of the central Klamath Mountains, and its paleolatitude is to be compared with the paleolatitude of Permian strata of the Eastern Klamath terrane. Laboratory studies of the paleontology (Blome) and the paleomagnetism (Mankinen) of the chert samples are in progress.

2. Revision of a preliminary geologic map of the Red Bluff 100,000 quadrangle (Open-File Map 84-105), which covers the tectonically complex junction of the Coast Ranges, Klamath Mountains, Great Valley, and Cascade Range provinces, was begun. The map is co-authored with M.C. Blake, Jr., D.S. Harwood, E.J. Helley, A.S. Jayko, and D.L. Jones and is being prepared for publication in the USGS Miscellaneous Investigations Map series. The writing of a report describing the geology and tectonic development of the Klamath Mountains, for publication in the USGS Bulletin series, was continued during this report period.

Reports

No reports this period.

10/90

Coastal Tectonics Western United States

9910-01623

Kenneth R. Lajoie
Branch of Engineering Seismology and Geology
U.S. Geological Survey
345 Middlfield Road MS 977
Menlo Park, California 94025
(415) 329 -5747, 329-5641

Investigations

1. Deformed Pliestocene marine strandlines, Santa Cruz County
2. Coseismic marine strandlines and Holocene sea level
3. Cosiesmic marine strandlines, southern Alaska (G. Plafker project chief)
4. ESR-dating fossil marine shells (with T. Furutani)
5. U-series dating fossil solitary corals (with J. Wasserberg and M. Stein)

Results

1. Previous analysis of relative strandline elevations correlated the Cement, Highway-1 and Davenport strandlines in northern Santa Cruz County (Bradley and Griggs, 1974) with the 120, 102 and 85-ka sea-level highstands, respectively (Hanks and others, 1984). However, this analysis ignored the minor Greyhound strandline, which lies above and intersects with the major Highway-1 strandline. It also ignored a similar relationship between in southern Santa Cruz County where the minor 2nd strandline lies above and intersects the major 1st strandline (Alexander, 1952). Because the 1st strandline is the southern extension of the Highway-1 strandline, the 2nd strandline must correlate with the Greyhound strandline.

   A higher (older) strandline can intersect a lower (younger) strandline on a tilted coastline only if the sea-level highstand that produce the former was lower that the highstand that produced the latter. It is widely accepted that the penultimate interglacial highstand at 210 ka was about 15 m lower than the last interglacial highstand at 120 ka. Consequently, the Greyhound-2nd strandline probably correlates with the 210-ka highstand and, as originally suggested (Bradely and Griggs, 1974), the Highway-1 strandline, not the Cement strandline, correlates with the 120-ka highstand. U-series dates on solitary corals from the Davenport strandline should help resolve any remaining uncertainty in the ages of these strandlines. The revised age of the Highway-1 strandline decreases the minimum calculated uplift rate for the northern Santa Cruz County coast from about 0.4 to 0.2 m/ka.

A recent paper (Anderson, 1990) claims that the surface deformation pattern produced by the Loma Prieta rupture is similar to the long-term deformation pattern reflected in the convex-upward longitudinal profiles of emergent strandlines in the southern part of Santa Cruz County (Alexander, 1952), and concludes that the rupture was a characteristic event that occurs every 800 years. However, the convex-upward profiles in both data sets merely reflect the broadly embayed coastline superimposed on a SW-tilting structural block. Any seaward tilt would produce a convex-upward profile along the embayed coastline. The three mapped strandlines (1st, 2nd and 3rd in ascending order; Alexander, 1952) are actually warped in a concave-upward pattern with their elevations increasing non-linearly to the NE, toward the San Andreas fault. However, the fold axes of the warps in each strandline are not parallel to the fault, nor to each other. Relative strandline elevations correlate the 3rd strandline south of Aptos with the 320-ka sea-level highstand, but with the 420-ka highstand north of Santa Cruz. This discrepancy suggests that there is a previously unrecognized structural complication between Aptos and Santa Cruz. In Summary, the strandline data suggest that the Loma Prieta rupture was not necessarily a characteristic event, regardless of whether or not it occurred on the San Andreas or a subsidiary fault. The preferred model is that the long-term uplift and seaward tilt reflected in the strandlines results from numerous overlapping and somewhat random uplift events, not from similar (characteristic) events. If the Loma Prieta event was not characteristic, it could not have been forecast.

2. Emergent and submergent marine strandlines record vertical cosiesmic movement along many tectonicaly active coastlines throughout the world. However, to derive an accurate tectonic history from these relative sea-level records, the sea-level history must be known. Unfortunately, the sea-level history over the last 5 to 6 ka (the period of time over which sea level has been close to its present position) is poorly known. A theoretical model developed on this project yields past sea-level elevations from a sequence of tilted Holocene strandlines if the original elevation of just one of strandlines is known. A complete sea-level history can be derived if both the age and original elevation of one strandline are known. On a coastline where historical cosiesmic uplift has occurred, the original elevation of the lowest strandline is known (0 m). Consequently, the original elevations of the prehistoric strandlines can be determined if the entire sequence was tilted in a uniform manner. Unfortunately, when the model is applied to data sets from several coseismically tilted coastlines, no consistent sea-level pattern emerges. In fact, no data set produces a reasonable sea-level history. Obviously, the coastlines were not tilted in a uniform manner, suggesting that the fault-rupture events which produced the strandlines were not characteristic. Collectively, the data suggest that characteristic fault rupture is a myth, at least along megathrust boundaries where most of the analyzed data were derived.

3. At least five submerged beds of fresh-water peat (muskeg) with rooted tree stumps are interbedded with beds of tidal-flat silt in the upper 8 m of the Copper River delta in southern Alaska. This stratigraphic sequence reflects episodic tectonic uplift and interseismic subsidence over the last 3 to 4 ka. The net submergence probably reflects roughly equal amounts of crustal subsidence (tectonic plus isostatic) and eustatic sea-level rise. The unequal spacing between peat beds suggests that the size of and time between uplift events are irregular.

4. To better understand the ESR spectra from Pleistocene fossil shells, several older carbonate specimens have been analyzed. Surprisingly, systematic differences in the Mn superfine lines of the ESR spectra clearly reflect the relative ages of 0.7, 1.0, 1.9 and 2.4 By carbonatites. The lines broaden and eventually split with increasing age, indicating that the spectra represents two wave forms that gradually go out of phase as the calcite lattice changes, or as the Mn distribution changes with time. Experiments with shell samples reveal that ESR spectra are far more sensitive than X-ray analysis in detecting minor aragonite-to-calcite alteration. Analysis of the nacreus layer from a Cretaceous pelecypod shell shows less alteration than in most Pleistocene shells.

5. An experiment to evaluate the feasibility of dating Pleistocene solitary corals using the recently developed high-precision mass-spectrometer U-series technique has produced promising results, but has left some important questions unanswered. Multiple analyses of samples from specimens known to be the same age (connected during growth) show that different sample preparation procedures effect the resultant ^{230}Th-^{234}U date significantly. Dates from carefully cleaned samples are about 10 % higher than dates from poorly cleaned samples, suggesting that ^{234}U is probably associated with contaminating silicate detritus. Analyses of well cleaned samples of numerous specimens from the same outcrop yield a 10 % spread in ages. Theoretically, the technique has a resolution of 2 ka at 100 ka. Consequently, the 13 ka spread in dates from the same bed reflects real age differences or sample variability. The latter seems more likely.

Reports

Lajoie, K,R., Conlan, L.M.,Furutani, T. T., Ponti, D.J. and Saxton, J. L., in press, Intra- and inter-shell variability of amino acids in fossil *Saxidomous* shells from Goleta, California (abs): GSA Abstracts with Programs.

Plafker, G., Lajoie, K. R. and Rubin, M., in press, Radiocarbon dating of coseismic uplift events, southern Alaska: Radiocarbon.

Latest Quaternary Surface Faulting in the Northern Wasatch to Teton Corridor (NWTC)

14-08-0001-G1396

James McCalpin
Department of Geology
Utah State University
Logan, UT 84322-4505
(801) 750-1220

Investigations

1. Trenching the 12 m-high fault scarp which runs through the eastern part of Afton, Wyoming (southern segment of the Star Valley fault).

Results

1. At last! I got permission to trench the Star Valley fault, in the back yard of a residence in Afton, Wyoming (future paleoseismologists thank Mrs. Ruby Kennington, age 85).

2. The trench exposed stratigraphic evidence for three large (3-4 m) paleoseismic displacements in the last 15 ka (Fig. 1). Radiocarbon samples that constrain the age of the latest two events are now being processed; results are expected by Oct. 26, 1990.

3. The trench was visited by ca. 30 geologists on a pre-meeting field trip associated with the Geol. Soc. of Amer., Rocky Mtn. Section Meeting in Jackson, WY, on May 19, 1990. About 20 townspeople also attended the field review.

Reports

McCalpin, James, Piety, L.A and Anders, M.H., 1990, Late Tertiary and Quaternary faulting north and south of the eastern Snake River Plain. Part 1. Latest Quaternary faulting and structural evolution of Star Valley, Wyoming, in Roberts, Sheila (ed.) Geologic Field Tours of western Wyoming and parts of adjacent Idaho, Montana and Utah: Geological Survey of Wyoming, Public Information circular no. 29, p. 5-14.

Anders, M.H., Rodgers, D.W., McCalpin, J.P. and Haller, K.M., 1990, Late Tertiary and Quaternary faulting north and south of the eastern Snake River Plain. Introduction., in Roberts, Sheila (ed.) Geologic Field Tours of western Wyoming and parts of adjacent Idaho, Montana, and Utah: Geological Survey of Wyoming, Public Information Circular no. 29, p. 1-4.

McCalpin, James, in press, Late Quaternary faulting in the northern Wasatch to Teton Corridor, Utah, Idaho, and Wyoming: Geol. Soc. Amer., Abstracts with Programs, Annual Meeting, Dallas, TX.

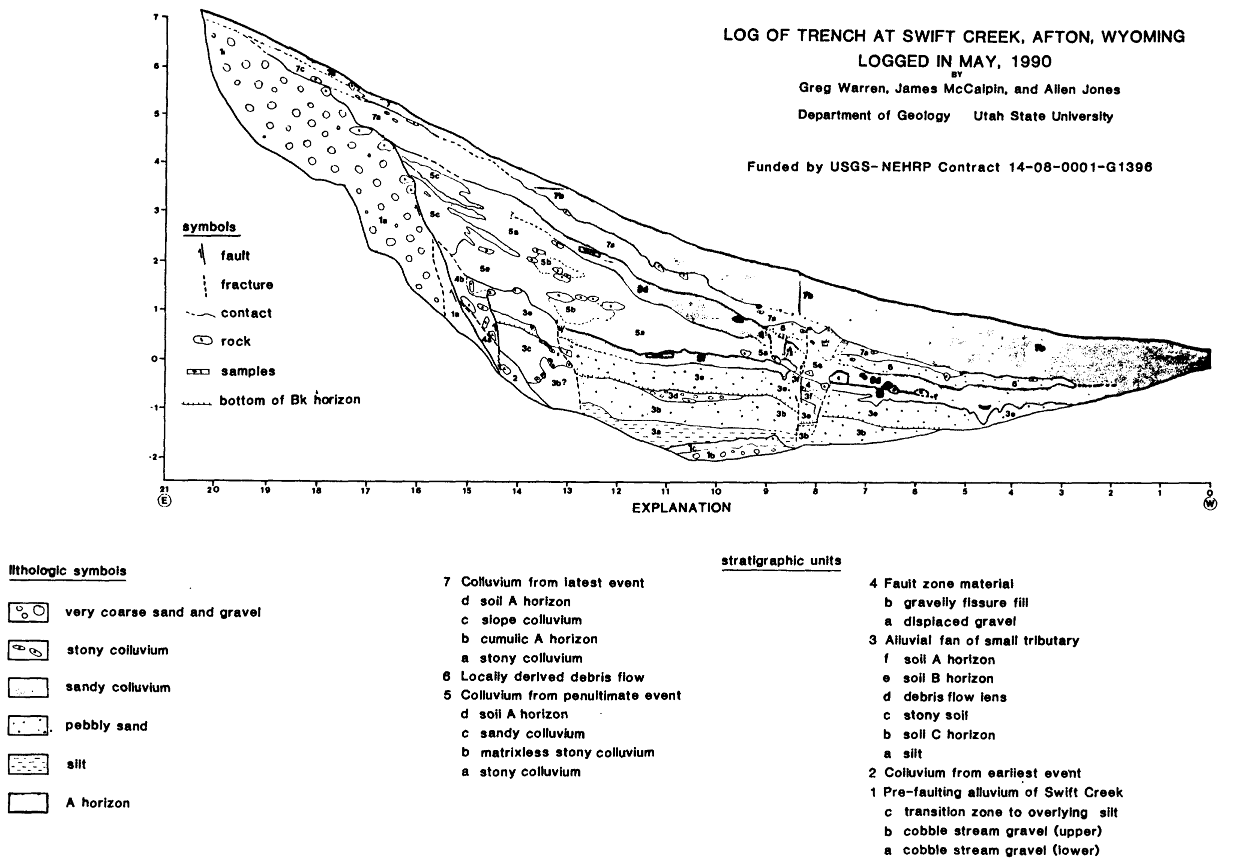

Fig. 1. Log of a trench across the southern segment of the Star Valley fault at the mouth of Swift Creek, Afton, Wyoming. Three colluvial wedges downslope from the main fault zone (15 m on log) suggest three paleoseismic ruptures created the 9.6 m of surface offset here. Radiocarbon samples from the two linear boxes in units 3f and 5d are currently being analyzed.

ACTIVE MARGIN TECTONICS, PACIFIC NORTHWEST REGION

9910-04492

P. A. McCrory

Branch of Engineering Seismology and Geology
U.S. Geological Survey
345 Middlefield Road, MS 977
Menlo Park, California 94025
(415) 329-5677 or (FTS) 459-5677

Investigations

Document recent tectonic deformation in the vicinity of the Puget Sound metropolitan area and relate it to the earthquake potential in this region.

Results

1. FY90 research focused on tectonically deformed sediments exposed along the coast of the Quinault Indian Reservation, Washington. Preliminary stratigraphy has been constructed for three key sedimentary sequences within the Quinault Formation: the Point Grenville, Taholah, and Duck Creek sections. The next task will be to determine the age of these sequences so as to understand the rates at which the sedimentary units are being compressed and tilted.

2. Rock samples collected in FY89 are being reprocessed to concentrate microfossils for analyses of age and uplift data.

3. Analyses of rock samples collected in FY89 for age and uplift data are in progress.

Reports

None this reporting period.

NORTHERN SAN ANDREAS FAULT SYSTEM: PALEOSEISMIC AND SLIP RATE STUDIES IN NORTHERN AND CENTRAL CALIFORNIA

9910-04483

CAROL PRENTICE

BRANCH OF ENGINEERING SEISMOLOGY AND GEOLOGY
345 MIDDLEFIELD RD, MS 977
MENLO PARK, CA 94025
415-329-5690

Investigations

1) Investigations of the San Andreas and related faults in northern and central California to determine timing of prehistoric earthquakes and average Quaternary slip rates. 2) Investigations of the Loma Prieta earthquake.

Results

1) Studies of excavations at two sites are yielding paleoseismic data for faults of the San Andreas system in northern and central California: 1) on the Carrizo Plain along the San Andreas fault in central California, and, 2) along the Maacama fault near Ukiah, CA. Excavation sites along the peninsular segment of the San Andreas fault are being evaluated for paleoseismic and slip rate potential. Results from the first two sites are summarized below:

An excavation across the San Andreas fault on the Carrizo Plain in central California has yielded evidence for at least six earthquakes. The most recent earthquake is known from historical records to have occurred in 1857. This study shows that an earthquake prior to 1857 occurred after the deposition of a unit with a corrected radiocarbon age of 1365 ± 165 AD. The third event back occurred before the deposition of a unit formed in 1190 ± 80 AD. All six events occurred after the deposition of a unit that is about 3000 years old. These data imply a long recurrence interval for this fault segment.

The excavation at the City of Ten Thousand Buddhas, in Talmage, near Ukiah, California, exposed a sequence of marsh, fluvial and lacustrine deposits overlying a paleosol developed on Pleistocene (?) gravel. The Maacama fault, clearly expressed in the older gravels, has not caused any brittle deformation of the overlying Late Holocene section. The section instead has been warped.across the fault zone. Relations indicate that only one warping event has occurred. Results of radiocarbon dating suggest that there has been an earthquake in the last three to four hundred years, and this is the only earthquake to have occurred in the last six to eight hundred years. Further work at this site is expected to yield additional paleoseismic data for the Maacama fault.

2) Investigations following the Loma Prieta earthquake of October, 1989, included mapping of ground fractures and study of the historical record to compare the effects of the 1906 earthquake along this segment of the San Andreas fault with the effects of the 1989 earthquake. In this region in 1906, as in 1989, many large ground cracks opened up in the Summit Road and Skyland Ridge areas. No surface rupture occurred along the San Andreas in 1989; it is not possible to determine from the published report documenting the effects of the 1906 earthquake whether of not surface rupture occurred along the main trace of the San Andreas fault at that time. Left-lateral offset was documented (off the main trace of the San Andreas fault) in 1906 near the Morrell ranch; a smaller amount of left-lateral offset occurred on this same fracture as a result of the 1989 earthquake. Ongoing research into the archival and other historical information available for 1906 is providing new insights into the observations made in the southern Santa Cruz Mountains after the 1906 earthquake. Field work and analysis of aerial photographs suggest a youthful, through-going fault for this region, but no clear-cut evidence for 1906 rupture has been found so far.

Reports

Prentice, C.S. and Schwartz, D.P., 1990, Surface fractures associated with the 1906 and 1989 earthquakes: 1906 and 1989 compared; *in* Schwartz, D. P. and Ponti, D. J., *eds:* Field Guide to Neotectonics of the San Andreas Fault System, Santa Cruz Mountains, in Light of the 1989 Loma Prieta Earthquake, Seis. Soc. Am. Annual meeting. U.S.G.S. Open-File Report 90-274.

Schwartz, D.P., and Prentice, C.S., 1990, Surface fractures in the Loma Prieta area, CA; 1906 & 1989: [abs.] Seismological Society of America, 1990.

Schwartz, D. P., Prentice, C. S., and Fumal, T., Geologic constraints on earthquake recurrence models, Santa Cruz Mountains segment, San Andreas fault zone [abs.] *in press* EOS.

The Bootheel Fault, Southeastern Missouri, and Its Relationship to the New Madrid Seismic Zone

14-08-001-G1772

Eugene S. Schweig, III
Center for Earthquake Research and Information
Memphis State University
Memphis, TN 38152
(901) 678-2007

Objective:

Although the New Madrid seismic zone is the site of the greatest historical earthquakes in eastern North America, the surface expression of the causative fault(s) for these earthquakes has never been found. However, during a comprehensive remote sensing examination of the New Madrid seismic zone (Marple, 1989) a discontinuous linear feature was discovered that may be the surface expression of at least one of the coseismic faults of the New Madrid earthquakes of 1811 and 1812 (Figure 1). We now call this feature the Bootheel lineament. The objectives of this study are to demonstrate whether the lineament is indeed a fault, and, if it is a fault, to characterize it in terms of its length, geometry, and displacement, and to determine whether or not it has ruptured prior to 1811.

Results to date:

During the latest reporting period we have been mapping the Bootheel lineament in more detail, revealing a much more complex trace than presented in earlier reports (Figure 1). We also have recently obtained a radiometric date on a tree stump from the second trench site. The tree stump was located immediately below the surface buried by liquefied sand in the graben area of the second trench. The sand in one of the dikes flowed around the stump (Figure 2), and thus the wood predates the earthquake that liquefied the sand. The stump was radiometrically dated at 505±75 years by means of ^{14}C analysis. This is compatible with other data suggesting that the latest tectonic activity on the lineament dates from 1811 and 1812.

Four more trenches are being excavated in October and November, 1990. Two of these are along features that have the potential to show the amount of lateral offset, if any, that exists along the Bootheel lineament.

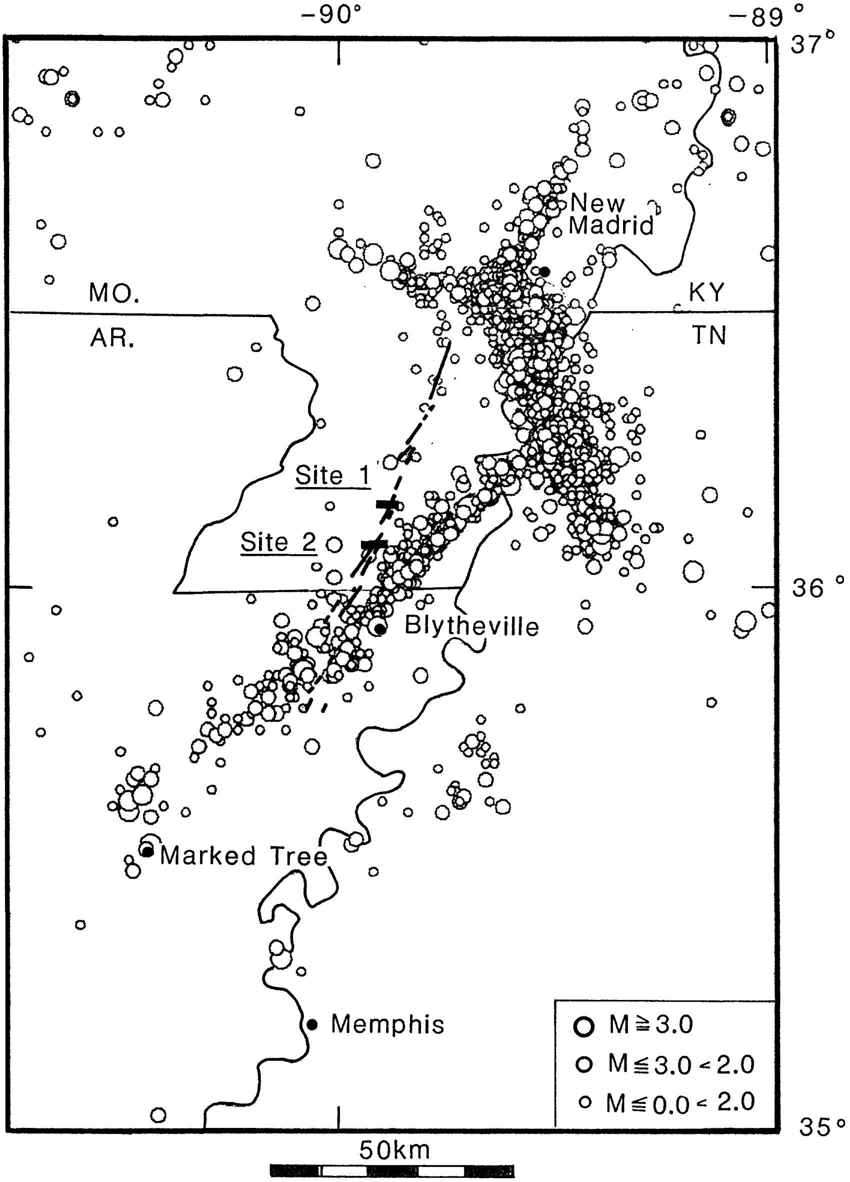

Figure 1: The Bootheel lineament shown in relation to the New Madrid seismic zone (1974-1987). The sites of the first two trenches are also shown.

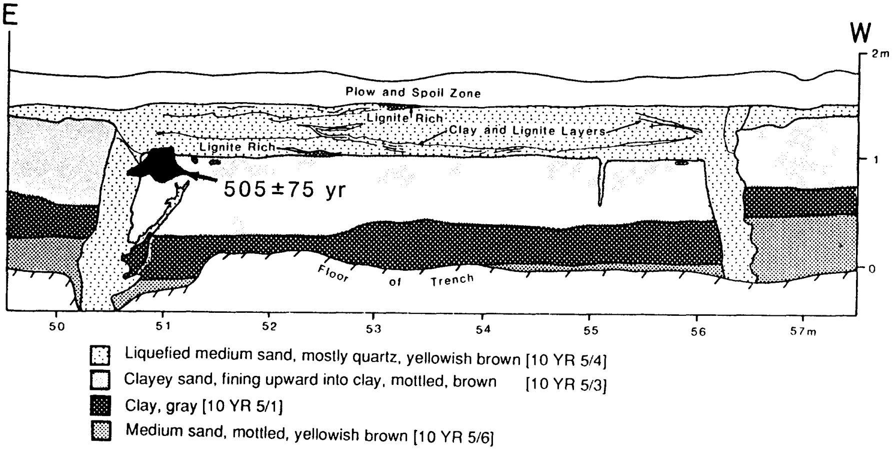

Figure 2: Log of a portion of the trench across the Bootheel lineament at site 2 (see Figure 1 for location). The downdropped block between the two sand dikes underlies the trace of the lineament. The location of the dated tree stump, projected from the opposite wall of the trench, is also indicated. Horizontal scale is meters from east end of trench.

Reports:

Marple, R.T., 1989, Recent discoveries in the New Madrid seismic zone using remote sensing [M.S. thesis]: Memphis, Tenn., Memphis State University, 81 p.

Marple, R.T., and Schweig, E.S., III, 1989, Remote sensing of alluvial terrain in a tectonically active setting of the midcontinent: the New Madrid seismic zone: Geological Society of America Abstracts with Programs, v.21, p. A372.

Schweig, E.S., III, and Jibson, R.W., 1989, Surface effects of the 1811-1812 New Madrid earthquake sequence and seismotectonics of the New Madrid seismic zone, western Tennessee, northeastern Arkansas, and southeastern Missouri *in* Vineyard, J.D., and Wedge, W.K., eds., Geological Society of America 1989 Field Trip Guidebook: Missouri Division of Geology and Land Survey Special Publication 5, p. 47-67.

Schweig, E.S., III, and Marple, R.T., 1989, The Bootheel lineament in southeastern Missouri and northeastern Arkansas: a co-seismic fault of the New Madrid earthquakes?: Geological Society of America Abstracts with Programs , v. 21, p. A186.

Schweig, E.S., III, and Marple, R.T., 1990, The Bootheel lineament, northeastern Arkansas, and the New Madrid seismic zone, *in* Guccione, M.J., and Rutledge, E.M., eds., Field guide to the Mississippi alluvial valley, northeast Arkansas and southeast Missouri: Friends of the Pleistocene South-Central Cell, p. 265-277.

Schweig, E.S., III, and Marple, R.T., The Bootheel lineament: A possible coseismic fault of the great New Madrid earthquakes: submitted to *Science*.

PALEOSEISMOLOGICAL STUDIES IN SOUTHERN CALIFORNIA

Grant Number 14-08-0001-G1789

Kerry Sieh
Seismological Laboratory
California Institute of Technology
Pasadena, CA 91125
(818) 356-6115

During the six month period ending October 1990, I and my graduate students, in collaboration with Carol Prentice of the U. S. Geological Survey, have made progress in several areas:

1) Bidart Site

Knowledge of the dates of the past few great earthquake ruptures in the Carrizo Plain would increase the likelihood of successful forecasts of future great earthquakes along the southern half of the San Andreas fault. Currently, intervals are believed to range from about 250 to 450 years, based upon our knowledge of the long-term slip rate and geomorphic evidence for the amount of slip during the past several earthquakes (Sieh and Jahns, 1984). This suggests that the Carrizo segment of the fault has a very low probability of rupturing in the next few decades. It also suggests that the next few Parkfield earthquakes are unlikely to trigger a great earthquake involving rupture of the Carrizo segment.

Unfortunately, the geomorphic basis of this important conclusion is tenuous. Thus, we have sought to date and characterize the past several earthquakes more convincingly. To this end, we excavated and logged one wall of a trench across the Carrizo segment of the San Andreas fault in May and July 1989. During March and April 1990 we reopened the trench and logged the opposite wall. This confirmed our earlier findings that several large rupture events are recorded by these sediments. These ruptures are clearly indicated by upward truncations of fault planes and facies variations in alluvial fan and pond deposits. The characteristics of the sediments are such that we are confident that we have a complete record of at least the latest three events. Within the past year we received the results of radiocarbon analyses of samples collected from the trench. The radiocarbon dates indicate that two slip events have occurred at the Bidart site since about 1260 A.D. The carbon sample that was dated at 1260 A.D. was considerably below the horizon of the penultimate event. Thus the data are consistent with our earlier suspicions that the past three ruptures of the Carrizo segment of the San Andreas fault may correlate with ruptures documented at Pallet Creek that occurred around 1100 A.D., around 1480 A.D. and in 1857 A.D.

We have also recognized evidence for large events at five distinct horizons deeper in the trench. Radiocarbon dates constrain the first of these to about 3000 yrs BP. The second and third occurred between about 3000 and 1800 years BP, and the fourth and fifth occurred between about 1800 years BP and about 700 years ago. The occurrence of these five large faulting events in the past 3,000 years suggests an average recurrence interval of about 500 years, although the interval would be less if we do not have a complete record.

3) Phelan Site

Dextral offsets of small stream channels in the Carrizo Plain occur in rough multiples of 10 meters (Sieh, 1978). This observation is the basis for the interpretation that 10 meters is the magnitude of slip associated with each large earthquake produced by this section of the fault. If this interpretation is correct, this section of the fault must rupture about every 250 to 450 years (Sieh and Jahns, 1984).

In order to test this interpretation, Lisa Grant, several other graduate students and I continued 3-D excavations of an alluvial fan/channel complex that crosses the San Andreas fault in the Carrizo Plain. During March 1990, we excavated and logged two new trenches at this site. In combination with three trenches that were dug at this site earlier, the new trenches revealed two buried channels, the projections of which are each offset 6.3 to 7.9 meters. Radiocarbon analysis of carbon samples collected from these channels bracket the age of the channels. We exposed one of the channel offsets in a 3-D excavation in September 1990. Thus, we confirmed the 7-meter offset and placed constraints on the amount of dextral warp within a few meters of the fault trace. This excavation appears to support the hypothesis that the Carrizo Plain segment of the San Andreas fault ruptures in large-magnitude slip events spaced relatively far apart in time. However, we are still analyzing the large amount of data we collected in September, so our conclusions are tentative.

4) Garlock fault

Graduate student Sally McGill has submitted to JGR a paper that characterizes the most recent slip events along the eastern Garlock fault, based on offset geomorphic features. Along the easternmost 90 km of the fault, the smallest offsets cluster around 3 m, indicating that the latest earthquake on this portion of the fault was produced by about 3 m of left-lateral slip. Larger offsets along this part of the fault, especially in Pilot Knob Valley, cluster around values consistent with 2 to 4 m of slip in each of the past six events. Farther west, near Highway 395, offset geomorphic features suggest that the past two earthquakes on this stretch of the Garlock fault were produced by about 7 m of slip, whereas the third event back was produced by about 4 m of slip.

Based on the geomorphic data, on the geometry of the Garlock fault, and on the precedents set by historical strike-slip earthquakes, a number of distinct rupture scenarios are plausible. These range from rupture of the entire Garlock fault in a single event of magnitude Mw=7.8, to separate rupture of the eastern and western segments of the fault with magnitudes Mw=7.5 and Mw=7.6, respectively, to separate rupture of even shorter segments, producing earthquakes of magnitudes Mw=7.0 to Mw=7.5.

In conjunction with the available slip-rate data for the Garlock fault, the geomorphic data suggest that recurrence intervals ranging from 250 yr to 1000 yr are plausible for individual segments of the Garlock fault. One plausible slip-rate model for the Garlock fault implies recurrence intervals of about 1000 yr for the portion of the fault near Highway 395, about 420 yr in Searles Valley, about 600 yr in Pilot Knob Valley, and about 1000 yr from the Quail Mountains to the eastern end of the fault.

In order to determine the recurrence interval more directly, Sally excavated two trenches across the Garlock fault in Searles Valley in the Spring of 1990. Several very small samples of carbon will constrain the dates of the four events she recognized in these excavations.

Evaluation of the use of compressive growth structure in Earthquake hazard assessment

14-08-0001-G1699

John Suppe and Richard Bischke

Dept. of Geological and Geophysical Sciences
Princeton University
Princeton, NJ 08544
(609) 258-6769

Investigations:

1) Investigate balancing techniques that determine fault geometry and position in the subsurface.
2) Identify active thrust faults and construct balanced cross sections of their geometry.
3) Utilize growth fault-bend and fault-propagation fold theory to determine the long term kinematic history and slip rates along blind thrust faults.

Present Results:

Two common fold styles exist throughout the world under compressive environments, the symmetric fault-bend folds and the asymmetric fault-propagation fold (FPF) types, although other styles and geometries exist (Suppe, 1983 and 1985). Field investigations and theoretical considerations suggest two end-member types of fault-propagation folds: constant thickness FPF in which the thickness of the horizons are constant from the fold crest and through its frontal limb (Fig. 1), and fixed axis FPF in which layer thickness either thicken or thin across the frontal limb and crest of these asymmetric structures (Fig. 2; Suppe and Medwedeff, 1990). In constant thickness FPF axial surfaces A-A' generally migrate relative to each other and with respect to surrounding existing and recently deposited (growth) sediments, whereas in the fixed axis model axial surface A is locked relative to surrounding materials. These kinematic relationships permit an interpreter to distinguish between the different fold types, particularly where the fold is growing contemporaneous with (growth) sediments that cover the flanks of the structure (Suppe et al., 1990). Suppe and Medwedeff (1990) have investigated 19 well constrained folds throughout the world in order to determine how these folds conform to theory (Fig. 3). Most of the folds appear to obey the constant thickness theory, while several folds appear to conform to the fixed axis theory. We are currently investigating the Oak Ridge structure (Figure 4) which is located in the Ventura basin, California between the South Mountain and Saticoy oil fields. Well log, seismic, and surface data agree very well with theory and constrain the interpretation to suggest that a blind thrust fault ramps off a bedding plane decollement at a depth of about 5 km. Also notice that in this balanced interpretation the preexisting Oak Ridge normal fault has been folded by the Oak Ridge Anticline, presently bounding its frontal limb. Unfolding the anticlinal structure predicts that the Oak Ridge normal fault initially dipped at 65-70° which is consistent with the initial dip of many normal faults (Xiao and Suppe, 1989). Furthermore, seismic imaging of the structure in a down plunge position (Figure 5) shows a geometry of the growth strata that agrees with the predictions of fault-propagation folding (Figure 6). Continuing studies are seeking to obtain the stratigraphic and structural control to precisely constrain long-term slip rates.

References

Suppe, J., 1983. Geometry and kinematics of fault-bend folding, Amer. Jour. Sci., v. 83, p. 648-721.

Suppe, J., 1985. Principles of Structural Geology, Prentice-Hall, N.J., 537p.

Suppe, J. and D.A. Medwedeff, 1990. Geometry and kinematics of Fault-Propagation folding, Eclogae Geol. Helv., v. 82, Laubscher volume, in press.

Suppe, J., G.T. Chou and S.C. Hook, 1990. Rates of folding and faulting determined from Growth Strata, in Thrust Tectonics, K.R. McClay ed., Unwin Hyman, Publisher, in press.

Xiao, H. and J. Suppe, 1989. Role of compaction in Listric shape of Growth Normal Faults, AAPG.Bull., v. 73, p. 777-786.

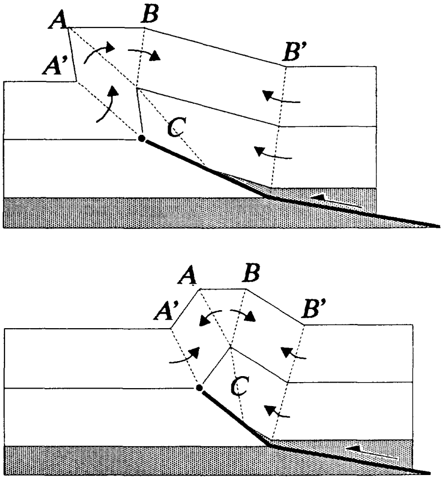

Constant thickness model

Figure 1

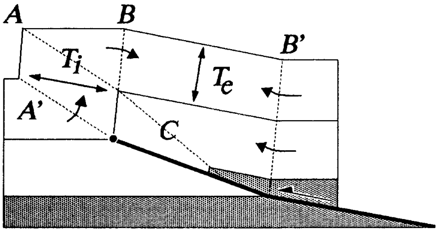

thickening

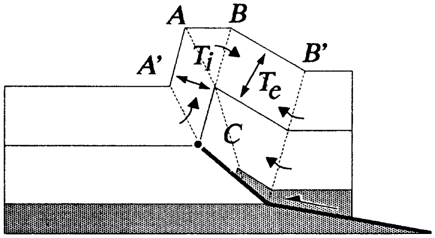

thinning

Fixed axial surface model

Figure 2

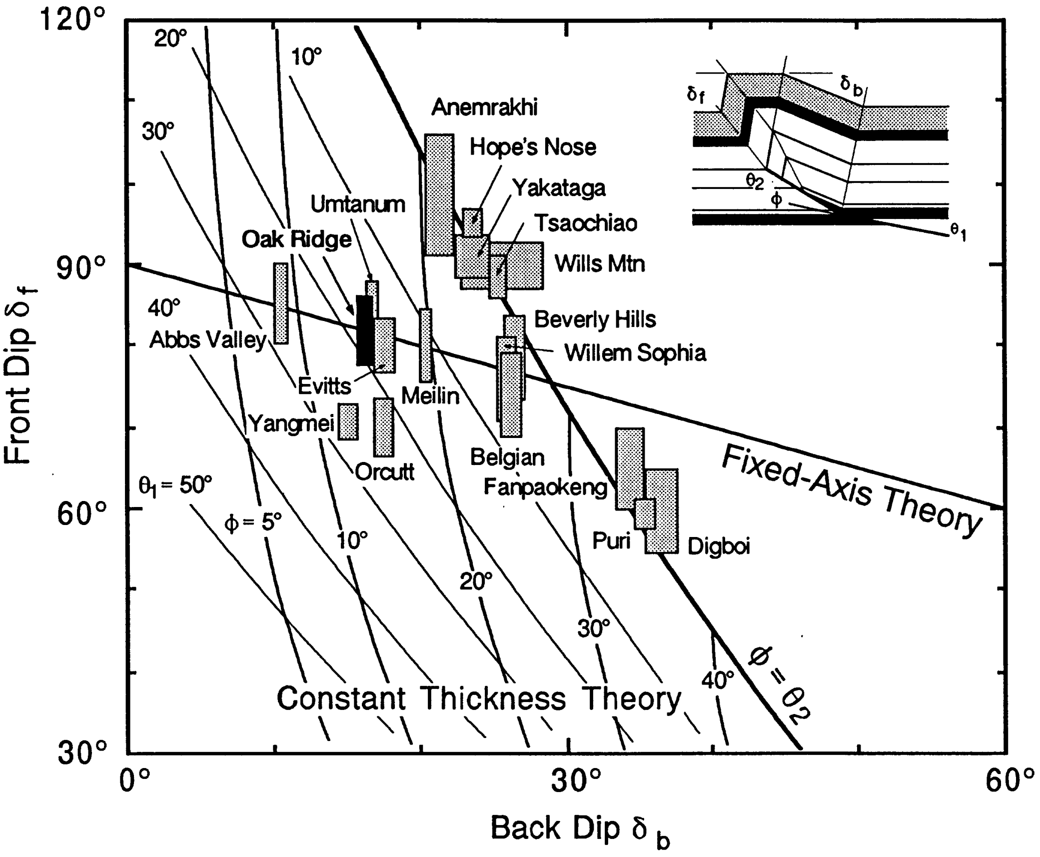
120°
90°
60°
30°
0°
30°
60°
Front Dip δf
Back Dip δ b
20°
10°
30°
40°
θ1 = 50°
φ = 5°
10°
20°
30°
40°
Anemrakhi
Hope's Nose
Yakataga
Tsaochiao
Wills Mtn
Umtanum
Oak Ridge
Beverly Hills
Willem Sophia
Abbs Valley
Evitts
Meilin
Yangmei
Orcutt
Belgian
Fanpaokeng
Puri
Digboi
Fixed-Axis Theory
Constant Thickness Theory
φ = θ2
δf
δb
θ2
φ
θ1

Figure 3

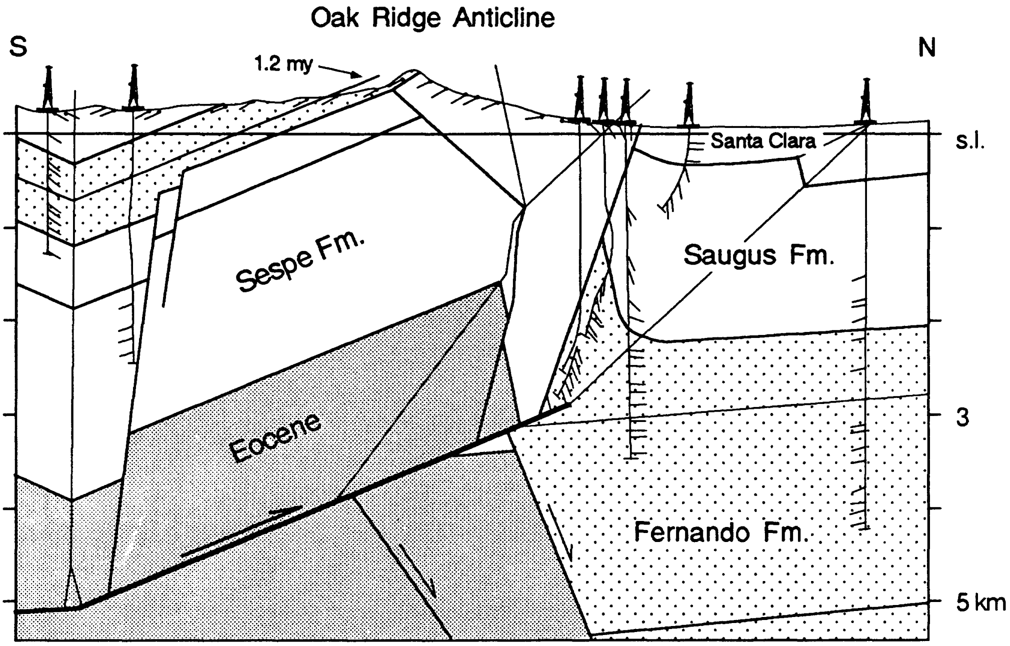

Ventura Basin, California

Figure 4

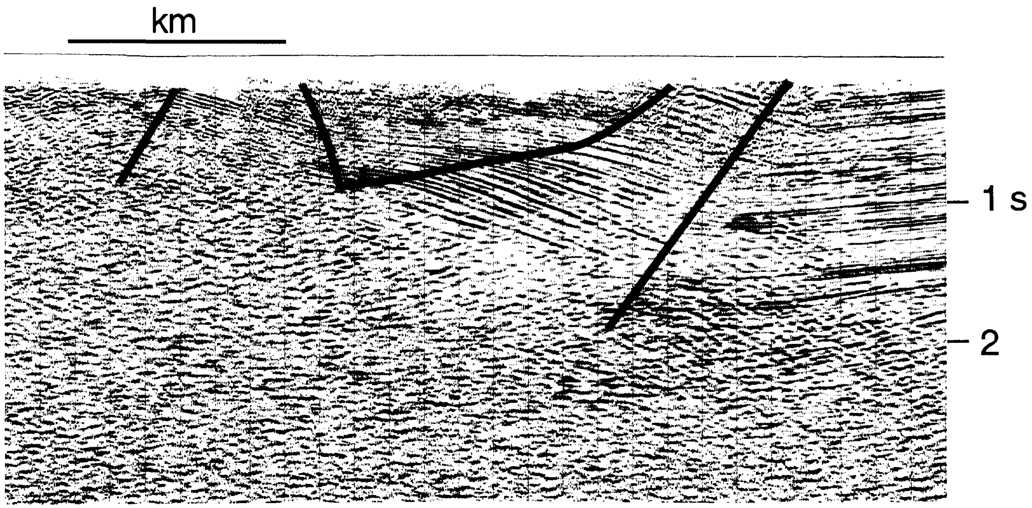

Figure 5

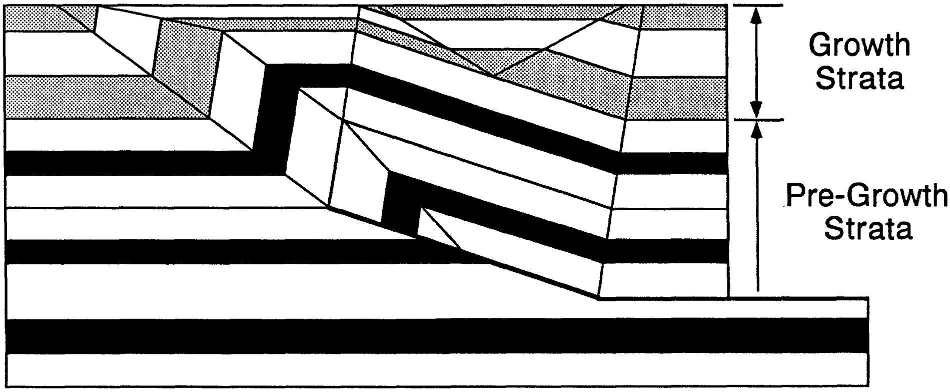

Figure 6

Paleomagnetic Investigations of Non-Brittle Deformation along Active Faults

Agreement No. 14-08-0001-G1814

Kenneth L. Verosub
Department of Geology
University of California - Davis
Davis, California 95616

(916) 752-6911 or 0350

Data from an earlier paleomagnetic study of two units sampled in a trench across the San Andreas fault at Pallett Creek imply that in the last three earthquakes at this site a significant amount of the movement across the fault had been taken up by non-brittle deformation. If the phenomenon observed at Pallett Creek occurs frequently elsewhere, we may have been seriously underestimating the earthquake potential of active faults. The purpose of this project is to determine whether evidence for the importance of non-brittle deformation can be found at other sites besides Pallett Creek. If such evidence exists, it is important to determine the extent to which the slip is being underestimated and the width of the zone that is being affected by the non-brittle deformation. If evidence for non-brittle deformation is not found at other sites, the results from Pallett Creek are still relevant to the earthquake history of the San Andreas Fault and to the evaluation of the earthquake risk in southern California. Therefore this project is also addressing the question of whether a different analysis of the data from Pallett Creek can lead to an alternate interpretation of the amount of non-brittle deformation observed there.

Our primary research effort involves paleomagnetic sampling of fine-grained material in trenches that expose active strike-slip faults. Within a given trench, selected units will be sampled at the fault and at various distances from the fault. At the present time, we are contacting other researchers to locate trenches that have been opened and logged either by U.S.G.S. personnel or by NEHRP-funded researchers from private industry and academic institutions.

Continuation of Paleoearthquake Study in the New Madrid Seismic Zone

14-08-0001-G1791

Steven G. Wesnousky
Center for Neotectonic Studies
University of Nevada
Reno, Nevada 38152
702-784-6067

Objective: For purposes of flood control and land reclamation, the U.S. Army Corps of Engineers has recently reexcavated and widened an extensive set of drainage ditches within the Saint Francis drainage basin. The majority of the ongoing and planned excavations cut through the meisoseismal zone of the great 1811-12 New Madrid earthquakes. The 1811-12 earthquakes produced extensive liquefaction within the New Madrid Seismic zone at the time of the earthquakes. Evidence of that liquefactiction still exists in the geologic record. The ditches provide an opportunity to systematically examine and document the geological record of liquefaction in the New Madrid Seismic Zone. The objective of this study is to document liquefaction phenomena exposed in the ditches and determine whether or not evidence for pre-1811-12 earthquakes exists.

Progress: The contour and shading within the inset of Figure 1 shows the region where liquefaction deposits (i.e. extruded sands) attributed to the 1811-12 earthquakes still comprise greater than 1% and 25% of the ground cover, respectively. The ditches are situated on braided stream terrace deposits associated with the retreat of the last glaciation and, hence, on a surface that has been relatively stable during the last 6 thousand to 10 thousand years. The upper few meters of the stratigraphy of the braided stream terrace deposits and visible in the ditches is generally quite simple, consisting of very fine to fine sands overlain by a clay and silt-rich topstratum of low permeability. Toward identifying possible evidence of paleoliquefaction, we have walked the length of the reexcavated ditches in Figure 1 and searched for breaches in the clay-rich topstratum. In this manner, we systematically identfy sites of sandblows and sand dikes. Those sections of the ditches showing a greater concentration of liquefaction phenomena are later logged in greater detail. More specifically, we establish benchmarks that may later be reoccupied and use a *Total Station* to survey the upper and lower contacts of the clay-rich topstratum or 'clay cap'. The surveying serves to document the general character of liquefaction phenomena along the ditches and permanantly document their location for later study by ourselves and others in the future.. Sections of the ditches we have logged in this way are labeled Log 1, Log 2, and Log 3 in Figure 1. Currently, we are extending the logging eastward along the Pemiscot Bayou and northward to the vicinity of New Madrid. The pervasive nature of liquefaction is illustrated by the numerous breaches of the clay-rich topstratum by liquefied sands observed in the Log 2 pictured in Figure 2. Towards looking for evidence of pre-1811-12 liquefaction, ruptures or breaches in the 'clay cap' are further cleaned off by hand shovel or backhoe to be photographed and logged in detail. Two sites for which we have completed detailed logging are labeled Sites 1 and 2 in Figure 2,respectively. At both Sites 1 and 2, as well as others along Log 2 and 3 in Figure 1, evidence of only 1 major liquefaction event is recognized. A buried log recovered from the section in site 1 was radiocarbon dated at about 5,000 years B.P. Very weak soil development upon extruded sands is characteristic of all liquefaction features documented thus far. The simplest hypothesis to explain the observations thus far collected is that only one major liquefaction event has occurred in this area during at least the last 5,000 years, and that liquefaction event is most reasonably attributed to the 1811-12 sequence of earthquakes.

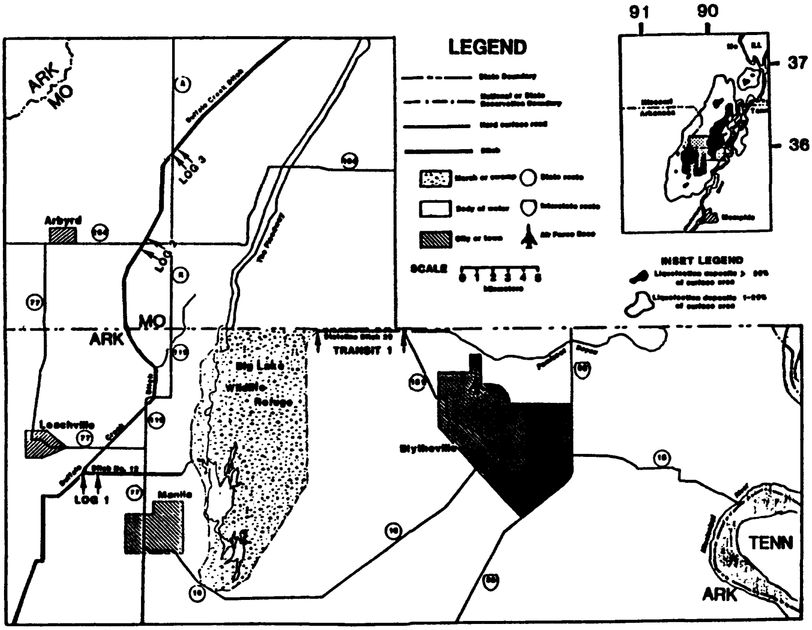

Figure 1.

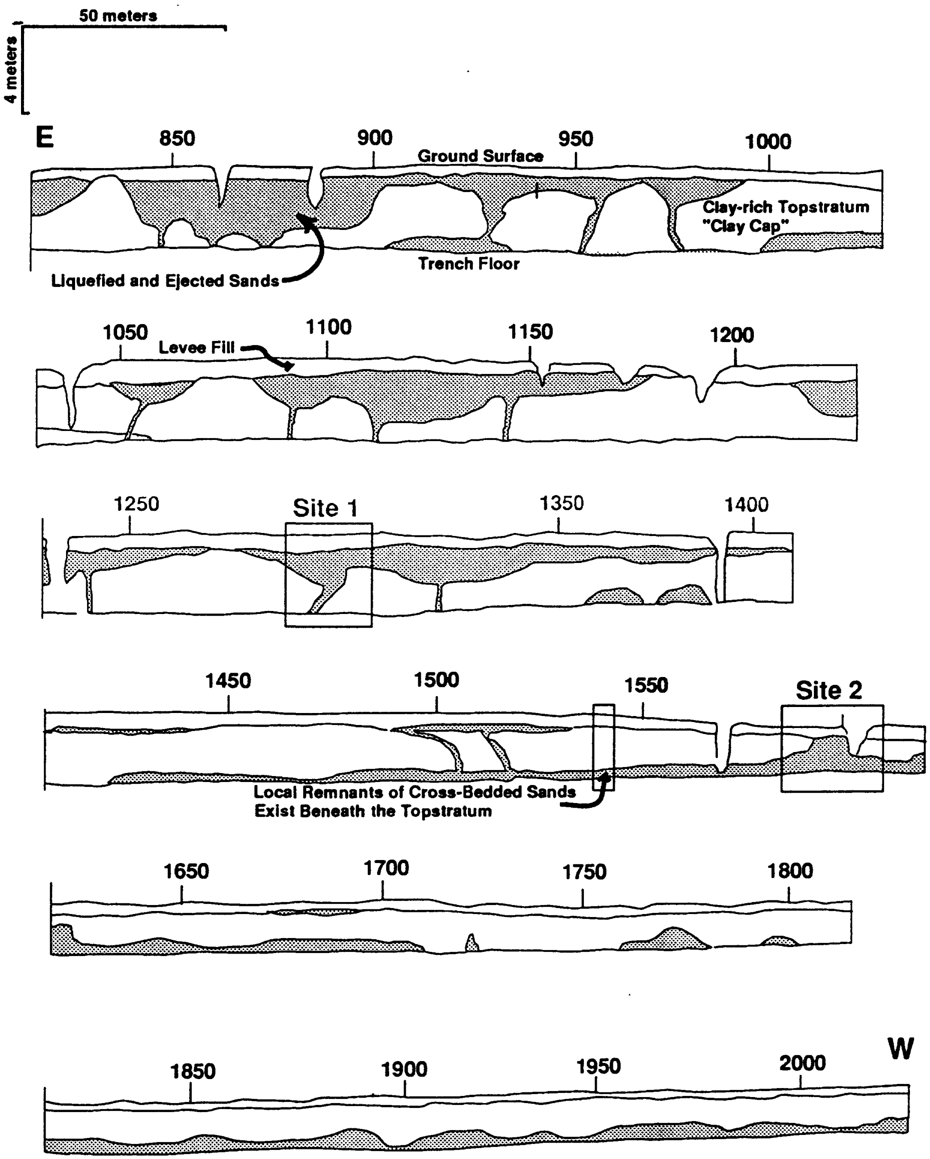

Figure 2. Log of the south side of Ditch No. 12. Locality shown in Figure 1.

Convergence Rates Across Western Transverse Ranges

14-08-0001-G1372 and -G1798

Robert S. Yeats and Gary J. Huftile
Department of Geosciences
Oregon State University
Corvallis, OR 97331-5506
(503) 737-1226

Investigations

A new retrodeformable cross section from the Simi fault, just west of Simi Valley, to the San Gabriel fault (F-F′ on Figure 1) was constructed by Prof. Lu Huafu of Nanjing University. This section crosses the Santa Clara Valley near the eastern ends of the surface traces of the San Cayetano and Oak Ridge faults and the western end of the Santa Susana fault. The cross section addresses the transfer of displacement from one major fault to another near a possible segment boundary.

Two cross sections were completed across the central Ventura basin (A-A′, B-B′) and retrodeformed to the top of the Saugus Formation. The cross sections document the displacement transfer between active surface reverse faults and blind thrusts. The western cross section crosses the active, north-dipping Red Mountain fault. The eastern cross section crosses Ojai Valley where there is no active, north-dipping reverse fault, and displacement is taken up on a blind thrust. A third cross section (C-C′) is in preparation across the north-dipping western San Cayetano fault. These three cross sections will be published together.

Other cross sections in preparation are (1) South Mountain to Timber Canyon, crossing the Oak Ridge and San Cayetano faults (D-D′), (2) eastern Oak Ridge to the Modelo lobe of the San Cayetano fault (E-E′), (3) central Santa Susana fault near the Gillibrand Canyon lateral ramp to the San Gabriel fault (G-G′), and (4) eastern Santa Susana fault at Aliso Canyon field to the San Gabriel fault (H-H′).

Results

The east Ventura basin fold belt consists of a fold train cut by south-dipping reverse faults which are, from north to south, the Santa Felicia, Oak Canyon, Hasley, Holser, and Del Valle faults. The Santa Felicia fault overrides and postdates the San Gabriel fault. The San Gabriel fault now dips east, but prior to Pliocene and Pleistocene deposition, the fault dip was essentially vertical. The two southern faults (Holser and Del Valle) are the largest, and the folds cut by them have the greatest structural relief. The south-dipping faults are best explained as backthrusts above north-dipping blind thrusts that are part of the San Cayetano fault system. Surface displacement on the San Cayetano fault west of Piru Creek gives way eastward to the east Ventura basin fold train and to the blind thrusts, of which only the backthrusts are expressed at the surface.

Below the two blind thrusts that are directly related to the south-dipping backthrusts from the Holser fault northward is the Santa Susana fault which produces the Del Valle backthrust and extends southward to the surface at Oakridge oil field, where it overrides an older strand of the Oak Ridge fault.

Convergence on sections A-A' and B-B' in the last 300±100 ka, the age of the top of the Saugus Formation, is 5.9 km and 4.5-5.5 km respectively. Post-Saugus shortening rates are 1.5-3.0 cm/y along A-A' and 1.1-2.7 cm/y along B-B'.

Reports

Huftile, G. J., 1991, Thin-skinned tectonics and oil accumulation of the Upper Ojai Valley and Sulphur Mountain area, Ventura basin, California: in press, American Association of Petroleum Geologists Bulletin.

Huftile, G. J., in prep., Displacement transfer between surface reverse faults and blind thrusts, central Ventura basin, California: to be submitted to Tectonics.

Huftile, G. J., and Yeats, R. S., in prep., Cenozoic structure of the Piru 7½-minute quadrangle, California: to be submitted to USGS as an open-file report.

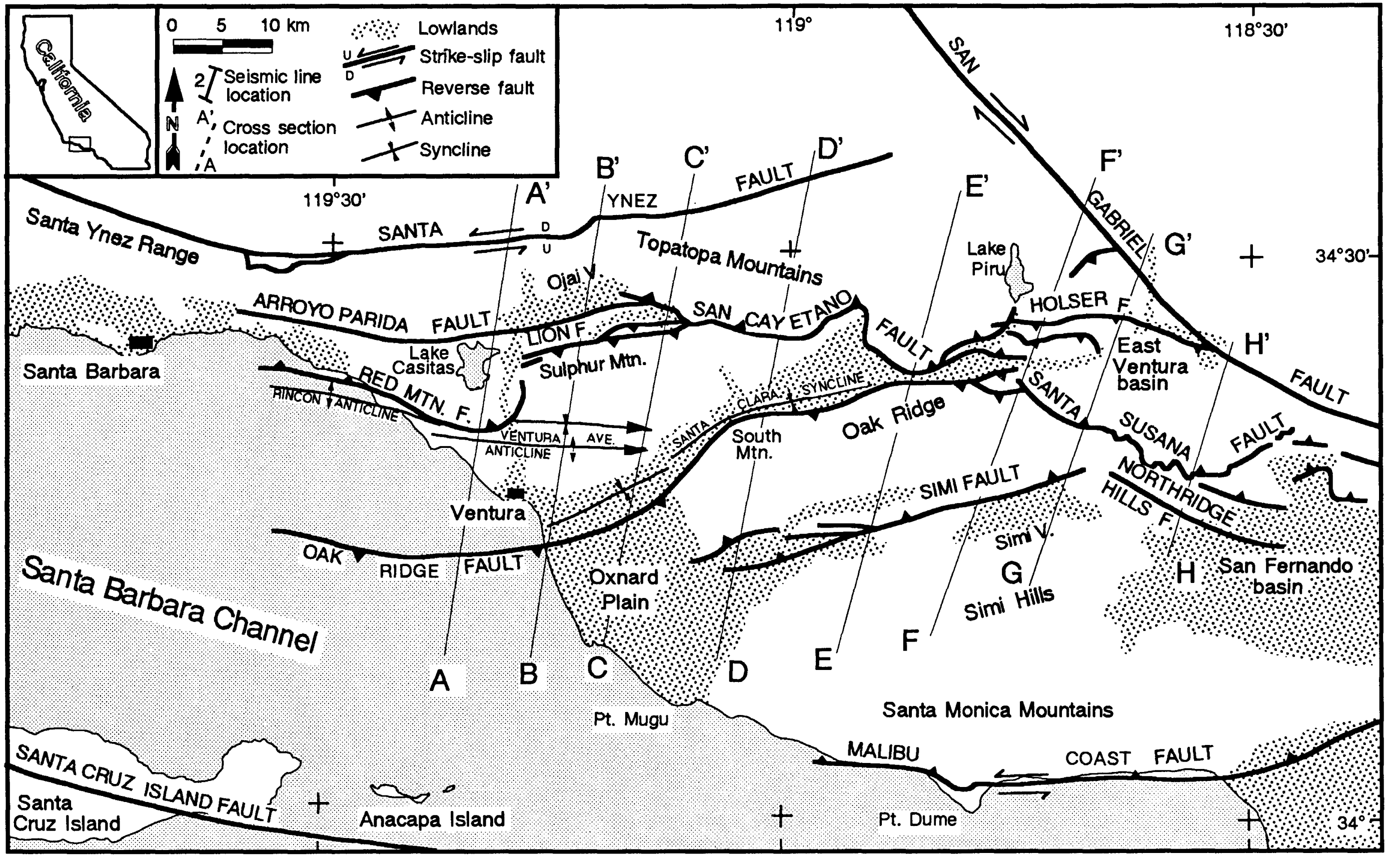
California
0 5 10 km
Seismic line location
2
N
A'
A
Cross section location
Lowlands
Strike-slip fault
U
D
Reverse fault
Anticline
Syncline
119°30'
119°
118°30'
34°30'
34°
Santa Ynez Range
SANTA YNEZ FAULT
Topatopa Mountains
Ojai V.
ARROYO PARIDA FAULT
LION F.
SAN CAYETANO FAULT
Sulphur Mtn.
Lake Casitas
Santa Barbara
RED MTN. F.
RINCON ANTICLINE
VENTURA AVE. ANTICLINE
Ventura
SANTA CLARA SYNCLINE
South Mtn.
Oak Ridge
OAK RIDGE FAULT
Oxnard Plain
SIMI FAULT
Simi V.
Simi Hills
SAN GABRIEL FAULT
Lake Piru
HOLSER F.
East Ventura basin
SANTA SUSANA FAULT
NORTHRIDGE HILLS F.
San Fernando basin
Santa Barbara Channel
Santa Monica Mountains
Pt. Mugu
MALIBU COAST FAULT
Pt. Dume
SANTA CRUZ ISLAND FAULT
Santa Cruz Island
Anacapa Island
A'
B'
C'
D'
E'
F'
G'
H'
A
B
C
D
E
F
G
H

Figure 1.

On-Line Seismic Processing

9930-02940

Rex Allen
Branch of Seismology
U.S. Geological Survey
345 Middlefield Road, MS 77
Menlo Park, California 94025
(415) 329-4731

Investigations and Results

All RTP software is working on an INMOS system with 3 linked processors. Some bugs remain, but all parts pass individual checks, and at present I am working on what I believe to be the last few problems of communication between Pickers and Associator. Expansion of the system to use as many processors as required for any size seismic net is easy. Currently tests are run with a fake data set to simulate network operation. We expect to be running with actual data from an A/D converter in about six weeks.

The A/D is being built in-house to interface with the INMOS processors. Grey Jensen and Jim Ellis have encountered no serious problems with this design and expect it to be completed soon.

The Mk I RTP's at Menlo Park and the University of Utah have continued to operate satisfactorily, as have the Mk II's at Menlo Park and Caltech.

Long Baseline Tiltmeters: Southern California

14-08-0001-G1790

John Beavan
Lamont-Doherty Geological Observatory of Columbia University
Palisades, New York 10964
(914) 359-2900

Investigations

We operate a 535 m long-baseline half-filled water tube tiltmeter at Piñon Flat Observatory (PFO) in the San Jacinto Mountains of southern California. This is used in conjunction with a similar instrument operated by the University of California, San Diego (UCSD), to investigate:

(1) sources and magnitudes of noise affecting the tilt signal;
(2) water level sensor design and reliability;
(3) methods of referencing tiltmeter to depth;
(4) interpretation of tilt signal.

Results (November, 1990)

1. Tiltmeter Operation and Sensor Development

The LDGO tiltmeter continues to perform reliably, requiring little maintenance. Development of a simple absolute sensor (USGS Open File Report 90-54, pp 163-165, 1989) has been accelerated by our new engineer, and the prototype is in its final stages of completion for installation in California in January 1991. The power requirements have been reduced to about 250 mA at 12 V; since most of the electronics can be turned off between samples this makes the instrument easily operable from batteries for extended periods of time. Circuit boards are currently being made, and the mechanical parts for the end reservoirs are already made and only require coating before being ready for installation.

2. Tiltmeter Data Analysis

The tiltmeter data analysis was discussed in USGS Open File Report 90-334, pp 165-168. The micrometer intercomparison experiment between the LDGO and UCSD tiltmeters has now been terminated. The LDGO interferometers continue to collect data. We plan, in conjunction with UCSD, to publish the full results from the PFO long-baseline tilt experiment during 1991.

Crustal Deformation Measurements in the Shumagin Seismic Gap, Alaska

14-08-0001-G1792

John Beavan
Lamont-Doherty Geological Observatory of Columbia University
Palisades, NY 10964
(914) 359 2900

Investigations

1. Twelve short (~ 1 km) level lines are measured every one to three years within the Shumagin seismic gap, Alaska (Figures 1 and 2). Surface tilt data are interpreted in terms of tectonic deformation and earthquake hazard at the Pacific-North American plate boundary.
2. Six absolute-pressure sea-level gauges are operated in the Shumagin Islands in an attempt to measure vertical deformation associated with the Aleutian subduction zone.
3. The sea-level data are transmitted by satellite in near real time, and are examined for possible tectonic signals. Noise studies are used to determine the relative usefulness of different types of measurement, and to evaluate the minimum size of tectonic signal visible above the noise. Our data are compared with other crustal deformation data from the Shumagin gap.

Results (October 1990)

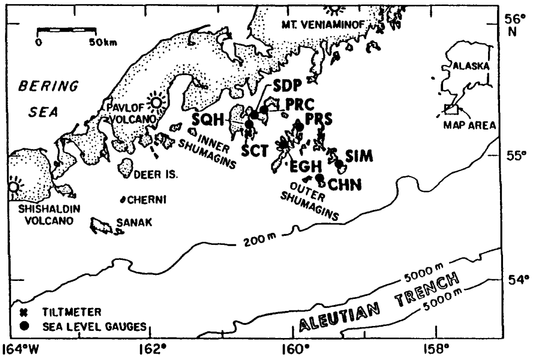

Figure 1. Location of the Shumagin Islands with respect to the trench and the volcanic arc. Depth contours are in metres. The seismic gap stretches from approximately Sanak Island in the west to about 30 km east of the Shumagin Islands. Also shown are the sites of six sea-level gauges operated by LDGO and one by the National Ocean Survey (at SDP). Level lines of approx. 1 km aperture are located on many of the Shumagin Islands, and on Sanak Is.

Field Report (3-28 July, 1990)

The 1990 field season was very successful, despite a run of poor weather during the second set of low tides (when the sea-level gauges are serviced). Our major accomplishments were:

- The pair of perpendicular level lines on S.E. Sanak Island (at the western end of the seismic gap) were remeasured for the first time since their installation in 1988. The tilt rate appears to be significantly greater on these lines than on those at the eastern end of the seismic gap (Figures 3, 4), but with only two measurements it is not yet possible to place great significance on this result. Differences in behavior at either end of the gap have been suggested by Hudnut and Taber [1987].

- The two-component leveling network on N.W. Sanak was successfully measured (this was installed in 1989, but not measured due to poor weather).
- A self-contained sea-level gauge was designed, and three were built and installed at the three sites where we have had the worst record of cable damage. These gauges will store a little over a year's data at 12 minute sampling; the data cannot be recovered until the following field trip.
- The other three sea-level sites continue to transmit data in real time via the GOES satellite. All are operating at the time of writing.
- The solid-state backup recorders we installed at three sites last year proved useful. Well over a month of data would have been lost from site Simeonof due to an early-June failure in the satellite transmitter, but these data were successfully recovered from the backup. There were 1989-90 failures at two other sites that were not backed up.
- Little leveling was done in the Shumagins proper. Two lines were measured fully, and another was measured in one direction only. None of these showed significant deviation from their past behavior (Figures 2, 3; Table 1).
- We made a number of GPS measurements in the Shumagins, using three Trimble 4000SST receivers purchased by Lamont with 50% NSF cost sharing. We took several days of simultaneous data in the Inner (Sand Point) and Outer (Simeonof & Chernabura) Islands, in order to test our receivers and to compare results with previous TI-4100 measurements at these sites by USGS. We used a mode of operation in which the GPS receivers were left to run unattended for up to a week at a time - a tremendous manpower savings over a conventional GPS survey. We also took a further week of data at Sand Point as part of an Alaska-wide campaign that included GPS measurements at all NASA's Alaskan VLBI sites, and with ties to a large GPS experiment in northern Europe. (The GPS part of our fieldwork was supported in part by NASA.)

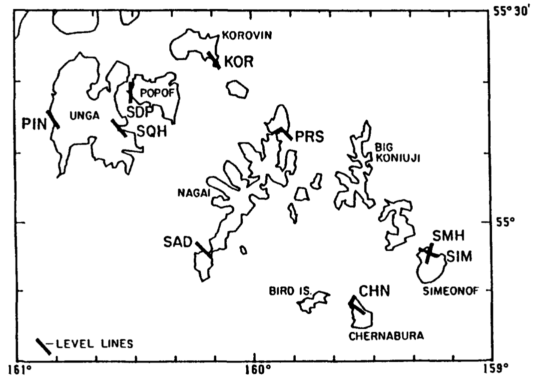

Figure 2. The Shumagin Islands, showing the locations and directions of first-order level lines, whose lengths vary between 600m and 1200m. The resultant of the data from lines SDP and SQH is used to estimate the tilt direction in the Inner Shumagins. The resultant of SIM and SMH is used for Simeonof Island. The lines at CHN and PRS each consist of two approximately straight sections in different azimuths, with benchmarks at the junction. This non-linear geometry allows tilt direction to be estimated at these sites. Two sets of perpendicular level lines have also been installed on Sanak Island, at the western end of the seismic gap (see Fig. 1). One of these, at the SE end of the island was measured in 1988 and 1990. The other, at the NW end, was first measured in 1990.

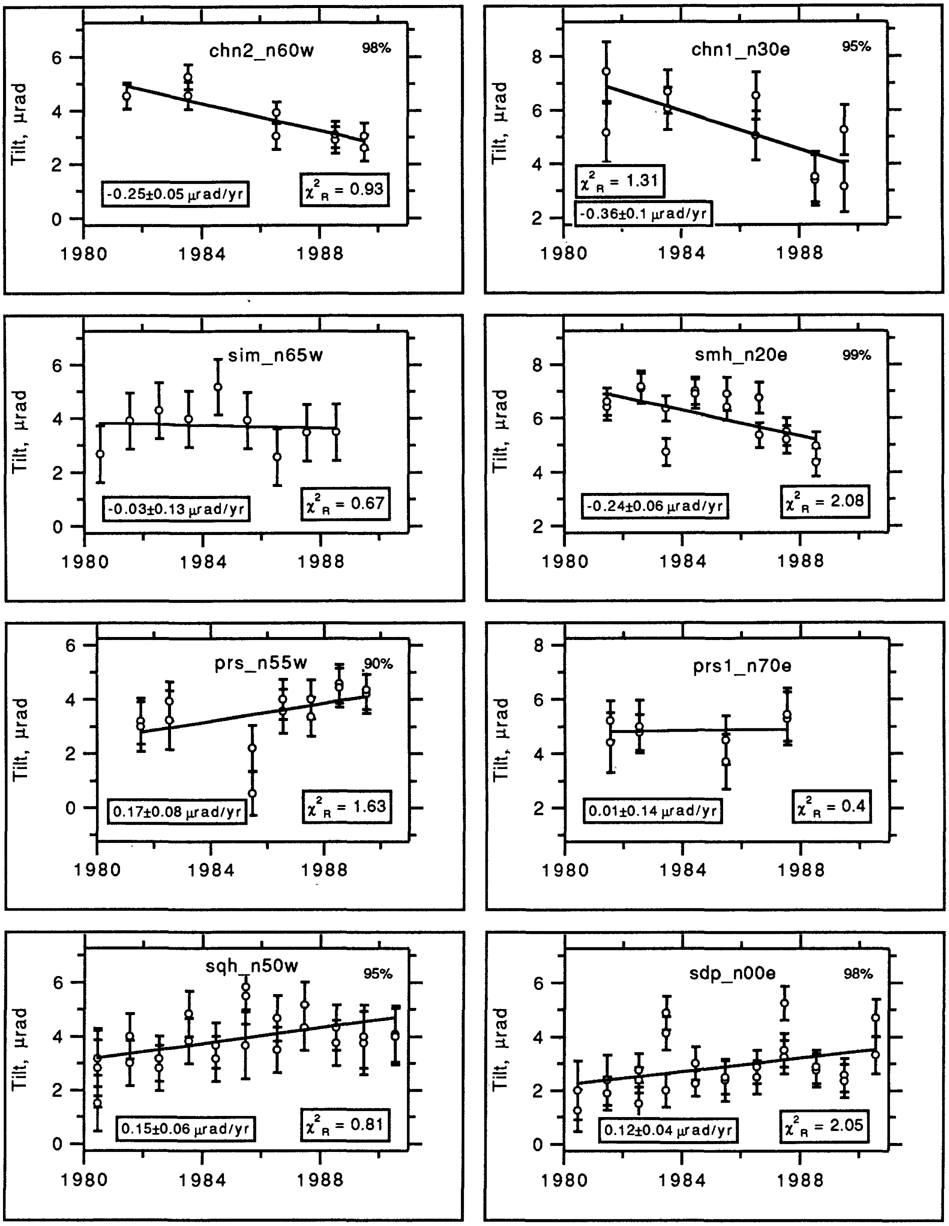

Figure 3. 1980-90 leveling history from those lines in the Outer (1st & 2nd pairs), Central (3rd pair) and Inner (4th pair) Shumagin Islands where the tilt direction as well as rate can be resolved. Tilt rates, their 1 sigma error bars, and the reduced chi-square statistic are shown. If the tilt rate is significantly greater than zero at the 90% or higher confidence level, this value is also shown at upper right. Upward trends on the plots represent relative ground uplift in the direction give in the plot title. Note the tendency for arcward tilting in the Outer Islands, and trenchward tilting in the Inner and Central Islands.

Table 1. Shumagin Seismic Gap 1980-90 tilt rates

Site	Interval	Rate (µrad/yr)*	Azimuth*	Confidence**
Inner Shumagins				
SQH/SDP	1980-90	0.15±0.05	-38°±30°	98%
PIN	1980-90	0.03±0.05	NW†	-
KOR	1980-89	-0.01±0.07	NW†	-
Central Shumagins				
PRS/PRS1	1981-89	0.21±0.14	-17°±36°	-
SAD	1980-89	0.13±0.12	NW†	-
Outer Shumagins				
SIM/SMH	1980-88	-0.24±0.06	18°±31°	99%
CHN1/CHN2	1980-89	-0.44±0.09	-5°±9°	98%
Sanak Island				
SAL1/SAL2	1988-90	1.22±0.71	-43°±20°	-

* Positive rates indicate relative uplift towards the given azimuth

** Level of confidence that tilt rate is different from zero, if > 90%.

† Level line in only one azimuth, so tilt determined only in that azimuth

Errors quoted are 1 standard deviation.

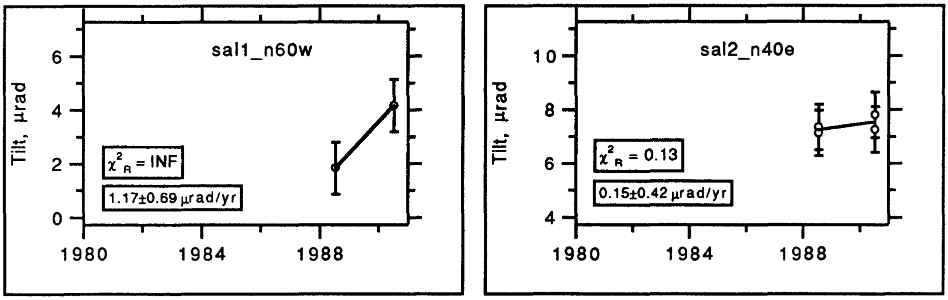

Figure 4. 1988-90 leveling history from the level lines at Salmon Bay, S.E. Sanak Island. See Figure 3 caption for details. Based on just two sets of measurements, the tilt rates appear substantially higher here than in the Shumagin Islands at the eastern end of the seismic gap.

Discussion

About half the individual level lines show non-zero tilting at a high level of confidence. However, the pattern of tilting is consistent with arcward tilting in the outer islands and trenchward tilting in the inner and central islands. This pattern is also consistent with our sea level results [Open File Report 90-334, pp 169-174], which indicate sinking of the central islands with respect to both the inner and outer islands. Even though the tilt and relative sea level rates are small, the consistency of the pattern leads us to believe that real deformation is occurring, and hence that the small horizontal strain signal observed by Lisowski et al. [1988] cannot be explained by aseismic subduction in the Shumagin seismic gap. Further evidence is supplied by the NASA VLBI results [Sauber & Bell, 1990] which indicate 1984-90 WNW motion of Sand Point at about 6 mm/yr, significantly different from zero at the 3σ level. This rate, and the tilt and strain rates, are substantially lower than would be predicted from simple models of subduction. We do not yet have a good explanation of these facts, though it remains possible that the low rates are connected with viscoelastic coupling that slows the deformation rates towards the end of the seismic cycle [Thatcher & Rundle, 1984; Rice & Stuart, 1989; see discussion in Lisowski et al., 1988]. The historical seismicity evidence [e.g., Boyd et al., 1988] continues to suggest that a major earthquake is to be expected in this region. Other factors that tend to support this hypothesis are an accelerating moment release rate in the area and a recent outer rise compressional event.

References

Boyd, T.M., J.J. Taber, A.L. Lerner-Lam and J. Beavan, 1988. Seismic rupture and arc segmentation within the Shumagin Islands seismic gap, Alaska, Geophys. Res. Lett., 88, 201-204.

Hudnut, K.W. and J.J. Taber, 1987. Transition from double to single Wadati-Benioff seismic zone in the Shumagin Islands, Alaska, Geophys. Res. Lett., 14, 143-146.

Lisowski, M., J.C. Savage, W.H. Prescott and W.K. Gross, 1988. Absence of strain accumulation in the Shumagin seismic gap, Alaska, 1980-1987, J. geophys. Res., 93, 7909-7922.

Rice, J.R. & W.D. Stuart, 1989. Stressing In and Near a Strongly Coupled Subduction Zone During the Earthquake Cycle (abstract), Eos, 70, 1063.

Sauber, J. and L. Bell, 1990. The Subduction Zone Process in Alaska, NASA CDP P.I. Working Group Meeting, Greenbelt, MD, Oct 25-26 1990.

Thatcher, W. & J.B. Rundle, 1984. A viscoelastic coupling model for the cyclic deformation due to periodically repeated earthquakes at subduction zones, J. geophys. Res., 89, 7631-7640.

High Temporal Resolution of Crustal Deformation with GPS

14-08-0001-G1673

Yehuda Bock
Institute of Geophysics and Planetary Physics
Scripps Institution of Oceanography
La Jolla, CA 92093
(619) 534-5292
E-Mail: BOCK@BULL.UCSD.EDU

Objectives:

GPS surveying has the potential to provide crustal deformation precursors for the prediction of large earthquakes and, in particular, to allow the *rapid and dense* monitoring of coseismic and post-seismic strain transients which would add to our fundamental understanding of the physics of the earthquake process. The goal of this research is to develop and evaluate the capability of surveying *spatially dense, small- and possibly medium-aperture, three-dimensional geodetic networks, in near real-time with several millimeter-level accuracy* using kinematic-type GPS techniques.

Data Collected:

(1) In May 1990, we collected GPS data near at 12 marks along a 12 km profile crossing the San Andreas fault at Parkfield. We used four Trimble 4000 SST receivers. Two receivers were held fixed at the endpoints of the profile for a six hour period while the other two receivers surveyed the remaining 10 marks in the so-called pseudo-kinematic mode. These intermediate marks were surveyed twice, each time for approximately 30 minutes. These data have been analyzed and indicate that short, repeated site occupations provide similar precision to long static occupations. The profile will be re-surveyed in November, 1990.

(2) In July 1990, we collected kinematic GPS data with Trimble 4000 SST receivers along two profiles across the Sumatran fault, one profile in West Sumatra near Bukittinggi, and another profile in North Sumatra, west of Lake Toba.

(3) In October 1990, we collected kinematic data on a small test network in San Diego county designed to test the compatibility of data collected with Ashtech XII and Trimble 4000 SST receivers. As ground truth, we leveled the heights between the marks and measured the distances with a Wild DI-2000, to a precision of about 1 mm.

(4) Since April 1990, we have been collecting data from three Rogue SNR-8 receivers located at Scripps Institution of Oceanography, Piñon Flat Observatory and Jet Propulsion Laboratory as part of the Permanent GPS Geodetic Array (PGGA) (Shimada and Bock, 1989; Bock et al., 1990 a,b; Lindqwister and Bock, 1990). We are using these data to support our investigations of the temporal resolution of GPS.

Example of high temporal resolution

We refer to data item 3 above. We analyzed the Ashtech to Ashtech baseline using six hours of dual-frequency data sampled every 30 seconds. This solution provides the integer phase ambiguities among the different combination of doubly-differenced stations and satellites. To determine the temporal resolution of position, we analyzed the data every 20 epochs (10 minutes of data), 4 epochs (2 minutes of data) and 1 epoch. That is, we estimated independent relative positions at these three different time intervals, keeping fixed the phase ambiguities determined from the solution of the complete data set. These position determinations were restricted to intervals during which at least five satellites were visible. In the 1 epoch case, the number of observations are 4 L1 and 4 L2 doubly-differenced observations and the number of parameters are three (the three-dimensional relative position). The results of these tests are shown in Figures 1-4 for north, east, height and length components of the baseline. For each component, the horizontal line indicates the result of the six hour solution. The length and height agree to a millimeter with the ground truth.

It is clear from this test that GPS is capable of high temporal resolution of position. This is particularly apparent in the determination of the length component which has an rms of 2 mm even at a resolution of 1 epoch. The other component have an rms of about 5 mm at 1 epoch resolution. The 1 epoch case has powerful implications for the accurate positioning of moving platforms, on land, at sea and in the air. In particular, a single roving receiver can provide rapid and accurate "point" positions with respect to a regional continuously tracking network such as the PGGA in California.

We are extending these type of investigations to the 10 km and 100 km range of baseline lengths, using improved orbits from the PGGA analyses.

References:

Bock, Y. and S. Shimada (1990), "Continuously monitoring GPS networks for deformation measurements," in Global Positioning System: An Overview, proc. IAG Symposium 102, Y. Bock and N. Leppard (eds.), Edinburgh, Scotland, August 7-8, 1989, Springer Verlag, in press.

Bock Y. (1990), "Spatial and temporal resolution of kinematic GPS," *Eos Trans. AGU*, *71*, 483.

Bock, Y., U.J. Lindqwister, J.A. Scheid, G. Blewitt, W.G. Melbourne, S.J. DiNardo, T.P. Yunck, C.L. Thornton, T.H. Dixon, F.K. Wyatt, D.C. Agnew, J-B. Minster, B.H. Hager, R.W. King, T.A. Herring, T.H. Jordan, K.E. Sieh, K.W. Hudnut and D.D. Jackson (1990), "Permanent GPS Geodetic Array in California", *Eos, Trans. Amer. Geophys.Union, 71,* 477.

Lindqwister, U.J. and Y. Bock (1990), "Development of a permanent GPS geodetic array in California for continuous monitoring of crustal motion", *Eos, Trans. Amer. Geophys. Union, 71,* 858.

Bock, Y., F. Wyatt, D.C. Agnew, J.-B. Minster, W. Gurtner, P. Henkart, S. Shimada, S.S.O. Puntodewo, K. Stark, D. Rosenblatt, Z.-K. Chen and P. Worcester (1990), "Continuous monitoring of crustal strain using GPS in Southern California", GPS '90 meeting, Ottawa, Canada, September 3-7, 1990, in press.

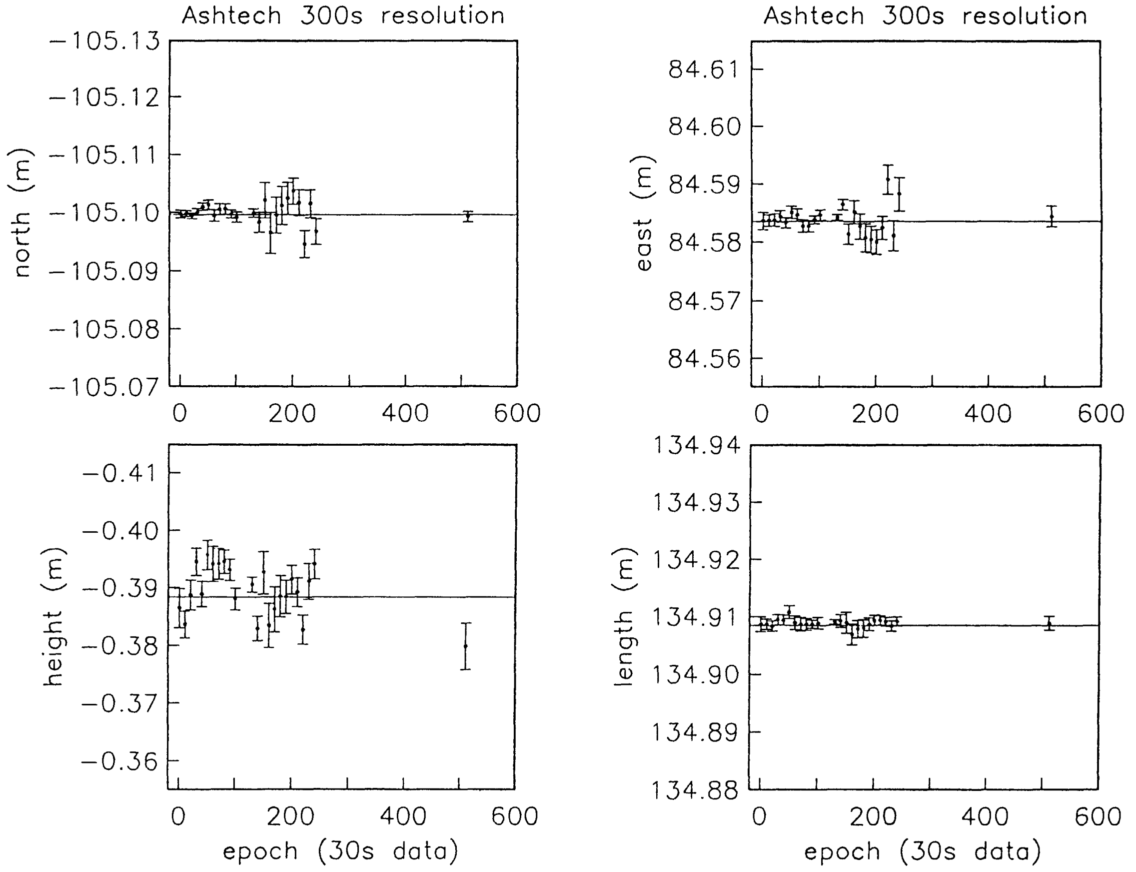

Figure 1: Independent position determinations of the Ashtech-Ashtech baseline at 300 s resolution (10 epochs). Error bars are scaled formal errors.

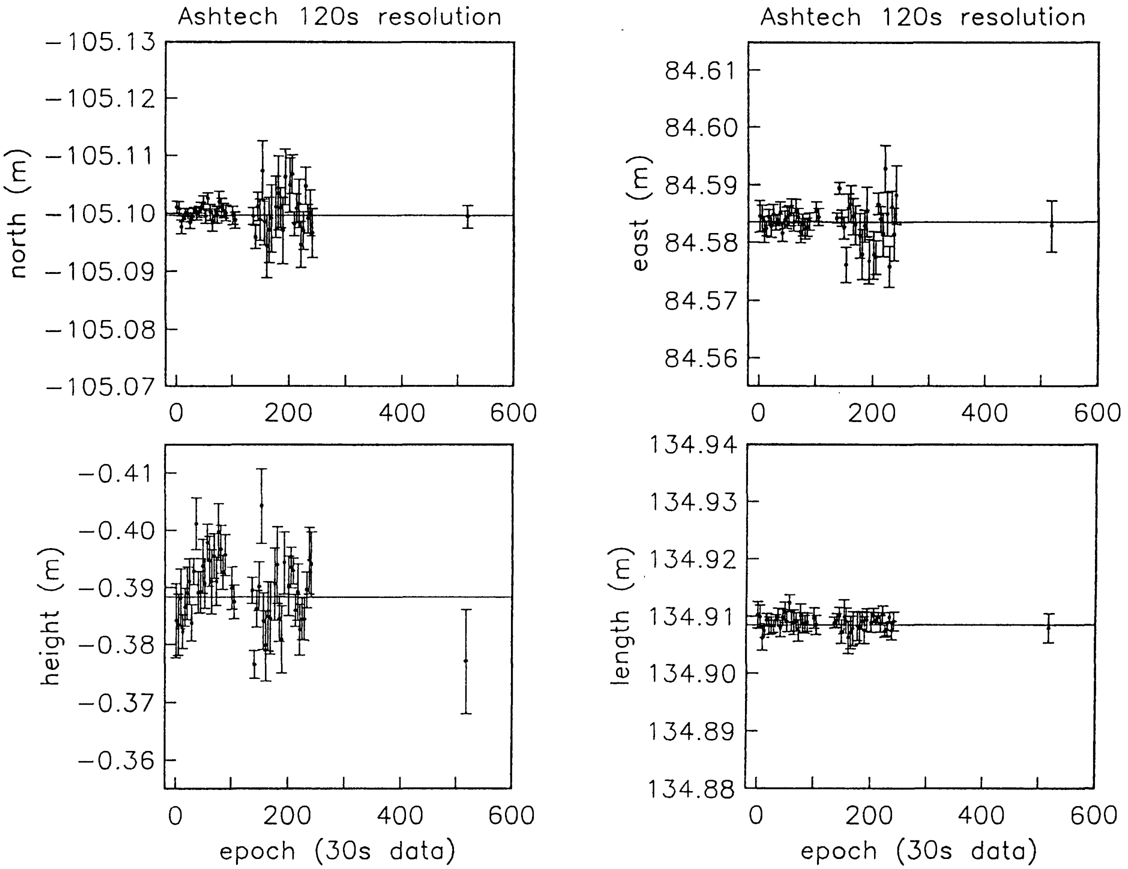

Figure 2: Independent position determinations of the Ashtech-Ashtech baseline at 120s resolution (4 epochs). Error bars are scaled formal errors.

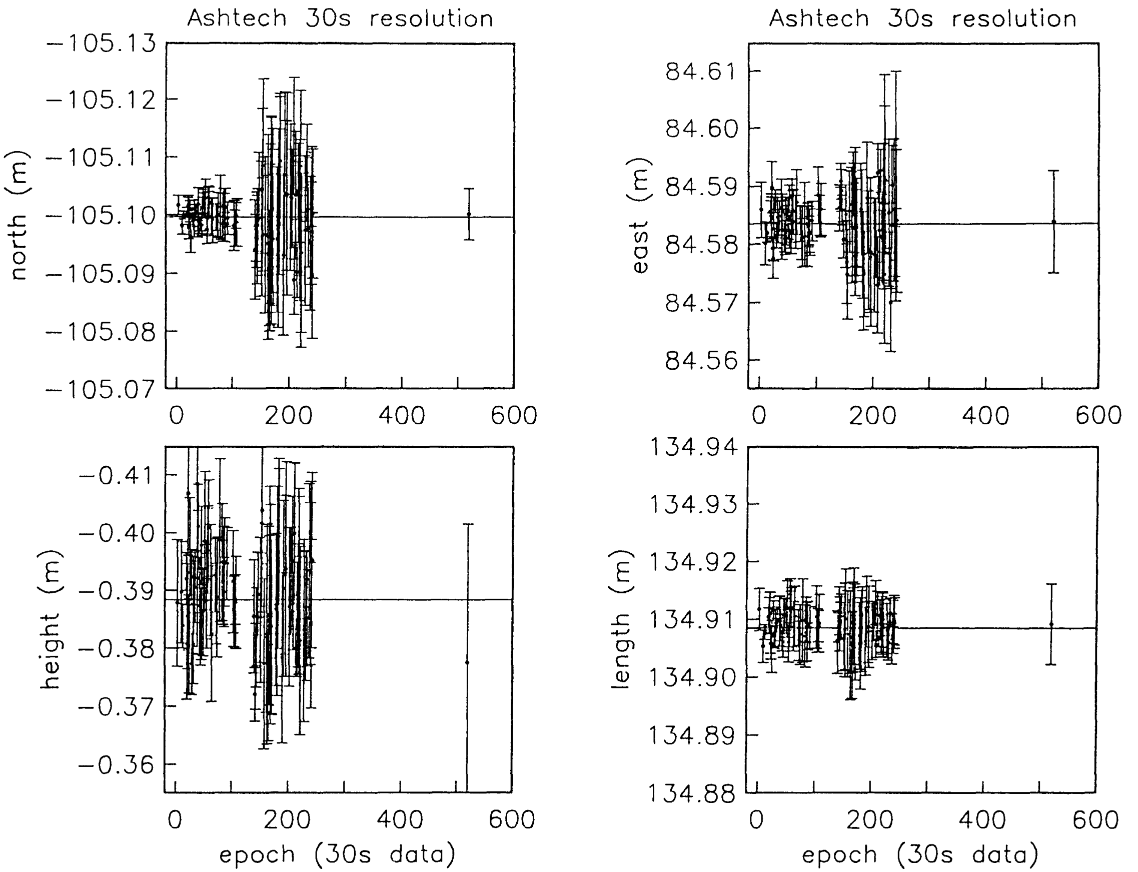

Figure 3: Independent position determinations of the Ashtech-Ashtech baseline at 30 s resolution (1 epoch). Error bars are scaled formal errors.

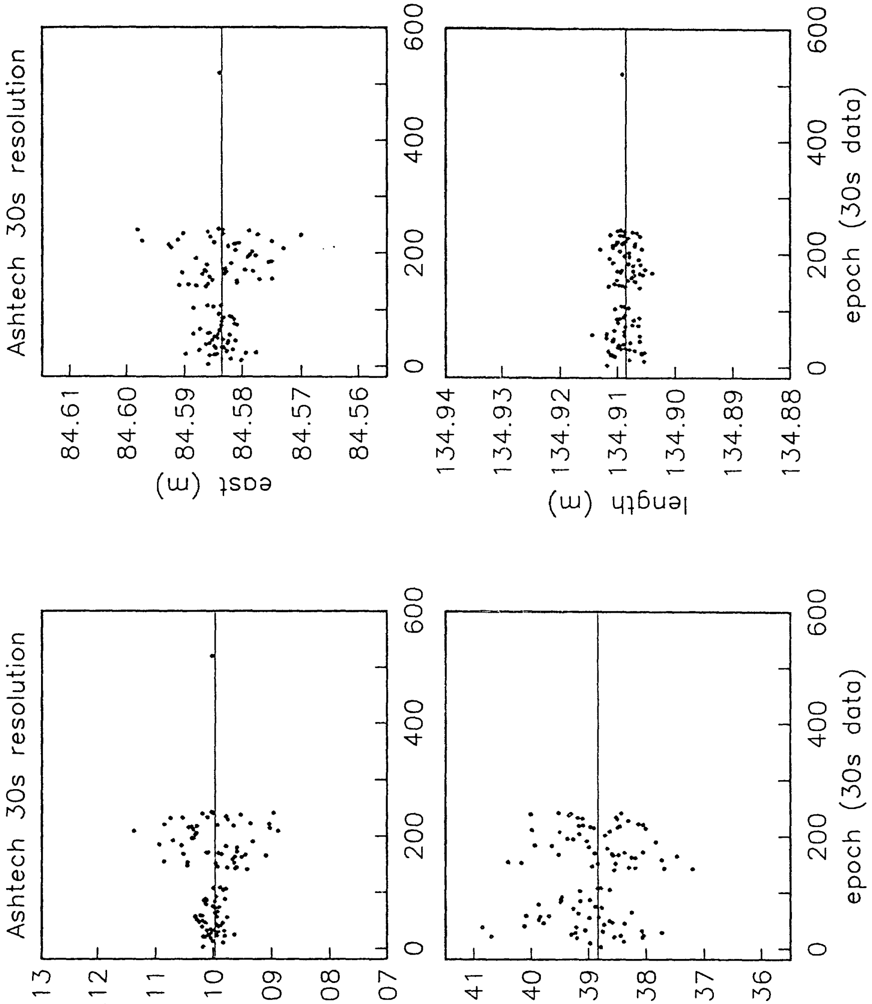

Figure 4: Independent position determinations of the Ashtech-Ashtech baseline at 30 s resolution (1 epoch). Error bars are given in Figure 3.

FAULT ZONE TECTONICS

9960-01188

Katherine S. Breckenridge, Robert O. Burford
Branch of Tectonophysics
U.S. Geological Survey
345 Middlefield Road, MS 977
Menlo Park, California 94025
(415) 329-4849

Investigations

[1] Directed maintenance of creepmeter and alinement array networks in California.

[2] Updated archived creep on the USGS *Low Frequency* computer.

[3] Monitored creepmeter data for possible earthquake precursors, primarily in the Parkfield, California area, site of the USGS-California State earthquake prediction experiment, and in the San Juan Bautista, California region.

Results

[1] Currently 30 extension creepmeters, one contraction meter, and 7 strong-motion creepmeters are operating; 22 of the extension meters, the contraction meter, and all 7 strong-motion meters have on-site strip chart recorders. Of the total 38 instruments, data from 29 are telemetered to Menlo Park (Figures 1,2). Surveys of the alinement array network will be discontinued for the foreseeable future due to a combination of budget cuts and the loss of key personnel, including former project chief Sandra Schulz Burford. Richard Liechti is independently overseeing creepmeter maintenance.

[2] Fault creep data from USGS creepmeters along the San Andreas, Hayward, and Calaveras faults have been updated through mid-September, 1990, and stored in digital form (1 sample/day). Telemetry data are also stored in digital form (1 sample/10 minutes), and can be merged with daily-sample data to produce long- or short-term plots.

[3] Parkfield creep data are being closely monitored to detect changes in rate which, although significant within the context of the historic record, may fall outside the established alert criteria. Data from six instruments along the San Andreas Fault between San Juan Bautista and Melendy Ranch are being examined to characterize changes in fault slip before and after the October 17, 1989 Loma Prieta earthquake.

Reports

Schulz, Sandra S., Catalog of Creepmeter Measurements in California from 1966 through 1988, U.S. Geological Survey Open-File Report 89-650.

Breckenridge, K.S. and Burford, R.O., 1990, Changes in Fault Slip Near San Juan Bautista, California Before the October 17, 1989 Loma Prieta Earthquake - A Possible Precursor? (abstract submitted to American Geophysical Union for Fall 1990 meeting).

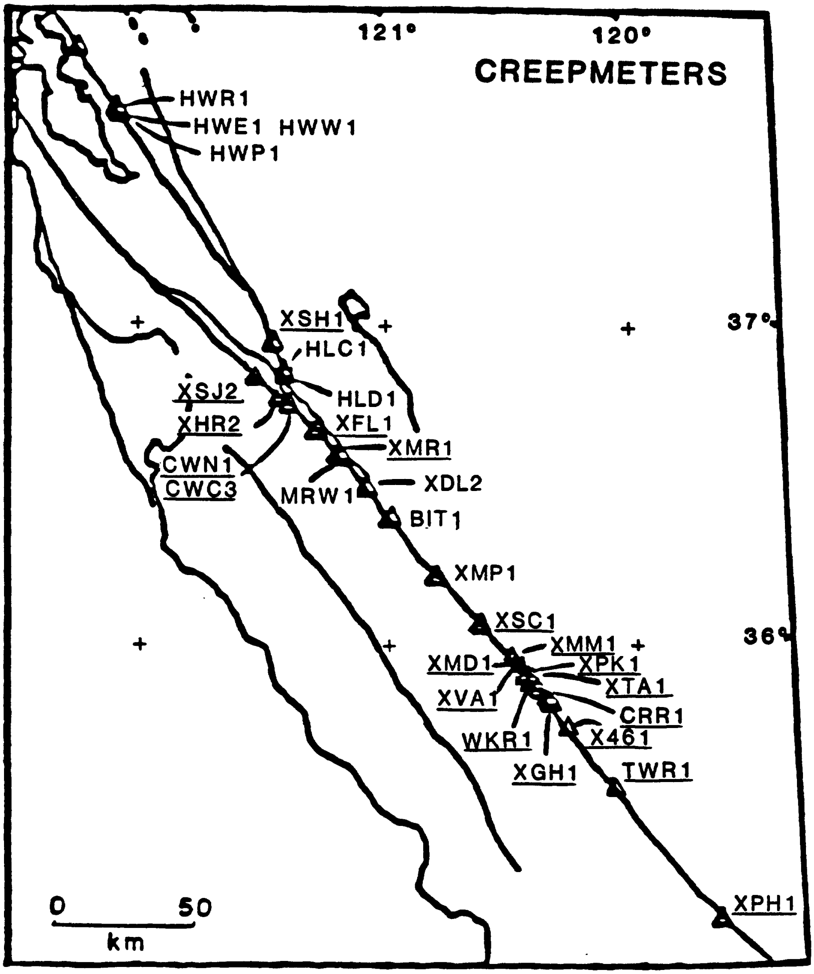

FIGURE 1

USGS creepmeter stations in northern and central California. Instruments with underlined names transmit on telemetry. NOT SHOWN: XRSW, XHSW on the Southwest Fracture near Parkfield (See Figure 2). Strong-motion creepmeters are located in vaults at XMM1, XMD1, XVA1, XTA1, X461, XRSW, and XHSW.

Creep and Alinement : Parkfield, CA

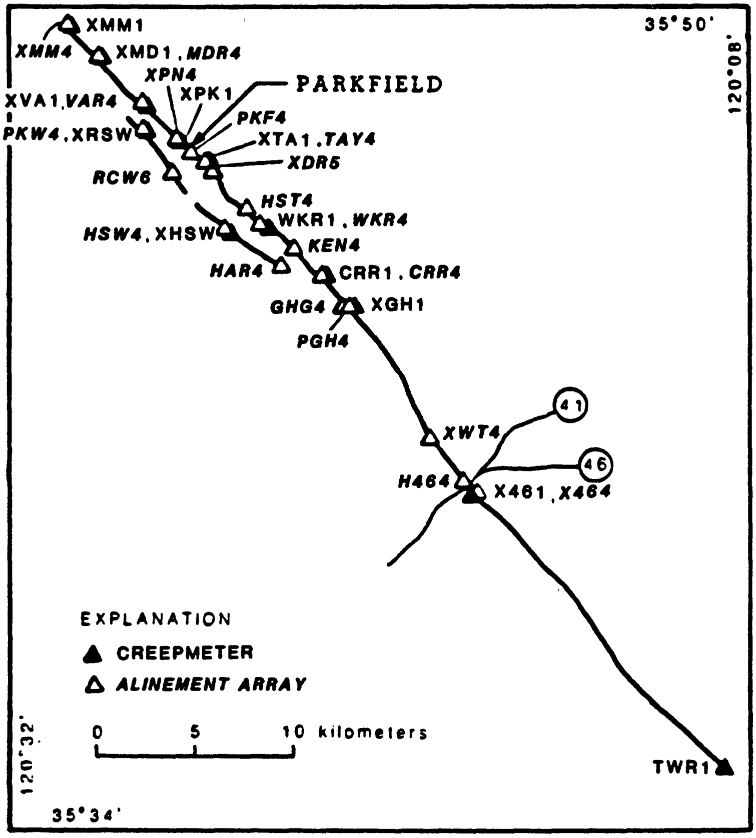

CREEPMETER AND ALINEMENT ARRAY SITES IN PARKFIELD
MARCH 1988

FIGURE 2

Remote Monitoring of Source Parameters for Seismic Precursors

9920-02383

George L. Choy
Branch of Global Seismology and Geomagnetism
U.S. Geological Survey
Denver Federal Center
Box 25046, Mail Stop 967
Denver, Colorado 80225
(303) 236-1506

Investigations

1. NEIC reporting services. Methods of analyzing broadband data are being introduced into NEIC operations. Broadband data are now routinely used to increase the accuracy of some reported parameters such as depth and to compute additional parameters such as radiated energy. These parameters, along with waveform plots of broadband data, are published in the Monthly Listing of the Preliminary Determination of Epicenters.

2. Rupture process of large- and moderate-sized earthquakes. We are using digitally recorded broadband waveforms to characterize the rupture process of selected intraplate and subduction-zone earthquakes. The rupture processes thus delineated are used to complement seismicity patterns to formulate a tectonic interpretation of the epicentral regions.

3. Teleseismic estimates of radiated energy and strong ground motion. On a world-wide basis, the relative paucity of near-field recording instruments hinders the prediction of strong ground motion radiated by earthquakes. We are developing a method of computing radiated energy and acceleration spectrum from direct measurements of teleseismically recorded broadband body waves. From our method, the maximum expectable spectral level of acceleration and lower bounds of stress drops can be made for any event large enough to be teleseismically recorded.

Results

1. Reporting services. The NEIC now uses broadband waveforms to routinely: (1) resolve depths of all earthquakes with $m_b > 5.8$; (2) resolve polarities of depth phases to help constrain first-motion solutions; (3) computed radiated energies for all earthquakes with $m_b > 5.8$; and (4) present as representative digital waveforms in the monthly PDE's. In the Monthly Listings of the Preliminary Determination of Epicenters covering the interval October 1989-April 1990, depths using differential arrival times from broadband waveforms were computed for 64 earthquakes; radiated energies were computed for 67 earthquakes.

2. Rupture process of earthquakes. Source characteristics of the Loma Prieta, California, earthquake of 18 October 1989 were studied with global digitally recorded broadband data. Besides the static parameters such as focal mechanism and depth, we are deriving the rupture history, radiated

energy, and associated stress drops. In modeling the displacement and velocity waveforms, we find that the stress release of the earthquake was spatially heterogeneous. The moment release of the earthquake occurred in four identifiable subevents: the initial subevent had a negligible moment, while the second, third, and fourth subevents released one-third, one-half, and one-sixth of the total moment. In analyzing teleseismically derived acceleration data, we find an acceleration spectral level of 1.6 cm^2/s, implying a stress drop of 51 bars.

A study of the Armenian earthquake of 7 December 1988 in collaboration with the German Geological Survey has been finished. The earthquake was a complex rupture; from the broadband data, we can resolve the source functions of three subevents. From the distribution of aftershocks and the derived focal mechanism, we infer that the causative faults have different strikes. The relative locations of these subevents indicate a fault zone that has a bend.

3. Strong ground motion of intraplate events. We have applied our algorithm for the computation of acceleration spectra to a series of shallow intraplate earthquakes. Most of these events are characterized by a flat spectral level at high frequencies but an intermediate slope before an ω^2 falloff at low frequencies. The high-frequency spectral levels of these intraplate earthquakes are the same as the levels of subduction-zone earthquakes with the same seismic moments, although the spectral shapes are different.

Reports

Choy, G. L., 1990, Global digital data--Interpretation of the earthquake mechanism from broadband data: Proceedings of the Pacific Rim Congress 1990, v. 2, p. 11-18.

Choy, G. L., and Boatwright, J., 1990, Source characteristics of the Loma Prieta, California, earthquake of October 18, 1989 from global digital seismic data: Geophysical Research Letters, v. 17, p. 1183-1186.

Choy, G. L., Boatwright, J., and LaVonne, C. K., 1990, Teleseismic estimates of radiated energy from global seismicity of 1986-1988 [abs.]: EOS (American Geophysical Union, Transactions), v. 71, p. 258.

Choy, G. L., and Bowman, J. R., 1990, The rupture process of a multiple main shock sequence--Teleseismic, local and near-field analysis of the Tennant Creek earthquakes of 22 January 1988: Journal of Geophysical Research, v. 95, p. 6867-6882.

Choy, G. L., and Kind, R., 1990, A preliminary broadband body-wave analysis of the Armenia S.S.R. earthquake of 7 December 1988: Geologisches Jahrbuch (in press).

Choy, G. L., Presgrave, B. W., and LaVonne, C. K., 1990, Broadband seismogram analysis--The Ethiopian double earthquake of 20 August 1989, in Semi-Annual Technical Report: U.S. Geological Survey Open-File Report 90-267, p. 10-12.

Southern California Earthquake Project

90-9930-01174

Thomas H. Heaton
Branch of Seismology
U.S. Geological Survey
525 S. Wilson Ave.
Pasadena, CA, 91106
FAX: 818-405-7827

Introduction

This project covers almost all of the activities of the Pasadena Office of the U.S. Geological Survey. This is a large and complex project that includes the operation of the 250-station Southern California Seismic Network (SCSN), response to major southern California earthquake sequences, and basic research in earthquake physics.

Investigations

1. Operation, maintenance, development and recording of the Southern California Seismic Network consisting of 220 U.S.G.S. telemetered seismometers and 66 seismometers telemetered from other agencies. All stations are recorded on the CUSP digital analysis system.

2. Routine Processing of Southern California Network Data. Routine processing of seismic data from stations of the cooperative southern California seismic network was continued for the period April 1990 through September 1990 in cooperation with scientists and staff from Caltech. Routine analysis includes interactive timing of phases, location of hypocenters, calculation of magnitudes and preparation of the final catalog using the CUSP analysis system. About 800 events were detected in most months with a regional magnitude completeness level of 1.8.

3. Development and testing of an automated real-time earthquake location capability that is fast, reliable, uses data from all network stations, and is not dependent on exotic hardware.

4. Collaboration with Caltech to develop a network of very broad band seismic stations in southern California.

5. Prediction Probabilities from Foreshocks. When any earthquake occurs, the possibility that it might be a foreshock increases the probability that a larger earthquake will occur at the same site within the next few days. It is intuitively obvious that the probability of a very large earthquake should be higher if the potential foreshock were to occur on or near a fault capable of producing that very large mainshock, especially if the fault is towards the end of its seismic cycle or if the background rate of seismic activity is particularly low. In this study, the probability of a major earthquake

characteristic to a particular fault, given the occurrence of a potential foreshock near to that fault is analytically derived from basic tenets of probability theory.

6. Teleseismic surface waves recorded on the network. Record sections were constructed for teleseismic Rayleigh waves (15 to 25 sec. period) recorded on both the southern and northern California seismic networks.

7. Network recording of sonic booms. We have used the arrival times of the shock waves from supersonic aircraft flying over the Southern California Seismic Network, in order to estimate the trajectory, velocity, and height.

8. Loma Prieta source inversion. We have collaborated on an investigation of the rupture history of the 1989 Loma Prieta earthquake by inverting strong motion and teleseismic waveforms.

9. Amplitudes and travel-time delays for teleseismic P-waves. We have observed a correlation between the amplitudes and residual time delays for teleseismic P-waves recorded by the Southern California Seismic Network. Possible explanations for this observation were investigated.

10. Analysis of waveform data from aftershocks of the 1990 Upland earthquake (M_L 5.5) recorded on a small aperture array. About 50 small aftershocks were recorded during a 10-day period following the mainshock, on a two-dimensional, 5-station, GEOS array with spacings of 50 to 100 meters.

Results

1. Operation and maintenance of field stations and recording systems continued with little failure during this reporting period. Time varying attributes of the system are completely recorded on a data base (DBASE III). Documentation of the system and changes to the system continued to be developed by the preparation of semi-annual network bulletins.

2. Routine Processing of Southern California Network Data. The projects to upgrade the southern California seismic network are continuing. To increase the accessibility and research potential of the seismic data, a series of semi-annual Network Bulletins have been issued since 1985. These bulletins provide information about how to access data from the network, problems with the data, details of the processing computer systems, and earthquakes in southern California. As part of this project, documentation of past and present station configurations has been compiled. Reconfiguration of station electronics to maximize the dynamic range and frequency response of the stations is continuing. The average dynamic range of most of the short period vertical seismometer stations in the network is now 40-50 dB. The gains on the stations are now staggered (some very high. others quite low) to

maximize the overall dynamic range of the network. At the lowest gains, 7 force balance accelerometers are now being telemetered and digitized within the short period network.

3. Development of Real-Time Analysis Systems. A software program (PICKLE) has been developed that runs in parallel with the existing online data aquisition system on a DEC MicroVAX computer. This developing system locates about 3 times as many earthquakes as our previous 64-station RTP. In addition, amplitudes from low-gain and force-balance accelerometers are now used in the calculation of magnitude.

4. Deployment of very broad band seismic systems. We are collaborating with Caltech to complete deployment of 6 very broad band stations within southern California by the end of 1990. Our prototype station, PAS, has been in operation since 1988 and Goldstone (GSC) became operational in August 1990. Stations are scheduled for installation this fall at Pinion Flat, Santa Barbara, Isabella, and the San Bernadino mountains. All stations have 24-bit digitizers for very broad band channels and also have strong motion channels for a total dynamic range exceeding 200 db. Data is telemetered via high speed modem by an implementation of Gopher on Caltech's Sun computers. Data logging is triggered by both QED messages from NEIC and RTP messages from the Southern California Seismic Network. Data from these systems is available either by direct telephone access or through Internet.

5. Prediction Probabilities from Foreshocks. In this study, the probability of a major earthquake characteristic to a particular fault, given the occurrence of a potential foreshock near to that fault is analytically derived from basic tenets of probability theory. The data needed to compute this probability are 1) the rate of background activity on that fault, 2) the long term probability of a large earthquake occurring on that fault, and 3) the rate at which foreshocks precede the large earthquakes. We compute the probability with an expression that includes the parameters of time, magnitude and spatial location. We assume that foreshocks to San Andreas earthquakes will follow the average properties of foreshocks to moderate earthquakes in California. We thus assume that 1) the rate of mainshock occurrence after foreshocks decays rapidly with a 1/t type behavior and that most immediate foreshocks occur within three days of their mainshock, 2) that foreshocks and mainshocks occur within 10 km of each other, and 3) that the percentage of mainshocks preceded by foreshocks increases linearly as the magnitude threshold for foreshocks decreases, with 50% of the mainshocks preceded by foreshocks with magnitudes within 3 units of the mainshock's magnitude within 3 days. This derivation is applied to the San Andreas, Hayward, San Jacinto and Imperial faults. We assume that at the scale at which we are examining the faults, all sections of the fault are equally likely to contain the epicenter of the mainshock (and thus the foreshocks). We use the long-term probabilities of a large earthquake from the Working

Group on California Earthquake Probabilities (1988). The short-term probability that a M5.0 earthquake on the San Andreas fault will be followed by a large earthquake within 3 days ranges from a low of 0.2% from Point Arena to Cape Mendocino to a high of 24% in the Carrizo Plain (Figure). By comparison, the probability that any M5 in California will be followed by a M7.5 within 3 days is 0.08%. The rate of background activity along the major faults varies more than the long term probabilities and thus leads to greater variations in the short term probabilities. Alert levels have been proposed for commutation with the California Office of Emergency Services.

6. Teleseismic Rayleigh waves recorded on California seismic networks. Large magnitude (M>7.2) earthquakes generate large enough Rayleigh waves (15-25 sec. periods) to be recorded on the short-period California regional networks. We have digitized FM tape recordings of these surface waves from several earthquakes and for several hundred stations. We find that the surface waves are very coherent as they travel across California, but significant variations in phase velocity can readily be seen. We are using these observations to map average crustal velocity structure.

7. Sonic booms. We developed a computer program to determine the trajectory, velocity, and height of supersonic aircraft from the arrival times of their sonic booms. We analyzed the shock waves from 6 space shuttle landings and a flight of the SR-71 Blackbird. Figure 1 shows four examples of the travel time data and the best fitting trajectories. Examination of the errors in fitting the observed arrival times indicates that the trajectory direction can be determined within an accuracy of several degrees in azimuth and a few kilometers in lateral offset. The average velocity can be determined within a few tenths of a Mach number. Altitude is the least resolvable parameter, with uncertainties of 5 to 10 km.

8. Loma Prieta source inversion. Inversion of strong motion and teleseismic waveforms for the slip history of the 1989 Loma Prieta earthquake indicates bilateral rupture with oblique slip on a 70° dipping plane (probably the Sargent fault). There is compelling evidence that the main rupture was preceded by a foreshock (magnitude 3.5 to 4.5) about 2 seconds before the main initiation of rupture. Large regions of slip were centered 6 km northwest and 6 km northeast of the hypocenter. There appears to be relatively little slip in the region directly updip from the hypocenter.

9. Teleseismic P-waves amplitudes and travel times. The relative amplitudes and travel time residuals for teleseismic P-waves recorded on the short period net show a correlation between increasing amplitude and increasing travel time. Using 13 events, well-distributed in azimuth and recorded on 50 to 100 stations, Figure 2 shows a plot of the logarithm of the relative amplitude versus travel time residual. Although there is

a large amount of scatter, a linear regression analysis indicates a change in amplitude of about a factor of two for a change in travel time of one second. Part of this trend can be explained in terms of the local velocity (impedance) at each site. However, at some sites the strong azimuthal dependence of the amplitudes and travel time residuals suggests that structures in the mantle may contribute to this phenomenon.

10. Geos array at Upland. Aftershock data from the 28 February Upland earthquake and recorded on a small-aperture, 5-station Geos network show significant variations in waveforms over the 50 to 100 meter spacing of the stations. The array recorded aftershocks with a with a wide range of depths and backazimuths, and it should be possible to identify the source of complexities in the waveforms using the combined data set.

Publications

Hauksson, E., L. Jones, J. Mori, R. Clayton, T. Heaton, H. Kanamori, D. Helmberger, 1990, The Southern California Seismic Network: Report to the U.S. Geological Survey, U.S. Geol. Surv. Open File Rep., submitted.

Heaton, T., 1990, The physics of earthquake rupture, EOS, Fall 1990.

Jones, L., and K. Sieh, 1990, Short-term earthquake hazard assessment for the southern San Andreas fault, U.S. Geol. Surv. Open-File Rep., submitted.

Kanamori, H., J. Mori, D. Anderson, and T. Heaton, 1991, Seismic excitation by the Space Shuttle Columbia, J. Geophys. Res., submitted.

Mori, J., 1991, Estimates of velocity structure and source depth using multiple P-waves from aftershocks of the 1987 Elmore Ranch and Superstition Hills, California, earthquakes, Bull. Seism. Soc. Am., submitted.

Wald, D., D. Helmberger, and T. Heaton, Analysis of the 1989 Loma Prieta earthquake from inversion of local strong motion and broadband teleseismic data, EOS, Fall 1990.

Wald, L., D. Given, J. Mori, L. Jones, and L.K. Hutton, 1990, The Southern California Network Bulletin; January - December, 1988, U.S. Geol. Surv. Open-File Rep. 90-499.

Wald, L., D. Given, L. Jones, L.K. Hutton, 1990, The Southern California Network Bulletin; January - December, 1989, U.S. Geol. Survey Open-File Rep. 90-483.

Wald, L., and T. Heaton, 1991, LG and RG waves on the California regional networks from the December 23, 1985 Nahanni earthquake, J. Geophys. Res., submitted.

Figure Captions

Figure 1. Arrival times data (sec) and estimated flight paths for aircraft that caused strong sonic booms. The flight pattern is shown by hyperbolas that represent 20 second isochrons. For the space shuttle cases, the square marks the landing site at Edwards Air Force Base.

Figure 2. Logarithm of the relative amplitude versus travel-time residual for P waves from 13 teleseismic events. The average amplitude for each event was normalized to 1.0. The travel times were calculated with respect to the Herrin tables. For each event, the average time residual was subtracted from each residual to normalize the average value to 0.0. The line is a least squares regression which gives a slope of 0.32.

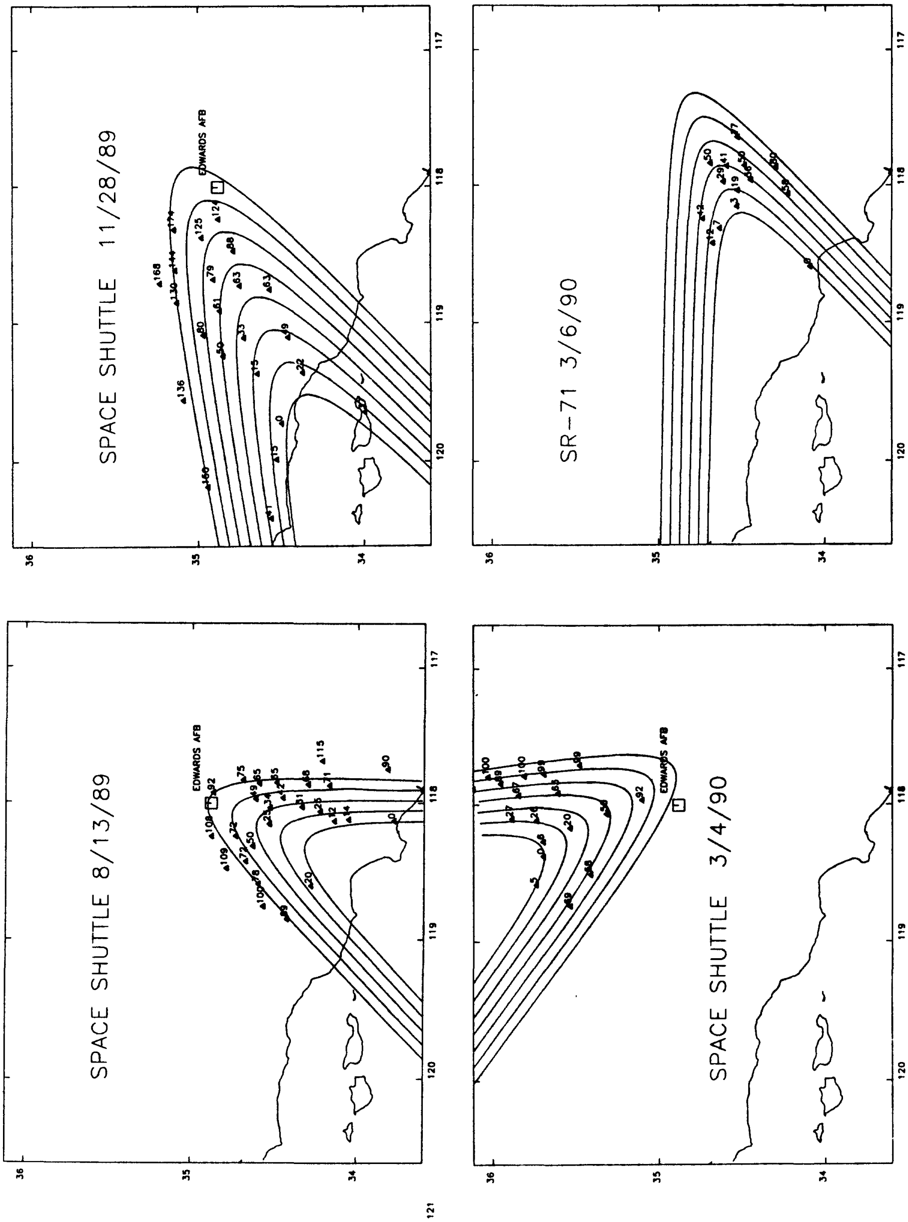
SPACE SHUTTLE 11/28/89
EDWARDS AFB
SR-71 3/6/90
SPACE SHUTTLE 8/13/89
EDWARDS AFB
SPACE SHUTTLE 3/4/90
EDWARDS AFB
36
35
34
117
118
119
120
121

Figure 1

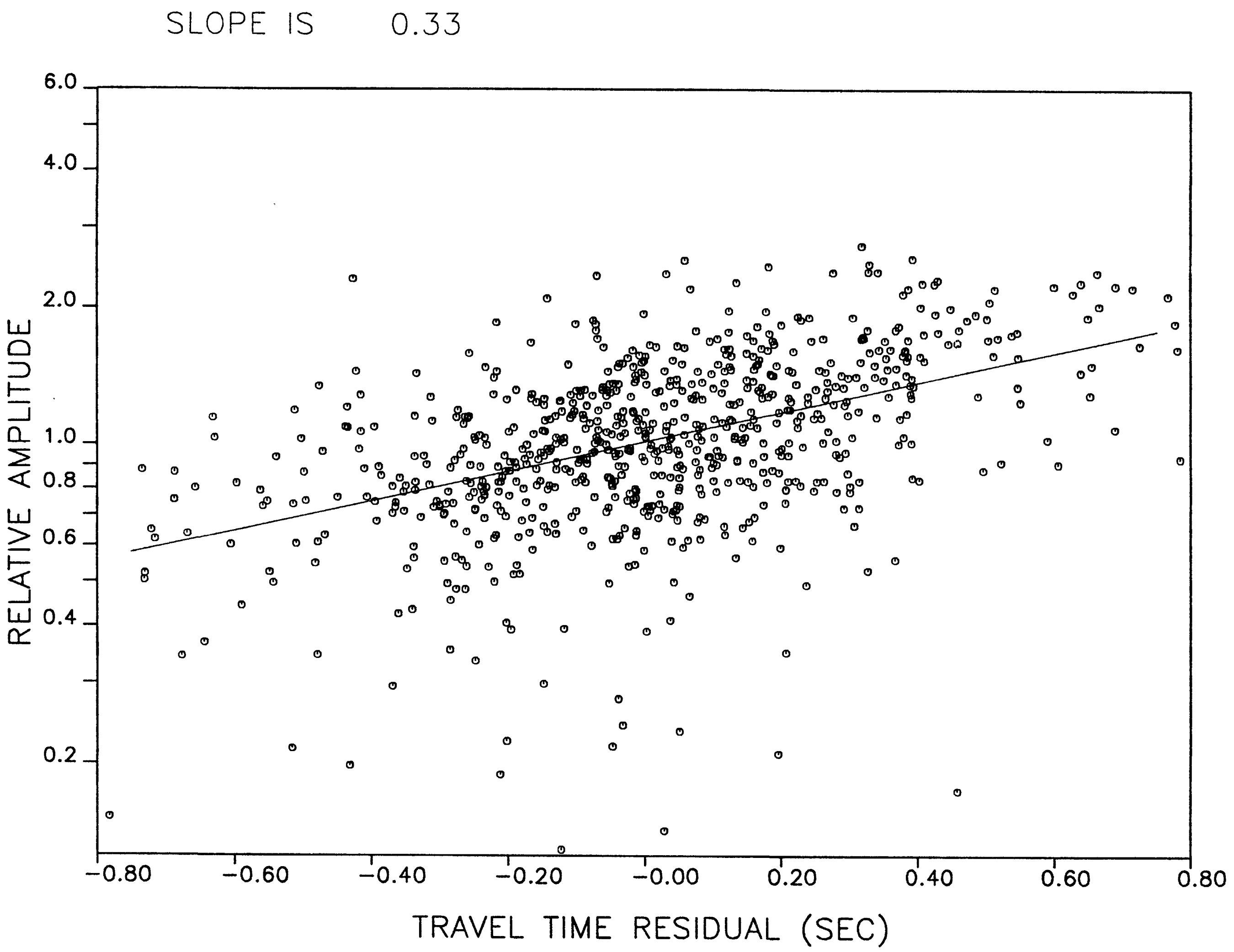
SLOPE IS 0.33
RELATIVE AMPLITUDE
6.0
4.0
2.0
1.0
0.8
0.6
0.4
0.2
TRAVEL TIME RESIDUAL (SEC)
−0.80
−0.60
−0.40
−0.20
−0.00
0.20
0.40
0.60
0.80

Figure 2

Instrument Development and Quality Control

9930-01726

E. Gray Jensen
Branch of Seismology
U.S. Geological Survey
345 Middlefield Road - Mail Stop 977
Menlo Park, California 94025
(415) 329-4729

Investigations

This project supports other projects in the Office of Earthquakes, Volcanoes and Engineering by designing and developing new instrumentation and by evaluating and improving existing equipment in order to maintain high quality in the data acquired by the Office. Tasks undertaken during this period include repair and modification of Seismic Group Recorders (SGR's), blasters and accessories, development of a master clock and construction of an RTP digitzer interface, among other things.

Results

The SGR's which have been modified with timers for refraction seismology returned from a successful experiment in Kenya. The recorders were tested and repaired. The new electronic blasters were modified to correct problems encountered in the field. The SGR's were then deployed around the Brooks Range in Alaska for the TACT '90 experiment in July. Both the recorders and the blasters performed well. The recorders and associated equipment were then used in a PASSCAL experiment in Minnesota during August.

A prototype master clock was constructed. This will design will be incorporated into the electronic blaster. Three units will be constructed as stand alone clocks. Software for the clock is under development. A prototype field seismic digitizer was constructed as part of the digital seismic data collection system development.

All of the hardware for a interface between the new transputer-based RTP (under development by Rex Allen) and a Tustin digitizer has been assembled. This includes an PC-AT compatible computer, a DMA interface card, transputer link interface card and a parallel I/O card. When programmed, the PC will transfer seismic data digitized by the Tustin via the DMA interface to memory buffers. Time information will be read-in through the parallel card. The data will then be transferred to the transputers through the link card. Software development is in progress.

Four electrostatic field strength meters were rehabilitated along with several strip chart recorders. These will be deployed by Chi-Yu King on nearby faults to correlate the electrostatic field with earthquakes. Site visits were made to repair or modify field equipment in the Parkfield and Mammoth areas. Among these was the repair of the Reftek Model 44 which is the central unit for the digital seismic network in Parkfield. As a result, the computer there is now collecting clean data from all nine stations where before about half had noise spikes and blank periods.

Reports

Fischer, F. G., 1990, An electronic blaster for use in refraction seismology, *U. S. Geological Survey Open-File Report 90-429.*

Jensen, E. G., 1990, A six-channel seismic amplifier, *U. S. Geological Survey Open-File Report 90-346.*

State of Stress in the Rupture Zone of Large Earthquakes

Grant No. 14-08-0001-G1773

Hiroo Kanamori
Seismological Laboratory, California Institute of Technology
Pasadena, California 91125 (818) 356-6914

Investigations

1. Resolution of Fault Models Determined From Teleseismic Body Waves
   by Masayuki Kikuchi and Hiroo Kanamori
2. Rupture Patterns of Recent Major Earthquakes
   by Hong Kie Thio, Kenji Satake, Masayuki Kikuchi, and Hiroo Kanamori

Results

1. Resolution of Fault Models Determined From Teleseismic Body Waves

Teleseismic body waves are extensively used to determine the rupture pattern of earthquakes. The rupture pattern is represented by a distribution of subevents on the fault plane, and the location, size and the mechanism of the subevents are determined with inversion of teleseismic body waves. If the mechanisms of the subevents are allowed to vary, and if no constraints are imposed on them, the inversion becomes very unstable, and the solution is inevitablly nonunique. We have developed a procedure to explore the range of allowable solutions and appropriate constraints. In this procedure a network of grid points is constructed on the t-*l* plane, where t and *l* are, respectively, the onset time and the distance from the epicenter of a subevent; the best-fit subevent is then determined at all grid points. Then the correlation is computed between the synthetic waveform for each subevent and the observed waveform. The correlation function as a function of t and *l*, and the best-fit mechanisms computed at each grid point depict the character of allowable solutions and facilitate a decision on the appropriate constraints to be imposed on the solution.

2. Rupture Patterns of Recent Major Earthquakes

We have made preliminary analyses of body and surface waves of recent major earthquakes, the 1990 Sudan, Iran and Philippines earthquakes. We used the data from the IDA/IRIS, NARS, Yellowknife and GEOSCOPE arrays. In general, the results from body-wave inversions and surface wave inversions are consistent, except that the moments from body waves are smaller, up to a factor of three, than the moments determined from surface waves.

The Sudan earthquake sequence occurred just outside the area of mapped normal faulting which comprises the western branch of the East African Rift (EAR), in an area with very little background seismicity. The first event on May 20 had a moment of 5×10^{26} dyne-cm and the mechanism was purely strike-slip corresponding to a left-lateral movement along the NW-SE nodal plane. This event was followed four days later by two large events, the second being similar in size to, but having a longer source duration than, the May 20 mainshock. For these events, however, we found normal faulting along the ENE-WSW striking nodal planes. None of the Sudanese events shows much source complexity. The strike-slip mechanism of the first event contrasts sharply with the predominantly normal-fault mechanisms which are found for the EAR earthquakes.

However, if the NW striking plane is the actual fault plane, then this event can be understood in terms of transform movement parallel to a nearby lineament which has been interpreted as a left lateral fault zone connecting the eastern and western branches of the EAR.

Contrary to the Sudan events, the Iran event shows considerable source complexity. The moment is 1×10^{27} dyne-cm, an order of magnitude larger than the 1988 Armenian event, and was mainly released in three subevents, all with strike slip mechanisms corresponding to right lateral movement along the strike of 215°. The first main subevent is preceded by a smaller initial subevent. This earthquake is one of the largest recorded events in this part of Iran and its mechanism is quite different from that of earlier events. The moment tensor also differs from the cumulative moment tensors calculated for this region by various authors, but when we include this event in those cumulative moment tensors the result is not significantly different from the earlier studies.

The Philippines earthquake is the largest and most complex event of the ones under study. The moment amounts to 4.9×10^{27} dyne-cm and the mechanism is again strike-slip, with left-lateral movement along a strike of 335°. Rupturing seems to have occurred over a time interval of up to 70 seconds with many subevents. The aftershock distribution indicates that the eastern branch of the Philippines fault ruptured, although there was also activity along the western branches. For the largest aftershock which occurred the next day we found a thrust mechanism along the nodal plane with a strike of about 220°. This aftershock is located where the eastern branch of the Philippines fault bends into a northerly trend; the difference in mechanism between the main shock and this aftershock as well as the very occurrence of the aftershock could be related to that bend. The existence of a major strike-slip fault close to a zone of active thrusting along the east coast of Luzon suggests that strain partitioning is taking place in this region.

This study is still in progress, and more details will be reported in the final report.

Publications

Kikuchi, M., and H. Kanamori, Inversion of Complex Body Waves, Submitted to the Bull. Seismol. Soc. Am., 1990. (Preprint available.)

Kanamori, H., and K. Satake, Broadband Study of the 1989 Loma Prieta Earthquake, *Geophys. Res. Lett.*, *17*, 1179-1182, 1990.

Satake, K., and H. Kanamori, Fault Parameters and Tsumani Excitation of the May 23, 1989, MacQuarie Ridge Earthquake, *Geophys. Res. Lett.*, *17*, 997-1000, 1990.

FAULT MECHANICS AND CHEMISTRY

9960–01485

C.–Y. King
Branch of Tectonophysics
U.S. Geological Survey
345 Middlefield Road, MS/977
Menlo Park, California 94025
(415) 329-4838

Investigations

[1] Water temperature and radon content were continuously monitored at two water wells in Parkfield, California.

[2] Water level was continuously recorded at six other wells in central California.

[3] Water temperature and electric conductivity were periodically measured, and water samples were taken from most of these wells and two springs in San Jose for chemical analysis.

[4] Cumulative slip distribution for a long sequence of slip events along a laboratory fault is studied.

Results

In cooperation with Drs. H. Wakita and J. Igarashi of the University of Tokyo, we replaced the aging radon monitor at Miller Ranch in Parkfield, installed another radon monitor at Mission Farm Campground in San Juan Bautista, and installed a set of water–level and barometric–pressure instruments at San Francis Retreat in San Juan Bautista.

No significant geochemical changes were recorded during this report period.

Reports

Rydelek, P.A., Knopoff, L., and King, C.–Y. (1990). Comments on "Migration of historical earthquakes in California." by C.–Y. King and Z. Ma, *Pure and Applied Geophysics*, v. 133, p. 547–551.

King, C.–Y. and Luo, G., 1990, Variations of electric resistance and H_2 and Rn emissions in concrete blocks under increasing uniaxial compression, *Pure and Applied Geophysics* v. 134, p. 45–56.

CALIFORNIA AND HAWAII SEISMICITY STUDIES

Project 9930-03563
for the period April 1, 1990 through September 30, 1990

Fred W. Klein
Branch of Seismology
U.S. Geological Survey MS 977
345 Middlefield Rd.
Menlo Park CA 94025
FTS 459-4794

Investigations

The overall objective is to look for long-term seismicity and tectonic patterns in the Northern California and Hawaii earthquake catalogs. The two catalogs are in very different states of self-consistency and usefulness for research, however. Accordingly, the Hawaiian work uses a completely reprocessed catalog and focuses on research. The Northern California effort presently involves cleaning up the raw phase data and developing methods for reprocessing this data into a self-consistent catalog. This reprocessing is necessary before many types of research become meaningful. The emphasis is on applying methods developed for Hawaiian processing and earthquake display to the California catalog.

The Hawaiian seismic investigation consists of a thorough study of earthquake focal mechanisms in the upper mantle beneath Hawaii. The goal is to determine the state of stress, nature of lithospheric flexure and interaction of the volcanic system with the lithosphere. This work includes a detailed study of the vertical magma conduit feeding Kilauea Volcano's shallow (3-7 km depth) magma reservoir. The seismically active conduit extends downward to about 55 km to the top of the magma source region. Earthquakes in the surrounding lithosphere below 15 km depth reflect deformation and stress imposed by the volcanic edifice above.

The work on the Northern California earthquake catalog is being shared by several colleagues in the branch. This project has assumed responsibility in several areas: (1) Develop a data base of seismic station data and apply it to the reprocessing of the earthquake catalog. (2) Develop a computer file system or data base for storing both raw and processed earthquake phase data. (3) Develop and modify the HYPOINVERSE earthquake location program to handle the various tasks needed for Northern California processing. (4) Integrate existing and develop new regional crustal velocity models into a multiple model system for processing earthquakes from anywhere in California. (5) Organize a system for recognizing earthquakes needing human reprocessing, dividing the catalog into regions of equal numbers of events to reprocess, and supervising individuals to reprocess each area. (6) Prepare earthquake animations for video presentations as needed on the Branch's Amiga computer.

These animations show the spatial distribution of earthquakes through animated movement and the time variation of seismicity with time-lapse map views. The animations have been used a) in research to visualize an earthquake catalog and look for patterns which are testable by more rigorous methods, b) for public and VIP visitor display, and c) to produce animated video tapes on major topics such as the Loma Prieta earthquake.

Results

The research on Kilauea's magma conduit suggests that the earthquakes require external sources of stress and are not simply generated by excess magma pressure, as with rift zone intrusions. Dramatic evidence for an external stress cause is the major drop in earthquake rate following the M=7.2 Kalapana earthquake in 1975. This event thus released stress in the entire volcanic system in addition to the rupture zone in Kilauea's south flank. Seismic gaps occur along the conduit centered at about 5, 13 and 20 km depths. The 3-to-7-km gap is the main magma reservoir, the 13 km gap appears to result from the layer of buried ocean sediments at the base of the volcanic pile, and the 20-km gap is present under the whole island. The latter may be a depth of low or "neutral" stress within the flexing lithosphere. Lateral extension is characteristic of the focal mechanisms within the volcanic pile (above the 13 km gap) and lateral compression occurs just below. Stresses are thus decoupled at the boundary of the volcanic pile with the underlying oceanic crust. Focal mechanisms below 20 km depth are similar to those in Kilauea's south flank and show southward motion of the upper block on a near-horizontal plane.

The reprocessing of the Northern California earthquake catalog is underway. Contributions from this project to date include: (1) Maintain a data base of seismic stations and their gains in and surrounding California has been assembled. (2) Enable the HYPOINVERSE location program to transparently handle several crustal models, magnitude scales, station delays and corrections and gain history. (3) Various routines to verify quarry blasts within the catalog and check for data completeness and regionally separate the catalog for specialized reprocessing.

Reports

Klein, F.W., Multiple crustal models for earthquake location in Northern California and surrounding areas, U.S. Geological Survey Open File Report, in preparation, 1990.

Klein, F. W. and Stephen G. Walter, Aftershocks of the Loma Prieta earthquake: computer animations (a video tape), U.S. Geological Survey Open File Report 89-669, 1990.

Operation of Borehole Tiltmeters at Pinon Flat Observatory, California and Analysis of Secular and Tidal Tilt

14-08-0001-G1765

Judah Levine
Joint Institute for Laboratory Astrophysics
Campus Box 440
University of Colorado
Boulder, Colorado 80309
(303) 492 - 7785

Objectives: To install borehole tiltmeters at Pinon Flat Observatory in Southern California; to compare the performance our instruments installed at three different depths; to analyze the data at secular and tidal periods; and to compare our results with those obtained from other instruments at the same site.

Results: We currently have three instruments installed at Pinon Flat Observatory and all three have been operating during this report period. The instrument in borehole BOC (the 122 m deep borehole) failed in July and was replaced. The installation in BOC has been somewhat more troublesome than the other two because of the continued accumulation of rust and metal chips at the bottom of the casing. The replacement instrument has a somewhat different bottom bracket designed to keep the instrument from resting on the chips. The data since that time have been somewhat quieter at intermediate periods (hours to days), but the longer-term signals are essentially unchanged. The data from BOC continues to be somewhat noisier than the data from the two shallower boreholes.

We have continued to inter-compare the data from our three instruments. We had hoped to be able to use data from the deeper installation of the Askania tiltmeter, but that instrument is not yet working reliably.

We have investigated two methods of comparing the instruments. In the first method, we construct transfer matrices that relate the observed tilts in any borehole to the corresponding measurements from another instrument. This approach makes no assumptions about the relationship between the admittances of the two instruments and assumes only that the two instruments are responding to a common excitation. In the second method, we expand the response of each instrument as a sum of the regional tilt signal plus admittances to various external effects (such as barometric pressure). The regional tilt signal is estimated using data from the other instruments at the site, including the long-fluid tiltmeter and the Askania device. Thus the first method is a purely phenomenological computation, while the second method models the responses in terms of various external excitations.

The power of either method resides in the stability of the model coefficients with time. Our results so far are quite encouraging; we find that all of the data from BOA can be modeled using a single admittance matrix, and that a similar matrix can be used for BOC. We are currently working on the data from BOB, and we do not have any results yet for that data set.

Summary of Data Collected: We acquire the data from our three instruments at PFO (2 channels/instrument) every 6 minutes. These same values are also transmitted to the PFO central recording trailer and are digitized and recorded there 12 times/hour.

CRUSTAL STRAIN

9960-01187

M. Lisowski, J.C. Savage, W.H. Prescott, N.E. King
Branch of Tectonophysics
U.S. Geological Survey
345 Middlefield Road, MS/977
Menlo Park, California 94025
(415) 329-4855

INVESTIGATIONS

The principal subject of investigation was the analysis of deformation in a number of tectonically active areas in the United States.

RESULTS

1. Strain Accumulation on the Olympic Peninsula, Washington.

A 20 × 30-km strain network in Olympic National Park has been surveyed with a Geodolite in September of 1982, 1983, 1986, and 1990. The measured principal strain rates are $\dot{\epsilon}_1 = 0.011 \pm 0.027$ and $\dot{\epsilon}_2 = -0.092 \pm 0.029$ μstrain/yr (extension reckoned positive) with the axis of greatest contraction directed N59°E ± 6.6°. The orientation of the contraction axis agrees reasonably well with the N68°E direction of plate convergence of the Juan de Fuca plate upon the North American plate. The measurement of strain in the Olympic Park network was undertaken as a test of 1972–1979 strain measurements made near Seattle. Both measurements indicate accumulation of east-northeast compression in northwestern Washington. Tide-gage measurements of relative sea level corrected for the eustatic sea-level rise and glacial isostatic rebound indicate an uplift rate of about 3 mm/yr on the west coast of the Olympic peninsula and about 0.4 mm/yr in the Puget Sound lowlands near Seattle. The uplift rates and measured strain rates are consistent with a subduction model in which the plate interface beneath the continental slope and continental shelf is locked but farther inland the interface slips continuously. The implication is that strain that will ultimately be released in a great subduction earthquake is now accumulating in western Washington.

2. Strain Accumulation Along the San Andreas fault in Southern California.

Five 6-line trilateration networks along the San Andreas fault have been surveyed frequently since 1986 using a Geodolite with aircraft monitoring of humidity and temperature. The accumulation of right-lateral shear strain across a vertical plane parallel to the local strike of the San Andreas fault is shown in Figure 1 for each of these networks. The linear fits to those strain accumulation plots are also shown in the figure. The linear fits provide a good fit to the observations. There may be a suggestion of a change in the rate of shear strain accumulation at Cholame in late 1989, but the precision of observation is not adequate to prove it.

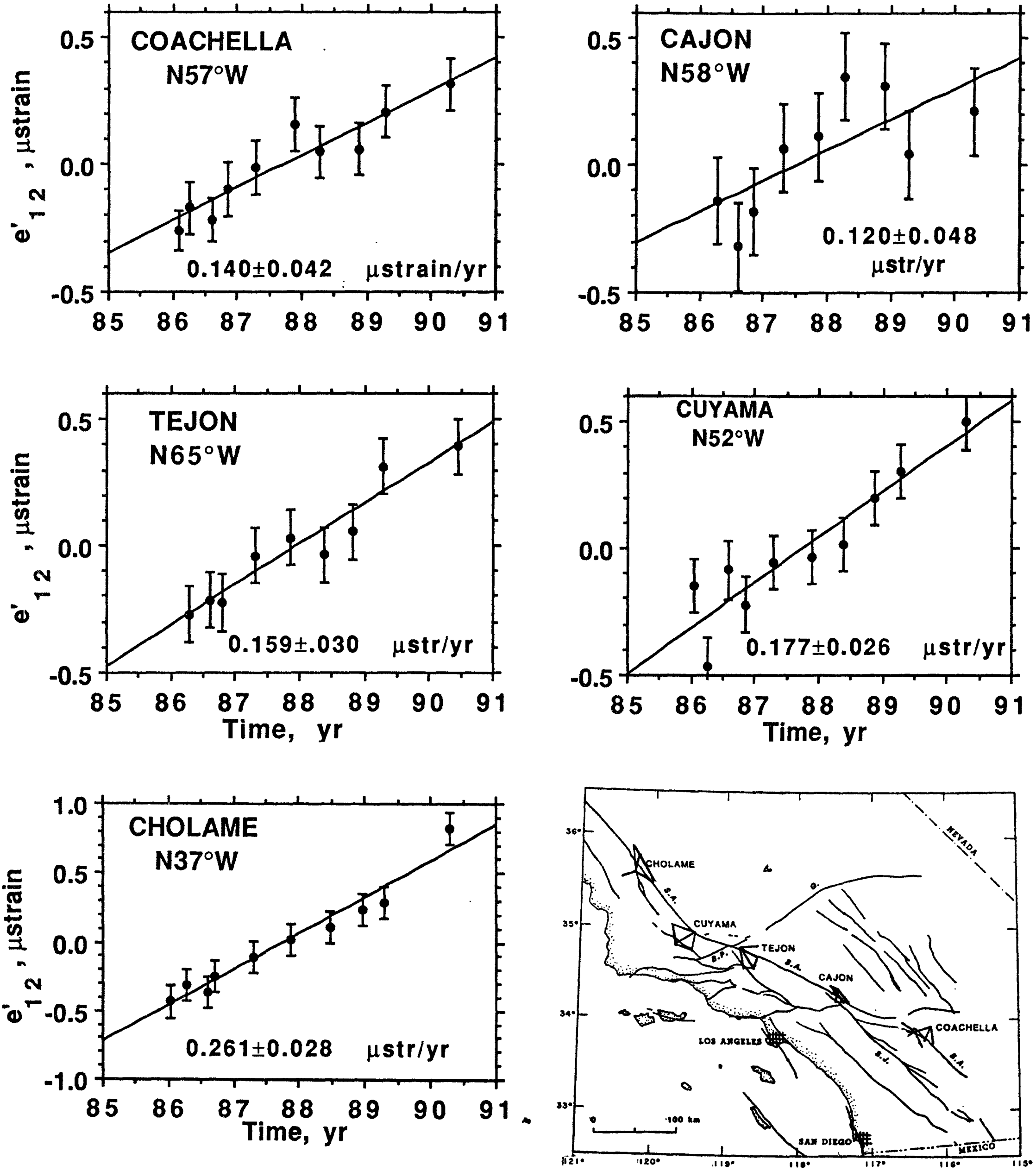

Figure 1. Right-lateral shear-strain accumulation as a function of time at five 6-line trilateration networks located along the San Andreas fault. The error bars indicate one standard deviation on either side of the plotted point.

3. Strain Accumulation Across the Wasatch Fault, Utah.

A trilateration network extending across the Wasatch fault near Ogden has been surveyed in 1972, 1973, 1976, 1978, 1981, 1984, 1987, and 1990. The average principal strain rates are $\dot{\epsilon}_1 = 0.033 \pm 0.009$ and $\dot{\epsilon}_2 = -0.009 \pm 0.010 \mu$strain/yr (extension reckoned positive) with the axis of greatest extension directed N90°E ± 5°. The accumulation of east-west extension is consistent with normal slip on the N10°W striking Wasatch fault. Although the average east-west extension is small ($0.033 \pm 0.009 \mu$strain/yr), it is several times larger than would be expected for the geologically determined secular slip rate of 1 mm/yr on the Wasatch fault. The observed strain accumulation is not significantly correlated with the fluctuations in the level of the Great Salt Lake.

4. Strain Accumulation Across the Denali Fault, Alaska.

Surveys of trilateration networks across the Denali fault at the Nenana River in 1982, 1984, 1988 and at the Delta River in 1975, 1979, 1982, and 1984 indicate a minor (0.1 ±0.04 μstrain/yr) northeastward uniaxial extension. The component of right-lateral shear-strain accumulation across the fault is not significant at the two-standard-deviation level. At the Delta River network the strain accumulation rate decreases rapidly with distance from the fault, but evidence for a similar decrease with distance from the fault is lacking at the Nenana River network. The strain accumulation rates inferred from trilateration are consistent with the VLBI (very long baseline interferometry) measurement reported by *Ma et al.* [JGR, in press, 1990] and support their contention that significant right-lateral shear is not accumulating along the Denali fault at the present time. *Savage et al.* [JGR, **80**, 1005, 1981] had earlier concluded erroneously that preliminary geodetic measurements at the Delta River network demonstrated right-lateral shear-strain accumulation. The absence of significant right-lateral deformation across the Denali fault in the 1975–1988 interval is in marked contrast with the abundant geomorphic evidence for Holocene right-lateral secular slip at the rate of 10 to 20 mm/yr on the Denali fault in this sector.

5. Revised Estimate of Shallow Slip Rate Across the Hayward Fault in Oakland, California.

The possibility of a relatively low creep rate across the Hayward fault in Oakland suggested by *Prescott and Lisowski* [Tectonophysics, **97**, 46, 1983] is not supported by new data. The 1947–1981 angle changes within a 6-km-wide triangulation-trilateration network spanning the Hayward fault indicates a shallow slip rate of 5.2±0.6 mm/yr. A similar rate, 5.7 ± 1.6 mm/yr, is calculated from the 1981–1990 average length change in a 5-km-long line that spans a 0.5-km-wide zone. These rates are similar to the 5.3 ± 0.9 mm/yr block motion rate deduced from the 1972–1988 average rate of length change in a 30-km-long Geodolite line that spans a 12-km-wide zone around the Hayward fault. The geodetically determined shallow slip rates are consistent with the 5 mm/yr creep rate determined by Jim Lienkaemper from offset cultural features on this part of the Hayward fault.

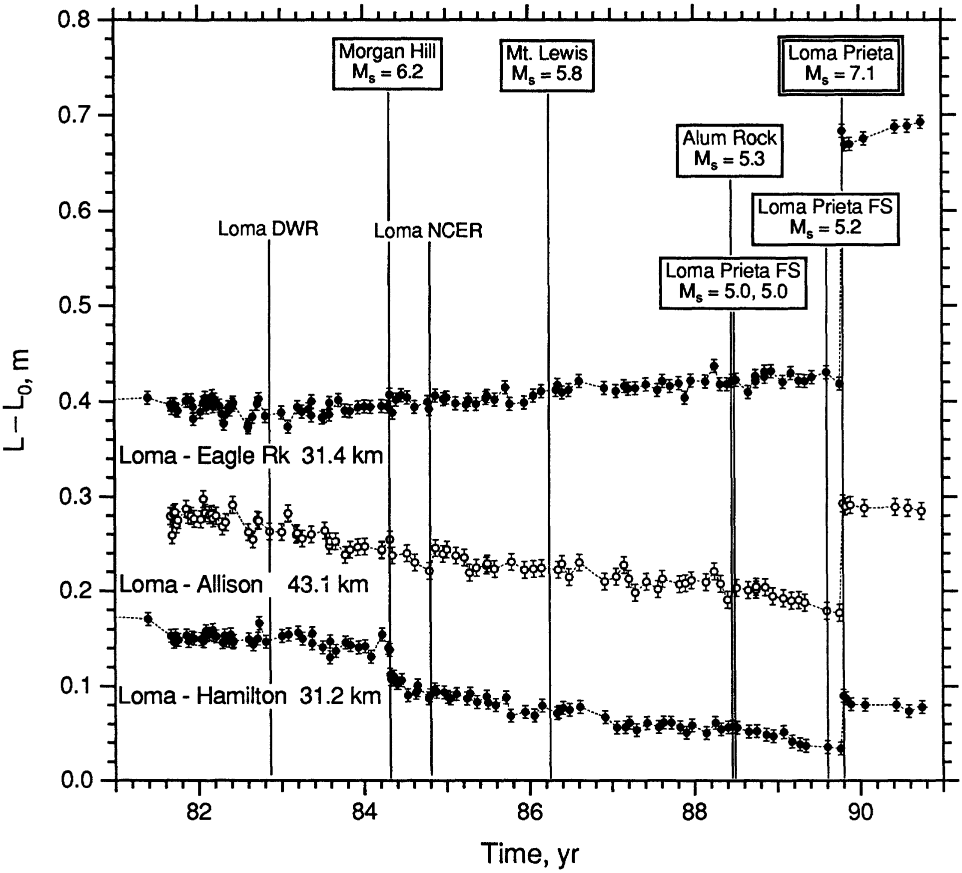

Figure 2. Time history of line lengths measured from a geodetic station located on Loma Prieta (the highest peak in the Santa Cruz Mountains). Vertical lines mark the times of nearby M> 5 earthquakes (boxes) and changes in the observing site. The error bars indicate one standard deviation on either side of the plotted point.

6. Deformation in the Year after the Loma Prieta Earthquake.

Geodolite measurements of distance from a geodetic station located 11 km from the epicenter of the Loma Prieta earthquake ($M_s = 7.1$; October 17, 1989) to three stations 30 to 40 km distant provide an unusually complete record of the deformation in the epicentral region of the earthquake (Figure 2). Possible changes in the rate of deformation prior to the earthquake were discussed by *Lisowski et al.* [GRL, **17**, 1211–1214, 1990]. The rates of line-length change in the lines Loma-Eagle and Loma-Allison appear to be slightly different in the year after the earthquake, but this difference is not yet significant. The largest change occured in the line Loma-Eagle, which crosses the rupture zone of the earthquake in an east-west direction. The 1984.8–1989.8 rate averaged 5.8 ± 0.6 mm/yr and the 1989.8–1990.8 rate averaged 20.2 ± 7.3 mm/yr.

Reports

Lisowski, M., W.H. Prescott, J.C. Savage, and J.L. Svarc, 1990, A possible geodetic anomaly observed prior to the Loma Prieta, California, earthquake *Geophys. Res. Lett*, **17**: 1211–1214.

Lisowski, M., W.H. Prescott, J.C. Savage, and M.J. Johnson, 1990, Geodetic Estimate of coseismic slip during the 1989 Loma Prieta, California, earthquake, *Geophys. Res. Lett*, **17**: 1437–1440.

Array Studies of Seismicity

9930-02106
David H. Oppenheimer
Branch of Seismology
United States Geological Survey
345 Middlefield Road - MS 977
Menlo Park, California 94025
415-329-4792

Investigations

1. Process, interpret and disseminate Loma Prieta seismic data.
2. Continue consolidation and clean-up of phase data of central California Seismic Network (CALNET) from 1969 through present.
3. Investigate seismic gaps along Rodgers Creek-Hayward fault system and the Concord-Calaveras-Sunol fault system.

Investigations

1. Efforts were directed toward completion of manuscripts describing the Loma Prieta aftershock data (see previous Semi-annual Technical Summaries and "Reports" below). Since processing of the October 1989 aftershock data is incomplete, this project maintains the most current data set for dissemination to the seismological research community. Data distribution continues to consume substantial project resources.

2. Progress continues to be made in the collection, organization, relocation, archiving, and documentation of CALNET earthquake data since 1969 (see previous Semi-Annual Reports). We have completed merging RTP and CUSP data for the latter half of 1986, when the Chalfant Valley sequence occurred, and thus the entire catalog from 1/69 through the present (with the exception of October, 1989) is assembled and complete. Preliminary quality checks to remove systematic errors in magnitude determination and gross blunders were begun, but we are unable at this time to estimate the amount of time required to rectify these problems. This data set is in much demand, and the project devotes considerable effort to answering data requests and inquiries from the public on seismicity in central California.

3. As reported in the previous Semi-annual technical summary, the 20 years of microseismicity in the San Francisco Bay area defines aseismic regions (gaps) which are thought to slip during main shock rupture. A report describing a seismic gap approximately 30 km in length along the Rodgers Creek fault zone north of the San Francisco Bay was prepared in collaboration with Karen Budding and David Schwartz of the U.S.G.S. The report describes the initial results of their paleoseismicity study within the gap and the historical seismicity of the region. Offset alluvial deposits yield a minimum slip rate of 2.1 to 5.8 mm/yr for the past 1300 years, and the maximum recurrence interval is estimated to be 248 to 679 years. Since the minimum elapsed

time since the last rupture is 182 years, this section of the fault may be approaching failure again.

A second area under study is the Concord-Calaveras-Sunol fault system east of San Francisco Bay. In April, 1990 a series of earthquakes occurred along a previously aseismic cross-fault structure linking the Concord and Calaveras faults. The earthquakes caused significant damage to local residential structures and prompted us to examine the relation of this seismicity to the potential for larger earthquakes on adjacent faults. To the north on the Concord fault exists a microseismic gap of approximately 25 km in length on which occurred a M5.5 earthquake in 1955. To the south on the Calaveras fault another 25 km gap exists terminating to the south at the Calaveras Reservoir. The last known M>5 earthquake to possibly rupture this segment occurred in 1864. A report is in preparation describing the seismogenic potential of this fault system and its seismotectonic significance.

Reports

Oppenheimer, D.H., Aftershock slip behavior of the 1989 Loma Prieta, California earthquake, *Geophys. Res. Let., 17*, 1199–1202, 1990.

Dietz, L.D., and W.L. Ellsworth, The October 17, 1989 Loma Prieta, California, earthquake and its aftershocks: Geometry of the sequence from high-resolution locations, *Geophys. Res. Let., 17*, 1417–1420, 1990.

King, G.C.P, A.G. Lindh, and D.H. Oppenheimer, Seismic slip, segmentation, and the Loma Prieta earthquake, *Geophys. Res. Let., 17*, 1449–1452, 1990.

Michael, A.J., W.L. Ellsworth, and D.H. Oppenheimer, Coseismic stress changes induced by the 1989 Loma Prieta, California earthquake, *Geophys. Res. Let., 17*, 1441–1444, 1990.

Oppenheimer, D.H., Forecasting main shock rupture location from microseismicity, in *PRC-US Bilateral Symposium on Xianshuihe Fault Zone and Field Geological Excursion, September 22-30, 1990, Program and abstracts*, 106–107, 1990.

Budding, K.E., D.P. Schwartz, and D.H. Oppenheimer, Slip rate, earthquake recurrence, and seismogenic potential of the Rodgers Creek fault zone, northern California: Initial results, submitted to *Geophys. Res. Let.*.

California Seismicity Studies

9930-02103

Paul A. Reasenberg
Donna Eberhart-Phillips
Mark V. Matthews

Branch of Seismology
United States Geological Survey
345 Middlefield Road - MS 977
Menlo Park, California 94025
415-329-5002

Investigations

1. Microclusters and Composite Clusters

Microclusters – small groups of earthquakes occurring close in time and space to each other – are easily recognized in the California earthquake catalogs. Most consist of a larger earthquake followed by one or more aftershocks. Of the 3656 microclusters identified in the central California catalog from 1969 to 1989, 89% consist of 5 or fewer events, and 63% consist of only 2 events. Their durations range from a few minutes to over a month, with 90% less than 3 days. Microclusters appear to occur in all the major fault zones in California, with approximately the same spatial and temporal distribution as the seismicity.

I assume that the interevent times in microclusters are random samples of the same physical processes governing the Omori decay of large earthquake sequences. A composite cluster is created by combining data for a subset of related microclusters, all drawn, for instance, from the same fault zone, crustal block or time period. The composite cluster consists of all the secondary events in the selected microclusters, with times shifted so as to preserve the time relative to their respective mainshocks. The Omori parameter, p^*, for the composite cluster represents the average decay process for the space-time region in which the consitituent microclusters occurred. The procedure is analogous to that of combining first-motion observations from a set of small earthquakes to obtain a composite focal mechanism. There, the small earthquakes are assumed to have a common mechanism. Here, the microclusters are assumed to be driven by a common seismogenic process.

Along the major fault zones in central California, p^* ranges from 0.6 to 1.2 ($\sigma \approx 0.1$). Along the actively slipping fault segments in the Bay area $p^* \geq 0.9$. In locked zones along the San Francisco Peninsula and east of the Calaveras fault $p^* < 0.9$. The deep, Loma Prieta segment of the San Andreas fault exhibited the lowest value ($p^* = 0.6$) in central California for the period 1969-1989. For the aftershocks of the Loma Prieta earthquake, the traditional (not composite) Omori parameter $p = 1.1$. In southern California, composite clusters for the crustal blocks northeast of the San Andreas fault and southwest of the San Jacinto fault exhibit p^* values in the range $1.1 \sim 1.2$, while the composite clusters for the San Andreas and San Jacinto fault zones have p^* in the range $1.3 \sim 1.8$. No significant differences in p^* were found among regions characterized solely by high or low heatflow. These results suggest that p^* in a region may be sensitive to the rate at which the region is able to accomodate a stress pulse by cold rheological processes such as fault creep. Thermal rheological (ductile) processes do not appear to be a factor. If so, p^* analysis may be useful for locating regions of high (and low) strain rate directly from the available microearthquake data. Furthermore, regions such as the Loma Prieta segment of the San Andreas fault, which exhibited the lowest value of p^* in California, and which are surrounded by regions of higher values of p^*, might be likely places for increased elastic strain accumulation (and a future strong earthquake).

2. Loma Prieta

In the Loma Prieta region, another three-dimensional velocity model has been obtained using a better data set. Refraction shots and earthquakes from the surrounding area were included to improve spatial distribution. Aftershock arrival times at temporary stations, as well as the CALNET stations, were also included. Three months of aftershocks were relocated in the 3D velocity model to obtain improved locations and compare to the velocity variations.

3. Velocity Structure and Seismicity

Taken together, studies of 3D velocity variations and seismicity at Loma Prieta, Parkfield, Morgan Hill and Coalinga show some consistent observations relating to rupture behavior. Variations in material property as imaged by heterogeneities in seismic velocity along fault are associated with variations in the character of rupture and variations in seismicity patterns. These results imply that velocity analysis may be an important tool for segmenting fault zones and delineating areas with expected large rupture. The fault zone appears as a simple vertical boundary in the creeping zone where there is a high level of microearthquake activity and where rupture behavior is temporally uniform. The velocity pattern of the fault zone is complicated where the fault is locked and characterized by rupture in moderate and large infrequent earthquakes. The rupture areas are limited by features observed in the seismic velocity models. At Loma Prieta, the high-velocity body along the northeast side of the fault can be directly related to the fault area that is inferred to have ruptured during the mainshock. At Parkfield, a high-velocity body along the southeast portion of the anticipated rupture area correlates with the area of maximum coseismic slip inferred by Segall and Harris (JGR, 1987) for the 1966 Parkfield earthquake. At Coalinga, the rupture terminated at the approximate boundary between Great Valley and Franciscan rocks.

Other velocity features appear to influence seismicity. At Loma Prieta, the most prominent off-fault clusters of aftershocks are associated with the positions of the low-velocity wedge above the mainshock and the northwest end the the high-velocity body. At Parkfield, on the northeast side of the fault, there is a large volume of relatively low-velocity material, which is inferred to be overpressured based on its velocity, resistivity and gravity. It adjoins the San Andreas at Middle Mountain, site of the anticipated mainshock hypocenter, and extends eastward toward Kettleman Hills, where rupture has been characterized by a slow earthquake with a high level of postseismic deformation.

4. Gravity

Since surface measurements of gravity provide information about rock density and density is strongly related to velocity, gravity may be useful for refining velocity models obtained from travel-time data. A method has been developed to invert gravity data for perturbations to the 3D velocity model. The gravity is upward continued 2 km so that a point-mass approximation is adequate. Gravity is calculated from a grid of point masses whose density is inferred from a regional velocity-density curve. Gravity residuals are related to changes in velocity and an iterative inversion solution for velocity is carried out. This method is now being applied at Parkfield. In the Salinian block, results correlate well with surface geology. On the northeast side of the SAF, the low-velocity area does not fit the observed gravity. Thus the low-velocities are most likely due to high pore-pressure, which can greatly reduce seismic velocity but has little effect on density.

Reports

Reasenberg, Paul A., Variations in the Omori Decay Parameter for "Composite Earthquake Clusters" in central California (abs.), Seismological Research Letters, 61, p.40 (1990).

Reasenberg, Paul A., Microclusters and Composite Clusters (abs.), EOS, in print, (1990).

Eberhart-Phillips, D., A. J. Michael, G. Fuis, and R. Luzitano, Three-dimensional crustal velocity structure in the region of the Loma Prieta, California, earthquake sequence from inversion of local earthquake and shot arrival times, Seismol. Res. Lett., v. 61, p. 48, 1990.

Michael, A. J., and D. Eberhart-Phillips, Correlation of heterogeneity in seismic behavior and seismic velocities, Seismol. Res. Lett., v. 61, p. 34, 1990.

Eberhart-Phillips, D., V. F. Labson, W. D. Stanley, A. J. Michael, and B. D. Rodriguez, Preliminary velocity and resistivity models of the Loma Prieta earthquake region, Geophys. Res. Lett., v. 17, p. 1235-1238, 1990.

Ekstrom,G., R. S. Stein, J. P. Eaton, and D. Eberhart-Phillips, Seismicity and geometry of a 110-km-long blind fault, 1: the 1985 Kettleman Hills, California, earthquake, submitted to J. of Geophys. Res., 1990.

Eberhart-Phillips, D., Three-dimensional P- and S-velocity structure in the Coalinga region, California, J. of Geophys. Res., v. 95, p. 15343-15363, 1990.

FLUID PRESSURE AND EARTHQUAKE GENERATION

Project #9960-04451

Evelyn Roeloffs, Eddie G. Quilty
Branch of Tectonophysics
U.S. Geological Survey
345 Middlefield Road, MS 977
Menlo Park, CA 94025
(415)329-4833

Investigations:

1. Real-time monitoring and processing of water level data from Parkfield, California as part of the Parkfield Prediction Experiment. Real-time monitoring of water level data from two sites near Palmdale, California. Water level data are processed in real time to remove tidal and barometric fluctuations, and the processed data are automatically screened for anomalous signals. A beeper monitoring system provides 24 hour a day automatic notification of water level anomalies near Parkfield.

2. Analysis of water level records and development of theoretical solutions to study response to fault creep, seismic waves, and barometric pressure. Searching of water level data for changes that may be related to to the earthquake generation process.

Results:

1. In cooperation with the USGS Water Resources Division, water level data from a network of 12 sites near Parkfield, California were collected throughout the reporting period. Water level data were also collected from two sites in the Mojave Desert. Site locations are shown in Figures 1a and 1b, and Raw water level, barometric pressure, and rainfall data are shown in Figures 2a-f.

2. A paper on the transfer functions relating barometric pressure to water level in the Parkfield area was completed. In this article we present time series of water level data from which barometric pressure effects have been removed using frequency-dependent transfer functions. We also investigated the stability in time of such transfer functions as determined using cross-spectral analysis on water level and barometer data, and we found that transfer functions determined from short stretches of data scatter more widely about the average transfer function than expected. At the Gold Hill site near Parkfield, the degree of scatter interferes with determination of the transfer function. Further work has identified sets of data from Gold Hill that produce a consistent transfer function in a limited sub-tidal frequency band.

3. One of us (ER) visited the All-Union Institute for Engineering Geology and Hydrogeology, near Moscow, and was able to study water level data from the epicentral region of the December 7, 1988 Spitak (Armenia) earthquake. Where

possible, the same types of analysis that are applied to the Parkfield water level data were applied to the Spitak data. The data are of special interest because Soviet scientists have identified water level changes in several wells that they believe to be intermediate-term precursors to the Spitak earthquake.

Reports:

Quilty, E.G., and E. Roeloffs, "Removal of barometric pressure effects from water level data", submitted to Journal of Geophysical Research.

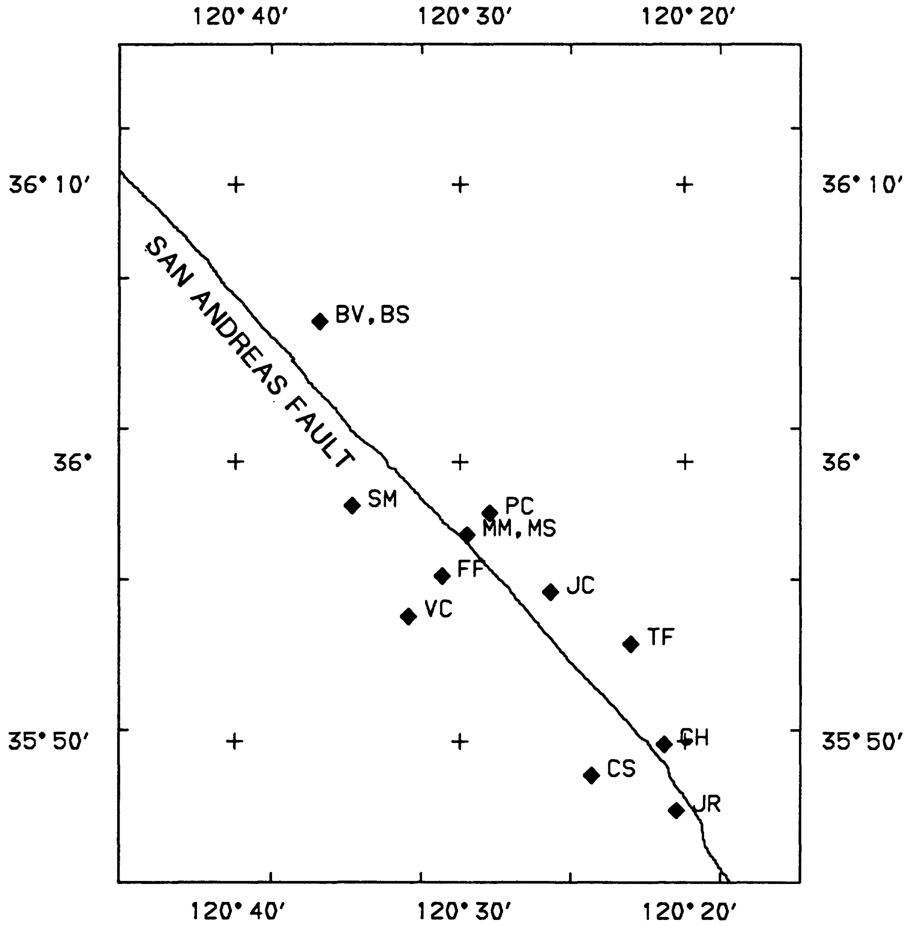

Figure 1. (a) Map showing water wells near Parkfield California, monitored as part of the Parkfield Earthquake Prediction Experiment.

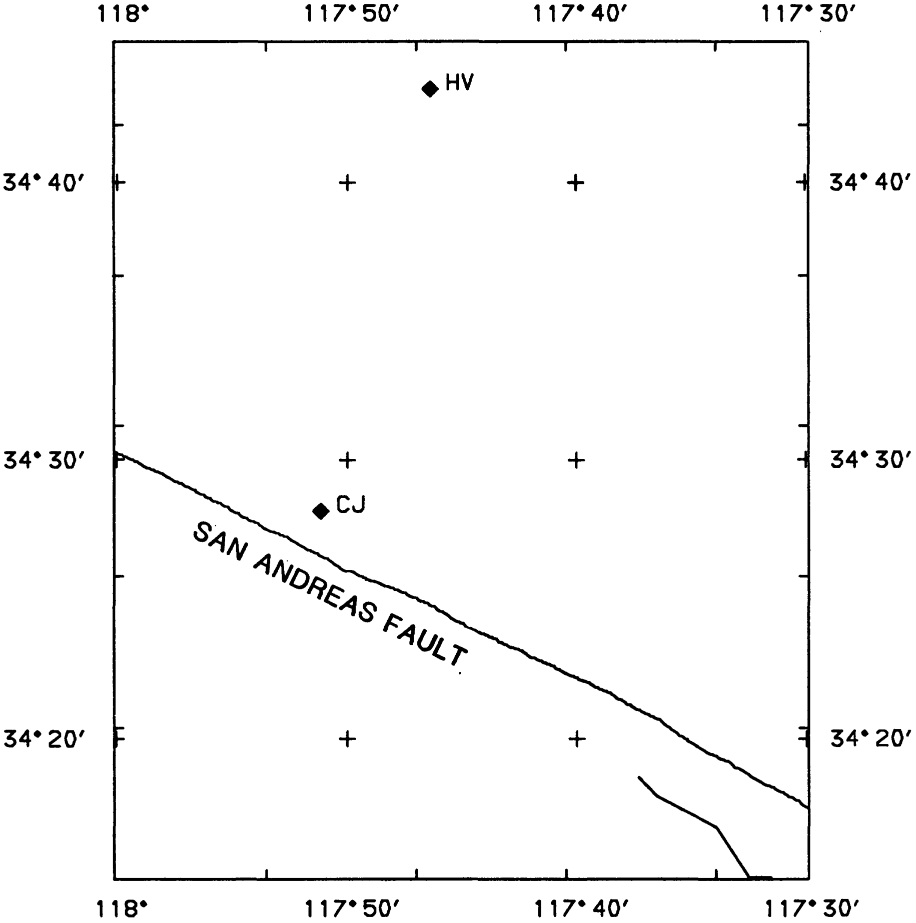

Figure 1. (b) Map showing wells HV and CJ near the Mojave segment of the San Andreas fault.

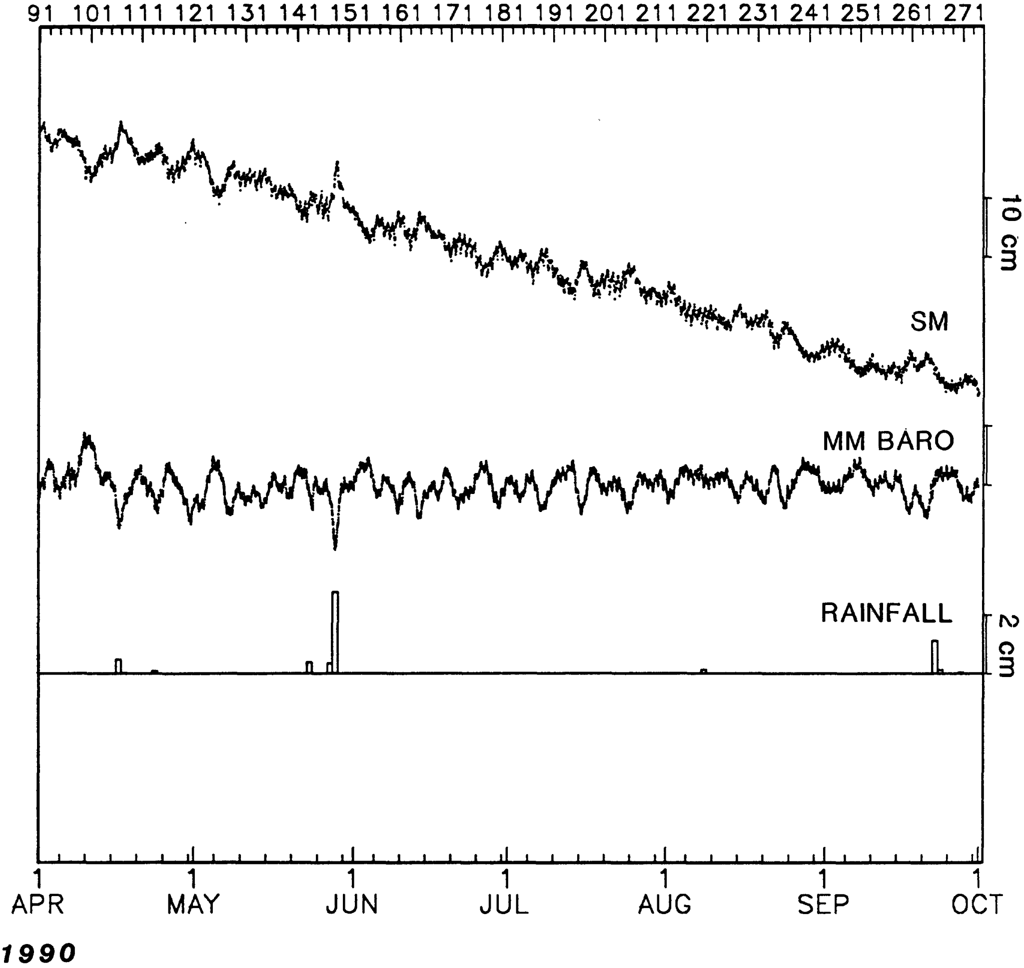

Figure 2. (a) Water level, barometric pressure, and rainfall records. Hourly values are plotted for water level and barometric pressure. Water level is in centimeters above an arbitrary datum. Barometric pressure is in centimeters of water with respect to an arbitrary datum. Bars indicate total rainfall in a 24 hour period. Site names are indicated at right.

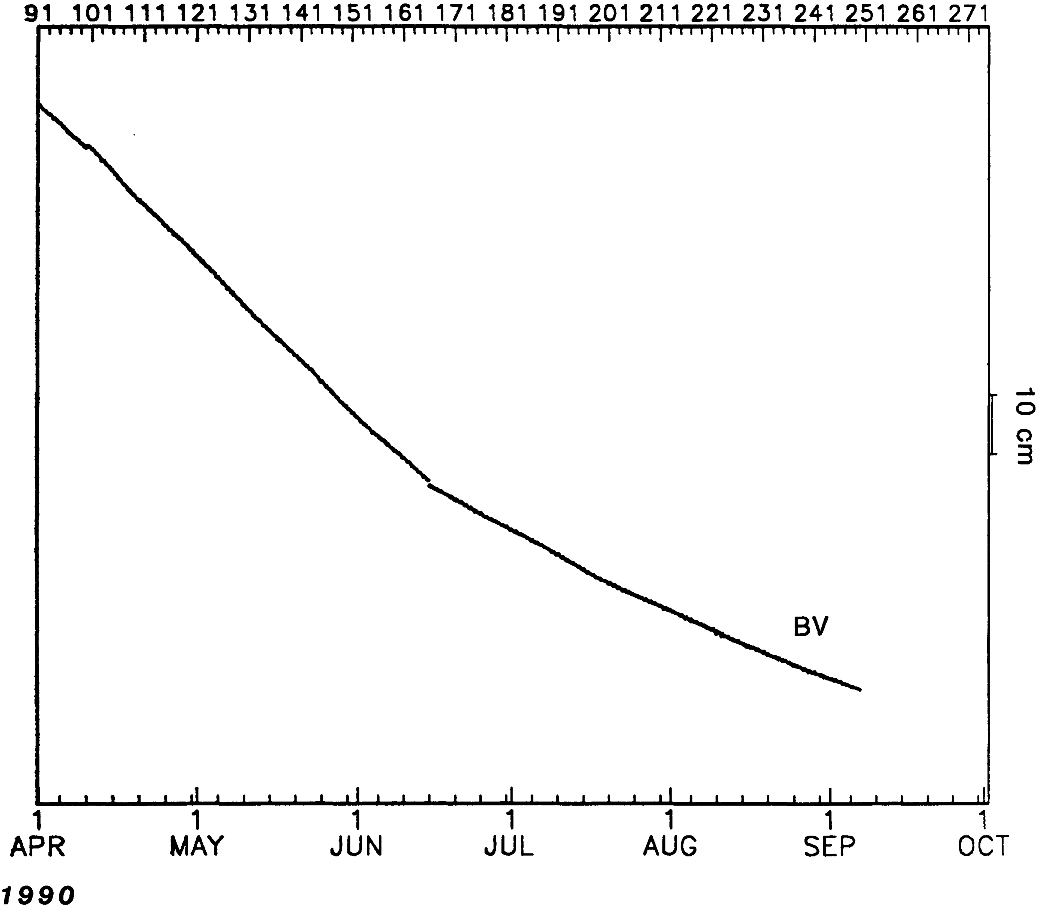

Figure 2. (b) Water level records plotted as in Figure 2(a).

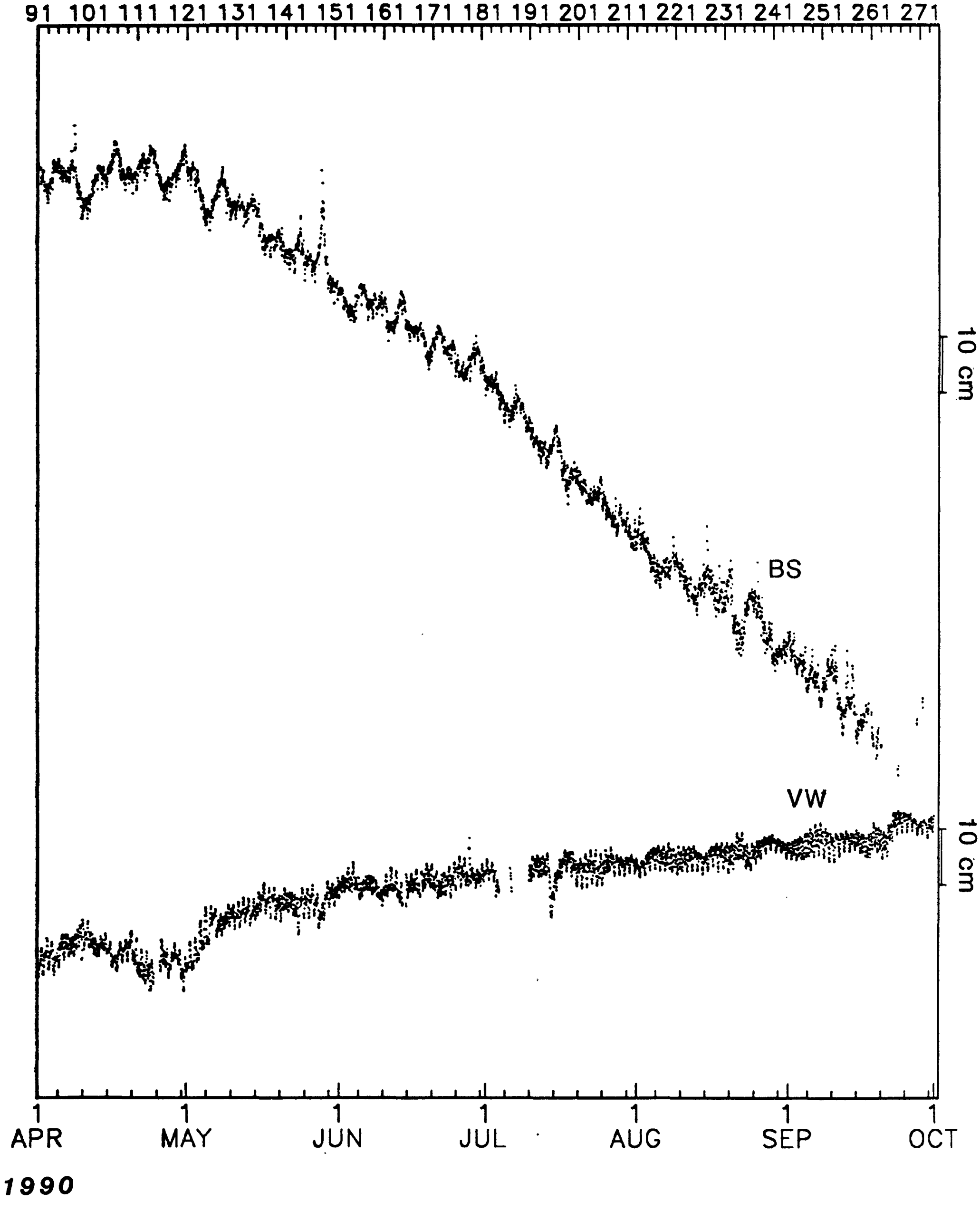

Figure 2. (c) Water level records plotted as in Figure 2(a).

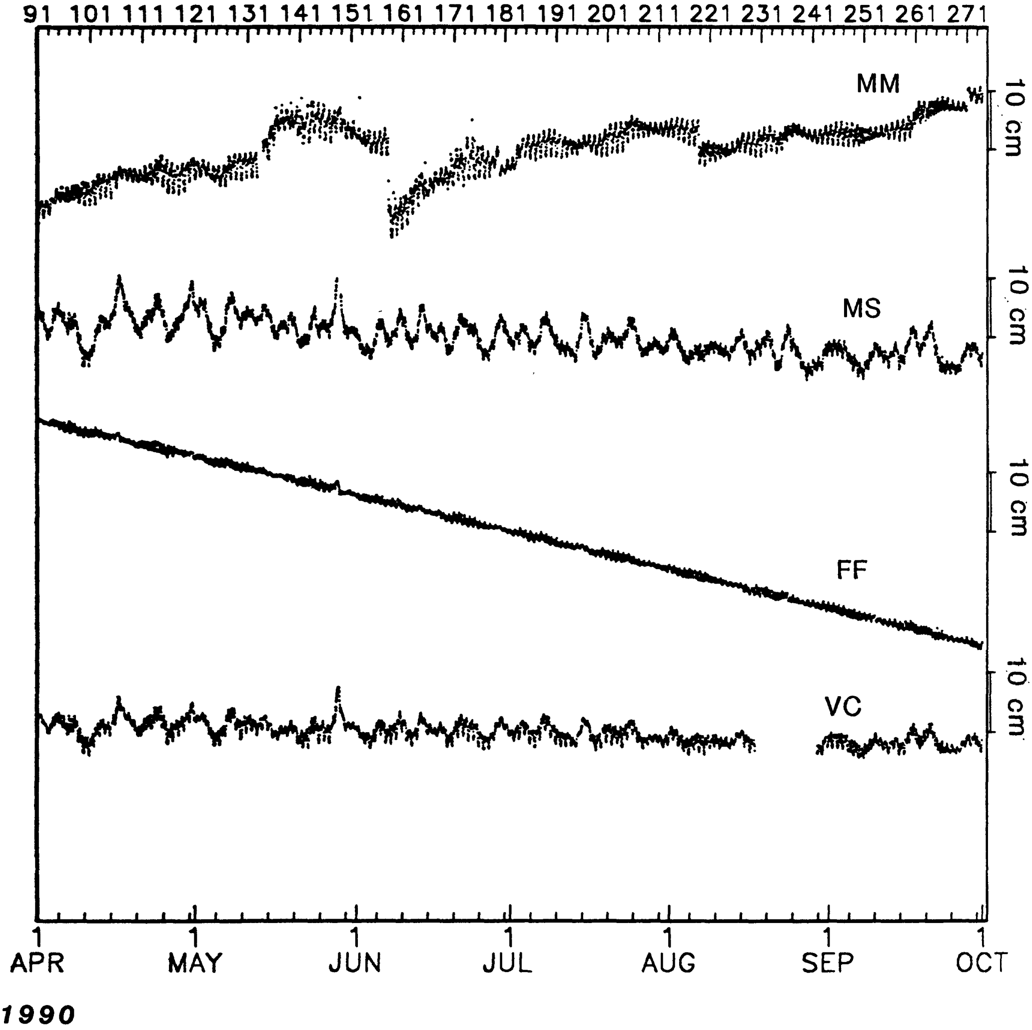

Figure 2. (d) Water level records plotted as in Figure 2(a).

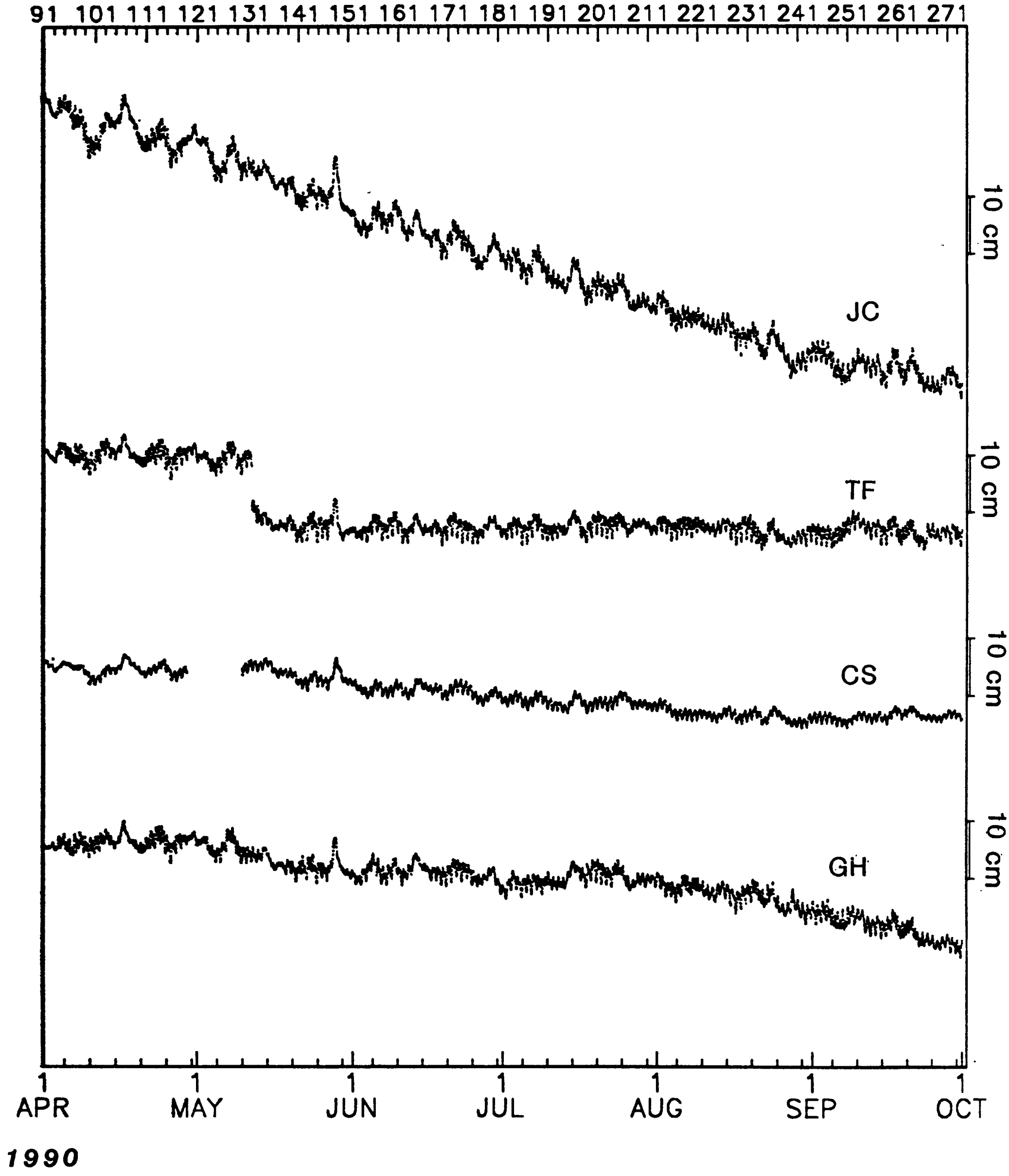

Figure 2. (e) Water level records plotted as in Figure 2(a).

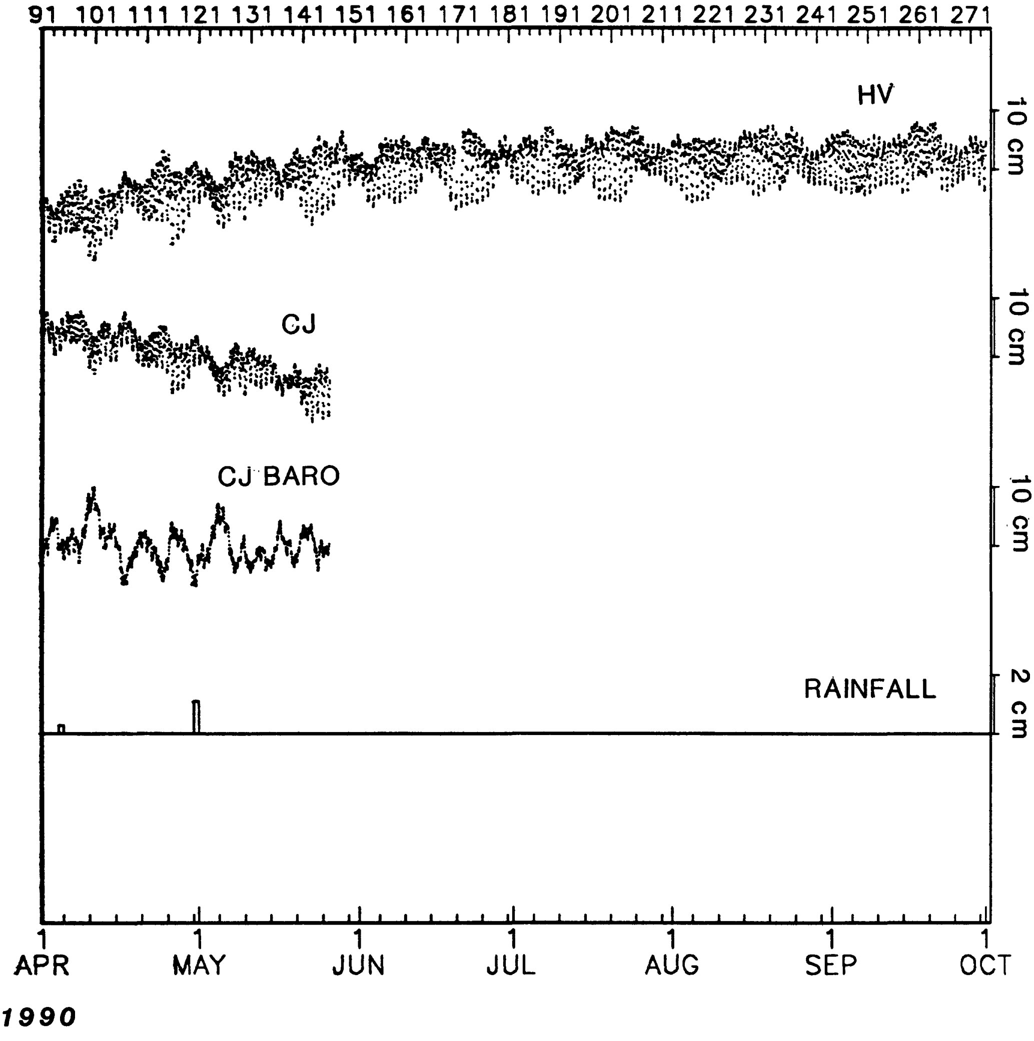

Figure 2. (f) Water level, rainfall, and barometer records plotted as in Figure 2(a).

Interpretation of Slip-Induced Water Well Level Changes at Parkfield

14-08-0001-G1691

J. W. Rudnicki
Department of Civil Engineering
Northwestern University
Evanston, IL 60208
(708)-491-3411

(For period April 16, 1990 to September 30, 1990)

Objective

Properly calibrated water wells can function as inexpensive and sensitive strainmeters. Solutions predicting water well level changes due to slip are needed to infer fault slip history and distribution from observed water well level changes. Recent solutions for pore pressure changes induced by fault slip have demonstrated that the coupling between deformation and pore fluid diffusion can strongly affect the response of the well to slip, particularly if the well is close to the fault, and, consequently, the inference of fault slip from water well level changes. The objective of this study is to assess effects of coupling between deformation and diffusion on the inference of fault slip from observed water well level changes and to include these effects in the analysis of observed water well level changes at Parkfield.

Results

We have examined coupled deformation-diffusion effects on five creep induced water level changes recorded in the deep interval of the Middle Mountain well from January 1989 to July 1990. The observed water level changes are characterized by a sharp drop and a slow recovery with magnitude of the change ranging from 11 to 15 cm. The slip history of the creep events for this portion of the San Andreas fault can be described by the following function suggested by Wesson [1988]:

$$u(t)=u_0(1-[C(b-1)u_0^{b-1}t+1]^{-\frac{1}{b-1}})$$

where u_0 is the final displacement, and b and C are constants. The values of u_0 , b, and C are obtained from data at two creepmeters near the well. The pore pressure response induced by such slip is calculated using Rudnicki's [1987] solution for instantaneous slip on an impermeable plane in a fluid-saturated porous medium. For values of the diffusivity consistent with those inferred from the analysis of the tidal response of the well, the calculated response history agrees well with that observed for each of the five creep events. The slow recovery of the water level response suggests that the magnitude of the coupling effects are not large at this site. Nevertheless, coupling seems essential since the recovery in the observed response is not easily explained by uncoupled solutions. Although shapes of the calculated and observed response agree well, the amplitudes of the water level change do not correlate well with the amplitudes of the slip for the different creep events. This implies that the amount and time history of slip are different at the earth's surface, where the creepmeters are installed, and at depth.

We have also conducted a preliminary reexamination of anomalous water level signals observed by Merifield and Lamar [1985] in three wells in southern California, one at Ocotillo Wells and two in the Borrego Valley. The original data records were digitized, interpolated and sampled hourly. Two charts of barometric pressure recorded at Anza Valley, which is about 50 km away, were also digitized and interpolated.

The water level data were processed by removing tidal and barometric effects. Unfortunately, the residuals are still large and it appears that the barometric pressure record at Anza Valley is sufficiently different from that at the well sites that it cannot be used to thoroughly remove barometric effects from the well response. Although the anomalies are apparent, the record is too noisy to make a detailed quantitative analysis profitable.

References

Merifield, P. M. and D. L. Lamar, Possible strain events reflected in water levels in wells along the San Jacinto fault zone, **PAGEOPH**, **122**, 245-254, 1985.

Rudnicki, J. W., Plane strain dislocations in linear elastic diffusive solids, J. **Appl. Mech.**, **54**, 545-552, 1987.

Wesson, R. L., Dynamics of fault creep, J. **Geophys. Res.**, **93**, 8929-8951, 1988.

Publication

Yin, J., E. A. Roeloffs, and J. W. Rudnicki, Coupled deformation diffusion effects on water level changes induced by fault creep at Parkfield, California (Abstract), submitted for presentation at Fall AGU, 1990.

Hydrogen and Other Non-Radon Geochemical Monitoring

Project #9980-02773

Motoaki Sato* and J. Michael Thompson**
Branch of Igenous and Geothermal Processes
U.S. Geoilogical Survey
* MS-959, Reston, VA 22092; ** MS-910, Menlo Park, CA 94025
(703) 648-6766, FTS 959-6766

INVESTIGATIONS

We continuously monitor soil hydrogen at 1.5 m depth along the San Andreas and Calaveras faults in central California. There are 4 telemetered monitoring sites in the Hollister area, and 7 telemetered sites in the Parkfield area (Fig.1). Five sites in the Parkfield area are equipped with duplicate sensors which are 17 m apart.

We also continuously monitor water conductivity, dissolved CO_2, and dissolved H_2 of pumped water at two wells, one drilled into the San Andreas fault zone (Taylor Ranch) and the other about 500 m from the fault (Miller Ranch). These sites are marked with filled triangles in Fig. 1.

RESULTS

Soil Hydrogen

The telemetered data from soil H_2 monitoring sites are compositely shown in Fig. 2. There were no major confirmed anomalies between April 1 and October 1, 1990, in spite of a series of D-level and a few C-level alerts issued on the basis of physical parameters.

Between May 6 and May 16 all the sites were visited for semmi-annual maintenance service. On this trip, the power supply electronics was modified at all solar-powered sites in an effort to reduce instrumental diurnal variations. Previously these sites had a 12V voltage regulator to provide a stable power, but when the storage battery voltage fell below about 13.5 V, the regulator failed to stabilize the voltage, giving rise to diurnal signal changes equivalent to as much as 100 ppm H_2 changes. Such large instrumental diurnal variations made the detection of subtle anomalous changes difficult. We replaced the 12V regulator with a 5V regulator and added a 5V/12V voltage converter, so that the supply voltage stays constant until the battery voltage falls below about 6.5V. Discontinuous changes in the hydrogen signal in mid-May at Twisselman Ranch, Gold Hill, Parkfield, Middle Mountain, Slack Canyon, and Melendy Ranch were due to this power supply circuitry change.

At Gold Hill and Middle Mountain, the vault temperatureor was also monitored. The thermometer circuit had to be removed eventually, however, because it interfered with other circuits by forming groundloops. Gold Hill was also equipped with an isolation amplifier which was not connected with a hydrogen sensor following the suggestion of Carl Mortensen. This dummy setup turned out to be very informative; it recorded diurnal changes of a magnitude similar to those of other sites. Although we had selected components that had smaller temperature coefficients than 100 ppm/°C, which would theoretically have produced less than 0.1% signal change for 20°C temperature change, the signal from the blank amplifier(Analog Device 284J, max. temco. 75 ppm/°C) actually varied by several percent. The blank signal change was not in phase with the solar panel voltage change but was in phase with the ambient temperature change.

Upon checking the records of past several years, we discovered that the battery voltages became considerably lower at the solar-powered sites where a duplicate sensor was added (Gold Hill, Middle Mountain, Parkfield). This symptom became worse after the power supply stability was enhanced by using the combination of 5V regulator and a DC voltage converter.

In conclusion, the soil hydrogen monitoring network needs the following improvements: (1) instead of the old-design 284J isolation amplifiers, newer amplifiers of higher temperature stability and power efficiency (such as Analog Device 5B30 signal conditioner) should be used at all sites; (2) an additional or a larger solar panel must be installed to supply enough power at solar-powered sites where duplicate sensor systems are operated; and (3) more frequent site visits must be made at least until most of the sites are upgraded and proven to be fully functional. The above three improvements must be carried out as soon as possible so that high quality data can be collected before the anticipated Parkfield earthquake strikes.

Water Geochemistry

The data recorded at Miller Ranch are shown in Fig. 3 and those recorded at Taylor Ranch in Fig. 4. Discontinuous changes that occurred in mid-May are due to servicing. The graddually increasing trend in water conductivity at Miller Ranch that happened in late summer was probably real, because the rancher started pumping irrigation water from the same well on account of severe water shortage. Probably the salt concentration in the ground water became increasingly higher due to evaporation and leaching.

Dissolved CO_2 and H_2 values were not collected under proper experimental conditions. In May, we discovered that somebody shut off the water supply valve for our experiment at Miller Ranch. This over-taxed the motor of the triplex metering pump, which pumps air and water into the degassing chamber at a fixed ratio. The CO_2 record probably reflects changes in the ambient CO_2 level inside of the instrumentation housing.

Taylor Ranch also sufferred from similar problems. Because of frequent power outages and water supply failures, the metering pump motor was worn out. All metering pumps including a spare are now inoperative. These water geochemistry monitoring sites were built using a one-time State of California funding. As we wait longer and longer for the earthquake to strike, the cost of maintenance becomes an increasingly serious problem. However, we will keep looking for more durable pumps which are rated for continuous duty and overload protected.

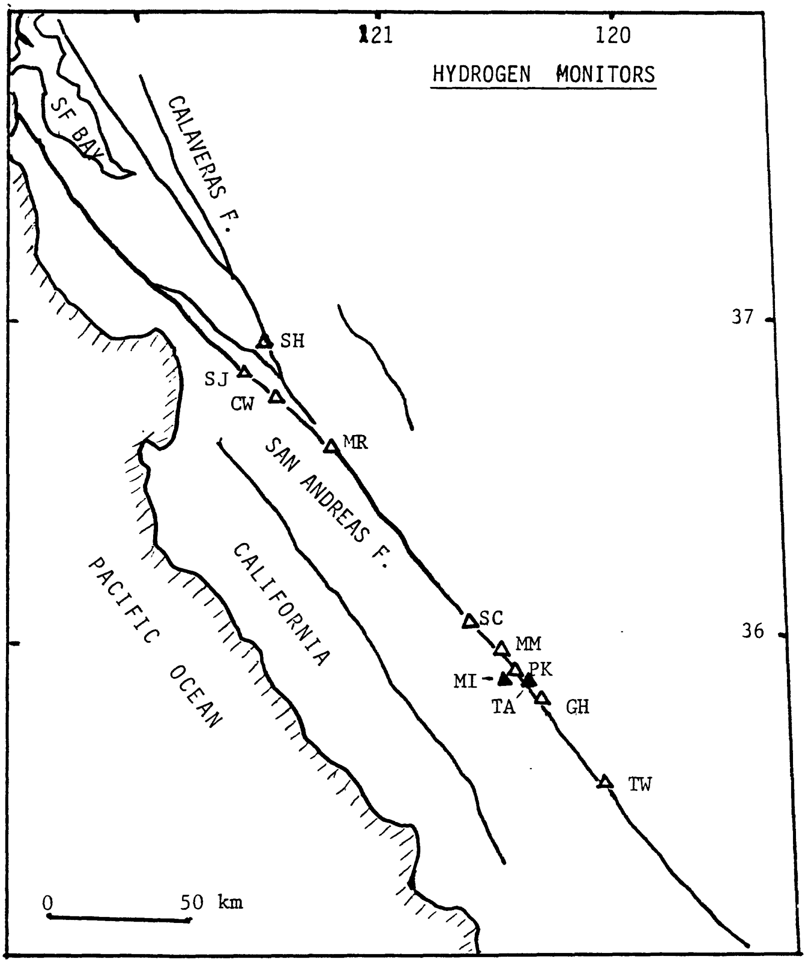

(Fig. 1) Location map for the hydrogen monitoring sites in central California. The sites marked with filled triangles also have other monitors for pumped water.

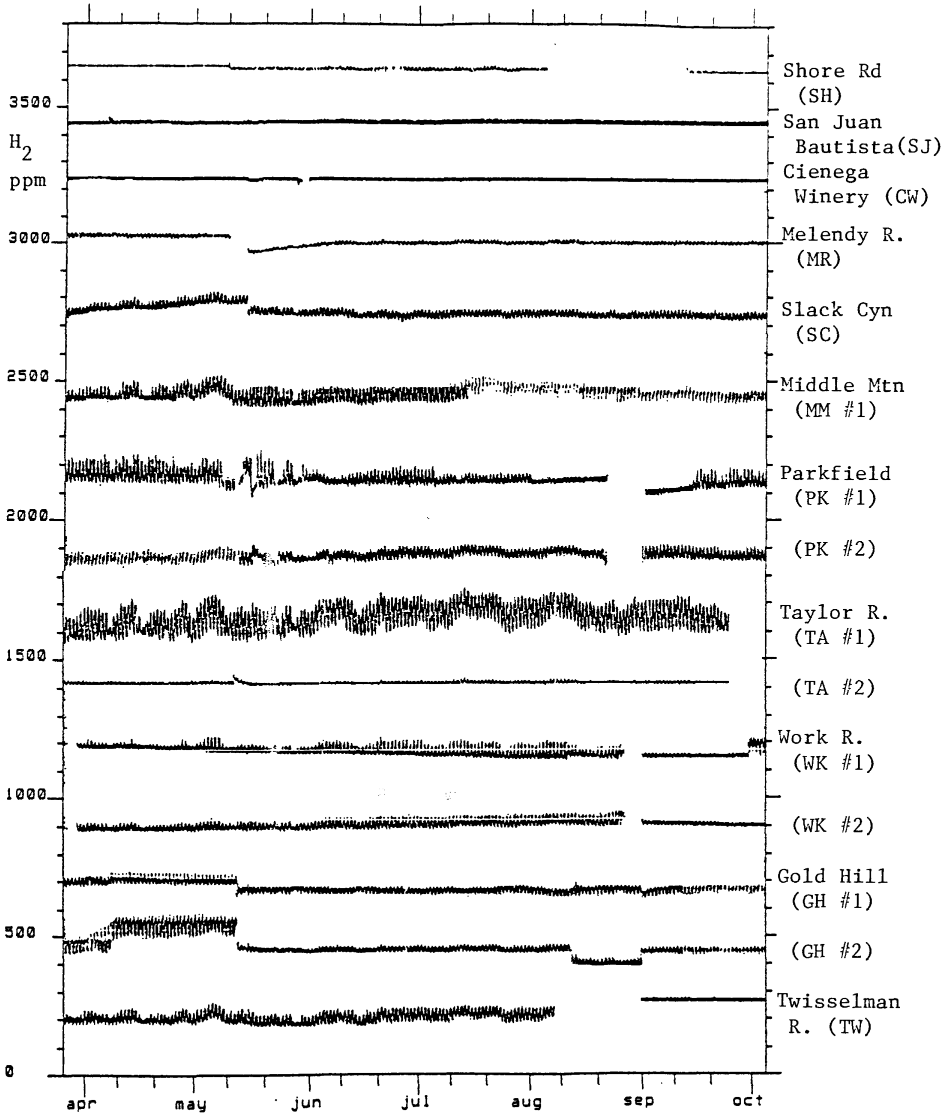

(Fig.2) Summary plot of soil hydrogen data recorded along the San Andreas and Calaveras faults in central California from April to October, 1990.

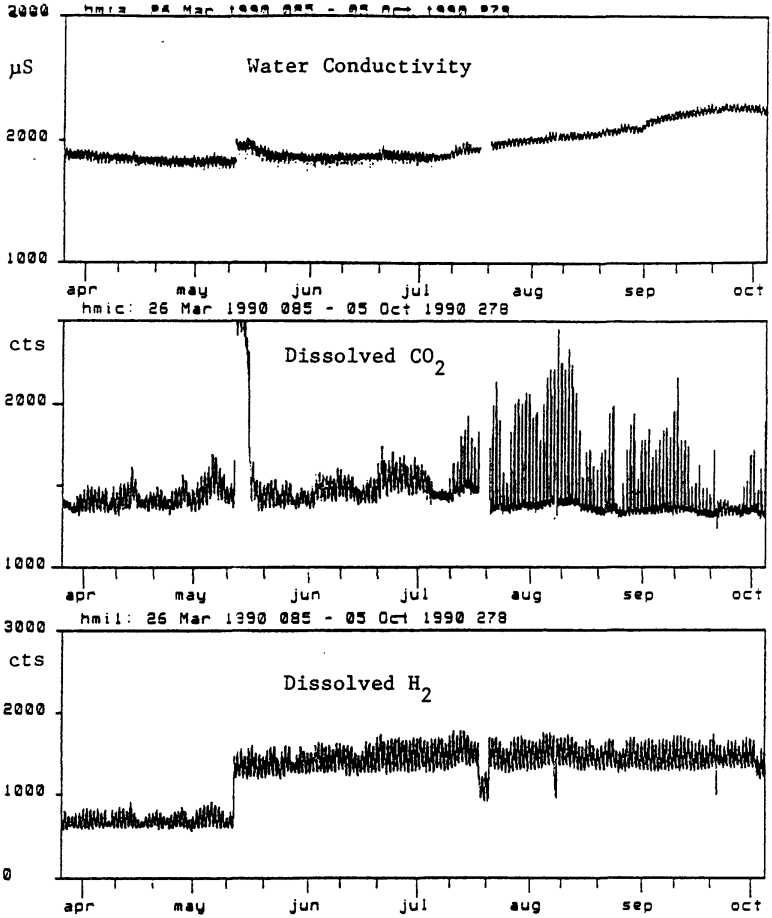

(Fig.3) Water geochemistry data recorded at Miller Ranch in the Parkfield area in central California between April and October, 1990.

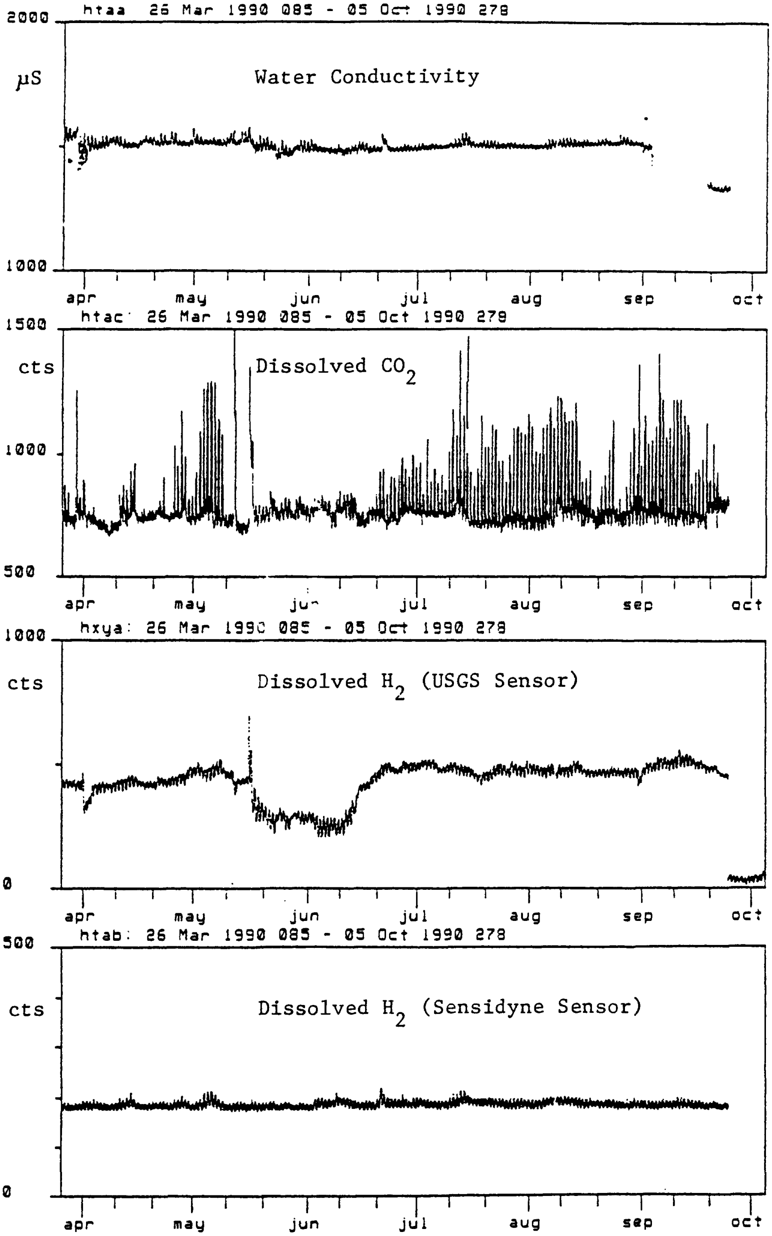

(Fig.4) Water geochemistry data recorded at Taylor Ranch in the Parkfield area between April and October 1990.

Quantitative Analyses of Shear-wave Polarizations and Inversion for Shear-wave Splitting Parameters

14-08-0001-G1767

Peter M. Shearer
Institute of Geophysics and Planetary Physics
Scripps Institution of Oceanography
University of California, San Diego
La Jolla, CA 92093
(619) 534-2260

Investigations

Our research in the last year has focused on developing quantitative methods for analyzing shear-wave polarizations, applying these techniques to data from three-component surface and borehole arrays, and evaluating recent claims that temporal changes in polarizations caused by shear-wave splitting may be useful in predicting earthquakes. Results of this work are described in detail in Aster et al. (JGR 95, 12449-12474, 1990) and Aster and Shearer (BSSA, submitted, 1990), abstracts for which are listed below:

Results

We analyze shear-wave polarizations from local earthquakes recorded by the Anza network in Southern California, using an automated method which provides unbiased and quantitative measurements of the polarization and the duration of linear motion following the shear wave arrival (the *linearity interval)*. Initial shear-wave particle motions are strongly aligned at four stations, a feature that is not predicted by focal mechanisms. The particle motion alignment is most likely caused by shear-wave splitting due to anisotropy beneath these stations, a result supported by the clear shear-wave splitting seen in a borehole recording near one of the Anza stations. These results are consistent with an earlier analysis of these data by Peacock et al. (1988). However, our analysis does not support claims (Crampin et al., 1990) that shear-wave splitting delay times at station KNW exhibit temporal variations which can be correlated with the occurrence of the North Palm Springs earthquake (M = 5.6) of July 8, 1986. Automatically determined linearity intervals scatter widely from 0.02 to 0.15 s and exhibit no clear temporal trends. We find a correlation between earthquake moment and the linearity interval, possibly a result of longer effective source time functions for the larger events. The inability to identify a distinct slow quasi-shear wave pulse for the vast majority of these events indicates that scattering strongly affects the particle motion, even in the very early shear-wave coda. Analysis of earthquake clusters with similar waveforms recorded at KNW shows that seismic Green functions are stable throughout the observational period and that most linearity interval variation is due to source and ray path differences between events. If shear-wave splitting is causing the observed delay times between horizontal components, the waveform stability for events in these clusters restricts any temporal changes in shear-wave splitting delay times to less than 5 to 10%.

Two borehole seismometer arrays (KNW-BH and PFO-BH) have been established in the Southern California Batholith region of the San Jacinto Fault zone by the U.S. Geological Survey. The sites are within 0.4 km of Anza network surface stations and have three-component seismometers deployed at 300 m, 150 m, and at the surface. We examine seismograms from local earthquakes in the time and frequency domain to assess the influence of the weathered layer on polarization properties and on the spectral content of high-frequency (2-200 Hz) seismic signals. We orient downhole horizontal seismometers to an accuracy within about 5 degrees using regional and near-regional initial P-wave particle motions. Shear waves recorded downhole at the KNW-BH indicate that the strong alignment of initial S-wave particle motions previously observed at the surface KNW Anza site (KNW-AZ) is not specific to that station and that the anisotropic effect extends below the weathered layer. The KNW-BH surface instrument, which sits atop a highly weathered zone, displays a significantly different (≈ 20 degree) initial S-wave polarization direction from that observed downhole and at KNW-AZ, which is bolted to an outcrop. Although downhole initial shear-wave particle motion directions are consistent with a shear-wave splitting hypothesis, good candidates for orthogonally-polarized slow shear-waves are generally elusive, even in seismograms recorded at 300 m. Free-surface reflected phases are not visible in the downhole records from near-vertical P- or S-waves at KNW-BH and initial arrivals show complexity that must arise either at the source or in scattering beneath the weathered layer. A cross-correlation measure of the apparent relative velocities of S_{fast} and S_{slow} horizontally polarized S-waves suggests shallow shear-wave anisotropy, consistent with the observed initial S-wave particle motion direction, of 2.3% ± 1.7% between 300 and 150 m and 7.5% ± 3.5% between 150 and 0 m. Signal-to-noise levels for $M \approx 2$ earthquake signals at both sites show significant increases in usable seismic bandwidth at depth due to a reduction in ambient noise levels downhole and (especially) to dramatically increased levels of high-frequency signal. Spectral ratios indicate that near-surface (between 0 and 150 m) material has a much larger influence on seismic signals than material between 150 and 300 m due to relatively low velocities and low Q. Forward modeling of high-frequency spectral ratios suggests $Q_\alpha \approx 5$ and $Q_\beta \approx 7$ between 0 and 150 m, increasing to $Q_\alpha \approx 19$ and $Q_\beta \approx 15$ between 150 and 300 m. Low-Q and low-velocity near-surface material forms a lossy boundary layer that is advantageous to the high-frequency borehole environment; not only are noise levels reduced, but reflections from the surface and near-surface are greatly attenuated. As a result, high-frequency recordings from below the weathered zone more nearly resemble those recorded in a whole space than would otherwise be expected.

Reports - 1990

Aster, R., Shearer, P., Berger, J., Seismic polarizations observed with borehole instruments in the Anza seismic gap, *Proc. 11th Annual AFGL/Darpa Symb.*, p. 8, 1990.

Aster, R., Shearer, P., Berger, J., Quantitative measurements of shear-wave polarizations at the Anza Seismic Network, Southern California — implications for shear-wave splitting and earthquake prediction, *J. Geophys. Res.*, **95**, 12449-12474, 1990.

Aster, R., Shearer, P., Fletcher, J., Shear-wave observations using borehole instruments at Anza, southern California, *Proc. Fourth International Workshop on Seismic Anisotropy, Edinburgh*, 1990.

Aster, R., Shearer, P., Fletcher, J., Shear-wave splitting and limits on temporal anisotropy variation at Anza, southern California, *Proc. Fourth International Workshop on Seismic Anisotropy, Edinburgh*, 1990.

Aster, R., Shearer, P., High-frequency seismic polarizations and site effects observed in boreholes in the San Jacinto Fault Zone, Southern California, *Bull. Seismol. Soc. Am.*, submitted, 1990.

An Absolute Long-Base Tiltmeter with Vertical Anchoring

14-08-0001-G1336

Frank K. Wyatt, Hadley O. Johnson,
Mark A. Zumberge, and Duncan Carr Agnew
Institute of Geophysics and Planetary Physics
University of California, San Diego
La Jolla, California 92093-0225
(619) 534-2411

This research project supports work on the design and development of a long baselength tiltmeter intended for use in crustal deformation studies, including support for monitoring and evaluating this instrument against existing systems at Piñon Flat Observatory (PFO). In general for long-base tiltmeters to be useful in crustal deformation measurement, they must be stable, engineered for ease and reliability of use, and suitable for installation in a variety of locations. We have been working toward these ends for the past few years, with most of our recent efforts focussed on field testing of equipment designed to operate unattended—at minimal cost to the quality of the data. We completed construction of a new 550-m instrument at the beginning of 1990, and are just beginning to have enough data from it to draw some conclusions about its design.

The most difficult problem in the development of highly stable systems for deformation measurement is deciphering what part of the observed signals are due to the earth and what part due to instrument instability. Our oft-repeated refrain for encouraging development work at PFO is that at this site we have a sufficient collection of high quality instruments to permit the direct comparison and evaluation of new systems. In this situation, however, our new instrument was constructed to fulfill two roles: first as a test system, and second as a monitoring device complementary to existing measurements at the site. For the second role it was installed at 90° to the existing pair of extremely stable EW long-base tiltmeters (run by LDGO and UCSD). To some degree this limits what we can say. Nevertheless we can use our geophysical prejudices and demand similar-quality signals from the different measurement systems and interpret any degradation in either short-term noise or long-term stability as a weakness of the new system.

Recent observations for one of the original EW long-base tiltmeters (design: circa 1982) and the new NS instrument are presented in Figure 1. Overall, the new, fully automated system and the older manual tiltmeter appear to behave about equally well. Owing to continued work on the instrument vaults for the new instrument its record has many gaps. The long-term tilt rate for the new instrument is comparable to the other one, and the short-term noise (days and shorter) only slightly worse. As mentioned in our previous summary report an important virtue of the new generation of continuous deformation monitors—to some degree offsetting their cost and effort involved in construction—is the immediate constraint they provide on the rate of secular deformation. Even over longer baselines, say 10 km, it would take many years of leveling to get similar results, and for GPS measurements (to address an important alternative) it would take much longer.

We are sure some of the long-term signal is due to instrument drift. Small, inexpensive electrolytic tiltmeters are used at both ends of the long-base system to keep the fluid-height-sensing optics aligned. Any drift in these is reflected in the final output of the tiltmeter. The good news is that this drift is monitorable, can be removed from the final record, and (best of all) diminishes with time. Another source of error is from the optical-fiber anchoring system used to measure and correct for end-monument instability. (The earlier instruments have evacuated pipes extending to depth and use discrete optics to form a Michelson interferometer: extremely accurate but very difficult to built.) All conventional anchoring schemes have trouble accurately monitoring long-term displacements of order 100 μm over distances of 50 m or so. Because our optical-fiber anchoring system is a new technology we are especially uncertain of its quality. The redundancy of measurements at PFO provides us with a check on this. In particular, the north end of the new instrument shares a vault with an extension of the original east-west tiltmeter; this ultimately should allow us to constraint its end-monument motion independently of the fiber measurements.

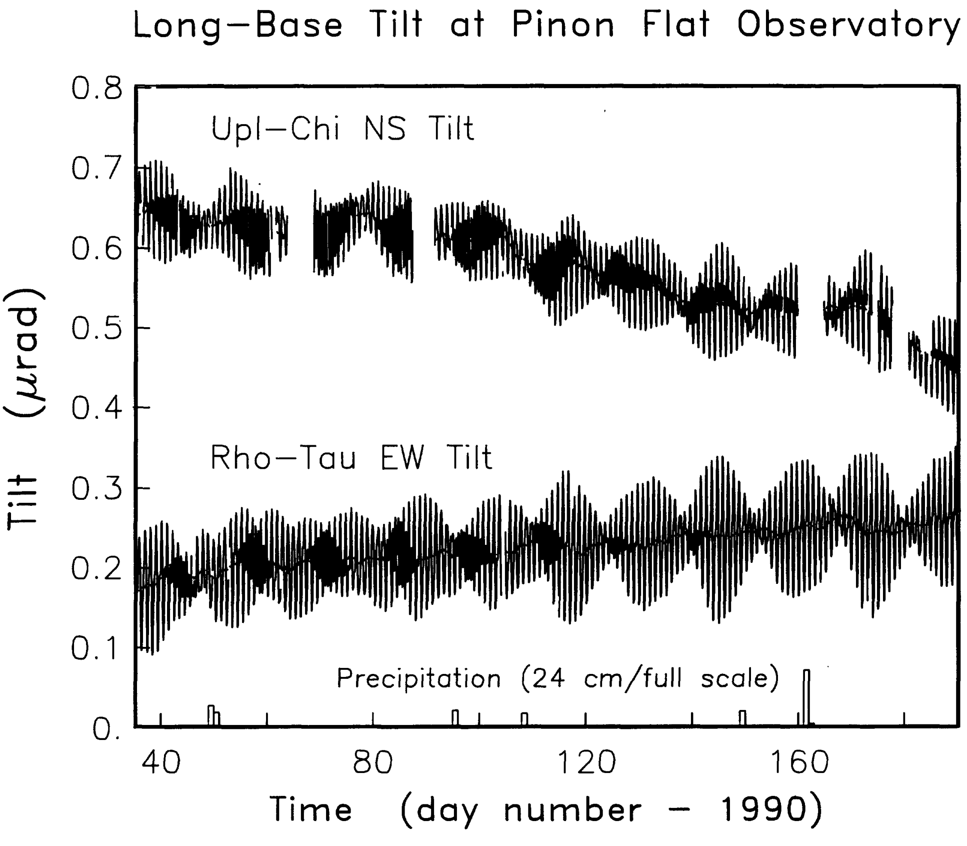
Long-Base Tilt at Pinon Flat Observatory
Upl-Chi NS Tilt
Rho-Tau EW Tilt
Precipitation (24 cm/full scale)
Tilt (μrad)
0.8
0.7
0.6
0.5
0.4
0.3
0.2
0.1
0.
40
80
120
160
Time (day number - 1990)

Figure 1

Piñon Flat Observatory: Comparative Studies and Geophysical Investigations

14-08-0001-G1763

Frank K. Wyatt, Duncan Carr Agnew,
and Hadley O. Johnson
Institute of Geophysics and Planetary Physics
Scripps Institution of Oceanography
University of California, San Diego
La Jolla, CA 92093-0225
(619) 534-2411

This grant provides support for collaborative studies with several USGS-sponsored investigators conducting research at Piñon Flat Observatory (PFO). One aim of this work is to evaluate instrumentation developed for the measurement of ground deformation, the idea being to simultaneously operate a number of continuously recording sensors, and small geodetic arrays, and, by direct intercomparison, to identify the merits and limitations of the various techniques. The other aim is to use the combined results to learn about the earth. Good progress has been made in evaluating the instruments in a common setting and in establishing better bounds on the behavior of the crust in this tectonically active area.

Below we list some of the research groups sponsored by the USGS NEHRP who are currently active at the site, those with whom we are working on collaborative studies.

Air Force Geophysics Laboratory (AFGL)

The AFGL program at PFO is self-supporting, in fact a provider of funds of the overall program. The borehole tiltmeters provided by the AFGL have provided valuable data for comparison with the other borehole tiltmeters. Our plans for early 1991 include adding a second AFGL sensor at the site, (in the 25-m-deep borehole that was previously monitored by an Askania borehole tiltmeter). During its tenure, the Askania tiltmeter gave consistent results, even upon reinstallation at a different azimuthal orientation; we believe we know ground truth for this borehole, at least as recorded by an Askania tiltmeter. Any discrepancies shown by the AFGL sensor will thus help us understand sources of error in borehole tilt measurements.

Carnegie Institution of Washington

This project involves the evaluation of data from three borehole volumetric strainmeters (CIA, CIB, and CIC). Two of these systems (CIB and CIC) are no longer operating, apparently because of cable-seal leakage at the instrument package which is cemented in place. From the beginning the data from all the sensors showed gradually slowing compression caused (we assume) by curing of the cement around them. The initial compressional signal on CIA ended in late 1985, four years after installation, and was followed by expansion. The most obvious feature in recent times was an especially rapid expansion commencing in the fall of 1986, reversing abruptly to compression in early 1987, with an apparent recovery to the earlier trend by 1988. Because of the other strain measuring systems at the site we know this 0.6 $\mu\varepsilon$ signal was not of broad extent. It is tempting to suggest that this event had some hydrologic cause, especially since the rapid expansion began just after the drilling of holes for some

USGS seismometers, about 130 m away. However, the water-level data from the same borehole (which is open to within a few meters of the dilatometer) does not suggest any direct correlation between local pore-pressure and observed volumetric strain. The water level began falling before the dilatometer event began and reached an equilibrium level (despite disturbances from drilling and earthquakes) while it was still going on, remaining invariant during the 1987 swing in apparent strain. This stable record seems to rule out any simple diffusion of pore-pressure changes from the area of drilling as described by Kümpel (1988, *EOS*, **69**, 1193). Outside of this event these instruments have done much to confirm the general finding as to the remarkable stability of secular strain accumulation.

Joint Institute for Laboratory Astrophysics

Two ~30-m-deep borehole tiltmeters run by this group (in boreholes BOA and BOB) functioned well from their installation in early 1986, until November 1987, when a nearby lightning strike destroyed the electronics in these instruments (and all other electronics in the area). Two new sensors were reinstalled in the late spring of 1988, with one of these needing further replacement in the spring of 1989. The data from these installations and the Askania tiltmeter show a surprising variability in their earth-tide response, and this is the subject of ongoing investigations. The earth tides, being roughly the same amplitude as the anticipated annual crustal tilt signal near a fault zone, but of relatively short period, are an important "calibration" signal. Dr. Carl Gerstenecker, of University of Darmstadt (FRG), spent three months this year in San Diego working on this and the Askania data, uncovering many instrumental sources of tidal variation.

In an attempt to understand better the reduction in borehole tilt noise with depth (ref: Wyatt *et al.* (1988), *JGR*, **93**, 9197-9201), a JILA team in 1988 prepared a 120-m-deep fully cased hole for a third JILA tiltmeter. Owing to a lack of funding, installation of an instrument in this hole was not done until the summer of 1989. Results from this hole, like those from the similarly deep Askania installation are troubled by the presence of debris in the fully cased borehole.

Lamont-Doherty Geological Observatory

The instrument operated with this group is a 535-m Michelson-Gale water-tube tiltmeter, which has produced excellent data since its refurbishment by Dr. John Beavan late in 1987. The long-term tilt rates from this instrument now seem to be quite similar to the rate measured by the parallel UCSD long-base tiltmeter (0.10 μrad/yr down to the west), and a final intercomparison is promised for next year.

Schiltach Observatory

This project involves deployment and evaluation of an Askania tiltmeter, loaned to us by Dr. Walter Zürn of the University of Karlsruhe. The sensor was first operated in a 25 m deep hole (borehole KUA). The instrument was installed on 1985:346 (only two weeks after cementing in the casing) and produced high-quality records until its failure from the lightning strike mentioned previously. With advice from Dr. Zürn we were able to dismantle, repair, and reinstall this instrument; it was put back into borehole KUA in the summer of 1988. In the summer of 1989 we removed the instrument for more work on its electronics after we discovered a systematic change in its gain over the course of a year (following an idea suggested to us by Dr. Joachim Kümpel). This particular instrument is an early model, without active feedback electronics, so any instability in the electronics can easily translate to a gain change.

In parallel with this lab work we completed work on a 120-m-deep borehole for this sensor. Much effort was needed to obtain a precise gyroscopic measurement of the down-hole alignment assembly, as the work proved far more difficult than we imagined. Tiltmeter operation in this fully cased borehole (called KUB) has been complicated by the need to deal with the rain of fine metal-scale that showers the bottom of the borehole whenever anything is lowered in; this scaling is the result of corrosion inside the casing.

University of California, San Diego

This year, under a two-year grant, we completed the installation of a North-South long-base tiltmeter at PFO (see summary for G1336). This instrument is roughly perpendicular to the first UCSD instrument and shares an end-vault with the extension of it. Data from these orthogonal sensors will be especially useful in evaluating the borehole tilt measurements made at or near PFO.

One major setback this summer was the flooding of vault TAU (the middle vault of the extended EW tiltmeter) and loss of the equipment in it. This occurred during a flash-flood, when water entered the vault via a trench recently dug by another Scripps group (working under our direction) in anticipation of adding more sensors to the vault. As the middle vault in the EW instrument, the measurements made at this location were not critical, but this was still an unwelcome accident.

University of Queensland

The three-component borehole strainmeter, run by this group has continued to run well, with perhaps some down-hole problem with one of the sensors. This instrument is installed at a depth of 151 m is capable of measuring shear as well as areal strain, and so is largely immune to the effects of grout curing which control much of the long-period dilatometer record. Gladwin (1987, *USGS Open File Report 88-16*, 345-351) has presented the secular records from this instrument, and pointed out a surprising change in strain rate seen on it at the time of the North Palm Springs earthquake. Prior to this shock the rate of NS tensor shear strain (e_{12}, 1-axis east) was a large 0.6 $\mu\varepsilon$/yr, but after this earthquake it fell to less than 0.1 $\mu\varepsilon$/yr, a value more in keeping with local geodetic results. Surprisingly, during this same time period the areal strain e_A maintained a steady rate of -1.5 $\mu\varepsilon$/yr, indicating no gross change in the net compressional strain impressed upon the instrument by grout curing. We are studying this interesting change in response by comparing the data from this instrument with the laser strainmeter records from PFO and also with the geodetic measurements made over the site (see below).

U.S. Geological Survey – Crustal Deformation

Over the past few years several precise geodetic surveys have been made in the area around PFO. The longest-running of these is the Pinyon single-color Geodolite network, part of the larger Anza net, surveyed by the USGS Crustal Strain group of Drs. J. C. Savage, M. Lisowski, and W. H. Prescott. This network (observed since 1973) has served as the low-frequency constraint on the continuous strain measurements made at PFO, and shows that in one direction (EW) the strains over PFO are nearly equal to those occurring over the fault traces of the nearby San Jacinto and San Andreas Fault systems. With the community's increasing dependence on GPS it now seems there will be but one more Geodolite measurement of this network (probably in May 1990) whereupon succeeding measurements will be made with GPS. We have begun making GPS measurements to some of the Geodolite monuments and are working with members of the USGS on combining a GPS survey with the final

Geodolite survey to get as concurrent GPS/Geodolite measurements as possible.

In 1986, Dr. J. Langbein set up a 2-color geodimeter network which extends across Pinyon Flat and is surveyed roughly quarterly. This array spans 4-km distances, and so is intermediate in length scale to the 20-km lengths of the Geodolite network, and the ~500-m-long lines of the observatory instruments. As more surveys have been done, results from this 2-color network generally appear to be converging onto the long-running Geodolite values for the Flat — though with some unexpectedly large uncertainties. We have made some GPS measurements to a few of the end points in this array, to begin to sort out the absolute distances between the monuments (something not given by the Two-color instrument) and to better understand the merits of the two systems.

We have benefited tremendously in these projects from the contributions made by NASA/JPL, NGS and the Riverside County Flood Control and Water Conservation district in their geodesy programs at the site.

For three years, beginning in 1986 Dr. R. Stein (USGS) directed the leveling of a 14-km-long, reference-calibration line across Pinyon Flat (with a loop going through PFO). We are hopeful that we can get USGS/NGS support to run this line next year as the leveling data over this five-year interval would prove valuable in understanding the continuous tilt measurements made at the observatory.

Piñon Flat Observatory: A Facility for Studies of Crustal Deformation

14-08-0001-G1764

Frank K. Wyatt, Duncan Carr Agnew,
and Hadley O. Johnson
Institute of Geophysics & Planetary Physics
Scripps Institution of Oceanography
University of California, San Diego
La Jolla, CA 92093
(619) 534-2411

This grant supports the operation of Piñon Flat Observatory (PFO) as a research center for the study of crustal deformation in an area of active faulting. Through this grant, the U.S. Geological Survey provides 50 percent of the funding needed both for running the 160-acre facility and for maintaining the reference-standard instruments there. Matching funds are provided by a grant from the National Science Foundation. The work done at PFO includes establishing the accuracy of instruments designed for measuring various geophysical quantities by comparing results from them with data from the best available continuously recording deformation monitors. Such comparison then provides for an accurate record of strain and tilt changes in the area near the observatory, between the active San Jacinto fault and southern San Andreas fault systems. All of this effort is intended to foster development of precision instrumentation and from this an improved understanding of the earth. Particularly for crustal deformation studies, more accurate measurements are needed for a better understanding of the mechanics of faulting. The site continues to be utilized by roughly 20 different research teams, the most recent efforts focusing on GPS and seismic correlation/waveform studies.

As noted in the previous semi-annual report, we were able to use the reference-standard instruments at PFO to show that a burst of earthquakes on the San Jacinto fault in late 1989 and early 1990 was not accompanied by significant amounts of deep aseismic slip; specifically, for uniform right-lateral slip along the fault over the distance covered by the December earthquakes the aseismic moment release must have been less than 3×10^{16} N-m, five times the seismic moment release. If deep slip triggered this burst of activity, it could not have been much larger than the results it produced. Without these data—available in few other places—speculation on such an aseismic slip episode would be extremely hard to avoid.

There has been no continuance of this unusual activity along this fault, so we do not have as interesting a story for this report period. Instead we focus on some other projects that have made use of the facilities provided by this grant. One activity during this time has been a very useful contribution made at no cost by Mr. W. Young of the Riverside County Flood Control and Water Conservation District (RCFCD): an accurate map of the observatory. This has been done photogrammetrically, with aerial photography and photogrammetric reduction being done by RCFCD, with ground control done by us using GPS receivers. The resulting map (shown greatly reduced in the Figure 1) has better than 1′ horizontal accuracy and 2′ vertical contours. We expect it to be extremely useful in planning work at the site. One by-product (done by the Riverside County Surveyor) is an accurate location of the boundaries of the property.

In speaking of the "reference standard" instruments we have usually meant the laser strainmeters and long-base tiltmeters. It would seem appropriate to add to this list the continuous GPS receiver now operating at this site. This project, though largely funded by NASA, has benefited considerably from the existence of the facility, since in the initial stages the receivers have needed regular visits to maintain full operation. A Trimble receiver was installed in February 1990, and replaced by a Rogue receiver on March 1990, which has operated (with some interruptions) through the present. Ties have been made between this receiver and the VLBI site, thus making this receiver suitable for use as a fiducial station.

Another project that has made use of the facility is a closely-spaced array of short-period seismometers to study high-frequency seismic signals — a joint project of researchers from UCSD, the USGS, Indiana University, and the University of South Carolina. A total of 58 3-component sensors were installed; these were all put in shallow trenches, assuring they were secured to solid material below the top meter or two of weathered rock. (One benefit to the aerial mapping mentioned above was the precise location of all these trenches). Most of the sensors were installed in a 6×6 square grid, 44 m on a side, centered over the deep-borehole seismometer array; the other 22 sensors formed two perpendicular lines each 220 m long. All seismometers were recorded on a common time base at 250 samples/sec, and, during the two-month period of operation, recorded over 300 local and regional earthquakes, providing a large dataset for studies of waveform coherence at high frequencies. One reason for doing this work at PFO was the homogeneity of the local geology–a granodiorite batholith–which should minimize local effects. Another was the prior installation of the borehole seismometers. But most important was the existence of the facilities supported by this grant; this project made good use of the existence of the PFO facility in providing ease of permitting, power, shelter, freedom from vandalism, and minor logistical support, without which the whole effort would have been far more costly.

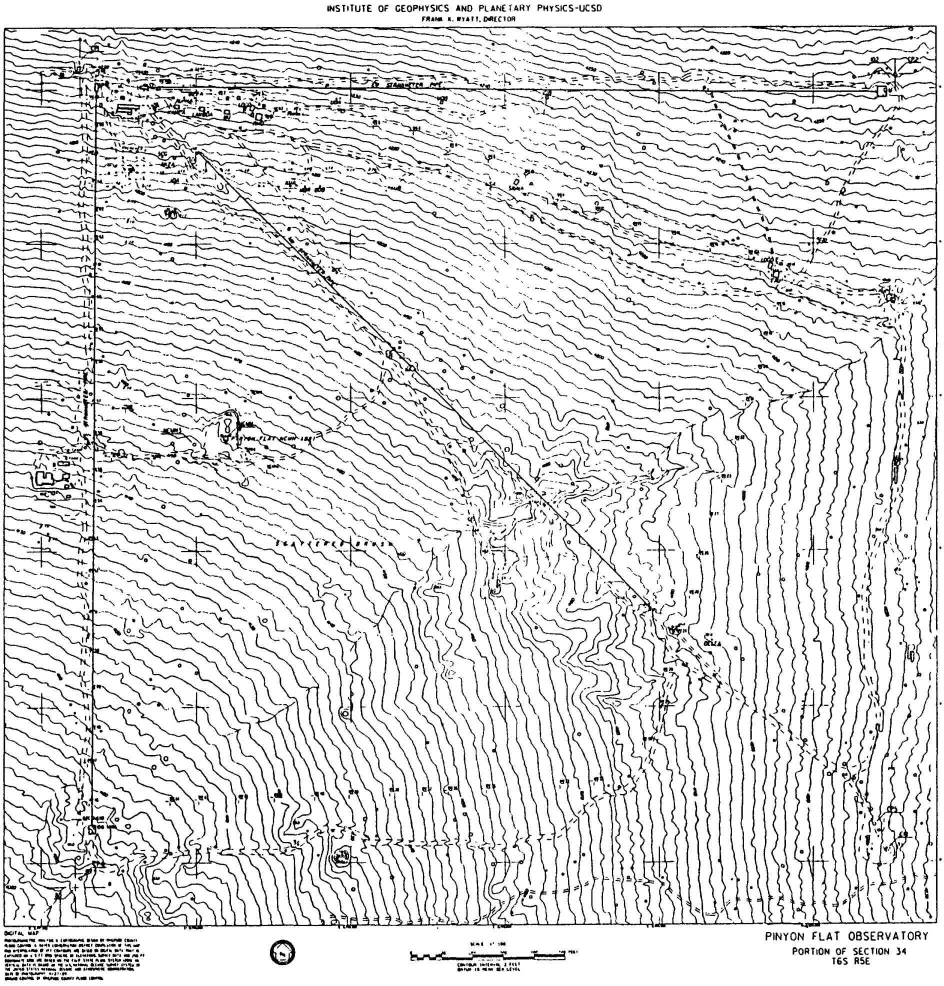
INSTITUTE OF GEOPHYSICS AND PLANETARY PHYSICS-UCSD
FRANK K. WYATT, DIRECTOR
STRAINMETER PIPE
SCATTERED BRUSH
DIGITAL MAP
SCALE 1" = 100'
FEET
CONTOUR INTERVAL 2 FEET
DATUM IS MEAN SEA LEVEL
PINYON FLAT OBSERVATORY
PORTION OF SECTION 34
T6S R5E

Figure 1

Continuation of Creep and Strain Studies in Southern California

#14-08-0001-G1666

Clarence R. Allen and Kerry E. Sieh

Seismological Laboratory
California Institute of Technolgoy
Pasadena, CA 91125
(818) 356-6115

This project improves and maintains creepmeter and slipmeter instrumentation along the San Andreas fault and Imperial fault in southern and central California. Also, numerous alignment arrays across the San Andreas fault and other active faults are monitored. Primarily, during the past six months, maintenance and servicing of the instruments has been performed.

Creepmeter data are telemetered to Caltech from several stations, and recent work has improved the satellite telemetry. These efforts have resulted in a substantially lesser need for field maintenance for these instruments during the past year. We are in the process of modifying our data-retrieval software to work with changes in the GOES satellite telemetry.

Since April 1990, we have maintained our creepmeters and slipmeters as follows. In late May 1990, the following creepmeters on the Imperial fault were serviced: Ross Road, Heber Road, Tuttle Ranch, and Harris Road. After this, the following creepmeters on the southern San Andreas fault were serviced: Salt Creek, Mecca Beach, and North Shore. In early June, the battery was replaced at the Salt Creek creepmeter. In late September 1990, the following slipmeters were serviced: Lost Lake (near Cajon Pass), Jack Ranch (Parkfield area), and Twisselman Ranch (Cholame segment). Servicing in October 1990 will include the Salton Trough creepmeters.

Of the alignment arrays, only Dixieland has been resurveyed since our last semi-annual report. The last major resurvey of the alignment arrays was in March 1989, during which a total station EDM was used to measure distances as well as angles in all of the arrays along the southern San Andreas fault, Imperial fault, and Superstition Hills fault at Imler Road. Numerous new arrays were also installed along the southern San Andreas fault, Superstition Hills fault, Elmore Ranch fault, and Extra fault during early 1989.

Acceleration, Velocity, and Volumetric Strain from Parkfield GEOS Network

9910-02089

Roger D. Borcherdt, Malcolm J. Johnston, C. Dietel,
G. Glassmoyer, and Allan Lindh
Branch of Engineering Seismology and Geology
345 Middlefield Road, MS 977
Menlo Park, California 94025
(415) 329-5619

Investigations

- Maintain GEOS array near Parkfield, CA to serve as a strong-motion array to provide broad-band, high-resolution measurements of the mainshock as well as an array to provide measurements of pre-, co-, and post-seismic strain and displacement field pertubations for purposes of earthquake prediction.
- Maintain up-to-date archive of all events recorded in anticipated rupture zone.
- Develop theoretical basis and models to interpret colocated measurements of volumetric strain and seismic displacement fields.

Results:

- An array of 15 stations has been maintained at 95 percent or greater reliability since July, 1987. An up-to-date digital data archive is being maintained and summarized in monthly internal USGS reports. (See previous reports for detailed description of the array.) Events recorded along Parkfield segment of study zone during time interval indicated are summarized according to magnitude and depth (Table 1). Examples of colocated measurements of volumetric strain (Figures 1 and 2; traces 1, 2, and 3), ground velocity (Figure 1, traces 4, 5, and 6), and ground acceleration (Figure 2; traces 4, 5, and 6) for a magnitude 4 event are shown.

Reports

Borcherdt, R.D., Johnston, M.J.S., and Glassmoyer, G., 1989, On the use of volumetric strain-meters to infer additional characteristics of short-period seismic radiation: *Bulletin of the Seismological Society of America*, v. 79, p. 10,106-10,230.

(See projects Borcherdt *et al*., (9910-02689 and 9910-03009) and Johnson for related reports.)

10/90

TABLE 1

HYPO-71 LISTING: PARKFIELD EARTHQUAKES RECORDED ON ONE OR MORE GEOS STATIONS FROM NOVEMBER 1,1989 TO MAY 15, 1990.

```
8911 3  758 28.85 36  0.07 120 32.97   3.17    1.98 11 175   5.0 0.02  0.6  0.7
8911 4 1329 31.68 35 52.50 120 25.61   9.06    1.36 12 107   2.5 0.04  0.5  0.6
891112  553 13.45 35 47.67 120 21.04  10.02    2.05 28  66   6.3 0.09  0.3  0.6
891214 1227 28.07 35 31.15 120  4.69  12.40    2.05 29 129   6.6 0.11  0.3  0.4
891215 1311 28.21 35 58.00 120 31.04  11.43    1.74 21 135   2.1 0.05  0.5  0.4 S
891216  3 1  4.61 35 31.37 120  4.36  12.79    2.46 29 133   6.2 0.07  0.3  0.4
891223 2213 54.39 35 46.17 120 18.54   5.02    2.21 29  61   6.8 0.08  0.2  0.4
90 125  838 16.12 35 57.59 120 29.86  11.55    1.85 19 138   0.4 0.05  0.4  0.3
90 131 1033  1.96 35 55.34 120 28.22   5.46    1.68  9 157   3.5 0.03  0.5  1.0
90 131 1052 43.04 35 55.33 120 28.30   5.37    1.69  9 155   3.4 0.02  0.5  1.0
90 210  856 53.87 35 44.61 120 17.57  13.75    1.89 25  48   4.1 0.06  0.3  0.4
90 326 1941 11.26 35 59.43 120 32.64   4.74    1.91 13 181   5.2 0.05  0.5  0.4
90 331 1533 32.97 35 59.58 120 33.21   5.44    1.92 15 177   4.4 0.08  0.6  0.4
90 4 3 1632 38.36 35 59.62 120 33.08   5.68    1.80 10 180   4.6 0.06  0.6  0.4
90 4 7 1627 57.19 35 58.51 120 33.12   4.98    1.96 16 129   4.6 0.06  0.3  0.4
90 4 8 1758 10.63 36  2.77 120 36.59  10.22    2.55 43  66   6.8 0.11  0.2  0.5
90 425  914  5.36 36  1.46 120 35.83   8.55    2.43 36  64   4.3 0.12  0.3  0.4 S
90 427 1853 12.71 36  2.36 120 34.84   8.38    2.10 20 134   6.3 0.06  0.4  0.5
90 429  636 25.89 36  1.95 120 35.39   9.19    1.66 20 165   5.3 0.06  0.5  0.7
90 511 10 4 30.03 35 55.77 120 29.37   6.02    2.25 31 125   1.7 0.11  0.3  0.4 S
90 512 1742 49.21 36  2.55 120 36.64   5.59    2.83 35  85   6.4 0.08  0.2  0.4
```

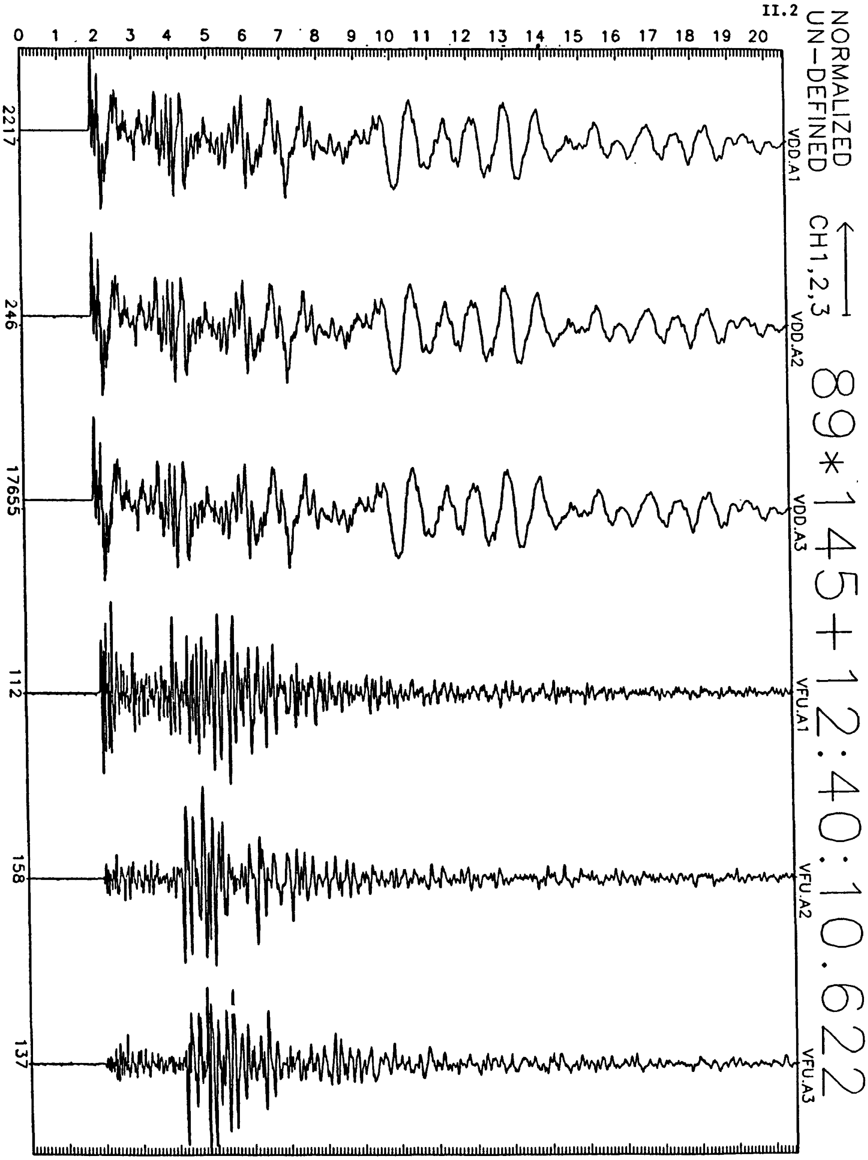

Figure 1

9901-02089

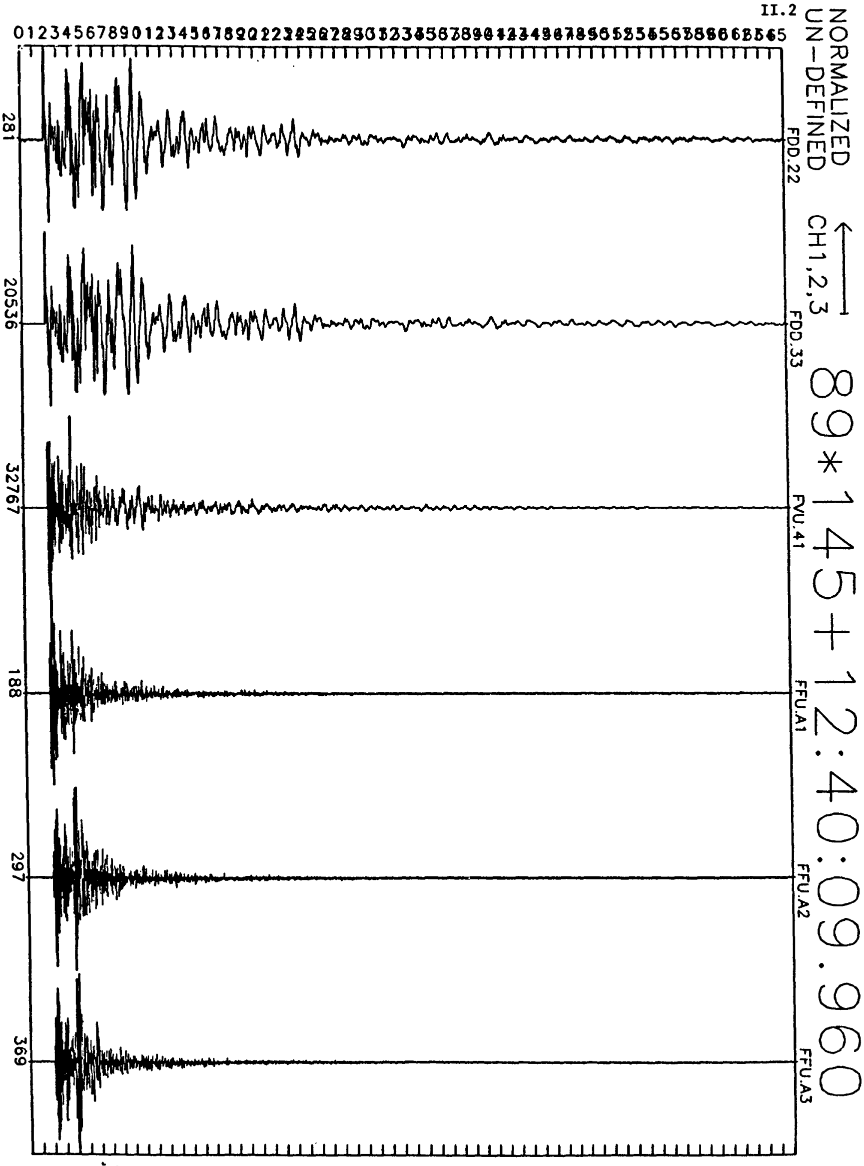

Figure 2

9910-02089

Seismic Studies of Fault Mechanics

9930-02101

William L. Ellsworth
Lynn Dietz and Randall White

Branch of Seismology
U.S. Geological Survey
345 Middlefield Road - MS 977
Menlo Park, California 94025
415-329-4784

Investigations

1. Reassessment of earthquake probabilities in the San Francisco Bay Region in the light of the Loma Prieta earthquake.
2. Completion of work on Central American seismicity.
3. Loma Prieta earthquake response.

Results

1. In 1988 a Working Group convened by the National Earthquake Prediction Evaluation Council (NEPEC) issued a report assessing the long-term probabilities of large earthquakes along the San Andreas fault system. NEPEC organized a new working group following the 1989 Loma Pritea earthquake to reexamine the probabilities of large earthquakes in the San Francisco Bay region, in light of new interpretations or physical changes resulting from the Loma Prieta earthquake, and new data developed since the 1988 report.

   We now estimate the chance of one or more large earthquakes in the San Francisco Bay region in the coming 30 years as about 67 percent.

   Considerable uncertainty remains about the association of the 1989 fault rupture and prior activity along the San Andreas fault system in the southern Santa Cruz mountains, and much of our current research program is aimed at reassessing the seismicity and tectonics of this region in the light of all the historical data.

2. Seismicity within the interior of the Caribbean Plate in Central America and along the Caribbean-North American (CARB-NOAM) plate boundary in Guatemala is dominated by crustal activity concentrated in a nearly continuous belt along the axis of principal Quaternary volconoes. This narrow belt (≤20 km wide) shows approximately east-west extensional faulting, with some evidence for both left-latereal strike-slip faulting on faults striking perpendicular to the zone, and right-lateral strike-slip faulting along arc-parallel faults. Since 1900, more than 30 earthquakes (M≥5.7) have occurred along the volcanic chain. At most, only three can be associated with volcanic activity.

   Most of the seismic slip along the CARB-NOAM plate boundary is accomodated along the Montagua and Chixoy-Polochic faults. Activity since 1538 accounts for a relative slip rate of about 13 mm/a. Several additional mm/a of motion may be occurring in the extensional faulting regieme between the volcanic zone and the CARB-NOAM boundary, where earthquakes M≥7¼ occurred in 1733 and 1765. Seismicity along the volcanic chain appears to be compatible with the interpretation of the volcanic zone as a leaky right-lateral shear zone, driven by a small but non-negligible oblique component of convergence between the Caribbean and Cocos plates.

3. Response activities to the Loma Prieta earthquake continued during this period and were highlighted by the conception, creation and publication of the magazine-style supplement "The next big earthquake in the Bay Area may come sooner than you think" by Peter Ward. We provided many forms of assistance ranging from ideas for contents, layout and figures, to reviewing and editing numerous drafts, to chasing down items for the biblography. Our press conference releasing the Working Group report was well received by the national press and public alike.

Reports

Dietz, L.D., and Ellsworth, W.L., 1990, The October 17, 1989 Loma Prieta, California earthquake and its aftershocks: geometry of the sequence from high-resolution locations: Geophysical Research Letters,v. 17, p. 1417-1420.

Michael, A.J., Oppenheimer, D.H., and Ellsworth, W.L., 1990, Coseismic stress changes induced by the 1989 Loma Prieta, California earthquake: Geophyiscal Research Letters, v. 17, p. 1441-1444.

White, R.A., in press, Microseismicity and seismic networks of Central America: Neotectonics of North America, Seismicity Section, Decade of North American Geology Associated Volume (GSMV-1), 30 p.

Working Group on California Earthquake Probabilities, 1990, Probabilities of large earthquakes in the San Francisco Bay Region, California: U.S. Geological Survey Circular 1053, 51 p.

DENSE SEISMOGRAPH ARRAY AT PARKFIELD, CALIFORNIA

9910-03974

Jon Fletcher and Paul Spudich
Branch of Engineering Seismology and Geology
U.S. Geological Survey
345 Middlefield Road, MS 977
Menlo Park, California 94025
415/329-5628 or 415/329-5654

Investigations

1. Recording of local and regional seismicity.
2. Data-base creation and data archiving.
3. Correction of instrument problems.
4. Calibration of site delays at the array elements.

Results

1. The array has been running continuously with 13 of 14 stations functional for the last 11 months, except for occasional down time for instrument maintenance. The array has recorded about 250 local events (distance less than 60 km, Figure 1) and about 270 events at greater epicentral range (Figure 2).

2. As we are accumulating large amounts of data from the array, we have implemented a data management scheme based on the commercial database SYBASE. We investigated the compatibility of various commercially available databases with our needs. Our criteria were that the database should reside on the computer which is mainly used for data processing. In addition, it should interface with evaluation and archival programs both from above as a director of processing steps and from below as a receiver of information generated by evaluation and archival procedures. While many databases fulfilled the first requirement, we selected SYBASE because it provided interfaces to FORTRAN and other user-developed programs and procedures. In addition, it can acquire and store large binary objects such as seismograms. Since acquiring SYBASE in May, we have developed a database structure which encompasses the hard- and software information needed for data evaluation, as well as seismological parameters determined from catalogs and through data evaluation programs. Currently we are filling the database with parameters from past data as well as continuously updating it as new events occur. We have successfully linked SYBASE with our event

association program and with F. Klein's program QPLOT, and we can now select data based on combinations of parameters involving hypocentral coordinates, theoretical slownesses, etc, and we can plot the retrieved information conveniently.

3. We have three instrumental problems that have yet to be resolved. First, we have not yet been able to bring the 14th station on line owing to telemetry problems, but the lack of this station does not compromise the mission of the array significantly because the station is rather redundant, being one of a cluster of three instruments within 25 m of each other. The second problem is that four of the analog-to-digital converters are different from the remainder in the array, which causes those four stations to have lower gains and signal-to-noise ratios than the other stations. This problem should be solved shortly. The third problem is an instrumental timing problem. In December of 1989, we installed new clocks in each array element and nominally our inter-element timing has been good since then. However, we have been experiencing crystal aging problems in the timekeeping circuit supplied by Reftek. The center frequency on the phase-locked loop circuit drifts too far on elements P04 and P12, causing their timing to be bad. We should have this problem fixed in October of 1990.

4. Before we can form beams from the seismic data to examine the spatial and temporal variations of coda-Q, we must determine the dependence of site delays upon wave back-azimuth and incidence angle at each array element. In effect, we must remove the time delays in the wave fronts caused by lateral variations of earth structure beneath the array. It is necessary to do this before forming beams from the data, because the beams would be defocused if each site introduced an additional unknown time shift into its data. It is important to note that all the data we have recovered previously can be used to study coda-Q once we have determined these station delays. Additionally, we can check the overall performance of the timekeeping circuit since December by examining the relative P-wave arrival times of events occurring very close to each other. To do this, it has been necessary to wait until we have accumulated a good collection of recordings of events having nearly identical back-azimuths and incidence angles at the array (such as Loma Prieta aftershocks). When we have verified that the instrumental timing has been stable, then we can measure the time delays for a set of events well distributed in back-azimuth and incidence angle. These time delays can then be compensated for when beams of the data are formed.

Reports

None for this reporting period.

10/90

Figure 1: Events recorded at PDA

Distance < 60 km

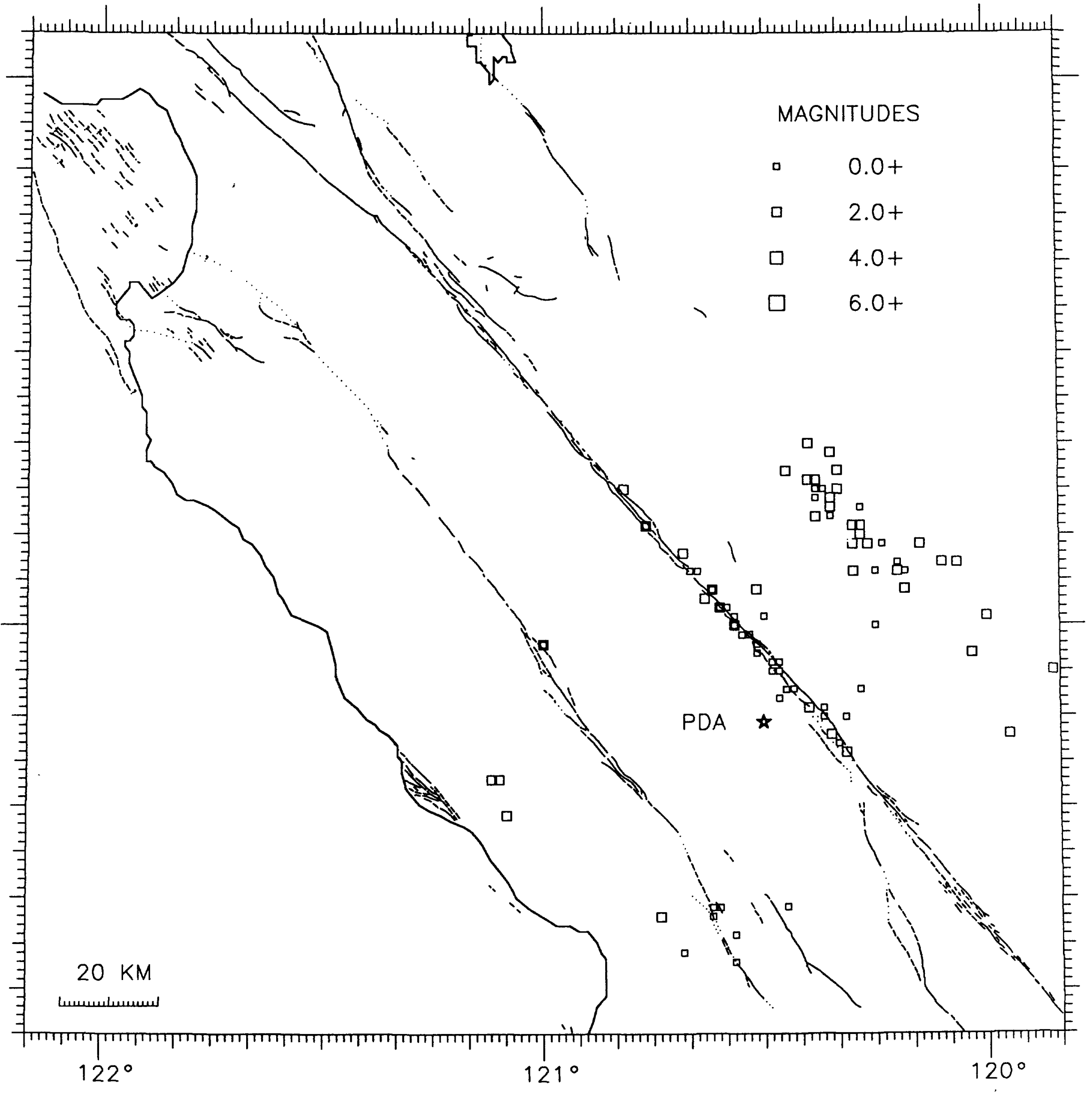

9910-03974

Figure 2: Events recorded at PDA

Distance > 60 km

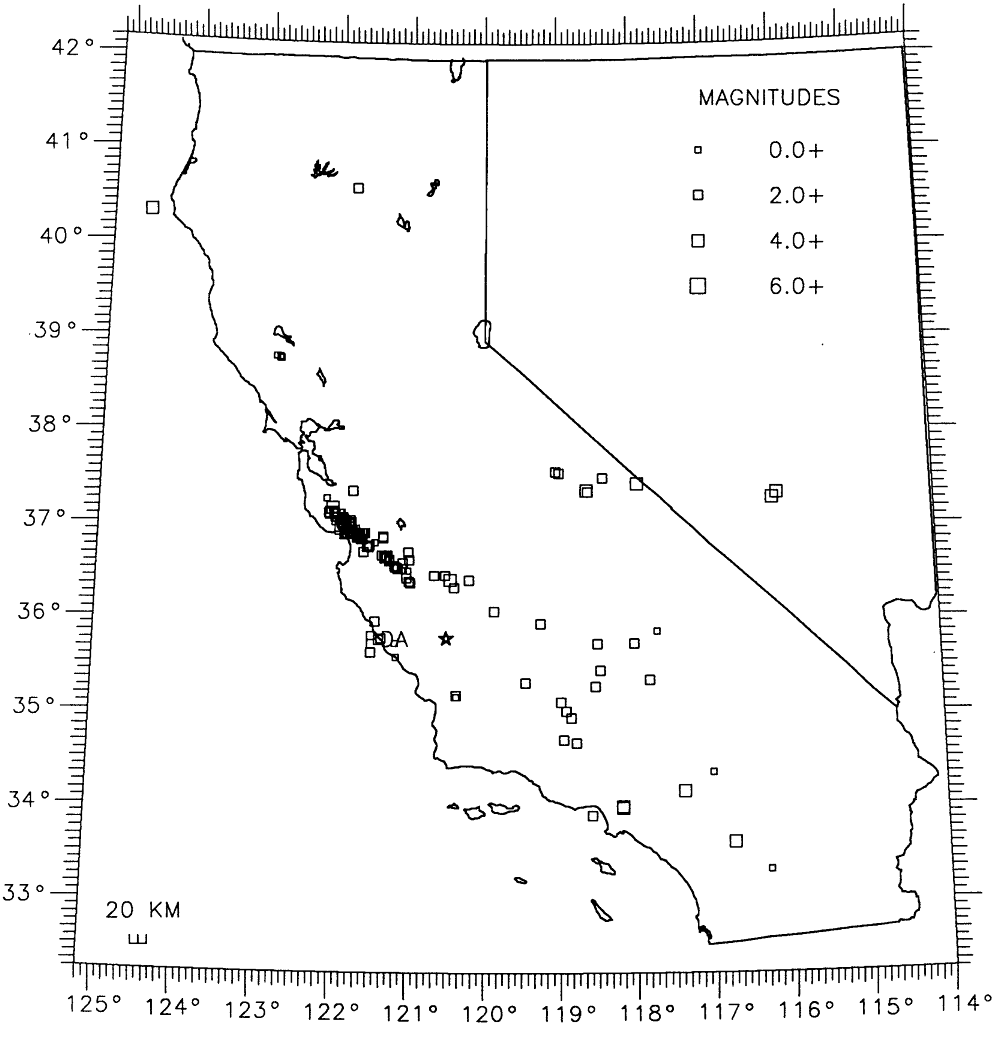

Theodolite Measurements of Creep Rates on San Francisco Bay Region Faults

14-08-0001-G-1676

Jon S. Galehouse
Department of Geosciences
San Francisco State University
San Francisco, CA 94132

(415) 338-1204

We began to measure creep rates on San Francisco Bay region faults in September 1979. Amount of slip is determined by noting changes in angles between sets of measurements taken across a fault at different times. This triangulation method uses a theodolite to measure the angle formed by three fixed points to the nearest tenth of a second of arc. Each day that a measurement set is done, the angle is measured 12 times and the average determined. The amount of slip between measurements can be calculated trigonometrically using the change in average angle.

We presently have theodolite measurement sites at 23 localities on active faults in the San Francisco Bay region (see Figure 1). Most of the distances between our fixed points on opposite sides of the various faults range from 50-275 meters. The precision of our measurement method is such that we can detect with confidence any movement more than a millimeter or two between successive measurement days. We remeasured most of our sites about once every two to three months prior to the 17 October 1989 Loma Prieta earthquake. Following the quake, we established new Sites 22, 23, and 25 on the San Andreas fault northwest and southeast of the epicentral area (see Figure 1). We also began more frequent measurements on sites on the San Andreas fault (14, 10, 22, 23, 25), on the Hayward fault (17, 13, 12, 2, 1), and on the Calaveras fault in the Hollister area (6, 4). These more critical sites are now being measured about every six to seven weeks. The following is a brief fault-by-fault summary of our movement measurements through 4 October 1990. Included are brief statements regarding the effect of the Loma Prieta earthquake on creep rates at each measurement site.

SAN ANDREAS FAULT (See Figure 2) - We have been measuring horizontal slip on the San Andreas fault at Site 10 in South San Francisco for over ten years and at Site 14 at the Point Reyes National Seashore Headquarters for over five years. Both sites have shown virtually no net slip and neither was affected by the 17 October 1989 earthquake thus far.

In November 1989, we began measuring a USGS site (our Site 22) in Woodside that had not been remeasured for several years. Our results compared to unpublished USGS measurements in 1977 show that virtually no surface slip occurred between 16 February 1977 and 4 November 1989. Less than 2 millimeters of right slip has occurred between 4 November 1989 and 6 September 1990.

We also established in November 1989 a new measurement site (23) on the San Andreas fault near the southeastern end of the aftershock area near San Juan Bautista. Virtually no slip has occurred at this site between 18 November 1989 and 1 September 1990. In July 1990, we established a new site (25) on the San Andreas fault just south of the aftershock zone. This site is on the creeping portion of the fault and has already moved over 5 millimeters between 21 July 1990 and 1 September 1990.

Our site 18 (not shown on Figure 1) in the Point Arena area has averaged less than a millimeter per year of right slip since January 1981.

In summary, the San Andreas fault at our measurement sites does not appear to have been affected by the Loma Prieta earthquake in the year since October 1989. We are, however, continuing our measurements about every six to seven weeks.

HAYWARD FAULT (see Figure 3) - We have been measuring horizontal slip at five sites along the Hayward fault for about the past ten to eleven years and have determined that the right-lateral creep rate is about 4 to 5 mm/yr. Although the creep characteristics (steady, episodic, or seasonal) differ from site to site, the overall rates are similar. None of these five sites on the Hayward fault showed anything particularly unusual either before or after the 17 October 1989 earthquake.

In February 1990 we established a new site (24, not shown in the figures) on the Hayward fault on Camellia Drive in Fremont, just southeast of our Site 1. Although relatively rapid creep has been reported for this site in recent years, we have measured virtually no creep at all (through 16 September 1990). Perhaps this site moves episodically and has been in a dormant phase since we began measuring it.

CALAVERAS FAULT (see Figure 4) - We have been measuring horizontal slip at two sites on the Calaveras fault in the Hollister area for about eleven years. Slip at both sites has been rather episodic with intervals of relatively rapid right slip typically lasting a couple months or less alternating with longer periods of time when little net slip occurs. More specifically, Site 4 along Seventh Street in Hollister has had ten episodes of relatively rapid right slip of about 5 millimeters or more since September 1979. Alternating with these times of relatively rapid movement are intervals of little net movement typically lasting about 8-12 months with one lasting two years between January 1986 - January 1988. The Loma Prieta earthquake occurred during an interval of slower movement that had persisted for about a year. The earthquake apparently triggered up to 14 millimeters of right slip at Seventh Street (see Figure 4). Overall the rate of right slip is about 7.1 to 7.6 mm/yr for the past 11.0 years.

Slip at Site 6 along Wright Road just 2.3 kilometers northwest of Site 4 has included 12 episodes of relatively rapid right slip of about 5 millimeters or more since October 1979. Intervals of little net movement typically last about 3-12 months with one lasting about a year and a half between June 1985 - December 1986.

The Loma Prieta earthquake occurred during an interval of slower movement that had persisted for about a year at Wright Road (similar to the situation at Seventh Street). The earthquake apparently triggered up to 12 millimeters of right slip. The overall rate of slip at Wright Road is about 11 to 12 mm/yr for the past 10.9 years. This rate is the fastest of any of our sites in the San Francisco Bay region and is about 4 to 5 mm/yr faster than the rate at nearby Seventh Street. It is possible that undetected surface movement may be occurring outside our 89.7 meter-long survey line at Seventh Street.

After the rapid slip triggered by the Loma Prieta earthquake, both sites in the Hollister area returned to the slower mode of movement which has persisted for about eleven months thus far (through 23 September 1990). A more detailed discussion of the effect of the Loma Prieta earthquake on the Calaveras fault in the Hollister area was published in Geophysical Research Letters (Galehouse, 1990). The paper also discusses the effect of the Morgan Hill earthquake in 1984. No immediate surface displacement had occurred at either of our Hollister area sites when they were measured the day after the Morgan Hill earthquake in 1984. However, within the following 2.5 months, both sites showed over a centimeter of right slip which was followed by a relatively long interval of slower slip (see Figure 4).

CONCORD - GREEN VALLEY FAULT (see Figure 5) - We began our measurements at Site 3 and Site 5 on the Concord fault in the City of Concord in September 1979. Typical movement characteristics on the Concord fault are intervals of relatively rapid right slip of about 7-10 millimeters over a period of a few months alternating with intervals of relatively slower right slip over a period of several years.

It appears that the Loma Prieta earthquake and the 1990 swarms of earthquakes near Alamo had no effect on the Concord fault at our measurement sites in the City of Concord.

We began measuring Site 20 on the Green Valley fault near Cordelia in June 1984. Large variations tend to occur at this site between measurement days, possibly because logistical considerations resulted in our survey line being particularly long (335.8m). However, our results suggest that the Green Valley fault behaves similarly to the Concord fault which is along trend to the southeast, i.e., relatively rapid right slip in a short period of time (months) alternating with relatively slower slip over a longer period of time (years). The Green Valley fault was in a period of relatively slow movement for the first 20 months of our measurements, averaging a few millimeters per year of right slip. In early 1986, however, the fault slipped right-laterally more than a centimeter. This was followed by about three years in which the net slip was less than a millimeter per year. Sometime after 6 August 1989, the Green Valley fault entered into another phase of relatively rapid right slip that is still continuing. Seven measurements since then indicate right slip of about two centimeters, a rate much higher than occurred during the first five years of our measurements. It may be only coincidental that the onset of this latest phase of relatively rapid movement occurred within a couple months of the Loma Prieta earthquake.

RODGERS CREEK FAULT - We measured a site on the Rodgers Creek fault in Santa Rosa from August 1980 until we had to abandon it for logistical reasons in January 1986. During these 5.4 years of measurements, no significant surface slip occurred and we concluded that the Rodgers Creek fault was not creeping at this site.

In September 1986, we established a new site (SF-21) on the Rodgers Creek fault near Penngrove (see Figure 1). Although variations of several millimeters tend to occur from one measurement day to another, the net movement after 17 measurements through 16 June 1990 was virtually zero and the Loma Prieta earthquake does not seem to have had any immediate effect. However, preliminary results from measurements in early August and early October 1990 suggest that the Rodgers Creek fault at Site 21 may have begun to creep. We are continuing our measurements to see whether this is indeed the case or whether the preliminary results are simply due to larger than usual surface variations.

WEST NAPA FAULT - We began our measurements at Site 15 in Napa in July 1980. No net slip had occurred after 46 measurements over the next ten years, although variations did occur from some measurement days to others. The Loma Prieta earthquake did not have any immediate effect at this site. Similarly to the situation at our site on the Rodgers Creek fault, preliminary results from measurements in early August and early October 1990 indicate that the West Napa fault may have begun to creep. We are continuing to check this possibility.

OTHER FAULTS - Not much, if any, net slip appears to have occurred at our two sites along the Antioch fault since May 1980 and November 1982. However, much subsidence and mass movement creep occur both inside and outside the Antioch fault zone and it is probable that these nontectonic movements obscure any tectonic slip that could be occurring. Our two sites on the Seal Cove-San Gregorio fault have shown virtually no net slip since November 1979 and May 1982. The Loma Prieta earthquake appears to have had no noticeable effect on the rate of movement at any of our sites on the Antioch and Seal Cove-San Gregorio faults.

PUBLICATION

Galehouse, J.S., 1990, Effect of the Loma Prieta earthquake on surface slip along the Calaveras fault in the Hollister area: Geophysical Research Letters, vol. 17, no. 8, pp. 1219-1222.

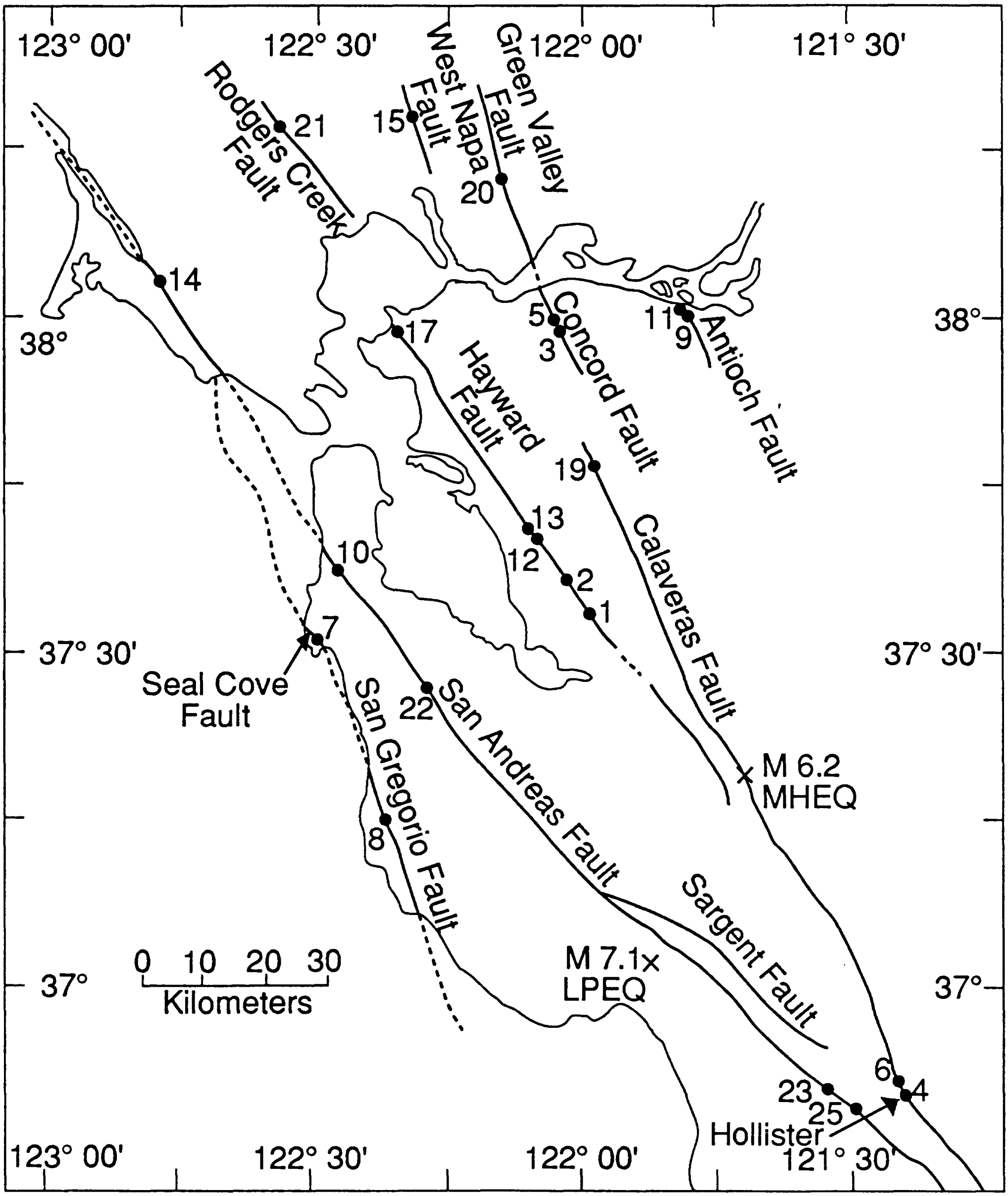

Figure 1. Numbered dots are San Francisco State University theodolite measurement sites. Epicenters and magnitudes are indicated for the 24 April 1984 Morgan Hill earthquake (MHEQ) and the 17 October 1989 Loma Prieta earthquake (LPEQ).

SAN ANDREAS FAULT

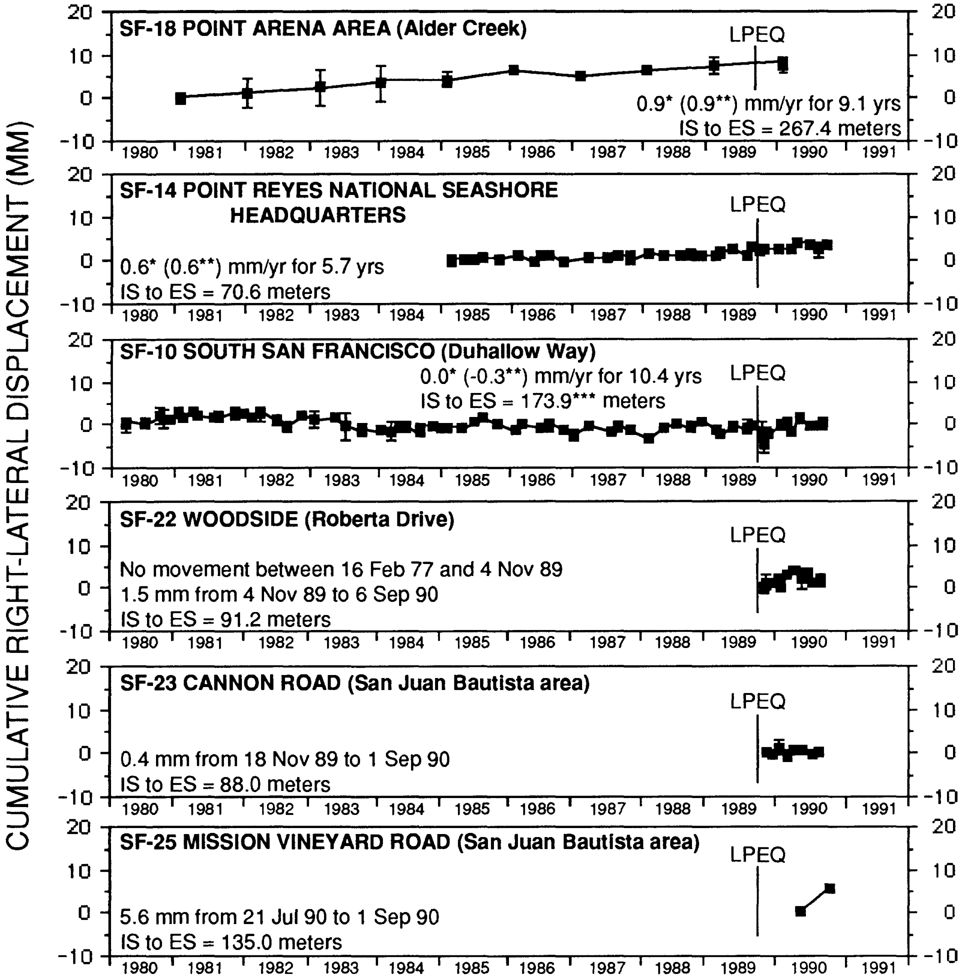

LPEQ = Loma Prieta Earthquake of 17 Oct 89
* Simple average ** Least-squares average
*** Extended to 207.5 meters on 15 Nov 89

Figure 2. San Andreas Fault Displacement (1980 - 1990)

HAYWARD FAULT

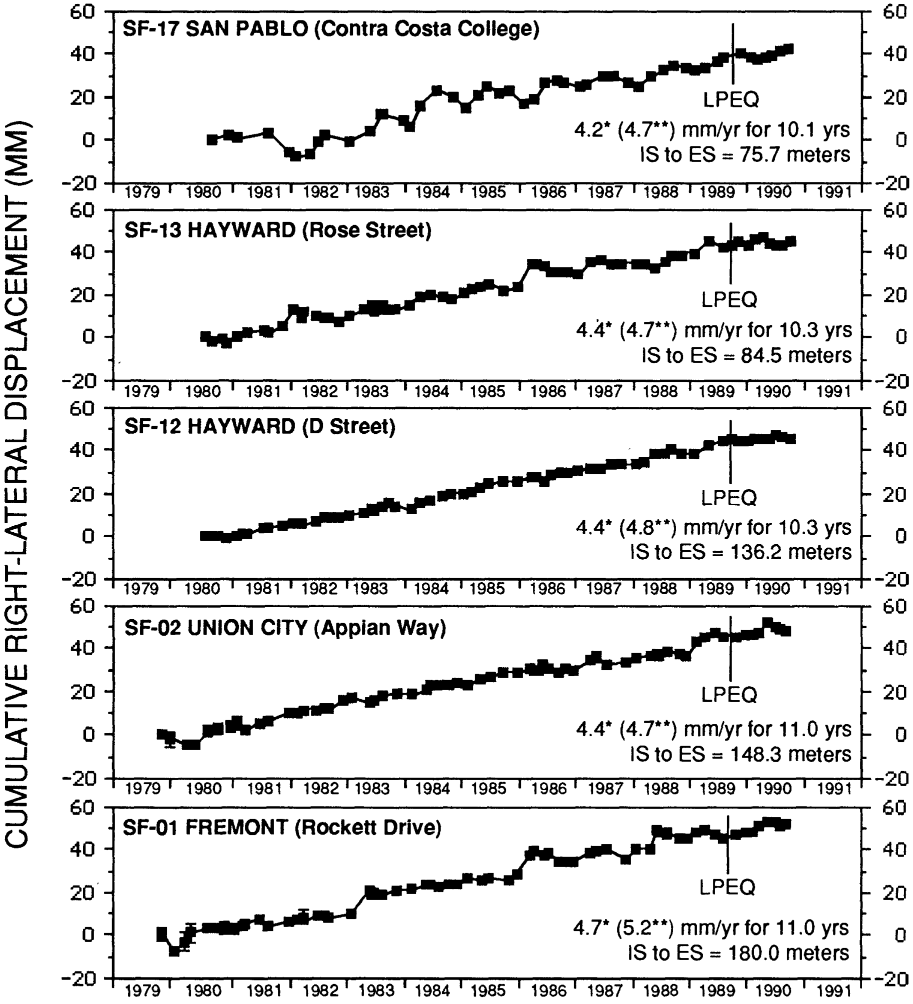

LPEQ = Loma Prieta Earthquake of 17 Oct 89
* Simple average ** Least-squares average

Figure 3. Hayward Fault Displacement (1979 - 1990)

CALAVERAS FAULT

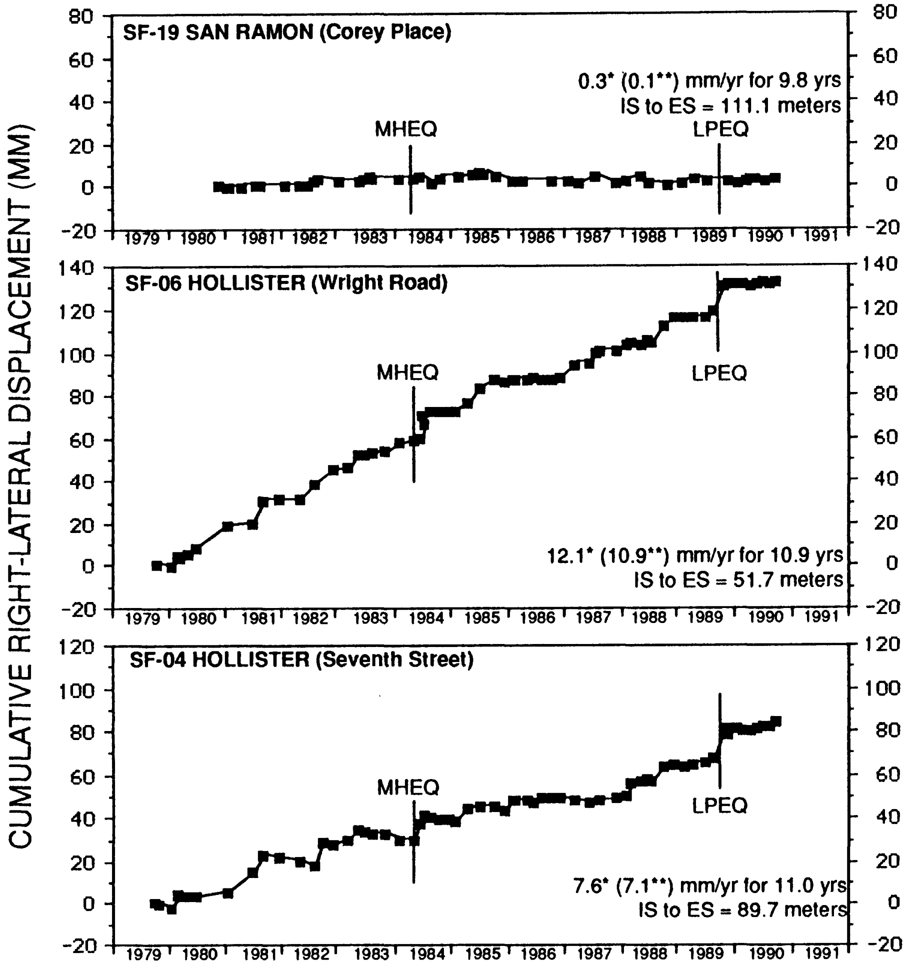

MHEQ = Morgan Hill Earthquake of 24 Apr 84
LPEQ = Loma Prieta Earthquake of 17 Oct 89
* Simple average ** Least-squares average

Figure 4. Calaveras Fault Displacement (1979 - 1990)

CONCORD - GREEN VALLEY FAULT

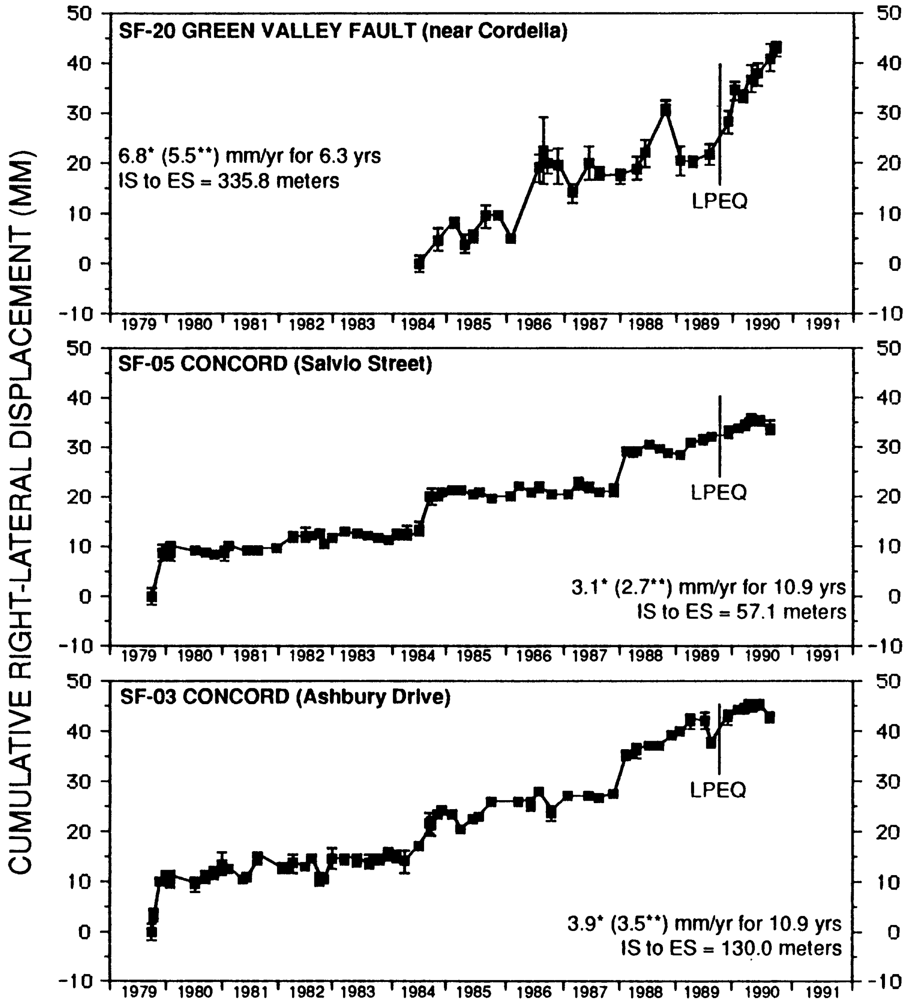

LPEQ = Loma Prieta Earthquake of 17 Oct 89
* Simple average ** Least-squares average

Figure 5. Concord - Green Valley Fault Displacement (1979 - 1990)

DEEP BOREHOLE PLANE STRAIN MONITORING
14-08-0001-G1376

Michael T Gladwin,

Department of Physics
University of Queensland
St.Lucia, 4067
AUSTRALIA.

ACTIVITIES

1. Data from the five borehole tensor strainmeters in California (at San Juan Bautista, Pinon Flat and three near Parkfield) has been regularly processed and analysed. Monthly reports on any anomalies in the strain record from the Parkfield sites have been presented to the regular Parkfield Project review meetings. Short term strain episodes have been investigated and catalogued for further study.

2. Procedures for calibration of individual gauge components of the tensor strainmeter has been further investigated. This involves comparison of gauge tidal data with theoretical tides, taking both ocean loading and topographical effects into account.

3. Long-term stability of individual tidal components of observed earth tide data have been investigated. This analysis is necessary to help in understanding complexities of gauge calibration and long-term coupling stability as well as possible tidal precursory effects for the Loma Prieta earthquake.

4. Analysis of the long and short term data associated with the Loma Prieta earthquake of October 17, 1989 has continued.

5. Investigation of strain events in the San Juan Bautista data has provided data for comparison with creep events monitored on a nearby creepmeter. This work is being carried out in conjunction with Ms. Kate Breckinridge at U.S.G.S, Menlo Park.

RESULTS

1. Data from tensor strainmeters installed in recently drilled boreholes tends to be dominated by exponential recovery processes. In the case of the San Juan data, this signal can be approximated by two exponentials, the first one clearly associated with grout cure with a period in the range 90-110 days, and a second exponential probably associated with recovery of the virgin stress field relieved at the borehole during drilling, with a time constant of approximately 1000 days. A technique has been refined for removal of these two exponentials from the data by a least square fitting procedure. An example of the raw data and the resulting residual is shown in Figure 1. In this case, data prior to March 1988 was used for the fit, and the shear strain shows stability to the 100 nanostrain level until mid-1988, when a clear change of gradient is evident.

Such a technique is useful for highlighting shear strain changes over time, provided all three instrumental gauges show similar behaviour. For most of the gauges in the other instruments, the second long period exponential is less evident, and can better be approximated by a linear term probably associated with long term creep of the borehole. A procedure similar to the above described method is being refined for these other instruments.

2. A number of short term strain transients have been observed in the data from San Juan Bautista. Figure 2 shows a typical episode in June, 1990 with tides removed and a linear trend removed from the data. An initial exponential change of shear strain, with a time constant of 60 minutes, is followed by a readjustment of strain over a period of approximately 2-3 days. This pattern is reasonably similar to perturbations in the creep data measured by a nearby creepmeter. Correlations of strain and creep episodes are being investigated further.

RELEVANT PUBLICATIONS

Gladwin, M. T., High Precision multi component borehole deformation monitoring. *Rev.Sci.Instrum., 55*, 2011-2016, 1984.

Gladwin, M.T., Gwyther, R., Hart, R., Francis, M., and Johnston, M.J.S., Borehole Tensor Strain Measurements in California. *J. Geophys. Res. 92.* B8 pp7981-7988, 1987.

Gladwin, M.T., Gwyther, R.L., Higbie, J.W. and Hart, R.G., A Medium Term Precursor to the Loma Prieta Earthquake? *(Submitted for Publication).*

Gladwin, M. T. and Hart, R. Design Parameters for Borehole Strain Instrumentation. *Pageoph.,123,* 59-88, 1985.

Gladwin, M. T., Hart, R., and Gwyther, R. L. Tidal Calibration of Borehole Vector Strain Instruments.*EOS, (Trans. Am. G. Un.) 66,* 1057, 1985.

Gladwin, M.T., and Johnston, M.J.S. Coseismic moment and total moment of the April 24, 1984, Morgan Hill and the January 26, 1986, Quiensabe earthquakes. *EOS,(TransAm.G.Un.), 67, R 308, 1986.*

Gladwin, M. T. and Wolfe, J. Linearity of Capacitance Displacement Transducers. *J.Sc.Instr. 46,* 1099-1100, 1975.

Johnston, M.J.S., Gladwin, M.T., and Linde, A.T. Preseismic Failure and Moderate Earthquakes. *I.A.S.P.E.I.* , Tokyo, August 19-30, S7-65, 35 , 1985.

Johnston, M. J. S., Linde, A.T., Gladwin, M.T., and Borcherdt, R.D. Fault Failure with Moderate Earthquakes. *Tectonophysics.* 144, 189-206, 1987.

Johnston, M.J.S., Borcherdt, R.D., Glassmoyer, G., Gladwin, M.T., and Linde, A.T. Static and Dynamic Strain during and following January 26, 1986, Quiensabe, California, Earthquake. *EOS,(Trans., Am. G. Un.), 67,* 16, 308, 1986.

Johnston, M.J.S., Borcherdt, R.D., Gladwin, M.T., Glassmoyer, G., and Linde, A.T. Static and Dynamic Strain during the M_L 5.9 Banning, California Earthquake on July 8, 1986. *EOS,(Trans. Am.G.Union),68*, 44, 1244 (1987).

Myren, G.D., Johnston, M.J.S., Linde, A.T., Gladwin, M.T. and Borcherdt, R.D. Borehole Strain Array near Parkfield, California. *EOS (Trans. Am.G.Union), 68,* 44, 1358 (1987).

Gladwin, M. T., Hart, R., and Gwyther, R. L. Continuous Regional Deformation Measurements Related to the North Palm Springs Earthquake of July 8, 1986.*EOS, (Trans. Am. G. Un.) 69* 1432, 1988.

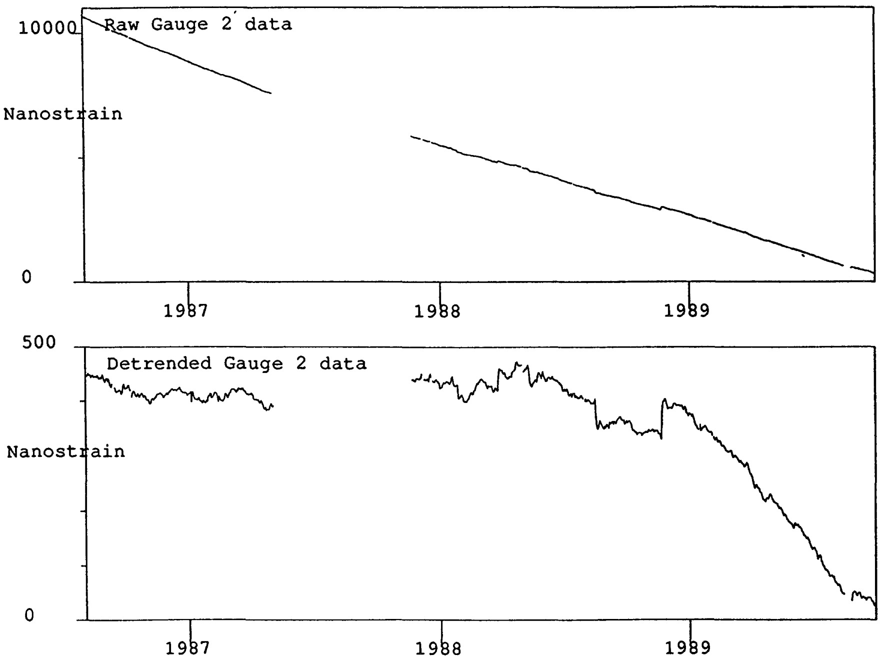

Figure 1

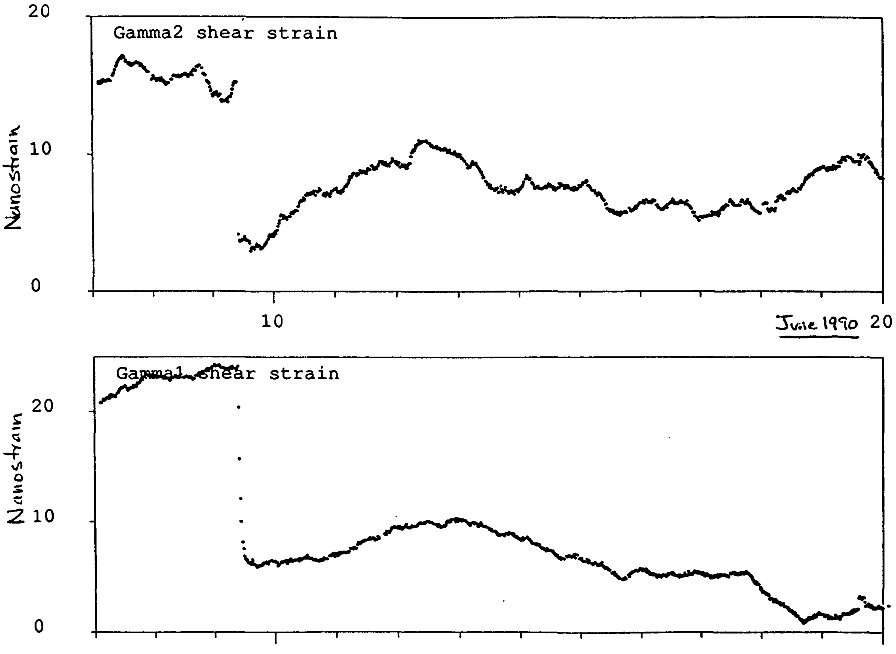

Figure 2

Parkfield Geophysics

9380-03074

Robert C. Jachens
U.S. Geological Survey, MS 989
345 Middlefield Road
Menlo Park CA 94025
(415) 329-5300

Investigations

1) Developed a 3-dimensional inversion scheme for magnetic data over flat-lying tabular bodies. The scheme is based on passing the magnetic anomaly data through a pseudo-gravity transformation, iteratively fitting a body shape to the pseudo-gravity anomaly, calculating the resulting magnetic anomaly from the modelled body, and adjusting the body depth to match the amplitude of the observed and calculated anomalies. The scheme makes use of the property that magnetic anomalies (arising from dipole sources) decay more rapidly with increasing distance from the source body than do gravity anomalies (arising from monopole sources).

2) With Andy Griscom, Clark Blake, Bob McLaughlin, and Carl Wentworth, investigated the attitudes of faults in the San Francisco Bay Region. Primary data sets used to constrain the fault attitude interpretations were the gravity and aeromagnetic data sets compiled as part of the Bay Region Project, augmented by data collected during the National Geologic Mapping Program's San Jose Sheet study and various groundwater investigations. In a few areas, seismicity data also were used to define the fault attitudes.

Results

1) The 3-dimensional inversion scheme was applied to the Parkfield aeromagnetic map which is dominated by anomalies from a large serpentinite body exposed in the New Idria dome and a widespread tabular body (probably also serpentinite) that extends northwest from Table Mountain more than 70 km. The latter body is 20-30 km wide and is truncated on the southwest by the San Andreas fault. The inversion scheme and the specific models are still undergoing testing but preliminary results suggest the following:

- a) The New Idria serpentinite has the shape of a thin flap in its western part but extends to mid-crustal depths as a north dipping thick slab in the southeastern part.
- b) The tabular body appears to underlie much of the Coast Ranges northwest of Table Mountain, probably attains a maximum thickness of 3-5 km, and bottoms at a depth of roughly 6 km at least near its northwest end.
- c) The tabular body extends beneath the Waltham Canyon fault, the Joaquin Ridge anticline, and the syncline located to the south of Joaquin Ridge, elements that all suggest substantial structural relief or vertical offset. Interestingly, the vertical tectonics do not appear to be reflected in the shape of the flat-lying tabular body.

2) Dips of principal northwest-striking faults of the south San Francisco Bay region, contrary to general view, do not seem to be vertical. Instead,

inspection and modelling of contoured gravity and aeromagnetic data indicate that substantial lengths of these strike-slip faults probably dip mainly to the southwest at angles of 70 degrees or less to depths of at least 5-10 km. In many places older rocks are placed over younger rocks, indicating a reverse component of slip. These faults include the Calaveras (60 degrees SW at Livermore Valley), Silver Creek (65 degrees SW at Silver Creek), Sargent, San Andreas (60 degrees SW at Hollister), Zayante (SW on northwest segment), and San Gregorio (NE at Pigeon Point).

Although some of the dipping segments are clearly associated with sinistral bends of the fault traces (which should produce local cross-fault compression) the widespread distribution of non-vertical faults implies general compression and shortening normal to the faults. Such compression is consistent with observed fault-parallel folding, thrusting normal to the San Andreas fault, and the general regime of northeast-southwest compression recently inferred for the Coast Ranges from earthquake focal mechanisms and other geophysical evidence.

Reports

Jachens, R.C., Griscom, Andrew, Blake, M.C., McLaughlin, R.J., and Wentworth, C.M., 1990, Cross-fault compression inferred from southwest dips of strike- slip faults in the south San Francisco Bay region, California: Geological Society of America Abstracts with Programs, v. 22, P. 31.

TILT, STRAIN, AND MAGNETIC FIELD MEASUREMENTS

9960-2114

M. J. S. Johnston, R. J. Mueller, G. D. Myren
Branch of Tectonophysics
U. S. Geological Survey
Menlo Park, California 94025
415/329-4812

Investigations

[1] To investigate the mechanics of failure of crustal materials using data from both deep borehole tensor and dilational strainmeters and near surface strainmeters, tiltmeters, and arrays of absolute magnetometers.

[2] To develop physical models of incipient failure of the earth's crust by analysis of real-time records from these instruments and other available data.

Results

[1] POSSIBLE CHNAGE IN EARTH TIDAL RESPONSE BEFORE THE OCTOBER 18, 1989, LOMA PRIETA M_L 7.1 EARTHQUAKE.

Modification of the elastic properties of fault zones prior to fault failure has long been expected and should be detected by changes in earth tidal response. High quality tidal strain recordings were obtained in the epicentral region prior to, and following, the October 18, 1989, M_L 7.1 Loma Prieta earthquake. These recordings were made in deep boreholes with both Sacks-Evertson dilational strainmeters (sensitivity 10^{-11}) and 3-component tensor strainmeters (sensitivity 10^{-9}). The closest dilatometer, SRLS, was 33 km to the south-east along strike from the epicenter of the earthquake but probably less than 10 km from the southern end of the final rupture. Tidal admittance (normalized by ocean-load corrected theoretical earth tides) has been calculated at 10 day intervals with a sliding 2 month data window of hourly averaged data starting in August, 1987 and ending in August, 1990. The coseismic offset is not included. During the 2-year period prior to the earthquake, the normalized M_2 amplitude may have increased in a linear manner by a few percent per year but scatter in these estimates (probably due either to small data gaps, incomplete removal of atmospheric pressure loading, and/or incomplete correction for ocean loading) is of the same order($\sigma = 2.5\%$). A least-square linear fit to these data prior to the earthquake indicates a rate of $2.9 \pm 0.5\%$/year. During the 2-month period immediately before the earthquake, M_2 amplitudes calculated at 10 day intervals from a sliding 15 day window of 10-min data have a standard deviation of 1.5%. We conclude that no significant variation in M_2 tidal admittance occurred before the Loma Prieta earthquake. Since fractional changes in strain tide amplitudes are proportional to changes in Poisson's ratio and inverse bulk modulus (Beaumont and Berger, 1974), this implies stability of these parameters at the few percent level during the two years before the earthquake. Following the earthquake, however, we have observed a uniform decrease with time in normalized M_2 amplitude that now totals more than 10%. This is probably a consequence of continuing fracture of fault zone materials to the south and beneath this instrument.

[2] POSSIBLE TECTONOMAGNETIC EFFECT OBSERVED FROM MID-1989, TO MID-1990, IN LONG VALLEY CALDERA, CALIFORNIA.

Precise measurements of local magnetic fields have been obtained with a differentially connected array of three proton magnetometers in the Long Valley caldera region since 1984. Two magnetometers are located inside the caldera with a third reference magnetometer located 26 kilometers southeast of the caldera. After correction for secular variation, it is apparent that an anomalous 2 nT decrease in the magnetic field has occurred from mid-1989 to mid-1990 at the magnetometer located closest to the center of the resurgent dome inside the caldera. During this period a significant increase in extensional displacement was observed on the 2-color geodimeter network within the caldera from October, 1989, to mid-1990 and a dramatic increase in seismic activity occurred from December, 1989 to July, 1990. The displacement data are consistent with a simple dilatational point-source model at a depth of about 8 km beneath the center of the resurgent dome and suggest the possibility of a magma chamber with active intrusion at this depth generating the micro-seismicity. A simple point-source mogi-type piezomagnetic model at this depth generates magnetic field perturbations of the same amplitude as those observed provided the Curie point isotherm is at a depth of less than 5 km. Other physical processes may also be contributing to the magnetic field in this region. Possible candidates are thermal demagnetization processes (Sasai, 1979), which may not be rapid enough to generate 2 nT in 1 year from a source 8 km deep, or electrokinetic effects (Fitterman, 1976) which require massive changes in the fluid flow regime at depth, the consequences of which may have been observed in deep wells monitored in the region.

[3] BOREHOLE STRAIN ARRAY IN CALIFORNIA

A network of 15 borehole strainmeters along the San Andreas fault zone and in the Long Valley Caldera continue to be monitored and maintained. All instruments are installed at depths between 117-m and 324-m and all are between 1-km and 5-km from the the surface trace of the fault. High frequency dilatometer data in the frequency range 0.005 Hz to 100 Hz are recorded on 16-bit digital recorders with least count noise less than 10^{-11}. Low frequency data from zero frequency to 0.002 Hz are transmitted through the GOES satellite to Menlo Park, CA, using a 16-bit digital telemetry system. At the USGS in Menlo Park the data are displayed in "almost real time" and are continuously monitored with detection algorithms for unusual behavior. Least-count noise is about $5*10^{-12}$ for the on-site digital recordings, and about $2*20^{-11}$ for the satellite telemetry channels. Earth strain tides, strain transients related to fault creep and numerous strain seismograms from local and teleseismic earthquakes with magnitudes between -1 and 6 have been recorded on these instruments. Static moments and total earthquake moments are determined from the co-seismic strains and total strain changes observed with the larger events.

[4] CROWLEY LAKE AND SAN ANDREAS LAKE WATER LEVEL MONITORING

Water level monitoring sites have been installed on Lake Crowley in the Long Valley/ Mammoth Lakes region and San Andreas lake on the San Andreas fault just south of San Francisco. These data provide differential water level measurements (tilt) with a measurement precision of less than 1 mm on baselines of 5 to 8 kilometers. Monthly averages of the data from San Andreas lake between 1979 and 1989 indicate a tilt rate of 0.02±0.08 microradians/yr (down S34°E).

[5] DIFFERENTIAL MAGNETOMETER ARRAY IN CALIFORNIA

We continue investigations of local magnetic fields and relationships to crustal strain and seismicity in the Parkfield region and in southern California. The network consists of 9 stations which are all sampled synchronously every 10 minutes and transmitted with 16-bit digital telemetry to Menlo Park, CA through the GOES satellite. Data are monitored daily with particular attention to the seven stations operating in the Parkfield region of central California.

[6] SEISMOMAGNETIC EFFECT GENERATED BY THE OCTOBER 18, 1989, M_L 7.1 LOMA PRIETA, CALIFORNIA, EARTHQUAKE.

A differentially connected array of proton magnetometers operated within the epicentral region of the October 18, 1989, M_L 7.1 Loma Prieta earthquake for 10 years from 1974 to 1986. The closest magnetometer station was located 7.3 km from the epicenter of the earthquake and within 3 km of the site where anomalous ULF magnetic noise measurements were observed. Following the earthquake, the magnetometers were reinstalled with sensors replaced in the original undisturbed sensor holders. Comparison of pre-1986 total intensity magnetic field data with data obtained during the months following the earthquake indicate local offsets of about 1 nT may have been generated at stations nearest the epicenter. Tests on other difference field data from 1983 to the present indicate that ofsetts determined in this way could be biassed, in worst case, by as much as 0.7 nT. The offsets can be generally, but not perfectly, fit with a simple seismomagnetic model of the earthquake for which 1.9 m of right lateral and 1.3 m of dip slip (south-west side up) occurred on a fault patch between 6 km and 18 km deep and 45 km long. The total rock magnetization is assumed to be 1.0 A/m. Since the offset has remained following the earthquake, an alternate explanation in terms of electokinetic effects is unlikely even though transient ground water flow occurred following the earthquake. Comparison of pre-1986 magnetic noise data and similiar post-seismic data does not indicate the change in total magnetic field noise measurements expected by aliasing of ULF (0.01 Hz - 10 Hz) magnetic noise in the vicinity of the Loma Prieta earthquake.

[7] NEAR-FIELD HIGH PRECISION STRAIN PRIOR TO THE OCTOBER 18, 1989, LOMA PRIETA M_L 7.1 EARTHQUAKE?

High resolution strain recordings were made in deep boreholes throughout California prior to, during, and following, the October 18, 1989, M_S 7.1 Loma Prieta earthquake. The nearest dilational strainmeters (sensitivity 10^{-10}) and 3-component tensor strainmeters (sensitivity 10^{-9}) were 37 km to 42 km, respectively, from the main shock. High quality data, including details of strain offsets, were recorded on both instruments through the earthquake. These data have been searched for indications of short-, intermediate-, and long-term strain redistribution and/or fault slip that might have indicated imminent rupture. Short- and intermediate-term changes in both tensor strain and dilational strain ($\leq$ several nanostrain, if any) during the minutes to months before the earthquake are at least 1000 times smaller than that generated by the earthquake itself. If short-term preseismic slip did occur at the nucleation point of the earthquake during the previous week, and if the type of slip is similar to that during the earthquake, its moment could not be more than 10^{24} dyne-cm. Stated another way, slip equivalent to that expected for a M 5.3 earthquake could have occurred in the hypocentral region without the strainmeters detecting it at these distances and azimuthal positions. Long-term strain changes appear to have occurred in mid-1988 and mid-1989. These changes were both followed by M_L 5 earthquakes in the hypocentral region on June 27, 1988, and August 8, 1989, respectively, and, since they correspond approximately to changes in geodetic strain rate over the epicenter, may indicate precursory strain redistribution in the epicentral region. Minor post-seismic strain recovery ($\approx$ 14%) occurred in the month following the main shock.

Reports

Johnston, M. J. S., A. T. Linde, and M. T. Gladwin, 1990. Near-Field High Precision Strain Prior to the October 18, 1989 Loma Prieta M_L 7.1 Earthquake. *Geophys. Res Lett.*, **17**, 1777-1780.

Lisowski, M., W. H. Prescott, J. C. Savage, and M. J. S. Johnston, 1990. Geodetic Estimate of Coseismic Slip During the 1989 Loma Prieta Earthquake. *Geophys. Res. Lett.*, **17**, 1437-1440.

Mueller, R. J. and M. J. S. Johnston, Seismomagnetic Effect generated by the October 18, M_L 7.1 Loma Prieta, California, Earthquake. *Geophys. Res. Lett.*, B17R, 2031-2034.

Zhan, Z., Fuxin, Y., M. J. S. Johnston, R. J. Mueller, and Gao Jintian, 1990, Analytical Comparison of Geomagnetic Total Field between Sino-US Stations, Proc. Int. Sym. Geomagnetism, April 17 - 20, 1990, Shanghai, China, 1-14.

Mueller, R. J., M. J. S. Johnston, and J. O. Langbein, 1990, Possible Tectonomagnetic Effect Observed from Mid-1989 to Mid-1990 in Long Valley Caldera, California. Trans. Am. Geophys. Un. (in press).

Johnston, M. J. S. and A. T. Linde, 1990, Possible Change in Earth Tidal Response Before the October 18, 1989, Loma Prieta M_L7.1 Earthquake. Trans. Am. Geophys. Un. (in press).

Johnston. M. J. S., 1990, Magnetic and Fault Crossing Geodetic Arrays in the Peoples Republic of China. PRC-US Bilateral Symposium on Xianshuihe Fault Zone and Field Geological Excursion, September 22-30, 1990. Chendu, China, p77.

GEODETIC STRAIN MONITORING

9960–02156

John Langbein
Branch of Tectonophysics
U.S. Geological Survey
345 Middlefield Road, MS/977
Menlo Park, California 94025
(415) 329–4853

Investigations

Two–color geodimeters are used to survey, repeatedly, geodetic networks within selected regions of California that are tectonically active. This distance measuring instrument has a precision of 0.1 to 0.2 ppm of the baseline length. Currently, the crustal deformation is being monitored within the south moat of the Long Valley caldera in eastern California, near Pearblossom, California on a section of the San Andreas fault that is within its Big Bend section and on Middle Mountain near Parkfield, California. Periodic comparisons with the prototype, two–color geodimeter are also conducted near Parkfield, California. These intercomparison measurements serve as a calibration experiment to monitor the relative stabilities of the portable and prototype geodimeters.

Results

1. Long Valley Caldera

The data from the Casa subnetwork (Figures 1 and 2) continue to show extension in response to inflation beneath the resurgent dome. However, on the baseline CASA–KRAKATAU, the extension rate has decreased to 37mm/a during March 1990 relative to the 75mm/a rate that started in October 1989. Because of its location and its high frequency observations, this baseline is particularly sensitive to changes due to inflation beneath the resurgent dome. To better understand the geometry of the inflation source, the entire network shown in Figure 1 was resurveyed in September 1990. The observed distance changes measured over the past year can be used to model the deformation. In particular, the geometry of the inflation resources inferred from the most recent data can be compared with the previous model of deformation derived from the data spanning mid–1983 to 1988. The initial attempt to model the most recent data implies that most of the deformation is a result of inflation at 8 km beneath the central part of the resurgent dome. In contrast, the data after mid–1983 needed two sources of inflation plus fault slip in the south moat of the caldera for a reasonable fit. Furthermore, although the deeper source was located beneath the central part of the resurgent dome, it had a source depth of 10 km which was primarily constrained by the releveling data along highway 395. The spatial distribution of two–color baselines was not dense enough to refine the estimate of depth for the earlier period of inflation. However, the more recent data appear to be fit best with an 8 km deep point source rather than the 10 km source. Furthermore, the older two-color data is also fit with a 8 km source, but the 8 km source is somewhat inconsistent with the earlier leveling data. To date, there is no long baseline leveling that spans the interval of the most recent episode.

2. Parkfield

In the previous report, I discussed the large fluctuations in areal dilatation from April 1989 through April 1990. Based on instrument calibration data, I attributed these variations to be caused by an instrument problem. However, as of mid-May 1990, the Parkfield two-color geodimeter has been repaired and the areal dilatation observed by this instrument is now "clean"

In May 1990, M. Wyss published two articles in *Nature* stating that both the rate of seismicity and the deformation rate decreased in late 1986 in the area just north of the town of Parkfield. In particular, he used data from 2 two-color geodimeter baselines, CAN and BARE. His metric consisted of picking a time and computing the secular rates before and after the time of interest. The metric consisted of the difference in rates. After reconstructing his algorithm, I ran many Monte Carlo simulations to quantify the probability that an observed rate change is significant. Because the variations in the observed displacements as a function of time do not exhibit the character of white noise, my simulations included both apparent seasonal variations and the contributions of $1/f^2$ noise. In my analysis, I concluded that the "anomaly" identified by Wyss is significant at the 80% level during late 1986. However, the highest confidence level of 90% is achieved in early to mid-1987 on both baselines. In my "correspondence to *Nature*" I point out several other factors that could degrade the significance. A possible man-made offset in distance data to CAN in late 1985 contributes a substantial uncertainty to any estimate of secular extension rates. The average rainfall decreased by 30% for the period spanning the data instead of the 10% claimed by Wyss. It is possible that the decrease in apparent tectonic deformation could be an artifact of decreasing soil moisture which is capable of displacing geodetic monuments. Finally, I used the analysis described above on data from all 18 baselines in the Parkfield two-color network. On the baselines to TABLE, HOGS and MID, I detected significant rate changes (> 95%) that preceded the Kettleman Hill Earthquake of August 1985. However, because the metric compares the secular rate before and after the time of interest, the anomalous rate should not be interpreted as a precursor, rather, the data preceding the earthquake had a different secular rate that the data after the quake.

Reports

Langbein, J., "Scientific correspondence to *Nature*", submitted June 1990.

J.O. Langbein, D.P. Hill, T.N. Parker, S.K. Wilkinson, and A.M. Pitt, Renwed inflation of the resurgent dome in Long Valley Cadera, California, from mid-2989 to mid-1990, abstract submitted to EOS.

Figure Captions

Figure 1. Map showing the location of all the baselines within and near the Long Valley caldera that are measured with a two-color geodimeter. The locations of the caldera, resurgent dome, Inyo craters, Crowley Lake and the major roads are also shown.

Figure 2. Changes in distances for the seven most frequently measured baselines within the caldera. These baselines use CASA as the central instrument station. The error bars represent ±1 standard deviation.

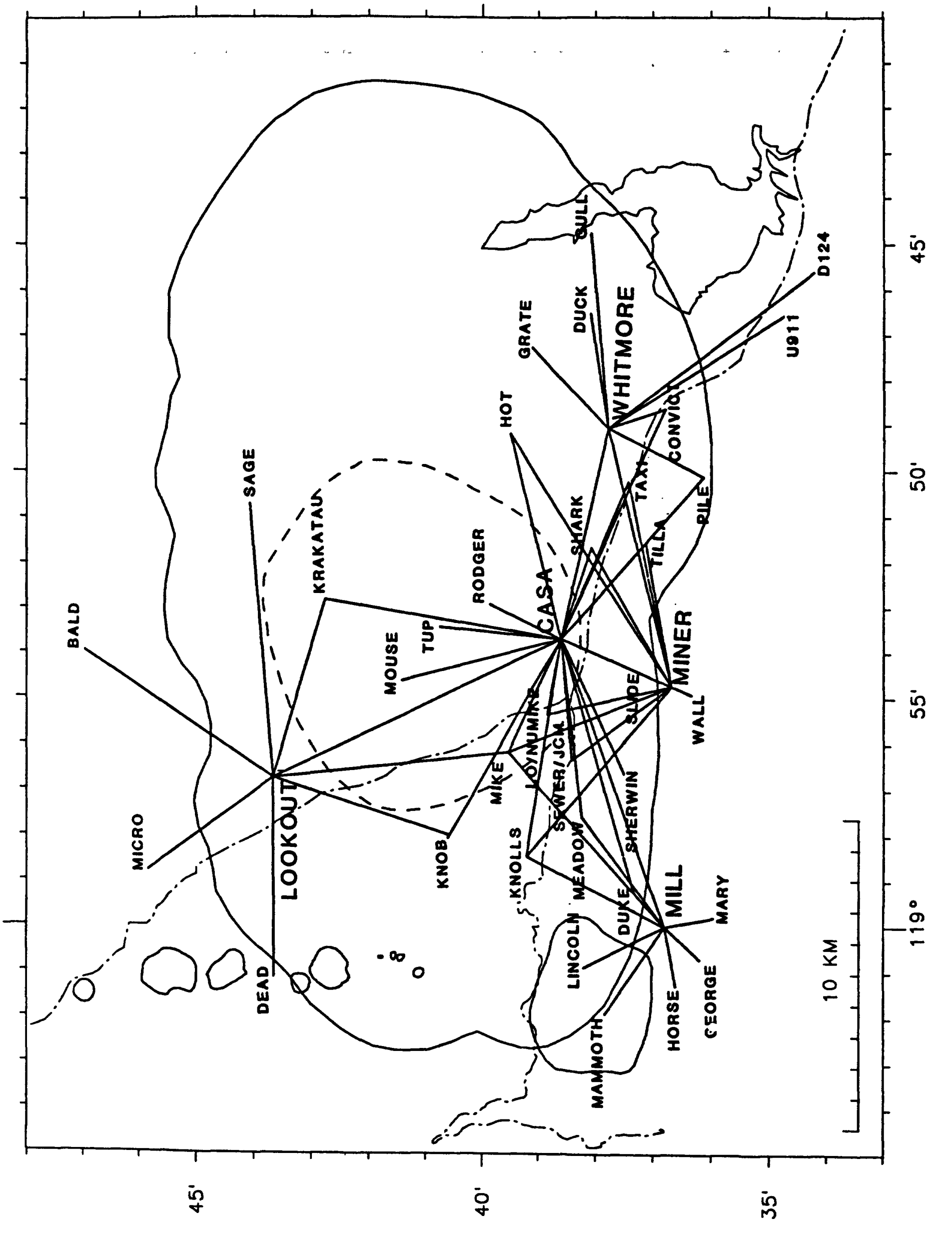
BALD
SAGE
KRAKATAU
RODGER
HOT
GRATE
DUCK
BULL
WHITMORE
D124
U911
CONVICT
TAXI
PILE
SHARK
TILLA
CASA
TUP
MOUSE
MINER
WALL
SLIDE
LOOKOUT
MICRO
DEAD
KNOB
MIKE
LO/NUMIKE
SEWER/JCM
SHERWIN
KNOLLS
MEADOW
MILL
MARY
DUKE
LINCOLN
MAMMOTH
HORSE
GEORGE
10 KM
45'
50'
55'
119°
45'
40'
35'

Figure 1

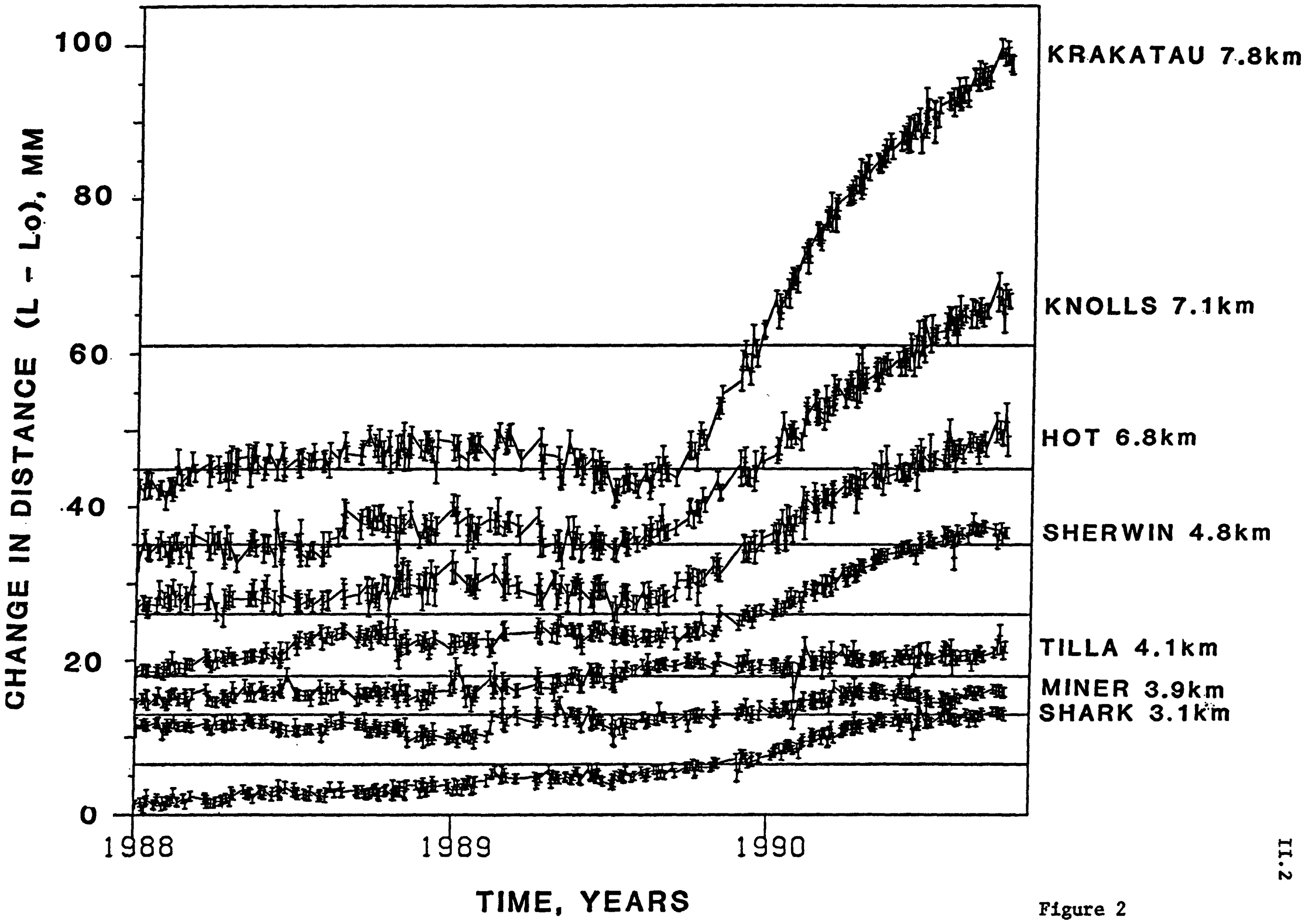
CHANGE IN DISTANCE (L - Lo), MM
100
80
60
40
20
0
1988
1989
1990
TIME, YEARS
KRAKATAU 7.8km
KNOLLS 7.1km
HOT 6.8km
SHERWIN 4.8km
TILLA 4.1km
MINER 3.9km
SHARK 3.1km

Figure 2

II.2

Microearthquake Data Analysis

1-9930-01173

W.H.K. Lee
U.S. Geological Survey
Branch of Seismology
345 Middlefield Road, MS 977
Menlo Park, California 94025
(415) 329-4781

Investigations

The primary focus of this project is the development of state-of-the-art computation for analysis of data from microearthquake networks. For the past six months I have been involved in:

(1) Using PC for Network Data Acquisition
A low-cost 128-channel PC data acquisition and recording system was implemented with the off-the-shelf hardware and a proto-type multiplexer designed by Jim Ellis. It became operational a few hours before the October 17, 1989 Loma Prieta earthquake and has recorded several thousand aftershocks. At the end of May, 1990, the PC hardware was upgraded from a 286 PC to a 386 PC with a 300-megabyte hard disk, and the proto-type multiplexer was replaced by an improved multiplexer due to J.R. Rogers. An off-line PC is networked to the online PC, and it is also used to collect teleseismic events (using an algorithm due to John Evans) when it is not used for offline duties. For the past few months, both PCs performed well in data acquisition.

(2) Applying non-USGS Plotting Software for Seismic Data Analysis
A 3-dimensional data viewing program (AcroSpin) for rotating, enlarging, or shrinking objects and data points was developed by David Parker of Acrobits, Inc. John Lahr and I wrote four programs to prepare hypocenter, coastline, text, and boundary data for the AcroSpin program so that earthquake data could be readily displayed and viewed in 3-dimensions.

A general plotting package (PixPlot and PenPlot) was developed by Ernest Lee (a high-school student) and Dean Tottingham (a college student). I have written a menu-driven interface to PixPlot so that plotting seismic data may be performed quickly. I have also collaborated with Nils Lahr (a high-school student) in writing a control program (DoPlot) so that data editing and plotting can be performed under an integrated and easy-to-use environment.

(3) Planning Seismic Instrumentation for Topical Volcano Studies

In collaboration with Bernard Chouet and Dave Harlow, I have assisted in planning seismic instrumentation for topical volcanic studies. Two portable arrays (one telemetered and one hardwired) are being implemented to meet the scientific objectives of volcano research.

Reports

Lahr, J.C., and W.H.K. Lee, 1990. User manual for DoPlot and QEdit, IASPEI Software Library, v. 2, p. 165-184.

Lahr, N. B., and W.H.K. Lee, 1990. User manual for DoPlot and QEdit, IASPEI Software Library, v. 2, p. 185-207.

Lee, W.H.K., 1990. Replace the HYPO71 format? Bull. Seism. Soc. Am., v. 80, p. 1046-1047.

Lee, W.H.K. (editor), 1990. "Toolbox for Plotting and Displaying Seismic and Other Data". IASPEI Software Library, Volume 2, Seis. Soc. Am., El Cerrito, CA.

Lee, W.H.K., 1990. User Manual for GoPlot, IASPEI Software Library, v. 2, p. 83-102.

Parkfield Prediction Experiment

9930-02098

Allan Lindh, Andrew Michael, Cathy Aviles, and Barry Hirshorn
Branch of Seismology
Office of Earthquakes, Volcanoes and Engineering
345 Middlefield Road, Mail Stop 977
Menlo Park, California
(415) 329-4778
(FTS) 459-4778

Investigations

1. Seismological research associated with the Parkfield Earthquake Prediction Experiment.
2. Analysis of USGS coda-duration measurements for magnitude determination.
3. Prepare weekly earthquake reports for Northern and Central California, distribute to press and public officials by FAX so that the reports are available on a timely basis.
4. Process RTP data to complete and final form on a daily basis.
5. Prepare on a timely basis merged monthly catalogs, including all CUSP and RTP data.
6. Continue ongoing work on long-term earthquake probabilities in California.
7. Research on the Loma Prieta earthquake.
8. Research on the seismicity of the S.F. Bay Area.

Results

1. A Real-time earthquake prediction experiment is underway at Parkfield and new seismological results add to our understanding of the fault at Parkfield.
2. Relationships between geologic structures revealed in three dimensional velocity models and earthquake ruptures are being developed.
3. Weekly reports have continued to go out every Thursday since February 1989.
4. Clean merged data is complete for January, 1989-September, 1990.

Reports

Aviles, C.A. and C.M. Valdes, 1989; Comparison of microearthquake source parameters in the preparation zone at Parkfield, California: 1977-1982 and 1984-1989, submitted to BSSA.

Nishioka, G.N., and A.J. Michael, 1990, A detailed study of the Seismicity of the Middle Mountain, CA zone, Bull. Seis. Soc. of Am., 80, 577-588.

Michael, A.J., 1990, Stress analysis of the Whittier Narrows, California, aftershock sequence: new techniques and results, J. Geophys. Res., submitted.

Michael, A.J., 1990, Energy constraints on kinematic models of oblique faulting: Loma Prieta versus Parkfield-Coalinga, Geophys. Res. Lett., 17, 1453-1456.

Michael, A.J., W.L. Ellsworth, and D.H. Oppenheimer, 1990h, Coseismic stress changes induced by the 1989 Loma Prieta, California, earthquake, Geophys. Res. Lett., 17, 1441-1444.

Eberhart-Phillips, D., V.F. Labson, W.D. Stanley, A.J. Michael, and B. Rodrigues, 1990i, Preliminary velocity and resistivity models of the Loma Prieta earthquake region, Geophys. Res. Lett., 17, 2035-2038.

Michael, A.J. and D.M. Eberhart-Phillips, 1990j, Correlation of heterogeneity in seismic behavior and seismic velocities, Earthquake Notes, abstract, 61, 34.

Oppenheimer, D.H., A.J. Michael, and W.L. Ellsworth, 1990k, Aftershock mechanisms of the Loma Prieta earthquake: a total stress drop event?, Earthquake Notes, abstract, 61, 46.

Eberhart-Phillips, D.M., A.J. Michael, G. Fuis, R. Luzitano, 1990l, Three-dimensional crustal velocity structure in the region of the Loma Prieta, California, earthquake sequence from inversion of local earthquake and shot arrival times, Earthquake Notes, abstract, 61, 48.

Michael, A.J., 1990m, Energy constraints on kinematic models of oblique faulting: Loma Prieta versus Parkfield-Coalinga, EOS, submitted.

Aviles, C.A. and A.J. Michael, Complications at the southern end of the 1966 Parkfield rupture zone, EOS, submitted.

Attachments:

A weekly seismicity report is attached as an example.

Seismicity Map for the San Francisco Bay Area
for the Week of 11 -- 18 October 1990

from the U.S. Geological Survey, Menlo Park, CA
data and text prepared by Allan G. Lindh
and Barry F. Hirshorn
graphics by Quentin W. Lindh

This was a normal week for seismicity in the San Francisco Bay area; for the seven-day period ending at 12am (PDT) on Thursday, 18 October 1990, the U.S. Geological Survey office in Menlo Park recorded 39 earthquakes of magnitude one (M1) and greater within the area shown in Figure 1. The largest event within the Bay area proper -- from San Jose north -- was a M3.3 event near Crockett at 7:06am on the 13th of October (Event #3 in Figure 1). There was a M2.1 event near this same location on 20 August 1990. There was also a pair of M2s on the Hayward fault near San Leandro on the 12th and 13th (#2 in Figure 1).

Elsewhere in the Bay area there was the usual scattering of small events along the Calaveras fault, although none larger than M2. The Loma Prieta aftershock zone heated up a little this week, with a M2.8 south of Los Gatos on the 12th (#1 in Figure 1), and a M2.5 near San Juan Bautista on the 15th (#5 in Figure 1). Farther east there was a M2.2 near Gilroy on the 15th (#6 in Figure 1).

Activity continued this week in the active zone north of Santa Cruz near Scott's Valley, with a M2.3 at 5:20am on the 14th (#4 in Figure 1). This event was 12 km deep, and was felt in the Monterey Bay area. This activity is too far west to be considered Loma Prieta aftershocks in the strict sense of the term, and they locate approximately mid-way between the surface traces of the Ben Lomond and Zayante faults.

South of San Juan Bautista, along the creeping portion of the San Andreas, there was the usual scattering of M2's, including one near Paicines, and a pair in the Bitterwater Valley. Farther east there was a single M2 near Coalinga.

There was a flurry of activity along the coast this week, most along or near the Sur-Nacimiento fault zone. The largest event was a M2.4 south of Big Sur on the 13th (#5 in Figure 2); there was also a M2.3 near Point Sur on the 16th (#7 in Figure 2).

In northern California there was the usual activity at the Geysers, including 2 events of M2+ (#2 in Figure 2). Farther north in the Coast Range, there was a M2.4 at 25 km depth beneath the north end of the Sacramento Valley on the 11th (#1 in Figure 2), and a M2.0 northeast of Red Bluff on the 15th (# 6 in Figure 2).

In the eastern Sierra Nevada activity continued near Mammoth Lakes. We recorded 44 events of M1.5 and greater within the area shown in Figure 3 this week, which is about the same as last week's total. There was an intense swarm just south of the town of Mammoth Lakes (#1 in Figure 3) on the 13th, which included a M2.4 (#2 in Figure 3). This was followed by a sequence of M2's inside the Long Valley Caldera along the northern extension of the Hilton Creek fault (#'s 3, 4 & 7 in Figure 3). There was also a pair of smaller events south of the Caldera on the 13th and 14th (#'s 5 & 6 in Figure 3)..

Farther north, there was a M2.5 southeast of Lake Tahoe on the 12th (#4 in Figure 2), and a M3.1 in southern Nevada on the 12th (#3 in Figure 3).

----ORIGIN	TIME----				-LAT	N--	--LON	W--	DEPTH	N	N	RMS	ERH	ERZ	N		DUR
YR	MON	DA	HRMN	SEC	DEG	MIN	DEG	MIN	KM	RD	S	SEC	KM	KM	FM	REMKS	MAG
90	OCT	11	736	22.13	40	8.92	122	13.33	25.25	11		.19	.9	1.4	12	KLA	2.4
90	OCT	11	1603	41.70	35	52.66	121	21.95	0.92	22		.11	.6	4.6	22	SSM	2.1
90	OCT	11	1817	40.03	35	34.52	121	15.11	1.25	20		.20	1.3	4.5	20	SSM *	2.1
90	OCT	11	1924	29.41	38	49.52	122	50.50	0.02	28		.20	.3	1.0	32	GEY *	2.1
90	OCT	12	113	22.68	37	30.46	118	24.63	7.92	14	2	.05	.4	.7	12	CHV	2.0
90	OCT	12	352	8.94	37	33.03	118	24.66	5.70	9		.03	.4	.6	9	CHV	2.0
90	OCT	12	850	11.43	38	21.33	118	8.22	2.30	25		.32	12.1	23.6	32	NEV -	3.1
90	OCT	12	953	5.55	38	49.73	119	51.03	0.02	15		.23	1.2	2.3	16	WAK *	2.5
90	OCT	12	1607	19.57	37	3.99	121	53.22	13.49	108		.11	.2	.3	99	LOM	2.8
90	OCT	13	233	18.96	37	43.70	122	6.95	4.88	33		.20	.3	.8	33	HAY	2.0
90	OCT	13	445	13.05	36	14.12	120	21.91	11.33	18		.16	.6	.9	18	COA	2.1
90	OCT	13	816	6.84	37	43.56	122	6.86	4.96	43		.18	.3	.8	44	HAY	2.1
90	OCT	13	1814	53.22	35	57.57	121	32.61	5.61	49		.20	.8	3.1	51	SSM	2.4
90	OCT	14	47	30.50	37	38.34	118	57.69	8.01	32		.12	.3	.5	32	SMO	2.4
90	OCT	14	48	38.21	37	38.37	118	57.56	7.41	25	1	.09	.3	.5	24	SMO	2.2
90	OCT	14	50	24.01	37	38.41	118	57.47	7.02	24		.09	.3	.5	24	SMO	2.8
90	OCT	14	50	37.18	37	38.57	118	57.72	7.34	19		.15	.7	1.0	19	SMO	2.3
90	OCT	14	51	15.15	37	38.56	118	57.44	6.86	20		.10	.4	.5	20	SMO	2.2
90	OCT	14	206	20.98	38	2.99	122	13.96	12.03	109		.24	.2	.3	99	CON	3.3
90	OCT	14	359	18.83	37	38.07	118	49.12	4.28	39		.14	.3	.6	48	HCF	2.7
90	OCT	14	543	12.91	37	39.52	118	50.78	6.90	27		.09	.3	.5	28	HCF	2.3
90	OCT	14	554	30.49	37	25.58	118	53.41	2.60	28	1	.08	.5	1.7	27	SIL	2.1
90	OCT	14	707	24.06	38	3.25	122	14.16	9.93	50		.20	.3	.7	50	CON	2.3
90	OCT	14	1220	15.40	37	4.52	122	1.23	11.83	88		.15	.3	.4	90	MON	2.3
90	OCT	14	1357	16.64	37	38.47	118	57.66	7.46	32		.12	.3	.5	33	SMO	2.3
90	OCT	14	2338	6.78	36	28.04	121	2.53	5.56	51		.12	.3	.8	53	BIT	2.2
90	OCT	15	16	47.71	37	38.29	118	57.40	7.88	25		.12	.4	.5	25	SMO	2.1
90	OCT	15	216	34.31	37	38.43	118	57.64	7.36	30		.16	.4	.6	42	SMO	2.5
90	OCT	15	348	19.28	37	32.61	118	52.39	4.77	24	1	.09	.3	.7	23	MOR	2.0
90	OCT	15	357	57.68	37	20.94	118	10.26	3.42	13		.07	1.0	2.0	13	WHI	2.2
90	OCT	15	821	0.17	36	53.27	121	35.88	5.12	80		.21	.3	.4	90	SJB	2.5
90	OCT	15	911	30.78	37	36.14	118	49.45	6.50	28		.12	.4	.6	29	HCF	2.2
90	OCT	15	937	42.32	36	26.61	121	0.20	4.26	18		.13	.5	2.6	19	BIT	2.1
90	OCT	15	941	2.70	36	39.97	121	17.32	4.89	48		.14	.2	.5	49	STN	2.1
90	OCT	15	1600	37.90	36	58.70	121	36.40	2.97	64		.20	.2	.6	70	SAR	2.2
90	OCT	15	1714	39.86	37	36.17	118	49.21	6.13	33		.11	.3	.5	34	HCF	2.4
90	OCT	15	1805	13.93	37	38.32	118	57.29	7.93	27		.11	.4	.6	28	SMO	2.2
90	OCT	16	158	22.48	40	32.03	121	39.26	10.21	16		.10	.4	.9	17	SHA	2.0
90	OCT	16	1215	42.05	36	9.15	121	34.36	8.66	60		.15	.3	.8	63	SUR	2.3
90	OCT	17	1320	2.76	38	45.56	122	43.49	1.62	34		.23	.3	.8	35	GEY	2.2

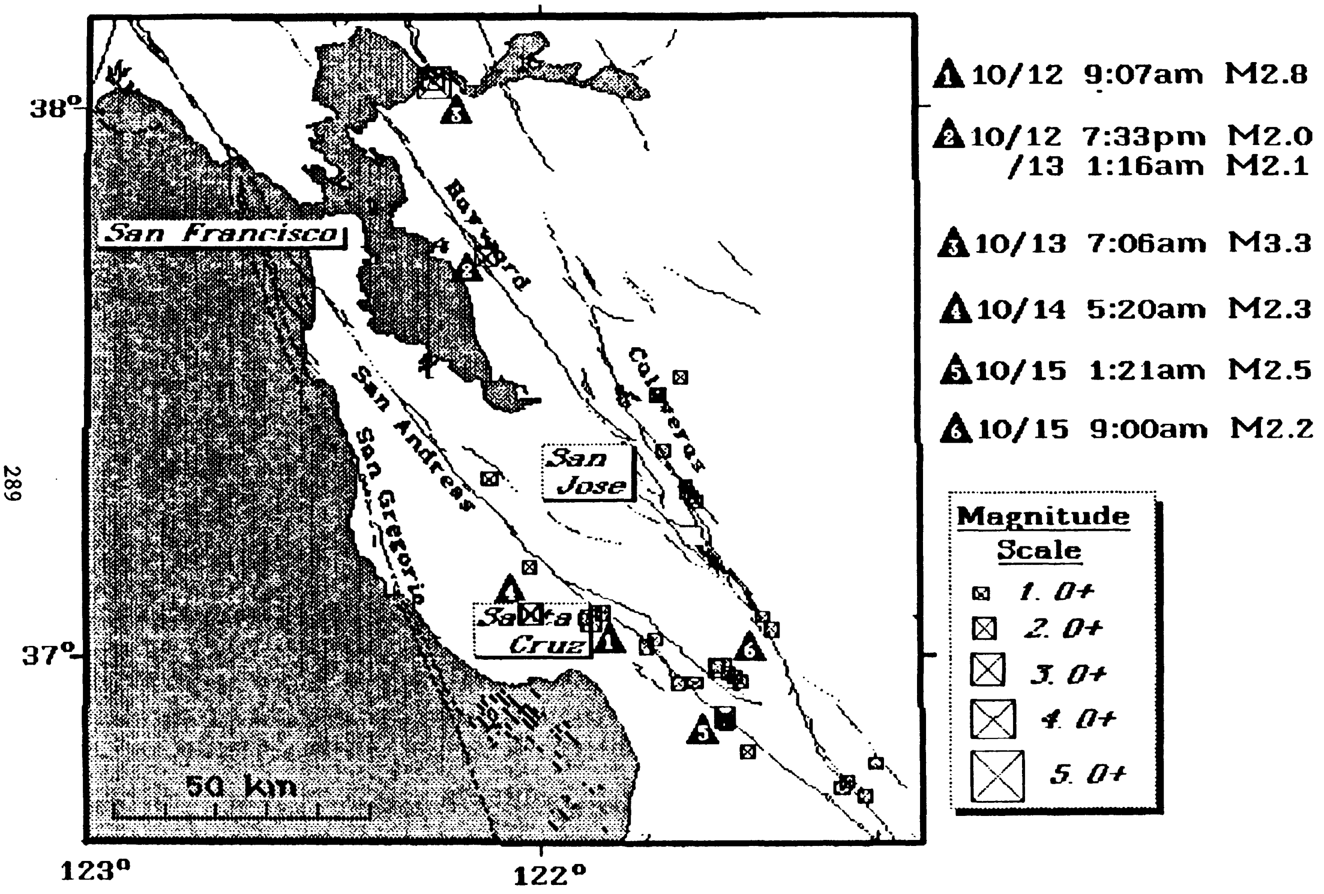
38°
37°
123°
122°
San Francisco
San Jose
Santa Cruz
Hayward
Calaveras
San Andreas
San Gregorio
50 km
1 10/12 9:07am M2.8
2 10/12 7:33pm M2.0
/13 1:16am M2.1
3 10/13 7:06am M3.3
4 10/14 5:20am M2.3
5 10/15 1:21am M2.5
6 10/15 9:00am M2.2
Magnitude Scale
1.0+
2.0+
3.0+
4.0+
5.0+

FIGURE 1

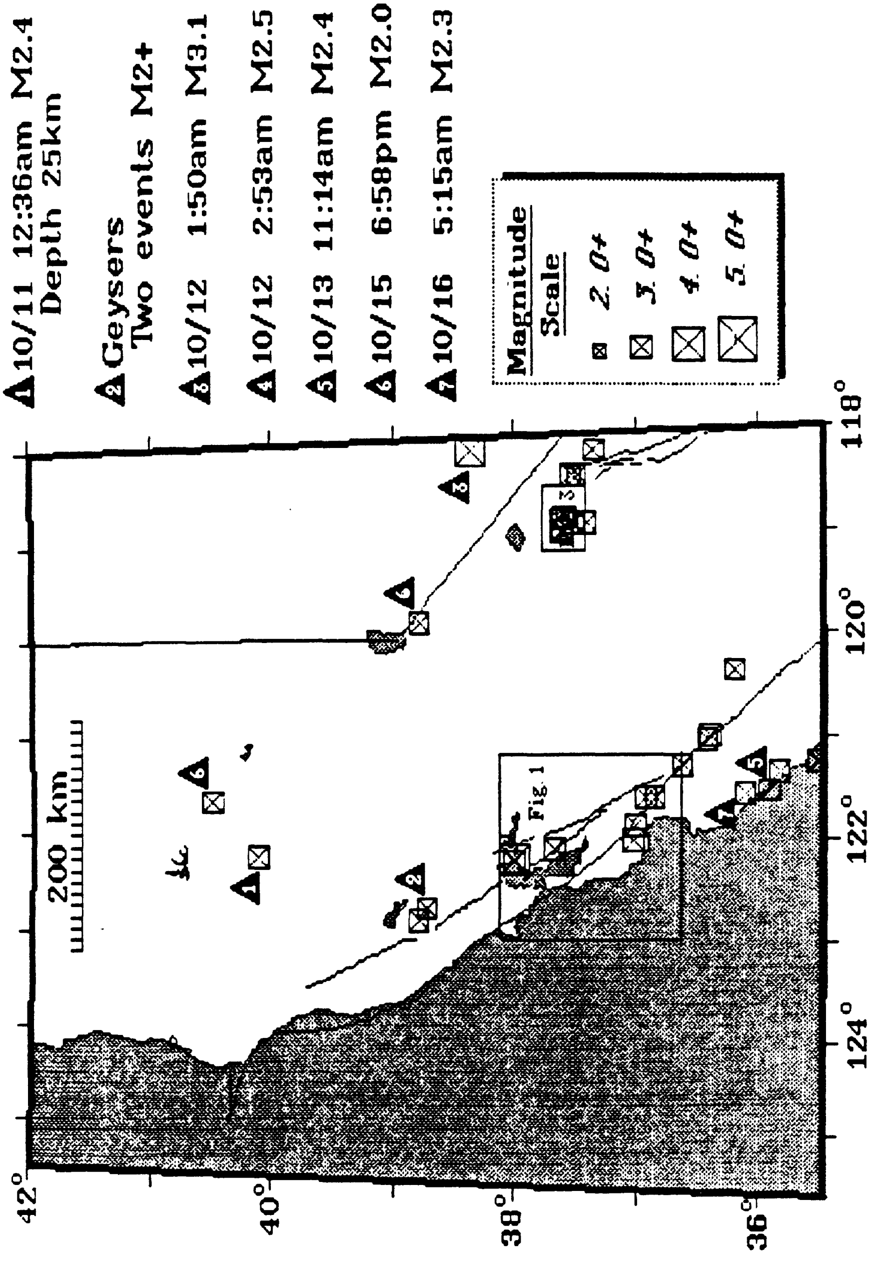
1 10/11 12:36am M2.4
Depth 25km
2 Geysers
Two events M2+
3 10/12 1:50am M3.1
4 10/12 2:53am M2.5
5 10/13 11:14am M2.4
6 10/15 6:58pm M2.0
7 10/16 5:15am M2.3
Magnitude Scale
2.0+
3.0+
4.0+
5.0+
200 km
Fig. 1
3
42°
40°
38°
36°
124°
122°
120°
118°

FIGURE 2

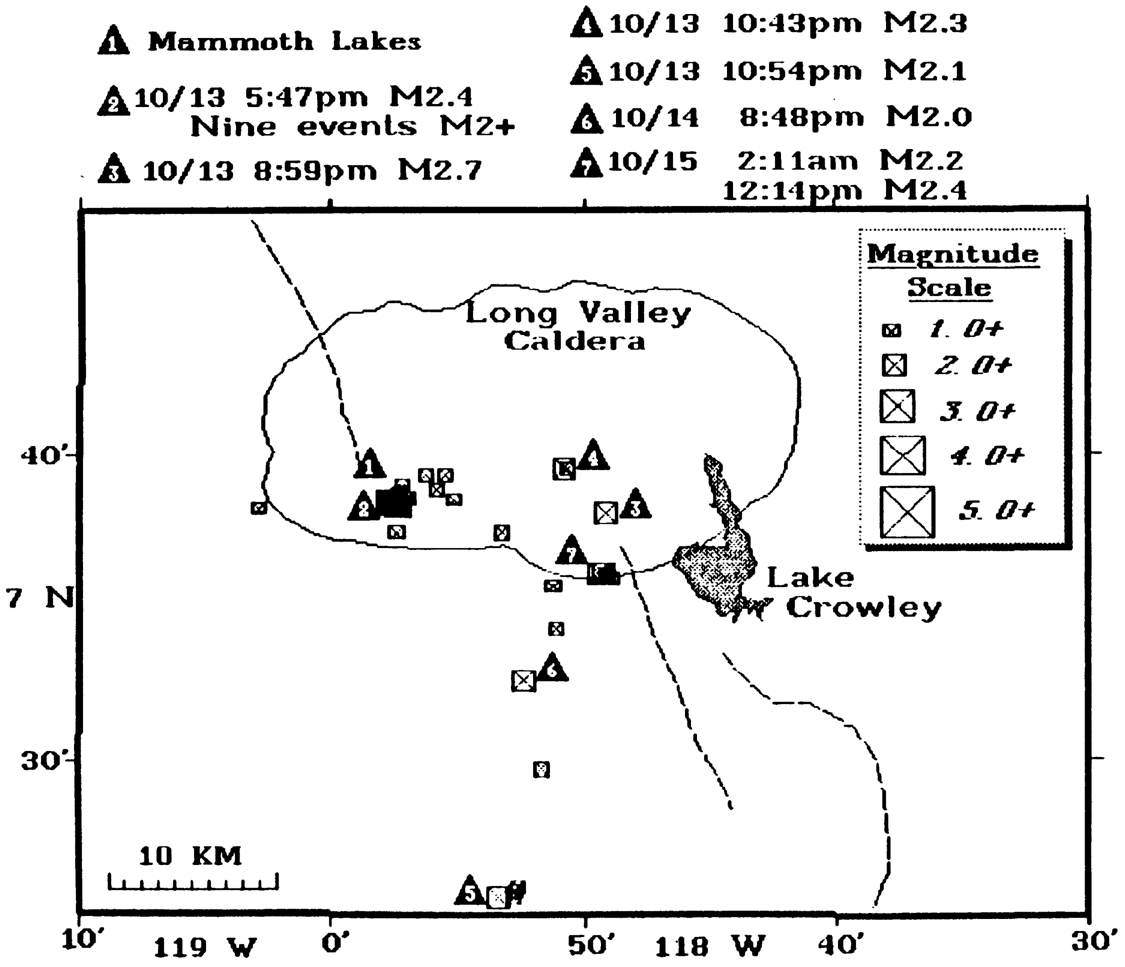
1 Mammoth Lakes
2 10/13 5:47pm M2.4
Nine events M2+
3 10/13 8:59pm M2.7
4 10/13 10:43pm M2.3
5 10/13 10:54pm M2.1
6 10/14 8:48pm M2.0
7 10/15 2:11am M2.2
12:14pm M2.4
Magnitude Scale
1.0+
2.0+
3.0+
4.0+
5.0+
Long Valley Caldera
Lake Crowley
10 KM
40'
7 N
30'
10'
119 W
0'
50'
118 W
40'
30'

FIGURE 3

SEISMIC WAVE MONITORING AT PARKFIELD, CALIFORNIA

14-08-0001-G1703

T.V. McEvilly, R. Clymer, T. Daley, B. Foxall, E. Karageorgi, A. Michelini
Seismographic Station, University of California, Berkeley, CA 94720
and
Earth Science Div, Lawrence Berkeley Lab, Berkeley, CA 94720

INTRODUCTION

Three programs of seismic wave measurements continue: Earthquake recording with the high-resolution seismic network (HRSN), begun in December, 1986; controlled-source monitoring with HRSN begun in June, 1987; and controlled-source experiments with the Varian well vertical array (VWVA), begun in November, 1987.

The HRSN (Figure 1) consists of ten, 3-component, borehole seismometers surrounding the 1966 Parkfield epicenter. Data-acquisition features digital telemetry with 125-Hz bandwidth and 16-bit resolution, and can operate in external-trigger *(i.e.,* controlled-source) or event-trigger (earthquake) modes.

The VWVA extends to 1400-m depth at a site 2 km from the San Andreas fault (Figure 1), close to the nucleation zone of the expected magnitude 6 Parkfield earthquake. While tests done shortly after installation indicated that the entire array was functioning, failure of deep connecting cables soon eliminated sensors below 968m. There is some indication of further degradation. The original November, 1987 survey results provide a 'benchmark' vertical seismic profile (VSP) using the full string, and have been published (Daley and McEvilly, 1990). The remaining instruments are adequate to proceed with all the proposed uses of the VWVA except the acoustic emission monitoring, as this array at the very bottom of the string was lost before any data were acquired. The array is recorded on a Sercel 338 96-channel reflection system.

INVESTIGATIONS

1) Earthquakes. Local microearthquakes of magnitude about -0.5 to about +2 are routinely recorded on scale. A 3-D velocity model and a high-precision relative hypocenter location procedure for clustered events with similar waveforms have been developed, which will allow high-resolution analysis of local earthquakes in this area (Michelini and McEvilly, 1991). The clusters are being studied for evidence of temporal changes in fault zone processes and properties, including anisotropy in cooperation with R. Aster of U.C. San Diego. Relocated events are being used to study failure processes, fault zone structure, and material properties within the Parkfield nucleation zone.

2) Controlled-source monitoring with HRSN. From June, 1987 through March 1990, the HRSN has been illuminated 29 times with S-waves of three polarizations at eight source positions throughout the study zone, using a shear-wave Vibroseis source, in an on-going monitoring program. The resulting data contain a temporal record of wave propagation characteristics throughout the nucleation zone. Albeit complexly encoded, the wave fields recorded contain the evidence for any nucleation-induced changes in velocities, attenuation or anisotropy, along with the ubiquitous seasonal effects of varying moisture content at the vibrator sites. Data reduction is accomplished at the University of California's Lawrence Berkeley Laboratory (LBL). A paper summarizing this study will be submitted in late 1990.

3) Controlled-source monitoring with VWVA. The VWVA data are a unique resource.

Analysis of local anisotropy and velocity structure using short-offset VSP's and 3-D generally anisotropic models is underway, the latter in cooperation with V. Cerveny, I. Psencik, and D. Gajewski. As part of this effort, an extensive multi-azimuth, multi-offset VSP survey has been conducted to extend the results of the more limited earlier study by Daley and McEvilly (1990).

Monitoring by occasional illumination of the VWVA from at least the four closest HRSN source sites plus an additional near-offset site has been integrated in a convenient manner into the routine HRSN data collection.

DATA COLLECTED

- Full-time, triggered recording of earthquakes has continued in the past six months. Event data are archived as IEEE-format binary files on 9-track tape with simple headers.
- Three vibrator data sets have been collected and the data reduced. Data after routine processing (edit, stack, correlation, gather by source site) are archived in SEGY format on 9-track tape.
- At VWVA, one monitoring data set was recorded in June.

RESULTS

1) *Earthquake studies:*.

- A paper on the 3-D modeling process and results has been accepted for publication by BSSA (Michelini and McEvilly, 1990), and is under final revision.
- Local Parkfield events have been picked and relocated with the 3-D model through September, 1990.
- In a major effort, we have defined, gathered, and archived clusters of events with similar waveforms. After relocating about 500 events through the 3-D model, spacial clustering analysis was accomplished with a commercial hierarchical clustering code (Becker and Chambers) using characteristic distances for cluster definition of 400-700 m. A visual search was then performed to identify clusters having characteristic waveforms. The result is 70-80 clusters defined within our network, with 2-18 events/cluster. About two-thirds of the total events are clustered. Many clusters span the three years of data collection.
- We have begun the automated picking of relative arrival times within clusters (using B. Foxall's cross-correlation, cross-coherence procedure), and high-precision relative relocation of events.
- We are working with Ivan Psencik of the Geophysical Institute, Prague on generalization of his 3-D dynamic ray tracing code to include vertical discontinuities. This will result in a major improvement of our ability to model the fault zone in Green's function studies.
- In the work with R. Aster, we are studying S-wave polarization variations within the clusters.

The archived clusters will be the basis for further studies:

- of rupture processes on small patches of the fault using either theoretical or empirical Green's functions (Foxall), and
- to search for temporal variations of fault-zone properties (Michelini).

2) *Controlled-source studies - HRSN.* The final working data sets for analysis are "time gathers": one source into one receiver gathered across calendar time, producing 720 files, each containing, at present, 29 similar traces. To analyze these gathers, methods have been developed to display waveform properties of windowed phases, of whole traces, and of entire time gathers. We have developed color-graphics displays of trace amplitude, frequency content, travel-time changes, and instantaneous trace attributes (signal strength and instantaneous frequency) and particle-motion parameters, and have been searching the data set for anomalous variations. Most displays to date show only seasonal variations. This effort is the subject of the paper to be submitted in late 1990.

The figures illustrate two examples of anomalous data of particular present interest.

- *Site 2 anomaly.* Several paths analyzed to date with the vibrator at site 2 - to MMN (NNW), to VCA (ESE), and to FRO (SSE) - show advances in travel time of 30-60 msec for a band of late phases, relative to an early measurement. Two other paths, 1-MMN (at 10-12 sec) and 4-VCA show similar but less pronounced effects. Figure 2 shows grey-scale displays of relative travel-time change (correlation lag) across time gathers in a moving window. The accompanying correlation function plots indicate data quality. The anomalies appear as dark zones at late times. Figure 3, showing windowed travel-time changes, shows that the advance does not appear on early arrivals, and is thus probably not a near-surface, seasonal effect as usually observed. Interestingly, path 2-SMN (NW) does *not* show an anomaly. Other paths examined (*e.g.*, 5-FRO and 2-SMN) do not show unusual variations.

In Figure 4, site 2 is shown with respect to the seismicity (relocated through the 3-D model). The cross-sections shown in Figure 4b indicate that the fault behaves differently in distinctly defined zones. In the vicinity of Middle Mountain, the segments of activity apparently dip to the southwest, possibly reflecting the bending of the fault, and events extend to 12-13 km depth. In the next zone to the south, the events are mainly clumped at 3-5 km depth. Fortuitously, site 2 lies on the boundary of these two zones, above the deeper events. The anomaly here at late travel times (possibly deeply backscattered returns) could indicate changes in material properties taking place at depth on the south edge of the preparation zone.

We are continuing to develop the data base necessary in the search for effects in more paths and source orientations. We hope to identify the wave types and ray paths with particle motion and frequency analyses.

- *Path 1-MMN P-wave anomaly.* Figure 5 shows relative window delays for several phases for path 1-MMN. All these phases show the same (seasonal) pattern through the April 1989 data, but beginning with the mid-June data (June 14, day 165), the P-arrivals become erratic with respect to the direct-S and the late (9-sec) arrival chosen, showing 35-40 msec oscillations. Perhaps coincidentally, a M3.7 earthquake occurred about 3 km southeast of site 1 on May 25 (day 145), between our April and June data points.

Two other experimenters observed interesting anomalies in slightly earlier time frames (both before the event). Park and Lee, 1990 of UC Riverside observed unusual resistivity anomalies, that they believe significant, from April 5-30 (days 95-120, or 40-25 days before the earthquake). These occurred on two dipoles extending from near EAD to the NW, straddling Middle Mountain (Site MMN). There was also an unusual tensor strain meter event at EAD and DonaLee (near JCN), from about March 20 to April 13, or days 79-103 (Gladwin, *et.al).*

3) Controlled-source studies - VWVA. The analysis of the initial VSP studies, showing up to 10% anisotropy in the vicinity of the well, has been published (Daley and McEvilly, 1990).

The recording system, on loan to LBL/UCB, was recalled by the owner in June, 1990. When the awaited Parkfield M6 event occurs, we will rent the system again for post-event acquisition.

Modeling of material properties using the multi-azimuth, multi-offset data set collected in December, 1989 has not yet begun.

References

Becker, Richard and John Chambers (1984). *S, An Interactive Environment for Data Analysis and Graphics,* Bell Telephone Labs.

Cerveny, V. (1985). The application of ray tracing to the propagation of shear waves in complex media, in *Seismic Shear Waves, Part A: Theory,* Gerhard P. Dohr, editor, Geophysical Press, London and Amsterdam, 1-124.

Gladwin, M.T., R. Hart and R. Gwyther (1989). Tensor strain in Parkfield, 1 January 1989 to 30 April 1989, in the Parkfield monthly data review for April 1989.

Park, Stephen and Tien Lee (1990). Electrical Properties, in the Parkfield monthly data review for September 1990 data, p 53.

Papers published or submitted

Daley, T.M., and T.V.McEvilly (1990). Shear Wave Anisotropy in the Parkfield Varian Well VSP, *Bull. Seis. Soc. Am.,* **80,** 857-869.

Michelini, A., and T.V.McEvilly (1991). Seismological studies at Parkfield: Simultaneous inversion for velocity structure and hypocenters using cubic B-splines parameterization, in press, *Bull. Seis. Soc. Am.*

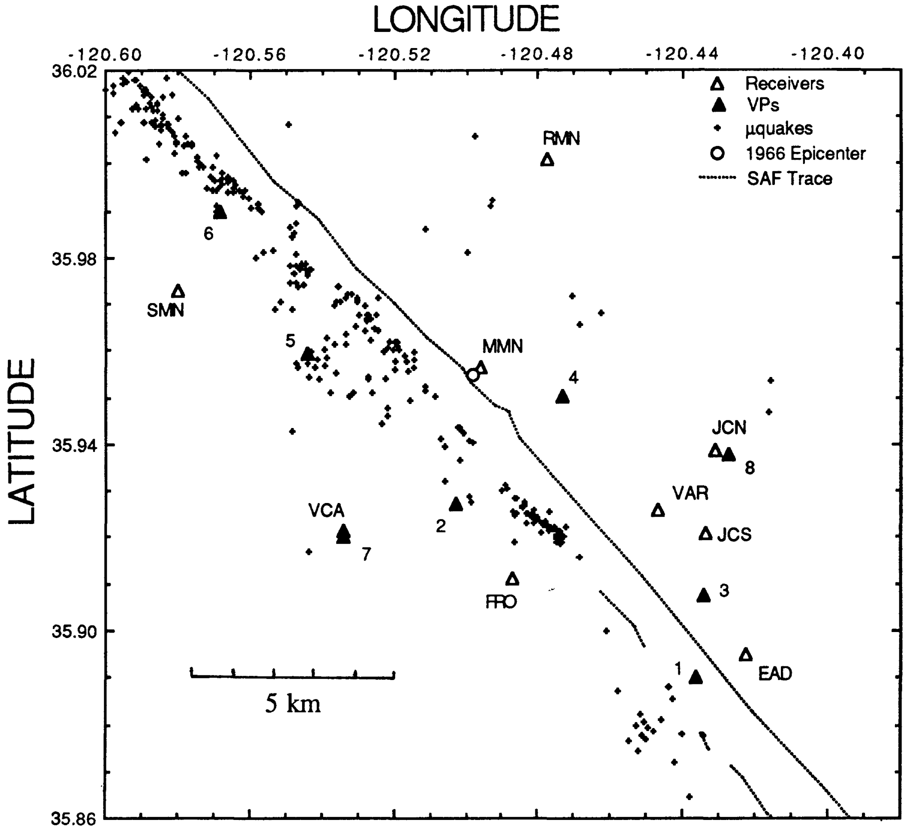

Figure 1. Parkfield location map, showing the High-Resolution Seismic Network (HSRN), controlled-source (vibrator) points, and 6/87-12/89 seismicity as relocated through the UCB 3-D velocity model.

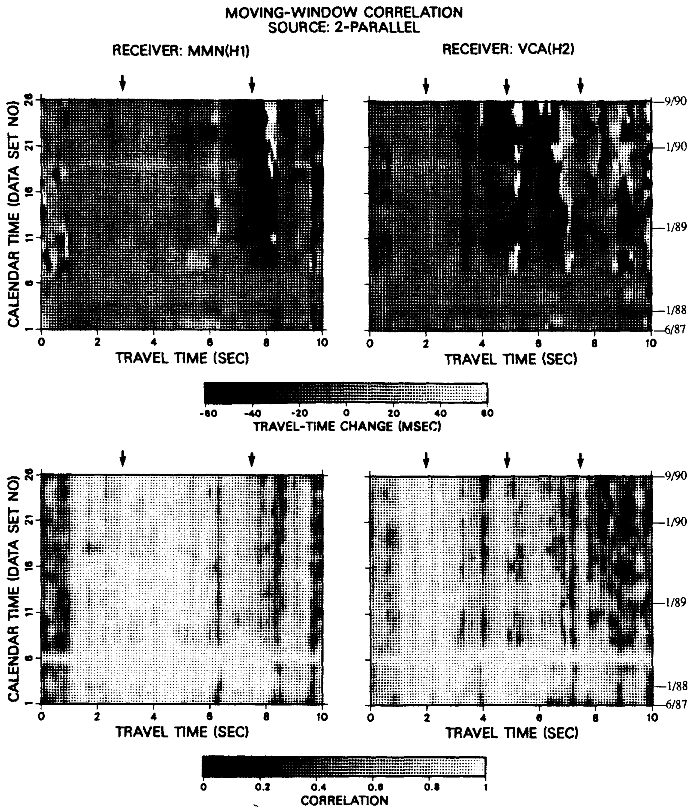

Figure 2. Upper: Travel-time change relative to data set 6 (April '88) by cross-correlation in a moving time window for two paths from source site 2. Note the late 30-60 msec advances (dark zones). Arrows indicate times of windowed phases in Figure 3. Lower: The correlation function gives an indication of the quality of the travel-time change calculations.

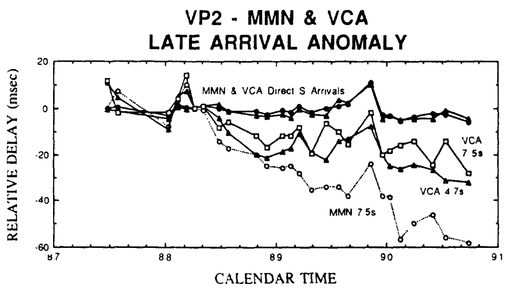

Figure 3. Travel-time change relative to data set 6 (April '88) of several windowed phases by a cross-correlation, cross-coherence technique (Foxall) on two paths from vibrator position 2. Window times are shown in Figure 2. Note the large variation in the late phases.

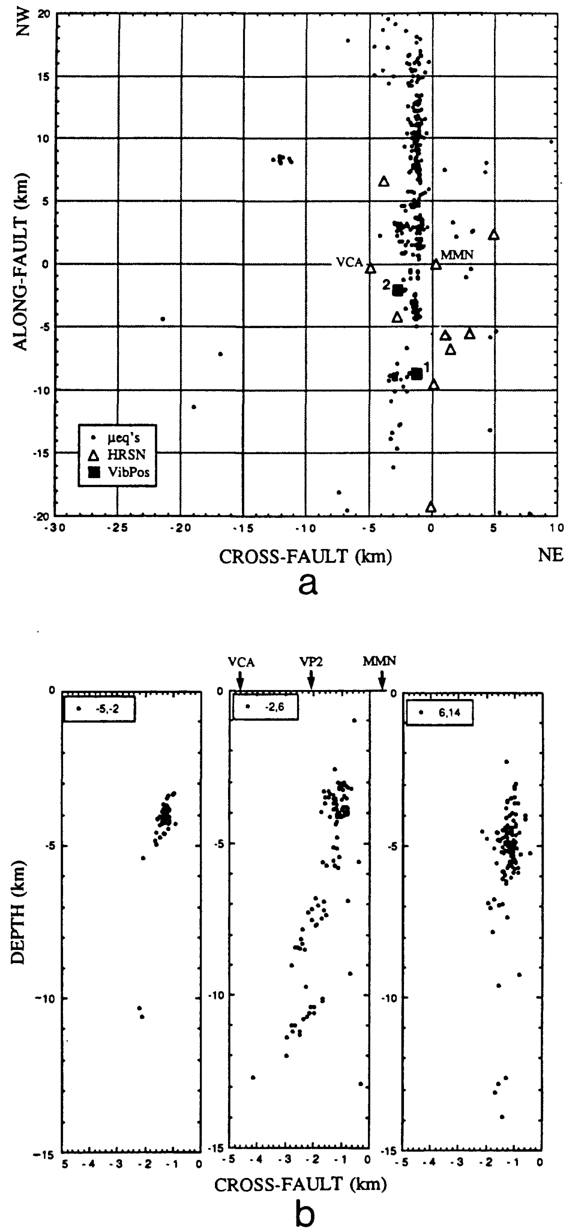

Figure 4. a. Plan view location map, oriented with the abscissa parallel to the San Andreas fault trace, and the origin of coordinates at the 1966 epicenter. Earthquakes (6/87-12/89) have been relocated through the 3-D model. b. Vertical cross-sections, with hypocenters from three bands along the fault, as indicated by the "along-fault" coordinates given in the inserts. The approximate projections of three sites are shown.

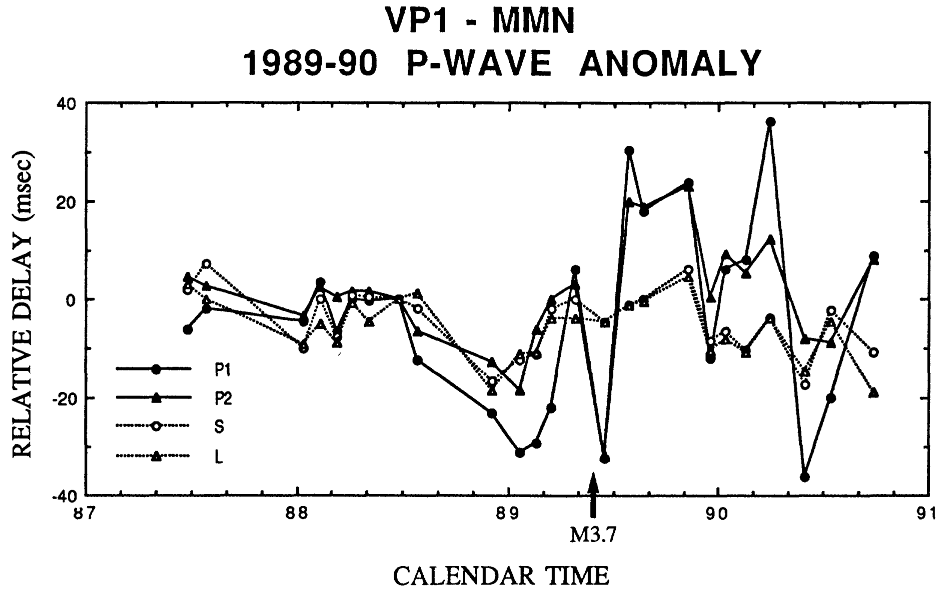

Figure 5. Travel-time change relative to data set 8 (June '88) of windowed phases on the path from vibrator position 1 to MMN. Phases P1 and P2 are the direct P-arrival picked on traces from both horizontal components, "S" is the direct shear-wave arrival, and "L" is a later phase at 9.0 sec. Note the erratic behavior of the P-arrival that first appears with the data point in mid-June, 1989. The arrow marks the time of a M3.7 event located approximately 3 km southeast of VP1 that occurred between the April and June 1989 measurements (see text).

Analysis of Crustal Deformation Along the Southernmost Segment of the San Andreas Fault System, Imperial Valley, California: Implications for Earthquake Prediction

14-08-0001-G1679

R.E. Reilinger
Earth Resources Laboratory
Dept. of Earth, Atmospheric, and Planetary Sciences
Massachusetts Institute of Technology
Cambridge, Massachusetts 02142
(617) 253-7860

INVESTIGATIONS

This project involves using geodetic observations in conjunction with other geophysical and geological information to investigate contemporary tectonic processes along the southernmost segment of the San Andreas fault system. Our primary efforts during the present contract period include:

1. Organizing and archiving GPS observations made in February/March 1990, and developing a uniform set of benchmark descriptions for all sites observed during this and previous surveys in the Salton Trough-Riverside County region.
2. Continuing analysis and interpretation of 1986, 1988 and 1989 GPS measurements in the Imperial Valley-Salton Trough with emphasis on regional strain accumulation and strain release associated with the 1987 Superstition Hills earthquakes.

RESULTS

1. From February 18 through March 9, 1990 a high precision GPS network was established along an approximately 400 km segment of the Pacific-North American plate boundary (Figure 1) from the Gulf of California in Northern Mexico to just south of the junction of the San Andreas and San Jacinto faults (~34°N). Participating institutions in the field campaign included: Caltech, CICESE, L-DGO, MIT, NGS, Riverside County, UNAVCO, U. of Mexico, U.T., Dallas, and U. of Nevada. A total of 103 primary stations were observed, most for 2 to 3 days. In addition half sessions (~3–4 hours) were observed at 31 sites near the San Andreas (Banning-Mission Creek segments), San Jacinto and Elsinor faults, and 5 sites were observed in a kinematic survey within a pre-existing EDM network straddling the Imperial fault in Northern Mexico (2 of these kinematic sites were also observed statically). Dense coverage (~5–10 km site spacing) was also established along the southernmost San Andreas and Imperial faults in S. California. Coverage extends to 150 km from the active fault systems.

   All data collected by university and Riverside County participants have been archived with the UNAVCO archiving facility under the direction of Dr. Judah Levine. UNAVCO is currently translating these Trimble data to RINEX format for distribution to participants in the Salton Trough- Riverside County experiment. In addition, descriptions are being generated in NGS format for all benchmarks in the STRC network. These descriptions will be made available to any interested group with the capability to respond in the event of an earthquake within the network.

2. Shawn Larsen has completed initial reduction of the 1988 and 1989 static GPS observations made with TI-4100 receivers using the Bernese 3 software at Caltech (reduction of 1989 Trimble data has been hampered by severe ionospheric disturbances during the campaign). Large station displacements between 1986 and 1988 are attributed to the November 24, 1987 Superstition Hills earthquake sequence. Displacements at 3 sites within 3 km of the surface rupture approach 0.5 m. Eight additional stations within 20 km of the seismic zone are displaced at least 10 cm. This is the first occurrence of a large earthquake (Ms 6.6) within a preexisting GPS network. Best-fitting uniform slip models of rectangular dislocations in an elastic half-space indicate 130 cm right-lateral displacement along the northwest-trending Superstition Hills fault and 30 cm left-lateral displacement along the conjugate northeast-trending Elmore Ranch fault. The geodetic moments are 9.4×10^{25} dyne-cm and 2.3×10^{25} dyne-cm for the Superstition Hills and Elmore Ranch faults respectively. Distributed slip solutions using Singular Value Decomposition suggest near uniform displacement along the Elmore Ranch fault and concentrated slip to the northwest and southwest along the Superstition Hills fault. A significant component of non-seismic secular displacement is observed across the Imperial Valley for the interval 1986-1988 which is attributed to plate-boundary deformation.

   To investigate strain accumulation across the Imperial Valley, station displacements are computed at 29 stations for the period 1986-1988 and 11 stations for the period 1988-1989. The earlier measurements indicate 5.9 ± 1.0 cm/yr right-lateral differential velocity across the Valley, although the data are strongly influenced by the Superstition Hills earthquake sequence. In addition, some measurements, especially those indicating large east-west displacements, are suspect for large errors (most likely in 1986 survey). The 1988-1989 GPS displacements are best modeled by 5.2 ± 0.9 cm/yr of plate boundary deformation, but rates calculated from conventional geodetic measurements (3.4 - 4.3 cm/yr) fit the GPS data nearly as well. There is evidence from GPS and VLBI observations that the present slip rate along the southern San Andreas fault is smaller than the long term geologic estimate, suggesting a lower earthquake potential than is currently assumed. Incorporation of the 1990 observations in this analysis should provide better resolution for strain accumulation across the valley as a whole as well as along individual faults.

PUBLICATIONS

Reilinger, R.E., J. Beavan, L. Gilbert, S. Larsen, K. Hudnut, C. Aiken, D. Ziegler, W. Strange, M. de la Fuente, J. Gonzalez, J. Stowell, W. Young, G. Doyle, G. Stayner, 1990 Salton Trough-Riverside County GPS Network, *EOS, Trans. Am. Geophys. Union, 71,* 477, 1990.

de la Fuente, M., J.J. Gonzalez, D. Ziegler, C. Aiken, The Northern Baja California GPS Campaign: First Epoch, *EOS, Trans. Am. Geophys. Union, 71,* 478, 1990.

Larsen, S., and R. Reilinger, Age constraints for the Present Fault Configuration in the Imperial Valley, California: Evidence for Northwestward Propagation of the Gulf of California Rift System, *J. Geophys. Res.*, submitted, 1990.

Larsen, S., R. Reilinger, H. Neugebauer, and W. Strange, GPS Measurements of Deformation Associated with the 1987 Superstition Hills Earthquakes, Imperial Valley, California, in preparation, 1990.

Larsen, S., and R. Reilinger, GPS Measurements of Strain Accumulation Across the Imperial Valley, California: 1986-1989, in preparation, 1990.

Larsen, S., Crustal Deformation in Southern California, Phd. Thesis, California Institute of Technology, Pasadena, California, 1990.

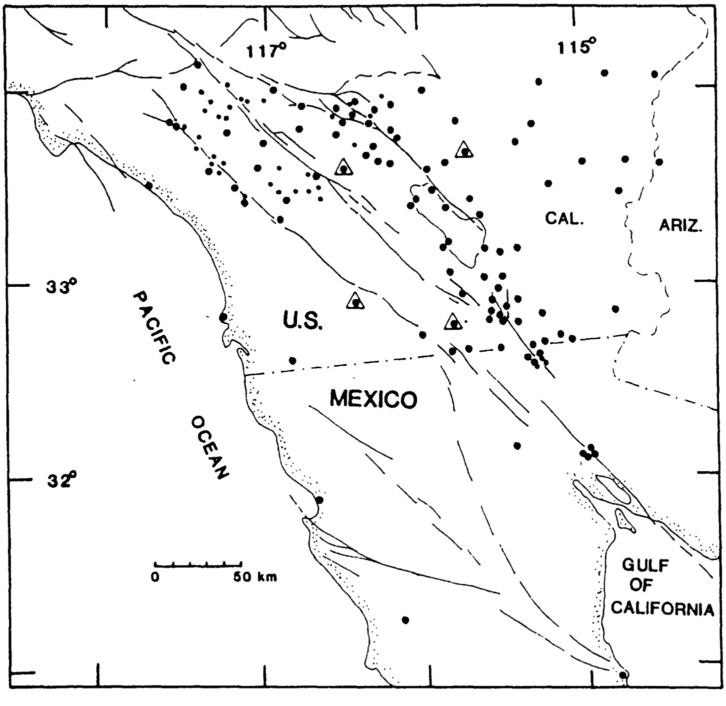

Figure 1. GPS stations observed during the 1990 Salton Trough-Riverside County campaign. Large dots show primary stations, small dots half-session and kinematic sites.

MECHANICS OF FAULTING AND FRACTURING

9960-02112

Paul Segall
Branch of Tectonophysics
U.S. Geological Survey
345 Middlefield Road, MS/977
Menlo Park, California 94025
(415) 329-4861

Investigations

1. Horizontal Deformation in the San Francisco Bay region (with Mike Lisowski).

2. Inverse theory for elastic dislocation models and analysis of crustal deformation around the San Andreas fault (with Mark V. Matthews).

Results

1. We compare the horizontal surface displacements in the Loma Prieta region that accompanied the great 1906 San Francisco earthquake with those occurring in the October 17, 1989 $M_s 7.1$ Loma Prieta earthquake. The 1906 displacements are determined from changes in horizontal angles and astronomic azimuths measured in the 1880's and again in 1906-7. In 1906 Loma Prieta, located in the middle of what was to become the rupture zone of the 1989 earthquake, was displaced one meter parallel to the trace of the San Andreas fault. This implies that the 1906 motion was nearly pure strike-slip, regardless of the dip of the fault plane. A joint solution for horizontal displacements during the 1989 Loma Prieta earthquake, determined from EDM, GPS, and VLBI measurements, shows that the displacement of Loma Prieta in 1989 involved subequal amounts of strike-slip and convergence. The surface displacements show that the 1906 earthquake was dominantly strike-slip, while the 1989 earthquake was highly oblique. If the two earthquakes occurred on the same fault plane, and the slip was in the direction of the resolved shear stress acting on the fault, then the shear stress would have had to have rotated significantly between the two earthquakes. If, on the other hand, the two earthquakes occurred on parallel faults with different dips, both events can be satisfied by a non-rotating stress state. Pre-1989 seismicity in the region outlines, albeit weakly, a vertical plane extending beneath the mapped trace of the San Andreas fault (Olson, 1990 GRL). Together the geodetic and seismic data are consistent with the 1906 earthquake occurring on a vertical fault and the 1989 earthquake on a southwest dipping fault. If correct, this conjecture has important implications for the evaluation of recurrence models and for present earthquake hazard.

2. We have been working to develop a theoretical foundation for inversion of crustal deformation measurements to estimate fault slip. Using elastic dislocation theory to derive

a "forward model" that describes deformation in terms of fault slip, we propose to handle the nonuniqueness inherent in the inverse problem of estimating slip from a small set of deformation measurements by finding slip estimates that minimize relevant measures of energy and stress concentration. In particular, we have sought estimates that minimize the most natural physical criterion: *stored elastic strain energy.* In the abstract context of elastic dislocation models, crustal deformation measurements are linear functionals of fault slip, usually expressed as "weighted averages" of slip, and often contaminated with nonnegligble measurement error. We have solved the energy minimization problem for functionals given by weighted averages in terms of the *traction-matching condition* (TMC). Let $\tau(\cdot; s)$ be the change in fault-surface traction accompanying slip, s. The TMC says that the slip distribution producing least elastic strain energy subject to a constraint of the form

$$\int_{\Sigma_0} s(\xi)w(\xi)d\Sigma(\xi) = c$$

is proportional to the slip distribution, W^* satisfying the traction-matching equation (TME): $\tau(\xi; W^*) = w(\xi), \quad \forall\xi \in \Sigma_0$. The TMC shows, for instance, that the least potential energy subject to a constraint on the *moment* of a slip distribution is given by the crack-like slip distribution with constant traction on the slipping part of the fault. For nonconstant weight functions, we must generally solve the TME numerically for the unknown, W^*.

We have found the criterion of minimum potential energy to be useful but not entirely satisfactory. We have demonstrated that potential energy bounds in dislocation models *impose no restriction on pointwise behavior of slip distributions.* An explanation for this undesirable property lies in the fact that a distribution with small elastic strain energy may have locally large stresses that exceed yield strength and give rise to significant plastic yielding. Thus, elastic energy may be a poor approximation of the total work required to achieve a given state of slip and deformation. In order to rectify this shortcoming, we have proposed to constrain local stress concentration as well as strain energy. We acheive this aim by defining a quadratic functional by

$$L(s) = \int [\tau(\xi; s)]^2 d\Sigma(\xi).$$

We may view $L(s)$, appropriately normalized, as a measure of *local energy* required to maintain a state of slip s. We have shown that $L(s)$ is proportional to the integrated,squared derivative of slip, and have thus been able to use the reproducing kernel structure of the Hilbert space of functions with square integrable first derivative to find slip estimates minimizing $L(s)$ subject to linear constraints.

Our application of the theory we've developed to date has been limited to a simple anti-plane slip model for coseismic deformation in the rupture zone of the 1906 San Francisco earthquake. We have inverted angle changes in a triangulation network in the vicinity of Point Arena, CA surveyed in 1891 and in 1907. Figures 2. a.-c. shows two sets of *basis functions* that form fundamental components of the slip estimate. These basis functions minimize the *self energy* (solid) and *local energy* (dashed) for fault-parallel antiplane displacement of the stations listed. In Figure 2. d., we show the basis function for the change in the angle from LANE to SHOEMAKER to SPUR. All basis functions in these figures were calculated assuming a faulting depth of 10 km. Though there are thirty data measured in this survey, our calculations show that there are only 9 linearly independent observations when we minimize global strain energy, and only 5 when we minimize local energy. Orthogonal basis functions spanning these 9 and 5 directions are shown, respectively, in Figures 3 and 4. Figure 5 shows two estimates of slip obtained by appropriate combination of the basis functions shown in Figures 3 and 4. Both estimates agree well with the observed coseismic surface offsets of about 5 m in the vicinity of Point Arena.

Reports

Segall, P., and M. Lisowski, Comparison of surface displacements in the 1906 San Francisco and 1989 Loma Prieta earthquakes, **Science** submitted, 1990.

Segall, P., and D. Richards, Displacements in the San Francisco Bay Area, California due to the 1906 earthquake, **EOS**, v. 71, n. 17, pp. 554, 1990.

Matthews, M.V. and P. Segall, Minimum strain energy inversions for fault slip, **EOS**, v. 71, n. 17, pp. 631, 1990.

Kronenberg, A.K., P. Segall, and G. Wolfe, Hydrolitic weakening and penetrative deformation within a natural shear zone, in Brittle-Ductile Transition in Rocks, the Heard Volume, Duba, A.G., W.B. Durham, J.W. Handin, and H.F. Wang eds, A.G.U. Geophysical Monograph 56, pp. 21–56, 1990.

II.2
Figure 1

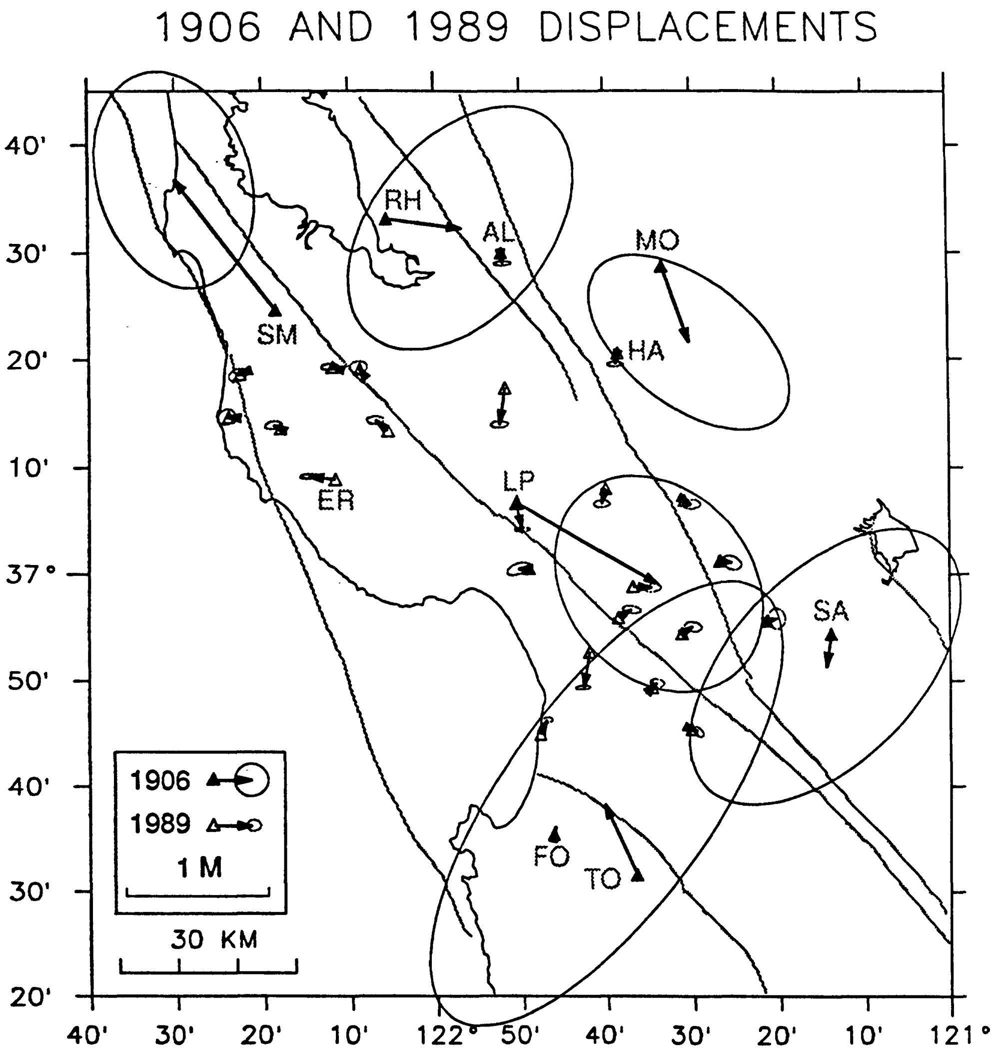

Figure ~~2~~ 1. 1989 Loma Prieta earthquake displacements (small error ellipses) compared to 1880's to 1906-7 displacements (large error ellipses). The 1989 displacements are from a joint solution using currently available electronic distance measurements (EDM), Global Positioning System (GPS) and Very Long Baseline Interferometry (VLBI) vectors. SM: Sierra Morena, RH: Red Hill, AL: Allison, MO: Mocho, HA: Mt. Hamilton, LP: Loma Prieta, ER: Eagle Rock, SA: Santa Ana, FO: Fort Ord, TO: Mt. Toro.

Figure 2

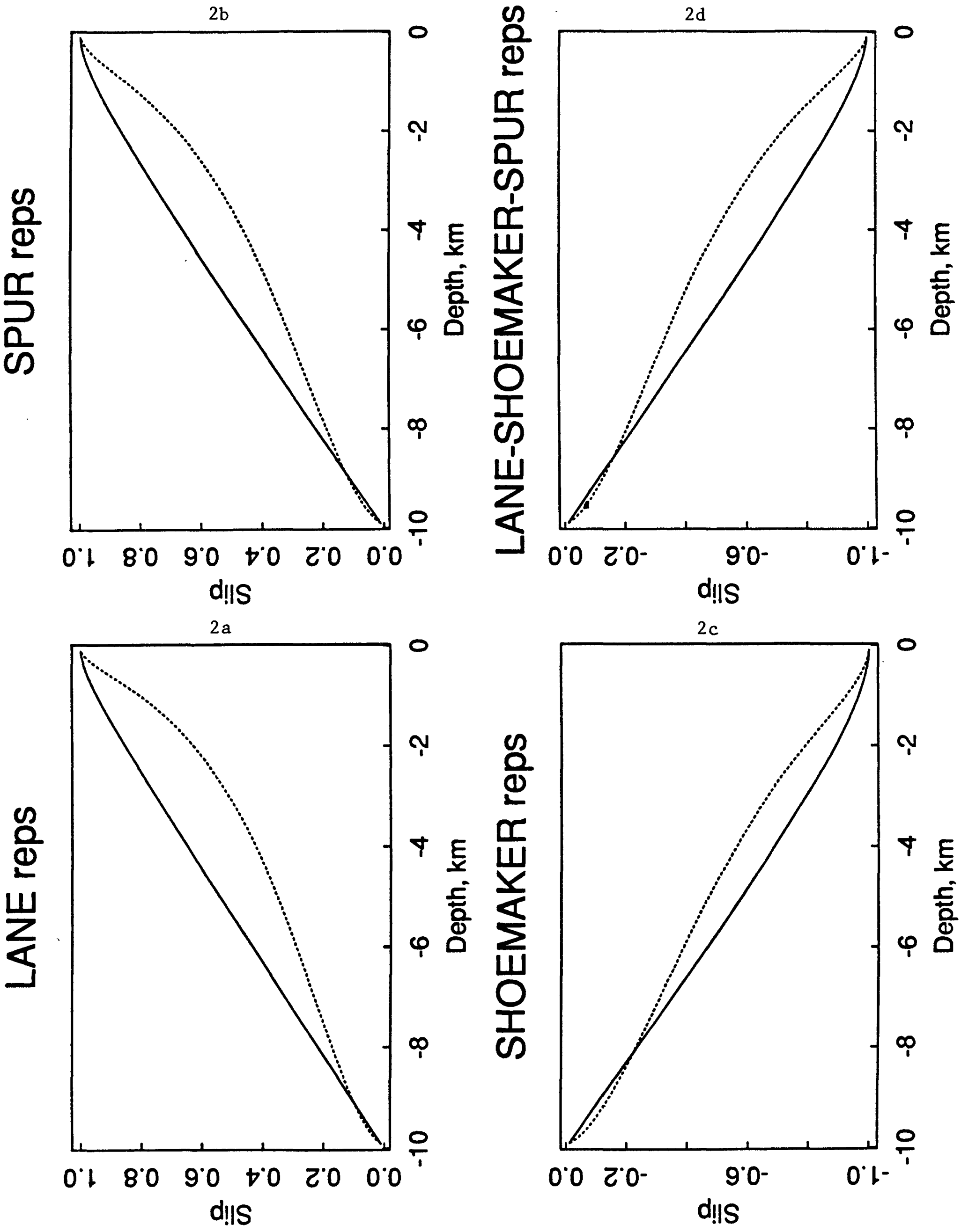
2a
LANE reps
2b
SPUR reps
2c
SHOEMAKER reps
2d
LANE-SHOEMAKER-SPUR reps
Slip
Depth, km
0
-2
-4
-6
-8
-10
0.0
0.2
0.4
0.6
0.8
1.0
-0.2
-0.6
-1.0

Figure 3

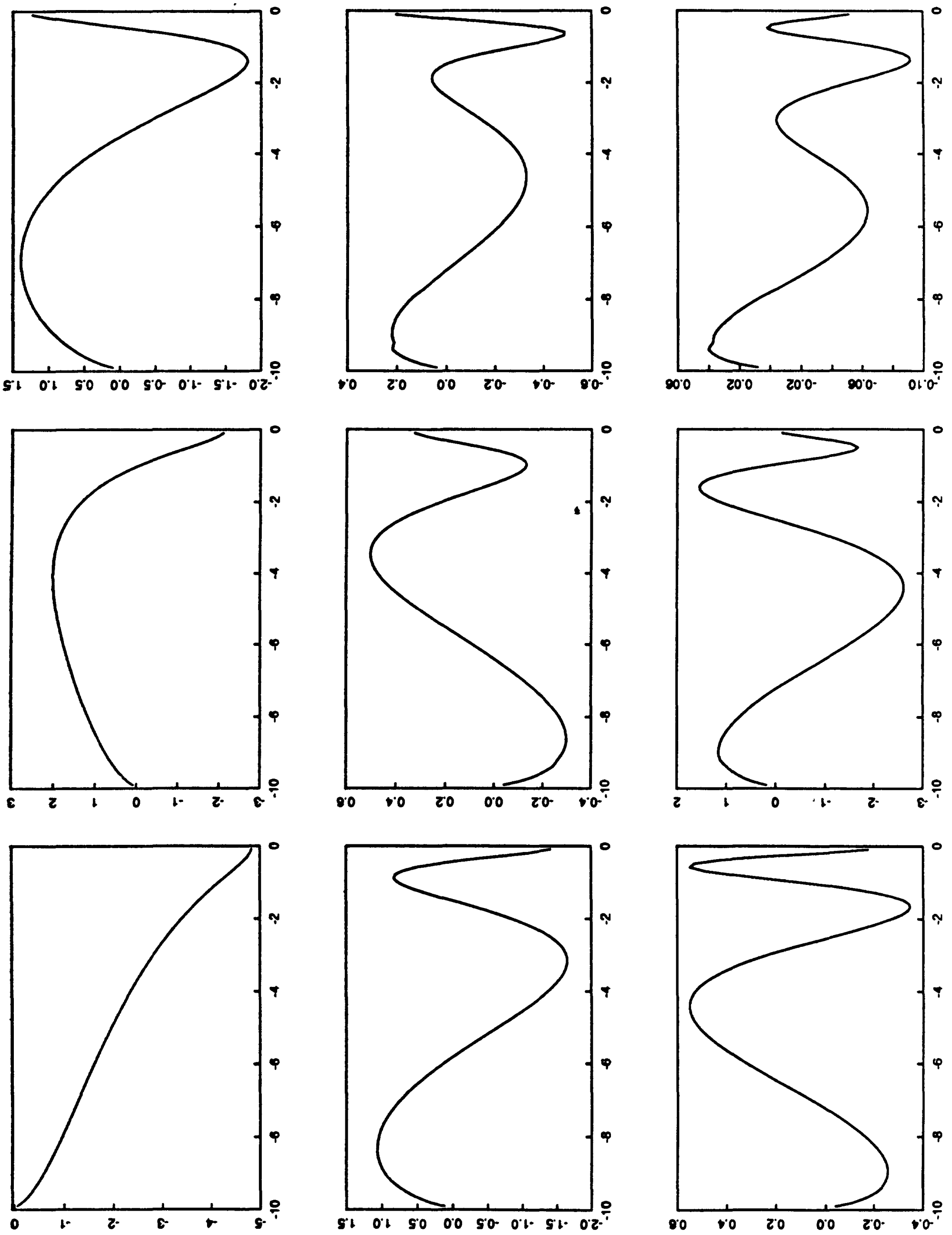
0
-2
-4
-6
-8
-10
-2.0 -1.5 -1.0 -0.5 0.0 0.5 1.0 1.5
-0.6 -0.4 -0.2 0.0 0.2 0.4
-0.10 -0.06 -0.02 0.02 0.06
-3 -2 -1 0 1 2 3
-0.4 -0.2 0.0 0.2 0.4 0.6
-3 -2 -1 0 1 2
-5 -4 -3 -2 -1 0
-2.0 -1.5 -1.0 -0.5 0.0 0.5 1.0 1.5
-0.4 -0.2 0.0 0.2 0.4 0.6

II.2
Figure 4

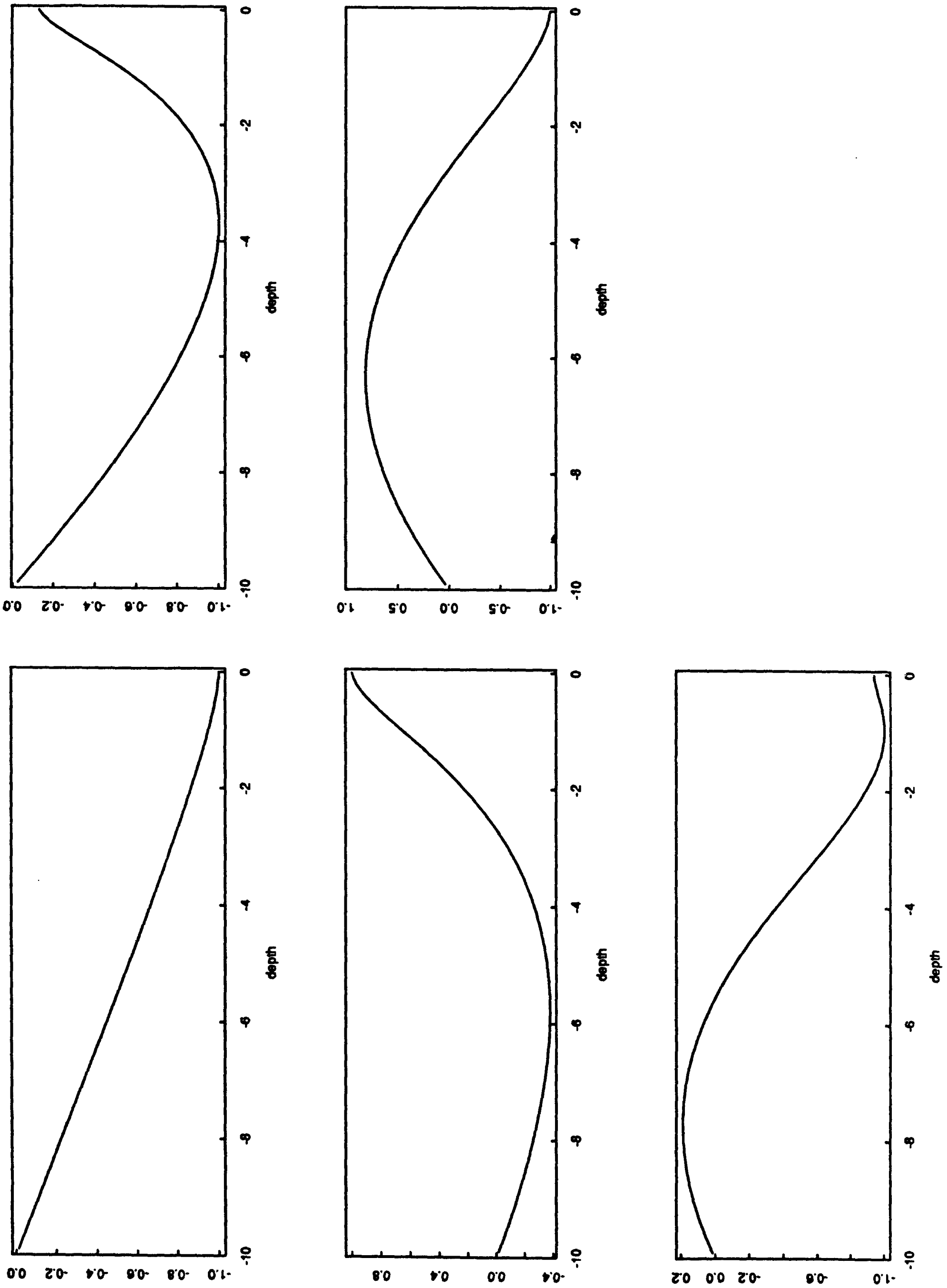
0
-2
-4
-6
-8
-10
depth
0.0
-0.2
-0.4
-0.6
-0.8
-1.0
1.0
0.5
0.0
-0.5
-1.0
0.8
0.4
0.0
-0.4
0.2
0.0
-0.2
-0.6
-1.0

II.2
Figure 5

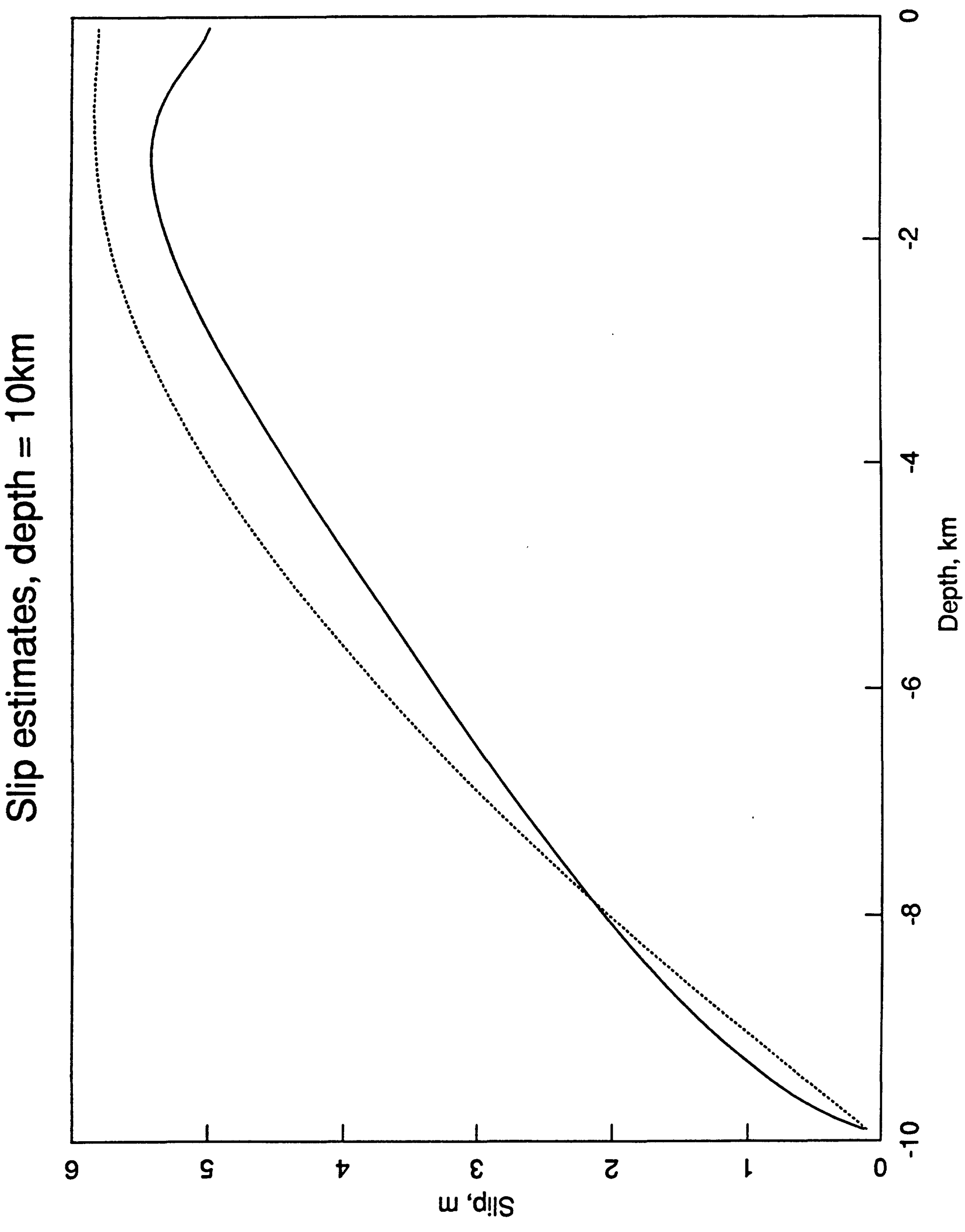

Geodetic Measurement of Coseismic Slip and Block Rotation in Southern California

Contract # 14-08-0001-G1805

Kerry E. Sieh and Kenneth W. Hudnut

Seismological Laboratory
California Institute of Technology
Pasadena, California 91125
(818) 356-6937 // hudnut@seismo.gps.caltech.edu

This project is primarily a data collection effort, the short-term aim being to increase the density of geodetic monumentation and measurement along the southern San Andreas fault. Longer-term goals are to accomplish this along other segments of faults in southern California as well, and to initiate a study of block rotation in the Salton Trough. We primarily utilize Global Positioning System (GPS) technology to perform high-accuracy surveys of relatively dense survey networks across active faults and folds. Beginning in 1991, this project will be merged with our Creep and Strain project and the Los Angeles Basin GPS project.

This project's funding began in February 1990. The first work accomplished with these funds was a cooperative survey from the Mexico/United States border through the Coachella Valley and throughout Riverside County. This project involved a large group, organized primarily by Rob Reilinger of MIT. Caltech's participation in this survey involved site selection and reponsibility for adding eleven new stations to the network in the Coachella Valley. The second project undertaken with these funds was a kinematic GPS survey of the UCSB monument array at Painted Canyon, combined with static measurements between this array, the Durmid Hill array (done by kinematic GPS in Dec. '89), and the fiducial station at Black Butte. These projects are described in our previous semi-annual report.

This report briefly describes work accomplished in the past six months on this project. Note that field work in the Coachella Valley becomes difficult in the summer months because of the intense heat during the day. Also, the ideal GPS satellite window has only recently begun to return to night-time here in California. Because of increased ionosphere activity during daylight hours, it is thought to be preferable to do GPS surveying at night. For these reasons, we loaned our receivers to UNAVCO for the three summer months. We are now, in early October, gearing up for this year's major field season in the Coachella Valley and Los Angeles region.

During the past few months, management and archiving of our data collected to date has been accomplished. We have also done preliminary processing of all our data with the Trimvec software. For the Los Angeles Basin study, data from the NGS data center have been obtained for the 1933 and 1979 surveys, and inverses from eccentric stations have been performed where needed. A preliminary report will be given by Hudnut et al. at the Fall 1990 meeting of the AGU, comparing these earlier surveys to the 1990 GPS survey.

The first data collection effort over the summer months was a collaborative GPS field project with Geoff Blewitt and Ken Hurst of the Jet Propulsion Laboratory (JPL). We reoccupied the Loma Prieta network and improved tie-ins to the USGS network of GPS stations there. This work was a further test of the Rapid Static Surveying technique developed at JPL, and provides the third set of measurements on this network since the Loma Prieta earthquake. Results from this third survey will reported by Hurst et al. at the Fall 1990 meeting of the AGU.

Second, during the month of September, our two GPS receivers were deployed for 19 consecutive days on the baseline between JPL and a new station atop the Palos Verdes

Peninsula. This was done to test the feasibilty of intermittent monitoring to study daily variations in apparent position, and to see whether errors can be substantially reduced by repeated measurement. Our goal in this work is to efficiently monitor long-term deformation at higher than usual GPS accuracies, utilizing precise (meter-level or better) orbits from the Permanent GPS Geodetic Array (PGGA) and >10 consecutive days' data. This approach will be taken in the Los Angeles Basin and elsewhere (e.g., the Coachella Valley) using GPS receivers as they are available.

Third, and perhaps most important, is our ongoing work in the Coachella Valley area along the southern San Andreas fault. During the past two weeks, we installed three arrays across the fault. Each array is framed by of two or more existing monuments that Caltech helped establish as part of the main GPS network in February 1990 with the Salton Trough - Riverside County (STRC90) Campaign. We have added about ten new monuments in each array, some of which are pre-existing monuments, but most of which were newly set by Caltech with a gas-powered hammering drill. A total of about 20 new monuments were set during September 1990. We are collaborating during Oct. 1990 with Riverside County Flood Control District (RCFCD) to survey in the positions of all these monuments using high accuracy static GPS measurement techniques. RCFCD is providing 6 experienced GPS surveyors, as well as 4-WD vehicles, to support this field work.

Our new arrays cross the San Andreas fault zone at three locations: 1) at Indio the array is a set of nested large quadrilateral figures (tied in to our near-fault total station geodetic figure at the Indio trenching site), 2) at Thousand Palms Canyon, the array crosses both main strands of the fault zone along a single profile, providing relatively dense GPS coverage, and 3) along Indian Avenue, a main north-south road from Palm Springs up to Morongo Valley, complementing the USGS small trilateration networks there.

Incidentally, RCFCD will also install a high-accuracy 30-station grid on a 100 sq. mile area in Palm Springs for one of their GPS-controlled mapping projects, and will make these data available to us. This grid will form a useful array for relatively detailed study of off-fault strain, and we plan to incorporate these data into our own data processing and archives. Furthermore, RCFCD will survey a quadrilateral array spanning the Elsinore fault with GPS and provide these data to us as well. They will be following our field procedures for primary stations on these projects of their own, which should assure high data quality.

Anticipated work during October and November 1990 will primarily involve our GPS surveying of the three new Coachella Valley arrays. Once this is accomplished, we plan to resurvey our array across highway 46, southeast of Parkfield. This array, surveyed by static and kinematic GPS in Dec. 1989, will be reoccupied in early November and tied in to the GPS monument installed by Caltech on Carr Hill in Parkfield. This work will be in collaboration with Mike Jackson and Yehuda Bock and will involve a mixture of static and kinematic GPS.

We will also be continuing to implement new releases of GPS processing software at Caltech, specifically for processing our Trimble data. Our goal is to replace routine processing of the data by Trimvec with software capable of attaining higher accuracy results. This includes the aim of rapidly and routinely achieving such results while in the field by obtaining precise orbits from the PGGA via modem and processing the data with our GRiD 386 and Macintosh SE/30 personal computers.

Low Frequency Data Network

Semi-Annual Report

S. Silverman, K. Breckenridge, J. Herriot
Branch of Tectonophysics
U. S. Geological Survey
Menlo Park, California 94025
415/329-4862
October 9, 1990

9960-01189

Investigations

[1] Real-time monitoring, analysis, and interpretation of strain, creep, magnetic, tilt and other low frequency data within the San Andreas fault system and other areas for the purpose of understanding and anticipating crustal deformation and failure.

[2] Enhancements to satellite-based telemetry system for reliable real-time reporting and archiving of crustal deformation data.

[3] Development and implementation of backup capablities for low frequency data collection systems.

[4] Specialized monitoring, including automated alerts, and display of data relevant to the Parkfield region.

Results

[1] Data from low frequency instruments in Southern and Central California have been collected and archived using the Low Frequency Data System. In the six months over over eight million measurements from over 100 satellite platforms have been received via satellite telemetry and subsequently archived by Low Frequency Network computers for analysis.

[2] The project has operated a configuration of an Integrated Solutions (ISI) V24S computer running under the UNIX operating system, with another ISI serving as data storgage backup. In addition, after the Loma Prieta earthquake, a Sun 3/280 was also used as a backup for the collection and storage of low frequency data. This backup was added due to the importance of maintaining operations and problems with maintenance of the ISI systems. Data from the Network are available to investigators in real-time and software for data display and analysis is readily available. Tectonic events, such as creep along the fault, can be monitored while still in progress. Also, periodic reports are produced which display data collected from various groups of instrumentation.

[3] The project continues to use a five meter satellite receiver dish installed in Menlo Park for retrieval of real-time surface deformation data from California and South Pacific islands. The GOES geostationary satellite together with transmit and receive stations make possible a reliable realtime telemetry system. Further expansion of the number of platforms monitored is ongoing.

[4] The project continues to take an active part in the Parkfield Prediction activities. Software has been written to provide scientists with automated alerts for signals which may indicate

anomolous tectonic activity. Kate Breckenridge is the monitor for Parkfield creep events, which includes contact via paging system during periods of increased activity. Stan Silverman is the alternate monitor for Parkfield strainmeter data, which also includes contact via paging system for alerts. Also, data collection and computer operations are automatically monitored for abnormal activity and project members are paged for in the event of problems with either.

[5] The project has continued to provide real-time monitoring of designated suites of instruments in particular geographical areas. Terminals are dedicated to real-time color graphics displays of seismic data plotted in map view or low frequency data plotted as a time series. During periods of high seismicity these displays are particularly helpful in watching seismic trends. The system is used in an ongoing basis to monitor seismicity and crustral deformation in Central California and in special areas of interest.

[6] A new computer system based on a Sun Sparcstation 1+ has been ordered to begin relieving the ISI system of primary data collection and analysis functions. The system will provide increased disk storage and industry standard hardware and software for reliability. The new system should be operational by January, 1991.

Parkfield Area Tectonic Framework

9910-04101

John D. Sims
Branch of Engineering Seismology and Geology
U.S. Geological Survey
345 Middlefield Road, MS 977
Menlo Park, California 94025
(415) 329-5653

Investigations

1. Field investigations of late Holocene and historic slip rates in the Parkfield and Carrizo Plain segments of the San Andreas fault.
2. Post-earthquake investigations of the 1989 Loma Prieta, California earthquake.
3. Field investigations of structural and stratigraphic relationships between late Cenozoic sedimentary units and underlying Franciscan and granitic basement in central California with emphasis on the Parkfield-Cholame area.

Results

1. We excavated 8 additional trenches (~125 m total length) at the Phelan Ranch site on the Carrizo Plain in May 1990. This phase of the study extended the search for more offsets, evidence of individual events, and additional study of the process of stream abandonment at the Phelan Site. The fault trace at the site is easily identified by geomorphic features. The trace is characterized by a pair of offset modern streams, an older abandoned and infilled stream channel, a graben, and a pair of beheaded streams. Off-sets of the modern streams measured by high precision surveys of their thalwegs show similar total offsets. The thalweg of the SE larger stream is offset 17.4 ± 1.6 m, and the offset of the NW smaller stream is 15.8 ± 0.6 m. In May our studies focused on the graben that lies across the right step-over in the San Andreas fault.

   Pull-apart basins on dextral strike-slip faults are associated with right step-overs that form tensional substructures. Excavations of the San Andreas fault (SAF) on the Carrizo Plain, central California reveal details of the development of a small pull-apart basin controlled by an en echelon right stepover of the SAF and subsequent filling of the depression with Holocene sediments. Juxtaposition of modern topographic features by right slip on the west trace of the SAF enhances the basin and its bounding fault scarps. Our excavations show that several en echelon strike-slip cross-faults transfer slip across the basin. Some of these cross-faults also show the usual paired normal and reverse faults seen on simpler strike slip faults.

   The step-over zone in which we excavated trenches reveals en echelon cross-faults whose aggregate displacement sums to about the total displacement of the SAF in this area. Our trenches reveal that as movement proceeds on the SAF zone new en echelon cross-faults are formed near the southeast end of the stepover and older ones are abandoned near the northwest end of the stepover. The excavations also show that at the NW end of the basin the west trace of the SAF dies out leaving an inactive extension to the NW. Slip is transferred by en echelon cross-faults to the east trace as the west trace dies out. The east trace of the SAF consequently shows increased displacement to the NW as the en echelon cross-faults release slip to it. The structural details seen in our excavations are similar to the model of basin development by en echelon strike-slip faults proposed by Rodgers (1980). However, the features in our excavations are more complex than those proposed by Rodgers and are probably better approximated by the non-constant offset model of Chinnery and Petrak (1968).

2. Following the 17 October 1989 Loma Prieta earthquake I began a project to study earthquake-induced liquefaction structures caused by the 1906 San Francisco earthquake, and the 1989 Loma Prieta earthquake and its April 1990 aftershock. The 1989 and 1990 events formed compound sandblows in sediments of Soda Lake near Watsonville, California. The objective of the project is to investigate areas that liquefied in response to shaking by the 1906 and 1989 earthquakes. I will compare relationships between structures formed in the 1906 and 1989 earthquakes and structures formed in Soda Lake by the 1989 Loma Preita earthquake and its 1990 aftershock.

   The study is intended to develop criteria for interpreting records of paleoliquefaction used for determining paleoseismic histories. There is no generally recognized set of criteria used to establish the completeness of a paleoliquefaction record. Few studies treat the problems of recognition and classification of liquefaction structures, and development of local recurrence intervals from evidence of paleoliquefaction (Sims, 1978a, 1978b). Accurate interpretation of liquefaction-induced deformation requires detailed examination and characterization of multiple liquefaction events of varying ages at a single site. Once characterized, criteria for the recognition, classification, and genesis of complex liquefaction structures can be developed. From these criteria complex cross-cutting relationships and the influence of other geological processes can be better understood. Most critical is to develop the ability to separate earthquake-induced structures from similar structures formed by other geologic processes. The relationships between liquefaction structures formed in 1989, 1906, and earlier can be used as a model of the relationships between multiple structures separated by long time intervals. Similarly, the structures formed in Soda Lake can be used as a model for structures separated by small time intervals. Thus, this work can form the basis, using physical relationships, for improving and expanding the interpretation of earthquake recurrence interval.

   Liquefaction induced by the Loma Prieta earthquake provides an excellent opportunity to study sediments affected by liquefaction. The Loma Prieta earthquake induced liquefaction in various types of sediments at numerous locations. Most importantly some of the largest aftershocks caused repeated liquefaction at some sites in the greater San Francisco Bay area. One of the sites, Soda Lake near Watsonville, Calif., reveals a rich record of multiple liquefaction events associated with the October main shock and a M 5.5 aftershock (Sims and Garvin, in prep.).

Soda Lake is a now inactive settling basin constructed in an abandoned meander loop of the Pajaro River near Watsonville, Calif. for the nearby Granite Rock Quarry (Fig. 1). The sediments in the basin are about 10 to 12 meters thick. The sediments accumulated in the last 30 to 40 years. These sediments were affected by two liquefaction events. The events, the 18 October 1989, M 7.1 Loma Prieta main shock and the 18 April 1990, M 5.5 aftershock, produced numerous fissures and sandblows. Sandblows that erupted during the 1989 main shock were easily distinguished from the sandblows erupted in the 1990 aftershock and the two generations were mapped. Excavations in the sediments of Soda Lake reveal a detailed stratigraphy through which numerous sand blows erupted. Vertical serial cross-sections of the excavated sandblows show they developed episodically. Two generations of surface cone and feeder dike features are easily defined (Sims and Garvin, in prep.). My investigations are the first to describe the morphology and sedimentary relationships of liquefaction structures at sites that experienced multiple liquefaction events. My investigation of the two liquefaction episodes and their compound structures illustrates the possible confusion that may occur if one is not aware of the physical relationships present in complex associations of liquefaction structures of variably differing ages. Other complexities can also be visualized; such as crosscutting of liquefaction features and their modification by fluvial, soil formation, and biological processes. These interactions must be understood before accurate assessments of paleoliquefaction events can be used to interpret paleoseismic history.

3. Geologic mapping of the Stockdale Mountain and Orchard Peak 7½-minute quadrangles is in progress. The Stockdale Mountain Quadrangle is about 60 percent complete and the Orchard Peak Quadrangle is about 40 percent complete.

4. A network of surveyed quadrilaterals, established on the San Andreas, White Canyon, Red Hills, Gold Hill, and Gillis Canyon faults in the Parkfield-Cholame area, totals 19 quadrilaterals. Fifteen quadrilaterals lie across the San Andreas, 2 on the White Canyon, and one each on the Red Hills and Gold Hill faults. These quadrilaterals are resurveyed every 2 months to gain background information on the sites prior to the next Parkfield earthquake.

Reports

Sims, J.D., Ito, Tanio, and Garvin, C.D., 1990, Holocene deposits in a right step-over on the San Andreas fault as a model for the development and propagation of strike-slip pull-apart basins: American Geophysical Union Transactions, EOS, v. , p. .

15 October 1990

Semi-Annual Technical Report XXXI

Modeling and Monitoring Crustal Deformation
9960-01488

Ross S. Stein, Wayne Thatcher, and Grant Marshall
Office of Earthquakes, Volcanoes, and Engineering
345 Middlefield Road, MS 977
Menlo Park, California 94025

415/329-4840, FTS 459-4840

INVESTIGATIONS.

Observed Vertical Deformation Associated With the Loma Prieta Earthquake. Coseismic elevation changes calculated from leveling observations are in qualitative agreement with the predicted vertical deformation computed with the fault model of *Lisowski et al.* [GRL, 1990]. Along the coastline, coseismic displacements are similar in shape to uplifted marine terrace profiles, a relationship predicted by *Anderson* [Science, 1990] and *Valensise & Ward* [Nature, 1990]. Anomalous deformation occurs where level routes cross the Sargent and San Andreas faults and where these crossings are correlated with shallow aftershock activity. Preseismic leveling surveys date from 1953 to 1989 and differ in quality from first to third order. Following the earthquake the National Geodetic Survey releveled 450 km of the survey routes in cooperation with the USGS and Santa Cruz County Public Works Department. Because coseismic time intervals between pre- and post-earthquake surveys range from 1 to 23 years, and because many of the routes traverse known subsidence basins, corrections for nontectonic processes were made to deduce the coseismic elevation changes. Errors were assigned to the coseismic data based on survey precision, and the uncertainty of the subsidence corrections.

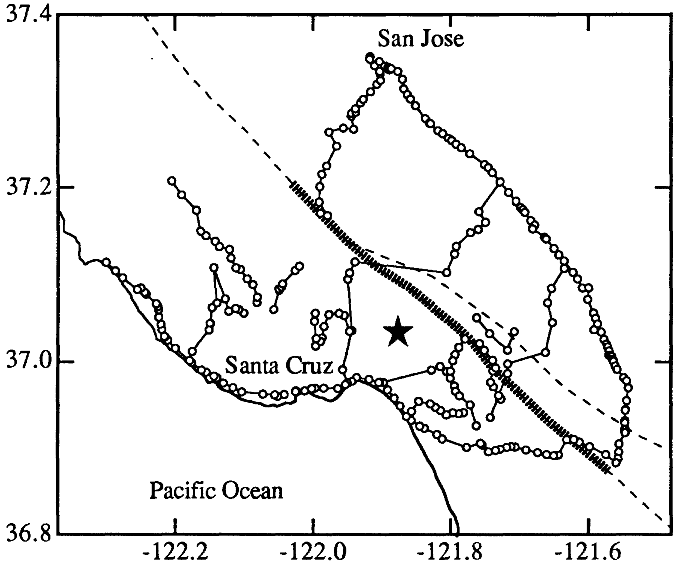

Contemporary, Holocene and Quaternary Deformation of the Asal Rift, Djibouti: Insights for the Mechanics of Slow-Spreading Ridges. The Asal rift bounding the African and Arabian plates provides a unique onshore analogue for slow-spreading midocean rifts; it displays a classical 10-km-wide rift valley with a central zone of fissures and about 15 inward-facing high-angle normal faults. Deformation accompanying a seismo-volcanic crisis in 1978 was measured by geodetic leveling. A highstand of Lake Asal has been extensively dated by ^{14}C, furnishing a record of the deformation since 7.4 ka (see figure). Only the central 4-5 faults slipped during the 1978 crisis. In contrast to expectations that faults become progressively inactive with distance from the rift axis, however, faults throughout the rift have been active during the Holocene. In fact, the slip rate of the central 2 faults (indicated by arrows) has slowed to 50% of its Pleistocene rate since 7.4 ka. There is no evidence for progressive block tilting with distance from the rift; fault dips are everywhere 70-85°. Because of negligible erosion and deposition in the hyper-arid Afar, the topographic profile provides a measure of the cumulative deformation since formation of the modern rift. We find that when the two profiles are scaled by a factor of 3.75:1, the Holocene profile closely resembles the topographic profile (see figure). This correlation suggests that the cumulative topography formed about 28 ka.

By comparing the 1978 coseismic fault slip to the Holocene slip rate, we estimate that earthquake repeat times for individual 5-10 km-long faults average 200 yr. Only 50% of the Holocene faults slipped in 1978, and thus the repeat time for grouped tectonic events, such as the 1978 crisis, is about 100 yr. The measured coseismic extension in 1978 was 1.7 m and the spreading rate is 17 mm/yr; this ratio furnishes independent evidence that tectonic events repeat every 100 yrs. We argue that half of the events occur in the central rift axis accompanied by volcanism, as in 1978; other events occur on the periphery of the rift without extrusion of lavas.

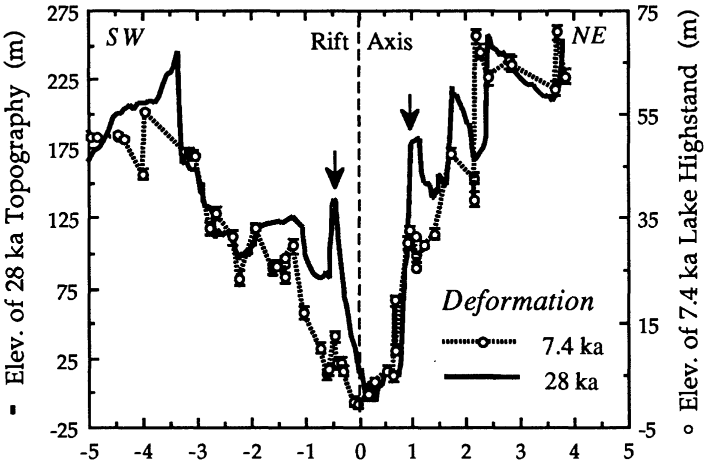

RESULTS

Seismicity and Geometry of a 110-km-long Blind Thrust Fault. How blind faults form, grow, and deform the rocks around them is central to understanding their prevalence and earthquake potential. Identification of active blind thrust faults is hindered by the absence of a surface fault trace, but they may be revealed by the presence of actively growing surface folds. Between 1982 and 1985, three $5.5 \leq M \leq 6.5$ earthquakes migrated 65 km along the north half of a string of Quaternary folds along the east front of the central California Coast Ranges. The fold chain, oriented parallel to the San Andreas fault 30 km to the west, accommodates part of the predicted 7 mm a^{-1} of contraction normal to the San Andreas fault. Because of excellent seismic, geodetic, and subsurface geologic data, this sequence provides an opportunity to illuminate the geometry of the folds and blind faults and to probe their mechanics. We relocated seismicity and determined focal mechanisms using a three-dimensional velocity model, and compared these results to the surface geology and seismic-reflection profiles across the fold. We also examined the vertical deformation accompanying and following the 1983 Coalinga earthquake.

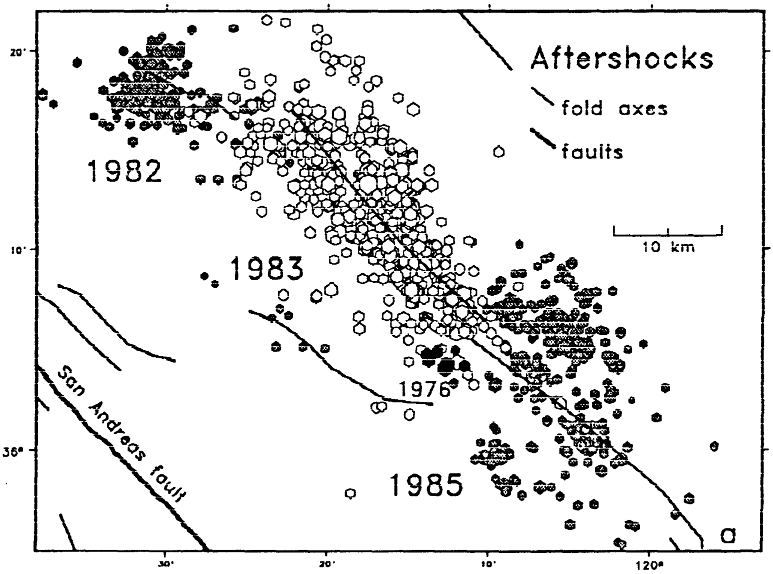

The main shocks display reverse slip perpendicular to the fold axes, and the aftershock zones abut at echelon offsets in the fold axes, suggesting that the folds conceal a continuous, segmented thrust fault. Background seismicity tends to concentrate at bends and breaks in the fold chain, sites that may correspond to tears and stepups in the thrust at depth. Several seismic-reflection profiles across the fold chain reveal thrust and reverse faults dipping toward the San Andreas fault at depths of 5-10 km with kilometers of cumulative slip, as well as high-angle reverse faults dipping away from the San Andreas fault in the anticlines with negligible cumulative slip. Coseismic uplift on or near the fold accompanied the Coalinga and Kettleman Hills North Dome earthquakes, suggesting that fold growth is episodic and coupled closely to repeated earthquakes on the underlying thrusts. The fold chain has been the site of several other 5.5≤M≤6.5 earthquakes during the 20th century, but none of these events has occurred in the south half of the chain. Thus, the next fold segment to the south, Kettleman Hills Middle Dome, has a high seismic potential. The postseismic deformation at Coalinga, amounting to 20% of the coseismic deformation during the first 4 years after the earthquake, is unusually large for an intraplate earthquake, and cannot be caused by shallow fault creep. One explanation for the postseismic deformation is upward and eastward propagation of the fault tip at the east front of the Coast Ranges.

The aftershock zones of the three main shocks are diffuse and occupy a region much larger than the sites of seismic slip. Aftershocks are found 5-7 km in front, above and below the fault tip, regions where the shear-strain increase caused by slip on the main fault exceeds ~20 ppm (equivalent to about 0.7 MPa). We argue that the diffuse aftershock distribution is a product of high, sustained off-fault stress caused by repeated displacement on faults that do not cut the free surface. The fault-tip stresses lead to the formation of secondary faults which can become sites of aftershocks and postseismic creep. The secondary faults near the tip of the thrust become part of a broad zone of fractures as the fault propagates through them, resulting in an unusually wide fault zone (Stein, Ekström, Eberhart-Phillips, and Eaton).

REPORTS PUBLISHED OR SUBMITTED DURING THIS PERIOD
(excluding abstracts):

Atwater, B.F., D.A. Trumm, J.C. Tinsley, R.S. Stein, A.B. Tucker, D.J. Donahue, A.J.T. Jull, and L.A. Payen, Alluvial plains and earthquake recurrence at the Coalinga anticline, *U.S. Geol. Surv. Prof. Pap. 1487*, 273-297, 1990.

Ekström, G., R. Stein, J.P. Eaton, and D. Eberhart-Phillips, Seismicity and geometry of a 110-km-long blind thrust fault, 1, The 1985 Kettleman Hills, California, earthquake, 49 p., submitted to *J. Geophys. Res.*, 1990.

Stein, R.S., and G. Ekström, Seismicity and geometry of a 110-km-long blind thrust fault, 2, Synthesis of the 1982-1985 California earthquake sequence, 50 p., submitted to *J. Geophys. Res.*, 1990.

Stein, R.S., Seismologists' blind faith in surface faults is being dispelled, *Earth in Space*, *2* (5), 8-9, 1990.

Yeats, R.S., A. Farah, M.A. Mirza, T. Nakata, M.R. Pandey, R.S. Stein, and K.S. Valdiya, The Himalayan frontal fault system, 26 p+1 plate, submitted to *Geological Character of Active Faults*, IGCP-206 Volume, Cambridge University Press, 1990.

Nearfield Geodetic Investigations of Strain across Faults in Southern California

14-08-0001-G1690

Arthur G. Sylvester
Department of Geological Sciences, and
Marine Science Institute
University of California
Santa Barbara, California 93106
(805) 961-3156

OBJECTIVE

The long-term, fixed purpose of this investigation is to search for and monitor the spatial and temporal nature of nearfield displacement across active and potentially active faults. Thus, we document pre-, co- and post-seismic displacement and aseismic creep, if any, especially where seismographic, paleoseismic and geomorphic evidence indicates current or recent fault activity. The geodetic arrays range in length from 300 m to 7000 m and are intermediate in scale, therefore, between the infrequent, regional geodetic surveys traditionally done by the National Geodetic Survey, and point measurements by continually recording instruments such as creepmeters, tiltmeters, and strainmeters. All leveling is done according to First Order, Class II standards, and horizontal surveys are done to First Order standards.

RESULTS

One of our primary objectives during the reporting period has been to test the capability of our Wild TC2000 total station distance meter to remeasure quadrilaterals for nearfield strain, and to remeasure leveled alignment arrays. We are still evaluating the data, but a preliminary conclusion is that we can achieve 1 ppm precision for horizontal measurements over periods as short as one day and as long as one year, and over distances up to 1000 m. Vertical reproducibility is about ± 2-4 mm, which is not acceptable for tectonic studies, and we prefer to rely on standard precise leveling that yields a reproducibility of ± 0.4 mm.

We surveyed 32 permanent bench marks along State Highway 203 through the town of Mammoth Lakes in the time period 21 to 28 August 1990. The objective of the survey was to determine vertical strain since the last previous survey that was done by the Cascades Volcano Observatory (CVO) in October 1989. Our results are similar to the CVO survey and by the National Geodetic Survey (NGS) in 1985, but dissimilar to those done by the NGS in 1986 and 1988. We concluded that little significant vertical strain occurred along the length of the line in the last 10 months since the 1989 CVO survey. More conservatively, we could conclude that little significant vertical strain has occurred since the first survey in 1985, and that the NGS surveys of 1986 and 1988 are contaminated with random and systematic errors that yielded an apparent uplift of 30 mm in the west half of the line between 1985 and 1989. We lack at present information on the quality and standards of the NGS surveys. Details and discussion of our results will appear in the Long Valley Monthly Report.

In the Parkfield area, we resurveyed level lines TURKEY FLAT, CAR HILL, PITT RANCH, and FLENGE FLAT and found no significant changes in bench mark heights since our previous resurveys in August 1989.

We releveled nearfield geodetic arrays LEWIS CREEK, MUSTANG GRADE, PINYON FLAT and WALLACE CREEK during summer 1990. LEWIS CREEK, which is in the center of the creeping segment of the San Andreas fault, continues to creep vertically at a rate of about 3 mm/yr. MUSTANG GRADE, also in the creeping segment, yields equivocal results. We are still processing the other arrays.

We have almost completed the programming of a new leveling adjustment program to run on Macintosh SE microcomputer. This is a major step forward for us, because it will replace a horseback program written for an old Apple II+ with its miniscule 128K of memory. Soon we will be able to process in one gulp our arrays that consist of 54 or more bench marks, and we have several of them waiting to be done.

A Vertical Deformation Sensor on the Southern San Andreas Fault

14-08-0001-G1786

Hadley O. Johnson, Frank K. Wyatt,
and Duncan Carr Agnew
Institute of Geophysics and Planetary Physics
University of California, San Diego
9500 Gillman Drive
La Jolla, California 92093-0225
(619) 534-2019

This grant supports the construction of a fiber-optic anchoring system near the Coachella segment of the San Andreas Fault—specifically, on the western flank of Durmid Hill, near the termination of this fault and its junction with the Brawley Seismic Zone. This area has been identified as one of the more likely initiation points for a great earthquake during our lifetime. The experiment involves measuring the differential vertical motion of four points in the ground from a depth of 5 m down to depths of 50 m. The goal of this temporary installation is to study the stability of the near-surface material in the region to determine if it is stable enough to support precise measurements of strain and tilt. Efforts at Piñon Flat Observatory have shown that observatory-based instruments can measure signals up to one thousand times more precisely than geodetic surveying techniques in the period range of months to minutes, while accurately recording the secular accumulation of deformation—provided that the instruments are adequately anchored to depth. Determining what depth is adequate in this area—as a first step toward consideration of more extensive instrumentation—is the aim of this project.

Because of the high accuracy needed for deformation measurements, we believe conventional extensometery using solid-rod or taut-wire sensors would not be adequate in this case. While using evacuated pipes and a laser interferometer would meet the accuracy requirements, it would involve complicated vacuum/optical systems and a much larger borehole. By using lengths of optical fiber for the light paths instead of evacuated pipes, we are able to make many differential measurements in the same borehole without needing cumbersome vacuum equipment–this, of course, makes the installation much less expensive. Another important advantage is that once the laser light has been sent into the fiber system all light-direction is permanently "hard-wired", with no discrete optical elements which would need frequent realignment, especially in a non-temperature-controlled setting such as this.

Construction at the field site began as soon as possible after preparation of the optical-fiber sensors (we were delayed by late delivery of the materials) which coincided with the end of the hot summer weather in the Coachella Valley—with its daytime temperatures of ~110°F in the shade. The field work has proceeded at a steady pace since mid-September. After first settling the land-use arrangement with a local resident our next step was to drill a borehole and install the fiber sensors to their proper depths. Based on the drilling results for several heat-flow holes (drilled nearby in the late 1960's), we were very concerned about how to drill to our target depth of 50 m. These earlier holes had often collapsed during drilling, and lost circulation to the surface. To avoid this we chose to use special drilling equipment which cased the borehole as it was being drilled; the side-walls of the formation could then never cave in. As it turned out, the drilling went fairly smoothly, though probably introducing large, local strains in the borehole side-wall, as the special drill bit was literally hammered through the ground with no boring action.

The fiber optic sensors (two each to four different depths, with one spare to each depth) were fabricated in our lab in San Diego prior to the drilling exercise. The individual fiber-arms of the interferometers were cut to length, a silver mirrored surface was chemically plated to their lower ends, and the fibers were permanently sealed against moisture. After drilling was completed, the full bundle of 12 fibers was lowered to the bottom of the open borehole and the operation of cementing them in place was begun. Initially we had planned to pump 5-foot vertical columns of very strong grout ("anchors") into the borehole, carefully placed at each of the four sensor depths. The intervals between these anchors was to be filled with packed sand. This elaborate scheme was devised because the bonding grout we originally considered using was so much stronger than the local material that filling the entire hole with grout risked making our measurements meaningless: we might end up measuring nothing more interesting than grout deformation. While planning the operation, we came to feel this scheme would be too difficult to accomplish under field conditions (that is, unless we had a lot more money). Instead, we experimented with various grout recipes (based on advice from John Boa, with the Army Corps of Engineers in Vicksburg) to reduce the grout's strength to match our estimate of the strength of the claystone/sandstone Borrego formation. We settled on a set of mix proportions and in the end filled the entire borehole with this "intermediate strength" grout formula. This approach had the enormous advantage of removing the need to accurately place small volumes of different materials in the borehole where, after all, you are nearly "blind" to what is going on.

After the sensors were safely grouted into the borehole, we started building the sub-surface vault for housing the optics and electronics. A large pit was excavated around the short section of surface casing sticking up from the borehole and our pre-assembled vault lowered into the hole. The vault is made of two 4-foot-diameter sections of drainage culvert tipped on end; these sit side-by-side with a "window" cutout connecting the two (see Figure 1). The taller of the two sections of culvert serves as an entrance-way while the short buried section will contain the laser, optics, and electronics necessary to make the differential displacement measurements.

We expect that we will complete installation of the sensors and begin recording data before the end of December 1990, about six-months later than we had originally planned.

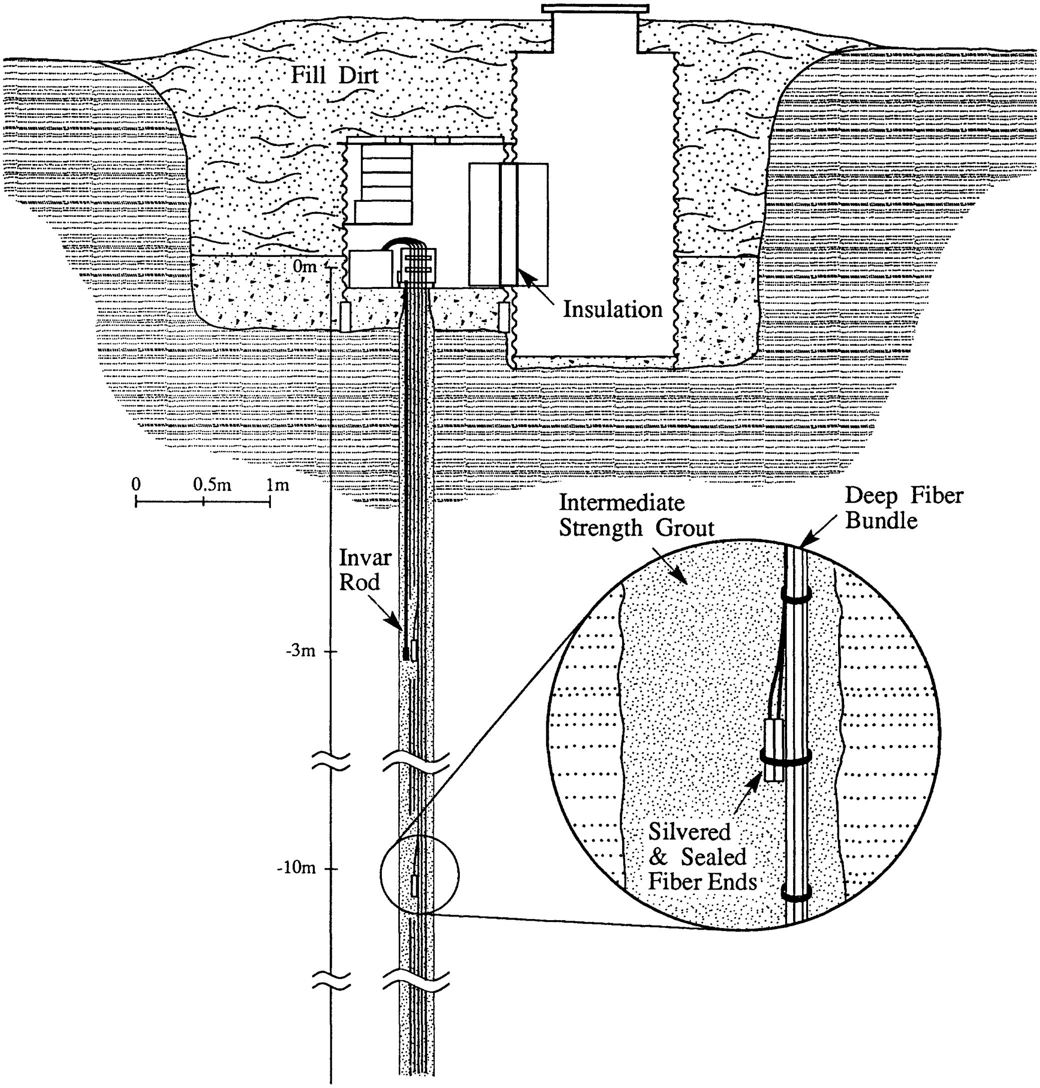
Fill Dirt
0m
Insulation
0
0.5m
1m
Intermediate Strength Grout
Deep Fiber Bundle
Invar Rod
-3m
-10m
Silvered & Sealed Fiber Ends

Figure 1

Friction Constitutive Behavior of Saturated Faults at Hypocentral Conditions

USGS 14-08-0001-G1768

Frederick M. Chester*

Lamont-Doherty Geological Observatory, Palisades, NY 10964; (914)359-2900.
(*Permanent address: Department of Earth & Atmospheric Sciences, St. Louis University,
3507 Laclede, St. Louis, MO 63103; (314) 658-3124.)

Investigations

The goal of the project is to determine the friction constitutive behavior of water saturated faults at hypocentral conditions through experimentation and constitutive modeling. Specifically, we are conducting triaxial friction experiments on wet and dry quartz gouge at normal stresses to 100 MPa and temperatures to 250 °C. Methods of testing include velocity stepping, slide-hold-slide and temperature stepping. Through such experiments we will determine the trade-off between slip rate and temperature, and the form of temperature dependence in rate and state dependent friction constitutive laws. Experiments are being conducted at water saturated and nominally dry conditions to determine the effect of water on frictional behavior, and in particular, to search for evidence of solution transfer at elevated temperatures and low sliding velocities.

Results

The first suite of experiments investigating velocity and temperature dependence of friction in quartz gouge at both wet and dry conditions has been completed. Using a servo-controlled triaxial apparatus, we sheared 1.5-mm thick layers of fine-grain (< 100 μm diameter) quartz gouge between rough steel surfaces to slip displacements of 10 mm, at a constant effective confining pressure of 20 Mpa, and under room-dry or water-saturated conditions. In each experiment the slip velocity was stepped between 4., 0.4 and 0.04 μm/s while temperature was maintained at a constant value between 22 and 85 °C. In some tests the temperature also was abruptly increased by 25 to 30 °C during a period in which the slip velocity was maintained at a constant 0.04 μm/s. We measured the transient and steady-state changes in frictional strength resulting from the imposed steps in temperature and velocity (e.g., Figs. 1 and 2).

Use of steel blocks in the sample assembly increases the thermal conductivity of the sample and allows rapid equilibration of temperature. A step in temperature of 25 to 30 °C to a new equilibrated temperature condition is achieved in less than 100 s. Thermal expansion of the sample column during temperature changes is significant: approximately 1 μm axial lengthening per °C temperature change. Expansion is measured by the transducer used to generate the feedback signal for displacement servo-control. Accordingly, we modify the command signal to achieve a constant shear displacement rate of 4 μm/s across the gouge layers during each temperature step. Corrections are based on separate calibration experiments, conducted under load feedback, that define the thermal expansion of the sample column during a standardized heating procedure.

Differential axial force is measured with a load cell positioned inside the pressure vessel (Fig. 3). As such, the components of the sample assembly contributing to the total resistance to slip are the 1) shear of the gouge layer, 2) deformation of the jacket, and 3) lateral slip between two steel spacers (Fig. 3). The jacket consists of a 5-μm thick copper foil inside a 2-mm thick sheet of lead. The spacer interface is lubricated with graphite powder to facilitate the lateral slip. Experiments have been conducted specifically to determine the time and temperature dependent strength properties of the jacket and graphite lubricated surface. Compared to the strength of the gouge and graphite, the velocity and temperature dependent strength of the jacket is negligible. The velocity and temperature dependent strength of the graphite lubricated surface is significant, and therefore characterizing the constitutive behavior of the graphite interface through numerical constitutive modeling is a necessary aspect of our present work. The graphite interface shows rate strengthening behavior, so the frictional behavior of the quartz gouge is more rate weakening than suggested by the raw friction data illustrated in Figures 1 and 2.

Presently, we are using the velocity and temperature dependent friction law proposed by Chester (1988) to describe the behavior of the quartz gouge. This friction law is based on the rate and state dependent law formulated by Dieterich (1979) and Ruina (1983), with assumptions regarding normal stress dependence following Rice and Gu (1983). The addition of temperature dependence assumes that the time-temperature relationship for the microprocesses producing velocity dependence are described adequately with an Arrhenius relationship. The single state variable law is given by:

$$\mu = \tau/\sigma = \mu^* + a[\ln(V/V^*) + Q_a/RT] + b\Theta$$

and

$$d\Theta/dt = (-V/L)[\Theta + \ln(V/V^*) + Q_b/RT],$$

where a and b are the friction parameters describing the direct and evolution effect, and Q_a and Q_b are the apparent activation energies for these effects.

The experiments clearly show that abrupt temperature changes produce direct and evolution effects characteristic of velocity dependent friction. Specifically, the changes in transient and steady-state frictional strength produced by a step increase in temperature are qualitatively similar to the response for a step decrease in slip velocity (Fig. 1). This behavior is consistent with the constitutive law described above.

The friction data also show that the quotient $\Delta\mu^{\text{instantaneous}}/\Delta\mu^{ss}$ for velocity steps is different than that for temperature steps (Fig. 2). This indicates different temperature-time relationships (different apparent activation energies) for the direct and evolution effects because $\Delta\mu^{\text{instantaneous}}$ reflects only the direct effect whereas $\Delta\mu^{ss}$ depends on both the direct and evolution effects.

The variation in frictional behavior between the dry and wet tests (Fig. 2) may be attributed to the gouge because the apparatus and jacket effects are the same in all experiments. In general, the magnitude of the direct and evolution effects is greater in wet quartz gouge than in dry quartz gouge. Our present work is aimed at quantifying the velocity and temperature dependence of friction in quartz gouge through numerical constitutive modeling of the experiments.

Reports

Chester, F. M., Temperature-time relationships for frictional strength of quartz gouge, AGU Fall Meeting, San Francisco, 1990.

Chester, F. M. and N. G. Higgs, Friction constitutive behavior of wet and dry ultra-fine grained quartz gouge at elevated temperatures, EOS Trans. Am. Geophys. Union, 71, 642, 1990.

References

Chester, F. M., Temperature and rate dependence of friction for faults, EOS Trans. Am. Geophys. Union, 69, 471, 1988.

Dieterich, J. H., Modeling of rock friction, 1, experimental results and constitutive equations, J. Geophys. Res., 84, 2161-2168, 1979.

Rice, J. R., and Gu, J. C., Earthquake aftereffects and triggered seismic phenomena, Pure Appl. Geophys., 121, 187-219, 1983.

Ruina, A. L., Slip instability and state variable friction laws, J. Geophys. Res., 88, 10,359-10,370, 1983.

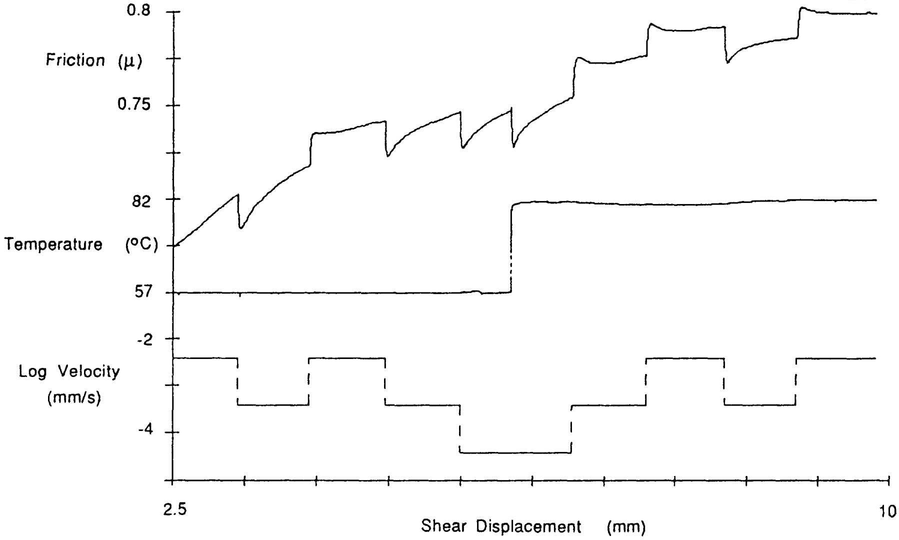

Figure 1. Representative results of a velocity and temperature stepping friction experiment. Quartz gouge sheared to 10 mm by stepping between velocities of 4, 0.4 and 0.04 μm/s at constant temperature, and between 57 and 82 °C while sliding at the lowest velocity. This is raw friction data uncorrected for jacket and apparatus effects. The friction response is similar for a step decrease in velocity and a step increase in temperature (compare steps at 5.5 and 6 mm shear displacement).

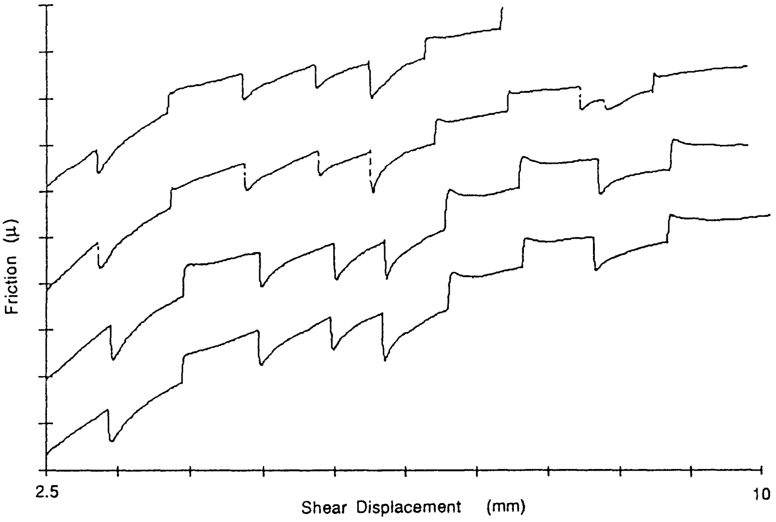

Figure 2. Frictional strength of quartz gouge in velocity and temperature stepping tests. Sequence of velocity and temperature steps are the same as that shown in Fig. 1; curves are shifted for clarity. Vertical scale is coefficient of friction, where 1 division equals .025. Top curve: dry, 57 to 82 °C temperature step. Second curve: dry, 22 to 57 °C. Third curve: wet, 57 to 85 °C. Bottom curve: wet, 22 to 57 °C.

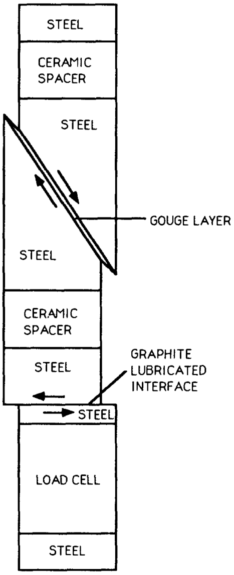

Figure 3. The sample column used in the temperature and velocity stepping experiments. Only the components between the two pistons and inside the pressure vessel are shown. Axial shortening of the column causes slip on the interfaces as shown. The differential axial load measured by the load cell reflects the resistance to slip in the gouge layer, strength of the jacketing used to isolate the specimen from the confining media, and the resistance to slip along the graphite lubricated interface. The graphite surface is located outside the sealed jacket.

Mechanics of Earthquake Faulting

9960-01182

James H. Dieterich
U.S. Geological Survey
345 Middlefield Road, MS 977
Menlo Park, California 94025
(415) 329-4867

INVESTIGATIONS

1. Wave propagation and onset of instability. Joint studies with V. A. Dubrovskii of the Institute of the Physics of the Earth, Moscow, U.S.S.R, were conducted on the theory of wave propagation and onset of instability along faults with rate- and state-dependent friction.

2. Friction experiments at a range of velocities and normal stresses. An initial series of direct shear friction experiments was completed by B. Kilgore, M. Blanpied and J. Dieterich. The experiments provide constitutive data at slip rates and normal stresses that previously could not be attained.

RESULTS

1. Wave propagation and onset of instability. We have studied the propagation of elastic waves along a fault with velocity- and displacement-dependent friction as a perturbation of uniform fault slip speed (Dubrovskii and Dieterich, 1990). Particle motion attenuates perpendicular to the fault and in this sense it consists of a generalized Rayleigh wave. Two critical wave lengths l_c, L_c, have been identified. If $l>l_c$ waves attenuate, if $l_c<l< L_c$ wave amplitude grows to instability and if $l> L_c$ instability takes place without oscillation.

2. Friction experiments at a range of velocities and normal stresses. Modifications of the direct shear testing sample configuration and improvements in the servo-control system have made possible friction experiments at previously unattainable normal stresses and slip rates (Kilgore and others, 1990). Normal stresses of 150 MPa, more than double of the maximum normal stress in previous experiments, were achieved using a raised sliding "button" sample configuration. This configuration generates confining stresses near the

sliding surface that help resist sample failure at the higher normal stresses. Constitutive properties were measured at steady-state sliding slip rates from $10^{-4}\mu$m/s (3mm/yr) to $10^{3}\mu$m/s and normal stresses of 5, 15, 30, 70 and 150 MPa.

Measurements of steady state velocity dependence ($\partial\mu_{ss}/\partial\log_{10}V$) on bare surfaces of Westerly Granite were obtained following a standard "run-in" of 6mm slip (Fig. 1). At normal stresses from 30MPa to 150 MPa, the velocity dependence of steady-state friction is negative resulting in velocity weakening behavior at all slip rates. At 15MPa normal stress, velocity weakening occurs at slip rates below 10µm/s, but switches to velocity neutral behavior at slip rates greater than 10µm/s. At 5MPa normal stress velocity weakening switches to strong velocity strengthening above 10µm/sec.

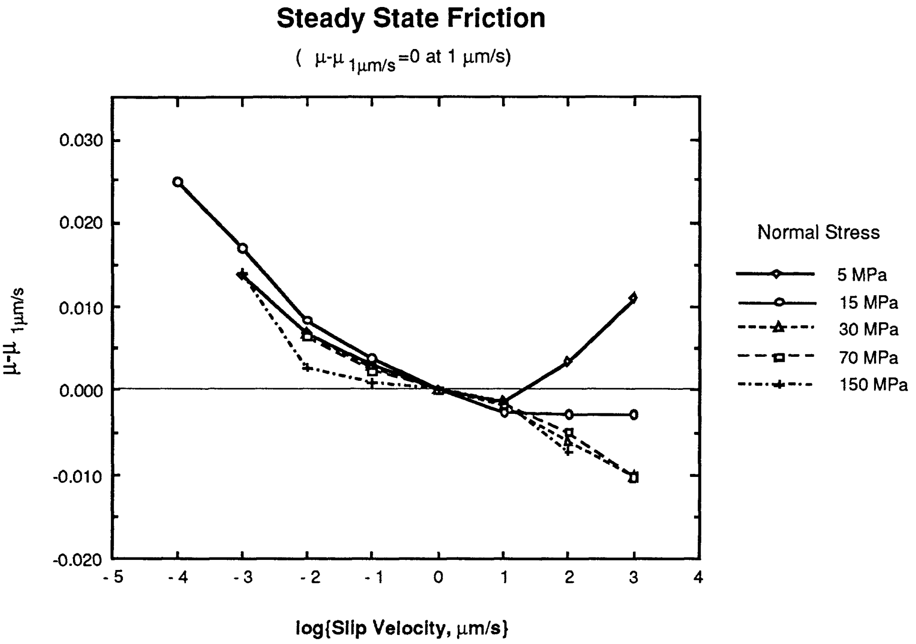

Figure 1. Dependence of steady-state friction coefficient, μ, on $\log_{10}$ slip speed and normal stress. $\mu_{1\mu m/s}$ is the steady state friction at 1µm/s.

The observations of velocity weakening imply the potential for unstable, stick-slip sliding at a wide variety of conditions. Limited observations at slip rates of 10^{-3} and 10^{-4} µm/sec.

indicate that at these low slip rates, velocity dependence becomes increasingly more negative as slip rates decrease. This suggests that an additional deformation mechanism; for example, crystal plasticity, pressure solution or subcritical crack growth may be activated at these low slip rates. The switch to velocity strengthening at high velocity and low normal stress implies that the onset of rapid slip at shallow fault levels would be arrested before resulting in true stick-slip behavior. The observed oscillatory creep at shallow levels on some natural faults may result from this switch in velocity dependence.

REPORTS

Blanpied, M. L., Lockner, D. A. and Byerlee, J. D., Experimental granite faults at hydrothermal conditions: implications for depth distribution of seismicity (Abstract, Submitted to 1990 Fall AGU).

Dieterich, J. H., 1990 Working Group Study on Probabilities of Earthquakes in the San Francisco Bay Region, California (Abstract, Submitted to 1990 Fall AGU).

Dieterich, J. H. and Linker, M. F., Effects of Variable Normal Stress on Rock Friction: Observations at 5 MPa Normal Stress (Abstract, Submitted to 1990 Fall AGU)

Dubrovskii, V. A. and Dieterich, J. H., 1990, Wave Propagation Along Faults and the Onset of Slip Instability (Abstract), Eos, Trans. AGU, **71**, 635.

Kilgore, B. D., Blanpied, M. L. and Dieterich, J. H., !990, Granite Friction Experiments at a Range of Velocities and Normal Stresses (Abstract, Submitted to 1990 Fall AGU).

Linker, M. F. and Dieterich, J. H., Effects of Variable Normal Stress on Rock Friction: Observations at 5 MPa Normal Stress (submitted to Jour. Geophys. Res.).

Stressing, Seismicity and Rupture of Slip-Deficient Fault Zones

14-08-0001-G1788

R. Dmowska and J. R. Rice (PI)
Division of Applied Sciences and Department of Earth and Planetary Sciences,
Harvard University, Cambridge, MA 02138
(617) 495-3452 and 3445

1. Investigations

1.1 Seismic behavior of the outer-rise has been investigated as a possible predictive indicator for large subduction earthquakes. Correlations with plate age, convergence rate and seismic coupling in the main plate interface were attempted. The work is in progress (Dmowska and Lovison, AGU San Francisco, 1990).

1.2 Large scale inhomogeneities along strike of coupled subduction zones have been investigated, as a continuation of our past work (see last two reports), with the use of $m_b > 5.0$ seismicity if available in the outer-rise and in the down-going slab at intermediate depths. The work shows promises for finding future areas of highest seismic moment release in zones that ruptured in large earthquakes before around 1960, that is in cases for which the distribution of asperities could not be assessed from the analysis of seismic radiation in the earthquake itself.

1.3 Finite element analysis of stress variations throughout the earthquake cycle have continued, in support of the subduction studies (above), and also for strike-slip models, in which case some effects of nonlinear creep rheology have been analyzed.

1.4 Implicit numerical methods for integration in time are being developed for analyzing crustal fault models with rate- and state-dependent friction laws in the fault zone, and some of these are now being tested. The hope is to find methods allowing significantly larger time steps than previous methods, and to incorporate them into finite element models of the crust.

1.5 The possibility is being evaluated that elevated pore pressure distributions within the crust, relating to plausible scenarios of pressure generation and fluid transport in and near fault zones that have lab-like friction properties, could account for not just the absolute weakness of the SAF, but also its relative weakness compared to the adjacent crust (which sustains maximum principal stress at a steep angle to the SAF, violating whatever failure criterion applies for the SAF).

2. Results

2.1 Seismic behavior of the outer-rise is a possible predictive indicator for large subduction earthquakes. It is known that the outer-rise breaks in tension adjacent to uncoupled subduction zones and in both tension and compression near coupled areas, where there are tensional events predominantly following large underthrust earthquakes and compressional events (much less frequent) grouped towards the end of the cycle. Our recent work (Dmowska and Lovison, EOS,1989) shows a high tendency of both tensional and compressional outer-rise events to occur in front of areas of highest seismic moment release (asperities) in the associated great thrust events. Here, for coupled subduction zones, we investigate the possible relation between seismic behavior of the outer-rise and the age of the incoming oceanic plate, rate of convergence and degree of coupling, using the data for earthquakes with $m_b \geq 5.5$ around the Pacific. The data set is limited as concerns important (for predictive purposes) years before and after large subduction events; however, some correlations emerge. Older oceanic plate (> 80 Ma) breaks usually with the presence of compressional outer-rise events, including large ones ($m_b \geq 6.0$), before large subduction earthquakes, and with tensional events predominantly afterwards. Very young oceanic plate (< 20 Ma) shows limited outer-rise activity, with earthquakes of smaller sizes ($m_b < 6.0$) that are predominantly tensional, and with only a few compressional events marking the mature segments ready to break in large subduction events. The response of medium-age plates (20 to 80 Ma) is more varied but these break predominantly in tension, with some compressional events present. The seismic behavior of the outer-rise seems not to correlate with the rate of convergence, but there is a weak correlation between the magnitude of outer-rise activity and seismic coupling.

Our preliminary results are shown in figure 1.

2.2 In our recent research we have investigated the influence of large-scale fault inhomogeneities in large subduction earthquakes on the style of deformation and seismic behavior of incoming oceanic plate and slab at intermediate depths during the earthquake cycle (Dmowska and Lovison, 1989). The zones of the large subduction events of Alaska 1964, Rat Islands 1965, Valparaiso 1985 and Colombia 1979 have been searched for earthquakes with mb>5.0 if available and for as long time periods as possible. It has been found that in general the seismicity in the incoming oceanic plate clusters in front of asperities (=areas of highest seismic moment release and strongest locking). It is usually lacking in areas adjacent to non-asperities, that is to zones that slip during the main event but with appreciably smaller seismic moment release , and possibly slip seismically/aseismically during the whole cycle. Similar behaviour occurs in the downgoing slab at intermediate depths, where seismicity during the cycle clusters (but less strongly than in the oceanic crust) next to asperities and downdip from them. We inferred that the locking of asperities did cause higher stresses associated with earthquake cycle itself to occur in areas adjacent to asperities, both updip and downdip from them, and that such stressing has been much less pronounced in the areas adjacent to non-asperities.

We have continued to investigate the influence of fault inhomogeneities on the seismicity in the outer-rise and down-dip in zones adjacent to asperities for two areas, where asperities have been smaller than in the large earthquakes investigated before, but still where their distribution has been known from the analysis of earthquakes itself . The areas were southern Kuriles and the area of Andreanof Island earthquake of 1986, with asperities found there by Schwartz and Ruff, 1987, and Schwartz et al. 1989, and Boyd and Nabelek, 1988, respectively. The results confirmed our previous observations of seismicity clustering both updip and downdip from asperities, and convinced us that such an approach opens the possibility of identifying the areas of highest seismic moment release in future subduction earthquakes.

Thus we have applied the approach to zones of unknown asperity distribution, with the aim of locating the asperities based on observations of outer-rise and down-dip seismicity alone, and we have analyzed the areas of the Chile 1960 and Aleutians 1957 earthquakes, identifying areas of future highest seismic moment release. Our results are still preliminary.

2.3 In a continuing collaboration with W. D. Stuart (USGS, Pasadena), we have used the ABAQUS finite element code to analyze stressing in and near a strongly coupled subduction zone during the earthquake cycle. Compared to our earlier work (Rice and Stuart, 1989), the more recent modeling has been based on a more refined grid with more distant boundaries, and with special treatment of the region at the downdip end of the seismic dislocation (although there remains a need for yet further grid refinement for accurate stress modelling in that area). Figure 2 shows a portion of a mesh, in the vicinity of the locked thrust zone. A solution based on linear Maxwell rheology in the mantle (dark portion of mesh) has been done for the fluctuating parts of the stress and displacement rate fields, i. e., the parts which average to zero over a cycle, and which are to be added to steady, long-term average tectonic fields to give the total stress and displacement rate. The upper part of figure 2 shows the extensional stress, S_{ext}, at various times throughout an earthquake cycle, along the middle plane of the ocean floor and descending slab; those regions are assumed to respond elastically to stress fluctuations on the time scale of the earthquake recurrence time, T_{cyc}. Other notation: V_{pl} is the time-averaged slip rate at the thrust zone; G = shear modulus; T_{relax} = Maxwell relaxation time assumed for mantle; Z = length of zone locked between earthquakes; x = epicentral position, from trench, for points along ocean plate/descending slab mid-plane. The curve sets are not continuous near x = 0 since the direction for S_{ext} is different in the two domains. These results provide a more accurate determination of stress fluctuations in the earthquake cycle than those that Dmowska et al. (1988) estimated using a simplified one-dimensional model. We find significant stress variations in the slab towards the trench and in the ocean floor, and also downdip in the slab adjacent to the base of the locked thrust zone. These are consistent with the observational results on seismicity variations in those regions associated with time through the earthquake cycle. Additional results, not shown here for brevity, show that the main fluctuation in stress in the vicinity of the trench and outer rise involve mostly extension/compression with little bending. These fluctuations thus superpose on the long term average tectonic field, which is thought to be dominated by bending in that region, to enable shallow extensional failures early in the cycle and deeper compressional failures at later stages, much as discussed by Dmowska and Lovison (1988).

Additional finite element modeling of stress variation throughout the earthquake cycle has been done for the strike slip situation. In those cases, we have begun to examine effects of power-law creep in the lower crust and underlying mantle, rather than just the linear Maxwell form used previously. Results are to be reported at a later stage.

2.4 Simpler models of slip on a fault (with rate- and state-dependent friction) between deformable continua, once discretized, reduce to the mathematical problem of solving $\Delta\tau_i = \Sigma_j K_{ij} (V_{pl}\Delta t - \Delta\delta_j)$ in successive small time steps, where τ is shear stress, δ is slip, K is an elastic stiffness matrix, and where the constitutive relations for slip, somehow approximated in a finite time step Δt, are used. In explicit methods, $d\delta/dt$ is known in terms of τ (and a state variable, the evolution of which is given by an associated differential equation) at the start of the step, and we may estimate the $\Delta\delta$ by multiplying by Δt, thus calculating the $\Delta\tau$. More sophisticated explicit methods, in actual use, use high order Runge-Kutta schemes. Such methods are accurate but require extremely small time steps and have not yet proven practical for use in crustal scale models with small state-evolution slip distances L, comparable to those of lab experiments. In an attempt to circumvent this difficulty, we have been examining implicit methods in which each $\Delta\tau$ is regarded as a function of the associated $\Delta\delta$, where the functional relation is dependent on the Δt and on the stress and state at the start of the increment, and is generated by some simple assumption which becomes exact as $\Delta t \rightarrow 0$. One promising candidate that we are exploring writes $\Delta\tau_i = F_i(\Delta\delta_i; \Delta t$, starting τ_i and state$_i)$ on the basis of treating each slip rate $d\delta_i/dt$ as constant during the increment and equal to its (unknown) value at the end of the increment. $\Delta\tau_i = F_i(\Delta\delta_i)$ is then substituted into the equations involving K above, which are then solved iteratively in a Newton-Rhapson scheme, or more directly by linearizing F in $\Delta\delta$ when Δt is not too large. This seems to be an advantageous method when applied to simple single degree of freedom systems, in that larger time steps (controlled by L and $d\delta/dt$ at the start of the step) can be taken. Working collaboratively with T. E. Tullis (Brown University), we are now examining the efficiency of such a method for complex multi-degree of freedom fault models, and its comparison against high order explicit methods now in the Stuart-Tullis code. The major drawback in the implicit method is that a system of simultaneous equations has to be solved in each time step, and this is to be traded against the significantly larger time steps hopefully allowed.

2.5 The San Andreas Fault is weak in an *absolute* sense, in that it moves under shear stresses far smaller than the most obvious reading of lab friction results (Byerlee law with hydrostatic pore pressure and friction coefficient f = 0.6 to 0.9) would seem to imply. It is also weak in a *relative* sense, in that the adjoining crust seems to be mechanically stronger. That is implied by the fact that the stress state in the adjoining crust, driving the SAF, has a horizontal maximum principal compressive stress direction which makes a steep angle to the trace of the SAF, much larger than the 25° to 30° expected from elementary frictional failure considerations (i. e., much larger than the angle $45° - 0.5 \arctan f$, with $f = 0.9$ to 0.6). Explanations of fault weakness may be based on weak fault zone materials (like some clays), on global effects of stress-transferring interactions between severely slip-weakening fault segments, and on elevated pore pressures. We find that pore pressure distributions which are high, and near to the normal stress, within a major fault zone, but lower in the adjacent crust, are consistent with both the absolute and relative weakness discussed. Further, the mechanics of a mature fault zone is such that stress components within it (other than those that act on planes with normals perpendicular to the fault) need not be identical to the stress components in the adjacent crust. That is shown to allow fault pore pressures to exist which may be higher than the least principal stress in the nearby crust, but lower than that within the fault, and thus not induce hydraulic fracture. Such a case is illustrated in figure 3 (Rice, 1990).

The type of pore pressure distribution discussed, leading to fault weakness, is shown to result from the assumptions that there is a supply of fluids, necessarily under near-lithostatic conditions, near the ductile roots of fault zones, and that fault zones are much more permeable than the adjoining rock for fluid transport in the middle crust. These assumptions have support in petrological studies of mineral alterations and fluid inclusions along exhumed faults, in the geochemistry of fluids exiting the earth near fault zones (sometimes identified, from ^{3}He/^{4}He ratio or, less reliably, from δ^{13}C, to have constituents of mantle origin), from crustal resistivity studies attesting to fluid presence in the lower crust, and from gravity and seismic velocity and attenuation studies of active faults. Also, nonlinear effects of a fault zone permeability that varies strongly with effective normal stress, as suggested by lab experiments, have been found. These include a tendency for the effective normal stress to become approximately independent of depth after a near-surface transition, and also the possibility of diffusive surges of pore pressure increase that propagate upwards through the crust in a slow wave-like manner.

References

Boyd T.M., and J.L.Nabelek, Rupture process of the Andreanof Islands earthquake, *Bull. Seism. Soc. Am.*, **78**, 1953-1673, 1988.

Dmowska R., and L.C.Lovison, Influence of asperities in zones of large subduction earthquakes on style of deformation and seismic behavior of incoming ocanic plate and slab at intermediate depths - Alaska 1964, Rat Islands 1965, Valparaiso 1985 and Colombia 1979, *EOS, Trans. Am. Geophys. Un.*, **70**, p.1063, 1989.

Dmowska R.,and L.C.Lovison, Intermediate-term seismic precursor for some coupled subduction zones, *Pure Appl.Geophys.*,**126**, N. 2-4, 643-664,1988.

Dmowska R., J.R.Rice, L.C.Lovison and D.Josell, Stress transfer and seismic phenomena in coupled subduction zones during the earthquake cycle, *J.Geophys.Res.*, **93**, NO. B7, 7869-7884,1988

Rice, J. R., Friction, pore pressure, and the apparent weakness of major faults (extended abstract), *Int. Symp. Earthquake Source Physics and Earthquake Precursors*, Tokyo, Nov. 1990

Rice J.R. and W.D.Stuart, Stressing in and near a strongly coupled subduction zone during the earthquake cycle, *EOS, Trans. Am. Geophys. Un.*, **70**, p.1063, 1989

Schwartz S.Y., J.W.Dewey, and T.Lay, Influence of fault plane heterogeneity on the seismic behavior in the Southern Kurile Islands Arc, *J.Geophys. Res.*, **94**, 5637-5649, 1989.

Schwartz S.Y., and L.J.Ruff, Asperity distribution and earthquake occurrence in the Southern Kurile Island Arc, *Phys. Earth Planet. Inter.*, **49**, 54-57, 1987.

SEISMIC BEHAVIOR OF OUTER-RISE FOR DIFFERENT SUBDUCTION SEGMENTS AS A FUNCTION OF AGE OF THE INCOMING OCEANIC PLATE AND CONVERGENCE RATE

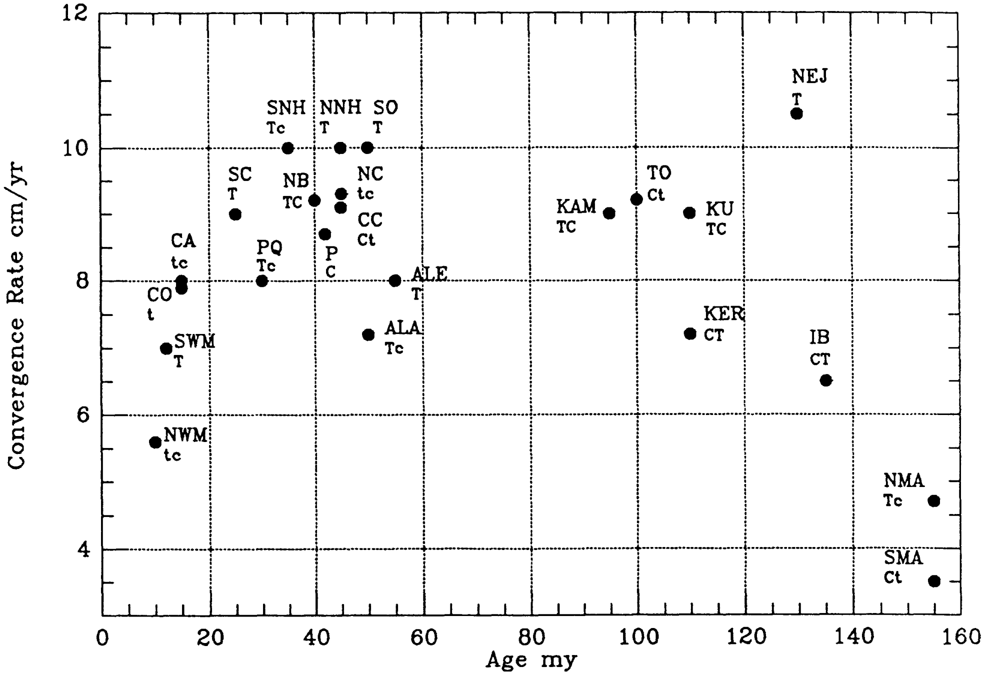

T: tensional events with mb ≥ 6.0
t: tensional events with mb < 6.0
C: compressional events with mb ≥ 6.0
c: compressional events with mb < 6.0

ALA - Alaska
ALE - Aleutian Islands
CC - central Chile
CA - central America
CO - Colombia
KAM - Kamchatka
KER - Kermadec
KU - Kuriles
IB - Izu-Bonin
NB - New Britain
NC - north Chile
NEJ - north-east Japan
NNH - north New Hebrides
NMA - north Mariana
NWM - north-west Mexico
P - Peru
PQ - Peru Quiet Zone
SC - south Chile
SO - Solomon Islands
SMA - south Mariana
SNH - south New Hebrides
SWM - south-west Mexico
TO - Tonga

Figure 1

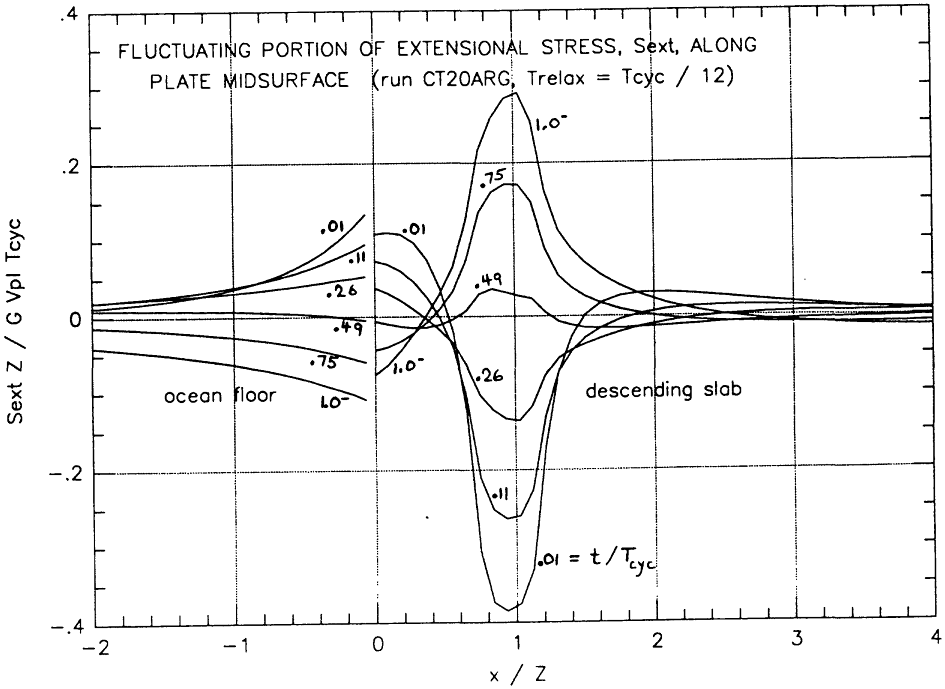
FLUCTUATING PORTION OF EXTENSIONAL STRESS, Sext, ALONG PLATE MIDSURFACE (run CT20ARG, Trelax = Tcyc / 12)
Sext Z / G Vpl Tcyc
x / Z
.4
.2
0
-.2
-.4
-2
-1
0
1
2
3
4
ocean floor
descending slab
.01
.11
.26
.49
.75
1.0-
.01
1.0-
.75
.49
.26
.11
.01 = t/Tcyc

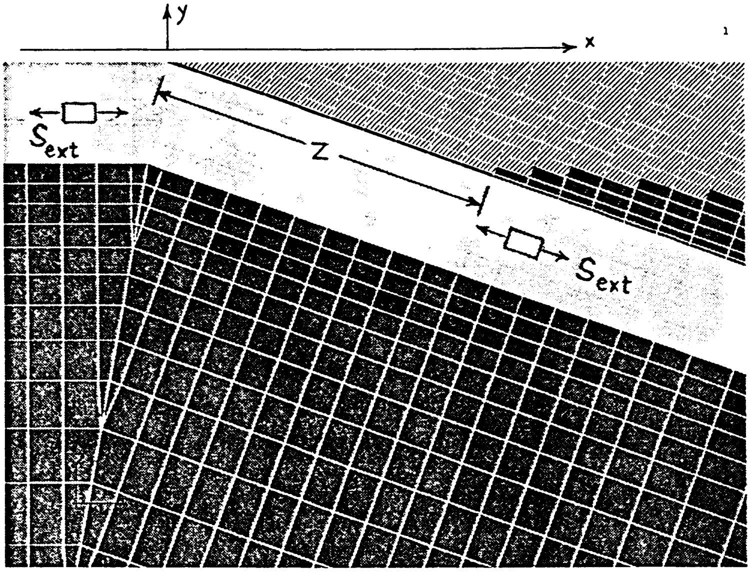
y
x
Sext
Z
Sext

Figure 2

Stress states in a vertical fault zone and in the adjacent crust; horizontal max and min principal stresses

(Illustrated as critical for *strike-slip* failure in the vertical fault zone and for *thrust* failure in the adjacent crust)

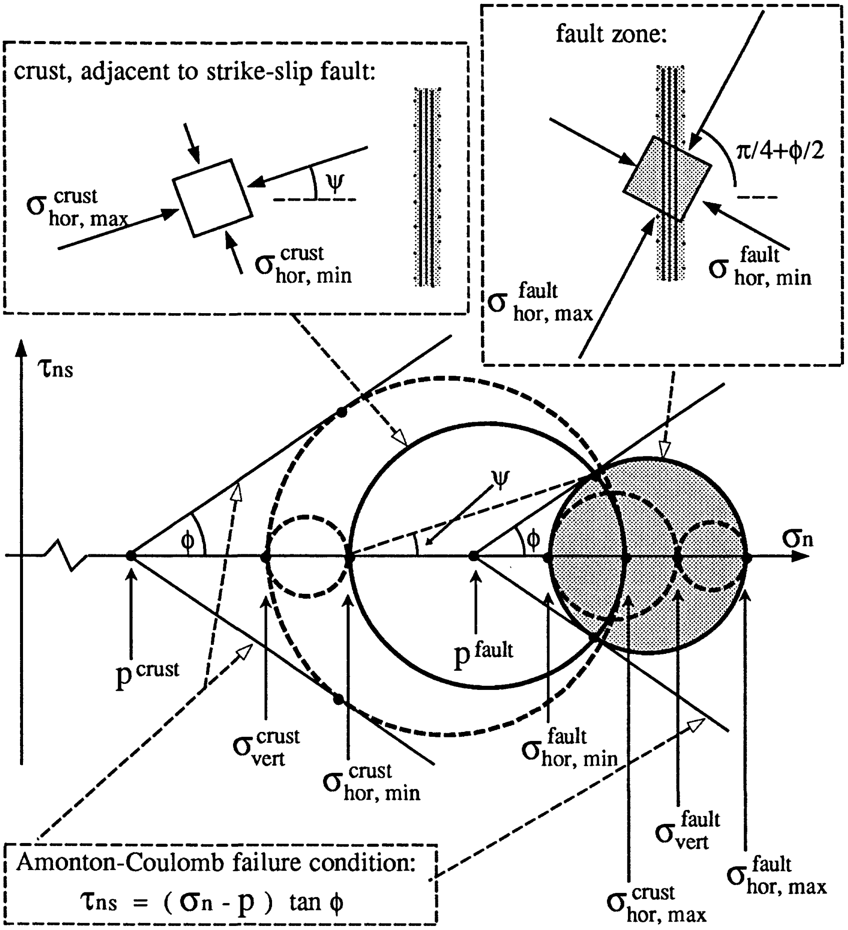

[Drawn for $\phi = 35°$ ($f = \tan\phi = 0.7$) and $\psi = 18°$; i. e., for the maximum σ direction in the adjacent crust making a 72° angle with the fault zone. Similar constructions are possible for arbitrarily small ψ, hence for the maximum σ direction arbitrarily near 90°, when p is near to $\sigma_{\text{hor, min}}$ in the fault zone.]

Figure 3

The Physics and Mechanics of the Brittle-Ductile Transition: Collaborative Research

Brian Evans and Teng-fong Wong, Co-Principal Investigators

USGS Grant # 14-08-0001-G1340
Dept. of Earth, Atmospheric, & Planetary Sciences
Massachusetts Institute of Technology
Cambridge MA 02139

USGS Grant #14-08-0001-G1352
Dept. of Earth & Space Sciences
State University of New York, Stony Brook
Stony Brook NY

Investigations:

The brittle-plastic transition is an important rheological horizon of the crust and upper mantle. We conducted an integrated laboratory study of the deformation mechanisms operating during the brittle-ductile transition, focusing on the micromechanics of semi-brittle flow, and the effect of variations in pressure, temperature and grain size on the strength of rocks deformed in the semibrittle field. Mechanical tests in the standard triaxial loading configuration were performed on several rocks with low porosity: Carrara marble, Solnhofen limestone, [both at room temperature and pressures up to 500 MPa] and Fredrich diabase [at 700-1000°C and pressures up to 500 MPa]. Additionally we investigated compaction behavior of two porous rocks [Berea and Boise sandstone] at room temperature and pressures up to 550 MPa. To complement the experimental investigations we also worked on crack nucleation owing to the stress concentrations around dislocation pileups and fluid inclusions using linear elastic fracture mechanics. An outline of the results and a list of publications and presentations are given below. The appendices contain reprints and preprints which present the results in detail.

The work was a collaborative effort between T.-f. Wong at SUNY Stony Brook and B. Evans at MIT and their colleagues and students. It was supported by the U. S. Geological Survey, Department of the Interior under award numbers 14-08-0001-G1340 (MIT) and 14-008-0001-G1352 (SUNY). This final report and the other publications which resulted from the project were developed under grants from the Department of the Interior, U. S. Geological Survey. However, the contents of those publications do not necessarily represent the policy of that agency, and you should not assume endorsement by the Federal Government.

Results:

The Brittle to Plastic Transition in Carrara Marble:

Samples of Carrara marble were deformed at room temperature to varying strains at confining pressures spanning the range in mechanical behavior from brittle to plastic in a very stiff triaxial deformation apparatus at MIT. Volumetric strain was measured during the experiments and the stress-induced microstructure was characterized quantitatively using optical and transmission electron microscopy. The range of confining pressure over which transitional (semi-brittle) deformation occurs is 30-450 MPa. The macroscopic initial yield stress is constant for confining pressures greater than 85 MPa, whereas the differential stress at the onset of dilatancy increases with pressure up to 300 MPa. The dilatancy coefficient decreases rapidly with increasing pressure up to 100 MPa, and then asymptotically approaches zero for pressures up to 300 MPa. The work hardening coefficient increases with pressure up to 450 MPa; the pressure sensitivity is greatest for pressures up to 100 MPa.

Deformation mechanisms include microcracking, twinning, and dislocation glide. Cracks and voids frequently nucleate at sites of stress concentration at twin boundaries, terminations, and at the intersection of twin lamellae. Geometries suggestive of crack tip shielding by dislocations are also observed. Crack density and anisotropy in samples deformed to axial strains of 3-5% in the semi-brittle field at pressures of 120 MPa and less are comparable to those in the pre-failure brittle sample deformed to an axial strain of 1% at a pressure of 5 MPa, although we detect a qualitative difference in the characteristic length of the cracks. The mean dislocation density at constant differential stress increases significantly for samples deformed at pressures of 230 MPa and greater. Qualitative TEM observations, however, indicate that dislocation glide occurs, at least on a local scale, in some grains in samples deformed in the semi-brittle field at 50 MPa confining pressure. An analysis of the energetics of deformation suggests that the ratio of brittle energy dissipation to total energy dissipation in samples deformed in the semi-brittle regime is at least 60% lower than for a pre-failure sample deformed in the brittle field.

Using the mechanical data, we determined the dilatancy factor, internal friction coefficient, and hardening modulus in both the brittle and the semi-brittle fields and calculated the critical hardening modulus at the onset of shear localization based on *Rudnicki and Rice's* [1975] model. The theoretical values for the critical modulus decrease with increasing confining pressure and are consistently negative for axisymmetric compression. The details of this study are presented in *Fredrich, Evans, and Wong* [1989].

Effect of Grain Size on the Brittle-Plastic Transition in Calcite Aggregates:

Finer-grained calcite rocks are known to have a higher transition pressure than coarser-grained aggregates, and thus, grain size may be an important parameter in delineating the confining pressures under which brittle, semi-brittle, and fully plastic flow occur. In the stiff press at MIT, we investigated the micromechanical basis for this phenomena. Triaxial experiments were performed at room temperature on four natural calcite rocks with grain sizes ranging over 3 orders of magnitude. Both the plastic macroscopic yield stress and the fracture strength increase with decreasing grain size, and the confining pressure at which the transition from work-softening behavior associated with macroscopic shear faulting to macroscopically stable, semi-brittle deformation occurs generally increases with decreasing grain size. The stress ratio σ_3/σ_1 at the brittle-plastic transition is apparently constant, i.e. independent of the grain size.

Brittle-Plastic Transition in Low Porosity Silicate Rocks:

Using the high temperature servo-controlled deformation apparatus at MIT, we have initiated a series of mechanical tests on a natural two-phase rock, Maryland diabase. Major phases in this rock of vanishingly low porosity include plagioclase feldspar and clinopyroxene; biotite and quartz occur as minor phases. Constant displacement rate tests are being conducted in a servo-controlled gas confining medium pressure vessel at temperatures of 800 and 900°C and confining pressures of 100 to 400 MPa. At 800°C and confining pressures of 300 to 400 MPa, the rock undergoes a transition in deformation mode from work softening behavior associated with shear localization, to stable work hardening behavior associated with distributed semibrittle flow. At 900°C, the transition occurs during the pressure interval of 100 to 200 MPa. We are presently conducting preliminary experiments to study the effect of varying initial water content. Particular attention is paid to the frictional characteristics of the high temperature faults, and the effect of small amounts of partial melt on the mechanical behavior. Fredrich and Evans will present the preliminary results at the 1990 Fall AGU meeting.

Acoustic emission measurements:

An acoustic emission (AE) system was set up in the Stony Brook rock mechanics laboratory.

The configuration of the AE counting system was described in detail by Zhang et al. (1990). We recently expanded this system to include 16 sets of discriminators and counters with amplitude threshold levels which can be preset over more than two orders of magnitude. We have successfully tested this new AE module, and our preliminary measurements of b-values during triaxial compression experiments are satisfactory. We have plans to modify this AE system so that it can be used in conjunction with a high-temperature gas rig or a solid medium Griggs rig.

AE measurements were conducted on Carrara marble, Berea sandstone and Boise sandstone. We observed very limited AE activity in Carrara marble samples deformed in both the brittle and the semi-brittle fields. The AE measurements were not helpful in providing insights on the micromechanical processes. In contrast, very high AE activity was observed in the sandstones. The AE measurments elucidate the grain-scale microcracking processes in connection with mechanical compaction and brittle-ductile transition in high porosity rocks (Wong, 1990b). Our AE measurements also help clarify several previously unresolved questions on high pressure embrittlement and shear-enhanced compaction (Zhang, Wong and Davis, 1990). We are in the process of formulating fracture mechanics models to interpret the AE data and microstructural observations.

Brittle Ductile Transition in Porous Rocks:

Using the triaxial deformation apparatus at Stony Brook, we also investigated the micromechanics of the brittle-ductile transition of porous rocks using AE measurements and scanning electron microscopy. The porosity and consolidation history of the sample have strong influence on the failure mode. The experimental results were compared with theoretical predictions of a fracture mechanics model formulated by Sammis and Ashby [1986] for cracks emanating from pores (see Wong, 1989 for details).

Stroh Crack Mechanism:

The interaction among dislocations, deformation twins and microcracks controls the micromechanics of the brittle-plastic transition. A mechanism often cited in the geologic literature is the Zener-Stroh mechanism involving microcracking induced by dislocation pile-ups. We formulated a fracture mechanics analysis of the propagation behavior of a Stroh crack under overall compression (Wong, 1990). Our analysis highlights several important differences between the compressive loading case and tensile loading case, especially with regard to microcrack stability and the important role of the lattice "friction"stress. In general, the propagation of a Stroh crack under compressive loading is expected to be stable.

Review of Recent Experimental and Theoretical Progress:

In the past two decades, major advances have been made in both the experimental observation and theoretical analysis of the brittle to ductile transition [see Horii and Nemat-nasser, 1985; 1986; Sammis and Ashby, 1986] . We recently completed a critical review [*Evans et al., 1989*] of recent progress focussing on four areas: phenomenological observations, microstructural studies, continuum models of shear localization, and micromechanical models of crack coalescence.

Publications:

Thesis:

Fredrich, J. T., Experimental study of the brittle to plastic transition in marble and diabase, PhD thesis, Massachusetts Institute of Technology, Cambridge, Sept. 1990.

Refereed Papers:

Evans, B., Fredrich, J. T., and Wong, T.-f., The brittle to ductile transition in rocks: Recent experimental and theoretical progress, in *The Brittle-Ductile Transition - The Heard Volume, Geophys. Monogr. Ser.* vol 56, edited by A. G. Duba, W. B. Durham, J. W. Handin, H. F. Wang, pp. 1-20, AGU, Washington, D. C., 1990.

Fredrich, J. T., B. Evans, and T.-f. Wong, Micromechanics of the brittle to plastic transition in Carrara marble, , *J. Geophys. Res.*, *94,* 4129-4145, 1989.

Fredrich, J. T., B. Evans, and T.-F. Wong, Effect of grain size on brittle and semibrittle strength: Implications for micromechanical modelling of failure in compression, *J. Geophys. Res.*, in press, 1990.

Wanamaker, B. J., T.-F. Wong, and B. Evans, Decrepitation and crack healing of fluid inclusions in San Carlos olivine, *J. Geophys. Res.*, in press, 1990.

Wong, T.-f. A note on the propagation behavior of a crack nucleated by a dislocation pile-up, *J. Geophys. Res.*, *95,* 8639-8646, 1990a.

Wong, T.-f. Mechanical compaction and brittle-ductile transition in porous sandstones, in press, J. Geol. Soc. London, special issue on "Deformation Mechanisms, Rheology and Tectonics", 1990b.

Zhang, J., T.-f. Wong, T. Yanagidani, and D. M. Davis, Pressure- induced microcracking and grain crushing in Berea and Boise sandstones: acoustic emission and quantitative microscopy measurements, in press, *Mech. Mat.*, 1990.

Zhang, J., T.-f. Wong, and D. M. Davis, High pressure embrittlement and shear-enhanced compaction of Berea sandstone: acoustic emission measurement and microstructural observation, *Proc. 31st U. S. Symposium Rock Mechanics, Denver,* 1990.

Papers presented at Meetings:

Fredrich, J., B.Evans, and T-f. Wong, The mechanics of semi-brittle deformation in Carrara marble, *EOS, Trans. Am. Geophys. Un.*, *68*, 1464, 1987.

Fredrich, J. T., B. Evans, and T.-f. Wong, Effect of grain size on the brittle-plastic transition in calcite aggregates, *EOS, Trans. Amer. Geophys. Un.*, *69,* 1417, 1988.

Wanamaker, B. J., B. Evans, and T.-f. Wong, Fluid Inclusion Decrepitation (Cracking) in San Carlos Olivine, EOS, Trans. Amer. Geophys. Un., 68, 1527, 1987.

Wong, T.-f., Effect of pressure on propagation behavior of microcracks nucleated by Stroh's mechanism, *EOS, Trans. Amer. Geophys. Un.*, *68,* 404, 1987.

Zhang, J., T.-f. Wong and D. M. Davis, Failure modes as a function of porosity and effective pressure in porous sandstone, *Geol. Soc. Am. Abst. Prog.*, *19,* 904, 1987.

Zhang, J., T.-f. Wong, and D. M. Davis, Hydrostatic compaction of porous rock and fracture mechancis analysis of grain crushing, *EOS, Trans. Am. Geophys. Un.*, *69,* 1464, 1988.

Strength Recovery in Rocks and Minerals: Collaborative Research

Brian Evans and Teng-fong Wong, Co-Principal Investigators
USGS Grant # 14-08-0001-G1806
Dept. of Earth, Atmospheric, & Planetary Sciences
Massachusetts Institute of Technology
Cambridge MA 02139

USGS Grant # 14-08-0001-G1807
Dept. of Earth & Space Sciences
State University of New York, Stony Brook
Stony Brook NY

Objectives:

Along geologic faults, repeated earthquake instabilities generate wear materials, which result in a thickening gouge zone as seismic slip accumulates. Seismologic observations suggest that faults may recover in strength during the aseismic period of the earthquake cycle. Field observations of fault zones indicate that minerals in the gouge, breccia, and wall rocks can participate in complex petrologic reactions which probably affect the mechanical properties of the fault.. The coupled effect of wear processes which occur during slip, and healing processes which operate in the interseismic period, may result in variation of seismic stress drop and productivity with recurrence time [*Kanamori and Allen,* 1985], tectonic environment [*Scholz,* 1990], and cumulative slip [*Wesnousky*, 1990]. It is important to have a fundamental understanding of the wear and healing mechanisms and their relation to fault instability. In this project we are investigating strength recovery by solution transfer processes in faulted samples of Carrara marble, Maryland diabase, and Sioux quartzite, and in quartz and calcite gouge.

Wear Processes and Fault Stability

Using conventional triaxial configuration, the frictional sliding behavior of a simulated gouge layer of ultrafine quartz was investigated as a function of slip in the laboratory. The sliding mode evolved from dynamic instability to stable sliding through several sequential stages, each of which had distinct dynamical behavior characteristic of a nonlinear system. Almost periodic, supercritical oscillations marked the onset of dynamic instability. Tens and sometimes hundreds of repeated stick-slip events ensued. The stress drop amplitude decreased monotonically with cumulated slip, and also with increasing load point velocity. As slip accumulated, a period doubling stage was observed, with the stress drop amplitude showing complex bifurcations. This was followed by quasi-static, periodic oscillations which ultimately led to stable sliding. The time scale of the dynamic instabilities is on the order of 0.1 msec. The frequency of the quasi-static oscillations was observed to be proportional to the load point velocity. The intercept from such a linear plot can be used to infer the characteristic slip L, which, according to our data, is several microns, comparable to the median particle size of the simulated quartz gouge. Our data also imply that the friction parameter $[A(B-A)]^{1/2}$ is on the order of 0.1 MPa [*Wong, Gu, and Yanigidani,* 1990].

Our experimental data suggest that dynamic rupture is very efficient in the generation of wear, and that the wear process by itself tends to stabilize the frictional sliding behavior from one seismic cycle to the next. Our experimental setup was designed to isolate this single mechanism. In geologic settings, fault healing processes are expected to be very important during the interseismic period. Such processes do not operate rapidly during room temperature friction experiments. Thus, there are two classes of evolutionary effects: short term effects which operate during periods of several hours at room temperature, and long term effects whose kinetics are slower and require either very long time periods at room temperature, or higher temperatures for typical laboratory time periods.

Short-term Evolutionary Effects

We have studied the short-term evolution effect as manifested by the effect of load point velocity on the frictional instability behavior. During the dynamic phase when we had repeated stick-slip events, the stress drop amplitude decreased with increasing load point velocity. One order of magnitude decrease in load point velocity results in about 30 to 50% increase in the stress drop.

Similar effects were observed in numerical simulations of the nonlinear dynamics of a single degree of freedom spring-slider system following a rate-and state-dependent friction law. We varied the loading velocity by 7 orders of magnitude, the stiffness by 2 orders of magnitude, the mass by 4 orders of magnitude and the velocity weakening parameter $(B-A)$ by a factor of 15. The nonlinear dynamic behavior is in qualitative agreement with that reported by *Rice and Tse* [1985]. For dynamic instability, the stress drop amplitude increases with decreasing stiffness and decreasing mass. In agreement with *Cao and Aki* [1985], our simulations show that the stress drop amplitude decreases with increasing loading velocity. We found an unexpectedly simple relation among stress drop, the loading velocity and the velocity weakening parameter. For fixed values of stiffness and mass, the computed stress drops expressed as a function of the natural logarithm of the loading velocity perturbation fall on a linear trend with a slope equal to $-2(B-A)$. Thus, for an order of magnitude increase in loading velocity, the stress drop decreases by about $4.6(B-A)$, which is comparable to our laboratory data. The numerical simulation results will be presented in the 1990 Fall AGU meeting [*Gu and Wong*, 1990].

To the extent that our simple system can be treated as an analog for earthquakes, our study shows that the velocity weakening parameter $(B-A)$ exerts control over the magnitude of the static stress drop which is by far stronger than that of loading velocity, stiffness or inertia. Along a fault with heterogeneous frictional behavior and multiple degrees of freedom. the variation of stress drop with loading velocity is expected to be more complex than what we observed. Some of the seismologic data may have to be interpreted using values of $B-A$ which are higher than laboratory measurements. The discrepancy may be attributed to interseismic healing processes not reproduced in short-term laboratory studies. A review will be given by *Wong* [1990] in a meeting on Earthquake Mechanics in Tokyo in November.

Long Term Evolutionary Effects

We have been investigating long term evolutionary effects in several systems. Most recently we observed fault healing in series of triaxial mechanical tests at temperatures ranging between 700-950°C in faulted samples of Fredrich diabase. In some of the tests, stable work softening was followed by an interval during which the strength first recovered and then exceeded that observed before softening. The modulus of the stress-strain curve during the recovered period was only slightly degraded in comparison to that observed prior to the softening event. One experiment exhibited two intervals of softening and recovery; correspondingly, two macroscopic faults were found to traverse the length of the sample. The stress-strain data suggest that elevated pore pressures induced shear localization. The fault may have established a high permeablity conduit to the atmosphere; perhaps causing the pore pressure to drop and the normal stress on the fault to increase. This interpretation is certainly not the only possible explanation, but it is clear from both the level of strength recovery and electron microscopy that physical "healing" of the fault has occurred. We are presently performing additional experiments to investigate further the time-dependent mechanical properties of fault zones at high temperatures *[Fredrich and Evans, 1990]*.

In a second suite of experiments we performed preliminary hot isostatic pressing of quartz powders saturated with water at temperatures from 600-850°C. For example, after hot pressing at effective pressures of 170 MPa for several days, the final porosities of the aggregates were from 7-20%. Compaction rates vary from 10^{-5} /sec to 10^{-8} sec at the end of the experiment. Pore fluid pressures were constant during a particular test, but ranged from 200 MPa to 400 MPa. Qualitative observations of the competency of the samples suggest that the compressive strength has increased by a substantial amount. Scanning electron microscopy shows that grain-grain contacts develop grain boundary regions or "necks" which increase in size during densification. New mechanical experiments which are in progress are designed to produce a lithified region of quartz gouge along an inclined sawcut within Sioux quartzite. The induration portion of the experiments will be done at high temperature, but initial tests of the strength of the resulting synthetic fault zone will be tested at room temperature.

References

Evans, B., and D. Lockner, Densification and Electrical Properties of Hot Pressed Quartz Aggregates, *EOS*, *70*, 1323, 1989.

Fredrich, J. T., and B. Evans, High Temperature Fracture and Flow of Maryland Diabase, to be presented at *Fall AGU Meeting*, 1990.

Gu, Y. and T.-f. Wong, The effects of stiffness, loading velocity, and inertia on the dynamics of a single degree of freedom spring-slider system, to be presented at *Fall AGU Meeting*, 1990.

Kanamori, H. and C. R. Allen, Earthquake repeat time and average stress drop, in *Earthquake Source Mechanics*, edited by S. Das et al., 227-235, 1985.

Rice, J. R., and S. T. Tse, Dynamic motion of a single degree of freedom system following a rate and state dependent friction law, *J. Geophys. Res.*, *91*, 521-530, 1986.

Scholz, C. H., *The Mechanics of Earthquakes and Faulting*, Cambridge University Press, 1990.

Wesnousky, S. G., Seismicity as a function of cumulative geologic offset: some observations from southern California, *Bull. Seismo. Soc. Am.*, *80*, 1374-1381, 1990.

Wong, T.-f., Stabilization of faulting by wear processes, *International Symposium on Earthquake Source Physics and Earthquake Precursors*, Tokyo, 1990a.

Wong, T.-f., Y. Gu, and T. Yanagidani, Stabilization of faulting by wear processes, to be presented at *Fall AGU Meeting*, 1990b.

HIGH-FREQUENCY SEISMIC AND INTENSITY DATA

9910-03973

Jack F. Evernden
Branch of Engineering Seismology and Geology
U.S. Geological Survey
345 Middlefield Road, MS 977
Menlo Park, California 94025
415/329-5627 or FTS 459-5627

Investigations

Investigating the quantitative relationships between maximum acceleration, velocity, and displacement *vs.* seismic intensity and seismic region.

Results

Strong-motion data of the San Fernando, Loma Prieta, and Imperial Valley earthquakes demonstrates the uniformity of the maximum acceleration *vs.* maximum velocity and the maximum acceleration or maximum velocity *vs.* intensity relationships for these three California earthquakes. In the course of the analysis of these data (as well as those below), it was clearly established that the proper statistical fitting relationship of the three used in the previous publication is that minimizing the sum of the perpendicular distances of all data points from the best fit line. On a log (ground motion) *vs.* intensity (RFI), the data over the full range of observation indicate a straight line relationship to be statistically tenable. The codes I have distributed to numerous users used one of the two incorrect relationships published earlier when converting predicted intensity to ground motion. Any who wish may request the new version of QUAK2 which uses the MPD relationships. Of interest is the demonstration that maximum velocity and maximum acceleration are not a function of site rock type when these quantities are plotted against site intensity.

Adding the strong motion data of the Chili 1985, Mexico 1985, and Irpinia 1980 earthquakes to the pot leads to the conclusion that there is a universally applicable intensity *vs.* maximum velocity curve, while intensity *vs.* maximum acceleration is regionally dependent, maximum acceleration at a given intensity being at least twice as high in the eastern United States as in western California.

All of the above analysis is in a paper now being considered for publication in the Bulletin of the Seismological Society of America.

Reports

No reports this period.

10/90

Mechanical Analysis of Large-Scale Folds Forming Above a Detachment

14-08-0001-G1700

Raymond C. Fletcher
Center for Tectonophysics
Texas A&M University
College Station, TX 77843
(409) 845-3251

Objective: For a class of earthquakes - e.g., the 1983 Coalinga Earthquake (M=6.7), the 1987 Whittier Narrows Earthquake (M=5.9)- the seismogenic faults occur within or are intimately related to large-scale folds which form above a shallowly-dipping basal detachment. The aim of the present study is to obtain a quantitative description of the mechanical environment of seismogenic faulting within large-scale folds, through theoretical modeling of fold initiation and growth, to apply the results to several natural structures, in order to test their value in interpreting the observed structure or the behavior in active fold growth, and to discuss the potential significance of the findings for the assessment of earthquake hazards.

Results: A study of the mechanics of sliding across a thrust ramp has been started to provide insight into the mechanics of "fault-bend folding", a process that is prominently employed in the interpretation and analysis of the form and kinematics of the fold and fault configurations implicated in fold-associated seismogenic faulting. Earlier studies (Berger and Johnson, 1980; Kilsdonk and Fletcher, 1989) obtained approximate solutions for stress and deformation in a deep isotropic viscous medium sliding across a thrust ramp. The method is accurate provided the thrust ramp has a dip of no greater than about 15°. The slip surface has been treated either as frictionless or as having finite sliding resistance at the thrust ramp (Berger and Johnson, 1980). The stress and deformation determined from the model does not take into account any regional contribution of horizontal compressive stress; the results therefore refer only to the anomaly associated with the presence of the thrust ramp. In this study, we consider: (i) a frictionless detachment, (ii) a layer of finite thickness, H, (iii) an anisotropic viscous medium to account for the relative weakness of the rock mass in bed-parallel shear, (iv) the effect of gravity through the induced topography, (v) the decay of topography by surface processes, and (vi) quasi-static viscoelastic transients. Features (v) and (vi) have not yet been implemented.

A base level for the study of quasistatic transients is provided by first studying the steady-state. The model is specified by three parameters. (1) $T/(2d)$ is the ratio of layer thickness to ramp width; results for $T/(2d) = 1$ and $T/(2d) \to \infty$ (half-space) are illustrated here. (2) $M = \eta_n/\eta_s$ is the ratio of the viscosity in layer-parallel shortening or extension to that in layer-parallel shear. If the layer is composed of two finely-interlayered isotropic media with viscosities η_1 and η_2 and volume fractions f_1 and f_2, $M \approx (f_1\eta_1 + f_2\eta_2)(f_1/\eta_1 + f_2/\eta_2)$. Maximum anisotropy is achieved for $f_1 = f_2 = 0.5$, for which $M \approx 0.25(1 + r)^2/r$, where $r = \eta_2/\eta_1$. Since a strength or viscosity ratio $r = 1/100$ is likely to be an extreme value for common rock types, $M \leq 25$. (3) $S = \rho g H/[2\eta_n(U/2d)]$ is the ratio of the lithostatic stress at the base of the layer to a stress associated with the deformation at the ramp, where U is the sliding velocity. This parameter determines the effect of gravity in suppressing the development of surface topography. For a 10 km layer, in which the stress associated with deformation at the ramp is ≈ 64 MPa ($U \approx 1$ cm/a, $2d \approx 10$ km, $\eta_n \approx 10^{21}$ Pa-s), $S \approx 4$.

Figure 1 shows the streamlines and fold form for two cases in which the layer thickness is much larger than the ramp width. Layering truncated by the ramp is assumed to have translated beyond the right edge of the region shown. The deformation for both the isotropic layer (M = 1) and the anisotropic layer (M = 10) is concentrated near the sliding surface. Layers thicken as they approach the lower flat-ramp corner, thin as they pass along the ramp, and finally thicken past the upper ramp-flat corner. A net thinning takes place in the lower layers, since the upper streamlines are more nearly planar. Contours of layer-parallel shortening/extension rates and layer parallel shear rates (Fig. 2) for these two cases show: (a) zones of layer-parallel shear centered at the ramp-flat corners; (b) the greater magnitude of shear in the case of the anisotropic layer, and its concentration into narrower regions that persist to greater heights; (c) layer-parallel thinning over the ramp, with thickening above the flats in the vicinity of the corners; and (d) the much smaller rates of layer parallel - thickening/thinning for the anisotropic layer.

Fold forms and changes in layer thickness are shown for a layer whose thickness is equal to the ramp width in Figure 3. The case S = 0 corresponds to a limit in which the upper surface is kept perfectly plane by surface processes. No perceptible changes in layer thickness occur. The fold form broadens in the isotropic case (M = 1), but does not perceptibly broaden in the anisotropic case (M = 10); the latter well approximates fault-bend fold form to the degree of approximation inherent in the analysis. Gravity tends to maintain a flat upper surface except in the immediate region of the ramp, where a well-defined fold is present. The variation in layer thickness is intermediate in degree between that in the halfspace case and that in the S = 0 case.

References:

Berger, P., and A.M. Johnson, First order analysis of deformation of a thrust sheet moving over a ramp. Tectonophysics, 70, T9 - T24, 1980.

Kilsdonk, B., and R.C. Fletcher, An analytical model of hanging-wall and footwall deformation at ramps on normal and thrust faults, Tectonophysics, 163, 153 - 168, 1989.

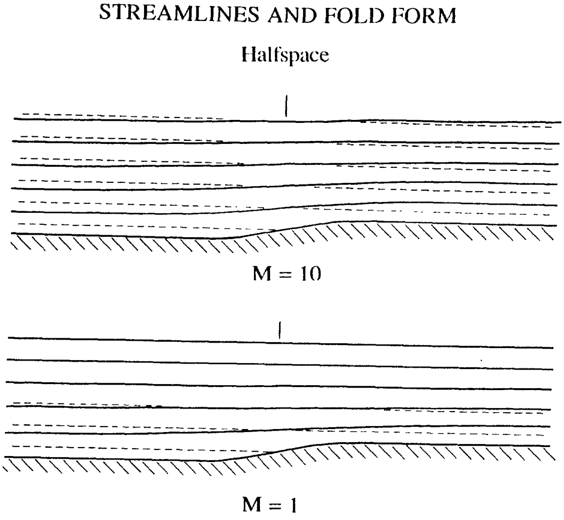

Figure 1. See text for further explanation.

STRAIN RATES

Halfspace

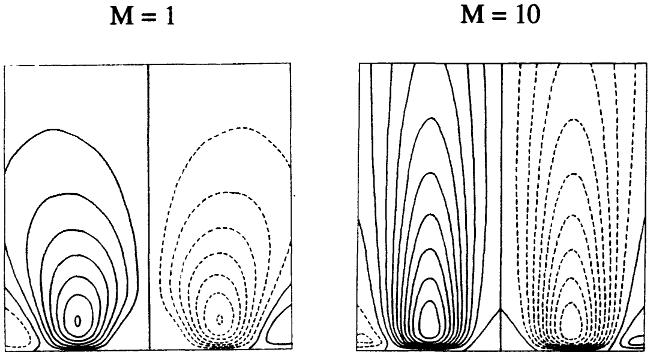

Layer-Parallel Shear, ε_{xz}

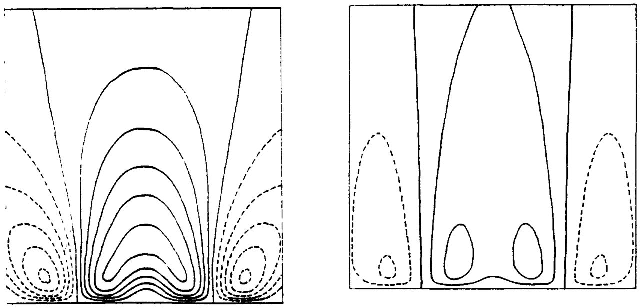

Layer-Parallel Shortening/Extension, ε_{xx}

Contour interval 10 in units:
Ramp Slope * (Sliding Velocity / Ramp Width)

solid lines: positive and zero values

Figure 2. See text for further explanation.

STREAMLINES AND FOLD FORM

Layer Thickness = Ramp Width

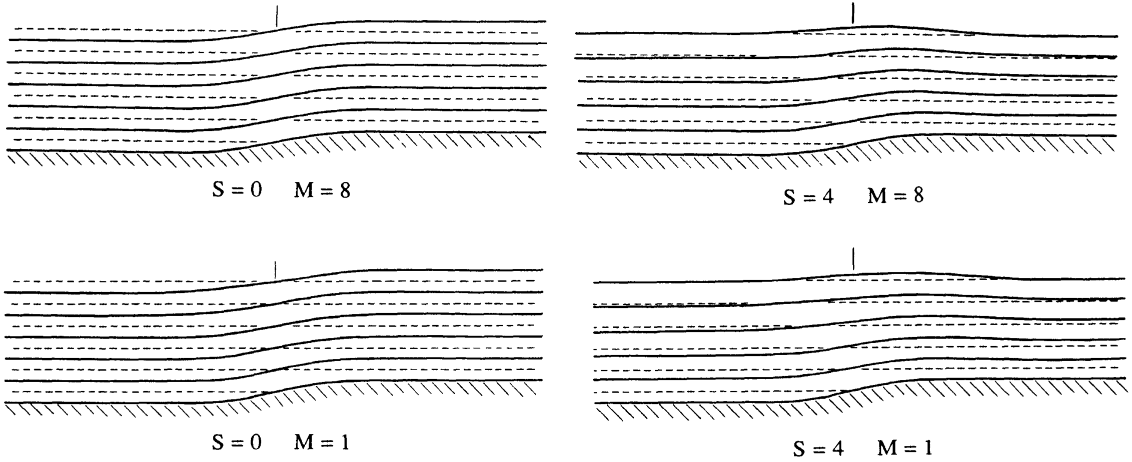

Figure 3. See text for further explanation.

Pressure Solution, Crack Healing and Crustal Stress

9960-04543

Stephen H. Hickman
Branch of Tectonophysics
U.S. Geological Survey
345 Middlefield Rd., MS 977
Menlo Park, CA 94025
(415) 329-4807

Investigations

1. To better understand the processes controlling the physical and temporal evolution of physical properties in the earth (e.g. permeability, seismic velocities, and density), the mechanisms and kinetics of solution-transport creep, and the micromechanics of friction and fault strengthening, we are beginning a detailed experimental study of pressure solution and crack healing under load in simple quartz/water systems. This study employs experiments with single crystals in well-controlled model geometries and experiments on polycrystalline aggregates.

2. Although knowledge of the pathways and rates for fluid migration in the earth's crust is critical to a full understanding of such diverse phenomena as the mechanics of rock deformation and faulting, metamorphic reaction kinetics, and heat and mass transfer by circulating fluids, the permeabilities of rocks at depths of greater than a few kilometers are almost completely unknown. To obtain more accurate information on rock matrix permeability at depth, we are making (together with David Lockner of the U.S.G.S., Menlo Park) simultaneous measurements of permeability and resistivity on cores recovered from the 12-km-deep Kola Deep Well in the Soviet Union. By making simultaneous permeability and resistivity measurements at a variety of confining pressures, we hope to quantify -- and perhaps correct for -- the effects of stress-relief cracking upon physical property measurements made on cores recovered from deep boreholes.

3. Although borehole breakouts have been widely used to study in-situ stresses, the extent to which variations in breakout geometry within a given well reflect variations in rock strength and the extent to which they reflect real fluctuations in the in-situ stress field is largely unknown. To improve our understanding of the mechanics of breakout formation, we have initiated a cooperative U.S./Soviet program to study the distribution, orientation, and morphology of breakouts from several deep and ultra-deep boreholes in the Soviet Union using borehole televiewer and oriented four- and eight-arm caliper logs together with laboratory strength measurements on cores.

Results

1. All components necessary for the single-crystal pressure solution and crack healing experiments have been designed and ordered. Assembly and testing of the completed high-pressure/temperature hydrothermal system will begin in early FY 1991.

2. As reported in the preceding technical summary, we have conducted constant flow-rate permeability measurements on three core samples taken from depths of 11.4 to 12.0 km in the Kola well. S. Hickman presented the results of these permeability investigations during a scientific exchange trip to the Soviet Union in the summer of 1990. At this time he was provided with 16 additional cores from the Kola well at a variety of depths, in addition to selected surface equivalents of these samples. We are presently seeking funds to continue our investigations on these samples.

A significant problem that we are currently addressing in this study is how to determine in-situ properties from samples that have undergone significant stress-relief cracking during coring. By making simultaneous measurements of permeability and electrical resistivity, and drawing on the equivalent channel model of Walsh and Brace (1984), we hope to devise a method for separating the effects of stress-relief cracks from those of the pre-existing crack population. In so doing we are assuming that the stress-relief cracks have different characteristics (aspect ratio, surface roughness, tortuosity, etc.) than the pre-existing in-situ cracks and thus effect physical properties in different ways. By assuming that fluid flow paths for permeability are the same as current paths for resistivity, the analysis of Walsh and Brace predicts that the slope of $\sqrt{(3kF)}$ *vs* log (P_{eff}) should be proportional to the rms channel roughness, where P_{eff} is the effective confining pressure, k is permeability, and F (equal to the resistivity of the rock divided by the resistivity of electrolyte) is the formation factor. Application of this approach to one of the three cores from the bottom of the Kola well showed a distinct break in slope at the predicted in-situ effective confining pressure, suggesting a fundamental change in the dominant crack population.

As an additional test of the applicability of the Walsh and Brace model, we have measured the change in porosity of the Kola samples as they were pressurized. From their analysis, the slope of a plot of $\sqrt{(3kF)}$ *vs* porosity change is the reciprocal of the specific surface area $(A_s/V)^{-1}$ of the equivalent channel, where A_s is the crack surface area and V the rock volume. Once again, we see a distinct break in slope near the estimated in-situ effective confining pressure. We believe that this approach shows promise in allowing us to identify the confining pressure corresponding to the transition between stress-relief-crack dominated and natural-crack-dominated behavior and, hence, make accurate determinations of in-situ matrix permeabilities. Similar tests will be conducted on cores recently obtained from the Kola well at a variety of depths, in conjunction with tests on the same rock types collected from the surface, to see if the transition pressures determined using the equivalent channel model scale with depth.

3. S. Hickman conducted a scientific exchange trip to the Soviet Union in the summer of 1990, during which time he visited the Kola and Krivoy Rog well sites, presented results from permeability investigations on the Kola core (see above), and conducted negotiations regarding future cooperative work both in rock mechanics and in the study of borehole breakouts and in-situ stress at these sites. During this trip, he also discussed possible collaborative in-situ stress studies in their 4-km-deep Tyrnyauz well in the Caucasus Mountains, near the site of the 1988 Armenian earthquake ($M = 6.9$). At this time, the Soviet Ministry of Geology provided him with an extensive suite of caliper and other geophysical logs from the Tyrnyauz and Krivoy Rog wells. In response to this visit, we have submitted a proposal to conduct a study of borehole breakouts and in-situ stress in both the Kola and Tyrnyauz wells, using 4- and 8-arm caliper logs, laboratory strength measurements, and borehole televiewer logs which we hope to conduct in FY 1991.

References Cited

Walsh, J., and W. Brace, The effect of pressure on porosity and the transport properties of rock, *J. Geophys. Res.*, *89*, 9425-9431, 1984.

Reports

Hickman, S., Field evidence for and against a weak San Andreas fault, *in* Proceedings of Symposium on Fault Mechanics and Transport Properties of Rocks, Cambridge, MA, 1990 (abstract).

Hickman, S., The strength of active faults in the Earth's crust and the high stress/low stress controversy, *Trans. Amer. Geophys. Union*, in press, 1990 (abstract).

Hickman, S., and B. Evans, Experimental pressure solution in halite: The effect of grain/interphase boundary structure, *J. Geol. Soc. London*, in press, 1990 (paper).

Hickman, S., and B. Evans, An experimental study of intergranular pressure solution and sintering using halite single crystals, *in*: Proceedings of SEG Workshop on Permeability, Fluid Pressure and Pressure Seals in the Crust., Denver, CO, 1990 (abstract).

Lockner, D., S. Hickman, J. Byerlee, V. Kuksenko, A. Ponomarev, and A. Sidorin, Laboratory-Determined Permeability of Cores from the Kola Deep Well, USSR, *in*: Proceedings of SEG Workshop on Permeability, Fluid Pressure and Pressure Seals in the Crust., Denver, CO, 1990 (abstract).

Earthquakes and the Statistics of Crustal Heterogeneity

9930-03008

Bruce R. Julian

Branch of Seismology
U.S. Geological Survey
345 Middlefield Road - MS77
Menlo Park, California 94025
(415) 329-4797

Investigations

Both the initiation and the stopping of earthquake ruptures are controlled by spatial heterogeneity of the mechanical properties and stress within the earth. Ruptures begin at points where the stress exceeds the strength of the rocks, and propagate until an extended region (''asperity'') where the strength exceeds the pre-stress is able to stop rupture growth. The rupture termination process has the greater potential for earthquake prediction, because it controls earthquake size and because it involves a larger, and thus more easily studied, volume within the earth. Knowledge of the distribution of mechanical properties and the stress orientation and magnitude may enable one to anticipate conditions favoring extended rupture propagation. For instance, changes in the slope of the earthquake frequency-magnitude curve (''b-slope''), which have been suggested to be earthquake precursors and which often occur at the time of large earthquakes, are probably caused by an interaction between the stress field and the distribution of heterogeneities within the earth.

The purpose of this project is to develop techniques for determining the small-scale distributions of stress and mechanical properties in the earth. The distributions of elastic moduli and density are the easiest things to determine, using scattered seismic waves. Earthquake mechanisms can be used to infer stress orientation, but with a larger degree of non-uniqueness. Some important questions to be answered are:

** How strong are the heterogeneities as functions of length scale?

** How do the length scales vary with direction?

** What statistical correlations exist between heterogeneities of different parameters?

** How do the heterogeneities vary with depth and from region to region?

Scattered seismic waves provide the best data bearing on these questions. They can be used to determine the three-dimensional spatial power spectra and cross-spectra of heterogeneities in elastic moduli and density in regions from which scattering can be observed. The observations must, however, be made with seismometer arrays to enable propagation direction to be determined. Three-component observations would also be helpful for identifying and separating different wave types and modes of propagation.

The stress within the crust is more difficult to study. Direct observations require deep boreholes and are much too expensive to be practical for mapping small-scale variations. Earthquake mechanisms, on the other hand, are easily studied and reflect the stress orientation and, less directly, its magnitude, but are often not uniquely determined by available data.

This investigation uses earthquake mechanisms and the scattering of seismic waves as tools for studying crustal heterogeneity.

Results

Because of conflicts caused by the Loma Prieta earthquake, travel, and field work, several semiannual reports for this project have been delayed. This report therefore covers activities in FY1990 and 1991.

Automatic Real-time Earthquake Monitoring

Monitoring central California earthquakes using data from the Allen-Ellis Real-Time Processor (RTP) has continued routinely. Following the Loma Prieta earthquake of October 18, 1989, data from these systems were critical in keeping scientists, disaster workers, and the public informed about earthquake activity. Unfortunately, however, the earthquake damaged the primary computer, and it performed unreliably during the critical first several weeks after the earthquake, so a workstation was acquired to take over as the main RTP processing machine. This computer has proven to be highly reliable, both because it is more modern and simpler than its predecessors, and because it is not being used as a general-purpose computer, but is dedicated to only the task of real-time earthquake monitoring. It's presence has had the additional benefit of allowing the branch's decade-old PDP-11/70, which had reached the stage of doing little else than acting as a third-level backup for RTP monitoring, to be eliminated.

The earthquake alarm software was re-written to make it easier to use. The driving table that defines the geographic regions, magnitude thresholds, etc., for alarms has been made easier to understand and to modify. Comments may now be placed in it, and it has a powerful macro facility that allows alarm rules to be written more compactly and readably, so they are clearer and easier to modify. An immediate benefit of these improvements was that several errors and inconsistencies in the tables were discovered and corrected.

The software was also modified to reduce the number of alarms during swarms. The previous behavior, which set of an alarm for each event in a swarm, caused the transmission of thousands of electronic mail messages, and severely slowed the computers. Now, the status of recent alarms is remembered, and the alarm is set off again only after enough new events occur to cause an alarm in their own right.

Chaos, Nonlinear Dynamics, and Earthquakes

A central fact about earthquake occurrence is that it is complicated and difficult to predict. Recent work on nonlinear dynamical systems, however, has shown that complicated behavior is not necessarily evidence of underlying complexity in a system, and have led to the development of methods that can often predict behavior of these systems a limited time into the future. The possible application of these ideas to earthquakes is an obvious and exciting possibility, but the knowledge and expertise that are needed are spread throughout many disciplines of mathematics and physics. To bring together experts from these many fields, Dr. John Rundle (Lawrence Livermore National Laboratory), Dr. Donald Turcotte (Cornell University), and I organized a 4-day workshop on the subject of "Physics of Earthquake Faults: Deterministic or Chaotic?" at the Asilomar Conference Center in February, 1989. This conference brought together 38 Earth scientists and 15 physicists and mathematicians, who shared their ideas with great enthusiasm is sessions that lasted far beyond the scheduled time each evening. It was widely felt that much fruitful cross-disciplinary research will be stimulated, and that it would be worthwhile to have another such meeting in two or three years to share the results of this work. A summary of the papers presented at the workshop was published in EOS, and a report by Christopher Scholz was published in Nature,

Volcanic and Geothermal Earthquake Mechanisms

In the last several years, evidence has accumulated that some earthquakes in volcanic and geothermal areas have mechanisms that can not be explained by shear faulting. The physical processes causing these "non-double-couple" events are not understood, although several suggestions have been made (tensile failure and simultaneous shear faulting, for example). It is likely that understanding these unusual earthquakes would help in predicting volcanic activity and in prospecting for and exploiting geothermal energy.

Ongoing swarms of earthquakes at Mammoth Mountain during the spring and summer of 1989 provided an opportunity to obtain high-quality recordings of volcanic earthquakes and study their mechanisms carefully. These swarms were notable for containing many rapid "bursts" of earthquakes occurring in an interval of a few seconds. Such behavior is unusual for earthquakes, and it is thought likely that it is caused by an unusual process, perhaps hydraulic fracturing. A network of 12 three-component seismometers and GEOS digital recorders was deployed for four days in June, 1989. The limited storage capacity of these instruments required that they be operated in a triggered mode, which proved not to be ideal for events that occur in rapid bursts. Nevertheless, dozens of earthquakes were recorded, including several on most of the instruments, and the records that were obtained are of high quality. Analysis of these data has required developing a large body of software for determining clock corrections and interactively processing digital seismograms (see below). Analysis of the Mammoth Mountain data is continuing at present. The final outcome of this experiment is expected to include accurate relative location of events within bursts, from which crack propagation may be resolvable, and higher-order moment tensor earthquake mechanisms, from which physical inferences can be drawn more easily than from conventional fault-plane solutions and first-order moment tensors.

The Hengill geothermal area in Iceland is probably the richest known source of non-double-couple earthquakes in the world. First motion data obtained in this area by Dr. Gillian Foulger of Durham University (U.K.) in 1981 first showed the anomalous nature of the earthquakes from this area, and tomographic analysis has now produced a three-dimensional model of the seismic-wave speed in the area. Working in cooperation with Dr. Foulger, we have used this model together with three-dimensional ray tracing methods to improve the accuracy of the first-motion analysis, and to show that the anomalous mechanisms are not an artifact of complex structure or event mislocation (see Figure 1).

One reason that non-double-couple earthquakes remain controversial and poorly understood is the lack of high-quality recordings of them. Dr. Foulger and I have now received support, from a G. K. Gilbert Fellowship, to deploy a dense seismic network at Hengill during the summer of 1991 to obtain digital three-component data, and have begun actively planning the details of the experiment. To test the instruments and the experimental procedure, a smaller network will be deployed at The Geysers geothermal area, California, during the Spring of 1991. Both deployments are expected to provide data of unprecedented quality bearing on the physical process causing geothermal and volcanic earthquakes. To optimize the layout pattern of the seismometers, we plan to use information about three-dimensional structure of the areas. Figure 2 shows how the structure at Hengill affects the points of emergence at the surface of seismic rays that leave an earthquake upward. Plots such as this show areas of focusing and de-focusing of seismic-wave energy, as well as regions where multiple arrivals and complicated signals are expected. We believe this will be the first time information of this type has been used in the design of a seismic experiment.

Interactively Processing Digital Seismic Data

Processing digital seismograms, such as those discussed above from Mammoth Mountain and Iceland, has always been a difficult task; digital data are inherently not well suited to human inspection and manipulation. Interactive computer programs are needed to make digital processing practical, but until recently, hardware adequate to the task was expensive. This problem has recently been solved, by the advent of cheap workstations with bit-mapped graphics displays. Public-domain software is available for processing digital seismic data on workstations, but this software currently lags behind the hardware in its development. To process the data collected at Mammoth Mountain in 1989, we have been forced to undertake an ambitious project of augmenting the capabilities of the AH (Ad Hoc) software, originally written at Lamont-Doherty Geological Observatory. In particular, we have modified the program sunpick in several ways. This program now is highly hardware-independent, uses a hardware-independent format for seismic data that achieves a factor of two saving in disk space, can handle multi-component data with variable start times, durations and sampling rates, and allows the measurement of multiple phases of arbitrary types from each seismogram. It has also been connected to hypocenter-location programs in a general, user-modifiable manner. Similar interfaces to focal-mechanism and waveform inversion programs are now under development.

References

Scholz, Christopher H., Global perspcctives of chaos, **Nature**, **338**, 459-460, 1989.

Reports

Rundle, John B., Bruce R. Julian, and Donald L. Turcotte, Are earthquakes deterministic or chaotic?, EOS, American Geophysical Union Trans., **70**, 880-882, October 3, 1989.

Julian, Bruce R., Nonlinear excitation of volcanic tremor by fluid flow (abs.), **EOS, American Geophysical Union Trans.**, **69**, no. 44, 1437, 1988.

Julian, Bruce R., Volcanic tremor as a nonlinear flow-excited oscillation, paper presented at workshop ''Physics of Earthquake Faults: Deterministic or Chaotic?'', Asilomar Conference Center, Pacific Grove, Calif., 13 Feb. 1989.

Julian, Bruce R., Are earthquakes chaotic?, **Nature**, **345**, 482, 1990.

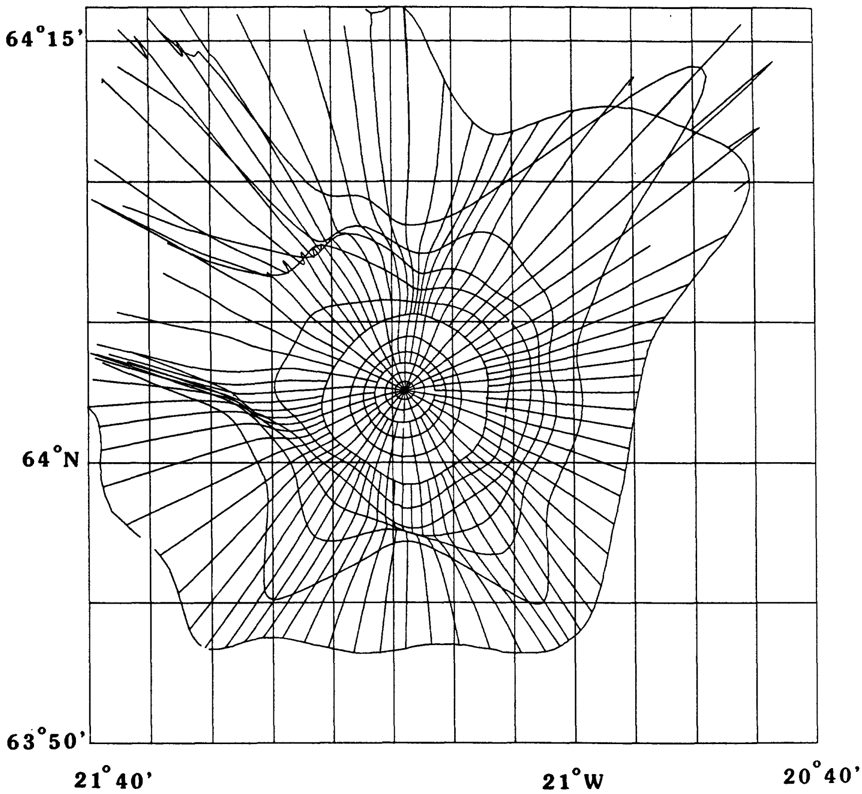

Figure 2: Map of Hengill geothermal area, Iceland, showing how rays from a 4-km-deep earthquake are distorted by complex structure. Curved lines are parallels and meridians on the upper focal hemisphere, as projected onto the surface along seismic rays in three-dimensional structure derived using tomographic methods. Parallels are plotted for take-off angles of 90°, 95°, 100°, 105°, 110°, 115°, 120°, 130°, 140°, 150°, 160°, and 170°. Meridians are spaced 5° apart in the outer part of the plot, and at 10° and 20 ° intervals for more nearly vertical rays. The anomalous spreading of rays traveling to the west is evident both here and in Figure 1.

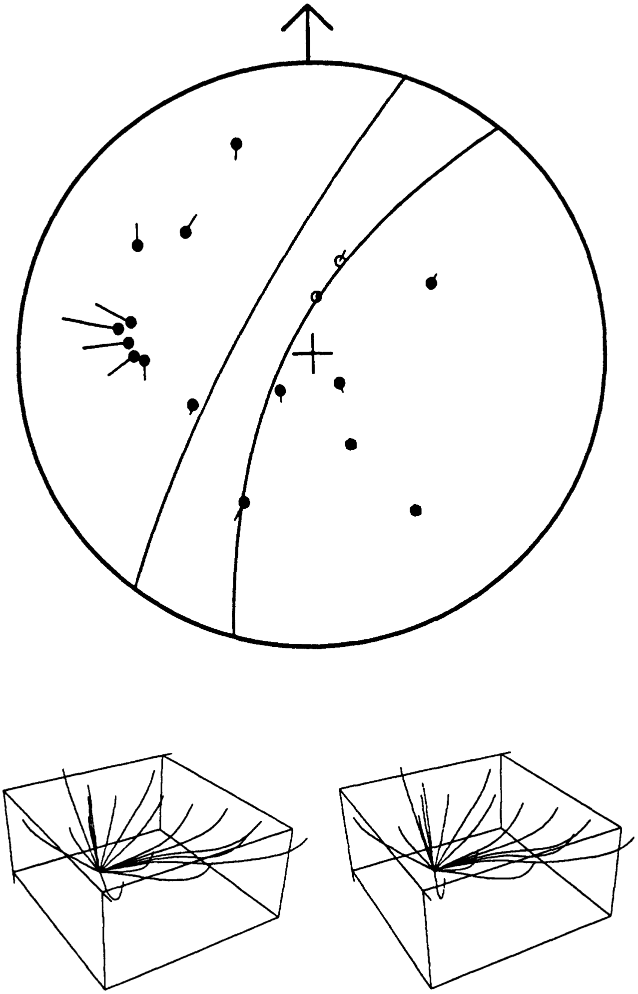

Figure 1: Top: Observed first motions from a non-double-couple earthquake at the Hengill volcanic complex, Iceland, showing effect of ignoring three-dimensional structural features in analyzing the focal mechanism. Solid circles: compressions; open circles; dilatations. Circles are plotted at the positions determined by tracing rays in three-dimensional structure. Lines emanating from circles show positions determined from one-dimensional regionally averaged model. The upper focal hemisphere is shown in stereographic projection.

Bottom: Stereoscopic view of three-dimensional ray paths used in determining focal-sphere positions plotted above. View is from slightly west of north.

EXPERIMENTAL ROCK MECHANICS

9960-11180

Stephen H. Kirby
Branch of Tectonophysics
U.S. Geological Survey
345 Middlefield Road, MS/977
Menlo Park, California 94025
(415) 329-4847

Investigations

A solicited paper for the journal *Science* was written concerning the thermodynamics and mechanics of deep earthquakes. This work follows up on earlier experimental studies on shear instabilities that occur in some minerals that undergo localized phase transformations.

Data analysis continued in our studies of the roles of hydrothermal alteration in the low sliding resistance of dunite in the presence of water.

Investigations into the properties of CO_2-rich fluids compared to basaltic liquids from which they exsolve continues with the goal of understanding the roles of the fluid in mantle fracture and earthquakes beneath volcanic centers like Hawaii.

Results

1. A comprehensive review of the thermodynamic state, expected mineral distribution, state of stress and high-pressure faulting behavior of deeply-subducting lithosphere was completed as a solicited General Report for the journal Science (Kirby, Durham and Stern, 1990). The conclusions are summarized in Fig. 1 that illustrates the roles of phase transformations in the occurrence of deep earthquakes in the sinking lithosphere. This work upsets the conventional view that deep earthquakes are generated solely by the equilibrium between the negative bouyancy forces that accompany the greater density of the slab and the viscous forces resisting plate penetration. Kinetic theory, recent experiments on the rates of mantle phase changes and seismic investigations have shown that a thin metastable wedge of olivine persists at depths below the

equilibrium reaction lines (Sung and Burns, 1976; Rubie et al., 1990). Low temperatures in the slab interiors permits olivine to decend below the equilibrium boundaries that at high temperatures mark the onset of transformations to denser phases. A recent study by Iidaka and Suetsugu (1990) has confirms the existence of the wedge in the subducting Pacific plate beneath Japan. Mark Richards and Chuck Wicks (1990) have detected a compressional-wave phase that they interpret as a shear wave converted at a phase boundary at 650-720 km depth in the Tonga and Izu Bonin subduction zones. This suggests that the olivine wedge does not persist below that depth range. This metastable wedge has two consequences. First, volume reduction in the lithospheric material that does transform to denser phases in the envelope around the wedge puts the wedge under a deviatoric compression parallel the wedge (Goto et al., 1987). Second, the wedge puts olivine in a thermodynamic state of extreme metastability while under high shear stresses. The olivine-spinel transformation is strongly exothermic and laboratory deformation studies (Kirby, 1987; Green and Burnley, 1989) show that similar transformation in other minerals that take place at lower pressures exhibit a type of shear instability that produces a bang in the laboratory, a process we term *transformation faulting*. This shear instability, unlike convention brittle fracture, is facilitated by pressure; no transition to ductile behavior is observed with increasing pressure. Within the wedge, this combination of high non-hydrostatic stresses and comparable critical shear stresses for transformation faulting, according to this hypothesis, causes deep earthquakes. The model explains a number of properties of deep earthquakes: their spatial distribution, some of their source characteristics and the lack of aftershocks of the type that occur at shallow depths. It also has important geodynamic implications.

2. Data analysis and library research continue in preparation for writing up the eventual JGR paper on the anomalously low sliding resistance of dunite under hydrothermal conditions.

3. A review of the relative physical properties of basaltic liquids and CO_2-rich fluids and of the phase relations of peridotite-CO_2-H_2O is in progress. This work is a follow up on the paper by Wilshire and Kirby (1989) that considered the roles of volatile fluids in fracture in the mantle based on observations of fractures in mantle-derived xenoliths.

References cited:

Akaogi, M., Ito, E. and Navrotsky, A., 1989, Olivine-modified spinel-spinel transitions..., J. Geophys. Res., v. 94, 15,671-15,685.

Goto, K, Suzuki, Z. and Hamaguchi, H., 1987, Stress distribution due to oivine-spinel phase transition in descending plate and deep-focus earthquakes, J. Geophys. Res., v. 92, 13,811-13,820.

Green, H.W. and Burnley, P., 1989, A new self-organizing mechanism for deep-focus earthquakes, Nature, v. 341, 733-737.

Helffrich, G.R., Stein, S. and Wood, B.J., 1989, Subduction zone thermal structure and mineralogy an their relationship to seismic wave reflections..., J. Geophys. Res., v. 94, 753-763.

Kirby, S.H., 1987, Localized polymorphic phase transformations in high-pressure faults and applications to the physical mechanmism of deep earthquakes, J. Geophys. Res., v. 92, 13,789-13,800.

Richards, M.A. and Wicks, C.W., Jr., 1990, S-P conversion from the transition zone beneath Tonga and the nature of the 670 km discontinuity, Geophys. J. Int., v. 101, 1-35.

Sung, C.-M. and Burns, R.G., 1976, Kinetics of high-pressure phase transformations ..., Tectonophysics, v. 31, 1-32.

Wilshire, H.G. and Kirby, S.H., 1989, Dikes, joints and faults in the upper mantle, Tectonopyhsics, v. 161, 23-31.

Reports

Kirby, S.H., Durham, W.B. and Stern, L.A., 1990, Phase transformations, Anomalous faulting and deep earthquakes: a new perspective, Submitted to the journal *Science* .

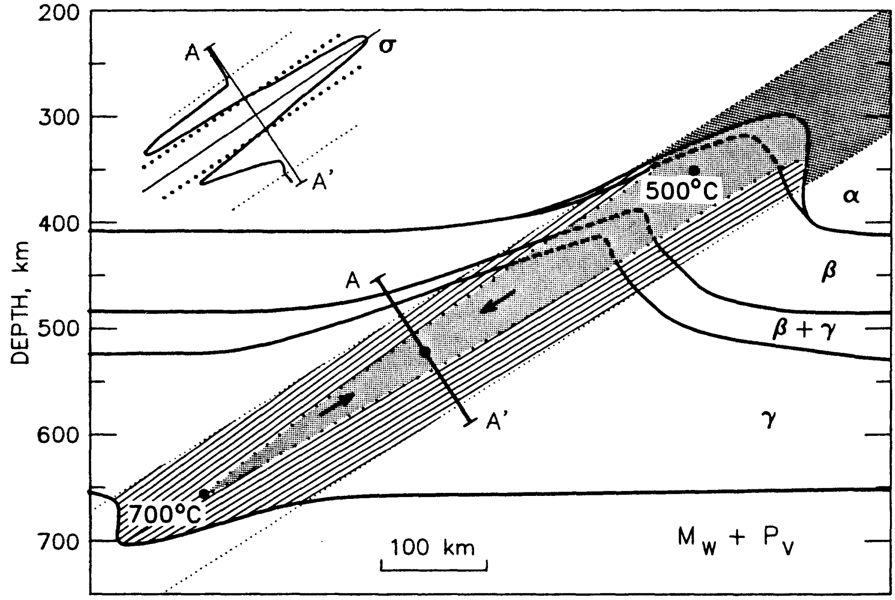

Fig. 1. Cross section showing the distribution of ferro-magnesian silicate phases in the subducting lithosphere based on the thermal model of Helffrich et al. (1989) and the phase relations of Akaogi et al. (1989). The positions of the maximum depths of the 500, 600 and 700°C isotherms are shown as filled circles. Also shown are the equilibrium α to α + γ and the α to β boundaries (dashed lines in the slab), a wedge of metastable olivine peridotite predicted by the kinetic model of Sung and Burns (1976) (light stipple), and regions of β- and γ-phase stability in the slab (ruled). The wedge-parallel compressive stress in the metastable olivine wedge (see inset) derives from the transformation strains in the envelope of lithosphere in which olivine has already transformed to spinel (Goto et al., 1987). Note that the region of olivine metastability, depending on the specific thermal model, generally corresponds to the depth interval for deep earthquakes (350-690 km).

ROCK MECHANICS

9960-01179

David Lockner
U.S. Geological Survey
Branch of Tectonophysics
345 Middlefield Road, MS/977
Menlo Park, California 94025
(415) 329-4826

Investigations

Laboratory experiments are being carried out to study the physical properties of rocks at elevated confining pressures, pore pressure and temperature. The goal is to obtain data that will help us to determine what causes earthquakes and whether we can predict or control them.

Results

Using USGS maps of recently active breaks, we have divided the San Andreas fault zone between Point Arena and Cajon Pass, California into geometrically defined segments of uniform strike that are bounded by bends and/or stepovers. Several recent seismological studies have emphasized the correlation between fault geometry and earthquake rupture patterns, and the Loma Prieta earthquake of October 17, 1989 provides a test of the appropriateness of our segment designations in the Santa Cruz Mountains. The lack of surface faulting accompanying the Loma Prieta earthquake precludes a direct comparison; nevertheless, both the main shock and the extent of rupturing as defined by the aftershocks appear to correlate well with our segment boundaries. The main shock is located downdip of a left (compressional) stepover, the northwestern termination of rupture is associated with a right (extensional) stepover, and the southeastern termination is associated with a 7° bend. The apparent correlation of the Loma Prieta earthquake rupture and the surface faulting pattern delineated by previous earthquakes suggests that the geometric discontinuities corresponding to the segment boundaries may extend throughout the seismogenic zone and affect fault motion.

Core samples from the Cajon Pass drillhole in Southern California show abundant evidence of hydrothermal alteration. One of the principal alteration minerals is zeolite laumonite, which both fills veins and occurs pervasively throughout the gneissic granodiorite host rock. It has been suggested that the presence of this mineral is correlated with the measured strength heterogeneity of the core samples. To test this suggestion, we have measured the frictional strength of laumontite gouge placed between sawcut surfaces of a granite sample, representing a laumontitic vein in a granite host rock. In this way we can determine the strength of the laumontite alone without the influence of the numerous natural and stress relief fractures present in the core samples. Frictional sliding experiments were conducted at room temperature under confining pressures of 30–450 MPa, at a displacement rate of 1 μ/s. Samples were tested under both dry and saturated (drained) conditions, using distilled water at fluid pressures of 10–150 MPa. Our results show that laumontite gouge supports typically high shear stresses similar to those of other crystalline rocks: The laumontite has a coefficient of friction between 0.65 and 0.80 over the range of pressures studied. The gouges reached a steady–state shear stress level and slid stably at all but the highest effective pressures, where stick–slip behavior was observed. Unlike typical clay gouges, the coefficient of friction of the laumontite was unaffected by the presence of water. These results show that laumontite is a strong mineral under the conditions explored in these experiments, and therefore any strength variations measured in the Cajon Pass core samples are probably not solely related to the presence of laumontite in the rocks.

The velocity dependence of rock friction is important in determining the stability of fault slip. We have completed a preliminary series of sliding experiments to measure velocity dependence for granite with both elevated temperature and pore water pressure, and find that these conditions cause a dramatic change in behavior comparied to either temperature or pore water pressure alone. We performeed triaxial sliding experiments on sawcut surfaces of Westerly granite with 0.5 mm simulated fault gouge (granite powder). Pore water pressure was controlled at 100 MPa and effective normal stress at 400 MPa. The temperature range tested was 22° to 600°C. Slip rate was stepped between 1 and 0.1 μ/s to measure the velocity dependence of steady state friction, $B = \Delta\mu_{ss}/\Delta \log V$. These conditions closely match those used by Lockner *et al.* [1], who deformed heated but dry granite powder and found little dependence of B on temperatures up to 845°C.

At room temperature the velocity dependence ($B = +0.009$ to $+0.020$) is similar to that seen in dry tests. However, in the range 150° to 350°C velocity dependence becomes negative (inducing oscillatory slip in some tests). Tests at 350°, 500° and 600° show a systematic trend from negative to very strongly positive velocity dependence ($B > +0.100$). The magnitude of B at 500°and 600° is much larger than that reported by Lockner *et al.* or by Stesky [2] for nominally dry granite; however, behavior similar to ours was inferred by Chester and Higgs [3] from experiments on saturated quartz powders. In addition, we observe a switch from strain hardening at lower temperatures to strain softening and decreased strength at $\geq$ 500°; this weakening also was not seen in the dry tests. Although we have yet to examine the gouge microstructure in detail, the data at the higher temperatures suggest the operation of a fluid–assisted deformation mechanism such as diffusive mass transfer or the retrograde reaction of feldspars to phyllosilicates.

Our results have intriguing implications for the distribution of seismicity with depth on faults such as the San Andreas. We find negative velocity dependence, and a tendency for stick–slip sliding in the approximate temperature range 100 to 300°C, which corresponds to the depth range of maximum seismicity (5 to 15 km) on the San Andreas fault.

Recent advances in the observation of nucleation and growth of macroscopic fault planes are presented. Based on the use of acoustic emission (AE) techniques. In the laboratory experiments, cylindrical samples of granite and sandstone were deformed in a triaxial apparatus at 50 MPa confining pressure. An electronic device was constructed which generated an output voltage proportional to AE rate. This device was incorporated in the feedback loop used to control axial stress. As a result, deformation experiments were conducted at constant AE rate rather than at the more conventional constant strain rate or constant stress conditions. By controlling AE rate, the post-failure stress curve was followed quasi-statically, extending to minutes or hours the fault growth process that normally would occur violently in a fraction of a second. In addition to this novel control syste, three-dimensional locations of AE events were determined by analyzing the relative arrival times of AE pulses recorded on a network of transducers attached to the sample. In this manner, as many as 40,000 AE events were located in the course of a single experiment.

While the details of fault formation varied from experiment to experiment, a number of features were consistantly observed. In all three granite experiments, the fault plane nucleated abruptly at a point on the same surface after peak stress. Prior to nucleation, microcrack growth was distributed evenly throughout the sample. From the nucleation site, the fault plane grew across the sample, accompanied by a gradual drop in axial stress. AE locations showed that the fault propagated as a fracture front (process zone) with dimension of 1 to 3 cm. As the fracture front passed, the AE from a given region would drop to a low level. If allowed to progress to completion, stress eventually dropped to the frictional sliding strength. Sandstone samples showed somewhat different response. A diffuse damage zone appeared prior to peak strength which gradually localized into an incipient fault plane. After passing through peak stress, this plane grew, as in the granite samples, to eventually bisect the sample.

We have conducted constant flow-rate permeability measurements on three core samples taken from the 12 km-deep well on the Kola Peninsula, USSR. All cores are from depths of 11.4 to 12.0 km. Pore pressures, P_{pore}, were held constant during each experiment and ranged from 112 to 117 MPa. By increasing confining pressure, P_{conf}, measurements were performed at effective confining pressures ($P_{eff} = P_{pore}$) ranging from 10 to 400 MPa. The measured permeabilities varied from approximately 10 μDa at a P_{eff} of 10 MPa to 0.1nDA at a P_{eff} of 300 MPa (Figure 1). By comparison, Bayuk *et al.* [1987] reported minimum permeabilities of 2 to 900 μDa at effective confining pressures of up to 120 MPa, using cores from depths of 3.7 to 9.9 km in the same well. Although the pore pressure at depth in the Kola Well is not well constrained, by assuming that the in-situ pore pressure follows the hydrostat, and using a confining pressure equal to the calculated overburden stress (317 to 333 MPa), our measurements, if taken at face value, indicate in-situ matrix permeabilities of 0.5 to 12 nDa for the three samples that we have studied. As discussed in Borevsky *et al.*[1987], however, there is evidence to suggest that the fluid pressures in the Kola well at depth may be considerably in excess of hydrostatic. If so, then the appropriate in-situ matrix permeabilities for these samples may be much higher (see Figure 1). On the other hand, if our estimates of in-situ pore pressures are correct, then the irreversible stress-relief cracking that appears to have occurred during sample retrieval suggests that our permeabilities are upper bounds to the in-situ matrix permeability. In either ase, the strong pressure dependence of permeability observed in our experiments indicates the importance of measuring permeability under realistic in-situ stresses and fluid pressures in order to obtain meaningful bounds on rock matrix permeabilities at depth.

Reports

D. Lockner, S. Hickman, J. Byerlee, V. Kuksenko, A. Ponomarev, A. Sidorin and B. Khakaev (1990), Laboratory–determined permeability of cores from the Kola deep well, *USSR, abst. Symp. on Perm., Fluid Pressure and Pressure Seals in the Crust, SEG*, Denver, CO, Aug. 5–8.

C. Morrow and J. Byerlee, (1990), Strength of laumontite from Cajon Pass, California, *EOS (Trans. Amer. Geophys. Union)* v. 71, pp. 626.

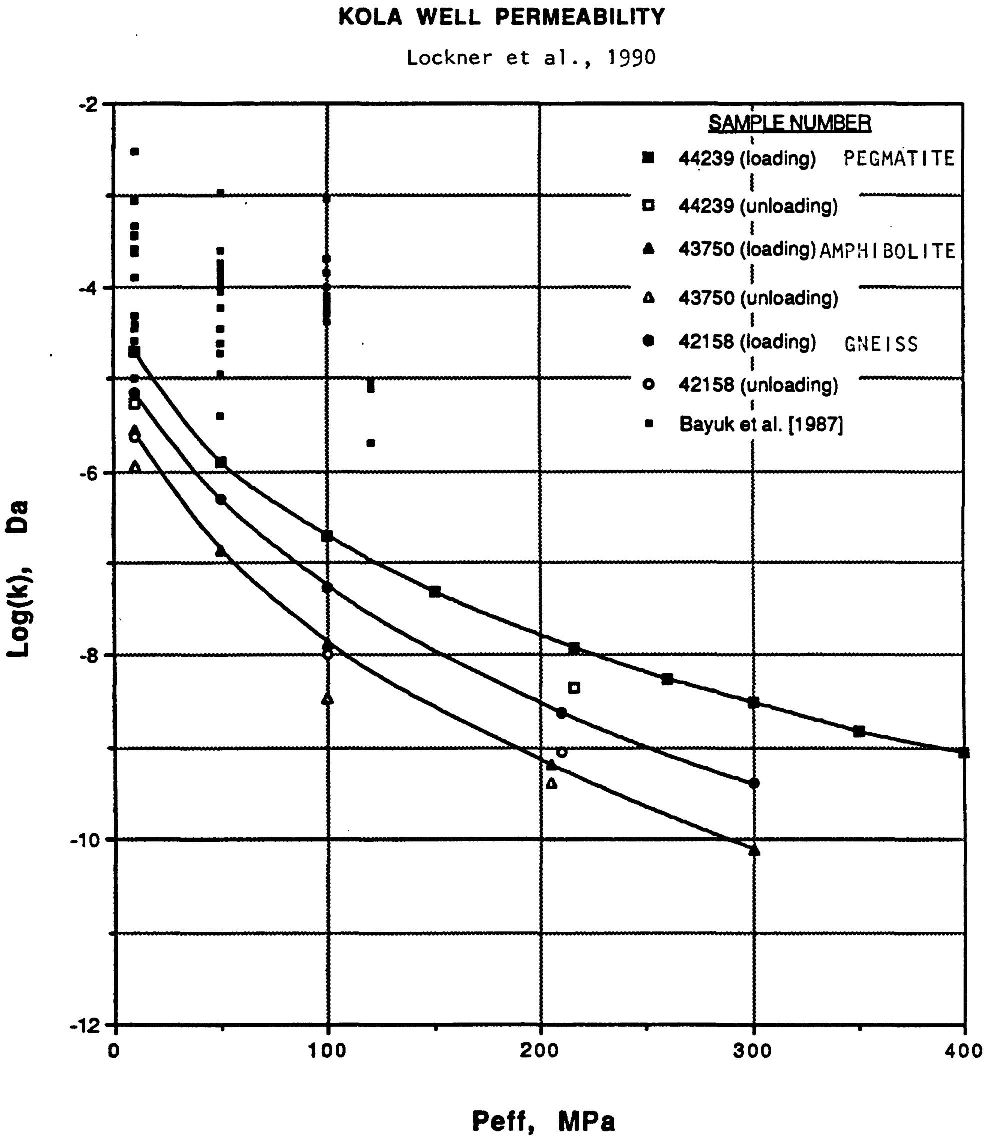

FIGURE 1: Permeabilitiy, k, in Darcies (1 Da = 10^{-12} m^2) as a function of effective confining pressure, P_{eff}, for three cores from the Kola Ultra-Deep well. Permeabilities are shown both during loading (filled symbols) and unloading (open symbols) for each sample; solid curves are fit to data collected during loading. Notice the small offsets between permeabilities measured during loading and unloading, indicating that the magnitude of permeability reduction resulting from cycling of confining pressure during these experiments is relatively minor. Uncertainties in k range from approximately ± 10% for permeabilities of 10^{-6} Da to ± 20% for permeabilities of 10^{-9} Da. Sample numbers 43750, 42158, and 44239 were recovered from depths of 11,386 m, 11,658 m, and 11,978 m, respectively. Also shown are permeabilities reported by Bayuk *et al.* (1987;) for cores recovered from shallower depths (3786 m to 9905 m) in the same well.

Accurate Three-Dimensional Calculations for Advancing Slip Zones in the Earth's Crust

(Joint funding with NSF Grant EAR-8707392)

J. W. Rudnicki and L. M. Keer
Department of Civil Engineering
Northwestern University
Evanston, Il 60208
(708)-491-3411

(For period April 16, 1990 to September 30, 1990)

Objectives

Understanding the mechanism by which slip is transmitted from depth to the surface and along the strike of the fault from freely slipping to locked zones is of great importance for understanding the earthquake process and for possibly anticipating damaging events. A major impediment to more accurate and realistic analyses has been the difficulty of making calculations for three dimensional cracked bodies. We are doing three-dimensional analysis of slip zones (cracks) in an elastic half-space to determine stresses and surface deformations due to the advance of shear faults into locked, or more resistant, portions of the shallow crust. The goal of these studies is to understand three-dimensional geometric effects on the intensity of stressing near the edges of slip zones. Ultimately, we hope to develop theoretical models for the advance of slip zones into and around slip resistant portions of the fault, focussing particularly on the effects of nonuniformities in the advancing slip front.

Results

Work during the earlier portion of the grant is summarized in the following abstract of a manuscript [Wu et al., 1990] submitted to the Journal of Geophysical Research:

"Free surface displacements, stress intensity factors and energy release rates are calculated for planar slip zones in an elastic half-space subjected to prescribed shear stress drop. Although the method can treat arbitrarily shaped planar zones and distributed stress drops, for simplicity, results are presented only for circular and elliptic zones and uniform stress drops. Calculations of the stress intensity factors and energy release rates for various geometries indicate that solutions for the half-space differ by less than 10% from those in the full space if the distance of the fault center from the free surface is greater than twice the vertical length of the fault. In addition, the influence of the free surface is greater for decreasing dip angle. For slip zones that are near the free surface and, especially, those that break the surface, there is a coupling between slip and normal relative displacement. That is, for a prescribed shear stress drop and zero normal stress change, slip induces relative normal displacement.

"As example applications, these solutions are used to reexamine coseismic geodetic data from three earthquakes: 1966 Parkfield, 1983 Borah Peak, and 1987 Whittier Narrows. The geometries, moments and stress drops are similiar to those inferred in previous studies using dislocation methods. However, the stress drop inferred here may be more reliable because stress drop is one of the parameters adjusted to fit the observed surface deformations. In addition, the method makes it possible to estimate the critical energy release rate at the termination of rupture. Values for the Parkfield, Borah Peak and Whittier Narrows earthquakes are 1.5×10^6 J/m^2, 1.2×10^6 J/m^2 and 2×10^8 J/m^2, respectively.

Current work has focussed on the development of an analytical solution for constant slip in a triangular region in an elastic half-space using the angular dislocation solution of Comninou [1973]. Because triangular elements can be used to model arbitrarily-shaped slip zones, this solution has advantages over the rectangular slip solution of Chinnery [1961]. For a vertical rectangular fault, the solution has been checked against that of Chinnery. However, solution for inclined faults is more difficult and we are still checking the results.

Although the constant slip triangular element cannot be used to obtain results for the stress intensity factors and energy release rate near the edges, it can be used to estimate stress drops. Comparisons with the crack (imposed stress drop) model agree within a factor of about two.

References

Chinnery, M. A., The deformation of the ground around surface faults, Bull. Seismol. Soc. Am., **51**, 355-372, 1961.

Comninou, M. A., Angular dislocation in a half-space, Ph.D. Dissertation, Northwestern University, Evanston, Illinois, 45 pp., 1973.

Publications

Kuo, C., M. Wu, J. W. Rudnicki, and L. M. Keer, Intepretation of coseismic deformation data using three dimensional crack (stress drop) models (Abstract), presented at NSF/USGS Workshop on Crustal Deformation Measurement and Earthquake Mechanics, Morro Bay, California. March 18-22, 1990.

Wu, M., C. Kuo, J. W. Rudnicki, and L. M. Keer, Modeling of coseismic surface deformation using non-kinematic approach (Abstract), Seismol. Res. Let., **61**, p. 38, 1990.

Wu, M., J. W. Rudnicki, C. Kuo, and L. M. Keer, Surface deformation and energy release rates for constant stress drop slip zones in an elastic half-space, submitted to J. Geophys. Res., July, 1990.

Heat Flow and Tectonic Studies

9960–01177

John H. Sass
Branch of Tectonophysics
U.S. Geological Survey
2255 North Gemini Drive
Flagstaff, AZ 86001
(602) 527-7226
FTS: 765-7226

Arthur H. Lachenbruch
Colin F. Williams
Branch of Tectonophysics
U.S. Geological Survey
345 Middlefield Road
Menlo Park, CA 94025
(415) 329-4879/4881
FTS: 459-4879/4881

Investigations:

A geothermal study of the Santa Maria Basin and environs is continuing. Preliminary heat-flow values have been determined for the onshore and offshore Santa Maria Basin. The analysis and interpretation of data from the Cuyama and western Ventura Basin is under way.

Apatite separates were delivered to Australia for fission-track analysis to investigate thermal history at Cajon Pass.

The significance of the vertical distribution of heat flow in the Cajon Pass research well has been assessed.

Precision temperature monitoring in the USL-Pearson well near Parkfield is continuing. Monitored temperatures remained stable over the past six months.

A manuscript on heat flow from Arizona and the Mojave Desert of California was prepared.

A heat-flow transect stretching from the California coast near Harmony through Parkfield to the Great Central Valley is being prepared.

Heat flow has been calculated for the DOE's Magma-Energy research well at Long Valley, California.

Temperature and thermal conductivity data from the Valles Caldera in northwestern New Mexico have been analyzed as part of a geothermal characterization of the caldera.

A new digital data-acquisition system has been installed in the Geothermal Studies Project well-logging truck.

A study of the gravity field and the topography of the Mojave-Sonoran Desert continued.

A manuscript on tectonic implications of eastern Sierra Nevada heat flow was submitted to *Tectonics*.

Temperature and thermal conductivity data from the NPRA are being used to estimate heat flow and subsurface temperature. USGS high-resolution temperature logs are supplemented by bottom-hole temperature data from petroleum exploration wells collected by *Blanchard and Tailleur* (1962).

Results:

Santa Maria. As part of the USGS Evolution of Sedimentary Basins Program, the Geothermal Studies Project is investigating the thermal regime of the Cuyama, onshore Santa Maria, offshore Santa Maria, and western Ventura Basins. To date, the Project has obtained temperature logs and collected core samples for thermal conductivity measurements from more than 50 idle oil wells in the Guadalupe, Santa Maria Valley, Cat Canyon, Orcutt Hill, Zaca, Lompoc, South Cuyama, Pt. Arguello, and Pt. Conception oil fields. The preliminary results reveal two significant aspects of thermal conditions in the Santa Maria province.

First, in many Santa Maria Valley wells, temperature gradients in the Plio-Pleistocene Careaga, Paso Robles, and Orcutt Formations (typically above 400 m depth) are depressed to nearly isothermal conditions. Temperatures in older formations (*e.g.,* Sisquoc, Monterey) are linear and yield conductive heat-flow values that are relatively constant with depth. The thermal consequences of refraction, vertical conductivity variations, sedimentation, relative sea-level changes, and groundwater flow have been considered as possible explanations. Simple analytical models suggest that shallow groundwater flow, active since at least the middle Pleistocene, accounts for most (if not all) of the heat loss. Relative sea-level changes and conductivity variations may be significant, but secondary, effects. These results suggest that equilibrium BHT data are unreliable indicators of true geothermal gradients in some parts of the Santa Maria Basin.

Second, preliminary heat-flow determinations from both onshore and offshore wells average 80 ± 10 $\mathrm{mW/m^2}$. These values are typical for the Coast Range heat-flow high to the north and contrast sharply with low heat flow (45 to 50 $\mathrm{mW/m^2}$) in the onshore Ventura Basin to the south. This places the southern boundary of the Coast Range anomaly somewhere in the Transverse Ranges. Research plans include an investigation of the location and nature of this transition. The persistence of high heat flow 20 m.y. after the passage of the Mendocino Triple Junction suggests that asthenospheric upwelling behind the Triple Junction may not be the sole significant heat source associated with evolution of the continental margin. The possible natures and magnitudes of additional heat sources are being studied.

Cajon Pass. Measured heat flow at Cajon Pass is consistent with predictions based on local site conditions and regional heat flow. With observations now ranging to a depth of $3^1/_2$ km, there is still no evidence for significant frictional heating anywhere on the San Andreas fault. The result supports the view, long suggested from heat-flow studies, that the fault is weak in spite of estimates based on Byerlee's law, isotropic strength, and hydrostatic fluid pressure that suggest a strength several times larger. Recent evidence (*Zoback et al.,* 1987; *Mount and Suppe,* 1987) that the maximum principal stress might be almost normal to the San Andreas fault would support the weak-fault model and add constraints over and above those imposed by heat flow; *e.g.* friction coefficients $\mu \lesssim 0.1$ or local fluid pressures greater than lithostatic, compared to $\mu \lesssim 0.2$ or fluid pressure greater than twice hydrostatic for the heat-flow constraint alone. Neither the general occurrence of such conditions nor the mechanics of a weak fault are readily explained by existing theory.

The balance of plate boundary forces around a weak fault depends on the basal traction coupling the seismic layer to the rest of the system; heat flow limits the coupling force across the fault to an insignificant $\sim 10^{11}$ N/m. The weak fault also precludes significant basal *driving* tractions, but it permits a large basal *drag* force which could result in a highly stressed seismic layer offering appreciable resistance to plate motion through its base. Such tractions could develop progressively if the fault weakens as it evolves; if they exist, they should cause an observable reduction in resolved shear stress and rotation of principal axes as the fault is approached. Heat-flow measurements should detect whether such basal tractions might be associated with basal decoupling and flow. Coupling at the base of the seismic layer is controlled by the rheological profile, the usual representation of which raises questions in applications to the San Andreas fault zone. First, the linear frictional portion through the seismic layer implies a resisting force on the fault much greater than the heat-flow limit permits. Second, the large stresses implied for the temperature-sensitive ductile layer could lead to shear-heating and weakening at plate-boundary strain rates. Third, in the ductile layer the stress is sensitive to whether deformation is concentrated in narrow vertical mylonite zones, as sometimes assumed in models of the earthquake cycle, or broadly distributed by bulk flow in a mid-crustal "asthenosphere." Horizontal basal shear stresses are of the same order as strike-slip stresses near the base of the seismic layer; they could result in bulk flow or horizontal detachment leading to a different pattern of long-term stress, strain rate, and dissipation and a requirement for decoupling and basal drag on the seismic layer in the near field. Results from the San Andreas fault taken with long-standing speculation about the orthogonal relation between oceanic transform faults and extensional spreading centers suggests that strike-slip transform faults might be anomalously weak in both continental and oceanic settings.

Parkfield Monitor. The Project's Long-Term Temperature Monitor (LTTM) has been operating in the USL-Pearson 1B (PRSN) well near Parkfield for approximately one year. During the first eight months of operation, the ±0.2 mK (±0.0002°C) resolution capability of the monitor was occasionally negated by the effects of extreme diurnal surface temperature variations and rain-related disturbances to the electronics. The surface electronics have been reconfigured, and the adverse effects of surface disturbances eliminated. Monitored temperatures have remained remarkably stable over the past six months. It is expected that activity along the San Andreas fault near Parkfield will generate an identifiable thermal-hydrologic signal that could provide premonitory information and data on strain-heating in the fault zone. These expectations will be tested by the onset of the long-awaited Parkfield earthquake.

Mojave-Sonoran Desert. More than 200 values of heat flow are now available from the crystalline terranes of southern California, the Basin and Range province of Arizona, and Paleozoic sedimentary rocks of the southwestern Colorado Plateau (CP). Heat flow ranges from about 5 mW m^{-2} on the CP near Flagstaff, Arizona, to more than 150 mW m^{-2} in the crystalline rocks bordering the Salton Trough in SE California. The heat-flow pattern within this region is complex and appears to be controlled by regional physiographic and tectonic features. Contemporary and Neogene tectonism appears to be responsible for the very high heat flow (>100 mW m^{-2}) associated with the Salton Trough and its neighboring ranges, the Death Valley fault zone and its southward extension, and zones of shallow (<10 km) Curie isotherms (as inferred from aeromagnetic data) in west-central Arizona. Low (<60 mW m^{-2}) heat flow in the Peninsular Ranges and eastern Transverse Ranges of California may be caused by thermal transients related to subduction and compressional tectonics. Relatively low heat flow (<80 mW m^{-2}) is also assocated with a band containing most of the metamorphic core complexes in Arizona. The regional variations in heat flow are mirrored in heat-flow - heat-production plots, but no statistically valid relation is apparent between heat flow and near-surface radiogenic heat production. This absence of correlation is attributable to the complex tectonic history, involving lateral movement of basement terranes, and heat sources and sinks of different strengths, ages, and durations.

Parkfield heat-flow transect. This transect represents an updating of region 5 (Figure 1, from *Lachenbruch and Sass,* 1980) with 24 additional holes in the fault zone near Parkfield and additional high quality data from the San Joaquin Valley. Preliminary results confirm the findings of Lachenbruch and Sass of a broad zone of high heat flow (about 90 mW m^{-2}) with no local thermal anomaly associated with the fault trace. Because of the lack of rock samples and the complicated and laterally discontinuous structure near the fault, the quality of the data from the Parkfield area is not high enough to document local variations in heat flow.

Long Valley. Well LVF 51-20 is near the center of the resurgent dome of the Long Valley Caldera. The well is planned for an ultimate depth of about 6 km, and the first phase, a large diameter (0.66 m) hole, was completed in the Bishop Tuff to a depth of 783 meters in early October of 1989. After the 0.51-m-diameter surface casing was grouted in place to 783 m, a smaller casing was set, and a 100-mm-diameter corehole was drilled between the depths of 783 and 839 m. A total of 10 temperature logs was run during casing and cementing of the large-diameter hole. Another log was run just prior to coring, and 4 logs were run during a 6-week period following completion of the corehole. The time series of 4 post-coring temperature logs was extrapolated to infinite time assuming a conductive decay of the drilling disturbance. The bottom-hole temperature of less than 50°C is surprisingly low for a region of such young and intense volcanic activity. In part, this low temperature may be the result of the shallow (200–300 m) hydrologic system being dominated by recharge. The interpretation of the temperature log between depths of 300 and 780 meters is complicated by the uncertainty in estimates of the formation porosity and thermal conductivity. Thermal conductivity was measured on 20 samples from the corehole. The harmonic mean conductivity of 2.26 W m^{-1} K^{-1} ± 0.13 (95% confidence limits) when combined with the corehole temperature gradient of 53°C km^{-1} yields a heat flow of 120 mW m^{-2}. This is a high value, but it is low compared to the current estimate of 640 mW m^{-2} for the average energy flux from the caldera.

Valles Caldera. Shallow thermal gradient data from the Quaternary Valles Caldera in the Jemez Mountains of New Mexico indicate that heat loss from the caldera is concentrated in its western half. The Sulphur Springs area, near the western margin of the resurgent dome of the Valles Caldera, was the site of the earliest and some of the most intensive exploration for geothermal resources in the caldera. In an earlier study we demonstrated that the conductive heat flow near the western margin of the Valles Caldera averages between 300 and 400 mW m^{-2}. We now have a combined total of 150 determinations of thermal conductivity on core segments from research wells VC-1, VC-2a, and VC-2b. These data are sufficient to characterize the thermal conductivity of the major rock types in the area. A high degree of alteration of tuffs from VC-2a and VC-2b relative to VC-1 is reflected by significantly higher thermal conductivities, generally greater than 2 W m^{-1} K^{-1}, for the tuffs in the VC-2 wells relative to an average tuff conductivity of 1 W m^{-1} K^{-1} for VC-1. Temperature data from VC-2a and VC-2b confirm surface indications that the Sulphur Springs area is the locus of vigorous hydrothermal activity. The hydrothermal systems in both wells are capped by relatively thin (60 and 200 m, respectively) near-surface conductive thermal regimes. Heat flows from these near-surface caps are 2.5 ± 0.5 W m^{-2} for VC-2a and 1.4 ± 0.15 W m^{-2} for VC-2b, several times the very high background heat flux in the western portion of the caldera. The probable source of these high heat-flow values is the intrusion of one or more shallow magma bodies during the post-collapse history of the caldera.

Data acquisition and reduction. The 15-year old Tektronix data-acquisition system in the logging truck has been replaced by a system based on a ruggedized PC with 80386 microprocessor. The new system allows faster logging speeds and the digital acquisition of new types of data (*e.g.*, line speed). In addition, the installation of commercial and in-house software packages enables personnel in the field to use all of the data analysis capabilities currently available in Menlo Park.

Mojave-Sonora topography, isostatic residual gravity, basement gravity, digital geology. [Saltus] Basin depth (modeled) maps were constructed for the Mojave-Sonoran study area (tied to the PACE transect). A basement residual gravity high correlates with the band of metamorphic "core-complexes" (which was found also to be a zone of low heat flow). Based on seismic refraction modeling (McCarthy *et al.*), it is reasonable to correlate the gravity highs with thickened ("upwarped") middle crust beneath the region of greatest surface extension.

North Slope. [Deming] Heat flow estimated from shallow (generally less than 600 m deep), high-resolution temperature logs ranges from a low of 27 ± 6 mW/m^2 in the Lisburne well in the foothills of the Brooks Range, to a high of 90 ± 19 mW/m^2 in the Atigaru well on the north coast. Heat flow is inversely correlated with topographic relief, suggesting possible disturbance by a basin-wide groundwater flow system. Similar flow systems have been hypothesized as possible mechanisms for the migration and concentration of oil (*Garven,* 1989) and formation of Mississippi Valley-type ore deposits (*Garven,* 1985), but their existence is controversial (*Fowler,* 1986).

Estimated equilibrium temperatures obtained by *Blanchard and Tailleur* (1982) from bottom-hole temperature data have been winnowed. Preliminary projection of these deep temperature data onto a N-S geologic cross-section through the basin shows curvature in the temperature field consistent with groundwater discharge near the coast. The hypothetical groundwater flow system may be controlled by the Paleozoic Lisburne and Endicott groups, both of which contain potential aquifers.

References cited:

Blanchard, D. C., and Tailleur, I. L., 1982, Temperatures and interval geothermal-gradient determinations from wells in National Petroleum Reserve in Alaska: *U.S. Geological Survey Open-File Report* **82-391**.

Fowler, A. D., 1986, The role of regional fluid flow in the genesis of the Pine Point Deposit, Western Canada Sedimentary Basin–a discussion: *Economic Geology,* **81**, p. 1014–1024.

Garven, G., 1985, The role of regional fluid flow in the genesis of the Pine Point Deposit, Western Canada Sedimentary Basin: *Economic Geology,* v. **80**, p. 307–324.

Garven, G., 1989, A hydrogeologic model for the formation of the giant oil sands deposits of the Western Canada Sedimentary Basin: *American Journal of Science,* v. **289**, p. 105–166.

Lachenbruch, A. H., and Sass, J. H., 1980, Heat flow and energetics of the San Andreas fault zone: *Journal of Geophysical Research,* v. **85**, p. 6185–6223.

Mount, V. S., and Suppe, J., 1987, State of stress near the San Andreas fault: Implications for wrench tectonics, *Geology,* v. **15**, p. 1143–1146.

Zoback, M. D., Zoback, M. L., Mount, V. S., Suppe, J., Eaton, J. P., Healy, J. H., Oppenheimer, D., Reasenberg, P., Jones, L., Raleigh, C. B., Wong, I. G., Scotti, O., and Wentworth, C., 1987, New evidence on the state of stress of the San Andreas fault system, *Science,* v. **238**, p. 1105–1111.

Reports:

Borns, D. J., Sass, J. H., and Schweickert, 1990, Proposed study of the Basin and Range from Death Valley to Yucca Flat: *Eos,* v. **71**, p. 1012–1013.

Lachenbruch, A. H., and McGarr, A., Stress and heat flow on the San Andreas fault: *U.S. Geological Survey Professional Paper,* in press, 1990.

Lachenbruch, A. H., and Sass, J. H., Heat flow from Cajon Pass, fault strength, and tectonic implications: Submitted to *Journal of Geophysical Research.*

Langseth, M. G., Lachenbruch, A. H., and Marshall, B. V., 1990, Geothermal observations in the Arctic region, in Grantz, Arthur, Johnson, L., and Sweeney, J. F., eds., *The Arctic Ocean Region:* Boulder, Colorado, Geological Society of America, Geology of North America, v. **L**, p. 133–151.

Osterkamp, T. E., and Lachenbruch, A. H., Current thermal regime of permafrost in Alaska and the predicted global warming, in *Proceedings, Workshop on "Climatic Change and Permafrost: Significance to Science and Engineering":* American Society of Civil Engineers, in press, 1990.

Saltus, R. W., and Lachenbruch, A. H., Thermal evolution of the Sierra Nevada–Tectonic implications of new heat-flow data: *Tectonics*, in press, 1991

Sass, J. H., Lachenbruch, A. H., Moses, T. H., and Morgan, Paul, Heat flow from a scientific research well at Cajon Pass, California: Submitted to *Journal of Geophysical Research.*

Williams, C. F., and Anderson, R. N., 1990, Thermophysical properties of the Earth's crust–*In situ* measurements from continental and ocean drilling: *Journal of Geophysical Research,* v. **95**, p. 9209–9236.

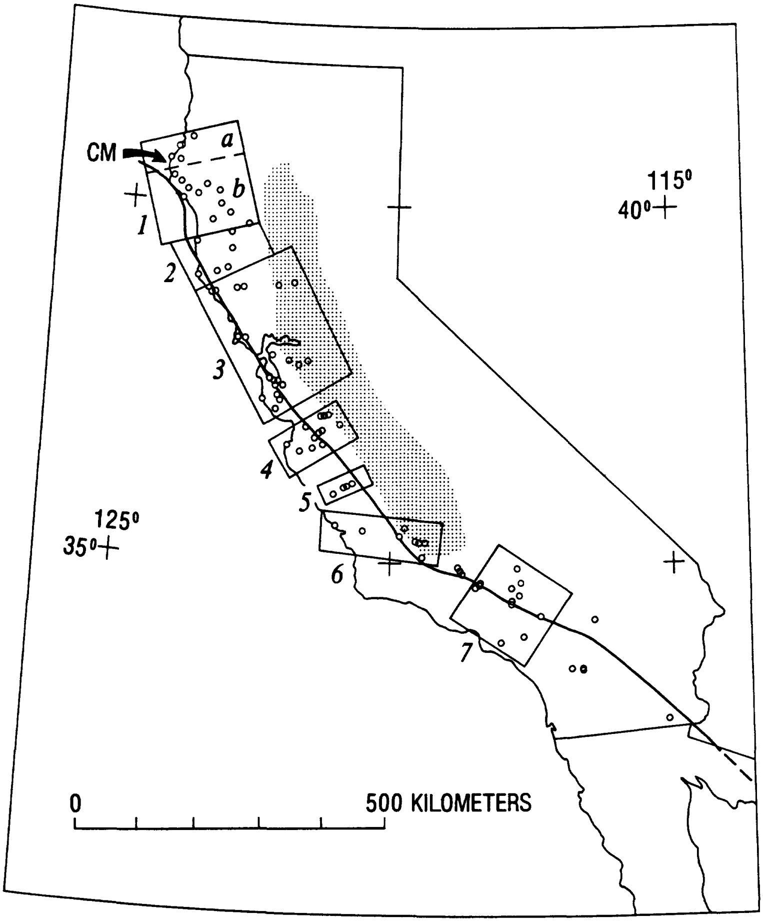

Figure 1. Outline of the state of California showing the trace of the San Andreas fault and heat-flow control (open circles). Stippled area is the Great Central Valley and boxes labeled 1 through 7 are sub-regions considered by Lachenbruch and Sass (1980).

Micromechanics of Rock Friction

USGS 14-08-0001-G1668

C.H. Scholz, G.N. Boitnott, W. Wang, N. Yoshioka, R.L. Biegel
Lamont-Doherty Geological Observatory
Palisades, New York 10964

(914) 359-2900 (x360)

We are continuing to develop a quantitative theory of friction and wear based on Hertzian elastic contact mechanics. The results of our investigation were presented in 3 abstracts at the Spring AGU conference, [Biegel, et al.; Boitnott et al.; Wang, et al. (1990)] and the Symposium on Earthquake Source Physics, Tokyo, 1990. The results of initial friction experiments and modeling are the subject of 2 manuscripts currently in preparation.

(1) A physically based semi-empirical model was developed which predicts the frictional properties of two rough surfaces in contact during shear (Boitnott, et al., 1990). Using the normal closure algorithum of Brown and Scholz (1985), the normal load imposed on individual asperities is calculated. Shear deformation of each asperity is then calculated using the elasticity solutions of Mindlin and Deresiewicz (1953). These solutions describe the development of slip at the contacts with application of a shear load. Finally, the macroscopic properties of the surface are computed by imposing a shear displacement and summing the forces on the individual asperities.

Geometric parameters from topography data are used to control the model. We found that an "asperity scale" coefficient of friction between 0.30 and 0.36 independent of normal load and surface roughness gives good agreement between model and data. Once a large population of contacts is sliding, the model underestimates the frictional strength, indicating displacement strengthening mechanisms have begun to operate. This begins after the first few microns of slip. With further slip, displacement hardening mechanisms begin to operate to raise the macroscopic friction coefficient to ~ 0.55 to 0.60. It is these mechanisms which are currently the object of our research.

(2) An experimental program is being conducted to investigate the effects of displacement dependent strengthening mechanisms by isolating and observing them individually. As a first step, we redesigned the displacement feedback system of our rotary apparatus by mounting the feedback transducer directly to the sample and across the joint. This has nearly eliminated the necessary solid sample correction for shear thus improving the signal-to-noise ratio. Also we have achieved a factor of five increase in slip distance capability for a single run, which is essential to solving the slip hardening problem.

Important to frictional displacement hardening is oblique contact of asperities. We are presently developing a model to incorporate this mechanism into the initial slip model. Using the elasticity solutions for oblique contact described by Mindlin, et al. (1953), we can extend our friction law into the slip hardening regime.

To measure the effects of each micro mechanism separately we have begun a series of friction experiments sliding westerly granite over polished sapphire. Polished sapphire, with a hardness of 9.0, does not scratch or indent under loading from granite, allowing slip to occur absent the strengthening mechanisms of oblique contact, indentation, ploughing, and (in the early stages of slip) wear. These results are being used to test the assumptions of the initial slip model from which the asperity scale coefficient was derived. It is essential that we confirm our previous findings before moving forward. The contribution of each micromechanism to the displacement strengthening process is being measured by sliding rough and smooth surfaces of granite over both polished sapphire and sapphire of different roughnesses. In this way we plan to model the effect of asperity interlock indentation and ploughing, and initial wear, each as a separate mechanism adding to the macroscopic friction force.

(3) The wear mechanism becomes increasingly important to friction with slip accumulation. To this end, an empirical wear law was developed which successfully predicts wear volume for different normal stresses and roughnesses. These results were presented at the Spring '90 AGU conference (Wang and Scholz, 1990). We are now using image analyzing techniques to calculate the ratio of damage to undamaged area on a surface. This information is then used to calculate the wear loss volume, the results of which can be checked with the actual measurements. Thus, a double check can be made of calculated wear loss. These results are also being compared with topography data in an attempt to calculate wear from the evolving surface geometry.

(4) Naoto Yoshioka stayed at Lamont-Doherty for July and August, 1990. Dr. Yoshioka has been instrumental in developing one of the two theories used to map topographic random processes from one dimensional profiles to two dimensional surfaces. His adaptation of the Yamada, et al. model (1978) to this experimental program is described in Yoshioka and Scholz (1989 a, b). His recent visit has been directed toward understanding the different mapping transformations used in the models of Brown and Scholz model (1985a) and Yoshioka and Scholz (1989a).

The Brown and Scholz models uses the moments of power spectral densities from upper and lower surfaces to combine them in to a composite topography following the method of Nyak (1971) and Adler and Firman (1981). Then the contact between the two surfaces is represented as a composite and a flat. The Yoshioka and Scholz model is an adaptation of the Yamada et al. method which treat the two surfaces separately, and maps directly from a topographic profile to predicted distribution of contacts between the surfaces. The object of Dr. Yoshioko's visit was to understand the differences between the 2 models and use them as reciprocal checks upon each other. His results are to be presented at the Symposium on Earthquake Source Physics, in Tokyo, Nov. 1990 (Yoshioka, et al. 1990).

References

Adler, R.J., and D. Firman, A non-Gaussian model for random surfaces, Philos. Trans. R. Soc. London, Ser. A., 303, 433-462, 1981.

Biegel, R.L., W. Wang, C.H. Scholz, G.N. Boitnott, N. Yoshioka, and T. Koczynski, Micromechanics of rock friction: 1. Experimental observations of early stages of slip, Trans. Am. Geophys. Union, 71, 630, 1990.

Boitnott, G.N., N. Yoshioka, R.L. Biegel, C.H. Scholz, and W. Wang, Micromechanics of rock friction 2: Quantitative modeling of initial friction with contact theory, Trans. Am. Geophys. Union, 71, 630, 1990.

Brown, S.R., and C.H. Scholz, Closure of random elastic surfaces in contact, J. Geophys. Res., 90, 5531-5545, 1985.

Mindlin, R.D., and H. Deresiewicz, Elastic Spheres in contact under varying oblique forces, J. Appl. Mech., 20, 327-344, 1953.

Nyak, P.R., Random process model of rough surfaces in plastic contact, Wear, 26, 305-323, 1973.

Yamada, K., N. Takeda, I. Kagami, T. Naoi, Surface density of asperities and real distribution of asperity heights on rubbed surfaces, Wear, 48, 5-20, 1978.

Yoshioka, N., G.N. Boitnott, R.L. Biegel, W. Wang, and C.H. Scholz, Micromechanics of the behavior of contacting surfaces: A new approach for rock friction, to be presented, Inter. Symp. on Earthquake Source Physics and Earthquake Precursors, Tokyo, Nov. 19-22, 1990.

Yoshioka, N. and C.H. Scholz, Elastic properties of contacting surfaces under normal and shear loads, 1, Theory, J. Geophys. Res., 94, 17,681-17,690, 1989.

Yoshioka, N., and C.H. Scholz, Elastic properties of contacting surfaces under normal and shear loads, 2, Comparison of theory with experiment, J. Geophys. Res., 94, 17,691-17,770, 1989.

Wang, W., and C.H. Scholz, Wear processes during frictional sliding of rock: A theoretical and experimental study, Trans. Am. Geophys. Union, 71, 409-676, 1990.

Systems Analysis of Geologic Rate Processes:

SPACE-TIME MODELS, COUPLED OSCILLATORS, AND GENETIC CODES: CALIFORNIA EARTHQUAKE RECURRENCE PATTERNS

9980-02798

Herbert R. Shaw and Anne E. Gartner
Branch of Igneous and Geothermal Processes, U. S. Geological Survey
MS-910, 345 Middlefield Road, Menlo Park, CA 94025
(415) 329-5245, 5209

Objective: The objective for this report period extends the ideas outlined in the two preceding reports; the strategy of our approach is elaborated more fully in the Report of 4/1/89-9/30/89 (NEHRP, Summaries, XXIX, p. 378-384).

Results: Progress toward automating the event sequence matrices described in previous reports was interrupted by a call to active duty for Gartner by her Naval Reserve Unit during the Persian Gulf situation. We have, however, manually constructed return maps of conditional occupancies of the 8-letter regional 'alphabet' for magnitudes $M \geq 5$ using chronological vectors based on CDMG catalogs of historical events to 10/25/1982, and NEIS Catalogs from 10/25/82 through 12/31/89. These are effectively maps of recurrences in a two-dimensional 8-cell state space, giving trajectories something like those in a pinball machine where the paths of motion of the ball between 8 pins are recorded, and where the incident trajectories and reflections off the walls represent 'the rest of the world'. The results are analogous to return maps of numerical dynamics. For example, there is a time series for a particular recurrence history in each cell that could be described by the methods of singularity analysis, as shown by Shaw and Chouet (1988, 1989) for time series constructed from the recurrence histories of seismic tremor in Hawaii.

In the present case, the space-time structure is spatially discrete (i.e., for the present purpose it is restricted to a nonfractal set of specific seismic regions) while being temporally multifractal, judging from graphical results in Shaw (1987a) and from the work of Shaw and Chouet cited above. The codification represented by our 8-letter 'recurrence alphabet' is analogous to phase portraits of a multiwell potential surface in which there are 8 minima of similar but not identical depths, and where the depths reflect the chosen range of earthquake magnitudes, hence numbers, of events (such a potential surface, in general, is probably multifractal, because the number of wells for a given range of magnitudes will be determined by the spatial variations of b-value data, which are fractal in nature). [Note: In some reiterations of letter-combination matrices we have simplified the spatial structure to a 5-letter code as the first-order description of discrete states, because three regions are of low relative probabilities and reasonably can be combined with two of the others; these regions are shown roughly by the trajectory patterns of large earthquakes in Figure 1 of Shaw and Gartner, NEHRP, Sum. Tech. Repts, XXIX, p. 384, 1989.]

To give perspective to concepts needed to describe self-organization in such a highly nonlinear network of coupled forces and flows, we use the analogy of a bistable oscillator (periodic motion in a two-well potential field) that responds to displacements in a nonlinear fashion. This is a useful analogy, because it applies to the response functions of many types of physical systems in which there are alternations between two stable positions, or loci of attraction, including such things as electronic resonator circuits, chemical resonators, and mechanical resonators of various kinds. A typical example of the latter is the gravitationally buckled elastic or viscoelastic beam driven parametrically by a time-varying external force. The model is useful because the trajectories of motion between the two (in this case) attractor basins can be visualized in terms of slip events separating the activated and relaxed states of a characteristic fault segment, and because the periodic and chaotic states of such bistable oscillators are related in familiar ways to the universal properties of many kinds of numerical attractor systems (circle maps, quadratic maps, Lorenz attractors, "dripping-faucet" attractors, and so on) that have been found to be applicable in virtually every field of geophysics (see review by Shaw, 1987b).

Ditto et al. (1989) describe a form of intermittency in the behavior of a bistable buckled beam in which there is a power-law scaling of times between events (times between excursions across a critical state relative to proximity of the periodic driving force to this "crisis"). This form of scaling also is characteristic of the Critical Golden Mean Nonlinearity (CGMN) of the sine circle map (Shaw, 1987b), which has a universal singularity spectrum with power-law scaling of times between events. The CGMN was found to be a reasonable model for the singularity spectra of time series representing the recurrence history of volcanic tremor analyzed by Shaw and Chouet (1989, 1990). Thus, this type of power-law universality represents a family of self-similar states that also includes the properties of self-organized critical phenomena of the types applied by Bak and Tang (1989) to the earthquake process based on the idea of power-law distributions of times between instabilities (their earthquake model is a variation of the 'sandpile model' of systems maintained near a critical state).

Recognition that the power-law scaling of times seems to be characteristic and universal in many systems near a critical state of organization suggests that the phenomenologies of the simpler systems of oscillators (the two-state resonator and coupled rotating oscillator) can be used as a guide to the regimes of periodic and chaotic behavior in networks of coupled nonlinear oscillators of many types. Therefore, it seems reasonable to suppose that trajectories in the return maps of our earthquake recurrence 'alphabet' also represent events that would scale in the same way as the above critical phenomena. Unfortunately, there are insufficient events per spatial state at magnitudes of 5 and above to perform singularity analyses. Therefore, we are currently inspecting the conditional probabilities for excursions between pairs and triplets of spatial states for indications of clustering and/or periodicity. When we use a model that has 5 spatial states, there are 10 pairs of 'quasi-bistable states'. We find that clustering, quasiperiodicity, and possibly phase locking, are suggested by the distributions of events per episode (i.e., per spatial state) and by the similarities of ratios of average events per episode among all spatial states relative to the total numbers of events per spatial state (emphasizing that each spatial state represents one of the seismic regions on a map of California and vicinity).

If we consider these average ratios to be analogous to the "winding numbers" of coupled oscillators (Shaw, 1987b), then we would tentatively conclude that the recurrence history of earthquakes in California is either crudely phase-locked among these five regions, or that the short sequences of states available for analysis in each region represent partial samples of a globally self-organized critical state that gives self-similar power-law scaling of recurrence times in each region. However, the main conclusion at this stage of analysis is that an expectation of parallels between different semantic descriptions of the earthquake process, involving mechanical ideas of coupled deformations, numerical concepts of systems of coupled oscillators, and linguistic and information theoretic measures of redundancy among codified states, appears to be confirmed for the space-time patterns of intermediate to large earthquakes in California. When we are able to represent these results by an algorithm, we plan to compare them, and possibly combine them in modular fashion, with other pattern-recognition studies of the type described by Keilis-Borok and Kossobokov (1990).

References:

Bak, P. and C. Tang, Earthquakes as self-organized critical phenomena, J. Geophys. Res., 94, 15635-15637, 1989.

Ditto, W. L., S. Rauseo, R. Cawley, C. Grebogi, G.-H. Hsu, E. Kostelich, E. Ott, H. T. Savage, R. Segnan, M. L. Spano, and J. A. Yorke, Experimental observation of crisis-induced intermittency and its critical exponent, Phys. Rev. Lett., 63, 923-926, 1989.

Keilis-Borok, V. I. and V. G. Kossobokov, Times of increased probability of strong earthquakes ($M \geq 7.5$) diagnosed by algorithm M8 in Japan and adjacent territories, J. Geophys. Res., 95, 12413-12422, 1990.

Shaw, H. R., A linguistic model of earthquake frequencies applied to the seismic history of California, U. S. Geol. Surv., Open-File Rep. 87-296, 1987a.

Shaw, H. R., The periodic structure of the natural record, and nonlinear dynamics, Eos, 68, 1651-1665, 1987b.

Shaw, H. R. and B. Chouet, Application of nonlinear dynamics to the history of seismic tremor at Kilauea Volcano, Hawaii, U. S. Geol. Surv., Open-File Rep. 88-539, 1988.

Shaw, H. R. and B. Chouet, Singularity spectrum of intermittent seismic tremor at Kilauea Volcano, Hawaii, Geophys. Res. Lett., 16, 195-198, 1989.

Shaw, H. R. and B. Chouet, Fractal hierarchies of magma transport in Hawaii, and critical self-organization of tremor, J. Geophys. Res., submitted, 1990.

FAULT PATTERNS AND STRAIN BUDGETS

9960–02178

Robert W. Simpson
Branch of Tectonophysics
U.S. Geological Survey
345 Middlefield Road, MS/977
Menlo Park, California 94025
(415) 329–4865

Investigations

Work described here was done in collaboration with Aleksander Sadovskii, a visiting scientist from the International Institute of Earthquake Prediction of the USSR Academy of Science. We explored the utility of gravity anomalies, topographic data, and a combination of the two called the S-parameter as predictors of earthquake locations for two areas in California. The northern California study area was a rectangle about 300 kilometers on a side centered on San Francisco. The southern California study area was a rectangle about 400 km in a north–south direction and 500 km in a east–west direction centered on Los Angeles.

Results

The value of the S–parameter at a site is defined to be the maximum value of the Bouguer gravity (in milligals) within a window around the site, plus a coefficient times the maximum elevation (in meters) within the same window ($S = b_{max} + C * e_{max}$). Commonly the coefficient C is chosen to be 0.1 mGal/m, which makes the S–parameter a close approximation to the free–air gravity in places where topography is gentle and the window effect (a 5 km window was used) is not important. Previous studies using this parameter have been described in Artem'ev *et al.* (1977), Caputo *et al.* (1983), Eaton and Sadovskii (1985), and Gorshkov *et al.* (1985).

We explored potential correlations of past earthquakes in our study areas with values of the S-parameter and its horizontal gradient. We also looked for correlations with topography, Bouguer gravity, and isostatic residual gravity anomalies as well as with horizontal gradients of these anomalies.

Results are intriguing, although questions remain as to how to quantify their statistical significance and how to possibly use them for defining risk. For example, in the northern study area, locations for which the isostatic residual gravity gradient is greater than 2.5 mGal/km occupy only 17 percent of the area, but contain 38 percent of the $m \geq 4$ earthquakes from 1969–1990. Thus, $m \geq 4$ earthquakes have occurred in these high–gradient locations 2.9 times more often than elsewhere in the area over the past 20 years.

This result makes geologic sense, because gravity gradients occur over changes in density at depth that can indicate the presence of structures including faults.

In general, no single parameter value (*i.e.,* S–parameter, gravity, topography, or their respective gradients) outperformed the others in our tests. Some worked well in one area and not in others. Results seemed to be sharpened if the approach was applied to a more homogeneous tectonic domain such as the Salton Trough instead of the entire southern California study area, but the question then arises how to best define the extent of such homogeneous domains.

Additional work could be directed toward understanding the best ways of choosing the extent of the study area and tuning the methods to a particular tectonic environment. Work also needs to be done to define ways of evaluating uncertainties in the results and quantifying their statistical significance. One useful aspect of the approach is that it focuses attention on regions that may not have experienced recent seismicity, but which share characteristics with regions that have. In some cases, more detailed geologic and geophysical studies of such regions would seem appropriate.

References Cited

Artem'ev, M.D., Rotvain, I.M., and Sadovskii, A.M., 1977, Recognition of places of possible occurrence of strong earthquakes, VII. Investigation of Bouguer anomalies for California and adjacent regions, in Pattern recognition and spectral analysis in seismology, Nauka, Moscow, *Vychislitel'naya Seismologiya*, n. 10, pp. 19–32.

Caputo, M., Marussi, A., and Sadovskii, A.M., 1983, Bouguer anomalies, topography, and seismicity of Italy, *Dokl, AN SSSR*, v. 272, n. 1, pp. 57–61.

Eaton, D. and Sadovskii, A.M., 1985, Gravity anomalies and epicenters of earthquakes with $M \geq 5$ in the zone of the central branch of the San Andreas fault system: *Vychislitel'naya Seismologiya*, n. 18, pp. 134–138.

Gorshkov, A.I., Niauri, G.A., Rantsman, E.Ya., and Sadovskii, A.M., 1985, Use of gravimetric data for recognition of places of possible occurrence of strong earthquakes in the Great Caucasus: *Vychislitel'naya Seismologia*, n. 18, pp. 127–134

MECHANICS OF LITHOSPHERE PLATES

9960–03419

William D. Stuart
Branch of Tectonophysics
U.S. Geological Survey
Pasadena, California 91106
818 405-7816
FTS 961-7816

Investigations

Pacific–North America Plate Interaction

This work attempts to reconcile two related problems. The first problem is the cause of the variation along strike and depth of the locking of the upper San Andreas fault. On the northern and southern sections the locking is firm, and thus conditions exist for the generation of great earthquakes. On the central section the locking is weak or absent, and slippage occurs as aseismic creep and small earthquakes.

The second problem is to determine the tractions and body forces that cause tectonic plates in contact along western North America to move relative to one another. The assumption made for the analysis of both problems is that plate boundary faults obey a pressure dependent constitutive law, and that this law links the two problems. That is, in principle fault properties are to be found simultaneously with plate motions.

Parkfield Prediction Methods

The goal of this work is to construct methods for trying to predict the next moderate Parkfield earthquake before it happens rather than after. There are two strategies. The first is to formulate an earthquake instability model for repeated earthquakes. The model simulates faulting and ground deformation for all parts of each cycle. In all models of this kind accelerating preseismic faulting and ground deformation occur, and such anomalies, if large enough to detect, could be the basis of experimental predictions. This work is in collaboration with T. Tullis, R. Simpson, and J. Rice. The second strategy is to construct a mechanical model that accounts for the seismic quiescence and rate changes of 2-color laser lines reported by Wyss, Aviles, Burford, Langbein, and colleagues.

Results

Pacific–North America Plate Interaction

As previously reported, a procedure has been developed to compute the stress and velocity fields for the Juan de Fuca plate as it interacts with the Gorda, Pacific, and

North America plates. The procedure makes the plane stress approximation and uses edge dislocations to represent strike slip and opening mode boundaries. Subduction is represented by a new approximation that maps three dimensional deformation into two dimensions.

Current research is development of the corresponding model for major faults in southern California, including the San Andreas, Garlock, and oblique thrusts bounding and within the Transverse Ranges. In a preliminary model it is found that the observed location and slip sense of the Garlock fault is obtained as a computed result. The oblique thrusts considered collectively are also a computed result if the model takes account of the subducting upper mantle slab reported by Humphreys and others.

The stress fields produced by the two models above will be used to study the locking of the San Andreas between the Mendocino triple junction and Tejon Pass, as described above and in the previous report.

Parkfield Prediction Methods

A second generation model now works and is being refined mainly by Tullis. One version of the model attempts to determine if the expected moderate Parkfield earthquake could have been delayed by the Coalinga and Kettleman Hills earthquakes.

One explanation for the rate changes of seismicity and geodetic lines at Parkfield is decreased loading rate on the upper part of the San Andreas between Parkfield and Slack Canyon. A loading rate decrease can be caused by new slippage on a sub-horizontal detachment fault at 10-15 km depth and adjacent to or intersecting the San Andreas. Such a fault would be expected to start slipping late in a seismic cycle.

Reports

Stuart, W. D., News and Views – Earthquakes: Parkfield slowing down, Nature, **345**, 383-384, 1990.

Stuart, W. D., Seismic quiescence at Parkfield due to detachment faulting, Nature, submitted.

Stuart, W. D., Buffer faults and seismic quiescence at Parkfield, EOS, Fall 1990 AGU meeting.

Tullis, T. E., Stuart, W. D., and Simpson, R. W., Instability model for Parkfield earthquakes, including the effect of New Indria, Coalinga and Kettleman Hills events, EOS, Fall 1990 AGU meeting.

STUDY OF THE CORRELATION BETWEEN WATER LEVEL FLUCTUATION AND RESERVOIR INDUCED SEISMICITY - PHASE I

14-08-0001-G-1713

Pradeep Talwani
Department of Geological Sciences
University of South Carolina
Columbia, SC 29208
(803) 777-6449

Objective: To study the role of lake level fluctuations on the mechanism of reservoir induced seismicity (RIS). We are continuing the preimpoundment studies near Bad Creek pumped storage facility in northwest South Carolina. Impoundment is planned for mid-December, 1990.

Investigations

In preimpoundment studies we have emphasized on the collection of background data on seismicity, hydrogeology, and geology of the area. Currently we are in the process of setting up the instrumentation to monitor pre and post impoundment seismicity and changes in the ground water conditions due to the influence of the reservoir.

Noise Surveys

A preliminary noise survey was conducted in Bad Creek area during the summer of 1989 in which 3 quiet sites were located. To seek other sites for permanent and portable stations we conducted additional noise surveys during summer 1990. Eighteen sites were investigated of which seven were found suitable (Figure 1). During the 2 month survey we also recorded (at various sites) about 30 construction blasts at the local quarries in the reservoir area. The traveltime data from the blasts are being used to obtain a local seismic velocity model.

Background Seismicity

Background seismicity at Bad Creek is being monitored using data from the Jocasse seismic network. Analysis of data for one year (August 1989 to August 1990) indicated low level seismicity at Bad Creek (with an average of two events of $M_L < 1.0$ per month). Due to the high noise level during construction activities some events may have been missed.

During the noise surveys (summer 1990), a portable seismograph at a site to the north of the regions near a local quarry recorded about 50 events ($M_L < 0$). This activity which was recorded on two separate occasions suggests that the local stresses are high. We plan to further investigate this site.

Seismic Instrumentation

We are in the process of moving four permanent stations from Montecello Reservior to Bad Creek. We are currently working on the logistics of transmitting and recording the data (Figure 1). Data from Bad Creek network will be telemetered to Jocassee and then to Columbia where it will be recorded. In addition to the permanent stations, we plan to deploy 10 PASSCAL digital instruments (DAS) for a six month period starting in December, 1990. These three component instruments will be deployed at suitable locations to monitor the expected epicentral growth following impoundment.

Geological Investigations

Detailed geological studies have been carried out by Malcolm Schaeffer and his team of geologists at Duke Power Company. Geologic mapping of the area around Bad Creek Project suggests the presence of vertical faults and several shear zones, dipping southeast and roughly parallel to each other (Figures 2 and 3). Two of these shear zones (E and F) intersect the bottom of the reservoir. We expect the shear zones and faults to be better conduits of pore pressure diffusion, the dominant mechanism that triggers RIS. Two observation wells have been drilled through these shear zones (#1 and 2). These wells were continously cored. These cores will be used for laboratory estimations of their elastic properties.

Based on well logging and core data from over 200 boreholes, lithologic sections were reconstructed to obtain depths to various rock units. These data will be incorporated in explaining the spatial pattern of induced earthquakes.

Hydrological Studies

Based on borehole observations a contour map of the anticipated depth of ground water level above the sea level was prepared. This information together with location and dip of shear zones has been used to locate the three wells. Two of these wells (#1 and 2) have been drilled in the Bad Creek reservior area (Figure 2 and 3) and the third (#3) is currently being drilled to the east. The first two wells intersect the shear zones at depths of 50-80 ft. It is anticipated that the third well will keep shear zone at a depth of about 250 ft. These wells will be open to the the shear zones in order to record pressure changes there.

We anticipate changes in the pore pressure due to water level fluctuations will be most pronounced in the shear zones and regions hydraulically connected to them. The pore pressure changes will be continually monitored to seek possible temporal association with the rate of water level fluctuations. Currently two wells have been completed and the third is being drilled. These wells will be instrumented using the pressure transducers fabricated by the Engineering Department of USC (Figure 4).

Changes in pore pressure will be continuously monitored using the pressure transducers installed in these wells.

The pressure transducer operates in the 0 - 100 psi (0 - 7 bar) range with an accuracy of 0.1%. The pressure transducer is isolated from the top by a packer. It is however open to the water in the fracture zone through the gravel. Pressure is transmitted to the data acquisition unit on intervals of 0.010 seconds. Data are stored in the data acquistion system for easy access - and are downloaded to a portable computer using RS232 port.

Development of theoretical model

We are developing a theoretical model to study the pore pressure changes due to the coupled effect of reservior loading and pore pressure diffusion associated with rapid lake level fluctuations. A study of these effects associated with the initial filling of Monticello Reservoir provided interesting insights into the mechanism of RIS.

Reports

Talwani,P., and Rajendran, K., 1990. Bad Creek Project: A field experiment in Reservoir induced seismicity - preimpoundment phase. Seism. Res. Let., 61, 41p (abst)

Talwani, P. Ownby,A., Rajendran K., Widdowson,M. and Schaeffer, M., 1990. Bad Creek Project: A progress Report (paper to be presented at AGU Fall meeting, 1990)

Talwani,P. Ownby,A. Rajendran, K. Widdowson, M. and Schaeffer, M., 1990. A field study of reservoir induced seismicity at Bad Creek, S.C., the preimpoundment phase (paper to be presented at the Eastern Section of the Seismological Soc. October, 1990)

Rajendran, K., Talwani,P., and Acree.,S. 1990. Stress modification mechanisms of reservoir loading and their relative roles in triggering earthquakes: A case study from Monticello Reservoir, S.C. (to be presented at the Eastern Section of the Seismological Soc. October, 1990)

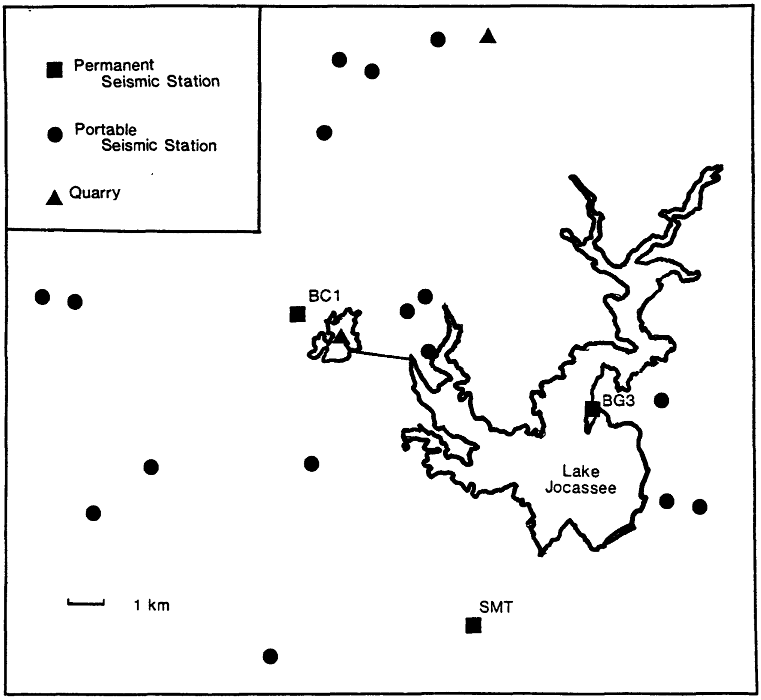

Figure 1. Shows location of sites occupied for noise survey and quarries in the vicinity of Bad Creek and Lake Jocassee

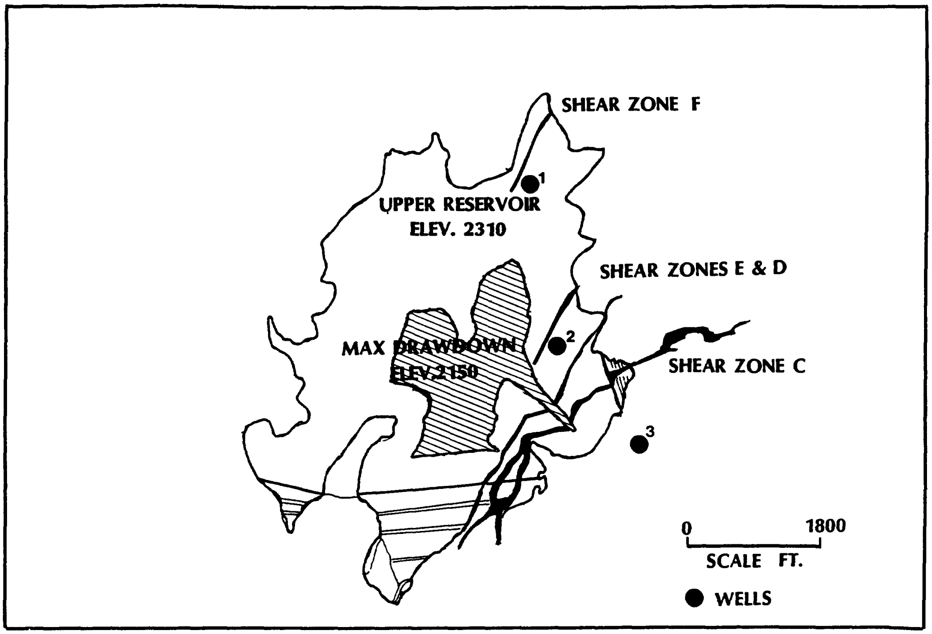

Figure 2. Location of shear zones in Bad creek area. The lake outline shows the extent of full pond (2310 ft) and stippled pattern shows the maximum drawdown (2150 ft). The numbers show the location of the observation wells.

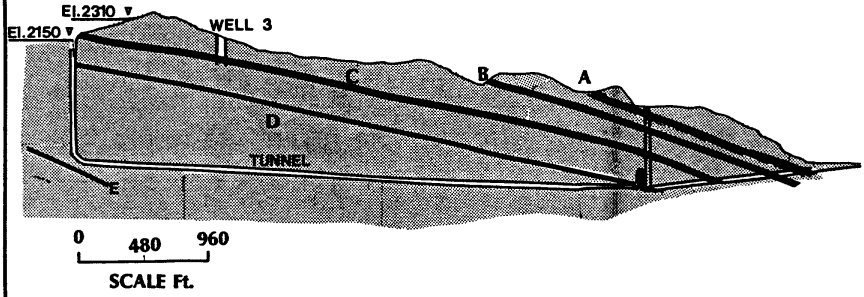

Figure 3. An east west cross section showing the location of the shear zones, the penstock tunnel and well no.3

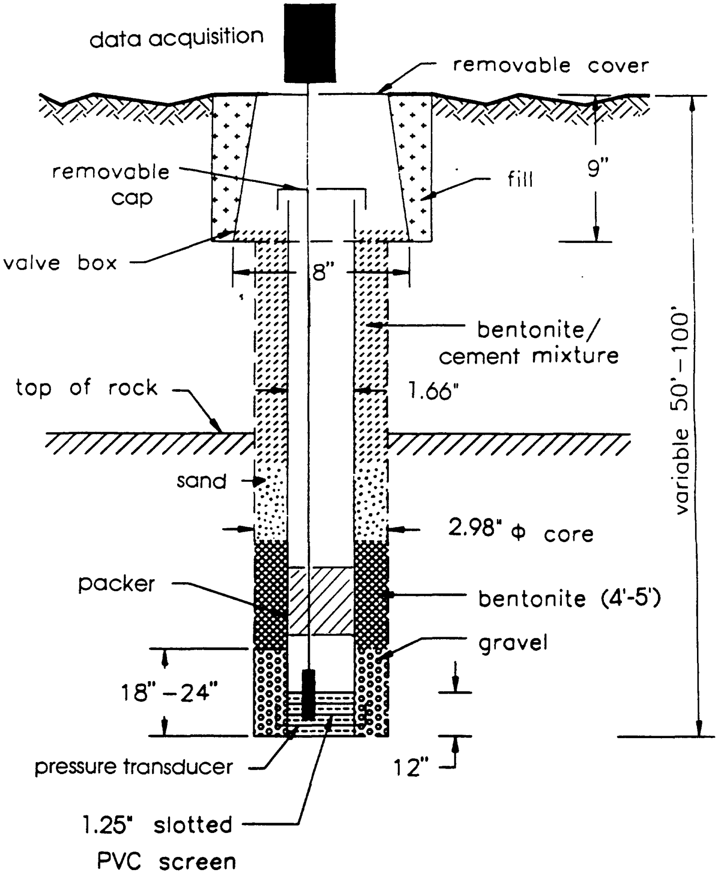

SEALED PIEZOMETER DETAIL

N.T.S.

Figure 4. Schematic drawing showing the cross section in one observation well with the piezometer and data acquisition system.

EXPERIMENTS ON ROCK FRICTION CONSTITUTIVE LAWS APPLIED TO EARTHQUAKE INSTABILITY ANALYSIS

USGS Contract 14-08-0001-G-1364

Terry E. Tullis
John D. Weeks
Department of Geological Sciences
Brown University
Providence, Rhode Island 02912
(401) 863-3829

INVESTIGATIONS:

1. Determination of the constitutive behavior of granite at large displacement.

2. Determination of the constitutive behavior of serpentinite.

3. Technical developments: completion and installation of bearing assembly to prevent sample misalignment; completion and use of new data acquisition system.

RESULTS:

1. With the completion and installation of our new bearing assembly to prevent axial misalignment of our samples (see item 3 below), we have continued our investigation of the velocity dependence of the frictional behavior of simulated granite gouge at large displacements. As we expected, the bearing assembly has eliminated the contamination of the sliding surfaces with Teflon that previously had been a severe problem. We now have measure-

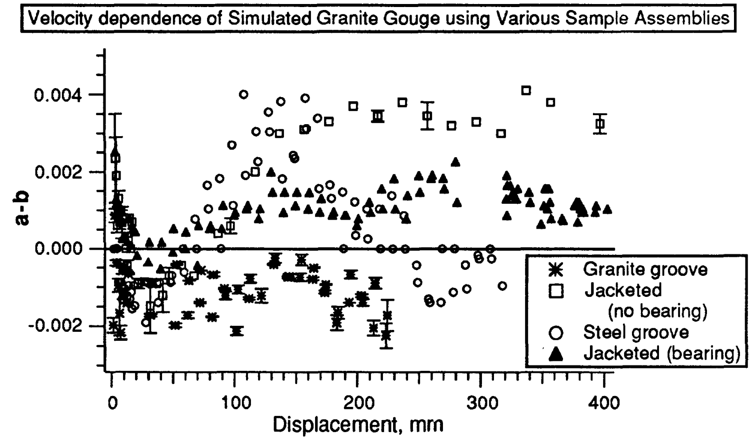

Figure 1. Velocity dependence of steady-state frictional strength of simulated granite gouge as determined using various different sample assemblies. Jacketed assemblies are run under confining pressure, granite and steel groove assemblies use a grooved sample to confine the gouge and have no jacket. Jacketed runs without the new alignment bearing have the potential for contamination of the sliding surface by Teflon from the jackets while groove runs have no jacket and no possibility of Teflon contamination. Groove runs, on the other hand, do not confine the gouge completely and lose gouge during the run, possibly preventing the development of mature fabrics in the gouge layer.

ments of the velocity dependence of frictional strength (**a-b**) of simulated granite gouge in four different assemblies: jacketed runs with confining prussure (and possible Teflon contamination), unjacketed runs with no confining pressure in which the gouge is contained in a grooved sample of steel or granite, and jacketed runs under confining pressure with the addition of the bearing assembly to prevent run-out of the sample rings. The behavior is similar in all cases for about the first 100 mm. After about 100 mm the velocity dependence is inconsistent, varying from velocity weakening in the granite groove runs to strong velocity strengthening in the jacketed confined runs lacking the alignment bearing (Figure 1).

Although the value of **a-b** in the confined runs with alignment bearing at displacements of a few mm is similar to values at displacements greater than about 100 mm, the detailed frictional response to a change in velocity is quite different. The new bearing assembly and new data acquisition system have improved the quality of the data so that we are able to analyze this difference much better than previously. We have long felt that our results usually require two state variables (the "active element" that produces the decays after a velocity change). In fact, the simulated gouge (Figure 2) requires a second state variable with a negative coefficient ($\mathbf{b_2}$). Such a negative $\mathbf{b_2}$ causes, in the case of a velocity increase, an upward decay, opposite to that which is considered "normal". The evidence for this negative $\mathbf{b_2}$ is particularly strong in the bottom trace in Figure 2, taken at a displacement of about 380 mm. We know of no way to combine the ringing below the previous

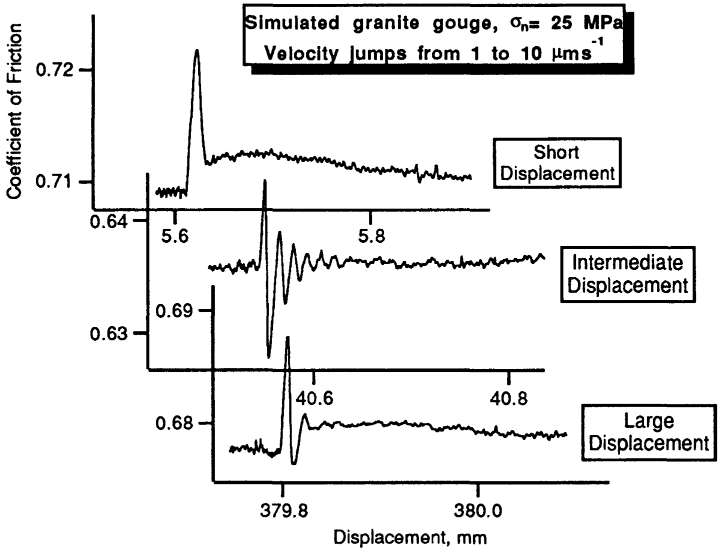

Figure 2. Development of response of frictional strength of simulated granite gouge to increase in load point velocity with increasing displacement. In each case, the velocity was increased from 1.0 to 10.0 μm s^{-1}. Short and long displacement traces exhibit velocity strengthening while intermediate trace shows approximately neutral response. Development of ringing indicates that the value of $\mathbf{b_1}$ has increased leading to short-term velocity weakening. In fact, inversion of the large displacement trace gives a set of parameters with $\mathbf{a\text{-}b_1} < 0$ while $\mathbf{a\text{-}(b_1\text{+}b_2)} > 0$.

steady state level that follows the velocity change with the overall velocity strengthening without resorting to a negative $\mathbf{b_2}$. While this enhances stability, it is still possible with a sufficiently large $\mathbf{b_1}$ to have what might be termed "short-term velocity weakening" and unstable behavior. In our experiments this negative $\mathbf{b_2}$ seems to develop slowly with displacement, along with an decreasing $\mathbf{a\text{-}b_1}$. We infer this from the change from velocity strengthening at small displacement, to nearly neutral steady-state response accompanied by strong ringing at intermediate displacement, to velocity strengthening with ringing at large displacement. The inference of "short-term velocity weakening" in the case of the large displacement trace in Figure 2 is supported by determination of constitutive parameters by least-squares inversion of the bottom trace. This gives values as follows: $\mathbf{a} = 0.00729$, $\mathbf{b_1} = 0.00777$, $L_1 = 1.9$, $\mathbf{b_2} = -0.00133$ and $L_2 = 7.58$; note that $\mathbf{b_1}$ is larger than $\mathbf{a}$, giving $\mathbf{a\text{-}b_1} = -0.00048$ while $\mathbf{a}-(\mathbf{b_1}+\mathbf{b_2}) = +0.00085$. The inversion was done using a computer program written by graduate student Linda Reinen.

2. It has been suggested that aseismic slip along segments of both continental and oceanic transform faults may be due to the presence of serpentine. Consequently, we have conducted a series of experiments to study the frictional behavior of serpentinite. We have previously reported the results of duplicate experiments at 25 and 50 MPa normal stress which yield consistent results. Initial experiments at normal stresses greater than 75 MPa showed sample misalignment and were therefore suspect. Recent experiments at these higher normal stresses were conducted using the ball-bearing alignment assembly which ensures proper sample alignment (see section 3, below). The experiments at 100 and 125 MPa normal stress display results similar to the low normal stress results (see Figure 3). We find that serpentinite exhibits velocity strengthening behavior at slow sliding velocities and velocity weakening at intermediate velocities. The transition in velocity dependence occurs in the range 0.03 to 0.1 microns/second. Because velocity strengthening is associated with stable sliding and velocity weakening may be associated with unstable sliding, these results indicate that faults containing serpentine should creep aseismically at typical rates of plate motion, but could produce earthquakes if forced to slide fast enough. This result is consistent over the full range of normal stress studied to date.

Results of experiments conducted by other workers on intact serpentinite samples indicate a transition from brittle to ductile behavior with increasing confining pressure, providing the temperature remains less than the dehydration temperature of serpentine. This would imply that at sufficiently high normal stress, we should see a transition to velocity strengthening at all velocities, and a change from shear stress depending linearly on normal stress to shear stress independent of normal stress. Our experiments up to 125 MPa normal stress indicate no apparent change in velocity dependence with increasing normal stress. In addition, the shear strength exhibits a nearly linear dependence on normal

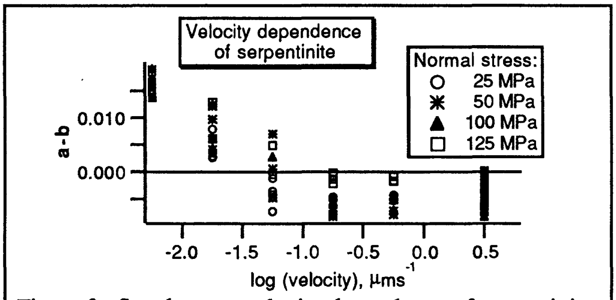

Figure 3. Steady-state velocity dependence of serpentinite.

stress. Apparently, normal stresses greater than 125 MPa are required for serpentinite to undergo the transition from brittle to ductile behavior; this is under continued investigation.

3. Two technical developments that improve the quality of data we collect have recently gone into routine use. We have now installed a ball-bearing assembly (described in volume XXX) to guarantee concentric alignment of the two sample rings. This was originally conceived to prevent contamination of the sliding surfaces with Teflon from the sample jackets caused by run-out of the sample rings, but has paid additional dividends as well. It has, in fact, eliminated the sliding surface contamination problem, and has also eliminated a wander in the measured frictional strength caused by slight eccentricity of part of the torsional drive system. In addition, the new assembly allows use of an internal LVDT to measure changes in sample length, simultaneously with use of an internal resolver to make very precise measurements of rotary displacements. Previously, these instruments could not be used at the same time. We have also recently switched to a new data acquisition and control system based on a Hewlett Packard workstation and data acquisition equipment. The resolution of our data is now limited entirely by instrument noise and drift. The increase in resolution over that furnished by the 13-bit analog-to-digital convertor in the old system is as large as a factor of ten for certain channels. The improvement is most readily seen in the traces of frictional response to velocity changes (as in Figure 2) which previously have had a range of about five least significant bits, giving it the stair-step appearance we have come to expect of digital data. It has also allowed us to resolve changes in sample length with velocity changes that were previously undetectable. The new workstation is much faster and provides more convenient handling of data. This report and its graphics, for instance, were prepared on a Macintosh computer with data extracted from archival records on the HP workstation and transferred over Ethernet. The manipulation of data on the workstation is far faster and more convenient than on our old DEC system because of the increase in computation speed and because of the many facilities provided by the UNIX operating system.

REPORTS:

Abstracts:

Reinen, L.A., and Weeks, J.D., Determination of rock friction constitutive parameters using a least squares inversion method, *Eos, Trans. Am. Geophys. Union, v. 71* , 636, 1990.

Weeks, J.D., Beeler, N.M., Tullis, T.E., Reinen, L.A. and Blanpied, M.L., Velocity dependence of frictional behavior of simulated granite gouge to large displacement, abstract accepted for AGU fall meeting, 1990.

Reinen, L.A., Weeks, J.D., and Tullis, T.E., The effect of normal stress and sliding velocity on the frictional behavior of serpentinite, abstract accepted for AGU fall meeting, 1990.

Papers:

Yund, R.A., Blanpied, M.L., Tullis, T.E., and Weeks, J.D., Amorphous material in high strain experimental fault gouges, *J. Geophys. Res., 95*, 15589-15602, 1990.

Reinen, L.A., and Weeks, J.D., Determination of rock friction constitutive parameters using a least squares inversion method, to be submitted to *J. Geophys. Res.*

Regional and National Seismic Hazard and Risk Assessment

9950-01207

S.T. Algermissen
Branch of Geologic Risk Assessment
U.S. Geological Survey
Denver Federal Center, MS 966
Denver, CO 80225
(303) 236-1611

Investigations

1. Improved measures of ground motion over acceleration and velocity are being investigated for mapping at a national scale.

2. Regional seismic source zones for a new generation of national probabilistic ground motion hazard maps are continuing to be revised, updated and documented.

3. Developmental work is continuing on the new seismic hazard and risk program, FRIENDLY. This program allows the analyst to perform probabilistic ground-motion hazard analysis interactively at a computer terminal. Conceptually, the ground-motion calculations are similar to those performed in the current program SEISRISK III. However, FRIENDLY is far more flexible with more sophisticated geometric treatments of fault sources.

Results

1. Project staff have been cooperating with the Building Seismic Safety Council, the National Center for Earthquake Engineering Research, and the Structural Engineers Association of California on identifying improved measures of ground motion for use in structural design. There is general agreement at this time that mapping of spectral response parameters (e.g. spectral acceleration and/or spectral velocity) rather than parameters such as peak acceleration will result in improved design procedures. Current work indicates that spectral response can be reasonably approximated with only two spectral response parameters, one at a short period of about 0.3 second and one at a longer period of about 1.0 second. Design procedures based on spectral response parameters have been proposed for use in the 1991 edition of the National Earthquake Hazards Reduction Program Recommended Procedures for the Development of Seismic Regulations for New Buildings.

2. Earthquakes in central and eastern North America with M 5.0 and larger appear to differ from earthquakes of similar magnitudes in the Precambrian Australian craton. Several of the Australian earthquakes were comparatively shallow and some produced historic surface ruptures. The differences imply that either the rupture process, the geological environment, or the stress environment differs between the two continental interiors. North America comprises a central a central stable Precambrian craton rimmed by late Proterozoic-early Paleozoic passive margins and aulacogens; younger orogens and margins are farther outboard. Seismicity in the central and eastern North America concentrates in the late Proterozoic and younger structures that rim the older, less active central craton. The only large, shallow, historic earthquake ruptured the surface at Ungava, Quebec (1989) in the central craton. Perhaps only the central craton is the North American analog to the Australian craton.

3. The next generation seismic hazard and risk computer program, FRIENDLY, has had limited use in ground motion calculations for project work. The options available for interactive use at a computer terminal continues to be expanded and documented.

Reports

Algermissen, S.T., Arnold, E.P., Steinbrugge, K.V., Hanson, S.L., and Hopper, M.G., 1990, Probabilistic and scenario losses to dwellings in California: U.S. Geological Survey Opern-File Report 90-323, 25 p.

Bender, B.K., 1990, Treatment of parameter uncertainty and variablility in seismic hazard maps: Earthquake Spectra [submitted].

Hopper, M.G., Leyendecker, E.V., Thenhaus, P.C., Stover, C.W., Algermissen, S.T., Reagor, B.G., Perkins, D.M., Hanson, S.L., Brewer, L.R., and Baldwin, F.W., 1989, Damage and intenisty survey of the October, 17, 1989 Loma Prieta earthquake: Eos, v. 71, no. 8, p. 288.

Leyendecker, E.V., Thenhaus, P.C., Campbell, K.W., and Hopper, M.G., Hanson, S.L., Algermissen, S.T., and Perkins, D.M., 1990, Preliminary assessment of the distribution of intensity and strong ground motion for the Loma Prieta Earthquake: Earthquake Spectra, Supplement to v. 6, p. 58-72..

Leyendecker, E.V., Thenhaus, P.C., Campbell, K.W., and Hopper, M.G., Hanson, S.L., Algermissen, S.T., and Perkins, D.M., 1990, Preliminary assessment of the distribution of strong ground motion and intensity for the Loma Prieta Earthquake: Interagency Committee on Seismic safety and Construction Special Report on the October 17, 1989, Loma Prieta Earthquake, in press.

Steinbrugge, K.V., and Algermissen, S.T., 1990, Earthquake losses to single family housing – California experience: U.S. Geological Survey Bulletin 1939-A, 65 p.

Steinbrugge, K.V., and Algermissen, S.T., 1990, California mobile homes (manufactured housing): Probable maximum loss (PML) and loss attentuation with distance: U.S. Geological Survey Bulletin 1939-B.

Wheeler, R.L., and Johnston, A.C., 1990, Nodal-plane dips, and their geologic associations in central and eastern North America [abs.]: Seismological Research Letters [submitted].

Wheeler, R.L., 1990, Seismicity and the Iapetan passive continental margin [abs.]: Geological Society of America Abstracts with Programs [submitted].

Holocene Paleoseismology of Coastal Washington State

9540-04004

Brian F. Atwater
U.S. Geological Survey at University of Washington AJ-20
Seattle, Washington 98195
(206) 442-2927 FTS 399-2927

INVESTIGATIONS

Precise radiocarbon dating of subsidence about 300 years ago. The goal of this dating to test synchrony of subsidence along hundreds of kilometers of coast. The materials dated are groups of rings from bark-bearing stumps of Sitka spruce killed by the most recent sudden subsidence. During the summer of 1990 I sawed ten samples from Willapa Bay and Grays Harbor. In addition, Minze Stuiver reported the first precise ages on spruce-stump samples collected previously from Willapa Bay and the Copalis River.

Did sand blows erupt through subsiding marshes and swamps underlain by thick bodies of loose, wet sand? They should have if strong shaking accompanied the subsidence; the goal of this work is to test for such shaking. During the summer of 1990 a team of geologists made a reconnaissance of liquefaction features in coastal southern Washington. The team consisted of Steve Obermeier and Brian Atwater (USGS), John Shulene (volunteer), Steve Palmer (Washington Division of Geology and Earth Resources), and Jim Phipps (Grays Harbor College). We visited most of the natural outcrops in areas likely to produce sand blows at estuaries in coastal southern Washington. In a separate but related effort, Shulene canvassed long-time residents of the Puget Sound city of Puyallup and the coastal sand spit west of Willapa Bay to determine the location of sand blows produced by the large Puget Sound earthquakes of 1949 and 1965.

RESULTS

Precise radiocarbon dating of subsidence about 300 years ago. Radiocarbon results on the next page (table 1) are consistent with subsidence around A.D. 1700, in the middle or late 1700s, or in the middle 1900s. This ambiguity is inherent in the radiocarbon dating of materials postdating the late 1600s. Ring-width pattern matching of western red cedar shows that the same subsidence occurred during or soon after the 1690s (D.K. Yamaguchi, C.A. Woodhouse, and M.S. Reid, written commun., 1990). A subsidence date around A.D. 1700 provides the simplest way to reconcile the radiocarbon ages with the tree-ring dates.

Did sand blows erupt through subsiding marshes and swamps underlain by thick bodies of loose, wet sand?

(1) Sand blows erupted about 1100 years ago at the Copalis River estuary (coastal southern Washington, near Grays Harbor). Although the sand blows about 1100 years ago did not coincide with appreciable subsidence at the Copalis River, subsidence of similar radiocarbon age occurred elsewhere in coastal Washington and northern Oregon.

(2) Among the five outcrops in which we found sand intrusions or volcanoes about 1100 years old at the Copalis River, none shows evidence for liquefaction during subsidence of that area about 300 years ago, even though the event responsible for this subsidence probably triggered a large tsunami. But the total length of these outcrops is 15 m--too little to preclude strong shaking during subsidence about 300 years ago.

(3) Liquefaction probably occurred along the western shore of Willapa Bay sometime between about 300 and 1700 years ago. I do not know if this liquefaction coincided with sudden coastal subsidence.

(4) The 1949 Puget Sound earthquake (magnitude 7.1) caused many sand blows in Puyallup but probably triggered none near the coast at Willapa Bay.

Table 1. Radiocarbon ages on rings from Sitka spruce probably killed by coseismic subsidence in coastal Washington state

Location	Lab no. QL-	Age		Rings dated (1=outside)		Earliest tree death in yr A.D.[2]
		^{14}C yr B.P.	Yr A.D.[1]	Range	Middle	
Copalis	4400	207+/14	1649-1677 1739-1804 1939-1954	30-49	40	1689-1717
Bay Center	4401	184+/14	1653-1690 1724-1810 1925-1954	30-35	33	1686-1723
Niawiakum	4404	219+/13	1647-1672 1745-1763 1767-1800 1943-1954	30-49	40	1687-1712
Niawiakum	4405	152+/30	1650-1950	1-20	10	after 1660

---

[1] At two standard deviations with error multiplier of 1.6, obtained from intercepts (method A of calibration program of Stuiver and Reimer)

[2] Sum of earliest calibrated age range and number of middle ring

REPORTS

Atwater, B.F., and Yamaguchi, D.K., 1991?, Sudden, probably coseismic submergence of Holocene trees and grass in coastal Washington state: manuscript intended for *Geology*; passed USGS review in September, 1990.

Shulene, J.A., 1990, Evidence of liquefaction in the Puyallup Valley: Washington Geologic Newsletter, v. 18, p. 15-16.

Depth to Bedrock map of the greater Tacoma area, Washington

9950-04073

Jane M. Buchanan-Banks
Branch of Geologic Risk Assessment
U.S. Geological Survey
David A. Johnston Cascades Volcano Observatory
5400 MacArthur Boulevard
Vancouver, Washington 98661
(206) 696-7996

Investigations

Most of report period spent on revising manuscript, Geologic Map of the Hilo 7 1/2' quadrangle, Island of Hawaii, as result of BWTR review.

Results

Small changes and a few data additions were made to Depth to Bedrock map. Completion of map delayed due to lack of marine seismic reflection profiles of sufficient depth to provide a bedrock depth. Marine seismic reflection profiles run by Sam Harding in 1988 is awaiting processing. Dialogue continues with WRD, Tacoma, in an attempt to arrange a possible co-purchase of seismic lines run by Western Geophysical in southern Puget Sound. Drawing of isopach lines showing depth to bedrock rely heavily on obtaining this data.

PUGET SOUND PALEOSEISMICITY

9950-04484

ROBERT C. BUCKNAM
U.S. Geological Survey
M.S. 966, Federal Center
Denver, Colorado 80225
(303) 236-1604

INVESTIGATIONS

Continued study of late Holocene uplift in the central Puget Lowland, Washington.

RESULTS

Stratigraphic relations and ^{14}C ages at Restoration Point, Bainbridge Island, Washington, (locality R, fig. 1) indicate that about 7 m of uplift occurred there less than 1,350-1,550 years ago (Bucknam and Barnhard, 1989). Similar data from a salt marsh 5 km to the north at Winslow (locality W) suggest that vertical deformation from the same event at that site was probably less than about 2 m. The surface of the Winslow marsh is at about mean higher high water and is underlain by about 2 m of peat. A 10-cm-thick interval of that peat collected at 160 cm depth gives a ^{13}C adjusted ^{14}C age of 1,670±60 yr B.P. (Beta-36044). Using the CALIB program of Stuiver and Reimer (1986) and a lab error multiplier of 1, the one-sigma calibrated age range for the sample is 1,520-1,690 cal yr.

Data collected thus far from the two sites show it is likely that the Winslow marsh was established prior to the nearby uplift at Restoration Point. Thus, the record of relative sea level in the stratigraphy of the Winslow marsh constrains the amount of vertical displacement that may have occurred at the site. Salt marsh plant fossils at several levels in the Winslow marsh section suggest that any vertical displacement since the marsh deposits began forming has been probably 1-2 m less than the tidal range of about 3.5 m. Radiocarbon and fossil samples collected in September 1990 should allow reconstruction of a detailed chronology and relative sea level history at the marsh.

The Winslow marsh is an important site for identifying possible structures associated with the uplift at Restoration Point. One of the major neotectonic features that has been recognized in central Puget Sound is a steep east-west-trending gravity anomaly that has been interpreted as a major fault zone, down to the north. Gower and others (1985) have inferred a possible Quaternary fault associated with that gravity anomaly (F on fig. 1). The relative sea level histories of the Winslow and Restoration Point sites, which lie on opposite sides of the inferred fault, may provide a basis for determining whether a few meters of late Holocene slip has occurred on the fault.

References Cited:

Bucknam, R.C., and Barnhard, T.P., 1989, Evidence of sudden late Holocene uplift in the central Puget Lowland, Washington [abs.]: Eos [Transactions of the American Geophysical Union], v. 70, p. 1332.

Gower, H.D., Yount, J.C., and Crosson, R.S., 1985, Seismotectonic map of the Puget Sound Region, Washington: U.S. Geological Survey Miscellaneous Investigations Map I-1613.

Stuiver, M., and Reimer, P.J., 1986, A computer program for radiocarbon age calibration: Radiocarbon, v. 28, p. 1022-1030.

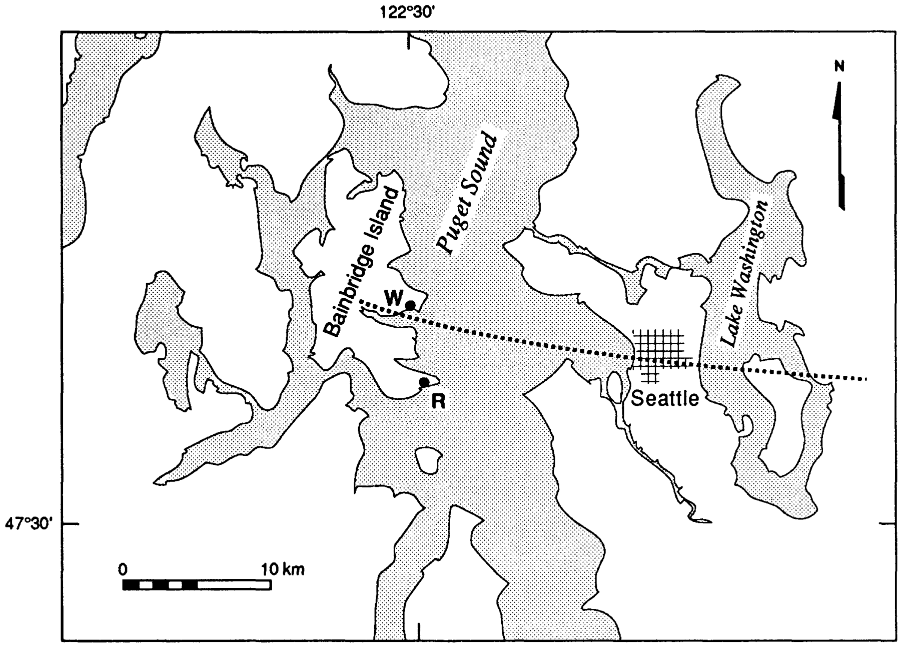

FIGURE 1. Central Puget Sound, Washington. R = Restoration Point site, W = Winslow site, heavy dotted line is possible Quaternary fault of Gower and others (1985).

Geology and Tectonic Evolution of the Western Transverse Ranges

9550-04063

Russell H. Campbell
Branch of Geologic Risk Assessment
U. S. Geological Survey
MS 922, National Center
Reston, Virginia 22092
(703)648-6784

Investigations

Recent project work has focused on the acquisition of digital geologic map data in preparation for compilation of a preliminary geologic database for the Los Angeles 1:100,000-scale quadrangle. Initial emphasis is on the southwestern 1/4 of the 1° x 30' quadrangle. Brief field investigations have addressed problems of stratigraphic correlation and structural continuity. Field investigations were conducted in cooperation with F. H. Weber of the CDMG. Preparation of the digital geologic map is a joint effort with R. F. Yerkes, USGS, BWRG.

Results

Several general and special-purpose geologic maps, which have recently been published at various scales (1:12,000 to 1:48,000) by the USGS and the California Division of Mines and Geology, have been digitized and are being edited for compilation at 1:100,000 scale. Digitizing of the geologic maps has been done manually in GSMAP and ARC/INFO, and by author scanning (using the Reston GIS-lab Tectronics scanner) followed by conversion to ARC/INFO. Editing to conform with compilation base scale and topographic contour representation is in initial stages. Digital images of the eight 71/2' quadrangle segments of the 1:100,000-scale composite topographic base were prepared by NMD, Menlo Park, as individual ARC/INFO files, by scanning (Scitex) and conversion to ARC/INFO.

Preliminary field investigations in the summer of 1990 indicate that intertonguing of similar marine sedimentary facies is common in the marine sequence that ranges from late middle Miocene to early Pliocene in age, and in various places, includes units assigned to the Monterey, Modelo, Castaic, Towsley, Repetto, and Pico Formations. Many of these units have been established on the basis of fossil ages; however, all include lithofacies representing deposition on submarine fans and quieter deep marine environments. Sedimentological study of the fans might yield a better understanding of the fault distribution and history on which late Pliocene and younger deformation has been imposed.

Structural significance of stratigraphic position, abundance, and spatial distribution of sills

Map relationships established in the Point Dume quadrangle (Campbell and others, 1970), the Malibu Beach and Topanga quadrangles (Yerkes and Campbell, 1980), and manuscript mapping by USGS and CDMG geologists in adjacent parts of the Santa Monica Mountains suppport the conclusion that major extensional tectonic activity was accompanied by basaltic and andesitic volcanism, beginning in middle middle Miocene time. (This coincides with the "basin-inception phase" of the evolution of the Los Angeles basin, as described by Yerkes and others, 1965). Although Conejo volcanism ceased by late middle Miocene time, the extensional deformation continued, probably episodically, into late Miocene (and possibly Pliocene) time. Subsequently, the stress field appears to have been reoriented so that deformation of the late Pleistocene and Holocene deposits (as well as contemporary seismic and aseismic deformation) indicates crustal shortening dominated by north-over-south reverse faulting.

Several relationships suggest that early phases of the extensional deformation (e.g., the detachment faulting) occurred in close association with intrusive activity related to the emplacement of the Conejo Volcanics (middle Miocene). Dikes and sills of basalt and andesite intrude the sedimentary strata that underly the extrusive volcanic strata. Sills and sill-like irregular bodies are largest and most abundant in the Vaqueros and Topanga Canyon strata, and the seem largest, thickest and most abundant where they are stratigraphically less than several hundred feet beneath the base of the Conejo Volcanics. The basal strata of the Conejo Volcanics include pillow breccias and aquagene tuffs together with intercalated marine siltstone and volcaniclastic sandstone; clear evidence of subaerial extrusive activity is lacking. These relations suggest there may have been no significant episode of uplift and subaerial erosion intervened between the close of marine sedimentation (as represented by the Topanga Canyon Formation) and the outbreak of Conejo submarine volcanism. A possible alternative to subaerial erosion as the origin of the unconformity at the base of the Conejo Volcanics is tectonic removal by detachment faulting on a low-angle surface, perhaps locally offset by high-angle faults. Because the pressure balance that permits sills to form (see McBirney, 1963, p. 465) would also reduce frictional resistance to low-angle faulting, the timing and extent of detachment faulting evidenced by the emplacement of the Tuna, Zuma, and Malibu Bowl thrust sheets may have been directly affected by episodes of intrusive activity as represented by the dikes and sills.

References Cited

Campbell, R. H., Blackerby, B. A., Yerkes, R. F., Schoellhamer, J. E., Birkeland, P. W., and Wentworth, C. M., 1970, Preliminary geologic map of the Point Dume quadranle, Los Angeles County, California: U.S. Geological Survey Open-File Report, Map 1:12,000

McBirney, A. R., 1963, Factors governing the nature of submarine volcanism: Bulletin Volcanologique, v. 26, p 464-469

Yerkes, R. F., and Campbell, R. H., 1980. Geologic map of east-central Santa Monica Mountains, Los Angeles County, California: U.S. Geological Survey Map I-1146, 1:24,000

Yerkes, R. F., McCulloh, T. H., Schoellhamer, J. E., and Vedder, J. G., 1965, Geology of the Los Angeles Basin, California -- an introduction: U.S. Geological Survey Professional Paper 420-A, 57p.

TECTONICS OF SEISMIC SOURCE ZONES, CENTRAL INTERIOR OF THE UNITED STATES

9950-04542

ANTHONY J. CRONE
Branch of Geologic Risk Assessment
U.S. Geological Survey
Box 25046, MS 966, Denver Federal Center
Denver, CO 80225
(303) 236-1595

INVESTIGATIONS

1. Crone and McKeown received funds to purchase Vibroseis™ seismic-reflection data across the fault systems that define the boundaries of the Reelfoot rift. These funds are part of the Loma Prieta earthquake relief funds that were specifically dedicated to studies in the New Madrid seismic zone (NMSZ).

2. Ellis began (a) investigating the potential for utilizing pre-existing small-diameter boreholes for conducting shallow hydraulic-fracturing stress measurements in regions around the NMSZ, and (b) developing plans for modifying existing slim-hole hydraulic-fracturing equipment for wireline operations.

3. Collins continued processing selected samples of well cuttings from Dow Chemical #1 Garrigan drill hole for analysis of insoluble residues.

4. Dart continued work on final versions of computer-generated subcrop, structural contour, and isopach maps of units within the Paleozoic section of the Upper Mississippi Embayment. In addition, he continued acquisition of existing drill-hole data, and updated the existing data base of drill-hole stratigraphic information as needed.

5. Diehl continued petrographic and scanning electron microscope (SEM) studies of drill core from the Dow Chemical #1 Garrigan drill hole and of drill cuttings from the Dow Chemical #1 Wilson drill hole.

6. Swolfs continued analyses of structural features in the Dow Chemical #1 Garrigan drill hole.

7. Cecil continued analysis and interpretation of potential field data to clarify structural relations across the Frontal Wichita fault system (FWFS) in the area of the Meers fault, southwest Oklahoma. In addition, she measured magnetic susceptibility and density (with Lee-Ann Bradley, BGRA) of handsamples collected in the field as well as drill cores (loaned from Ken Luza, Oklahoma Geological Survey) from holes adjacent to the Meers fault.

8. Collins began examination of thin sections and handsamples of core (on loan from Ken Luza, Oklahoma Geological Survey) from holes drilled adjacent to the Meers fault.

9. Ellis continued to evaluate and examine data on stress and the distribution of stress in south-central Oklahoma, and it's relationship to geologic structure and seismicity in the region of the FWFS.

10. Madole continued analysis of regional reconnaissance and detailed local studies of Quaternary alluvial stratigraphy in the vicinity of the Meers fault, southwestern Oklahoma.

11. As part of a USGS Gilbert Fellowship (FY 90-91), Crone and Michael Machette (BGRA) made preparations for field studies of two historic intraplate earthquakes in Australia that produced surface ruptures. The fieldwork is being conducted from August 19-October 13, 1990.

RESULTS

1. (Crone and McKeown) To date, efforts to identify and characterize seismic-source zones in the New Madrid region have concentrated on the areas of abundant microseismicity, which are primarily in the interior of the Reelfoot rift. The earthquake potential of the major fault zones along the margins of the rift is unknown, even though these zones are prominent structural discontinuities that likely extend through the upper crust. Assessing the earthquake potential of these faults is very important because the epicenter of an earthquake on one of these faults could be only 25 km away from Memphis, Tenn., the largest population center in the region. Furthermore, the microseismicity in the New Madrid region shows a weak alignment of epicenters along the southeastern margin of the rift, which may be evidence that these faults are capable of generating damaging earthquakes.

In the NMSZ, seismic-reflection data are the best (and commonly the only) means of identifying and characterizing deep, potentially seismogenic structures, because structural features in competent bedrock are concealed by a thick sequence of poorly consolidated Mesozoic and Cenozoic sedimentary rocks. These studies seek to characterize the structure of, and to document the amount and timing of, movement on the fault systems that bound the Reelfoot rift by interpreting about 126-line-miles of newly acquired seismic-reflection data. The procurement process for these data is nearly complete, and specific lines have been tentatively identified for purchase. Efforts will focus on the faults along the southeastern margin of the rift because of the hazard posed by earthquakes on these faults to the city of Memphis.

2. (Ellis) Contacts were made with personnel from State geological surveys in the area surrounding the NMSZ to search for existing small-diameter boreholes drilled for engineering or minerals exploration purposes, and to obtain contacts with drilling, mining, or quarry operators. Early feedback is encouraging in that such boreholes may exist in certain localities or that drilling activities resulting in potentially usable boreholes occur in areas of interest. An agreement was reached for the use of a small logging truck that can be outfitted to support shallow wireline hydrofrac measurements using existing slim-hole equipment.

3. (Collins) The insoluble residues of samples from 47 depth intervals from the Dow Chemical #1 Garrigan drill hole show no distinctive changes in the mineralogy or proportion of insoluble minerals that might serve as a tool for stratigraphic correlation. A special effort was made to treat the samples in a manner that would preserve soluble evaporite minerals such as gypsum, anhydrite, and phosphate fossil fragments. No evaporites have been found. Brachiopod fragments are currently being identified by M.E. Taylor (Br. of Paleontology and Stratigraphy, USGS). Identification of these fossils may provide the only stratigraphic correlation tool for the Garrigan drill hole.

Rock-fragment residues indicate cyclic transgressive and regressive events (see fig. 1). Insoluble minerals imply that the sedimentary units in the Garrigan drill hole were deposited in a near-shore, shallow, slightly reducing marine environment.

4. (Dart) Additional new drill-hole data were acquired and the existing Upper Mississippi Embayment drill-hole stratigraphic information data-base was updated. Work on the generation of a series of subcrop, structural contour, and isopach maps is nearing completion. This series will include approximately 32 maps, 29 of which are geologic interpretations of stratigraphic units of Paleozoic age and older that show a good correlation with interpreted units from seismic-reflection profiles.

5. (Diehl) Vertical fractures in the Dow Garrigan flaser-bedded sequence are crosscut by stratabound epigenetic mineralized fronts. Both the fractures and mineral fronts are rich in authigenic ferroan calcite. The mineral fronts contain coarse-grained pyrite, sphalerite, galena, and micron-sized particles that contain combinations of Au, Ag, Cr, Cu, Ni, or rare earth elements. Geochemical analyses by M.B. Goldhaber (Br. Igneous Processes, USGS) show an increase of total sulfur from $<=$ 0.01 weight %S in unaltered rock up to 1.05 weight %S in the mineral fronts. This trace mineralization indicates at least local migration of metalliferous fluids with the Reelfoot rift sediments.

Deformation of stylolites within the Dow Garrigan and Dow Wilson rock samples was accompanied by mineralizing fluids which deposited sphalerite, pyrite, thorite, and other rare earth minerals.

Barite and anhydrite occur as intergranular pore-filling cements and as fracture-filling minerals in the basal arkose in the Dow Wilson drill hole. Geochemical analyses by M.B. Goldhaber will determine if these sulfate minerals are evaporitic in origin or epigenetic.

6. (Swolfs) The Dow Chemical #1 Garrigan drill hole (AR-36; Dart, 1990) is the deepest hole drilled into the Blytheville Arch, a structurally uplifted feature centered in the Reelfoot rift of the Upper Mississippi Embayment. Computed 4-arm diplogs and accompanying electric logs have been used to establish major structural boundaries and discontinuities in the rock column (fig. 1). The deepest structural unit, 2.754-3.581 km (T.D.) subsea, is composed of mudstones and claystones dipping about 20° to the east and southeast. Two unoriented cores (C#3 - 3.394 km; C#2 - 3.028 km) recovered from this interval revealed a mineralized low-angle fault at 3.4 km and a pervasive calcite-filled vein set inclined at about 10° to the core axes. Diplog data enabled the orientation of core C#2 and the determination of the strike and dip of the high-angle vein set as N. 40° W. and 80° SW. (J.R. Howe, written commun., 1982).

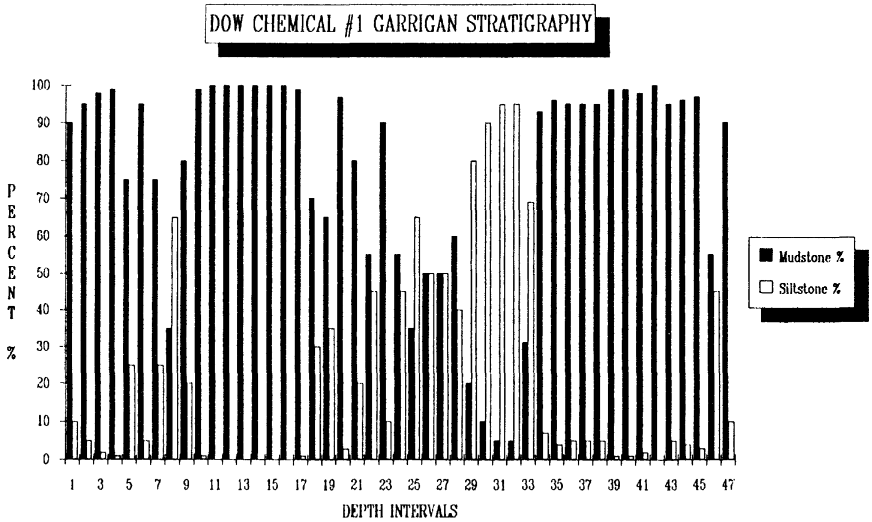

Figure 1. Generalized lithologies in the Dow Chemical #1 Garrigan drill hole compiled by D.S. Collins. Depth intervals start and end at 0.754 and 3.534 km, respectively. Each interval represents 18 m of cuttings spaced about 61 m apart.

The boundary near 2.754 km is a transitional one where dips decrease upward for about 21 m from 25° to less than 10° while maintaining a southeasterly dip direction. This feature may represent draping across a fault or dome. The top of the feature is to the west-northwest. This transition corresponds with an abrupt change in lithology (depth interval 34, fig. 1) from mudstone to siltstone. The interval between 2.754 and 1.748 km (depth intervals 18-33, fig. 1) is composed primarily of shallow-dipping (<10°) interbedded sequences of siltstone and shale (flaser?) deposits. Oriented core C#1 (2.349 km) contains two major sets of calcite-filled veins (Swolfs and others, 1990). Set #1 (N. 41° E.) is not observed in either core C#2 or core C#3. Set #2 in core C#1 strikes N. 35° W. and may correlate with the vein set observed in cores C#2 (N. 40° W.) and C#3. A fault located at 2.327 km has been identified on all available electric logs and has been characterized by a gas show during drilling (Howe and Thompson, 1984).

The section of mudstones above 1.748 km (depth intervals 10-17, fig. 1) is the site of a major drill-hole collapse just prior to coring C#1 (J.R. Howe, oral commun., 1990). Structural information of the logged section above this depth is sparse and incomplete.

7. (Cecil) Analyses of gravity, ground magnetic and VLF (very low frequency) electromagnetic data from several traverses across the Meers fault are completed. The potential field data suggest several features that may have bearing on the seismic potential of the Meers fault and other faults in the FWFS. These features include apparent splaying of the Meers fault beyond the end of the Holocene scarp (control of the northwest extent of rupture?), the presence of a dike-like body along approximately half of the Meers fault (mechanical influence on the rupture process?), considerable variability in the amount of offset of magnetic basement along the length of the Holocene rupture of the Meers fault (inhomogeneities that may influence the rupture process?), and possible definition of large blocks within the Wichita uplift (influence on stress distribution along the FWFS and within the Wichita Mountains?).

Lee-Ann Bradley completed dry and saturated density measurements on drill-core samples from wells adjacent to the Meers fault and from handsamples of exposed igneous rocks collected in the Wichita Mountains. The measured density values are generally typical of the rock types measured. Cecil measured magnetic susceptibility of the core samples. The susceptibility of the dike-like body is in the range of Roosevelt Gabbros measured elsewhere in the Wichita uplift. The susceptibility values and depths to different lithologies determined from the cores have been incorporated into the magnetic models across the Meers fault.

8. (Collins) Initial examination of handsamples and thin sections of the drill core adjacent to the Meers fault indicates that the dike-like body, interpreted from aeromagnetic data to be immediately south of the Holocene rupture, is a meta-gabbro or possible meta-andesite that shows a great deal of shearing and alteration.

9. (Ellis) Least-stress gradients, as reported in a 1973 study utilizing oil well hydraulic-fracturing treatment data, indicate a possible zone of relatively high stress magnitude in the south-central part of the State of Oklahoma. This apparent high stress zone corresponds spatially with the intersection of the FWFS and the McClain County fault zone, which in turn may represent the southern extension of the Nemaha uplift. The distribution of least-stress magnitudes in this zone is similar to the reported pattern of stress distribution near the intersection of artificial fractures in laboratory photoelastic experiments. The McClain County fault zone, near it's intersection with the FWFS, is also the site of elevated levels of contemporary seismicity, suggesting a possible relationship between seismicity, stress, and the intersection of major crustal fault zones that is consistent with the intersection theory for intraplate earthquakes.

10. (Madole) Preliminary correlation of alluvial units along East Cache Creek with units in the Red River valley, one of which contains the 620-ka Lava Creek B volcanic ash, supports the middle Pleistocene age previously assigned to the Porter Hill Alluvium of the Meers area (Madole, 1986, 1988). The Porter Hill Alluvium is apparently younger than 620 ka, but is significantly older than 130 ka. The amount of vertical displacement of the Porter Hill Alluvium on the Meers fault near Canyon Creek, a tributary to East Cache Creek, is approximately the same as the displacement of Holocene alluvium (Crone, 1990), indicating that the recurrence interval on this fault is very long.

11. Crone and Machette conducted about 2 months of fieldwork in central Australia as part of their Gilbert Fellowship. In September, they excavated several trenches across the scarps formed during the 1988 Tennant Creek earthquakes (M_s 6.3-6.7), Northern Territories, and the single scarp that formed during the 1986 Marryat Creek earthquake (M_s 5.8), South Australia. These earthquakes produced thrust-fault scarps. Crone and Machette are collaborating with J.Roger Bowman (Australian National University, Canberra) who is studying the seismicity associated with both earthquakes. Samples collected during the fieldwork will be submitted for thermoluminescence (TL) dating (John Prescott, University of Adelaide, Australia; Steven Forman, University of Colorado, Boulder), Electron Spin Resonance (ESR) dating (Kazuhiro Tanaka, Central Research Institute of Electric Power Industry, Abiko, Japan; Hugh Millard, Branch of Isotope Geology, USGS, Denver), and Uranium-trend dating (Dan Muhs and John Rosholt, Branch of Isotope Geology, USGS, Denver).

REFERENCES CITED

Crone, Anthony J., and Luza, K.V., 1990, Style and timing of Holocene surface faulting on the Meers fault, southwestern Oklahoma: Geological Society of America Bulletin, v. 102, p. 1-17.

Howe, J.R., and Thompson, T.L., 1984, Tectonics, sedimentation, and hydrocarbon potential of the Reelfoot rift: Oil and Gas Journal, November 12, p. 174-190.

Madole, Richard F., 1986, The Meers fault-- Quaternary stratigraphy and evidence for late Holocene movement, in Donovan, R.N., ed., The Slick Hills of southwestern Oklahoma--Fragments of an aulacogen?: Oklahoma Geological Survey, Guidebook 24, p. 55-67.

_____1988, Stratigraphic evidence of Holocene faulting in the mid-continent--The Meers fault, southwestern Oklahoma: Geological Society of America Bulletin, v. 100, p. 392-401.

REPORTS

Crone, A.J., 1990, Late Quaternary tectonism and intraplate seismicity in the central interior of the United States [abs.], Earthquake Seismology Symposium, Perth, Western Australia, September 5-7, 1990.

Dart, R.L., 1990, Catalog of drill-hole data from wells in the Paleozoic rocks of the Upper Mississippi Embayment: U.S. Geological Survey Open-File Report 90-260, 136 p.

Diehl, S.F., and Goldhaber, M.B., 1990, Microstructures in the Cambrian Bonneterre Formation and Lamotte Sandstone of southeast Missouri; sulphide occurrence in stylolites and extensional microfractures [abs.]: Workshop on application of structural geology to mineral and energy resources of the central region, Oct. 9, 1990, Golden, Colorado, Open-File Report 90-0508, p. 2-5.

Diehl, S.F., and Goldhaber, M.B., 1990, Trace mineralization in late Cambrian Reelfoot rift sediments: Dow Chemical #1 Garrigan drill hole, Mississippi County, Arkansas [abs.]: Geological Society of America, Abstracts with Programs, p. A137.

Jones-Cecil, Meridee, 1990, Ground-magnetic profiles across the Meers fault, SW Oklahoma--Quaternary reactivation of a late Paleozoic fault zone [abs.]: Geological Society of America, Abstracts with Programs, p. A18.

Jones-Cecil, Meridee, in press, Total-field aeromagnetic and derivative maps of the Lawton area, southwestern Oklahoma: U.S. Geological Survey GP-XXX-A, 2 sheets.

Jones-Cecil, Meridee, and Robbins, S.L., in press, Bouguer and isostatic residual gravity anomaly and derivative maps of the Lawton area, southwestern Oklahoma: U.S. Geological Survey GP-XXX-B, 3 sheets.

McKeown, F.A., Hamilton, R.M., Diehl, S.F., and Glick, E.E., in press, Diapiric origin of the Blytheville and Pascola arches in the Reelfoot rift, east-central United States--Relation to New Madrid seismicity: Geology.

Swolfs, H.S., McKeown, F.A., and Glick, E.E., 1990, Episodes of extension recorded in Cambrian rocks in the Reelfoot rift, Mississippi Embayment [abs.]: EOS [American Geophysical Union Transactions], v. 71, no. 17, p. 638.

SEISMOTECTONIC RESEARCH STUDIES

A.F. Espinosa
Branch of Geologic Risk Assessment
U.S. Geological Survey
Box 25046, MS 966, Denver Federal Center
Denver, CO 80225
(303) 236-1597

Investigations

1. Post-earthquake investigations were undertaken in the San Francisco Bay area after the October 17, 1989, Loma Prieta, earthquake. Follow-up field investigations have been conducted during the past year. The damage assessment was funded through the University of Colorado under an NSF Quick Response Research Grant. Direct field observations were made from one day after the earthquake to a week later, when the transition to reconstruction occurred. This data is being upgraded, edited and analyzed.

2. Continued investigations of damage in the Marina District of San Francisco, California. Critically damaged structures in the Marina District of San Francisco, California were analyzed in detail and a sample of other buildings throughout the study area that sustained moderate or light damage were evaluated. Field observations of damage, post-earthquake damage evaluations, documented engineering analyses, and field verifications of each structure were used to determine the degree of damage and its distribution. Structural type and building attributes affecting building resiliency (e.g. building footprint, framing system, age, height) were analyzed. Evidence of maintenance-related aspects which affect the structural integrity of buildings (e.g. dry rot, insect damage) were included in the analyses. Critically damaged building were examined for previous changes in structural integrity (e.g. post construction alteration of building framing systems, structural upgrade, or seismic retrofit).

3. Preparation of the geologic map-report for the Anchorage B-8 SE quadrangle Alaska, has begun and awaits field checking; further geologic interpretation is underway, as well as the beginning of text preparation which is intended to include extensive surficial geologic information that benefits from the ongoing studies of gradients of lateral moraines. This work aided correlation of geologic map units, both within this area and with type or reference deposits elsewhere in the region.

4. A continuous research study of the surficial geologic manifestations of the Chilean Tectonic Subduction Zone which were investigated in middle and southern Chile during part of an austral summer as part of a special USGS grant. Samples of several types of organic materials have been analyzed and their relation to submerged and emerged sediments is under study in cooperation with the Branch of Central Mineral Resources.

5. Focal-mechanism solutions and their distribution in Alaska and the Aleutian Islands for 889 earthquakes, which took place from 1927 through 1989, are being cataloged. A focal-mechanism parameter catalog is being prepared for publication.

6. A focal-mechanism distribution map for Alaska and the Aleutian Islands is being prepared for publication.

7. Post-earthquake study of $m_b(Lg) = 5.2$ southeastern Illinois earthquake of 10 June, 1987.

8. Continued study of relations among seismicity, tectonism and hydrothermal regime in the west moat of the Long Valley caldera, California.

9. Continued study of relations among seismicity, tectonism, and hydrothermal regime in Chile.

10. Initiated analysis of temperature and gamma-ray logs in a line of shallow (200 m) holes that cross the Imperial fault near El Centro, California with the objective of studying the hydrothermal effects of the Imperial Valley earthquake of October 15, 1979.

Results

1. Results from the post-impact damage-assessment study included the identification of critically important technical and societal factors that affected the damage assessment process. Significant environmental factors included aftershocks and asbestos in earthquake-damaged buildings. Significant social, economic, and legal concerns also influenced the building evaluation process (for example, liability, housing disputes, etc.).

2. Results from the building-by-building assessment of damaged structures show that while building type and design factors were important, that mitigation and maintenance-related issues were significant.

3. The collection of actual-loss data (not post-earthquake estimates) is still in process. Since few final decisions and little repair has been completed on severely damaged structures, the actual-loss figures are still being collected and analyzed.

4. For the Anchorage B-8 SW quadrangle, Alaska, map units have been described, interpreted, and map preparation and regional geologic framework aspects of the text almost completed prior to the impending technical review.

5. Stratigraphic interpretation of emerged and submerged tidal deposits southeast of downtown Anchorage, Alaska has resulted in the near completion of the pre-review stage of a USGS Bulletin presently entitled, The Girdwood Member of the Twenty Mile River Formation - late Holocene silt and peat stratigraphy, Turnagain Aram and vicinity, southcentral Alaska (Bartsch-Winkler, CMR).

6. A surficial geologic map of the Eklutna River drainage basin, Municipality of Anchorage, is nearing completion as reinterpreted from existing manuscripts and maps all for inclusion in a WRD, Alaska District, report on new Anchorage area water supplies.

7. Paper entitle, Evidence in intertidal deposits, Isla Chloe, southern Chile, for relative change in sea level during the late Holocene, was completed, reviewed, and has received Director's approval. Intended for publishing in symposium volume by the International Sedimentological Congress (Bartsch-Winkler, CMR). Oral presentation of same material given at their August 1990 Congress, Nottingham, England (Bartsch-Winkler CMR).

8. Reinterpretation of some early, provision surficial geologic maps and detailed airphoto interpretation of sectors of the Bulkana A-1 and Nebesna B-6 quadrangles, Alaska has been completed in cooperation with the Branch of Alaska Geology.

9. Paper entitled utility of intertidal peat and silt seque for determining earthquake recurrence intervals, upper Cook Inlet, southern Alaska, was completed and is being revised following technical review (Bartsch-Winkler CMR).

10. A preliminary analysis of precision temperature and gamma-ray logs in the MLGRAP #1 and #2 wells, Long Valley caldera, California has been open-filed along with the data (Diment and Urban, 1990a, b).

11. Due to lack of funds, shut down borehole geophysics lab in Golden and dispersed equipment among the Survey's needy. Gave logging truck to DOE (Sandia National Laboratory). Wrote an operations manual for the truck and logging system for Sandia (Urban and Diment, 1990a, b).

12. A preliminary analysis of precision temperature and natural gamma-ray logs obtained in 1980-81 in the line of shallow holes that crosses the Imperial Fault near El Centro, California indicates that: (1) temperature were noticeably depressed in the vicinity of the fault implying that water had flowed down the shallow part of the fault for a considerable period prior to the 1979 earthquake; and (2) elevated isotherms indicate that water is flowing up at El Centro which is near a seismic lineament that may be an extension of the Superstition Mountain fault. These results have been reported in an abstract (Urban and Diment, 1990b). Analysis is continuing in an effort to derive a suitable correction for the slight artesian flow observed in some of the holes.

13. An evaluation of a contractors' performance in digitizing the South Carolina Net earthquake data was completed. The results are reported in an administrative report. The report covers accessing the computer tapes, programs to read and plot the earthquake data, plots of the channels at various scales, and problems encountered.

14. The temperatures and thermal conductivity data for several drill holes in central Chile have been assembled and partially analyzed. The geologic background material has been obtained. Most of the information necessary to complete a report on the thermal regime of the area is in hand. However, detailed topographic maps necessary for terrain corrections have not been obtained yet.

Because of a lack of knowledge and understanding concerning the relation between North American mid-plate seismicity and the local and regional tectonic regimes, the occurrence of a moderate-sixed earthquake anywhere in the Eastern United States presents an important opportunity for study. The 10 June 1987 southeastern Illinois shock was such an event and the opportunity was not missed as several post-earthquake response teams converged on the epicentral region. Results from the combined efforts of the U.S.G.S. and the Center for Earthquake Research and Information (CERI), Memphis State University include:

15. Accurate locations of the later (1-1/2 to 5-1/2 days after the mainshock) aftershock foci which define a very compact cylindrically-shaped volume 0.8 km wide, 1.7 km long, and 3 km high. Duration magnitudes for those aftershocks range from -0.18 to 2.27.

16. Composite focal mechanism solutions determined from 47 events which exhibit a mix of reverse faulting motions (74% of the composite aftershocks) and main shock-like strike-slip movements. nodal planes of the reverse mechanisms strike throughout the northeast quadrant and have moderate dip angles. Strike-slip nodal planes are subvertical, striking northwest and northeast similarly to nodal planes of the main shock focal mechanism solution. *P*-axes from all solutions are easterly to east-southeasterly in azimuth and subhorizontal in plunge.

17. Selection of the northeast striking nodal plane as the preferred fault plane for the main shock focal mechanism solution based on the aftershock focal mechanism solutions and the northeast-trending aftershock zone.

18. A strong suggestion that the seismic potential of the host Wabash Valley zone may be greater than previously realized. It has MMI VII recurrence rates comparable to the New Madrid zone and, also similarly to that large zone, it has been the locus of earthquake-induced liquefaction affects.

Reports

Diment, W.H., and Urban, T.C., 1990a, Temperatures and natural gamma-ray logs obtained in boreholes MLGRAP #1 and #2, Mammoth Lakes, California: Data and preliminary interpretations: *U.S. Geological Survey Open-File Report* **90-460**, 135 pp.

Diment, W.H., and Urban, T.C., 1990b, Significance of precision temperature and natural gamma-ray logs of the MLGRAP boreholes, Long Valley caldera, California: *EOS, Transactions American Geophysical Union,*, v. 71, (submitted).

Espinosa, A.F., M. Hall, and H. Yepes, 1990, Seismicity and Tectonics, chapter, *in* the March 5, 1987, Ecuadorian Earthquake Post-earthquake study, edited by R.L. Schuster, *National Academy of Sciences, Washington, D.C.*, 15 pp.

Espinosa, A.F., J. Egred, M.G. Lopez, and E. Crespo, 1990 Intensity distribution, chapter, *in* the March 5, 1987, Ecuadorian Earthquake Post-earthquake study, edited by R.L. Schuster, *National Academy of Sciences, Washington, D.C.*, 20 pp.

Lopez-Arroyo, A., and A.F. Espinosa, 1990, Non-instrumental and instrumental intensity scales: their application to seismic hazard and risk assessment studies, *XII General Assembly of the European Seismological Commission, Practice of Earthquake Hazard Assessment Session, 17-22 Sept. 1990, Barcelona, Spain.*

Langer, C.J., and Bollinger, G.A., 1990, The southeastern Illinois earthquake of 10 June 1987: the later aftershocks, *Bull. Seis. Soc. Am.* (Submitted).

Langer, C.J., and Bollinger, G.A., 1990, The 1983 earthquake in Guinea, West Africa, *Conference Proceedings, natural Hazards in West and Central Africa, Lagos, Nigeria.*

Oaks, S.D. and A.F. Espinosa. A Multi-Parameter Vulnerability Analysis of Earthquake Damage, Part I: An Evaluation of the Marina District of San Francisco, California. Director's Approval 10/2/90.

Oaks, S.D. and T.D. O'Rourke, 1990, Structural Vulnerability in the Marina District of San Francisco, California; Analyses of Building Damage, Structural Attributes, and Related Geotechnical Factors, *EOS Transactions, American Geophysical Union,*, in press.

Urban, T.C., 1990, Evaluation of contractor performance in digitizing South Carolina network (SCNET) earthquake data: *U.S. Geological Survey Administrative Report*, 132 pp.

Urban, T.C., and Diment, W.H., 1990a, Logging truck operations guide: *U.S. Geological Survey Administrative Report*, 139 pp.

Urban, T.C., and Diment, W.H., 1990b, The shallow thermal regime near the Imperial fault after the October 15, 1979, Imperial Valley earthquake: Inferences of earthquake-induced change: *EOS, Transactions American Geophysical Union*, v. **71**, (submitted).

Yehle, L.A., Schmoll, H.R., and Dobrovolny, Ernest, 1990, Geologic map of the Anchorage B-8 SE and part of the B-8 NE quadrangles, Alaska: U.S. Geological Survey Open-File Report 90-238, 37 p., scale 1:25,000.

Soil as a time-stratigraphic tool

0-9540-03852

Jennifer W. Harden
Branch of Western Regional Geology
U.S. Geological Survey
345 Middlefield Road, MS 975
Menlo Park, California 94025
(415) 329-4949

Investigations

Rates of soil development in coastal and interior California as they relate to slip-rate studies in selected areas

Results

Data available from other USGS programs allowed an analysis of how rates of soil development vary over spatial and temporal scales. Results of studies in the southern Great Basin and Mojave semiarid regions indicate a 10 fold decrease in rates from the Holocene to Pleistocene. As many as six field and laboratory parameters indicate such significant temporal variation in the region. In comparison, such ten-fold differences were also found by Harden and Busacca in studies of soils in central California where soils receive about 3 to 4 times the annual precipitation. Temporal variation in rates is complexly related to climatic history, fluxes of dust, erosional history, weathering, and internal soil processes related to soil hydrology. In arid regions, soil genesis may be dominated by dust flux in initial stages of soil development (represented in data by Holocene chronosequences) and by changes in soil hydrology and erosion in later stages. In central California, soil genesis may be dominated by weathering and clay formation initially, with soil hydrology and erosion again being important in later stages of soil development.

In contrast to the 10-fold temporal variation in rates of soil development, rates within each the southern Great Basin-Mojave region and central California vary by an order of 2 or 3. Within each region, therefor, the spatial variation in rates appears to be less significant than temporal variation. Between regions, however, rates also vary significantly, by as much as a factor of 10 to 50. The implications of such an analysis are that dated soils must be studied within any region that requires correlation and dating by soils. Further research must identify boundaries of such regions within which rates are similar and between which rates vary significantly.

Reports

Harden, Jennifer W., 1990. Soil development on stable landforms and implications for landscape studies. Geomorphology vol. 3, p. 391-398.

Ground Motion Modeling in the Eastern U. S. With Emphasis on Effects of New Madrid Earthquakes on Memphis and St. Louis

14-08-0001-G1769

Robert B. Herrmann
Department of Earth and Atmospheric Sciences
Saint Louis University
3507 Laclede Avenue
St. Louis, MO 63103
(314) 658-3131

Investigations

This program is focused on the specification of representative time histories for future large New Madrid earthquakes at target sites of Memphis, Tennessee and St. Louis, Missouri. This will be accomplished by a combination of deterministic and probabilistic techniques for the generation of time histories. Because of the unique environment of sites within the Mississippi River flood plain, e.g., 1000 meter thicknesses of very low velocity materials, effort is first directed toward constraining the wave propagation properties of the surface material.

Results

1. A deterministic program which specifies the rupture time history on a fault plane and then generates time histories by summing Green's functions, has been completely rewritten into three separate programs. The first specifies the spatial distribution of moment release on the fault together with the time of the initiation of moment release on each fault subelement. The second program computes the distance and azimuth from each point on the fault plane to the target site. Finally, the third program sums the Green's functions, accounting for the varying radiation pattern of different elements of the fault plane.

This rewrite of an existing program was made to facilitate the use of inversions for moment release on fault planes available in the literature for actual large earthquakes. Thus the California earthquake can be transported to the eastern U. S. Another use is to use the output of the second program as the input of a program to sum random process theory time histories from the fault subelements to simulate ground motion near a large fault.

2. Model verification is underway to develop time histories for St. Louis from large New Madrid earthquakes, at present an $M_W = 7.5$ 1812 earthquake 265 km from St. Louis. Focal mechanisms of recent earthquakes are used to constrain the fault model. A smaller, magnitude 6.0 earthquake will also be modeled. This modeling is prompted by current, rabid interest in ground motions due to New Madrid earthquakes.

3. On September 26, 1990, an m_{Lg} = 4.6 earthquake occurred 175 km south-southeast of St. Louis near Cape Girardeau, Missouri. This earthquake was well recorded at the IRIS station at Cathedral Cave, Missouri. Using P-wave first-motion data, and well as the Very Broad Band channel data reprocessed into a 15-100 WWSSN seismogram, a seismic moment of 2.0- 3.0 E+22 dyne-cm was estimated by fitting complete synthetic histories obtained by wavenumber integration. Using this seismic moment, it was observed that the peak horizontal ground velocities at a distance of 176 km, agreed with the predictions of Ou and Herrmann (1990) for this seismic moment. Thus the introduction of modern instrumentation and the occurrence of a fortuitous earthquake are leading to verified ground motion estimation models for the region.

Publications

Ou, G.-B. and R. B. Herrmann (1990). Estimation theory for strong ground motion, *Seism. Res. Letters* **61,** 99-107.

Ou, G.-B. and R. B. Herrmann (1990). A statistical model for peak ground motion from local to regional distances, *Bull. Seism. Soc. Am.* **80,** (in press, December 1990).

Use of Temporal Correlation to Test a Proposed Seismic Origin for giant Landslides in Seattle, Washington

14-08-0001-G1776

Gordon C. Jacoby
Tree-Ring Laboratory
Lamont-Doherty Geol. Obs.
Palisades, New York 10964
(914) 359-2900

Patrick L. Williams
Earth Science Division
Lawrence Berkeley Laboratory
University of California
Berkeley, California 94720
(415) 486-7156

THE PALEOLANDSLIDES IN LAKE WASHINGTON

This investigation is studying large-scale landslides submerged in Lake Washington in Seattle. Slide blocks moved to 0 to ≥40 m depths by deep-seated translational gliding from adjacent steep slopes. The slides represent significant geohazards and may have been triggered by seismic events. Geomorphic features interpreted to be landslide head-scarps and terraced and hummocky topography are present in the adjacent upland area. Sonar confirms the presence of tilted blocks and chaotic bathymetric features in some near-shore areas around Mercer Island. There are trees on the landslides. These trees died due to drowning when the landslides collapsed into the lake. By radiocarbon analyses and tree-ring dating we are determining the dates of the landslides. The crossdating of the trees at different locations will establish the relative timing of different individual slides.

Preliminary efforts confirmed the location of the slides and established the presence of trees on the various slides. In addition, underwater methodologies were developed to obtain increment cores with a hydraulic system and for obtaining wedge sections from the trees with enough volume of wood for radiocarbon analyses.

Field sampling and surveys were conducted in the spring of 1990 to gain further information about the landslides in Lake Washington. The surveys were conducted using side-scanning sonar, depth recorder, and SCUBA diving. The surveys indicated multiple lobes of landslides at two locations. Another purpose of the side-scanning sonar survey is to aid in locating trees. In some portions of this preliminary survey the trees show up very well. In addition to taking 12 mm diameter cores from the trees we also cut wedges from the lower sides of the trees. These wedges provide enough material for radiocarbon dating and will generally preserve the outer rings better than a core sample.

Southeast of Mercer Island (Figure 1) detailed surveys indicate four distinct lobes. Radiocarbon dating indicates there may be three different events in this area. Radiocarbon dates for samples from this area are 1170 RYBP (+/-50), 1870 RYBP (+/-60), and 2840 RYBP (+/-60). West of Mercer Island there appear to be two different landslides. The surveys indicate a landslide with trees on it near the shore and a second landslide farther out, deeper and also with trees. Radiocarbon measurements support the hypothesis of two events in this area as shown on the map in Figure 1. Several samples are submitted for radiocarbon analysis from each area, south and west of Mercer Island. The results will be integrated with tree-ring crossdating to determine dates for the landslides.

TREE-RING DATING

Absolute crossdating has been established between six trees, all Douglas fir [*Pseudotsuga menziesii* (Mirb.) Franco] from slides A and B southeast of Mercer Island. This dendrochronological crossdating indicates parts of

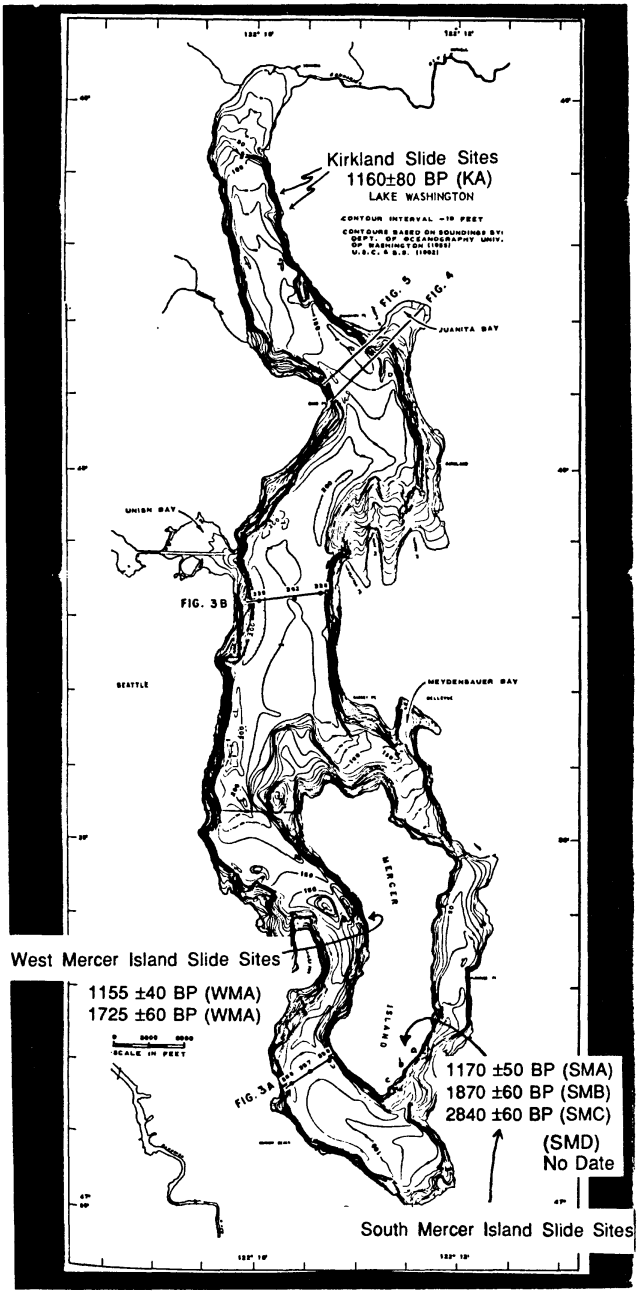

Figure 1: Bathymetric map of Lake Washington in Seattle, Washington. Landslide sites and radiocarbon dates shown for each slide area.

lobes A and B probably were emplaced at the same time. The samples include the outer rings of the remains of the trees but some outer wood, especially sapwood, may have decayed away. The crossdating shows all outer rings within 27 years of each other except for SMA-1 which extends 52 years beyond the outer year of any other sample. Tree SMA-1 was not rooted and is a relatively faster growing tree with wider rings than the other five. The other five were rooted and a radiocarbon date for one of the rooted trees is 1870 RYBP (+/- 60). There is another radiocarbon date from a rooted tree on slide A of 1170 RYBP (+/- 50) but this tree is a western redcedar [*Thuja plicata* Donn ex D. Don] and has so few rings and such uniform growth that it does not reliably crossdate with any other tree samples. The remaining tree samples from this area do not appear to crossdate with the first group. We thus have a 245-year "floating" chronology ending around 1870 RYBP from this location. Floating means that it is not absolutely dated to the exact year.

A second set of trees is tentatively crossdated and continuing analyses are underway to test these results. If substantiated this set will form another floating chronology of 289 years in length. It is crossdated with a sample having a radiocarbon date of 1155 RYBP (+/- 40). This set only comprises 5 samples from two different trees.

The crossdating is based on annual ring widths for the most part but width of latewood and qualitative comparisons of latewood density are also used for comparison. In several instances there are fire scars in the samples and these crossdate indicating fires in the stand that injured several trees simultaneously.

SONAR RESULTS TO DATE

Preliminary sonar surveys as noted above are of great use in locating the trees. Surveys southeast of Mercer Island and west of Mercer Island helped delineate the bottom topography and the areas with trees. Improved instrumentation would produce more detailed topography and individual tree locations. With the navigation information the position can be reoccupied and increase the divers' ability to locate and sample trees. Underwater visibility is limited and much time is spent looking for trees rather than sampling. Better tree locations would greatly increase diver efficiency in obtaining samples which is a limiting factor in results to date.

SUMMARY

Present results indicate a possibility of seven different landslides tending to cluster into three times over the past 3,000 years. Some of the landslide lobes may have resulted from the same event or be simultaneous over considerable distance. As sample productivity increases and radiocarbon dates are forthcoming the distribution in time and space will be resolved and related to other similar studies in the region.

PRESENTATION OF RESULTS

Williams, P.L. and G.C. Jacoby, Evaluation of possible seismic triggering of giant landslides in Seattle, Washington (abst.), EOS Trans. AGU, 70, 1332, 1989.

Jacoby, G.C., Williams, P.L. and Buckley, B.M. Timing and distribution of landslides in Lake Washington, Seattle: Geohazards of possible seismic origin (abst.), submitted to AGU, 1990.

Urban Hazards Seismic Field Investigations

9950-01896
9950-03816

K.W. King
Branch of Geological Risk Assessment
U.S. Geological Survey
Box 25046, Denver Federal Center, MS 966
Denver, CO 80225
(303) 236-1591; (303) 236-1605

INVESTIGATIONS

The objectives of this project are: (1) to maintain an operation-instrumentation readiness for opportunities to support research in the earth science and engineering fields, (2) to develop integrated techniques and methodologies for efficiently and effectively documenting and processing high quality digital seismic data, seismic reflection and refraction data, seismic and geological borehole data, and surface/structure response data,(3) to develop improved methods to investigate subsurface geologic structures and geologic/engineering parameters (4) To improve the understanding of how shallow underlying geology affects ground motion.

Specific goals for this reporting period were (a) to finalize the documentation of seismic data from the Loma Prieta earthquake, (b) Investigate the feasiability of using high-resolution-shallow reflection methods to map landslides from the Loma Prieta earthquake. (c) to field the high-resolution seismic reflection system with personnel to investigate potential earthquake source zones in the Mississippi embayment area. (d) to finalize the Puget Sound site response analysis, and (e) to investigate the seismic environs of Mesa Verde National Park and the Pueblo Grande Park in Phoenix, Arizona.

Field Laboratory Efforts

(a) The field calibrations, site locations, seismometer orientations and world time have been corrected on all Loma Prieta earthquake data. The data set is approximately 2 gigi-bytes in size are available in VAX format at the Golden facility. The data will be distributed on a CD in the near future. Preliminary analysis of the seismic data indicates that relative spectral ratios of ground response generally compare well with observed damage distribution resulting from the Loma Prieta earthquake and are correlatable with the subsurface geology.

(b) Five reflection profiles were run near the Summitt area on a suspected landslide from the Loma Prieta earthquake. The data has been preliminary analysed which indicate that the method may have mariot. Futher analysis is necessary.

(c) Seismic reflection profiles were made on the Bootheel Lineament which indicated gentle warping with maximum structural relief of about 20m beneath strands of the lineament. Eight seismic reflection profiles were made on the Crittenden County fault to help define the substructure in that area. The preliminary analysis has shown the data to be of high quality. Analysis is in progress. Five seismic reflection lines were run the the Crowley's Ridge, Arkansas area. The data are of high quality and are being analysed.

(d) The microearthquakes near Seattle have provided the best spectral ratio data to date. Because of funding limitations and project re-direction, data were recovered from only six sites. The data from the six sites have been analyzed an documented in a report. The report has been peer reviewed and will be part of a USGS journal report.
(e) The seismic field effort at the Pueblo Grande ruins and at the Mesa Verde Park for the USGS/NPS preservation team project is near completion. The data are now being analyzed.

PUBLICATIONS

King,K.W.,, Tarr, A.C., Carver, D.L., and Williams, R.A., 1989, Seismic ground response studies in Olympia, Washington and vicinity. (Director's Approval). (Submitted to and approved by BSSA).

Cranswick, E., K. W. King, P. Spudich, D. L. Carver, D. M. Worley, and R. Banfill (1990). Site response across the downtown Santa Cruz alluvial basin, EOS Trans., Am. Geoph. Union, **71**, no. 8, p. 287.

Cranswick, E., R. Banfill, K. W. King, R. Borcherdt, L. Bond, T. McCormick, and A. Johnston (1990). Processing digital seismograms in a Santa Cruz motel using locally rented IBM-PC-compatible microcomputers, EOS Trans., Am. Geoph. Union, **71**, no. 8, p. 287.

Andrews M., R. Banfill, D. Carver, M. Celebi, E. Cranswick, K. King, P. Spudich, and D. Worley (1990) Digital aftershock recordings of the October 17, 1989 Loma Prieta, California, earthquake, EOS Trans., Am. Geoph. Union, **71**, no. 8, p. 287.

Boore, D. M., S. Hough, S. P. Jarpe, and K. W. King (1990). Ground shaking from the 17 October Loma Prieta Earthquake, EOS Trans., Am. Geoph. Union, **71**, no. 8, p 290.

King, K. W., R. A. Williams, D. C. Carver, E. Cranswick, and D. M. Worley (1990) Site response and building damage in Santa Cruz, California, Seismological Society of America 85th annual meeting, May 2-4, 1990.

K. King, D. Carver, R. Williams, and D. Worley, E. Cranswick, and M. Meremonte (1990). Santa Cruz Seismic investigations Following the October 17, 1989 Loma Prieta Earthquake. U.S. Geological Survey Open-File Report 90-307.

K. King, R. Williams, D.Carver, and D.Worley, (1990) Site Response Studies in West and South Seattle, Washington, (Through peer review) for USGS Journal article.

E. Schweig, R. VanArsdale, K.Shedlock, E.Luzietti, and K.King, (1990), A Seismic Reflection Survey of the Bootheel Lineament in Missouri, abstract, fall meeting, AGU

R.VanArsdale, G.Scherer, E.Schweig, L,Kanter, R.Williams, K.Shedlock, and K.King, (1990), Seismic Reflection Survey of Crowley's Ridge, Arkansas, abstract, fall meeting, AGU

E.Luzietti, K.Shedlock, K.King, F.McKeown, E.Schweig, L.Kanter, and R.VanArsdale, (1990), A Seismic Reflection Survey of the Crittenden County Fault, northeast Arkansas, abstract, fall meeting, AGU

R. Williams and K.King, (1990), Seismic Reflection/Refraction Study of West Denver Pierre Shale, Ad.(in review).

CASCADIA SUBDUCTION ZONE: NEOTECTONICS OF THE ACCRETIONARY WEDGE AND ADJACENT ABYSSAL PLAIN OFF OREGON AND WASHINGTON

Contract 14-08-0001-G1800

Principal Investigator: LaVerne D. Kulm*
Co-Principal Investigator: Robert S. Yeats**
Graduate Research Assistant: Chris Goldfinger**

*College of Oceanography
**Department of Geosciences
Oregon State University
Corvallis, OR 97331
(503) 737-2296

Investigations

In this study, the overall objective is to characterize and determine the timing of deformational events in the subducting Juan de Fuca plate (abyssal plain) and deformation front (accretionary wedge) of the Cascadia convergence zone off Oregon and Washington. A neotectonic map is being constructed of the subducting oceanic plate, accretionary wedge, and adjacent continental shelf basins to identify the styles and areal extent of deformation. We are trying to identify and date discrete deformational events and relate them to the distribution of earthquakes on the subducting oceanic plate and in the subduction zone.

The GLORIA side-scan sonar map from the U.S.G.S survey of the EEZ off Oregon and Washington is serving as the base for the neotectonic map. We have acquired photographic prints of the bathymetry (i.e., older NOAA pre-SeaBeam bathymetry which was used for the GLORIA mosaics) from the U.S.G.S in Menlo Park, CA, for our base. All digital data obtained from the extensive and comprehensive 1989 SeaMARC-IA side-scan sonar survey off central and northern Oregon have been processed and adjusted to overlay the SeaBeam bathymetry acquired on previous cruises aboard the R/V ATLANTIS-II during 1987-1988. Numerous mosaics (scales ranging from 1:10,000 to 1:50,000) of the side-scan images have been completed for the survey area; they are being used to construct the neotectonic map. Approximately 1,000 km of the 2,000 km of 144-channel multichannel seismic reflection lines collected off central and northern Oregon in 1989 have been processed in the form of migrated time sections by our colleagues at the Hawaii Institute of Geophysics. Both of these Oregon surveys were funded by the National Science Foundation, Ocean Drilling Program, in a separate study of the continental slope and adjacent abyssal plain (44° 30' to 45° 20' N latitude).

Non-classified SeaBeam bathymetry in this region was acquired earlier in 1987 and 1988 with the ATLANTIS-II by Oregon State University in a study sponsored by the National Science Foundation. Pre-existing NOAA SeaBeam bathymetry off Oregon is becoming available in both published and pre-published form; it is being used to trace structures across the margin in this study. SeaBeam data, with the exception of some pre-1984 data along the deformation front, will remain classified off Washington. On the other hand, the Oregon bathymetry is unclassified, and it is extremely useful in tracing structures with seafloor expression between seismic reflection lines. Additional SeaBeam data are currently being collected by NOAA's vessel SURVEYOR along the south-central Oregon margin; it will be used in our study as soon as it is processed by NOAA in early 1991. All available seismic reflection records, both single-channel and multichannel, are being used to construct the neotectonic map of the Cascadia subduction zone. We still need to acquire larger copies of the seismic reflection records (than those displayed in the EEZ Atlas) from the U.S.G.S survey of the EEZ off Oregon and Washington to more clearly identify faults.

Gravity cores collected during the side-scan survey in 1989 were opened and logged at the OSU College of Oceanography Core Repository. We are exploring the appropriate biostratigraphic and radiocarbon methods of dating the several turbidite events displayed in each core.

An ATLANTIS-II/ALVIN cruise was conducted September 14-28, 1990 on the central and northern Oregon margin and abyssal plain. We were invited to conduct an ancillary study of selected fault zones by one of our colleagues from the University of California at Santa Cruz, who was the principal investigator of a separate study, and chief scientist of the cruise. Chris Goldfinger made one ALVIN dive on a NW-trending strike-slip fault that cuts the abyssal plain and intersects the accretionary wedge. LaVerne Kulm made one ALVIN dive in a faulted zone in an older portion of the accretionary prism. Four gravity cores were collected in the vicinity of the fault in an attempt to constrain the age of the fault. Precision depth records were made across other suspected fault zones in the abyssal plain.

Results

Neotectonic Map of the Accretionary Wedge and Adjacent Abyssal Plain Offshore Oregon and Washington

The neotectonic map presently being constructed utilizes all available seismic reflection data, SeaMARC side-scan, GLORIA side-scan, and SeaBeam bathymetry data. GLORIA imagery and SeaBeam bathymetry allow correlation of seismic structures over the map area, and they have been used to locate structural terminations, tear faults, changes in structural style and structural trends. The map will also show the relative ages of structures, constrained where possible by core samples and sedimentation-rate calculations.

Northwest-trending faults previously revealed with SeaMarc-1A side-scan (faults A, B, and C, described by Kulm et al., 1989; Appelgate et al., 1989; Goldfinger et al., 1989) have been traced landward through the accretionary wedge, up to 120 km along trend from the deformation front off central Oregon. Offset structures indicate left-lateral separation, the same as offset channels observed on the abyssal plain (Appelgate et al., 1989; Goldfinger et al., 1989). The seismic reflection style of these faults is also consistent with primarily strike-slip motion (i.e. lack of a consistent vertical sense of motion, near vertical dip, and flower structures). The length of these faults, and the involvement of both the subducting Juan de Fuca plate and the accretionary wedge suggest that they may represent segmentation boundaries in the Cascadia subduction zone.

Further examination of the detailed structure of fault A (45° 10' N latitude) with high-resolution side-scan imagery has revealed two additional seafloor channels offset in a left-lateral sense by fault A. With three offset features on the abyssal plain, and several more on the continental slope, we plan to calculate an approximate slip rate using dated cores collected near the fault in 1989 and 1990.

Examination of the "mud volcano" (Kulm et al., 1989; Appelgate et al., 1989; Goldfinger et al., 1989) using multi-channel seismic records and 2 km swath width side-scan show this structure not to be a mud volcano at all, but a north-plunging anticline. Apparently the structure evolved as a pressure ridge across a right step in the left-lateral fault A. Seismic reflection profiles suggest that the basement is offset by this structure. A previous ALVIN submersible survey in 1988 established that methane-rich fluids are venting from the pressure ridge, and that live chemosynthetic clams occur over much of it's southern flank. Fault A is actively venting fluids as documented by the abundant chemosynthetic animals. Fluids from the anticline contain a high ^{3}He content (23%) which suggests the fluids are derived from the basaltic slab of the subducting plate.

A second NW-SE trending fault (fault B) was imaged in side-scan on the abyssal plain to the south at 44° 52' N latitude. This fault crosscuts the base of a smaller "mud volcano" which is similar in appearance to the one associated with fault A, and is characterized by an escarpment that extends at least 5 km seaward from the base of the deformation front. Seismic records suggest that it also is a north-plunging pressure-ridge anticline across a right step in the fault. A multichannel seismic record across the fault suggests that fault B, like fault A, is a major fault zone with apparent basement offset.

A third fault (fault C) was clearly identified in a N-S multichannel seismic record at 44° 32'N latitude on the abyssal plain, 5 km seaward of the initial deformation front. Its orientation is now confirmed to be NW-SE, and it offsets the deformation front left-laterally. Displacement of the thick stratigraphic section appears to extend upward to the seafloor. The strata have the appearance of an evolving fold with probable seaward vergence. The fault appears to offset the basement, which is downthrown to the south or southwest.

Detailed study of SeaMARC side-scan images reveals that a second set of NE-trending faults intersect and offset the deformation front between 44°40' and 45° 00' N. This set of faults is much less well developed than the NW faults, and it has not, as yet, been traced more than 1-2 km into the accretionary wedge. Crosscutting relations with the northwest faults have not yet been determined.

Northwest-trending folds associated with faults A, B, and C have been identified in the accretionary wedge using seismic records and SeaBeam bathymetry. These folds, like the faults, are active structures deforming the seafloor. Further work should define the relationship of these folds to the strike-slip faults and to the dominant N-S structural grain of the accretionary wedge.

Submersible Investigations

ALVIN dives in September 1990 focused on the intersection of fault A with the deformation front. Direct observation of the scarp revealed a terraced, steep scarp, sloping 30°- 40°, thinly draped by hemipelagic sediment. No fresh breaks in the sediment cover were observed; however, this condition is also noted at the master decollement, and is explained by the high sedimentation rate, as well as erosion by relatively fast-moving currents as observed from ALVIN. Direct observation of the intersection of this fault with the deformation front (marginal ridge) shows that the fault is expressed as a series of splays in the initial ridge, and that the splay faults are sites of active fluid venting. Venting fluids have provided carbonate cement to the fault zones, creating hard brittle zones of unknown dimension within the accretionary wedge. Rock samples from these zones with abundant slickensides and mullions were recovered on several dives, suggesting that at least part of the accretionary wedge, at its seaward limit, is capable of brittle failure.

Cores

Two cores taken on the abyssal plain in 1989, seven km seaward of the deformation front at 44° 51', were found to contain ten distinct sand turbidites of probable Holocene age. These are the first cores from this area found to contain turbidites. These cores will be dated using radiocarbon and biostratigraphic methods, and compared to those used by Adams (1990). Adams has proposed that the presence of nearly identical turbidite sequences in channels with different source areas is evidence for regional triggering of turbidity currents, produced by great earthquakes. In order to test the hypothesis that these turbidites are the result of great Holocene earthquakes, our cores will be compared to those from Cascadia Channel, studied by Adams. If the turbidites found in our cores are derived from sources on the adjacent accretionary wedge, and if they can be correlated with those studied by Adams, this would strongly support his hypothesis. Because local sources for our turbidites are located 120 km south of the Columbia River, the source of the

Cascadia Channel turbidites, a correlation would require a regional trigger for both turbidite sequences. Four additional cores were taken in September 1990, along the base of the continental slope, in order to further test this hypothesis.

Reports

The following abstract was submitted to the Annual Meeting of the American Geophysical Union, San Francisco, CA which describes the research conducted during the first nine months of this NEHRP project:

Goldfinger, C., MacKay, M.E., Kulm, L.D., and Yeats, R.S., Neotectonics and Possible Segmentation of the Juan de Fuca Plate and Cascadia Subduction Zone off Central Oregon: EOS (submitted).

Additional results, which were reported earlier, are as follows:

Appelgate, T.B., Kulm, L.D., Embley, R.W., Fox, C.G., 1989, Surficial structure of the central Oregon convergent margin: results from a SeaMARC-1A sidescan sonar survey: EOS, v. 70, p. 1345.

Goldfinger, C., Appelgate, T.B., Kulm, L.D., and Yeats, R.S., 1989, Sidescan sonar imaging of probable active faults on the Juan de Fuca plate adjacent to the central Oregon continental margin: EOS, v. 70, p. 1329.

Kulm, L.D., Appelgate, T.B., and Fox, C., 1989, Sidescan survey of structures and fluid vent sites on the central Oregon margin and subducting Juan de Fuca plate: EOS, v. 70, p. 1345.

References

Adams, J., 1990, Paleoseismicity of the Cascadia Subduction Zone: Evidence from Turbidites off the Oregon-Washington Margin: Tectonics, v. 9, p. 569-584.

EEZ SCAN scientific staff, 1986, Atlas of the Exclusive Economic Zone, western conterminous United States, U.S. Geological Survey Miscellaneous Investigation I-1792. scale 1:500,000.

TEMPORAL AND SPATIAL BEHAVIOR OF LATE QUATERNARY FAULTING, WESTERN UNITED STATES

9950-04540

MICHAEL N. MACHETTE
Branch of Geologic Risk Assessment
U.S. Geological Survey, Box 25046, MS 966
Denver, Colorado 80225
(303) 236-1243

PURPOSE OF PROJECT

To define regional variations in the time-space partitioning of paleoseismic activity in the late Quaternary as a guide to understanding the accumulation and release of strain on faults in the Western United States. This project will serve as an umbrella for diverse but interrelated aspects of paleoseismicity in the western U.S. We will study selected faults that are critical to interpreting the paleoseismology and neotectonics in regions of active faulting. Our research will apply paleoseismologic studies to important problems on three different levels: (1) refine methodologies for dating fault movements that are applicable to a wide variety of tectonic problems and areas, (2) examine the long-term behavior and interaction of faults in a broad region (~20,000 km^2) that are exposed to the same regional stress field, and (3) study the time-space distribution of strain accumulation and release in the upper crust on a regional (province-wide) scale. Project members are R.C. Bucknam, A.J. Crone, K.M. Haller, and M.N. Machette.

INVESTIGATIONS

1. Bucknam continued photographic monitoring of the short-term natural degradation of the 1983 Borah Peak fault scarps using precision close-range photogrammetry that was initiated in 1985.

2. Haller and Machette started compiling a digital data base of Quaternary faults in the Western United States. Their first priority is to assemble data for a neotectonic transect of the northern Basin and Range province from the Wasatch fault zone (Provo, Utah area) to the Sierra Nevada frontal fault zone (Reno, Nevada area). We have defined the limits of our neotectonic transect as the corridor between 39° and 41°N. and 111° and 120°W. This east-west strip allows us to build upon the Wasatch fault zone study and 1°x2° quadrangle mapping in Utah by BGRA personnel (Anderson, Barnhard, Bucknam, Machette, Nelson, and Personius) and on previous mapping by Barnhard (Elko 1°x2°), Wallace (Winnemucca 1°x2°), and Bell (Reno 1°x2°) in Nevada. This leaves the Ely, Lovelock, and Millett 1°x2° quadrangles in Nevada as our main mapping objectives. We will be cooperating with personnel of the Nevada Bureau of Mines (John Bell and associates) and the Center for Neotectonics (Steve Wesnousky and associates).

3. Bucknam, Machette, and Crone completed mapping (1:24,000 scale) of the surficial geology associated with Holocene faulting along the east flank of the Fish Springs Range in western Utah.

4. Crone and Machette, as part of a USGS Gilbert Fellowship (FY 90/91), spent about one half of the reporting period preparing for field studies of two historic Australian intraplate earthquakes that produced surface ruptures. Fieldwork is being conducted from August 19 to October 15, 1990.

RESULTS

1. Preliminary interpretations of the faulting events recorded in two trenches along the Fish Springs fault indicate a complex history of latest Pleistocene and Holocene surface faulting. Our favored interpretation of the sequence of events indicates that Lake Bonneville probably had a strong influence on the temporal distribution of surface-rupturing earthquakes on this fault during the latest Quaternary. Stratigraphic relations in the trench provide evidence of four surface-rupturing events that postdate the high stand of Lake Bonneville. The inferred timing of these events indicates a temporal clustering of surface ruptures on the Fish Springs fault in latest Pleistocene to early Holocene

time. The proposed timing clusters two or three earthquakes in a 3,000- to 4,000-year time interval shortly after the catastrophic fall of Lake Bonneville to the level of the Provo shoreline.

2. Haller and Machette completed most of the field reconnaissance of late Quaternary faults in the Ely, Nevada, 1°x2° quadrangle. Data are being compiled from aerial photographs at a scale of 1:24,000 for publication at 1:250,000. In addition, the fault data are being digitized in BGRA's GIS Laboratory using ARCINFO software.

Most of the late Quaternary range-front normal faults in the Ely 1°x2° quadrangle flank the east side of the major mountain blocks in the sheet, and preliminary morphological comparison between scarps on alluvium in this quadrangle and scarps of known age in Utah indicates that there are no Holocene surface ruptures on the faults in the Ely quadrangle. The east half of the quadrangle is dominated by latest Pleistocene (10-30 ka) faulting and the west half by older faulting. Faults in the east half of the Ely 1°x2° quadrangle are expressed by nearly continuous scarps, either on bedrock or on alluvium. One of the most recently active structures, the 100-km-long fault on the east side of the Schell Creek Range, is characterized by younger faulting (~15 ka) along the middle part of the fault and older faulting at its ends. The entire length of the fault has had numerous faulting events prior to the most recent ones; however, the timing of these events cannot be estimated with any accuracy. It appears, at this time, that other faults in this half of the quadrangle have had faulting events roughly contemporaneous with those along the Schell Creek Range. In contrast, the faults in the west half of the quadrangle are characterized by discontinuous scarps, most of which are on bedrock. Those scarps that are on alluvium are subdued, and faulting only displaces the oldest deposits along the range front, which are assumed to predate the most recent pluvial episode.

3. The 1983 scarp from the Borah Peak, Idaho, earthquake has been monitored by close-range photogrammetry for nearly 5 years, from October 1985 to May 1990. Close-range photographs have been taken twice a year, in the fall and in the late spring. Analysis of those photographs shows that the scarp at the monitoring site retreated an average of 70 mm between October 1985 and October 1989, with over half of the retreat occurring between October 1985 and May 1986. This relatively large amount of retreat occurred during a winter with unusually high late winter precipitation. Generally below-normal winter precipitation since then has precluded testing the possible association of high winter and spring precipitation with an increased rate of scarp retreat. Definitive association of the rate of scarp retreat with climatic factors will require a long-term commitment to the monitoring, which will be possible using the low-cost procedures developed for this study.

4. Crone and Machette conducted about 2 months of fieldwork in Central Australia as part of their Gilbert Fellowship. In September, they excavated several trenches across the scarps that formed during the 1988 Tennant Creek earthquakes (M_s 6.3-6.7), Northern Territories, and the single scarp that formed during the 1986 Marryat Creek earthquake (M_s 5.8), South Australia. These earthquakes produced thrust faulting. The main objective of this study is to identify and date prehistorical ruptures on these faults. Crone and Machette are collaborating with J. Roger Bowman (Australian National University, Canberra, Australia), who is studying the seismology of both earthquakes. Samples collected during the fieldwork will be submitted in FY 91 for TL dating (John Prescott, University of Adelaide, Australia; Steven Forman, University of Colorado, Boulder), ESR dating (Kazuhiro Tanaka, Central Research Institute of Electric Power Industry, Abiko, Japan; Hugh Millard, Isotope Geology, USGS-Denver) and U-trend dating (Dan Muhs and John Rosholt, Isotope Geology, USGS-Denver).

REPORTS

Crone, A.J., 1990, Late Quaternary tectonism and intraplate seismicity in the central interior of the United States [abs.]: Earthquake Seismology Symposium, Perth, Western Australia, September 5-7, 1990.

Crone, A.J., and Haller, K.M., in press, Segmentation and the coseismic behavior of Basin-and-Range normal faults: Examples form east-central Idaho and southwestern Montana, U.S.A.: Journal of Structural Geology, 24 ms. p., 7 figs.

Machette, M.N., Personius, S.F., Nelson, A.R., 1990, Paleoseismology of the Wasatch fault zone, U.S.A. [abs.]: Earthquake Seismology Symposium, Perth, Western Australia, September 5-7, 1990.

Machette, M.N., Personius, S.F., Nelson, A.R., Schwartz, D.P., and Lund, W.R., in press, The Wasatch fault zone, Utah—Segmentation and history of Holocene earthquakes: Journal of Structural Geology, 23 ms. p., 5 figs, 4 tables.

DATABASE MANAGEMENT

9910-03975

Charles S. Mueller
Branch of Engineering Seismology and Geology
U.S. Geological Survey
345 Middlefield Road, MS 977
Menlo Park, California 94025
415/329-5646

Investigations

1. Develop new techniques for playback, processing, management, and export of seismic waveform data, with emphasis on large aftershock datasets collected with portable digital event-recording seismographs (*e.g.*, GEOS).

2. Design and implement relational databases for strong-motion and aftershock data.

Results

1. New datasets played back, processed, and archived:
   Aftershocks of the 17 October 1989 Loma Prieta earthquake.

2. Datasets exported:
   Imperial Valley, California, 1979 aftershocks — Institut de Physique du globe de Paris

Reports

Mueller, C., and Glassmoyer, G., 1990, Digital recordings of aftershocks of the 17 October 1989 Loma Prieta, California, earthquake: U.S. Geological Survey Open-File Report 90-503, 147 p.

10/90

EARTHQUAKE RECURRENCE AND QUATERNARY DEFORMATION IN THE CASCADIA SUBDUCTION ZONE, COASTAL OREGON

9950-04180

ALAN R. NELSON, STEPHEN F. PERSONIUS, AND SUSAN RHEA

U.S. Geological Survey
Branch of Geologic Risk Assessment
MS 966, Box 25046
Denver, CO 80225
(303) 236-1596; FTS 776-1596

INVESTIGATIONS

There are three components to this project: (1) Nelson's study of coseismic changes in late Holocene sea level as revealed by salt marsh stratigraphy, (2) Personius' study of fluvial terrace remnants along major Coast Range rivers to determine style and rates of late Quaternary deformation, and (3) Rhea's study of river and drainage basin morphology in the Coast Range to determine relative rates of tectonic uplift.

RESULTS

Recurrence of coeismic changes in sea level in central Oregon

Coring in several inlets on the eastern side of Coos Bay, central Oregon, revealed no evidence of sands that might have been deposited by tsunamis, such as those that might be expected following a large regional earthquake. These inlets are directly exposed to the wide, central part of Coos Bay, and if a large tsunami entered the bay it is very likely that sand would be deposited on the edges of these inlets. One or two peaty layers were encountered in cores adjacent to the forested sides of the inlets. At the most exposed site, fine pebbly sand beds were found at several levels in cores. But the sand beds were interbedded with mud units, and they did not directly overlie the peaty units. These sand beds are probably storm surge deposits because there is no evidence of sudden submergence prior to their deposition. A similar search for tsunami deposits in protected inlets in the northern South Slough arm of Coos Bay encountered either sequences containing no sand or sequences containing so much sand that possible tsunami deposits could not be distinguished from tidal sand deposits. The thick sand beds in these sequences limited core depths to 2-3 m; except in one core, only a single buried peaty soil was found in northern South Slough.

Detailed coring in Shinglehouse Slough in eastern Coos Bay and at our Winchester Creek site in southern South Slough shows that the buried peat between 50 and 100 cm depth at both sites lies on an abrupt unconformity, probably representing at least 0.5 m of emergence. The same stratigraphic relations are found at several other sites, suggesting the possibility of an uplift event of regional extent. A single ^{14}C age from the Shinglehouse Slough site suggests the unconformity may be >1000 years old. In contrast, detailed coring at 3 new sites in central South Slough shows that the buried peat at 50-100 cm depth has an abrupt upper contact and a gradational lower contact, like the contacts on most of the deeper peaty soils at sites in southern South Slough.

Thus, our most recent studies suggest that buried peaty soils of at least two different origins occur at the same depth at different sites in the Coos Bay area.

New sites with multiple buried peaty soils have been investigated in South Slough. Collaborative coring with four Japanese scientists (Yoko Ota (Yokohama State Univ.), Masatomo Umitsu (Nagoya Univ.), Kaoru Kashima (Kyushu Univ.), and Yoshiaki Matsushima (Kanagawa Prefectural Museum)) along transects in the Talbot Creek marsh in the southeastern part of South Slough revealed a sequence of 6 buried peaty soils, much like those at Winchester Creek, 2 km to the southwest. Only 2-3 buried soils were found in similar transects at two marshes in central South Slough. Sedimentologic, diatom, and AMS ^{14}C analyses of 7-cm diameter cores collected from the Talbot Creek marsh and from one of the central South Slough marshes should allow detailed correlation of these sequences. Such correlations are needed to determine whether all peaty soils were buried following coseismic events and, for those soils determined to have been submerged coseismically, whether coseismic events were regional or local.

Long core transects at two new sites in the Siuslaw River estuary confirm that sea level rise along this part of the coast has been gradual for the last 2000 years. A uniform, 2-to-4-m thick peat unit is widely distributed in South Inlet, on Cox Island, and in the mouth of the North Fork of the Siuslaw River. Sudden regional subsidence events of >0.3-0.5 m can be precluded in this area for at least the last 2000 years.

Late Quaternary deformation rates indicated by fluvial terraces in central Oregon

Personius is continuing to analyze fluvial terraces for evidence of late Quaternary deformation in the Oregon Coast Range. Radiocarbon analyses of Holocene terraces on the Umpqua, Smith, Siuslaw, and Siletz Rivers indicate relatively slow (0.2-0.6 mm/yr) rates of uplift (incision) of the central Oregon Coast Range. Incision rates appear to be higher in the upper parts of the drainages near the crest of the Coast Range. While not without some inconsistencies, thermoluminescence (TL) ages on fluvial sediment along the Umpqua River appear to yield similar rates for higher terraces. No evidence of active Holocene structures has been observed in the drainages examined in central Oregon, but an anticline in the underlying Eocene bedrock has warped older terraces (100-200 ka?) at one location along the Siuslaw River. A manuscript summarizing these studies is being prepared.

Differential uplift of the Oregon Coast Range

A manuscript summarizing Rhea's study of river valley and drainage basin morphology has been reviewed and is about to be submitted to *Geomorphology.* Evidence from changes in long profile, gradient, gradient index, pseudo-hypsometric integral, valley incision, and sinuosity fractal dimension for rivers in western Oregon supports an hypothesis of differential uplift within the Oregon Coast Range. Rivers were separated into three regional groups; those in the western Coast Range, the eastern Coast range, and the Klamath and Cascade Ranges. The general shape of the long profiles within the Klamath and Cascade Ranges were similar, as were those within the eastern Coast Range. Profiles for rivers within the western Coast Range show a greater diversity of form. Pseudo-hypsometric integrals for the western Coast Range have a wide scatter, whereas those for the eastern Coast Range and Klamath and Cascade Ranges have a narrow range. These observations suggest that deformation within the Klamath and Cascade Ranges is more or less spatially uniform but that deformation within the Oregon Coast Range is more variable. Valley entrenchment and high sinuosity suggest ongoing and concentrated uplift in the central western Coast Range. Generalizations about the morphometry within each regional group do not hold for the central Coast Range near 44.5°N where the Yaquina and Marys Rivers are located.

Differences in the morphometry of the Yaquina and Marys Rivers support a hypothesis that the central Coast Range is the locus of coastal synclinal tilting.

REPORTS

Nelson, A.R., and Personius, S.F., (in press), Great earthquake potential in Oregon and Washington--An overview of recent coastal geologic studies and their bearing on segmentation of Holocene ruptures in the central Cascadia subduction zone, *in*, Rogers, Kockelman, Priest, and Walsh, eds., Assessing and reducing earthquake hazards in the Pacific Northwest, *U.S. Geological Survey Professional Paper*, 69 ms. p.

Jennings, A.E., and Nelson, A.R., Foraminiferal assemblage zones in central Oregon salt marshes--Relation to marsh floristic zones and sea level: *Journal of Foraminiferal Research*, (submitted 7/90), 49 ms. p.

Rhea, Susan, River response to differential Quaternary uplift in the Oregon Coast Range: Geomorphology, (reviewed and about to be submitted, 10/90), 31 ms. p.

Earthquake Intensities

1. 14-08-0001-G1510

A.I. Qamar
R.S. Ludwin
Geophysics Program
University of Washington
Seattle, WA 98195
(206) 543-8020

Investigations

Tom Bodle completed a masters thesis entitled "The Relation of Earthquake Intensity to Surface Geology and Elevation in Western Washington State". Approximately 4000 intensity reports were analyzed from a shallow, M= 5.5 earthquake in 1981 and the 59 km deep M= 6.5 Seattle/Tacoma earthquake of 1965. Chi-squared tests were performed to check the association between geology and intensity and the results were mixed. For both earthquakes site geology was found to contribute significantly to the variation in earthquake intensity for the region around Olympia, WA. However, in the Seattle region, a significant dependence of intensity on geology was evident in the 1981 data but not in the 1965 data. One possible reason for the lack of a dependent relation in the 1965 data, favored by Bodle, is the ambiguity of questions in the questionnaire distributed in the Seattle region in 1965.

This year we have shifted the emphasis of the research to an investigation of historical earthquakes before 1928. The goal is to reestimate epicenter locations, focal depths and magnitude of early earthquakes from a library search of available earthquake reports. We are reviewing existing earthquake catalogs including Holden (1898), Earthquake History of the US, Bradford (1935), Townley and Allen (1939), Rasmussen (1967), Berg and Baker (1963), Milne (1956). We are reviewing all significant earthquakes before 1928 by compiling existing isoseismal maps, collecting reports to allow construction of new isoseismal maps, and reviewing reports of foreshocks/aftershocks. The presence of aftershocks may be a useful discriminant of earthquake depth in the northwest.

The following represents material examined so far:

Review of The **Oregonian**; A subject index (1850-1910) to the **Oregonian** created by Leslie Scott (**Oregonian** Editor during that period) allowed us to conveniently locate articles. This listing was referenced by Berg and Baker, but not by Rasmussen. We have transcribed all the articles verbatim; they will form an appendix to our final report and be available to future investigators.

Review of various newspapers for articles on specific earthquakes. All reports found have been transcribed verbatim, and will be available in our final report.

Review of **Washington Standard** articles referenced by Rasmussen.

Review of **Washington Historical Quarterly** for articles of interest.

Articles found of interest include reports of drowned forests in the Columbia Gorge (communicated to Robert Schuster (USGS)), and a second-hand contemporaneous account of the 1872 Ribbon Cliffs landslide.

The most interesting result we have had to date concerns an earthquake which occurred on May 1, 1882, that was reported to have intensity III in Portland by both Rasmussen and Berg & Baker but which appears to have been much stronger than previously believed. Accounts of this event in the **Oregonian** indicate that it was felt over a very considerable area, from Salem, Oregon to Port Townsend, WA with the strongest shaking in Astoria where reports indicate damage to crockery etc. on store shelves and considerable damage to plaster also. This earthquake apparently caused widespread alarm in Portland, although no damage was reported. We plan to report this earthquake at the December AGU meeting.

Publications

Bodle, T, The Relation of Earthquake Intensity to Surface Geology and Elevation in Western Washington State, masters thesis. Geophysics Program, University of Washington, Seattle, WA, 1990.

Abstracts

Bodle, T, The Relation of Earthquake Intensity to Surface Geology and/or Elevation in Western Washington State, Fourth Annual NEHRP Workshop, Seattle WA, April 16-19, 1990. of Washington, Seattle, WA, 1990.

Investigations of Site Response

9950-03899

A. M. Rogers
Branch of Geologic Risk Assessment
U. S. Geological Survey
Box 25046, MS 966, DFC
Denver, Colorado 80225
303-236-6978

Investigations

1.) Considerable effort continues on the editorship of USGS Professional Paper 1560 "Evaluating Geologic Hazards in the Pacific Northwest". During this period the introductory chapter was written.
2.) Programming to permit analysis of the Whittier Narrows data obtained from Sprengnther digital recorders using existing programs is now complete and the processing and analysis phase of this project is underway.

Reports

Rogers, A.M., Kockelman, W.J., Priest, G.R., and Walsh, T.J., in press, Assessing and Reducing Hazards in the Pacific Northwest, in "Evaluating Geologic Hazards in the Pacific Northwest", U.S. Geological Survey Professional Paper , 60 ms pages.

Deep Structural Complexity and Site Response in Los Angeles Basin

14-08-0001-G1684

Mrinal K. Sen*, Chandan K. Saikia and Joanne Yoshimura
Woodward-Clyde Consultants
566 El Dorado St.
Pasadena, CA 91101
(818)449-7650

(*Now at the Institute for Geophysics, University of Texas, 8701 Mopac Blvd., Austin, Tx 78759 , (512)471-0466)

INVESTIGATION:

The objective of the project is to derive seismic velocity models in different parts of the basin, characterize site effects and compute strong ground motion due to a hypothetical earthquake using semi-empirical simulation technique.

RESULT:

During the first year of the project, seismic velocity structures in different parts of the basin were derived by waveform modeling of small to moderate size earthquakes. Site effect was also studied by analyzing recordings of small aftershocks of the Whittier Narrows, California earthquake and the NTS seismograms recorded in the basin. Three papers (Sen 1990; Sen and Abrahamsson 1990; Saikia, Sen and Helmberger 1990) have been submitted for publication.

During the second year of the project, the following tasks are being carried out:

(1) Modeling of SH and SV waveforms of strong motion data from the largest (M=5.3) aftershock of the Whittier Narrows, California earthquake so as to derive the best fitting source parameters.

(2) Modeling of strong motion data from the Pasadena earthquake to derive the best fitting source parameters.

(3) Calibration of the simulation technique by forward modeling of the Whittier Narrows, California earthquake.

(4) Prediction of strong ground motion from a hypothetical moderate size earthquake in Los Angeles Basin.

As an example, we show in Figure (1) (taken from Yoshimura and Saikia 1990), the results of waveform modeling of tangential seismograms from October 4, 1987 aftershock of the Whittier Narrows, California earthquake. The figure shows a comparison between the recording and synthetic seimsograms for the best fitting source model. The objective was to derive the best fitting source parameters for this aftershock so that these recordings can be scaled and used later as empirical source functions in the simulation of strong ground motion due to a hypothesized earthquake in the Los Angeles basin. The one-dimensional model derived earlier (Sen 1990) was used to compute synthetic seismograms using wavenumber integration technique. The best fitting point source has a strike of 145^0 , dip of 60^0 , a rake of 148^0 and a moment of $1.1X\,10^{24}$ dyne-cm.

Next, we computed strong ground motion from a hypothetical magnitude 7.0 earthquake in the Los

Angeles Basin. A semi-empirical Green's function summation method was used. The records from the largest aftershock of the Whittier Narrows earthquake were used as empirical source functions and the model Sen (1990) was used to compute generalized ray theory Green's functions. Figure 2(a) shows the location of the postulated fault, the dimensions of the fault being length=30 km width=15 km. The following source parameters were used: dip = $30^0 N$, strike= 270^0 , rake = 90^0 , moment= $2.6X\,10^{26}$. The peak ground accelerations (average of two horizontals) for a particular slip distribution is ahown in Figure 2(c). Currently, the sensitivity analysis is being carried out for a suite of slip distribution, rupture velocity and rise time.

REFERENCES:

Hauksson, E (1990) Earthquakes, faulting and stress in the Los Angeles basin, In Press, JGR.

Saikia, C. K., Sen, M. K., and Helmberger, D. V. (1990) Analysis of NTS seismograms recorded in Los Angeles basin, submitted to JGR.

Sen, M. K. (1990) Modelin of wave propagation in northern Los Angeles basin, In revision, BSSA.

Sen, M. K., and Abrahamsson, N. A. (1990) Analysis of peak ground accelerations from small aftershocks of the Whittier Narrows, California earthquake, Submitted to BSSA.

Yoshimura, J., and Saikia, C. K. (1990) Source parameters of the October 4, 1987 Whittier Narrows aftershock, manuscipt in preparation for submission to BSSA.

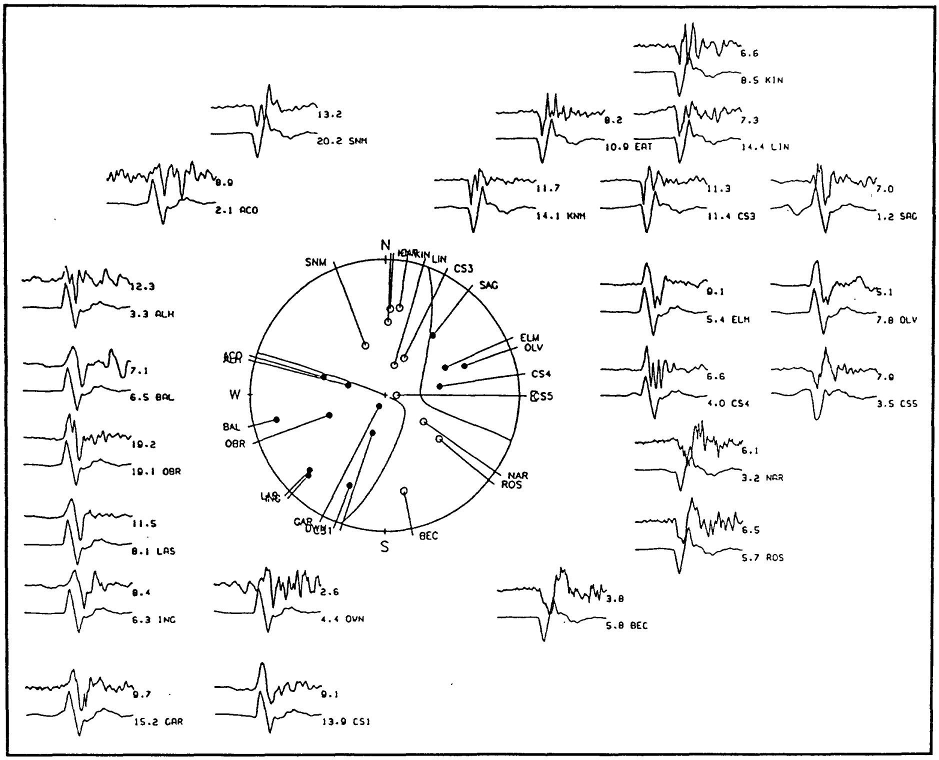

Figure 1. Results (Yoshimura and Saikia, 1990) from waveform modeling of SH seismograms of the October 4, 1987 aftershock of the Whittier Narrows, California earthquake.

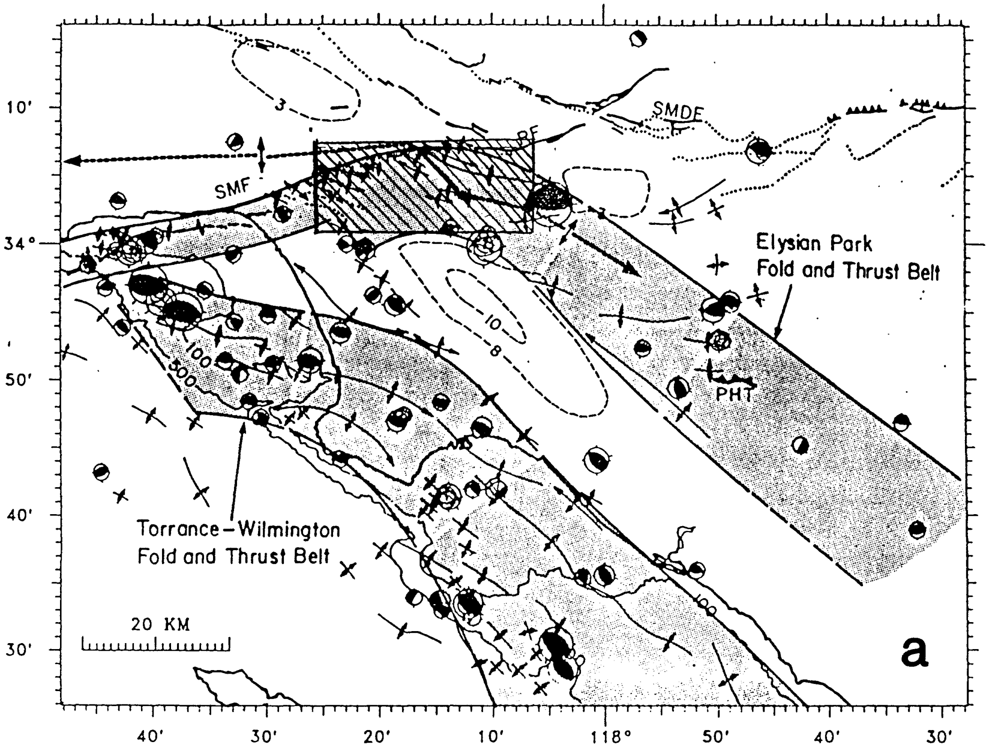

Figure 2(a). Location of the hypothetical fault used in the ground motion simulation is shown by hatched rectangle. The figure is taken from Hauksson (1990).

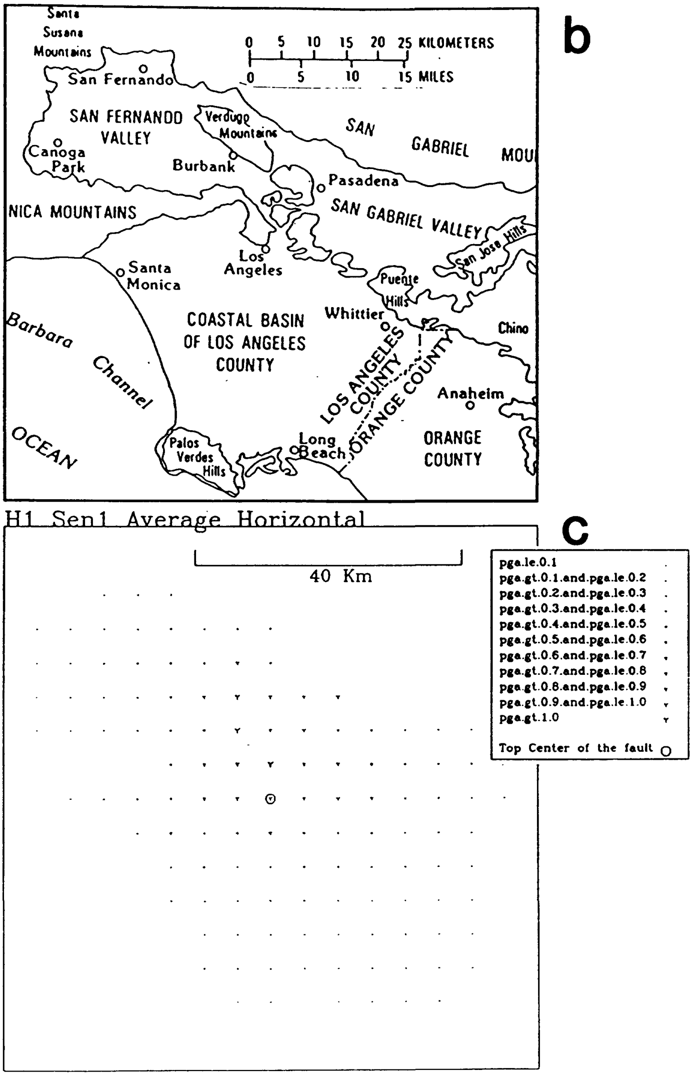

Figure 2(b). Map of the area under study.
(c). Ground motion (average of two horizontals) obtained by simulation; the top center of the fault is about 1 km north of down town Los Angeles.

EXPERIMENTAL AND ANALYTICAL INVESTIGATIONS OF THREE GRAVELLY SITES WHICH LIQUEFIED DURING THE 1983 BORAH PEAK, IDAHO EARTHQUAKE

USGS 14-08-0001-G1779

Kenneth H. Stokoe, II, José M. Roesset and Ronald D. Andrus
The University of Texas at Austin
Department of Civil Engineering
ECJ 9.227
Austin, Texas 78712
(512) 471-4929

Investigation

The primary objectives of this project are:

[1] Refine the characterization of gravelly soils which liquefied beneath the Pence Ranch during the 1983 Borah Peak, Idaho earthquake (Stokoe et al, 1988; Harder, 1988). Fully characterize sediments at two additional gravelly sites (Goddard Ranch and Larter Ranch) which also liquefied.

[2] Since there are no generally accepted guidelines for evaluating the susceptibility of soils which contain significant amounts of gravel, apply simplified liquefaction susceptibility procedures developed for sands to these gravelly sites, evaluate the usefulness of each procedure and propose guidelines for the future application of these procedures to gravelly soils in other parts of the world.

[3] Perform laboratory cyclic testing on 6-in. (15-cm) diameter reconstituted gravel specimens to determine G_{max}, the variation of modulus with strain amplitude and number of cycles of loading, and the threshold strain at which pore pressure generation is initiated.

[4] Develop a dynamic model from the results of the field and laboratory investigations combined with the limited amount of published data. Evaluate liquefaction susceptibility analytically at each site using both the cyclic stress and cyclic strain approaches.

Results

In August 1990, we conducted a variety of field investigations at the Pence Ranch, Goddard Ranch and Larter Ranch liquefaction sites. The field work included drilling, seismic testing, trenching, test pit excavations, in situ density and permeability testing, and sampling. Drilling consisted of 24 CPT soundings, 10 SPT boreholes, and 11 BPT soundings. Load cell measurements were made during several of the SPT tests. We will use the load cell data for energy calibration of the drill rig equipment. Downhole seismic tests were performed in one of the SPT boreholes at each site. Surface wave testing using the SASW method were conducted using hammers and bulldozers as sources. With the bulldozers, we were able to have geophone spacing ranging up to 160 ft (50 m). SASW testing was conducted along 12 arrays. The SASW method requires no boreholes and thus is well-suited for undisturbed testing of gravel. Trenches were excavated across the lateral spread near the hay yard at Pence Ranch and the gravel bar at Goddard Ranch. in these trenches, we logged the sediment profile, made descriptions of fissures, noted the structural relationship between sediment units and fissuring, and collected materials for radiometric dating.

In test pits excavated at all three sites, we conducted a total of 7 large ring density tests, 10 sand cone density tests, and 13 open-end permeability tests. The ring density tests were conducted using a 4-ft (1.2-m) diameter ring in the loose to dense gravels encountered within 6 ft (2 m) of the ground surface. Permeability testing was performed under contant-head conditions using 4-in. (10-cm) and 12-in. (30-cm) PVC pipes. A few intact samples of the gravelly soils were collected at the Pence Ranch and Goddard sites using an epoxy-based resin. These epoxy samples will be cut, polished and examined to define grain-to-grain structure. Bulk samples were collected with the aid of a backhoe, just below the water table in the loosest zones. About 4000 pounds (1800 kg) of gravelly soil samples were collected and transported to Austin. These samples will be used to accurately define grain size and construct 6-in. (15-cm) diameter gravelly specimens for laboratory cyclic testing. The large resonant column/torsional shear device to test these rconstituted gravelly specimens is presently under construction here at the University of Texas.

Data reduction during September involved the construction of a three-dimensional model of the soils underlying the Pence Ranch near the hay yard. This model is based on 10 CPT soundings, a trench excavated across the major fissure, and borehole sample data. A plan view of the region modeled, CPT test locations and trench excavation are shown in Fig. 1. CPT soundings were discretized into five units: 1) silty sand cap, 2) gravelly soil with $q_c < 50$ tsf, 3) gravelly soil with $50 < q_c < 100$ tsf, 4) gravelly soil with $100 < q_c < 250$ tsf, and 5) gravelly soils with $q_c > 250$ tsf (Note: 1 tsf = 95.8 kPa). A perspective view of the discretized CPT soundings is shown in Fig. 2. Continuous logs of CPT tip resistance and fiction ratio are shown with discretized layering along the CP1-CPC alignment in Fig. 3. With the aid of a recently developed solid modelling program developed by Mr. Norman L. Jones (1990), each unit boundary was approximated using interpolation and extrapolation contouring techniques. A fence diagram of the region modeled is shown in Fig. 4. The relationship of the water table to the stratigraphy is shown in a series of cross sections in Fig. 5. Much of the loosest zone, $q_c < 50$ tsf, lies below the water table. In the vicinity of CP2 and CPE the silty sand cap is over a meter thick. This thick cap, located so close to the water table and the loosest material, makes this area most vulnerable to liquefaction and provides an explanation for the location of the major fissure.

The model described in the preceding paragraph will be useful in correlating the other in situ tests conducted near the hay yard at Pence Ranch. Similar models will be developed for the Goddard Ranch and Larter Ranch sites.

REFERENCES

Harder, Jr., Leslie F., (1988), "Use of Penetration Tests to Determine the Liquefaction Potential of Soils During Earthquake Shaking," Ph.D. Dissertation, University of California, Berkeley, 565 p.

Jones, Norman L., (1990), "Solid Modelling of Earth Masses for Application in Geotechnical Engineering," Ph.D. Dissertation, The University of Texas at Austin, in preparation.

Stokoe, K.H., II, Andrus, R.D., Rix, G.J., Sanchez-Salinero, I., Sheu, J.C., and Mok, H.J., (1988), "Field Investigation of Gravelly Soils Which Did and Did Not Liquefy During the 1983 Borah Peak, Idaho, Earthquake," Geotechnical Engineering Report GR87-1, Civil Engineering Dept., The University of Texas at Austin, 206 p.

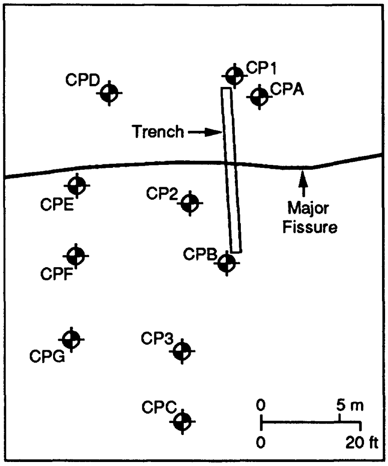

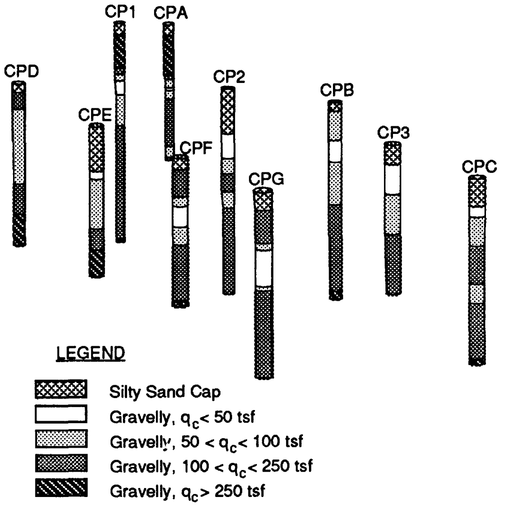

Fig. 1 Plan View of the Region Modeled Near the Hay Yard with Locations of CPT Soundings, Trench Excavation, and Major Fissure

Fig. 2 Perspective View of Discretized CPT Soundings Used in the Model

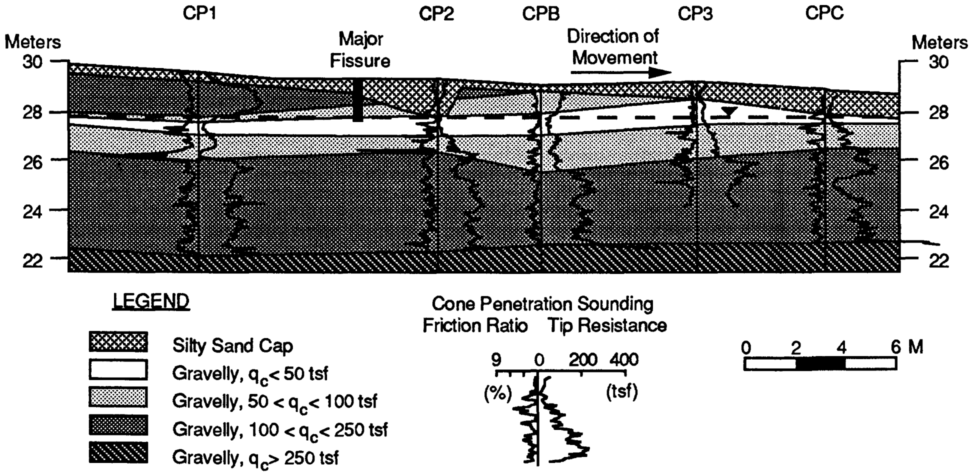

Fig. 3 Cross Section Along the CP1-CPC Alignment with Continuous Logs of CPT Tip Resistance and Friction Ratio

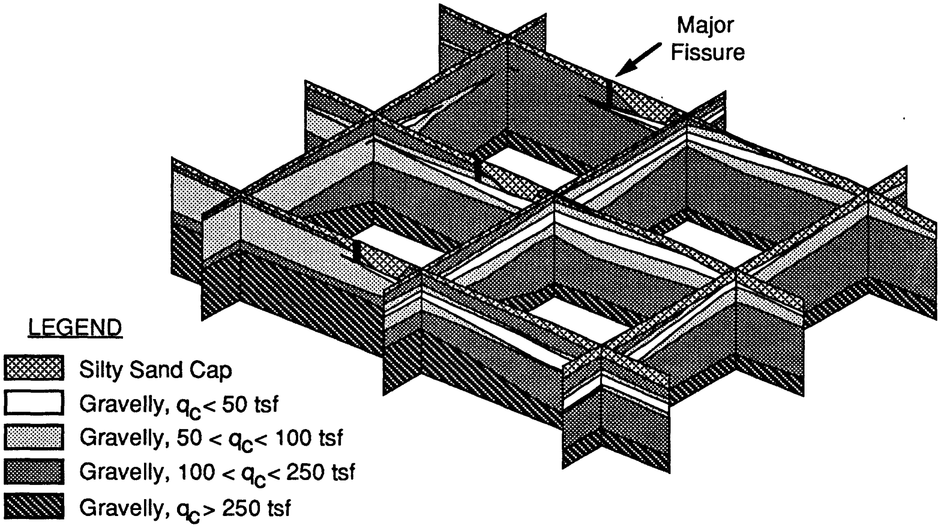

Fig. 4 Fence Diagram of Stratigraphy within the Region Modeled

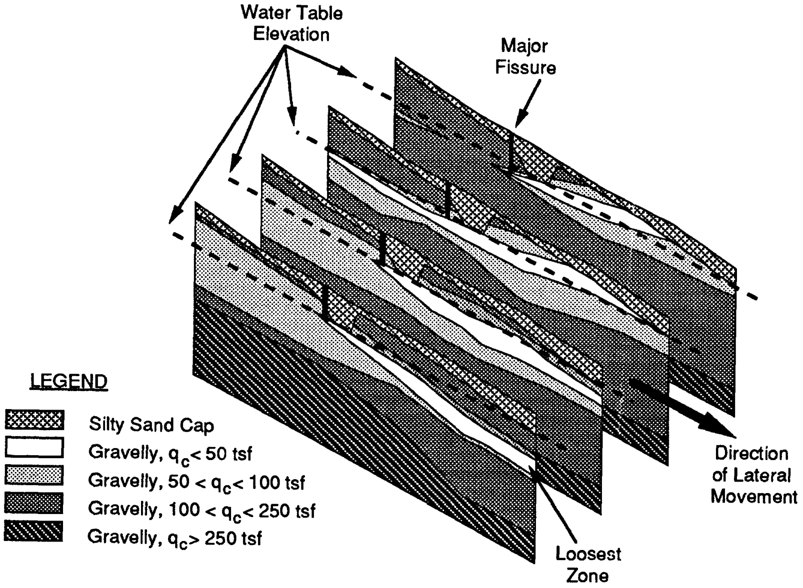

Fig. 5 Cross Sections of Region Modeled Showing the Relationship of the Water Table to the Stratigraphy.

Resonant Frequencies of Sedimentary Basins: Applications to Seismic Risk Evaluation

Contract USGS 14-08-0001-G1787

J.A. Rial & N. G. Saltzman

The University of North Carolina at Chapel Hill, Geology Department, Mitchell Hall,
CB#3315, Chapel Hill, NC 27599-3315; Tel: (919)9664553
E-mail: jar@antipode.geosci.unc.edu

INVESTIGATIONS:

Development of analytic and numerical methods to determine the natural frequencies of oscillation of three-dimensional models of sedimentary basins. The analytic methods are derived from similar problems in classical dynamics and quantum chemistry. The numerical approach uses a modification of the Rayleigh-Ritz variational method to determine the resonant frequencies in basins of arbitrary geometry.

Results

Analytically derived formulas to compute the eigenfrequencies of three-dimensional ellipsoidal sedimentary basins were described in a recent paper (Rial, 1989). For an ellipsoidal basin the eigenfrequencies of the most readily excited, high frequency bouncing-ball mode of oscillation (Mode II) were shown to be given by:

$$f = f_0 \{ (2n_z + 1) + (1/\pi) [(n_x + 1/2) \beta_1 + (n_y + 1/2) \beta_2] \} \qquad (1)$$

$$\beta_1 = \text{Arccos} (1 - 2 H/R_1) \qquad 0 \le \beta_1 \le \pi$$

$$\beta_2 = \text{Arccos} (1 - 2 H/R_2) \qquad 0 \le \beta_2 \le \pi$$

$$\text{with } \beta_1 \ne \beta_2 \text{ and } n_x, n_y, n_z = 0, 1, 2, 3, \ldots$$

R_1 and R_2 are the principal radii of curvature at the deepest point of the basin, whose geometrical center coincides with the origin of cartesian coordinates. $f_0 = v/4H$, where H is the basin's maximum depth at x=y=z=0, and v is the wavespeed in the sediments. We have computed the eigenvalues of arbitrarily shaped basins by the EBK or Poincare section method described in our previous report (Vol XXX; see also Keller, 1985; and Rial and Ling ,1990). Table I compares results of the eigenvalues obtained using the Poincare´ section method and the analytic solutions given by equation (1). Table I is for a triaxial ellipsoid and Tables II and III show results for nonseparable basins of cosine and gaussian shapes. Relative discrepancies between results for which there is an analytic solution are less than a fraction of 1% in most cases. Slightly larger discrepancies are due to the fact that the analytic results of equation (1) were obtained under the condition of paraxiality (Rial, 1989), i.e., valid for rays confined to the neighborhood of the basin's minor axis. The analytic results given by (1) should deteriorate as the eigentrajectory of the mode corresponds to initial rays with increasingly greater angles with the vertical. In general, and as expected, the discrepancies between analytic and EBK results decrease rapidly for modes with $n_z \ge 1$.

Table II shows results for a gaussian shaped basin. Table II includes an eigenfrequency upper bound, provided by the analytic results of an ellipsoid that has the same maximum depth as the gaussian and the same principal curvatures there. We use the 8/6/1 ellipsoid of Table I and construct the embedding gaussian from it. Since the total volume of the ellipsoid is smaller than that of the gaussian basin thus constructed, its eigenfrequencies must be an upper bound for the eigenfrequencies of the gaussian. Again, note that as the modes are confined closer to the axis (as n_z increases) all results tend to agree, since the eigenfrequencies of the vertical higher overtones under a given site do indeed depend on the local curvatures under the site, and not on the global geometry and/or extent of the basin.

Table III further illustrates results obtained for a cosine shaped basin. Again the upper bound eigenvalues are for an ellipsoidal basin that shares the same maximum depth and curvatures with the cosine basin. For any arbitrary basin it is useful, when applicable, to determine the analytic upper bound of the eigenvalues by constructing an embedded ellipsoid and calculating its eigenfrequencies by the use of formula (1) as suggested above.

To complement the EBK results and to obtain independent checks on the results, we used the variational K-S (Kutler and Sigillito, 1985) method, extended to three dimensional mixed boundary value problems. This method uses sums of basis functions to approximate the eigenmodes of a basin model. The coefficients of the basis functions in the sum are chosen so that they minimize the *a-priori/a-posteriori* eigenvalue error bounds. Codes for solution of the SH modes for three-dimensional basins of ellipsoidal, cosine, and gaussian shapes, using polynomial basis functions, have been developed.

The number of basis functions required to obtain the results presented here varied from 9 to 49 for two dimensional problems. For three dimensional problems, 64 basis functions were used although as many as 125 were required for high overtones. Table IV shows that our implementation of this method in two dimensions reproduces the Bard and Bouchon (1985) data without difficulty.

Table V shows eigenfrequencies for three-dimensional ellipsoids of different geometries obtained with the K-S method. The eigenfrequencies and eigenfunctions of an ellipsoid-shaped basin can be used as a good check because the analytic solutions are known. The results of the K-S method are in good agreement with the analytic results and with the results obtained with the Poincare section method.

Two types of error affecting the K-S results are numerical error and errors due to insufficient or inappropriate basis functions. Not much is known about the former, which is responsible for the occasional case where the K-S eigenfrequency range was very small and the true eigenfrequency was outside the K-S eigenfrequency range. The latter results in very large K-S eigenfrequency ranges. In our experience, this occurred mostly in the computation of higher modes and the approximate eigenvalues were nevertheless still very close to the true eigenvalues.

Current Effort

Since we have used independent analytical and numerical methods, our results can probably be used with confidence. The Poincare´ section method is the easier to implement, and extensions to compute the eigenfunctions too are presently under development, based on a method described by De Leon and Heller (1984). Also, its application to obtain the full elastic response of two-dimensional, arbitrarily shaped basins has been implemented and is presently being tested. The most severe limitation of the Poincare´ method is the inherent instability of any ray

TABLE I

8/6/1 ellipsoidal basin

MODE(*)	Poincare	Analytic f/f_0
(0 0 0)	1.094940	1.093193 (**)
(1 0 0)	1.177267	1.172980
(0 1 0)	1.207950	1.199794
(1 1 0)	1.307962	1.279580
(0 0 1)	3.093924	3.093193
(1 0 1)	3.173971	3.172980
(0 1 1)	3.206025	3.199794
(1 1 1)	3.284894	3.279580
(0 0 2)	5.094031	5.093193
(1 0 2)	5.171327	5.172980
(0 1 2)	5.203112	5.199794
(1 1 2)	5.282981	5.279580
(2 0 0)	1.263693	1.252766
(2 0 1)	3.255558	3.252766
(0 2 1)	3.318910	3.306395
(2 2 2)	5.474055	5.465967

TABLE II

Eigenfrequencies of a gaussian-shaped basin which has the same principal curvatures and depth at x=y=0 as an 8/6/1 ellipsoid. The ellipsoid is of lesser volume than the gaussian basin and tangent to it at x=y=0, z=-H. The gaussian basin is described by the formula $z = -H [\mathrm{Exp} [-\alpha x^2 - \beta y^2]$ where H is the maximum depth and α and β are constants.

MODE	Poincare	Upper Bound (8/6/1 Ellipsoid)
(0 0 0)	1.092325	1.093193
(1 1 1)	3.277253	3.279581
(2 0 0)	1.245022	1.252766
(0 2 0)	1.295846	1.306395
(2 2 0)	1.437640	1.465967
(0 3 0)	1.396581	1.412996
(3 3 0)	1.603512	1.652354
(4 4 0)	1.754662	1.838741
(5 5 0)	1.926742	2.025128
(6 6 0)	2.084287	2.211515
(4 4 1)	3.821851	3.838741
(4 4 2)	5.825840	5.838741
(4 4 4)	9.831758	9.838741

(*) Modes are described as integers (n_x n_y n_z)

(**) All values of the eigenfrequencies in this and in Tables II III and IV are for the dimensionless quantity f/f_0, where f is the eigenfrequency of the basin and $f_0 = v/4H$, where v is the wavespeed in the sediments and H is the maximum thickness of the ellipsoidal basin, which occurs at x=y=0.

TABLE III

Eigenfrequencies of a cosine-shaped basin which has the same principal curvatures and depth at x=y=0 as an 4/3/1 ellipsoid. The ellipsoid is of lesser volume than the cosine basin and tangent to it at x=y=0; z=-H. The cosine basin is described by the formula $z' = -H/2 [\mathrm{Cos} (\pi x/a) + \mathrm{Cos} (\pi y/b)]$ where H is the maximum depth and a and b the semiwavelengths

MODE	Poincare	Upper Bound (4/3/1 Ellipsoid)
(0 0 0)	1.186797	1.188604
(1 0 0)	1.338769	1.349465
(0 1 0)	1.394101	1.404951
(1 1 0)	1.541755	1.565812
(0 0 1)	3.187218	3.188604
(0 0 2)	5.187632	5.188604
(2 0 0)	1.489901	1.510327
(2 2 0)	1.889084	1.943020
(2 2 2)	5.929370	5.943020

TABLE IV

Comparison of results of the K-S method with numerical results reported by Bard and Bouchon (1985) for a two-dimensional cosine-shaped basin.

Aspect ratio (H/L)	F-K(*)	K-S	Bard & Bouchon
1.0	1.91833	2.010	----
0.8	1.71651	1.770	1.767
0.6	1.48620	1.54	1.537
0.4	1.21292	1.330	1.311
0.2	1.02058	1.150	1.140
0.1	1.00457	1.070	1.047

(*) Faber-Krahn minimum eigenvalue estimates for vibrating membranes
Faber, G (1923) *Sitz. Bayer. Akad. Wiss.* 169-72.
Krahn, E. (1924) *Math. Ann.*, **94**, 97-100.

TABLE V

Eigenfrequencies (f/fo) for several ellipsoids

Geometry (axes ratios)	MODE	K-S method	ε^2	Analytic
4/3/1	(0 0 0)	1.210	0.00004(*)	1.188604
	(2 0 0)	1.566	0.02	1.510327
	(0 2 0)	1.710	0.015	1.621298
	(2 2 0)	2.048	0.080	1.943003
2/2/1	(0 0 0)	1.399	0.00026	1.333333
	(2 0 0)	2.140	0.20	2.000000
2.5/2/1	(0 0 0)	1.352	0.00039	1.297656
	(2 0 0)	1.893	0.18	1.821616
3/2/1	(0 0 0)	1.322	0.00062	1.274840
	(2 0 0)	1.823	0.160	1.707534
4/2/1	(0 0 0)	1.289	0.0012	1.247097
	(2 0 0)	1.672	0.13	1.568820
5/2/1	(0 0 0)	1.270	0.002	1.230761
10/2/1	(0 0 0)	1.239	0.0045	1.198551
20/2/1	(0 0 0)	1.229	0.0057	1.182589

(*) $\min_{n} |(\lambda_n - \lambda_*)/\lambda_n|^2 \leq \Sigma M_{ij} c_i c_j / \Sigma N_{ij} c_i c_j = \varepsilon^2$

---

tracing scheme. The ray tracing method also becomes difficult to use in those cases where there exist strong symmetries in the basin's geometry that produce strongly periodic ray trajectories that do not fill the modal volume. Fortunately, it is for those highly symmetric, highly degenerate cases for which the variational Kuttler and Sigilito (1985) or K-S method seems to work best. Extension of the K-S method to computation of eigenfrequencies and eigenfunctions in general three dimensional and fully elastic problems is underway.

The figure in the next page shows a result were both the EBK and the K-S methods have been used to determine selected SH resonant modes in an ellipsoidal three-dimensional basin.

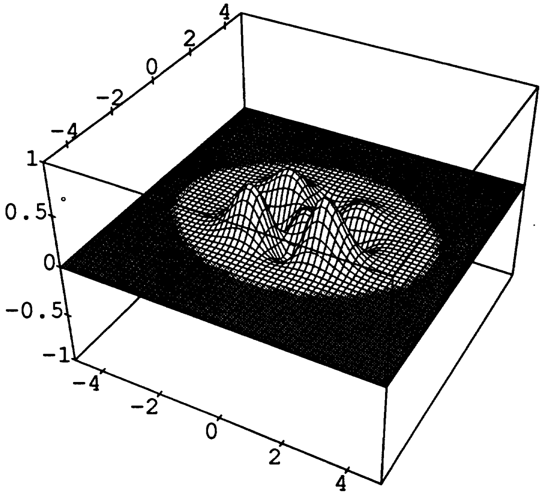

A resonant mode of oscillation of a model of an ellipsoidal basin filled with soft sediments -light color- imbedded in hard rock -dark color-. The relative dimensions of the basin's semiaxes are in the ratio 4/3/1. This is but one of a large number of frames computed to create an animated sequence that shows the oscillations of the ground in real time on a computer monitor.

REFERENCES

Bard, P. and M. Bouchon (1985): Bull. Seis.Soc. Am. **75**, 519-542

De Leon, N. and E.J. Heller (1984): *Phys. Rev.* **A30**, pp 5-18

Keller, J.B. (1985): *SIAM Review*, **27** (4), pp458-504

Kutler, J.R. & Sigilito (1985) ***Estimating eigenvalues with a posteriori/a priori inequalities***, Pitman, Boston.

Rial, J.A.(1989) : *Geophys. Jour. Int.*, **99**, pp81-90

Rial, J.A. and H. Ling (1990): *EOS (AGU)*, **71**, 466 (Abstract)

Weinstein, L.A. (1969) ***Open Resonators and Open Waveguides.*** The Golem Press, Boulder, Colorado.

Computer Graphics Laboratory

9950-04541

A. C. Tarr
Branch of Geologic Risk Assessment
U. S. Geological Survey
MS 966, Box 25046, Denver Federal Center
Denver, CO 80225
(303) 236-1605

INVESTIGATIONS

The objective of this project is to provide computer graphics services (such as access to Geographic Information System (GIS) software) to USGS geological hazards investigators. These services include (1) consultation on digital spatial data base design and data acquisition, (2) training in the use of GIS methods, (3) assistance in the assembly of large spatial data sets, and (4) research into advanced spatial data analysis topics.

Specific investigations conducted during the reporting period were (1) San Francisco Bay area digital spatial data sets, (2) Pacific Northwest geological hazards data base, (3) seismotectonic map of the Mississippi embayment, (4) Meers Fault, Oklahoma geologic map, and (5) ARC/INFO user interface development.

RESULTS

San Francisco Bay Area -- Topologically-structured data layers were constructed for three 30' X 60' quadrangles (Lodi, Napa, and Stockton) in the San Francisco Bay area from USGS Digital Line Graph (DLG) data files using ARC/INFO GIS software. These data layers will be added to a digital spatial data base being assembled for the San Francisco Bay area. The data base already contains hydrography, transportation (roads and trails, railroads, electrical transmission lines, pipelines, and ferry lines) data layers for five 30' X 60' quadrangles (Monterey, Palo Alto, San Francisco, San Jose, and Santa Cruz). In addition, hypsometric contours of the San Jose 30' X 60' quadrangle and geology of selected quadrangles in the Loma Prieta area have been added to the data base. The data base has been made available to USGS-sponsored studies of the San Francisco Bay area, including mapping of damaged structures in San Francisco and seismic response in Los Gatos, Santa Cruz, and Monterey County.

Pacific Northwest -- Augmentation of the geologic hazards data base of Puget Sound continues with the addition of hydrography and transportation data layers for Hoquiam, Port Townsend, and Victoria 30' X 60' quadrangles. The geology of the Seattle and southern half of the Tacoma 30' X 60' quadrangles are currently in the data base. The digital linework of the geologic contacts of the Port Townsend geologic map (Pessl and others, 1989) has been obtained from Western Mapping Center for conversion into ARC/INFO files. Completion of the northern half of the Tacoma quadrangle geology and combining the newly-acquired base data sets will permit construction of an entirely digital geologic map of the southern Puget Sound.

Mississippi Embayment -- In FY91, seismic hazards research begins anew in the New Madrid seismic zone and surrounding Mississippi embayment. One new project is construction of a seismotectonic map of the Mississippi embayment (Wheeler, this volume) utilizing GIS technology and digital spatial data. The seismotectonic map will portray numerous thematic data sets, such as seismicity, geology, depth to bedrock, and liquefiable sediments, on base data layers. During the reporting period, 1:100,000-scale DLG data for sixty 30' X 60' quadrangles, 1:24,000-scale DLG data for several hundred 7 1/2' quadrangles, and 1:250,000-scale Digital Elevation Model (DEM) data were obtained for an area encompassing the New Madrid seismic zone.

Meers Fault -- Maps of aeromagnetic and gravity anomalies of the Meers Fault area of Oklahoma (Cecil, unpublished data) required a digitized overlay of geologic contacts and mapped faults. Unfortunately, the only available map of the faults and contacts in the study was published without scale or projection; in addition, the scale varied unevenly across the map resulting in registration errors of hundreds of meters. Thus, the digitized linework was also distorted and could not be registered with the computer-generated aeromagnetic and gravity anomaly maps. Elimination of much of the distortion was possible by employing the GIS technique of piece-wise adjustment ("rubbersheeting") and by using township corners common to the geologic map and a scale-stable USGS greenline.

ARC/INFO User Interface -- Users of a powerful GIS software such as ARC/INFO are typically overwhelmed by the hundreds of commands available and by the extensive training period required to become a proficient user. Several currently available ARC/INFO user interfaces (ARCSHELL, ALACARTE, and MAPX) are being evaluated in the Computer Graphics Laboratory. ARCSHELL is a general interface developed by the manufacturer of ARC/INFO allowing access to all ARC/INFO commands from menus. ALACARTE is menu-driven digital map compilation tool developed by Wentworth and Fitzgibbon (unpublished software) which assists in compiling a digital geologic map. MAPX automates the complicated process of producing large, finished USGS maps entirely from digital spatial data. The goal is to refine and integrate these three interfaces to assist the occasional ARC/INFO user.

Quaternary Framework for Earthquake Studies
Los Angeles, California

9540-01611

John C. Tinsley
Branch of Western Regional Geology
U. S. Geological Survey
345 Middlefield Road MS-975
Menlo Park, California 94025
415-329-4928

Investigations

1. Geology and relative ground motion, Wasatch area, Utah:

Analysis of geologic and geophysical data from 43 sites in the Salt Lake Valley continues; writing of interpretive reports progresses as time can be borrowed from other projects. Studies involve comparisons of alluvium-to-rock spectral ratios in two period bands (0.2-0.7 sec, and 0.7-1.0 sec) with geologic parameters characterizing basin fill, including thickness of key stratigraphic intervals, degree of cementation of materials, shear-wave velocity, and other parameters correlative with site-dependent aspects of ground response (John Tinsley, Kenneth King, Rob Williams).

2. Regional Evaluation of Liquefaction

A. Monterey Bay Lowland and vicinity. Following the Loma Prieta earthquake, an exhaustive study of lateral spreading ground failures in natural deposits of the Salinas and Pajaro rivers and coastal estuaries was initiated with personnel from the Branch of Engineering Seismology and Geology helping to address the geotechnical aspects and personnel from the Branch of Geologic Risk Assessment helping to address the relevant ground motion parameters; Tinsley and Dupre provided mapping and stratigraphic analyses of the lateral spreading ground failures. The immediate goal was to evaluate the USGS liquefaction hazard mapping (scale 1:62,500) published by Dupre and Tinsley (1980) conducted according to the methodology of Youd and Perkins (1978). Additional goals included evaluating the in-situ properties of deposits that failed, in contrast to adjacent deposits that did not incur ground failure, to learn more of the suites of properties of materials that can produce the destructive effects of liquefaction. The US literature is sparse with respect to studies of lateral spreads. This study is reported elsewhere in this volume by Tinsley, Holzer, and Bennett in the section dedicated to the Loma Prieta earthquake.

B. Los Angeles and vicinity. A cooperative working agreement was concluded late this fiscal year with the Planning

Department of the City of Los Angeles supporting publication of USGS liquefaction hazard mapping at a scale of 1:24000, including the surficial geology, shallow groundwater data, and derivative hazard maps. This will complete the release of data mustered in support of the regional liquefaction mapping published in Tinsley and others (1985). The work will be in digital form, enabling revisions and updates to be made relatively easily. Also, a ground shaking hazards map of the Los Angeles 7.5' quadrangle produced using the methodology of Rogers and others (1985) is in progress.

Results:

1. The Salt Lake Valley ground response study has been stalled owing to a substantial investment of field time in the studies of the effects of the Loma Prieta earthquake and to a lack of funding specifically aimed at these ground response studies. The Wasatch area work should be progressing more rapidly, now that the Loma Prieta field studies are complete.

2a. The Monterey Bay area's liquefaction susceptibility mapping (Dupre and Tinsley, 1980) was robust with respect to lateral spreading ground failures, settlements, and sand "boils". The success of the mapping stems principally from two aspects: the mappers enjoyed (1) a thorough understanding of the stratigraphy of the fluvial and eolian systems in question, developed in the course of two Ph. D. dissertations and, (2) the benefits of hindsight and reports of liquefaction accompanying the 1906 earthquake and its aftershocks. The 1906 earthquake was about 60 time greater in terms of energy release and probably was at least 4 times greater in terms of duration of strong ground motion, compared to the recent Loma Prieta event. Moreover, the Loma Prieta earthquake followed 4 dry winters and the 1906 San Francisco earthquake followed a rather wet spring, so hillslopes and soils were much closer to being water-saturated in 1906 compared to 1989.

2b. Labor has been retained to assist with the revisions, compilations, and digitization of the maps showing liquefaction hazards in the City of Los Angeles.

Publications:

1. Dupre, W. R. and Tinsley, J. C., 1990, Geologic controls on liquefaction-induced ground failure in the Monterey Bay Area, California, during the Loma Prieta earthquake: Geological Society of America Abstracts with Programs, v. 22, no. 7, p. A188.

References cited:

Dupre, W. R. and Tinsley, J. C., 1980, Geology and liquefaction potential, northern Monterey and southern Santa Cruz

Counties, California: U.S. Geological Survey Miscellaneous Field Studies Map MF-1199, scale 1:62,500, 2 sheets.

Rogers, A. M., Tinsley, J. C., and Borcherdt, R. D., 1985, Predicting relative ground response in Ziony, J. I. (ed) Evaluating earthquake hazards in the Los Angeles region--An earth science perspective: U. S. Geological Survey Professional Paper 1360, p. 221-247.

Tinsley, J. C., Youd, T. L., Perkins, D. M., and Chen, A.T.F., 1985, Evaluating liquefaction potential in Ziony, J. I. (ed) Evaluating earthquake hazards in the Los Angeles region--An earth science perspective: U. S. Geological Survey Professional Paper 1360, p. 263-315.

Youd, T. L. and Perkins, D. M., 1978, Mapping liquefaction-induced ground failure potential: Proceedings of the American Society of Civil Engineers, Journal of the Geotechnical Engineering Division, v. 104, no. GT4, p. 433-446.

Propagating Rupture of the Whittier Narrows Earthquake

#14-08-0001-G1801

Ta-liang Teng

Center of Earth Sciences
University of Southern California
Los Angeles, CA 90089-0740
(213) 740-5838

INVESTIGATIONS

Research under this Contract concentrates on using data collected during the Whittier Narrows earthquake for studies on the nature of the source rupture. Theoretical formulation, software development, and extensive inversion of strong motion data are being carried out.

RESULTS

We have completed theoretical formulations and software development, and are in a process in performing extensive data inversion. We have overcome an important numerical difficulty with the inversion of large data sets and large number of model parameters. Typically, this type of inversion problem often involves the inversion of 1000 x 1000 matrices. This not only requires enormous amount of computer time, but also is very unstable numerically because of the ill-behaved matrices for which numerical accuracy is quickly lost as the dimension of the matrix becomes large. We have formulated the inversion by method of recursive processing. This cuts down the dimension of the matrices to about 100 x 100 (i.e., 1% of the original size) and significantly improves both on the speed(by a factor of 50 times) and on the accuracy. Presently, we have prepared strong motion data from different sources. Correction for the site effects is being carried out.

As we are gathering the Whittier Narrows strong motion data, we have also carried out a related research. Recordings from more than 100 free-field strong motion instruments in a region of 100 km x 100 km surrounding the 1987 Whittier Narrows epicenter are used to study the dependence of Richter magnitude on site conditions and local geology. A multitude of sites are involved, including basin sediments of different thickness, unconsolidated alluvium and fluvial deposits, consolidated sedimentary rocks, and basement rocks. The acceleration is integrated to give displacement. Upon an appropriate bandpass filtering, simulated Wood-Anderson records are obtained. M_L values of the Whittier Narrows earthquake are determined for all these free-field strong motion stations. Distribution of these M_L values, which range from 5.35 to 6.92, clearly reflects the site conditions and the local geology: high M_L values outline the deep Los Angeles basin and the San Fernando basin, and low M_L values are found over the Santa Monica Mountains and the San Gabriel Mountains. There is a positive correlation of the M_L value with the basin depth. The source radiation effect on M_L is not apparent perhaps because the Richter magnitude is based on the maximum displacement amplitude instead of the amplitude of the P or S arrival. The propagation path effect on the Richter magnitude is included in the A_0 term given by Richter. At large distance over regions of pronounced lateral inhomogeneity, the A_0 values given by Richter cannot adequately account for the propagation effect and some errors on M_L result. However, the average M_L value (5.95) approaches the published magnitude of 5.9 for the Whittier Narrows earthquake. A better M_L scale should measure the total equivalent energy of the displacement record with an appropriate site correction factor.

REFERENCES

Hauksson, E. and L. M. Jones, The 1987 Whittier Narrows earthquake sequence in Los Angeles, southern California: Seismological and tectonic analysis, J. Geophys. Res., 94, 9569-9590, 1989.

Hauksson, E. and G. V. Saldivar, Seismicity (1973-1986) and active compressional tectonics in the Santa Monica Bay, southern California, J. Geophys. Res., 94, 9591-9606, 1989.

Hauksson, E. and R. S. Stein, The 1987 Whittier Narrows earthquake: a metropolitan shock, J. Geophys. Res., 94, 9545-9547, 1989.

Hauksson, E., Earthquakes, faulting, and stress in the Los Angeles Basin, J. Geophys. Res., 95, 15365-15394, 1990.

Hauksson, E., T. L. Teng, T. L. Henyey, M. Robertson, J. K. McRaney and L. Hsu, Earthquake hazard research in the Los Angeles Basin and its offshore area, Annual Technical Report, submitted to the U.S. Geological Survey, December 1988, 90 pp.

Robertson, M. C. and E. Hauksson, Three-dimensional fine velocity structure of the Los Angeles Basin, Fall AGU meeting, 1989.

Li, S.B. and T.L. Teng, Dependence of Richter magnitude scale on site conditions and local geology, Fall AGU meeting, 1990.

Hisada, Y, S. Yamamoto, S. Tani, and T.L. Teng, Broadband seismograms on the Los Angeles Basin during the 1990 Upland earthquake, Japan seismological Society Fall meeting, 1990.

Teng, T.L. and J. Wang, Analysis of short-period waveform in the Los Angeles basin, Fall AGU meeting, 1990.

Su, F., S. Koyanagi, Y. Zeng, K. Mayeda, T.L. Teng, and K. Aki, A recursive stochastic inversion of site effect using coda waves, Fall AGU meeting, 1990.

A Search for Active Faults in the Willamette Valley, Oregon

14-08-0001-G1522

Robert S. Yeats
Department of Geosciences
Oregon State University
104 Wilkinson Hall
Corvallis, OR 97331-5506
503-737-1226

Investigations

Reconnaissance mapping of the Willamette Valley at 1:100,000 scale has been completed, and the results will be included in a USGS professional paper on earthquake hazards in the Pacific Northwest. Faults and folds deforming late Cenozoic alluvial deposits have been identified.

In July, 1990, a core hole through the alluvial deposits at the intersection of Interstate 5 and the Santiam River was logged by Ken Werner and Tom Popowski of OSU and Dave Weatherbee of USGS. The hole was funded by the Oregon Department of Transportation. The cores, along with those of two earlier holes at Sublimity and Corvallis, are being stored at OSU for future study.

Results

1. Proto-Willamette River and the North Santiam tectonic basin

A structure contour map of the base of unconsolidated late Cenozoic sediments in the southern Willamette Valley resulted in the recognition of the main channel of the proto-Willamette River. Figure 1 shows the subcrop of this channel beneath late Pleistocene outwash gravels of the Rowland Formation. The main channel is filled with sand and gravel deposits in contrast to the rest of the valley which is underlain by fine-grained overbank deposits ("blue clay" of water-well drillers). The overbank deposits are alluvial, not lacustrine as previously believed, as based on the presence of soil zones with rootlets in growth position, wood fragments, and the absence of laminations characteristic of lacustrine sediments.

The main channel, as marked by coarse clastic sediments and a low point in cross-valley profiles, enters the valley near Springfield, as do the present Willamette and McKenzie rivers. However, the channel is east of the present Willamette River. Northeast of Albany, the channel follows the North Santiam River, flowing northeast rather than southwest, as the North Santiam now does, and exits the North Santiam basin via a water gap occupied by an underfit stream, Mill Creek, east of Salem. A second channel underlies the present Willamette River north of Albany and extends west of Salem Hills, and enters the northern Willamette Valley at Salem; however, this channel lacks the coarse clastic deposits of the channel in the North Santiam basin. A subsidiary gravel-filled channel enters the southern Willamette Valley at Lebanon (ancestral South Santiam River).

The longitudinal profile of the base of the ancestral Willamette River channel shows evidence of deformation (Figure 2). The profile rises over the axis of the Harrisburg anticline in the underlying Eugene Formation (Figure 3). The profile also rises across a subsurface southeastern extension of the Salem Hills (Shelburn uplift), drops in the North Santiam basin, and rises across the Waldo Hills in the Mill Creek gap. The North Santiam basin is thereby identified as a tectonic basin, and the hills to the north and south are anticlinal uplifts (Figure 3).

The structure of the North Santiam basin has been mapped using structure contours on the top of the Columbia River Basalt Group (CRBG). This contact is preserved in the subsurface of the North Santiam basin and the Northern Willamette Valley and in the surface beneath volcanic and volcaniclastic rocks of the western Cascades (Sardine Formation). Where the top of the CRBG is not present, as in the Salem Hills and western Waldo Hills, isopachs of the CRBG were used to estimate the altitude of the top of the CRBG based on the known altitude of its base.

As a result, two previously unrecognized faults were mapped: the Mill Creek fault (MCF, Fig. 3) at the southern range front of the Waldo Hills and the Waldo Hills frontal fault on the north, following a prominent northeast-trending lineation. Separation on the Waldo Hills frontal fault decreases northeastward toward the Mt. Angel fault, discussed below.

2. Woodburn earthquakes and the Mt. Angel fault

In August, 1990, six small earthquakes with m_c = 2.0, 2.5, 2.4, 2.2, 2.4, and 1.4 were recorded by the IRIS/OSU broadband seismic station in Corvallis (COR, epicentral distance 68 km) and the Washington Regional Seismograph Network and shown to be located beneath the town of Woodburn in the northern Willamette Valley (Nabelek et al., 1990; Figure 4). Hypocenters are at a depth of about 29 km. These events occurred at the same place as three events in the 1980's with $m_c \leq 1.7$. The similarity of waveforms for the six earthquakes indicates essentially identical locations and mechanisms, so the spread of locations on Figure 4 is probably not real. The preferred composite focal mechanisms indicates right-lateral strike-slip faulting with a small normal component on a plane striking N-S and dipping steeply west.

The location and composite mechanism suggest that the seismicity is related to the Mt. Angel fault which cuts CRBG and overlying alluvial deposits, described in the previous NEHRP summaries of technical reports (Yeats, 1990). The Mt. Angel fault has been considered as part of the Mt. Angel-Gales Creek lineament, although proprietary seismic lines and structure contours on the top of CRBG do not show a connection between the Mt. Angel fault at Woodburn and the Gales Creek fault at Newberg, to the northwest (Figure 5).

The Mt. Angel fault is the southernmost of several zones of seismicity on northwest to north-northwest trending right-lateral faults; other zones include the Portland basin east of the Portland Hills-Clackamas River lineament (Yelin and Patton, preprint) and the St. Helens Seismic Zone (Weaver and Smith, 1983).

References:

Graven, E.P., 1990, Structure and tectonics of the southern Willamette Valley, Oregon: OSU MS thesis, in press.

Nabelek, J., Werner, K., Yeats, R., and Malone, S., 1990, The August, 1990, Woodburn, Oregon earthquake sequence: Constraints from broadband regional recording and geological implications: AGU Pacific Northwest Region Meeting, abstract.

Weaver, C.S., and Smith, S.W., 1983, Regional tectonic and earthquake hazard implications of a crustal fault zone in southwestern Washington: Journal of Geophysical Research, v. 88, p. 10,371-10,383.

Werner, K.S., 1990, I. Direction of maximum horizontal compression in western Oregon determined by borehole breakouts. II. Structure and tectonics of the northern Willamette Valley, Oregon: OSU MS thesis, in press.

Werner, K., Nabelek, J., Yeats, R., and Malone, S., 1990, The Mt. Angel fault: Implications of August, 1990, Woodburn, Oregon earthquake sequence: AGU Fall Meeting, abstract.

Yeats, R.S., 1990, A search for active faults in the Willamette Valley, Oregon, in Jacobson, M.L., compiler, NEHRP Summaries of Technical Reports v. 30, p. 530-536.

Yelin, T.S., and Patton, H.J., 1990, Seismotectonics of the Portland, Oregon region: submitted to Bulletin of the Seismological Society of America.

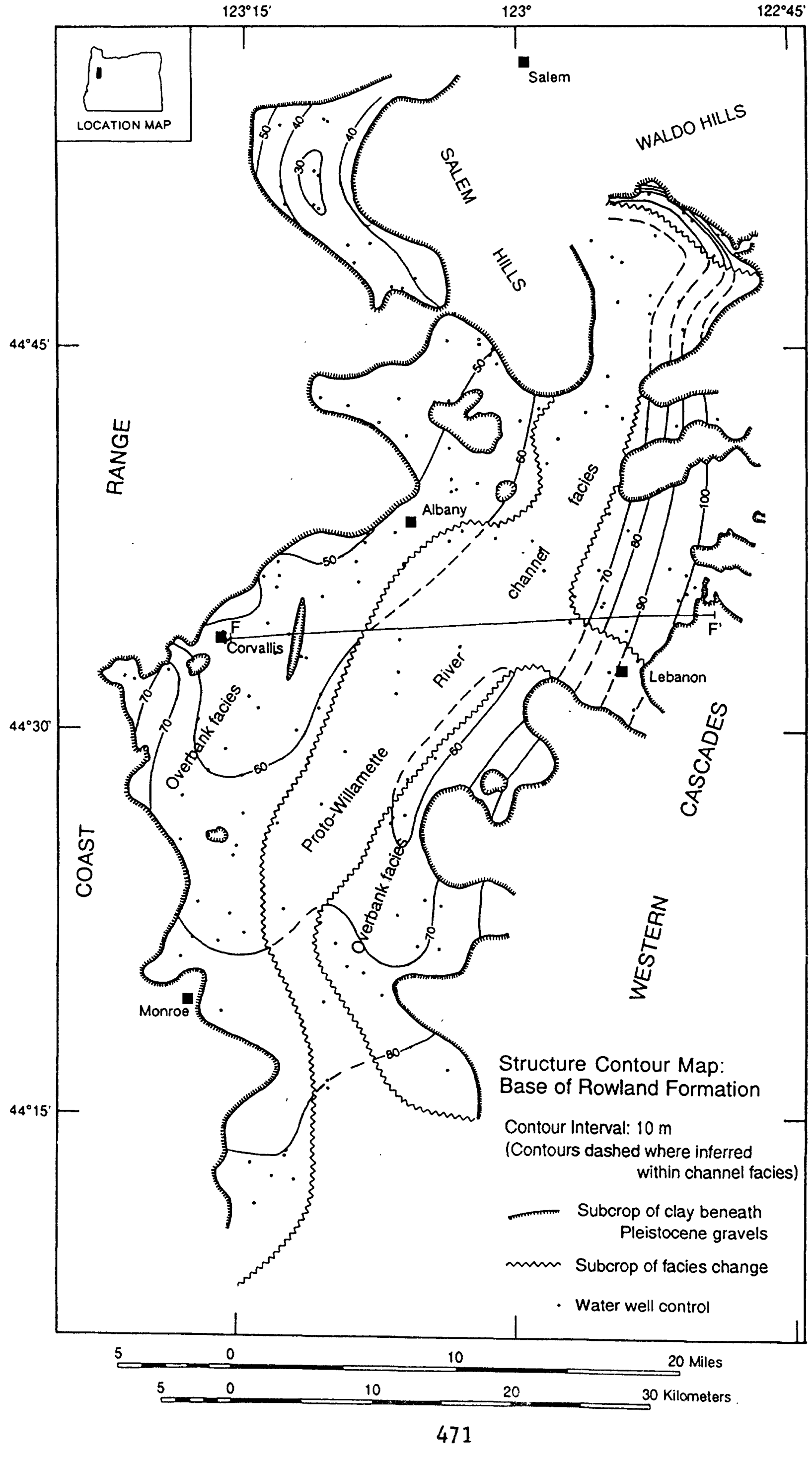

Figure 1. Facies map of pre-late Pleistocene outwash deposits in the southern Willamette Valley showing channel of proto-Willamette River and a side channel at Lebanon of the proto-South Santiam River. Note that channel facies extends east of Salem Hills whereas another channel with predominantly fine-grained sediment fill extends west of Salem Hills, the course of the modern Willamette River.

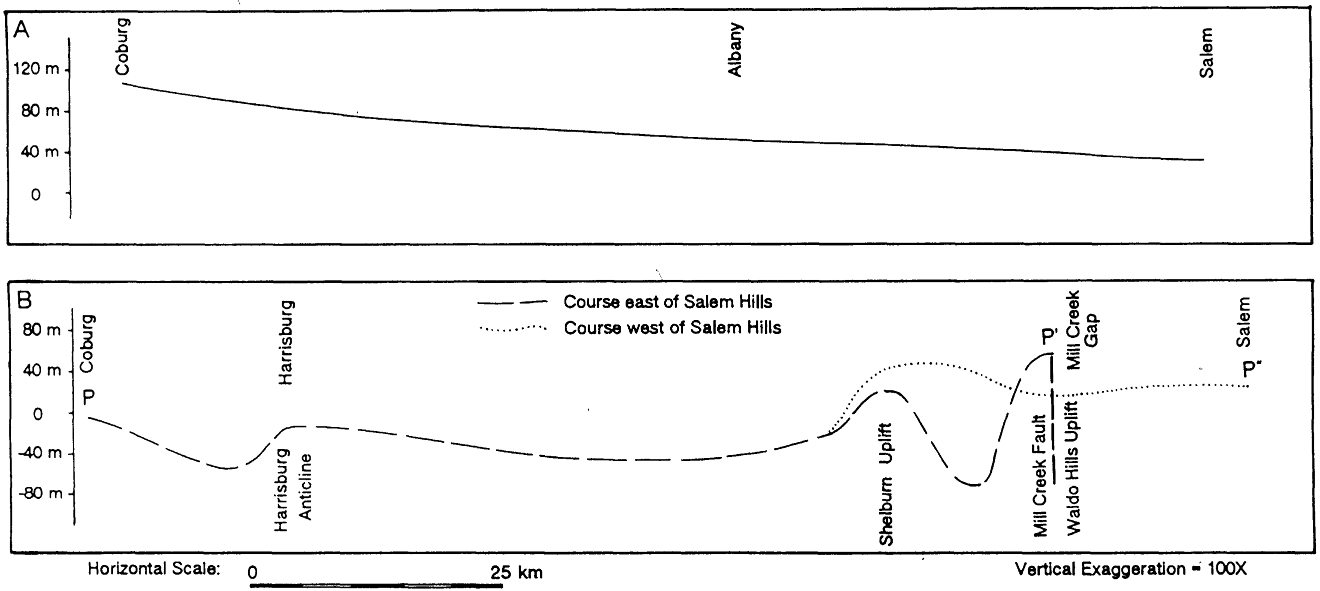

Figure 2. A. Longitudinal profile of modern Willamette River. B. Longitudinal profile of the base of the proto-Willamette River channel. Note deformation at Harrisburg anticline, Shelburn uplift, Waldo Hills uplift, and North Santiam River basin between the Shelburn and Waldo Hills uplift. Channel west of Salem Hills is also upwarped.

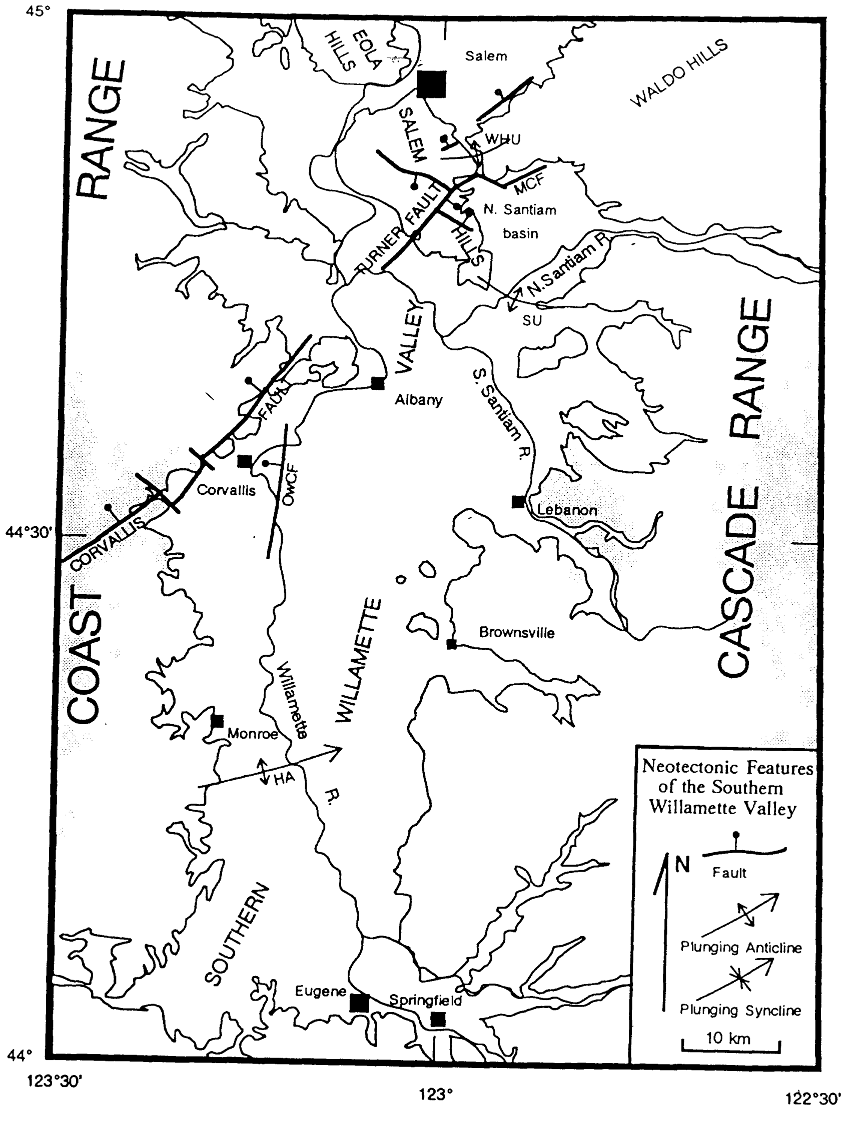

Figure 3. Structures in southern Willamette Valley deforming alluvial sediments of late Cenozoic age. HA, Harrisburg anticline; OwCF, Owl Creek fault; MCF, Mill Creek fault; WHU, Waldo Hills uplift.

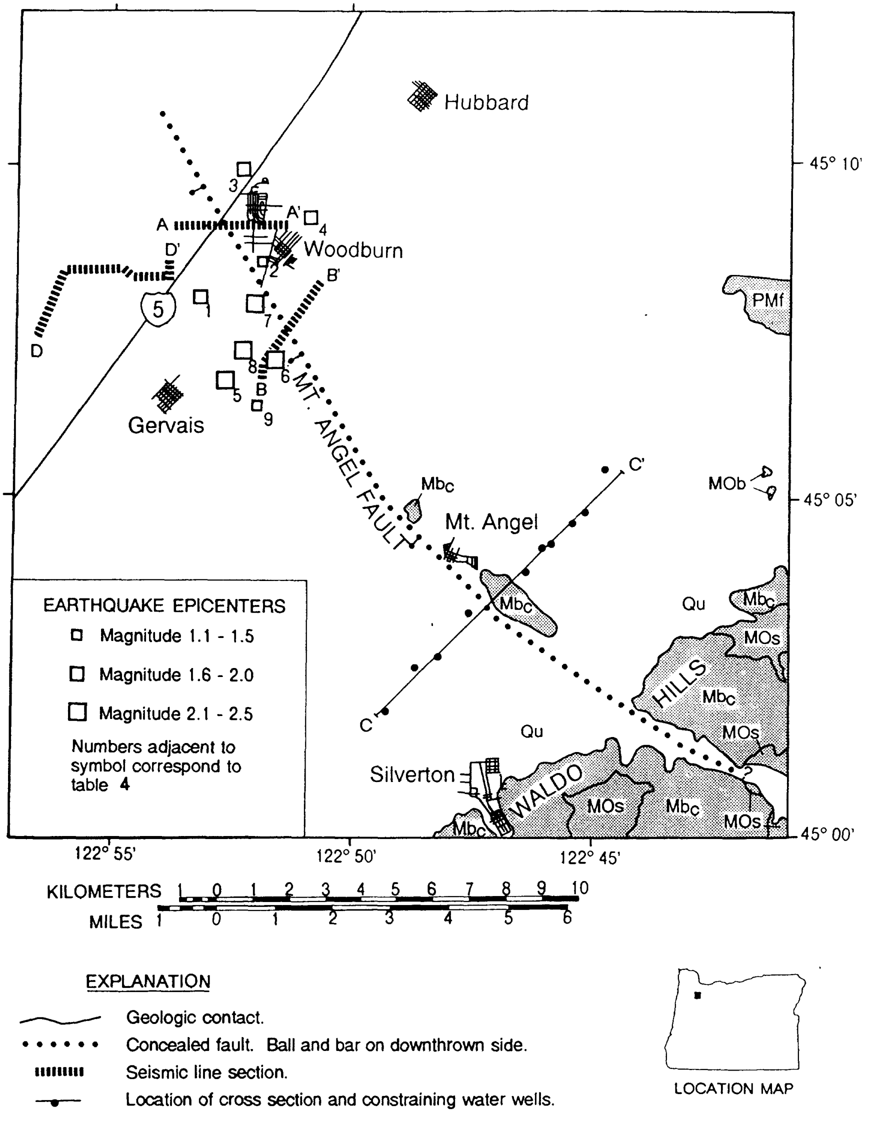

Figure 4. Mt. Angel fault, northern Willamette Valley, showing recent earthquakes near Woodburn. C-C¹ is line of cross section shown by Yeats (1990, p. 534), and B-B¹ locates seismic lines shown by Yeats (1990, p. 535).

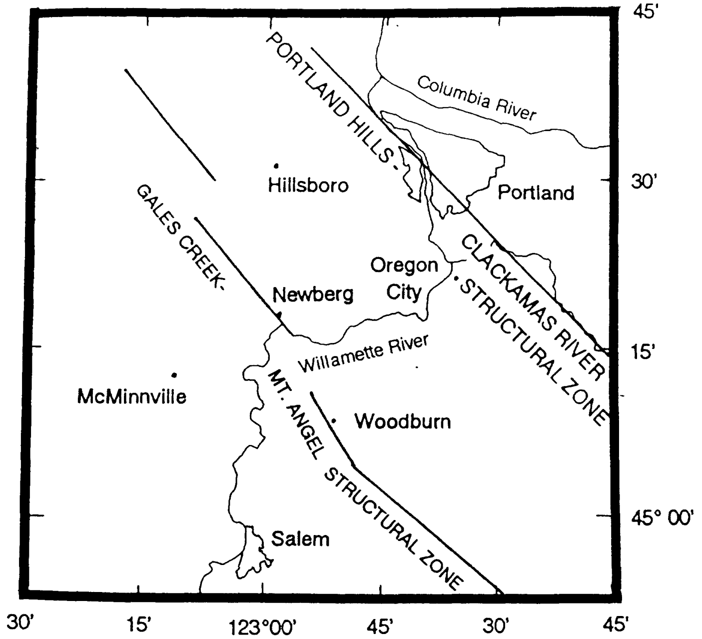

Figure 5. Gales Creek-Mt. Angel structural zone and Portland Hills-Clackamas River structural zone.

Intraplate Stress and Deformation

9930-02669

Mary Lou Zoback
U. S. Geological Survey
Branch of Seismology
345 Middlefield Road, Mail Stop 977
Menlo Park, CA 94025
(415) 329-4760

Investigations

1. Analysis of anomalies in the regional stress field which may be responsible for localizing intraplate seismicity.

2. Continued analysis of dipmeter logs from the Puget Sound and surrounding region. State of stress in the Cascade region is being investigated by analysis of vent alignments on recently published USGS maps of Quaternary volcanic vents. The regional state of stress is being inferred from a combined interpretation of the breakout data, earthquake focal mechanism data and from the vent alignments.

3. Continued compilation and upgrading of a global stress database being maintained at Menlo Park on a commercial database management system, dBase IV.

Results

1. Analyses of tectonic correlations in regions of intraplate seismicity invariably show a correlation with "continental rifts" or crustal zones with a history of extensional tectonics. A localized stress anomaly in the vicinity of a major crustal rift in Brazil, the Paleozoic Amazonas rift suggest a possible source of this correlation. Two moderate earthquakes (mb 5.1-5.5) in central Brazil have occurred in the past 25 years along the northern margin of the E-W trending Amazonas rift. These thrust events indicate N-S compression, a 90° local stress rotation relative to a general E-W maximum horizontal stress observed throughout the rest of the South American plate. The locations of these events and the inferred compression perpendicular to the axis of the rift suggest a causal relationship. Gravity data indicate an enormous (about 100 km wide) lower crustal dense body beneath this rift. Preliminary finite element modeling (with Randy Richardson at Univ. of Arizona) indicate that this dense "rift pillow" is capable of generating a compressive stress field perpendicular to the axis of the rift. Since both gravity and seismic refraction data indicate that lower crustal rift pillows are a common feature of modern and ancient rifts, we plan to extend the modeling to constrain the magnitude of the induced compression and also

to investigate the stress effect for rifts with a variety of orientations with respect to the contemporary regional stress field.

2. The state of stress withing the brittle crust in the Puget Sound basin and surrounding region region is characterized by NNE compression, not NE to ENE compression as would be inferred from convergence (subduction) of the Juan de Fuca plate. While strain may be accumulating on the subduction zone beneath this region, earthquake focal mechanisms (up to 20 km depth), wellbore breakouts (sampling the upper 2-3 km), and Quaternary geologic structures (primarily E-W trending anticlines) are all consistent with the NNE maximum compressive stress direction within the crust. Earthquake hazard related to this NNE compression and ongoing deformation of the upper crust can not be ignored in the assessment of earthquake risk in this region.

3. Currently more than 5000 stress data points reside in the World Stress Map database. Slightly more than half of the data come from earthquake focal mechanisms, roughly 30% come from wellbore breakout analysis, 10% from in-situ stress measurements and 10% from fault slip studies and volcanic vent alignments. The entire database will be release on floppy diskettes by the National Geophysical Data Center (NOAA) in early 1991.

Reports and Publications

Zoback, M. L. and Zoback, M. D., 1989, Tectonic stress field of the continental United States: Geological Society of America Memoir 172, p. 523-539.

Earthquake Loss Estimation of the City of Everett Lifelines

Agreement No. 14-08-0001-G1904

Donald B. Ballantyne
Kennedy/Jenks/Chilton
530 South 336th Street
Federal Way, WA 98003

(206)-874-0555

Introduction

This study is a demonstration project for estimating earthquake economic losses that result from lifeline failure. Lifeline earthquake vulnerability modeling specialists, working together with the lifeline operators in the Everett area, have developed seismic models to determine lifeline vulnerabilities to seismic hazards. Three earthquake events, representative of the Everett area, will be defined and the corresponding hazard levels will be estimated for the Everett vicinity. Based upon the seismic hazards and lifeline vulnerability models, lifeline responses to each of the three earthquake events will be estimated. Then, economic loss predictions to the Everett business community will be made. The loss predictions will include lifeline repair costs and loss of business opportunity costs incurred by both the lifeline operators and the community served by the lifelines. Predictions will be made for individual lifeline system failure effects and the effect of combined lifeline system outages. Additionally, loss mitigation recommendations will be made to the lifeline operators.

Everett Geography and Seismicity

Everett has been chosen as the study area because Everett's size and location and the recent interest in the seismicity of the Puget Sound area. Located about 20 miles north of Seattle, Everett's population is about 70,000. As shown by the map in Figure 1, Everett is bounded on the west by the Possession Sound and on the north and east by the Snohomish River. The limited number of lifeline paths into Everett provide for relatively simple lifeline models. Although the lifeline models are straight forward, Everett's moderate size allows the models to be representative of lifeline facilities in larger cities.

The two best documented earthquakes in the Puget Sound area occurred in 1949 and 1965 with respective magnitudes of 7.1 and 6.5. Both of these earthquakes occurred at depths of more than 50 kilometers beneath the Puget Sound region in the Juan de Fuca Plate. Recently, attention has also focused on the potential for large subduction earthquakes about 100 kilometers west of the Puget Sound area at the boundary between the overlying North American Plate and the Juan de Fuca Plate. Although large shallow earthquakes have occurred in the Cascade mountain range east of the Puget Sound region, a consensus has not been reached on the likelihood of large shallow earthquakes in the Puget Sound region.

For deep events in the San Juan de Fuca plate, return periods of 10, 35 and 110 years have been estimated for magnitude 6.0, 6.5 and 7.0 earthquakes. Return

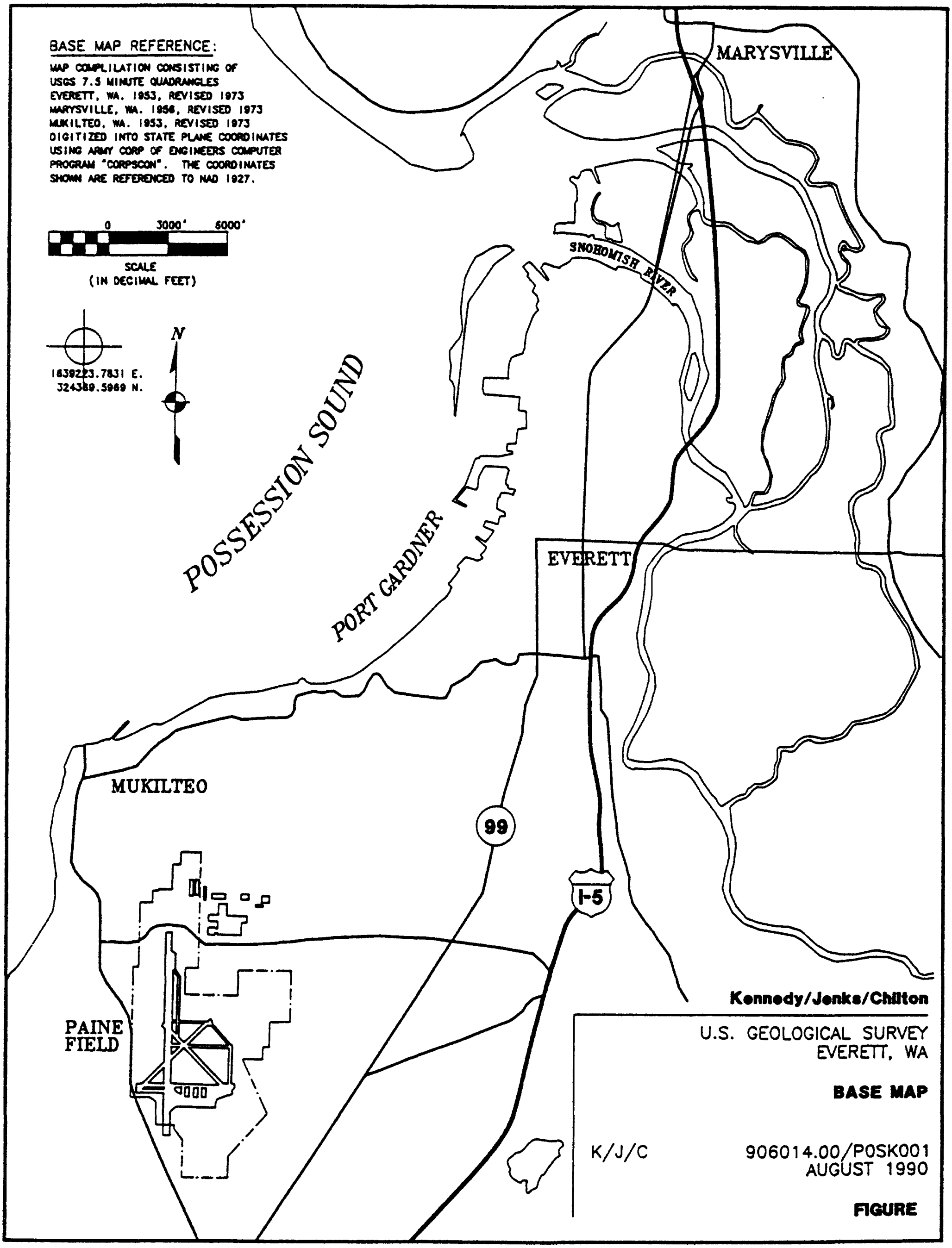

Figure 1. Everett Map

periods from about 300 to 1000 years have been estimated for subduction events west of the Puget Sound area which could exceed magnitude 8.0.

Everett Lifelines

There are six different lifeline categories: power, transportation, water, sewer, natural gas and communications. Power is provided by the Snohomish County Public Utilities District. Power is generated at the Bonneville Dam, located on the Columbia River, about 250 kilometers south of Everett. Because the power system in Everett is basically a distribution system, it is expected that the power system in Everett will be relatively resilient to earthquake hazards.

Because Everett is bordered on the west by the Possession Sound, there is not any access to Everett from the west. The Snohomish River limits northern and eastern access to and from Everett to Interstate 5 and Highway 529 on the north and Highway 2 to the east. Because the Snohomish River forms a delta with potential poor soil conditions in the regions to the north and east of Everett, the transportation routes through these regions may be vulnerable to earthquake generated hazards. Everett can be accessed from the south by either Interstate 5, Highway 99 or by one of several surface streets.

Everett's water is obtained from Lake Chaplain, a man made lake about 30 kilometers east of Everett. The water is treated at a treatment plant immediately south of Lake Chaplain and then piped through one of four transmission pipes into Everett. For many of the water service zones, there are redundant transmission sources. However, for the higher service zones, the Evergreen Way pump station is a key system component. The main transmission lines from the water treatment plant at Lake Chaplain are also critical system components.

In addition to providing water, the City of Everett Public Works Department also is responsible for wastewater treatment. The wastewater treatment plant is located in the northeast part of Everett on the eastern bank of the Snohomish River. Although there are a few key pump stations, such a pump station just west of the treatment plant, the wastewater collection system is mainly gravity fed.

Natural gas in piped into Everett from Northwest Pipelines in Clearview, Washington by Washington Natural Gas. The supply main is a 12 inch diameter welded steel pipe constructed in the 1950's. Flow is controlled throughout the Everett distribution network with regulator stations. All high pressure lines are either welded steel or plastic. The low pressure lines, some of which are still cast iron, are gradually being replaced by either welded steel or plastic pipe.

The primary local phone service provider in Everett is GTE. Long distance calls are distributed from central offices to the appropriate long distance provider's POP ("Point of Presence"). There are several alternate routes between adjacent US West Communications and GTE's Everett service area.

Everett Economy

The two major industrial complexes are Boeing's 747 assembly plant and a Scott Paper mill. Both Boeing and Scott are participating in the study and will provide estimates as to how lifeline outages would affect their operations.

Using the information provided by Boeing and Scott, in conjunction with specific economic data from the lifeline operators and general economic data obtained from various governmental sources, the economic impact for the entire Everett business community will be estimated in monetary terms.

Project Completion

It is anticipated that the project's results and findings will be completed in early 1991.

Frequency and Survivability Profiles of Highway Bridges Along the I-5 Corridor Between Everett, Washington and Salem, Oregon

14-08-0001-G1698

Prof. Ralph Alan Dusseau, Ph.D., P.E.
Wayne State University
5050 Cass, 1064 Mackenzie Hall
Detroit, Michigan 48202
(313) 577-3842

Objectives

The objectives during the second year of this project were to perform field ambient vibration measurements and laboratory data analyses on 30 to 50 typical highway bridge spans along interstate highways I-5, I-205, and I-405 between Everett, Washington and Salem, Oregon. The purpose was to determine the fundamental frequencies and to estimate the modes of vibration for a representative sample of bridge spans along these interstate highways.

Bridge Spans Analyzed

The bridge spans that were analyzed were chosen to reflect, as closely as possible, the actual distribution of bridge span type and length for the 1,000 bridges along I-5, I-205, and I-405 in western Washington State and northwestern Oregon. The 53 bridge spans that were analyzed are summarized in Table 1. These spans included 2 steel girder spans, 2 reinforced concrete T-beam spans, 9 reinforced concrete slab spans, 19 reinforced concrete box-girder spans, and 21 prestressed concrete girder spans. For safety reasons, only underpasses with wide sidewalks were chosen for field ambient vibration measurements. The traffic along I-5, I-205, and I-405 was deemed to be to heavy to permit safe measurements on highway overpasses. Wide sidewalks were necessary to facilitate safe access to the bridge span without disruption of vehicular traffic.

Field Measurements

For each bridge span that was analyzed, field ambient vibration measurements were taken using eight signal transducers: six seismometers and two accelerometers. The signal output from these eight transducers was amplified and then recorded on an FM tape recorder. For safety reasons, all transducers were placed on the bridge sidewalks. The initial configurations of these transducers were as shown in Fig. 1a for each bridge span. Because the vertical direction was assumed to be the most flexible for each bridge span, three seismometers were oriented in that direction with one at midspan, one at a quarter point, and one at a support. In order to cover the full range of potential bridge frequencies in the vertical direction, the two accelerometers were also oriented in the vertical direction with one at midspan and one at the quarter point. Two seismometers were oriented in the transverse direction with one at midspan and one at the quarter point. The longitudinal direction was assumed to be the least flexible and only one seismometer (located at midspan) was oriented in the longitudinal direction. After completing the measurements on the 21 prestressed concrete girder spans, the configuration of the accelerometers was changed as shown in Fig. 1b.

Preliminary laboratory analyses of the prestressed concrete girder data indicated very little difference between the signal outputs of the vertical seismometers and accelerometers. Thus the accelerometers were moved (as depicted in Fig. 1b) to the support (with one oriented in the transverse direction and one in the longitudinal direction) to obtain new information on the bridge span responses at this location.

Laboratory Data Analyses

Laboratory analyses of the data recorded in the field are currently being conducted. In these analyses, the recorded signal output from each transducer is played back through a spectrum analyzer and a fast Fourier transformation (FFT) is performed. The final results are plots of signal amplitude versus frequency from which the frequencies of the bridge span at the given location and in the given direction can be read directly. These analyses also include comparisons of phase and coherence between pairs of transducer signals. These comparisons aid in estimating the mode shape associated with each fundamental frequency. The final results of these laboratory data analyses will be presented in the April 1991 Summary of Technical Reports.

TABLE 1. BRIDGE SPANS MEASURED AND ANALYZED UNDER AMBIENT VIBRATION LOADING

BRIDGE TYPE	BRIDGE NUMBER	BRIDGE NAME	BRIDGE LENGTH, feet	TOTAL NO. SPANS	SPAN NO.	SPAN LENGTH, feet
Steel Girder	5/526.1	STEEL HILL U-XING	644.00	6	1	61.50
					2	155.00
Reinforced Concrete T-Beam	5/413	BERKELEY STREET U-XING	99.00	2	1	49.50
					2	49.50
Reinforced Concrete Slab	5/417	CLOVER CREEK	68.80	3	1	20.90
					3	20.90
					2	27.00
	5/428	S 56TH STREET U-XING	204.00	4	1	45.00
					4	45.00
					2	57.00
					3	57.00
	5/425	S 84TH STREET U-XING	140.75	2	1	70.38
					2	70.38

TABLE 1. (continued)

BRIDGE TYPE	BRIDGE NUMBER	BRIDGE NAME	BRIDGE LENGTH, feet	TOTAL NO. SPANS	SPAN NO.	SPAN LENGTH, feet
Reinforced Concrete Box-Girder	5/596	NE 185TH STREET U-XING	249.66	4	4	45.00
					1	54.00
	5/418	BRIDGEPORT WAY U-XING	293.56	4	1	59.28
					4	59.28
	405/17	BENSON ROAD U-XING	276.92	4	1	60.46
	5/419	CARLYLE ROAD U-XING	317.00	4	4	68.00
	5/596	NE 185TH STREET U-XING	249.66	4	2	75.33
					3	75.33
	405/57 S	NE 124TH STREET U-XING	442.00	4	4	78.00
	405/17	BENSON ROAD U-XING	276.92	4	2	78.00
					3	78.00
	5/418	BRIDGEPORT WAY U-XING	293.56	4	2	87.50
					3	87.50
	5/419	CARLYLE ROAD U-XING	317.00	4	3	90.50
	405/50 N	NE 72ND PLACE U-XING	417.62	4	3	97.81
	405/50 S	NE 72ND PLACE U-XING	429.40	4	3	102.70
	405/50 N	NE 72ND PLACE U-XING	417.62	4	4	111.00
	405/50 S	NE 72ND PLACE U-XING	429.40	4	4	112.00
	405/57 S	NE 124TH STREET U-XING	442.00	4	3	143.00

TABLE 1. (continued)

BRIDGE TYPE	BRIDGE NUMBER	BRIDGE NAME	BRIDGE LENGTH, feet	TOTAL NO. SPANS	SPAN NO.	SPAN LENGTH, feet
Prestressed Concrete Girder	5/457	PORT OF TACOMA RD UC	297.75	4	1	40.91
	5/630	41ST STREET U-XING	260.00	4	4	42.50
	405/42	MAIN STREET U-XING	260.00	3	3	52.00
	5/457	PORT OF TACOMA RD UC	297.75	4	4	54.84
	5/615	164TH ST S W U-XING	322.50	4	1	55.50
	5/605	220TH ST S W U-XING	337.90	4	1	55.98
	5/602	236TH ST S W U-XING	318.50	4	4	60.00
	5/615	164TH ST S W U-XING	322.50	4	4	67.00
	405/42.5	NE 4TH STREET U-XING	136.76	2	1	68.38
					2	68.38
	5/630	41ST STREET U-XING	260.00	4	3	73.50
	5/602	236TH ST S W U-XING	318.50	4	1	74.50
	5/605	220TH ST S W U-XING	337.90	4	4	77.97
	5/602	236TH ST S W U-XING	318.50	4	2	92.00
	405/42	MAIN STREET U-XING	260.00	3	1	93.50
	5/615	164TH ST S W U-XING	322.50	4	2	100.00
	5/457	PORT OF TACOMA RD UC	297.75	4	2	101.00
	5/605	220TH ST S W U-XING	337.90	4	2	101.98
	5/656	MARSHALL ROAD U-XING	217.00	2	1	108.50
					2	108.50
	405/42	MAIN STREET U-XING	260.00	3	2	114.50

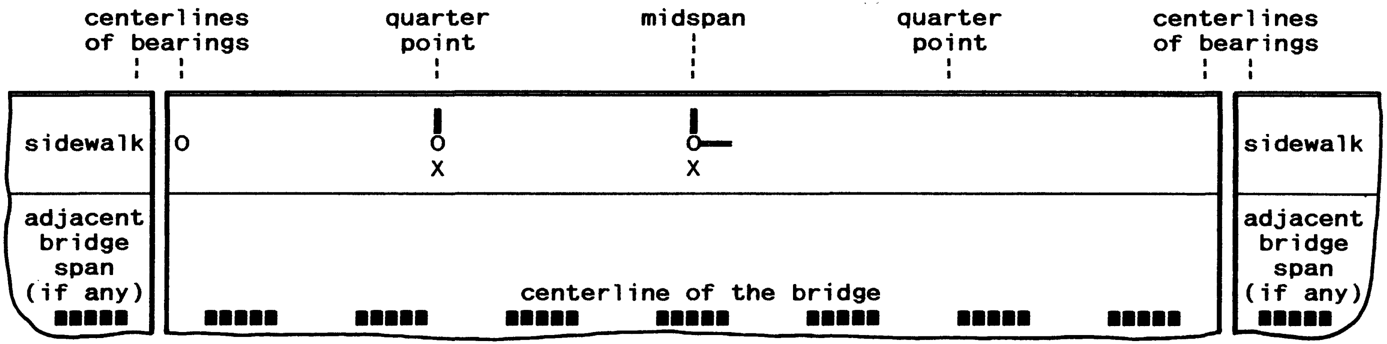

a. Initial Configuration

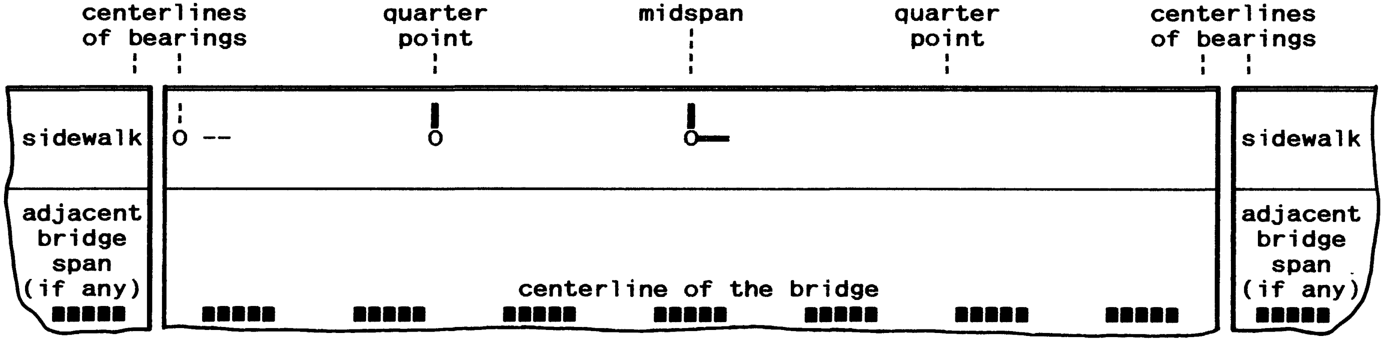

b. Revised Configuration

Legend:

O	vertical seismometer	X	vertical accelerometer
═	longitudinal seismometer	¦	longitudinal accelerometer
▌	transverse seismometer	--	vertical accelerometer

FIGURE 1. PLAN VIEW OF BRIDGE DECK SHOWING CONFIGURATIONS OF MEASUREMENT TRANSDUCERS

LATE QUATERNARY FAULTING, SOUTHERN SAN ANDREAS FAULT

9910-04098

Michael J. Rymer

Branch of Engineering Seismology and Geology
U.S. Geological Survey
345 Middlefield Road, MS/977
Menlo Park, CA 94025
(415) 329-5649

Investigations

1. Monitoring nail quadrilaterals after the 1989 Loma Prieta earthquake.

2. Continued investigation of the Quaternary history of the San Andreas fault in the Coachella Valley, with special emphasis on structure and stratigraphy.

Results

1. Data recorded at small-aperture nail quadrilaterals across both the San Andreas fault and newly formed dominantly extensional cracks to the southwest of the fault were reanalyzed using programs and generous help of M. Lisowski. The new analyses, using a variation-of-coordinants procedure, result in slightly different amounts of fault/crack motions than reported in the last semi-annual technical report. The two sites on the San Andreas fault, near the southeast and northwest ends of the aftershock zone, both showed about 5±2 mm of right-lateral component of postseismic slip; sites across dominantly extensional cracks in the Summit Road area showed from 4 to 10±2 mm of left-lateral component of postseismic slip. However, these new afterslip values do not change the basic conclusion that the lack of tectonic coseismic surface rupture associated with the Loma Prieta earthquake was not followed by large postseismic slip.

2. Paleomagnetic samples were run through a cryogenic magnetometer by J. Boley for analysis of magnetostratigraphy and study of tectonic rotations in the Indio Hills. Analysed samples are from sites in the southeast and central parts of the Indio Hills. The two sites were reported on in 1987 from preliminary data sets (Rymer, Boley, and Weldon, EOS, v. 87, p. 1507). The new data sets give a greater number of sample locations for both sites and extend the stratigraphic range of the southeastern section. Preliminary checks of the data indicate that the inferred tectonic rotations reported in 1987 are valid. Furthermore, the extended stratigraphic range of the southeastern section indicates at least one magnetic reversal within the Matayama revered chron that will aid in more precise determination of stratigraphic age of the deposits.

Reports

Rymer, M.J., 1990, Near-fault measurement of postseismic slip associated with the 1989 Loma Prieta, California, earthquake: Geophysical Research Letters, v. 17, no. 10, p. 1789–1792.

INVENTORY AND POST-EARTHQUAKE FUNCTIONALITY OF EMERGENCY RESPONSE RESOURCES: FIRE SERVICE OPERATIONS IN THE PUGET SOUND AREA

Award Number 14-08-0001-G1693

Charles Scawthorn, S.E.
EQE Engineering, Inc.
595 Market Street
San Francisco, CA 94105
(415) 495-5500

and

Jane Preuss, Urban Regional Research, Seattle, WA 98101
Kevin Coppersmith, Geomatrix, San Francisco CA 941105

Objective. This is the second of a three part program to estimate post-earthquake emergency response demand and capacity in the Puget Sound Area. Year One developed estimates of damage to fire stations within urban portions of the Puget Sound area. Estimated impacts on post-earthquake functionality of the Puget Sound area's fire service were made, particularly vulnerable facilities which might be cost-effectively upgraded were identified, and a methodology for application elsewhere were developed. Year Two's objective is to estimate post-earthquake emergency response demand in the Puget Sound Area. The focus is upon the City of Seattle to (1) utilize seismic hazard information, (2) select a Pilot Project Area and inventory a high-hazard class of building, and (3) based on the inventory, select several examples of this building class and develop vulnerability functions for estimation of damage and collapse. Lastly, (4) estimate damage for this high-hazard building class.

YEAR ONE RESULTS

Post-Earthquake Functionality. Historically, damage to stations and other critical facilities has impaired post-earthquake functionality. Fire stations have sustained damage in the 1906 San Francisco, 1925 Santa Barbara, 1933 Long Beach, 1964 Alaska, 1971 San Fernando, 1983 Coalinga, 1984 Morgan Hill, and 1989 Loma Prieta (San Francisco) earthquakes. The 1987 Whittier earthquake resulted in demolition orders for two fire stations (just as two were demolished following the 1983 Coalinga earthquake). Unless specially reinforced, the large open ground/floor apparatus areas and doors make fire stations, as a structural type particularly vulnerable, to lateral forces. Prior to 1976, the Uniform Building Code did not identify fire stations as requiring special reinforcement for earthquake forces. A survey of fire stations in the Puget Sound Region indicates a large number of older fire station structures (Figure 1). Facilities were cataloged, and rated as to their seismic vulnerability. Utilizing the estimated ground motions at each site due to specific scenario earthquake events, damage and likely loss of functionality of the fire service, the residual capacity has been estimated, as displayed in Figure 2.

Particularly Vulnerable Facilities. Based upon the results of the inventory process, there are a few areas where relativley high concentrations of severe impacts indicate further engineering review to determine if seismic retrofit action is required. These areas are downtown Seattle, and downtown Tacoma, and are depicted in Figure 2.

General Methodology. A general methodology which can be used as a preliminary assessment tool for ascertaining the general vulnerability of a particular fire station to earthquake damage has been developed. The survey form has been adapted from the *ATC-21 Rapid Visual Screening of Buildings for potential Seismic Hazards: A Handbook*, and *ATC-22 A Handbook for Seismic Evaluation of Existing Buildings*, and is intended for use by non-engineers. For regions of relatively low-seismicity, the ground motion parameters are estimated based upon the *1988 edition of NEHRP Recommended Provisions for the Development of Seismic Regulations for New Buildings.* This methodology can be used by fire departments throughout the U.S. as a first order method to estimate the need for a seismic retrofit program.

YEAR TWO

Earthquake Hazards Map. In year two, the project focuses on the city of Seattle, in a program to synthesize available seismic hazard information for shaking, liquefaction, landslide, tsunami and seiche, and building vulnerability into an earthquake hazards map. A mapping in the San Francisco Bay Area, by the Association of Bay Area Governments (ABAG, 1987) has proved to very useful to local governments, and a similar synthesis is needed in the Seattle Area.

Pilot Project Area. Based upon the results of this mapping, a Pilot Project Area will be selected, and one high-hazard class of building inventoried (a reinforced Concrete mid-rise building is the preliminary choice). Even relatively new but non-ductile reinforced concrete (RC) buildings can sustain severe damage, as illustrated by the near-collapse and total loss of the Olive View hospital in the 1971 San Fernando event, or the similar great damage to the County Services Building in the 1979 Imperial Valley event. Thus, buildings of relatively "modern" vintage (ie, 1960's or '70's) as well as buildings of the inter-war years, may still be seismically very vulnerable. The Pioneer Square/Duwamish/West Seattle area, an industrial area in south central Seattle, is the preliminary Pilot Project Area, to be confirmed in the initial stages of the project. Vulnerability functions of this building class are being developed using techniques previously developed by the Principal Investigator.

Damage Estimation in Pilot Project Area. Using the vulnerability functions developed, an estimate will be made as to the damage in the Pilot Project Area, for this high-hazard building class.

Implications of Results. The projected third year of this study would extend the methods and findings of the Pilot Project Area to the majority of the city of Seattle, to provide an estimate of building damage and collapse. This damage estimate, including the demands for fire and trapped victim response, would form the basis for estimation of emergency response demand. This would be compared against post-earthquake functionality (the first year findings) to determine the net shortfall in emergency response, for a major Puget Sound earthquake.

Year Built of Fire Stations Inventoried
Puget Sound Urban Areas (64 Stations)

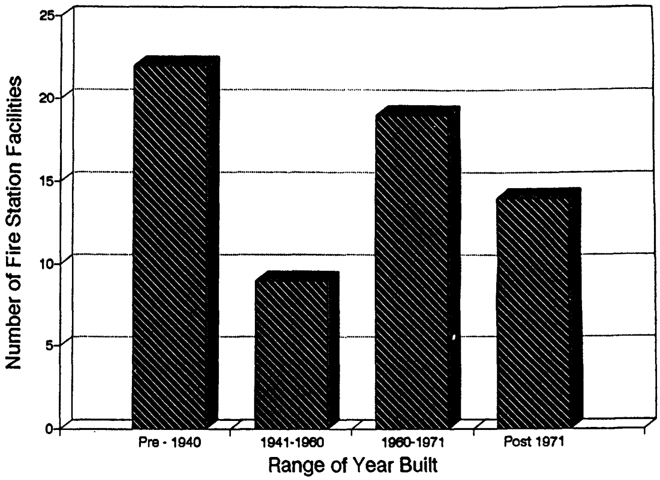

Breakdown By Structural System
Puget Sound Urban Areas (64 Stations)

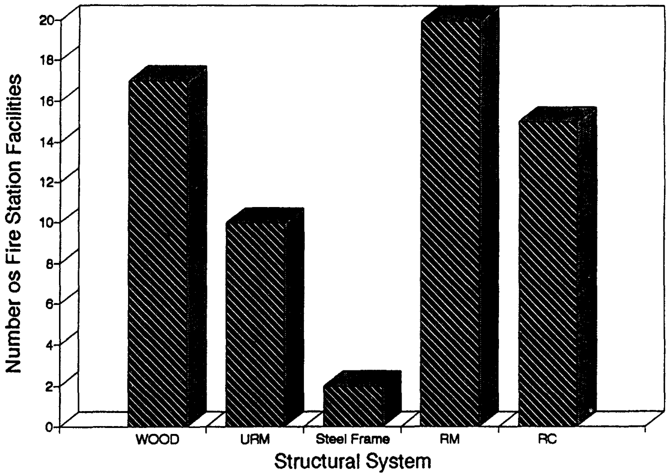

Figure 1

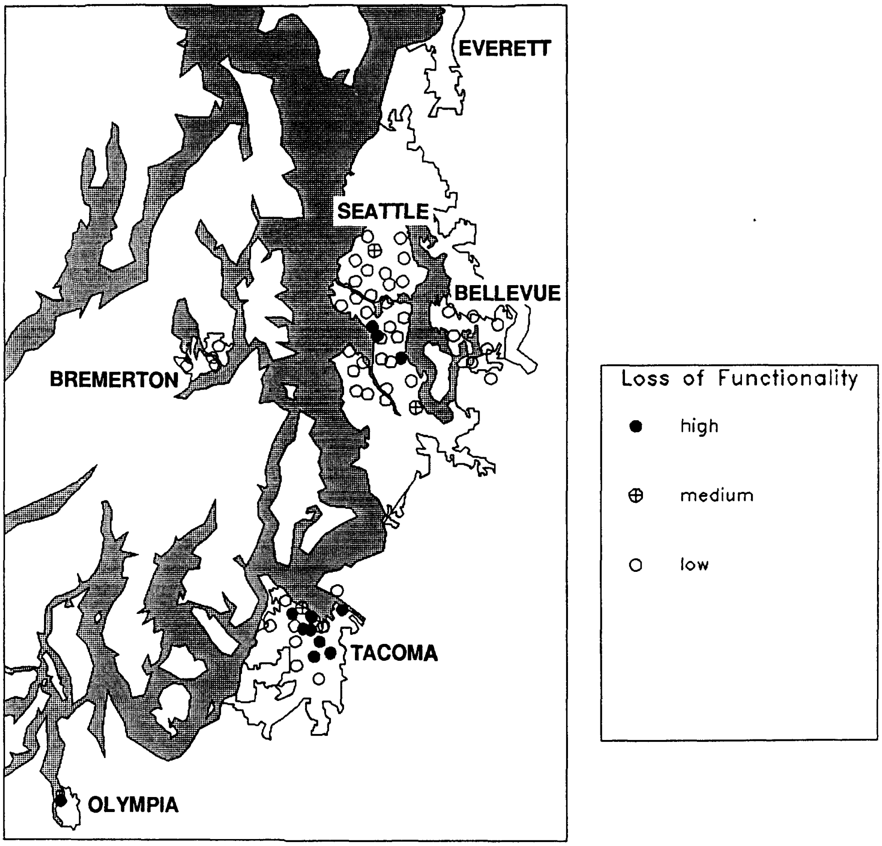

Figure 2: Functionality of Fire stations following scenario M_W 7 $^1/_2$ Earthquake near Seattle

Wasatch Front and Intraplate Recurrence

9910-04102

David P. Schwartz
Branch of Engineering Seismology anf Geology
U. S. Geological Survey
345 Middlefield Road, MS 977
Menlo Park , CA 94025
(415) 329-5651

Investigations

The objective of the project is to define earthquake recurrence models for intraplate extensional environments. Work focuses on evaluating the degree to which recurrence on fault segments is time dependent or Poisson, quantifying periods of quiescence between active cycles on faults, and evaluating temporal clustering on adjacent fault segments during active cycles. This information forms the basis for formulating approaches for long-term forecasting, including probabilistic analysis, of intraplate normal faults.

Results

Available Wasatch fault zone (WFZ) paleoseismologic data for the past 6 ka have been used to estimate 50- and 100-year Poisson and time-dependent probabilities for a M 7 earthquake along the WFZ. Five of the six active fault segments have produced M 7 events during an earthquake sequence that began about 1.4 ka and has continued to about 300 years ago. Only the Brigham City segment, with an elapsed time of 3.6 ka, has not had an event during this most recent temporal cluster. The occurrence of 15 to 17 M 7 events during the past 6 ka, yields 50- and 100-year Poisson probabilities (P_{50} and P_{100}) of 0.12-0.13 and 0.22-0.25, respectively, for an event anywhere along the WFZ. Within the current active sequence the average repeat time of 183-220 years (5-6 events in 1.1 ka) and the 75-400 interval between successive events yields Poisson probabilities of P_{50} 0.16-0.24 and P_{100} 0.29-0.42. Poisson probabilities provide no information on the location of the next WFZ event. Time-dependent conditional probabilities are based on the geologic behavior of individual fault segments. For some segments (Salt Lake, Provo), ^{14}C estimates of repeat times are quasi-periodic and proportional to slip per event and the long-term slip rate (about 1 mm/yr). Other segments (Brigham City, Nephi, Weber(?)) appear to release accumulated slip in two relatively closely spaced (<1 ka) earthquakes followed by longer intervals. Therefore, no one single recurrence model appears to be appropriate for all segments. The most recent faulting episode on the Brigham City segment occurred as two events, 3.6 +/-0.25 and 4.8 +/-0.25 ka ago, with 1.5-2 m slip per event. The direct recurrence time estimate is 3-4 ka per episode (3-4m/ (1 mm/yr)) and the 50- and 100-year conditional probabilities are 0.03 and 0.07, respectively. For comparison, 100 year probabilities for the other Wasatch segments, based on their segment-specific recurrence times, are less than 0.02. Rupture of the Brigham City segment would complete the current active sequence along the WFZ.

Reports

Nishenko, S.P. and Schwartz, D.P., Preliminary estimates of large earthquake probabilities along the Wasatch fault zone, Utah (abs): Submitted to Fall 1990 AGU.

Fault Segmentation: San Andreas Fault System

9910-03983

David P. Schwartz, Thomas E. Fumal, Karin E. Budding, and Ray J. Weldon
Branch of Engineering Seismology and Geology
U. S. Geological Survey
345 Middlefield Road, MS 977
Menlo Park , CA 94025
(415) 329-5651

Investigations

The objective of the project is to quantify the behavior of the San Andreas fault between Tejon Pass and San Bernadino, and in the Santa Cruz mountains, and of the Rodgers Creek fault, with regard to segmentation, recurrence, slip rate, and slip per event. These parameters form the basis for long-term earthquake forecasting.

Results

1. San Andreas fault-Wrightwood, CA. a) Four trenches were excavated during June and July, 1990. These were extensions of deep trenches originally excavated across the secondary fault zone at the site in 1988. and allowed us to trace and correlate deep stratigraphic units between the main and secondary fault zones. b) Digitizing of all trench logs made to date has been initiated This will enable us to retrodeform the faulted and folded stratigraphic sequence and place tighter structural and stratigraphic constraints on the approximately twelve events that we have tentatively identified for the past 1300 years of record at this site. c) High-precision radiocarbon dates from the University of Washington have been obtained for the upper four peats at the site. The ages of these peats bracket the third and fourth most recent events at Wrightwood. Using the new dates and the historical record, our best estimates of the timing of the four most recent events at Wrightwood are: AD 1857, 1812, 1670-1720, and 1525-1630. These differ from the earthquake chronology at Pallett Creek, 25 km to the north, reported by Sieh and others (1989). Our dates suggest a more regular recurrence, with interevent times of less than 200 years.

2. San Andres fault-Santa Cruz mountains. Investigations have continued on the comparison between 1906 and 1989 surface fracturing. We have studied the accounts of 1906 faulting, the geomorphology of the fault zone, and a trench across the fault. 1906 fracturing between Lexington Reservoir and San Juan Bautista was poorly described; no documented right lateral surface faulting along this fault segment was reported, and it is unclear whether any occurred. However, analysis of aerial photographs asnd surface mapping show that, except for a 6-km-long section of the fault across landslide-controlled slopes west of Los Gatos Creek, the San Andreas fault zone has a well-defined, geomorphically young surface trace through the Santa Cruz mountains. Trenching near the south end of the 1989 aftershock zone exposed displaced late Holocene ponded alluvial deposits. The San Andreas fault zone in the Santa Cruz mountains appears to be characterized by features that indicate recent, repeated strike-slip surface faulting in contrast to 1989. If the Loma Prieta event occurred occurred on a rupture surface continuous with the surface trace, downdip segmentation and a variable mode of strain release (deep and shallow) are required. Alternatively, the source of the 1989 event may not have been the main San Andreas fault.

3. Rodgers Creek fault zone. Seismicity data show a seismic gap along the Rodgers Creek fault between Santa Rosa and San Pablo Bay. Initial results of paleoseismic investigations within the gap, using offset channels in late Holocene deposits as piercing points, indicate a *minimum* slip rate of 2.1 to 5.8 mm/yr for the past 1300 years. The preferred range for the *maximum* recurrence interval is 248 to 679 years. A debris flow and gully at the site have been offset 2 +0.3, -0.2 m during the most recent event. Historical seismicity data indicate a *minimum* elapsed time of 182 years since the most recent event. Ten new charcoal samples from trenches excavated in April 1990 have been submitted for accelerator mass spectrometry dating.

Reports

Budding, K.E., Schwartz, D.P., and Oppenheimer, D. H., Slip, rate, earthquake recurrence, and seismogenic potential of the Rodgers Creek fault zone, northern California: initial results (submited to Geophysical Research Letters, August, 1990).

Fumal, T. E., Weldon, R.J., and Schwartz, D.P., 1990, Recurrence of large earthquakes along the San Andreas fault at Wrightwood, California (abs): Seismological Research

Letters, v. 61, no.1, p. 44.

Schwartz, D.P., and Prentice, C. S. 1990, Surface fractures in the Loma Prieta area, CA: 1906 and 1989 (abs): Seismological Research Letters, v.1 no.1, p.16.

Schwartz, D.P. and Ponti, D.J. (editors), 1990, Field guide to neotectonics of the San Andreas fault system, Santa Cruz mountains, in light of the 1989 Loma Prieta earthquake: U. S. Geological Survey Open-File Report 90-274, 38 pp.

Earthquake Hazards Studies, Metropolitan Los Angeles-Western Transverse Ranges Region

9540-02907

R. F. Yerkes
Branch of Western Regional Geology
345 Middlefield Road MS 975
Menlo Park, CA 94025

Investigations and results

1. Historic earthquakes (W. H. K. Lee and Yerkes). This work recessed in favor of (2) below.

2. Geologic studies (P. K. Showalter, C. M. Wentworth, and Yerkes). Open filed digital map of 1400 exploratory wells drilled in the Los Angeles 1:100,000 quadrangle, with accompanying table of geologic data, as a precursor to a digital geologic map of the quadrangle, part of the Southern California Study Unit (NGM Task 1.2.4).

Completed to review stage full-color digital geologic map of the Thousand Oaks 1:24,000 quadrangle, including digital records of exploratory wells and fossil localities, as first element of the digital geologic map of the Los Angeles 1:100,000 quad. Digital files for the adjoining Calabasas 1:24,000 quad are about half completed, and compilation of the next-in-order Canoga Park 1:24,000 quad nearly completed.

Reports

Yerkes, R. F., and Showalter, P. K., 1990, Preliminary map of exploratory wells showing bottom-hole geology and oil fields, Los Angeles 1:100,000 quadrangle, southern California: U.S. Geological Survey Open File Report 90-____.

Expert Synthesis and Translation of Earthquake Hazard Results —A Book for Non-Scientists in the Wasatch Front Region

14-08-0001-G1671

W. J. Arabasz and D. R. Mabey
Department of Geology and Geophysics
University of Utah
Salt Lake City, Utah 84112-1183
(801) 581-6274

Investigations

This "implementation" project is part of the culmination of recent NEHRP focus on Utah's Wasatch Front region. The goals of the project have been: (1) to coordinate with the scientific investigators who have worked in the Wasatch Front earthquake-hazards program—in order to develop a synthesis of important technical information, (2) to produce intermediate-level summaries from those discussions, and finally, (3) to "translate" the technical information into a book on the earthquake threat in Utah for non-scientists. The book has been designed to appeal to (i) the general public (who must encourage and support elected and appointed officials to make decisions on implementing earthquake-hazard-reduction measures), (ii) teachers and students, and (iii) decision-makers themselves.

Results (April 1-September 30, 1990)

- Revision and completion of "Consensus Document"—*A Guide to Reducing Losses from Future Earthquakes in Utah*—(task 2). This document summarizes available technical information on the earthquake threat in Utah and was distributed at the Sixth Annual Wasatch Front Earthquake Conference (Salt Lake City, June 11-12, 1990).
- Successful negotiations with the Utah Geological and Mineral Survey (UGMS) for production support and publication of our book as a so-called "trade title" (task 3) for general readership in Utah. Contributing support from the UGMS will enable printing of a high-quality book for public appeal, yet allow a significantly reduced retail price. (Agreement by the University of Utah Press to co-publish the book with the UGMS is still pending.)
- Ongoing collection of resource materials, illustrations, and writing as part of completion of draftscript.

(Note: During the report period, a no-cost extension was requested and granted for this award. The project completion date is June 30, 1991.)

NEAR-SURFACE LITHOLOGIC AND SEISMIC PROPERTIES

9910-01168

J.F. Gibbs
W.B. Joyner
Branch of Engineering Seismology and Geology
U.S. Geological Survey
345 Middlefield Road, MS 977
Menlo Park, California 94025
415/329-5631 or 415/329-5640

Investigations

Measurements of seismic velocity and attenuation to determine the effect of local geology on strong ground motion and to aid in the interpretation of seismic source parameters.

Results

1. A program has begun to measure seismic velocities in boreholes at U.S.G.S. strong motion stations that recorded the Loma Prieta earthquake of 17 October 1989. To date most of the sites have been permitted for drilling and a drilling contract is being finalized. We anticipate drilling and logging approximately 15 sites over the next year.

2. The study being conducted from data obtained at Gilroy strong motion stations 1 and 2 is continuing. Besides borehole Q_s measurements at station 2 (10.2 ± 3.2) in last report, the spectral decay parameter κ has been determined from records of the Coyote Lake earthquake $M_L = 5.9$ of 6 August 1978 and the Loma Prieta earthquake $M_L = 7.1$ of 17 October 1989. Spectral trends are nearly linear (between 2-20 Hz) for recordings at station 1 (rock) and at station 2 (alluvium) for the Coyote Lake earthquake. The resulting Kappa values are 0.02117 and 0.06620 respectively. For the Loma Prieta earthquake the spectrum from recordings at station 1 has a linear trend but at station 2, the spectrum has a pronounced sage between 6 and 9 Hz. The resulting Kappa values are 0.05758 at station 1 and 0.05714 at station 2 with the slope constrained between 2-20 Hz.

Reports

No reports this period.

10/90

The Implementation of an Earthquake Hazard Mitigation Program in Salt Lake County: Phase II

Contract Number: 14-08-0001-G1797

Investigators: Gary Madsen, Loren Anderson,
and Gerold Barnes

Utah State University, Logan, Utah 84322-0730

(801) 750-1233, (801) 750-2775, (801) 468-2061

Investigations:

This is the second phase of a project to further develop an earthquake hazard preparedness program for Salt Lake County involving public officials, community groups, and the general public. The program is being designed to create heightened awareness of earthquake problems, generate public acceptance of earthquake hazard reduction programs, and establish an earthquake hazard mitigation plan for the county. We have already accomplished three primary tasks: 1) assessing earthquake hazard reduction priorities of public officials in the county, 2) assessing public awareness and understanding of earthquake hazards, and 3) developing an educational program for Salt Lake community groups. The second phase of the project began January 1, 1990. The final tasks are: 4) implementing the education program with materials designed for three distinct audiences (volunteer organizations, the business community, and local government officials), and 5) evaluating the program's effectiveness.

Results:

Activities during the last six months have been directed toward presenting the earthquake education videotape to numerous Salt Lake Valley public officials, community groups and the general public. The videotape was designed to create heightened awareness of earthquake problems in Salt Lake County, generate public acceptance and support for earthquake risk reduction programs, and to further promote hazard mitigation planning among public officials. Two methods were employed to present the videotape. The first was to develop ten copies which could be checked out from the Salt Lake County Planning Division Offices. This was facilitated by newspaper articles in the Desert News and Salt Lake Tribune which identified the contents of the video and where it was available for check out. During a six month period it was checked out by numerous groups including individual families, church groups, schools, neighborhood community groups, businesses, hospitals, realtors, public officials, and community councils. In all, over thirteen hundred persons viewed the video through this check-out method.

The second method was to personally show the video to a broad range of community, professional and government groups. These included the Utah Advisory Council on Intergovernmental Relations, Cache County emergency preparedness seminar, the Thirty-Second Annual Concrete Conference, the Salt Lake County Commissioners and the Salt Lake Council of Governments. Responses to the video have been very encouraging. Numerous copies also have been disseminated to other professionals who are incorporating the video into their educational programs.

As a result of the widespread acceptance and use of the video throughout Salt Lake County, it was felt it was important to produce another one which would have a larger statewide focus. At this time we have been able to secure state support from the Office of Planning and Budget and the Utah Geological and Mineral Survey for this expanded effort.

EARTHQUAKE RISK REDUCTION PROSPECTS:
PUGET SOUND - PORTLAND ASSESSMENT

Grant 14-08-0001-G1778
12/16/89-12/15/90

Peter J. May
Associate Professor
Political Science DO-30
University of Washington
Seattle, WA 98195
(206) 543-2780

Objective: This research has the broad objective of providing an understanding of the opportunities and problems associated with local earthquake risk reduction within the Puget Sound and Portland areas. The current research addresses professional practices and their relationship to local policies. It is aimed at providing a better understanding of the role of the professional standards of architects, geotechnical and structural engineers, and other design professionals in influencing local earthquake risk reduction.

Summary of Research : Information has been collected within the Pacific Northwest about: (a) the role of different professional associations for design professionals in influencing risk reduction practices, (b) state licensing and registration requirements as they relate to professional practices, and (c) design professionals' perceptions of changes in practice over time. Interviews were completed during summer 1990 with officials from 17 local chapters of different professional associations, and with 27 architects and structural engineers.

Summary of Results: The direct impact upon seismic safety of professional recommendations about building design is mediated by variation in practice reflective of differing personal philosophies, experience, training, and sensitivity to earthquake risks. Various public and private regulatory mechanisms help to avert poor seismic design practice of which the major factors are code enforcement and liability considerations. The indirect impact through the influence of various chapters of professional associations is important as a conduit for technical information, but the earthquake network in the Pacific Northwest is too fluid to have sustained policy impact in stimulating change in state or local policy.

The key policy issue stemming from this research is the prospective role of the design professions in enhancing local earthquake risk reduction. The research findings concerning the relationship between codes and practice suggest substantial change in seismic safety would not occur -- even if warranted by new evidence concerning increased risk -- without requisite code revisions and governmental adoption of new codes. Given this situation, the code ultimately becomes a restriction on the extent to which efforts to alter or extend professional practice will enhance earthquake risk reduction. The clear implication is that professional practice is most effectively altered by adopting appropriate seismic building code provisions and by strengthening existing code provisions.

Papers/Presentations based on this research:

"Loss Estimates as Unknown Numbers," Presentation at the USGS-FEMA NEHRP Workshop, Seattle, Washington, April 17-19, 1990.

"Earthquake Risk Reduction: Implementation Prospects for the Puget Sound and Portland Areas," in Proceedings of the Fourth U.S. National Conference on Earthquake Engineering, May 20-24, 1990, Palm Springs, CA, pp. 259-268.

"Design Professions and Earthquake Policy," Draft working paper; Seattle, WA: Department of Political Science, University of Washington, October 1990.

Washington Division of Geology and Earth Resources Earthquake Hazard Reduction Program

Agreement No. 14-08-0001-A0509

Timothy J. Walsh and Stephen P. Palmer
Washington Department of Natural Resources
Division of Geology and Earth Resources
Mail Stop PY-12
Olympia, WA 98504

(206) 459-6372

The Washington Division of Geology and Earth Resources (DGER) is actively investigating earthquake hazards statewide, and presently receives funding from the National Earthquake Hazard Reduction Program (NEHRP) to conduct earthquake hazard mitigation studies. DGER has concentrated its earthquake program on mapping Quaternary deposits in the Puget Sound region subject to seismically-induced ground failure, and on increasing the public's awareness of earthquake hazards in Washington state.

A main focus during this last year was the development of liquefaction susceptibility maps for King County, the most populous county in Washington state. Geotechnical boring data (Standard Penetration Test blow counts, grain size curves, and field descriptions) are being compiled from public data sources such as the King County Building and Land Development agency and the Washington Department of Transportation. These data will be used to evaluate the liquefaction potential of various Quaternary deposits that can be mapped regionally. DGER staff also provide advice and preliminary evaluations of liquefaction and seismically-induced landslide potential to other local government agencies in the Puget Sound region.

A study of liquefaction in the city of Puyallup was performed during this last year. Liquefaction features, including sand blows and lateral spreading, caused by the 1949 (M 7.1) and 1965 (M 6.5) earthquakes were widely reported throughout the Puget Sound region. Precise locations of liquefaction phenomena that occurred in Puyallup during these earthquakes have been obtained through recent interviews with a number of longtime residents. Standard Penetration Test (SPT) data and grain size analyses obtained from geotechnical borings near these sites allowed delineation of three potentially liquefiable soil units. Puyallup was at the same hypocentral distance (65 km ± 2 km) from both the 1949 and 1965 earthquakes. Liquefaction-related phenomena were commonly reported for the 1949 earthquake, but only a single site of sand blow activity was reported for the 1965 event. The critical peak ground accelerations (PGA's) required to cause liquefaction for M 6.5 and M 7.1 earthquakes were back-calculated from the geotechnical boring data. These critical PGA's ranged from 0.10 g to 0.20 g for the liquefiable soil units in question. During the 1965 earthquake a PGA of 0.08 g was measured at both Tacoma and Seattle, which are at hypocentral distances of 65 km and 67 km, respectively. These measured PGA's are less than the minimum critical PGA (0.10 g) estimated from the SPT data and sieve analyses. It was concluded that the 1965 earthquake did not produce the ground acceleration and duration of strong shaking necessary to cause liquefaction in Puyallup. This study provides some validation of the methodology that will be employed in evaluating liquefaction potential throughout the Puget Sound region.

Increasing the public's awareness of earthquake hazards in Washington state is an important activity within DGER, as the Division's primary charter is to disseminate geologic information to the public. This mandate is often carried out by the direct response of the Division's geological staff to oral or written inquiries by members of the public. Information Circular 85, "Washington State Earthquake Hazards", is typically sent as part of the response to questions regarding earthquakes and seismic hazards, and over 3000 copies of Information Circular 85 were distributed during the last year. DGER also maintains a comprehensive public library on the geology of Washington state, and is expanding the reference section pertaining to earthquake-related topics.

Besides the technical publications and maps produced and distributed by the Division, the quarterly Washington Geologic Newsletter provides a vehicle for disseminating earthquake information. On average, one article on an earthquake-related topic is published in each issue, as well as a listing of all new library acquisitions. DGER staff prepared a one page summary of "Earthquake Tips" which was published in the Thurston/Mason Counties telephone book, and will be included in phonebooks for Pierce, Kitsap, and Lewis Counties.

A second avenue for increasing public awareness of earthquake hazards has been the Division's participation and presentations at technical workshops and meetings. Also, DGER staff give informational talks on the Pacific Northwest earthquake potential and earthquake hazard reduction to requesting organizations and businesses. Finally, DGER staff organized the 4th Annual NEHRP Workshop on Earthquake Hazards in the Pacific Northwest that was held on April 17-19, 1990, in Seattle, and attended by over 300 people. By continuing to provide timely and accurate geologic information to the public, DGER will contribute to earthquake hazard mitigation in Washington state.

Global Seismograph Network

9920-02398

Howell M. Butler
Branch of Global Seismology and Geomagnetism
U.S. Geological Survey
Albuquerque Seismological Laboratory
Building 10002, Kirtland AFB-East
Albuquerque, New Mexico 87115
(505) 844-4637

Investigations

The Global Seismograph Network (GSN) presently consists of 11 SRO/ASRO, 12 DWWSSN, 81 WWSSN and 7 IRIS-I type recording stations located in 58 countries and islands throughout the world. The primary objective of the project is to provide high-quality digital and analog seismic data for fundamental earthquake investigations and research, enhancing the United States capabilities to detect, locate and identify earthquakes and underground nuclear explosions in support of test ban issues. Technical and operational support is provided as funds permit to keep the GSN operating at the highest percentage of recording time possible. This support includes operational supplies, replacement parts, repair service, modifications of existing equipment, installation of systems and on-site maintenance, training and calibration. A service contract provides technicians to perform the support requirements as well as special projects such as on-site noise surveys, site preparations, and evaluation and testing of seismological and related instrumentation.

On-site Station Installation/Matinenance

1. ANMO - Albuquerque, New Mexico - Five mainenance visits.
2. BCAO - Bangui, Central African Republic - One maintenance visit.
3. CCM - Cathedral Caves, Missouri - IRIS-I installed.
4. MATO - Matsushiro, Japan - IRIS-I installed.
5. Due to reduced project funding considerations, maintenance visits have been curtailed during this period. The systems at Bogota (BOCO), Columbia, and Lembang (LEM), Indonesia, have had catastrophic failures and will remain inoperative until funding is available for maintenance or replacement of the current system at those locations.

Results

The Global Seismograph Network continues with a combined total of 111 WWSSN/SRO/ASRO/DWWSSN/IRIS-I stations. The main effort of this project, as funding permits, is to furnish the types of support at a level needed to keep the GSN at the highest percentage of operational time in order to provide the improved geographical coverage with analog and digital data from highly sensitive short-period and broadband seismic sensor seismograph systems. Seventy-five WWSSN stations have been converted from photographic recording to thermal recording. Thirty-eight stations operate with six components. Five station, BKS, FVM, GSC, HON and LUB, continue with photographic recording. The seven IRIS-I stations are Albuquerque, New Mexico; Kipapa, Hawaii; Matsushiro, Japan; Cathedral Caves, Missouri; Harvard, Massachusetts; Corvallis, Oregon; and Pasadena, California.

U.S. Seismic Network

9920-01899

Marvin A. Carlson
Branch of Global Seismology and Geomagnetism
U.S. Geological Survey
Denver Federal Center
Box 25046, Mail Stop 967
Denver, Colorado 80225
(303) 236-1500

Investigations

U.S. Seismicity. Data from the U.S. Seismic Network (USSN) are used to obtain preliminary locations and magnitudes of significant earthquakes throughout the United States and the world.

Results

As an operational program, the USSN operated normally throughout the report period. Data were recorded continuously in real time at the National Earthquake Information Center's (NEIC) main office in Golden, Colorado. At the present time, 80 channels of SPZ data are being recorded at Golden on develocorder film. This includes data telemetered to Golden via satellite from both the Alaska Tsunami Warning Center, Palmer, Alaska, and the Pacific Tsunami Warning Center, Ewa Beach, Hawaii. A representative number of SPZ channels are also recorded on Helicorders to give NEIC real-time monitoring capability of the more active seismic areas of the United States. In addition, 18 channels of LPZ data are recorded in real time on multiple pen Helicorders.

Data from the USSN are interpreted by record analysts and the seismic readings are entered into the NEIS data base. The data are also used by NEIS standby personnel to monitor seismic activity in the United States and world wide on a real time basis. Additionally, the data are used to support the Alaska Tsunami Warning Center and the Pacific Tsunami Warning Service. At the present time, all earthquakes large enough to be recorded on several stations are worked up using the "Quick Quake" program to obtain a provisional solution as rapidly as possible. Finally, the data are used in such NEIS publications as the "Preliminary Determination of Epicenters" and the "Earthquake Data Report."

Development is continuing on an Event Detect and Earthquake Location System to process data generated by the USSN. We expect the new system to be ready for routine operational use during 1990. At that time, the use of develocorders for data storage will be discontinued. Ray Buland and David Ketchum have been doing the developmental programming for the new system. A VAX 3800 will be used as the primary computer of the Event Detect and Earthquake Location System.

Five stations of our pilot VSAT Network have had new equipment installed to use the new U.S. National Seismic Network VSAT system with the Master Earth Station located in Golden, Colorado. Three of the stations are the former RSTN sites at McMinnville, Tennessee, St. Regis Falls, New York, and Black Hills, South Dakota, which are now operated by the Branch of Global Seismology and Geomagnetism. The fourth site is the former AFTAC Array near Boulder, Wyoming, and the fifth site is at what was formerly the Newport Observatory, Newport, Washington, which is no longer a manned site. In addition, VSAT's have been installed at the Albuquerque Seismic Laboratory and at the former World Wide site at Bergen Park, Colorado.

Instrumentation of Structures

9910-04099

Mehmet Celebi
Branch of Engineering Seismology and Geology
U.S. Geological Survey
345 Middlefield Road, MS 977
Menlo Park, California 94025
(415) 329-5623

Investigations:

1. The process of selection of structures to be recommended for strong-motion instrumentation has continued in Orange County, Hawaii, and Puget Sound (Seattle), Reno (Nevada), and Puerto Rico. This effort has also been exended to Salt Lake City.

2. The process to design instrumentation schemes for selected structures has continued. Permits for a structure in Orange County, Calif. have been obtained. Current efforts are being made to obtain permits for structures in Hawaii and Seattle.

3. The process of implementation of instrumentation for those structures for which instrumentation schemes have been designed has been completed in Anchorage, Alaska and Orange County, California. The strong-motion recording systems in these buildings are now operational.

4. Non-destructive dynamic testing of Salt Lake City and County Building is to be carried out progressively to evaluate the dynamic characteristics of the building before and after being rehabilitated by base isolation.

5. The minimal instrumentation in a building in Alhambra, southern California, has been upgraded to contain extensive instrumentation to acquire sufficient data to study complete response modes of the building. A set of records is obtained during the Uplands earthquake. This will be compared with the Whittier (October 1, 1987) earthquake data which was codetype.

6. Agreements have been made with UCLA to convert the wind-monitoring system in the Theme Buildings in Los Angeles (previously financed by NSF) into a strong-motion monitoring system. Plans are being made to implement the conversion.

7. Studies of records obtained from instrumented structures are carried out. In particular, the records obtained during the October 1, 1987 Whittier Narrows earthquake from 1100 Wilshire Finance Building (Los Angeles), the Bechtel Building (Norwalk), and the Santa Ana River Bridge (base-isolated) are being investigated. Papers and open-file reports are prepared.

8. Studies of records obtained from instrumented structures during the October 17, 1989 Loma Prieta earthquake are carried out. In particular, Transamerica Building in San Francisco and Pacific Park Plaza in Emeryville have been investigated. Papers are prepared.

Results:

1. The Hawaii committee on strong motion instrumentation of structures has completed its deliberations and a draft report is being prepared.
2. A final report of the Puget Sound (Seattle) advisory committee for strong-motion instrumentation has been completed.
3. Papers resulting from study of records obtained from structures are prepared.
4. An invited talk given on Seismic Monitoring of Structures at the NCEER, Buffalo, New York (April 1990).
5. Invited talks on records from structures given in Taipei and Tokyo.
6. Invited talk on structural instrumentation and data given at U.C. Berkeley on April 30, 1990.
7. Invited talk on structural response records to be given in ASCE Congress in November 1990 (San Francisco).

Reports:

Celebi, M., 1989, Seismic monitoring of structures--objectives and analyses of records from structures: U.S.-Japan Panel, (Wind and Seismic Effects), May 1989.

Celebi, M., and Safak, E., 1990, Study of earthquake records from select tall buildings: completed invited paper for Tall Buildings Conference, November, 1990.

Celebi, M., Safak, E., and Youssef, N., 1990, Coupled torsional response of a unique building: Proceedings, National Conference on Earthquake Engineering, 4th, Palm Springs, California.

Celebi, M., 1990, Types of structural damage, in Effects of the Loma Prieta earthquake on the Marina District, San Francisco, Ca.: U.S. Geological Survey Open-File Report 90-253.

Celebi, M., and Safak, E., 1990, Study of earthquake records from select tall buildings: Tall Buildings Conference, Hong Kong, November 1990 (invited paper).

Celebi, M., and Safak, E., 1990, Recorded seismic response of Transamerica Building (Part I-Data and Preliminary Analysis), paper in review.

Safak, E., and Celebi, M., 1990, Recorded seismic response of Transamerica Building (Part II-System Identification), paper in review.

Celebi, M., and Safak, E., 1990, Recorded seismic response of Pacific Park Plaza (Part I-Data and Preliminary Analysis), paper in review.

Safak, E., and Celebi, M., 1990, Recorded seismic response of Pacific Park Plaza (Part II-System Identification), paper in review.

Celebi, M., and Safak, E., 1991, Recorded responses of two tall buildings during the 10/17/1989 Loma Prieta (California) earthquake: ASCE Structures Congress, April 29-May 1, 1991, Indianapolis, Indiana, invited paper.

Safak, E., and Celebi, M., 1990, Analyses or recorded responses of two high-rise buildings to Loma Prieta main shock, paper in review.

10/90

Earth Structure and its Effects upon Seismic Wave Propagation

9920-01736

George L. Choy
Branch of Global Seismology and Geomagnetism
U.S. Geological Survey
Denver Federal Center
Box 25046, Mail Stop 967
Denver, Colorado 80225
(303) 236-1506

Investigations

1. Effects of Earth structure on NEIC reporting services. The NEIC now uses broadband data to routinely compute parameters such as depth from differential arrival times, radiated energy, and arrival times of late-arriving phases. To assure the accuracy of source parameters derived from waveforms, we are developing corrections for the effects of wave propagation in the Earth.

2. Use of differential travel-time anomalies to infer lateral heterogeneity. We are investigating lateral heterogeneity in the Earth by analyzing differential travel times of phases that differ in ray path only in very narrow regions of the Earth. Because such phases often are associated with complications near the cusp or caustic, their arrival times cannot be accurately read without special consideration of the effects of propagation in the Earth as well as additional processing to enhance arrivals.

3. Use of body wave pulse shapes to infer attenuation in the Earth. In previous work, we developed techniques to determine the depth- and frequency-dependence of attenuation in the Earth. Resolution of this frequency dependence requires analysis of a continuous frequency band from several Hz to tens of seconds as well as consideration of the contributions of scattering and slab diffraction to apparent broadening of a pulse. We are now in the process of documenting Q for surface events and for events at different depths.

Results

1. Effects of Earth structure on source parameters. Body waves that touch internal caustics in the Earth are distorted in a way that can be mathematically corrected by Hilbert transformation. The correction for this pulse distortion has generally not been recognized in the practice of record interpretation. We are evaluating the effect on phases that are commonly read by analysts and the possible effect on tomographic inversions which take reported arrival times of body waves on face value.

2. Use of differential travel-time anomalies to infer lateral heterogeneity. We have developed a source-deconvolution technique that resolves differential travel times of body waves near cusps and caustics. Application of this algorithm to PKP waves sampling the inner core suggests that regional velocity variations exist within the upper 200 km of the inner core. The regional variations are consistent with those obtained from global inversions of absolute PKP times. We are reading high-quality arrival times of PcP and branches of PKP, corrected for propagation effects. This accumulation of data can be used to determine if propagation phenomena have biased the catalog data which have been used to derive models of lateral heterogeneity.

3. Use of body wave pulse shapes to infer attenuation in the Earth. The frequency-dependent Q model of Choy and Cormier (1987) has been crucial to the practical implementation of some algorithms that are used to compute source parameters. It was incorporated into the semi-automated version of the algorithm of Boatwright and Choy (1986) for use by the NEIC in computing radiated energies of earthquakes with $m_b > 5.8$. This Q model also provided the crucial attenuation correction in the technique described by Choy and Boatwright (1988) and Boatwright and Choy (1989) which derives acceleration spectrum from far-field broadband data. We are now attempting to separate intrinsic attenuation from scattering in waveforms. We synthesize waveforms using a method that simultaneously models causal attenuation and source finiteness. Under the assumption that intrinsic attenuation can be described by minimum phase operators, we can attribute discrepancies in the waveforms to scattering.

Reports

Choy, G. L., 1990, Global digital data--Interpretation of the earthquake mechanism from broadband data: Proceedings of the Pacific Rim Congress 1990, v. 2, p. 11-18.

Choy, G. L., and Boatwright, J., 1990, Source characteristics of the Loma Prieta, California, earthquake of October 18, 1989 from global digital seismic data: Geophysical Research Letters, v. 17, p. 1183-1186.

Choy, G. L., Boatwright, J., and LaVonne, C. K., 1990, Teleseismic estimates of radiated energy from global seismicity of 1986-1988 [abs.]: EOS (American Geophysical Union, Transactions), v. 71, p. 258.

Choy, G. L., Presgrave, B. W., and LaVonne, C. K., 1990, Broadband seismogram analysis--The Ethiopian double earthquake of 20 August 1989, in Semi-Annual Technical Report: U.S. Geological Survey Open-File Report 90-267, p. 10-12.

Reanalysis of Instrumentally Recorded United States Earthquakes

9920-01901

J. W. Dewey
Branch of Global Seismology and Geomagnetism
U.S. Geological Survey
Denver Federal Center
Box 25046, Mail Stop 967
Denver, Colorado 80225
(303) 236-1506

Investigations

1. Relocate instrumentally recorded U.S. earthquakes using the method of joint hypocenter determination (JHD) or the master event method, using subsidiary phases (Pg, S, Lg) in addition to first arriving P-waves, using regional travel-time tables, and expressing the uncertainty of the computed hypocenters by means of confidence ellipsoids on the hypocentral coordinates.

2. Evaluate the implications of the revised hypocenters on regional tectonics and seismic risk in the U.S.

3. Use JHD to study foreign earthquake sequences that have unusual potential to shed light on issues that are important to seismic-hazards analyses in the U.S.

Results

D. W. Gordon continues to investigate seismotectonic relationships in the Northern Great Plains region (lat 37° N.-49° N., long 94° W.-105° W.), on the basis of the available earthquake data and an evolving plate-tectonic model of the Precambrian basement. The model characterizes the region as a collage of fault-bounded terranes, among which are Archean microcontinents, accreted volcanic-arcs, intracratonic sedimentary basins, and an aborted continental rift (Sims, P. K., 1990, U.S. Geological Survey MAP 1-1853-A). Sets of northwest- and northeast-trending Precambrian wrench faults, some of which were evidently reactivated in the Phanerozoic, crisscross the region.

The historical data base covering the region spans about 130 years and, excluding foreshocks and aftershocks, contains about 200 earthquakes (Maximum Intensity III or larger, and/or m_b 3.0 or larger). The regional catalog is approximately complete at the magnitude (m_b) 3.5 level for the period since 1900. On average, shocks of this size or larger occur in the region every 1.5 years. Earthquake reporting in the region was very inconsistent before 1900; about two-thirds of the events listed in the regional catalog represent the period since 1925. The largest historic earthquakes in the region have had magnitudes in the 5.0 to 5.5 range.

Due to imprecise epicenters and focal depths, one-to-one correspondence between individual earthquakes and faults can seldom be established.

However, the overall distribution of seismicity exhibits remarkable spatial agreement with the principal Precambrian faults and suture zones in the region. For example, the distribution of epicenters of a dozen light shocks in South Dakota and northeastern Nebraska suggests that they are associated with the Reservation fault, a northwest-trending Precambrian fault reactivated in the Phanerozoic. The relatively well-located epicenters of about 20 minor to light earthquakes are concentrated along similar, northwest-striking, faults in south-central South Dakota. In general, with few exceptions, clusters of epicenters coincide with areas of significant basement structure.

Macroseismic data from earthquakes in the region suggest that the Precambrian terranes and associated crustal structures have a significant influence on isoseismal patterns. Relatively broad suture zones between terranes seem to control the configurations of isoseismals, in that seismic intensity apparently falls off more rapidly across suture zones than it does within terranes. In some cases. Precambrian wrench faults sharply define the boundaries of meizoseismal zones. Isoseismals of well-observed shocks show great complexity. In isoseismal maps of widely felt earthquakes occurring in the past six decades, lobes of anomalously high intensity tend to follow the axes of major elongate structural elements such as the Midcontinent Rift System.

Reports

Dewey, J. W., 1990, The 1954 and 1980 Algerian earthquakes--Implications for the characteristic-earthquake model of seismicity: EOS (American Geophysical Union, Transactions), v. 71, p. 560.

Dewey, J. W. (in press), Joint epicenter determination for earthquakes occurring over several decades--A case history from northern Algeria: Proceedings, Symposium on the Seismicity, Seismotectonics, and Seismic Risk of the Ibero-Maghrebian Region, University of Madrid.

Dewey, J. W. (submitted), the 1954 and 1980 Algerian earthquakes--Implications for the characteristic-earthquake model of seismicity: Bulletin of the Seismological Society of America.

Global Seismology

9920-03684

E. R. Engdahl
and
J. W. Dewey
Branch of Global Seismology and Geomagnetism
U.S. Geological Survey
Denver Federal Center
Box 25046, Mail Stop 967
Denver, Colorado 80225
(303) 236-1506

Investigations

1. Travel-Time Tables. Develop new standard global travel-time tables to locate earthquakes.

2. Arrival-Time Data. Coordinate planning for an International Seismological Observing Period (ISOP)--a time interval during which there would be enhanced reporting of arrival-time data.

3. Earthquake Location in Island Arcs. Develop practical methods to accurately locate earthquakes in island arcs.

4. Subduction Zone Structure. Develop techniques to invert seismic travel times simultaneously for earthquake locations and subduction zone structure.

Results

1. Travel-Time Tables. The standard travel-time tables used by seismological agencies such as the National Earthquake Information Center (NEIC) in Golden, Colorado, USA, and the International Seismological Centre (ISC) in Newbury, U.K., are the Jeffreys and Bullen tables published in 1940. These tables were developed over the period 1930-1939, making use of reported arrival times of seismic phases at a sparse global network of stations for which time keeping was frequently not reliable.

Although the limitations of these tables (Jeffreys and Bullen, 1940), especially in the proper identification of later arriving core phases, have been recognized for some time, no other tables provide such a complete representation of the P, S, and core phases. A major effort to improve P-wave travel times was made in 1986 based on the use of well-timed underground nuclear explosions as well as earthquakes (Herrin, 1968). Subsequently, a number of studies were made to try to improve knowledge of S times, either directly (Hales and Roberts, 1979; Randall, 1971) or via P-S differential times (Uhrhammer, 1971).

The ISC has built up a major data base of the station readings used in establishing earthquake locations. This data set now extends over more than 20 years (1964-1988) with over 6 million arrival-time readings at nearly

3,000 seismic stations. This set of arrival times has been made available in digital form, originally on magnetic tape and recently for the period 1964-1987 on CD-ROM. Although the geographic distribution of stations is somewhat patchy and most sources occur in a limited number of seismic zones, the cumulative data set gives a good coverage of the interior of the Earth. The ISC data has played an important role in the development of recent Earth models such as PREM (Dziewonski and Anderson, 1981) and in studies of the lateral heterogeneity of the Earth (see e.g. Inoue et al., 1990).

With the extensive ISC data set for a period where station time can be determined accurately, it is feasible to construct a set of travel-time tables for the major seismic phases with greater precision than Jeffreys and Bullen (1940) could attain. In 1987, the International Association of Seismology and the Physics of the Earth's Interior (IASPEI) requested its Subcommission on Earthquake Algorithms to propose a suitable set of table times for use in global earthquake location. Kennett and Engdahl (1990) describe the progress which has been made in the generation of such tables and presents a set of summary tables for the main seismic phases. The primary form of the tables is a computational algorithm.

2. Arrival-Time Data. Participated in Workshop on Seismological Instrumentation and Data Analysis in Africa at the IASPEI/ICL/Unesco Regional Assembly in Nairobi, Kenya. Presented paper on the International Seismological Observing Period (ISOP) in Africa. ISOP is a specific time interval designated for enhanced international cooperation in the collection and dissemination of observatory measurements from the global seismographic network. The ISOP project is sponsored jointly by IASPEI, by the IUGG Inter-Association Commission on the Study of the Earth's Deep Interior (SEDI), and by the Inter-Union Commission on the Lithosphere (ICL). The primary goal of ISOP is to strengthen the international infrastructure that supports current seismological practice and increase the cooperation among nations that operate seismological observatories.

Measurements reported by the existing global network and compiled by agencies such as the ISC are providing new information about earthquakes and Earth structure of fundamental importance to the Earth Sciences. A goal of the ISOP is to collect improved sets of observatory data; in particular, the ISOP will encourage the measurement and reporting of high-frequency later-arriving phases from specific earthquakes selected for detailed observation by cooperating stations during a fixed ISOP period. Toward this goal, current reporting practice by African observatories will be reviewed and plots of arrival-time data reported to the ISC presented.

The deployment of advanced digitally recording instrumentation provides an unprecedented opportunity to enhance the methods of seismogram interpretation and seismic parameter extraction through implementation of digital processing methods at seismic observatories worldwide. It must be ensured that this new information will be available to the seismological community at large. It is believed that this purpose is best served with an ISOP that promotes the development toward increased on-site analysis at digital stations. Examples of how interactive processing of digital data can be accomplished on low-cost PC's at African digitally recording stations were presented.

Improvements in seismology require truly international cooperation, and the educational aspects of seismological practice form one of the goals of the ISOP. Thus, workshops will be needed to train analysts in ISOP procedures and to introduce them to modern techniques and applications of the data. Participants will thus benefit from theoretical results and practical experience that are of direct relevance to their own work. Participation of African countries in ISOP workshops is anticipated.

3. Earthquake Location in Island Arcs and
4. Subduction Zone Structure. In the particular case of the NW Pacific, results of P delay-time tomography do not show sufficient resolution in the down-dip direction of subduction zones to provide a conclusive answer to the question of slab penetration. An attempt was made to improve the resolution in the down-dip direction by the incorporation of pP phases. Van der Hilst and Engdahl (1990) showed that: (1) pP waves sample Earth structure that is not adequately sampled by the direct phases (e.g., shallow structure below back-arc regions); (2) pP rays are oblique to rays of direct P, which is especially important when the latter sample mantle structure only in selected directions; and (3) pP data give better constraints on focal depth.

It is important to note that the ISC delay times of phases other than P may not be consistent with ISC hypocentral parameters which are determined from direct P travel times. In addition, if there are few stations at regional distances (e.g. in the case of the Izo Bonin and Mariana subduction zones), part of the slab signal will be removed from the ISC/NEIC P data and will be mapped into the (mis)location of the earthquakes. In the present study, pP and P phase data were used to relocate ISC hypocenters prior to the actual tomographic inversion. Both for the relocation and for the inversions, IASP91 was used as the reference model, which is more appropriate for the mantle beneath the NW Pacific than the Jeffreys-Bullen model. This reduces reference model artifacts in the tomographic images. With the relocated earthquakes, the IASP91 model, and approximately 2,300,000 P and 70,000 pP delay times (1964-1989) computed for the new hypocenters, linearized tomographic inversions were performed. The relocation procedure and present images of the subduction zone below the NW Pacific are addressed. Differences between inversions of P and pP data, and of P delay times only, are focused on. Important conclusions are: (1) The reduction of the data variance due to relocation in the IASP91 model is of the same order of magnitude as reductions typically obtained upon 3D inversion. (2) Due to relocation, the new P data contain more information about subduction zones than the original ISC data. As a consequence, velocity perturbations associated with subducted lithosphere have higher amplitudes (4-5 percent) than in previous studies (3 percent). (3) The spatial resolution in the tomographic images improved significantly due to incorporation of pP data and the "smearing" of anomalies in the direction of P rays is decreased. (4) High P-wave velocities are imaged in the lower mantle below the Japan and Kurile subduction zones. (5) In contrast to results of earlier inversions of ISC P delay times using ISC hypocenters, with the present method no high velocities are imaged in the lower mantle below the Izo Bonin and Mariana subduction zones.

Reports

Kennett, B.L.N., and Engdahl, E. R., 1990, Travel times for global earthquake location: Geophysical Journal International (submitted).

Van der Hilst, R. D., and Engdahl, E. R., 1990, On the use of PP and pP data in delay time tomography: Geophysical Journal International (submitted).

Systems Engineering

9920-01262

Gary Holcomb
Branch of Global Seismology and Geomagnetism
U.S. Geological Survey
Albuquerque Seismological Laboratory
Building 10002, Kirtland AFB-East
Albuquerque, New Mexico 87115
(505) 844-4637

Investigations

Engineering development to improve the quality of seismic instrumentation.

Results

As part of a contract with Sandia National Laboratories, a series of evaluation tests was conducted on the Guralp CMG-3S borehole sensor system. This study is aimed at identifying noise levels and the sources of noise within this instrument system. The data has been analyzed and an Open-File Report of the results has been written and is being reviewed.

A study of potential error sources in analyzing data obtained from side-by-side seismometer evaluations has been completed. These error sources include sensor misalignment, numerical precision in the data processing, and model applicability. An Open-File Report describing this study has been written and released.

A set of Teledyne BB-13 sensors is undergoing evaluation in the Albuquerque Seismological Laboratory vault. These measurements have revealed excessive noise in the system amplifiers, which the manufacturer is currently attempting to reduce.

Probabilistic Earthquake Assessment

9920-01506

Stuart P. Nishenko
Branch of Global Seismology and Geomagnetism
U.S. Geological Survey
Denver Federal Center
Box 25046, Mail Stop 967
Denver, Colorado 80225
(303) 236-1500

Investigations

1. Improve current probabilistic estimates for earthquakes within the United States and the circum-Pacific region.

2. Development of an operational methodology to provide rapid and reliable estimates of damage caused by moderate and large United States earthquakes.

Results

1a. Analysis of seismograph network data, earthquake catalogs from 1727 to 1982, and paleoseismic data for the central and eastern United States by Nishenko and Bollinger (1990) indicate that the Poisson probability of a damaging earthquake (magnitude $\geq$ 6.0) occurring during the next 30 years is at a moderate to high level (0.4 to 0.6) (see table 1). When differences is seismic wave attenuation are taken into account, the central and eastern United States has approximately two-thirds the likelihood of California to produce an earthquake with comparable damage area and societal impact within the next 30 years.

1b. As a consequence of the magnitude 7.1 Loma Prieta earthquake of 17 October 1989, the Working Group on California Probabilities was reconvened to review and, as necessary, revise the findings of the 1988 Working Group report (WGCEP, 1988) for the San Francisco Bay Region. The Bay Area Working Group report (WGCEP, 1990) now estimates that the chances for one or more large earthquakes in the San Francisco Bay region is about 0.67 during the next 30 years.

1c. Study of historic great earthquakes along the Peru subduction zone indicates significant variations in the size of events during the last 400 years. Modified Mercalli intensity and tsunami wave heights for earthquakes in this century are compared with the 29 October 1746 and 20 October 1687 earthquakes by Beck and Nishenko (1990). The great 1746 event occurred along the same segment of the subduction zone as the 24 May 1940 ($M \approx 8$) and 17 October 1966 (M_W 8.1) earthquakes, and is estimated to have a magnitude (M_W) of 8.8 on the basis of the ratio of near-field tsunami wave heights (using the 1746 and 1966 events). The 1687 event probably ruptured the 3 October 1974 (M_W 8.1) segment as well as the adjacent segment to the south where there is at present a gap between the 1942 and 1974 rupture zones. In contrast to the simple, single asperity nature of 20th Century earthquakes, these older and larger events may represent multiple-asperity ruptures along the Peru subduction zone.

2. Work during FY90 concentrated on identifying and implementing methodologies for the actual computation of earthquake effects. While we used the algorthms of Everenden and Thomson (1988), there is no reason why other ground motion algorthms cannot be used as they become available. The primary problem encountered during the first year is not with the ground motion models, but rather with the availability of digital geologic maps with sufficient resolution to provide a socially useful product. Local site geology plays an important role in modifying ground motion and must be taken into account. For FY91 we are planning to integrate the ground motion algorithms with a Geographic Information System (GIS). The GIS provides the necessary geologic digital data base with sufficient resolution at a variety of scales for our needs.

Table 1. Conditional probability estimates for earthquakes in the central and eastern United States. Probabilities are given for an earthquake of equal or greater magnitude during the next 10, 30, 50, and 100 years. New England, Southeast U.S., and New Madrid refer to the regional seismograph network data. Combined row gives the probabilities of at least one event within the above three regions. CEUS and ENA are the central and eastern United States and eastern North America (south of 55°N). See Fig. 1 for network and catalog locations.

Region	1990 to 2000		1990 to 2020		1990 to 2040		1990 to 2090	
	$m_b \geq 6.0$ $M \geq 6.1$	$m_b \geq 7.0$ $M \geq 7.4$	$m_b \geq 6.0$ $M \geq 6.1$	$m_b \geq 7.0$ $M \geq 7.4$	$m_b \geq 6.0$ $M \geq 6.1$	$m_b \geq 7.0$ $M \geq 7.4$	$m_b \geq 6.0$ $M \geq 6.1$	$m_b \geq 7.0$ $M \geq 7.4$
New England	0.08	0.01	0.21	0.03	0.33	0.04	0.55	0.08
Southeast	0.11	0.02	0.30	0.04	0.45	0.07	0.70	0.14
New Madrid	0.13	0.02	0.34	0.05	0.50	0.08	0.75	0.15
Combined	0.29	0.04	0.64	0.11	0.81	0.18	0.97	0.33
CEUS catalog	0.16 to 0.22	0.01 to 0.02	0.41 to 0.53	0.03 to 0.07	0.58 to 0.72	0.05 to 0.11	0.83 to 0.92	0.10 to 0.20
ENA catalog	0.31 to 0.39	0.03 to 0.05	0.67 to 0.78	0.10 to 0.14	0.85 to 0.92	0.16 to 0.23	0.98 to 0.99	0.29 to 0.40

Reports

Beck, S., and Nishenko, S. P., 1990, Variations in the mode of great earthquake rupture along the central Peru subduction zone: Geophysical Research Letters, v. 17.

Everenden, J. F., and Thomson, J. M., 1988, Predictive model for important ground motion parameters associated with large and great earthquakes: U.S. Geological Survey Bulletin 1838.

Nishenko, S. P., and Bollinger, G. A., 1990, Forecasting damaging earthquakes in the central and eastern United States: Science, v. 249, p. 1412-1416.

Working Group on California Earthquake Probabilities, 1988, Probabilities of large earthquakes occurring in California on the San Andreas fault: U.S. Geological Survey Open-file Report, 88-398, 62 p.

Working Group on California Earthquake Probabilities, 1990, Probabilities of large earthquakes in the San Francisco Bay region, California: U.S. Geological Survey Circular 1053, 51 p.

Global Seismograph Network Evaluation and Development

9920-02384

Jon Peterson
Branch of Global Seismology and Geomagnetism
U.S. Geological Survey
Albuquerque, New Mexico 87115-5000
(505) 844-4637

Investigations

Continued work in support of the Eurasian Seismic Studies Project.

Results

Following receipt of an export license, equipment was ordered for a broadband seismograph system to be installed at an observatory near Garni, Armenia, U.S.S.R. The system being assembled is a somewhat modified Soviet version of the IRIS/USGS broadband seismographs being deployed in the Global Seismograph Network. It will consist of STS-VBB seismometers with 24-bit, 20 sample per second encoding, GS-13 short-period seismometers with 16-bit, 100 sample per second encoding, and an IRIS/USGS type of data acquisition and recording system, except that nine-track tape drives will be used in place of cartridge recording. Twelve channels of data will be recorded: three-component short period in a triggered mode, three-component broadband in a continuous mode, plus long-period and very long-period signals derived from the broadband data channels. All of the data will be locally accessible from the data buffer which has sufficient capacity to store at least 24 hours of continuous broadband data. A PC-based data processing system to be furnished with the seismograph system will provide station personnel with the capability to capture and store events of interest for off-line analysis. A site visit to the Garni Observatory was made in September to survey available facilities and complete plans for training and installation.

In a reciprocal arrangement, the USSR side is preparing to install a borehole seismograph system at the Albuquerque Seismological Laboratory. A 12-inch borehole has been completed successfully, and contracts have been awarded for construction of a small building and for a 220 volt, 50 Hz power system. A meeting was held in Moscow during September to complete plans for the installation scheduled for November.

Digital Data Analysis

9920-01788

Stuart A. Sipkin
Branch of Global Seismology and Geomagnetism
U.S. Geological Survey
Denver Federal Center
Box 25046, Mail Stop 967
Denver, Colorado 80225
(303) 236-1506

Investigations

1. Moment Tensor Inversion. Apply methods for inverting body phase waveforms for the best point-source description to research problems.

2. Other Source Parameter Studies. Apply methods for inverting body phase waveforms for distributed kinematic and dynamic source properties.

3. Aftershock Source Properties. Examine mainshock and aftershock source properties to study the mechanics of aftershock occurrence.

4. Broadband Body-Wave Studies. Use broadband body phases to study lateral heterogeneity, attenuation, and scattering in the crust and mantle.

5. Earthquake Recurrence Statistics. Use earthquake recurrence statistics and related parameters to better understand the earthquake cycle and study how they can be used for prediction and forecasting purposes.

6. Earthquake Location Studies. Study techniques for improving the robustness, honesty, and portability of earthquake location algorithms, and participate in the construction and implementation of new standard travel-times for routine earthquake location.

7. NEIC Monthly Listing. Contribute both fault-plane solutions (using first-motion polarity) and moment tensors (using long-period body-phase waveforms) for all events of magnitude 5.8 or greater when sufficient data exists. Contribute waveform/focal-sphere figures of selected events.

Results

1. Moment Tensor Inversion. A Professional Paper on the 1983 Coalinga earthquake has been published. In our contribution we demonstrate, using a time-dependent moment-tensor inversion algorithm, that the strike of the fault plane rotated clockwise by approximately 10° during rupture. May 1990 was notable for the large number of unusual earthquakes. We are studying several of these earthquakes (in the Alaska Peninsula, Sakhalin Is., southern Sudan, and Romania) using the digitally recorded long-period and broadband body waves. A study of structural complexity in seismogenic zones using earthquake mechanism catalogs is underway. The differences in

mechanism for nearby earthquakes are quantified and compared to the differences expected based on the uncertainties in the moment-tensor solutions. In areas where the differences exceed those expected we hypothesize that these differences are due to variations in the orientation of the fault surface(s).

2. Other Source Parameter Studies. Linear and nonlinear methods of waveform inversion are being implemented to determine the fault-rupture history of large earthquakes. Results from a recent nonlinear inversion of teleseismic P-waveforms and strong-motion data recorded for the 1978 Tabas, Iran, earthquake suggest that this event ruptured mostly within the upper 15 km of the crust and occurred as a series of up to three distinct subevents. In addition, a linear method that inverts for the total slip as a function of position on the fault has been applied to broadband teleseismic waveform data recorded for the October 1989 Loma Prieta earthquake. The same procedure is also being employed in the study of several recent large earthquakes along the Mexico subduction zone.

3. Aftershock Source Properties. Work is continuing on the comparison of aftershock locations with distribution of fault slip derived from observed waveform data, especially for interplate thrust events.

4. Broadband Body-Wave Studies. A data set of relatively broadband shear-wave data has been assembled for the purpose of studying deep discontinuities in the Earth. Another data set has being assembled for the purpose of identifying near-receiver scattering of seismic waves. Software for both studies is being developed. While trying to recover broadband ground displacement we discovered that, when deconvolving an instrument response, unless one explicitly takes into account the properties of the filters being used, either bias or increased uncertainty in the results can be introduced, especially when taking integral measures of the displacement pulse. A new optimal method for deconvolving the instrument response has been developed that avoids the pitfalls inherent in the methods currently used.

5. Earthquake Recurrence Statistics. A paper has been submitted for publication in which the "generic," characteristic earthquake, recurrence interval, probability density function model has been extended to provide a marginal distribution for recurrence intervals which is independent of the uncertainty in the median recurrence interval. This permits the estimation of a single preferred value for the conditional earthquake forecast probability.

6. Earthquake Location Studies. As a result of participation in an IASPEI working group, tau-p travel time programs were provided on a UNIX platform. Subsequently, the tau-p package was modified to support the generation of a reference Earth model. The software has been updated to include the most current proposed IASPEI Earth model, and the number of travel-time branches has been doubled. Work is currently being done on making this code more accessible (ie. cleaner user interface, documentation, specialized code to run on various computers). A journal article on the statistics of teleseismic body-wave travel-time residuals has been submitted for publication. The results are leading to the development of new algorithms using robust

estimation techniques. In this work the statistics of travel-time residuals, which are well known, are being applied directly in the location algorithm. This has lead to improving the meaningfulness of the estimated errors in the locations and in earthquake magnitude. The estimated errors in the earthquake origin time are now being examined. A study of the statistics of later arriving phases will also be undertaken.

7. NEIC Monthly Listing. Since January 1981, first-motion fault-plane solutions for all events of magnitude 5.8 or greater have been contributed to the Monthly Listings. Since July 1982, moment-tensor solutions and waveform/focal-sphere plots have also been contributed. In the last six months, solutions for approximately 93 events have been published. An atlas of European seismicity is in preparation. A special map showing the seismicity of the New Madrid region was made for a member of Congress. A complete compilation of Mediterranean Sea seismicity is being prepared.

Reports

Buland, R. P., 1991, Residual statistics: Bulletin Seismological Society of America (submitted).

Buland, R. P., and Nishenko, S. P., 1991, Preferred earthquake forecasts and conditional earthquake prediction: Bulletin Seismological Society of America (submitted).

Hartzell, S. H., and Mendoza, C., 1990, Simultaneous inversion of strong-motion records and teleseismic P-waveforms for fault slip and rupture times of the 1978 Tabas, Iran, earthquake [abs.]: Seismological Research Letters, v. 61, no. 1, p. 34-35.

Hartzell, S. H., and Mendoza, C., 1991, Application of an iterative least-squares waveform inversion of strong motion and teleseismic records to the 1978 Tabas, Iran, earthquake: Bulletin of the Seismological Society of America (submitted).

Sipkin, S. A., 1990, Use of seismic-source-parameter catalogs to determine the roughness of a seismogenic zone [abs.]: Abstracts, ESC Workshop on Earthquake Source Mechanism and Seismotectonics, Madrid, Spain.

Sipkin, S. A., 1990, Moment-tensor solutions for several unusual earthquakes in May 1990 [abs.]: EOS (American Geophysical Union, Transactions) (in press).

Sipkin, S. A., and Lerner-Lam, A. L., 1990, Pulse-shape distortion introduced by broadband deconvolution [abs.]: EOS (American Geophysical Union, Transactions) (in press).

Sipkin, S. A., and Needham, R. E., 1990, Kinematic source parameters of the 2 May 1983 Coalinga earthquake determined by time-dependent moment-tensor inversion and an analysis of teleseismic first motions, in The Coalinga, California, earthquake of May 2, 1983: U.S. Geological Survey Professional Paper 1487, p. 207-213.

Seismicity and Tectonics

9920-01206

William Spence
Branch of Global Seismology and Geomagnetism
U.S. Geological Survey
Denver Federal Center
Box 25046, Mail Stop 967
Denver, Colorado 80225
(303) 236-1506

Investigations

Studies carried out under this project focus on detailed investigations of large earthquakes, aftershock series, tectonic problems, and Earth structure. Studies in progress have the following objectives:

1. Explore the consequences of the slab pull force acting at the zone of plate bending that is downdip of the lower end of an interface thrust zone (W. Spence and W. Z. Savage).

2. Determine the tectonic consequences at the western U.S. caused by heating of the stalled Farallon plate.

3. Describe the evolution of aftershock series of the great 1957 Aleutian arc earthquake (with T. Boyd and E. R. Engdahl).

4. Describe the evolution of the aftershock series of the great 1974 Peru earthquake (with Charley Langer).

Results

1. Interface thrust zones typically have dips in the range 8-15°, whereas lithospheres that are subducted into the mantle typically have dips in the range 40-70°, giving an average dip increase in the mantle of about 45°. These dip increases often occur within 40-60 km of plate length. These zones of sharp dip increases (slab bends) have not been given much attention because generally they lack large earthquakes. This is in sharp contrast to the well-studied zones of bending beneath oceanic trenches where there are frequent normal-faulting earthquakes. It has been noted by Ruff and Kanamori (1983) that great, interface thrust earthquakes terminate their downdip ruptures at the updip part of mantle slab bends. Spence (1987) showed that the slab pull force is the primary force that causes shallow, subduction earthquakes. The mantle slab bend acts as a pivot for the summed slab pull force of the more deeply subducted plate. In this study, we model the stress distribution in the mantle slab bend, acting under a slab pull load. We find that the observed lack of earthquakes in the mantle slab bend is due to ductility there. However, the strength of the work-hardened ductile portion of the slab bend is more than sufficient to transmit the slab pull load into the shallow subduction zone, thereby producing much of the stress that ultimately will be relieved by a subduction style earthquake.

2. Because the Laramide Rockies were eroded to a largely featureless surface by about 40 Ma, explanations are needed for the modern elevations and tectonic character of the Rockies, the Colorado Plateau, and the Basin and Range. Taking the sub-horizontal Farallon plate to have remained in place after the Laramide orogeny and to have been warmed by the underlying asthenosphere leads to the required explanations. One consequence of warming of the Farallon plate is the trend towards higher-melting point volcanics that derive from the Farallon plate. The present low velocity zone of the upper mantle is the relict Farallon plate. The 90-km-thick plate underwent expansion due to this heating and to the formation of partial melt within the plate. This expansion and that due to heating of the overlying plate led to isostatic uplift of about 1.8 km, with about 3/4 of this uplift due to expansions of the Farallon plate. The uplifted welt has tended to gravitationally spread westwards since about 20 Ma.

3. Aftershocks of the 1957 Aleutian Islands earthquake are being relocated and magnitudes are being determined. Tectonic interpretations of the space-time evolution of aftershock series, including the vigorous sequence near the Aleutian trench, are in progress.

4. Aftershocks of the 1974 Peru earthquake are being relocated to verify focal depths and the space-time development of the aftershock series, as previously determined using another velocity model and another location algorithm.

Reports

Boyd, T., Engdahl, E. R., and Spence, W., 1990, Aftershock distribution of the 1957 Aleutian Islands earthquake [abs.]: EOS (American Geophysical Union, Transactions) (in press).

Spence, William, and Gross, R. S., 1990, A tomographic glimpse of the upper mantle source of magmas of the Jemez lineament, New Mexico: Journal of Geophysical Research, v. 95, p. 10,829-10,849.

Spence, William, 1990, Post-Laramide tectonics and the relict Farallon plate: Science (submitted).

United States Earthquakes

9920-01222

Carl W. Stover
Branch of Global Seismology and Geomagnetism
U.S. Geological Survey
Denver Federal Center
Box 25046, Mail Stop 967
Denver, Colorado 80225
(303) 236-1500

Investigations

One hundred and sixty-five earthquakes in the United States and Puerto Rico, were canvassed by a mail questionnaire for felt and damage data during the period April 1, 1990 to September 30, 1990. Seventy-two of these earthquakes occurred in California, 52 in Alaska, and 40 in eighteen other states, and 1 in Puerto Rico.

Compilation is proceeding on the Professional Paper "Seismicity of the United States, 1568-1989" with an estimated completion date of December 1990.

The Earthquake Data Base System (EDBS) managed by Glen Reagor has added new catalogs and improved the worldwide coverage of earthquake data.

Results

Five earthquakes caused minor damage during this period--three in California and two in Washington. All were intensity VI with damage consisting of cracked chimneys, broken windows, minor cracking of plaster or dry wall, and the fall and breakage of some glass objects in stores and homes.

The EDBS has been updated through the current PDE and through March 1990, Monthly Listing. Eight new catalogs have been added to the EDBS and the Canadian catalog updated through 1987.

The new catalogs are:

1. DNAG - Decade of North American Geology, 1500-1985 covering North and Middle America.
2. GREAT - Magnitude 7.0 or larger earthquakes, worldwide, 1904-1977.
3. INDIA - Felt earthquakes for the Indian Peninsula, 1939-1900.
4. ITALY - Earthquakes in Italy and adjacent areas, 1400 B.C.-1984.
5. MEAST - Earthquakes in the Middle Eastern Countries, 1900-1983.
6. PERU - Instrumentally located earthquakes in Peru, 1900-1984.
7. SISRA - Earthquakes in the Andrean Mountains Countries, 1471-1981.
8. WCAFR - Earthquakes in continental West Africa and adjacent oceanic areas, 1615-1984.

The EDBS is continuing to be highly used as a data source by engineering firms, scientists, architects, law firms, universities, and by individuals for personal research.

United States Earthquakes, 1985 (Bulletin) is in press. USE, 1986, has been compiled and a manuscript is in progress.

Reports

Highland, L. M., Stover, C. W., Hopper, M. G., Thenhaus, P. C., and Algermissen, S. T., 1990, Intensity studies, in Rymer, M. J., and Ellsworth, W. L., eds., The Coalinga, California, earthquake of May 2, 1983: U.S. Geological Survey Professional Paper 1487, p. 349-358.

Global Seismicity Mapping

9920-04321

Susan K. Goter
Branch of Global Seismology and Geomagnetism
U.S. Geological Survey
Denver Federal Center
Box 25046, Mail Stop 969
Denver, Colorado 80225
(303) 236-1506

Investigations

1. State Seismicity Maps. Produce and distribute seismicity maps on shaded, elevation-tinted state map bases.

2. U.S. Seismicity Map. Produce and distribute a full-color seismicity map of the United States on a shaded, elevation-tinted map base.

Results

1. State Seismicity Maps. The aim of the state seismicity maps is to provide the most complete picture possible of where earthquakes have occurred historically in relation to geographic, geomorphic, and cultural features. This is accomplished by selecting or compiling an earthquake database that is then plotted and printed on a shaded, elevation-tinted base map.

Since this project began in 1988, state seismicity maps have been completed for California, Hawaii, and Alaska. Work is currently underway to produce a similar map for the state of Utah. This map will display earthquakes that occurred between 1884 and 1989. Although the magnitude threshold for earthquakes plotted on the map varies throughout the historical record, the lower magnitude cut-off for earthquakes that occurred after 1962 is 2.5. Epicenter symbol sizes plotted on the map are scaled into four magnitude categories. Earthquakes that occurred since 1975 are distinguished on this map from earlier events by the intensity of color of the epicentral symbol.

The resulting full-color maps are distributed to the research community worldwide, as well as to each high school in the state covered by the map.

2. U.S. Seismicity Map. Work is currently underway on a full-color seismicity map of the United States. The map is expected to be produced at a scale of 1:3.5 million on an Albers Equal Area map base.

The resulting maps will be distributed to the research community worldwide and will be available for purchase.

Reports

Goter, S. K., 1990, Seismicity of Utah, 1884-1989 (in preparation).
Goter, S. K., 1991, Seismicity of the United States (in preparation).

Date Processing, Golden

9950-02088

Robert B. Park
Branch of Geologic Risk Assessment
U.S. Geological Survey
Box 25046, MS 966, Denver Federal Center
Denver, CO 80225
(303) 236-1638

Investigations

The purpose of this project is to provide the day-to-day management and systems maintenance and development for the Golden Data Processing Center. The Center supports Branch of Geologic Risk Assessment with a variety of computer services. The systems include a PDP 11/70, a VAX/750, a VAX/780, two MicroVAX's, two SUN servers, 5 SUN workstations, and a PDP 11/34. Total memory is 40 mbytes and disk space is approximately 7 G bytes. Peripherals include four plotters, ten mag-tape units, an analog tape unit, two line printers, 5 CRT terminals with graphics, and a Summagraphic digitizing table. Dial-up is available on all the major systems and hardwire lines are available for user terminals on the upper floors of the building. Users may access any of the systems through a Gandalf terminal switch. Operating systems used are RSX11 (11/34's), Unix (11/70), RT11(LSI's) and VMS (VAX's).

Results

Computation performed is primarily related to the Hazards program; however, work is also done for the Induced Seismicity and Prediction programs as well as for DARPA, ACDA, and U.S. Bureau of Reclamation, among others.

The data center supports research in assessing seismic risk and the construction of national risk maps. It also provides capability for digitizing analog chart recordings and maps as well as analog tape. Also, most, if not all, of the research computing related to the hazards program are supported by the data center.

The data center also supports equipment for online digital monitoring of Nevada and Colorado Western Slope seismicity. Also, it provides capability for processing seismic data recorded on field analog and digital cassette tape in various formats.

National Earthquake Information Service

9920-01194

Waverly J. Person
Branch of Global Seismology and Geomagnetism
U.S. Geological Survey
Denver Federal Center
Box 25046, Mail Stop 967
Denver, Colorado 80225
(303) 236-1500

Investigations and Results

The Quick Epicenter Determinations (QED) continues to be available to individuals and groups having access to a 300- or 1200-baud terminal with dial-up capabilities to a toll-free WATS number or a commercial telephone number in Golden, Colorado. It is also accessible via GEONET and public TYMNET. The time period of data available in the QED is approximately 3 weeks (from about 2 days behind real time to the current PDE in production). The QED program is available on a 24-hour basis, 7 days a week. From April 1, 1990, through September 30, 1990, there have been 8,954 logins to the QED program. A daily QED message, 7 days behind real time, is transmitted to 22 different agencies in the U.S. and throughout the world via electronic mail, including a scientific bulletin board operated by Dr. Francis Wu at the State University of New York at Binghamton. This bulletin board is accessible by anyone who is connected to BITNET. The daily QED message is also distributed to another 13 agencies via U.S. government communications (VADATS/DTS/AUTODIN), including worldwide distribution on the communications system of the World Meteorological Organization.

NEIS is making extensive use of electronic mail for data acquisition. Data are now being received via GEONET, TYMNET, internet, BITnet, DECNET/SPAN and uucp on a regular basis. Agencies sending data to NEIS via electronic mail include the following:

U.S. Bureau of Reclamation, Denver
Geological Survey of Canada, Ottawa
Geological Survey of Canada, Sidney, BC
Universidad Autonoma de Mexico, Mexico City
Universidade de Sao Paulo, Brazil
University of Bergen, Norway
Instituto Nazionale di Geofisica, Rome, Italy
Centro Cultura Scientifica Ettore Majorana, Erice, Sicily
Centre Seismologique Euro-Mediterraneen, Strasbourg, France
University of Thessaloniki, Greece
Kandilli Observatory, Istanbul, Turkey
Harvard University, Cambridge, MA (Centroid, Moment Tensor Solutions)
Graefenberg Observatory, Germany

In addition, the following agencies contribute data to the PDE program by computer file transfer or remote login via the computer networks:

USGS Alaska Seismic Project, Menlo Park
USGS/California Institute of Technology, Pasadena
USGS Fredericksburg Observatory, Corbin, Virginia
USGS Guam Observatory, Mariana Islands
University of California, Berkeley
University of Southern California, Los Angeles
University of Washington, Seattle
John Carroll University, Cleveland, Ohio
North Illinois University, DeKalb
Oklahoma Geophysical Observatory, Leonard

Data acquisition by electronic mail is in the process of being established with the Bureau Central Seismologique Francaise in France.

Telegraphic data are now being exchanged with the USSR on most larger earthquakes. The Soviet data are being received from the Central Seismological Observatory, Obninsk, under the auspices of the World Data Center system. Our designation as World Data Center A for Seismology played a key role in permitting this exchange to be established.

Data from the People's Republic of China via the American Embassy continue to be received in a very timely manner and in time for the PDE publication. We continue to receive four stations on a weekly basis from the State Seismological Bureau of the People's Republic of China. The Bulletins with additional data are now being received by floppy disk in time for the Monthly.

Special efforts are being made to receive more data from the Latin American countries on a more timely basis. The increased availability of telefax is permitting much more interaction with Latin American countries than in the past.

We have rapid data exchange (alarm quakes) with Centre Seismologique European-Mediterranean (CSEM), Strasbourg, France, and Instituto Nazionale de Geofisica, Rome, Italy, and Sicily, and data by telephone from Mundaring Geophysical Observatory, Mundaring, Western Australia and Pacific Tsunami Warning Center in Honolulu. The geophysical laboratory in Papeete, French Polynesia contributes a single-station estimate of seismic moment within about 24 hours of a large event in the Pacific region.

The Monthly Listing of Earthquakes is up to date. As of September 30, 1990, the Monthly Listing and Earthquake Data Report (EDR) have been completed through May 1990. The total number of events published for the period December 1989 through May 1990 was 8,050. The number of events located for 1989 was 14,604. By comparison, for 1970 only 4,353 events were published in the PDE for the entire year. Radiated energy, moment tensor, P-wave first-motion and broadband depth solutions continue to be determined by the USGS when possible and published in the Monthly Listing and EDR for any earthquake having an m_b magnitude ≥ 5.8. Centroid moment tensor solutions contributed by Harvard University continue to be published in the Monthly Listing and EDR. Waveform plots are being published for selected events having m_b magnitudes $\geq$ 5.8.

The Earthquake Early Alerting Service (EEAS) continues to provide information on recent earthquakes on a 24-hour basis to the Office of Earthquakes, Volcanoes and Engineering, scientists, news media, other government agencies, foreign countries, and the general public.

Fifty releases were made from April 1, 1990, through September 30, 1990. In the United States, the most newsworthy earthquake was a magnitude 4.6 quake in Cape Girardeau, Missouri, on September 27. This was because of the prediction of a major earthquake in the New Madrid area on December 4, 1990. The most significant foreign earthquakes were:

Date	Magnitude	Country
April 5, 1990	7.4 MS	Mariana Islands
April 18, 1990	7.4 MS	Minahassa Peninsula
April 26, 1990	6.9 MS	Qinghai Province, China
May 20, 1990	7.2 MS	Sudan
May 24, 1990	6.8 MS	Sudan
May 24, 1990	7.0 MS	Sudan

The main shock on May 20 is believed to be the largest earthquake ever recorded in the Sudan and the second largest in the East African rift system.

Date	Magnitude	Country
May 30, 1990	6.4 MS	Peru
May 30, 1990	6.7 m_b	Romania
June 14, 1990	7.0 MS	Panay, Philippine Islands
June 20, 1990	7.7 MS	Western Iran
July 6, 1990	5.8 m_b	Java
July 13, 1990	5.6 m_b	Hindu Kush Region
July 16, 1990	7.8 MS	Luzon, Philippine Islands

Reports

Monthly Listing of Earthquakes and Earthquake Data Reports (EDR); six publications from December 1989 through May 1990. Compilers: W. Jacobs, P. Chang, J. Minsch, R. Needham, W. Person, B. Presgrave, W. Schmieder.

Preliminary Determination of Epicenters (PDE); 26 weekly publications from April 5, 1990 through September 26, 1990, 36-90, numbers 11-90 through 36-90. Compilers: W. Jacobs, P. Chang, J. Minsch, R. Needham, W. Person, B. Presgrave, W. Schmieder.

Quick Epicenter Determination (QED) (daily): Distributed only by electronic media.

Person, Waverly J., Seismological Notes: Bulletin of the Seismological Society of America, v. 80, no. 3, July-August 1989; v. 80, no. 4, September-October 1989; v. 80, no. 1.

Monthly Listing of Earthquakes, in Seismological Research Letters, Eastern Section, SSA, v. 61, no. 1, January-March 1990; v. 61, no. 2, April-June 1990 (Microfiche): Compilers: W. Jacobs, P. Chang, J. Minsch, R. Needham, W. Person, B. Presgrave, W. Schmieder.

Person, Waverly J., Earthquakes, in Earthquakes and Volcanoes, v. 21, no. 3, January-February 1989; v. 21, no. 4 May-June, July-August, September-October 1989.

Seismic Review and Data Services

9920-01204

James N. Taggart
Branch of Global Seismology and Geomagnetism
U.S. Geological Survey
Denver Federal Center
Box 25046, Mail Stop 969
Denver, Colorado 80225
(303) 236-1506

Investigations

This project distributes copies at cost of filmed seismograms from the Worldwide Standardized Seismograph Network (WWSSN), the Canadian Standard Network (CSN), and various stations with historical (pre-1963) records. In addition, the project receives and processes the original WWSSN analog seismograms for photography, and afterward returns them to the stations.

Results

Six hundred station-months of WWSSN seismograms were processed during fiscal year 1990. The seismograms were received from the stations, reboxed, stamped, collated, sent to the contract photographer, returned from the photographer, and mailed back to the stations after the films passed quality control requirements. Problems with the old government-owned camera and photographic contractor's employee turnover caused delays through much of the year. Copies of CSN seismograms on 35mm reels were received on schedule from the Geological Survey of Canada. No films of historical seismograms were added to the archives this year.

The number of active stations in the WWSSN continues to decline, partly as a result of the replacement of the 1960 vintage analog seismographs with modern broadband digital systems. The quality of the recent data from the active WWSSN stations is still very good because these stations are operated by well-trained staffs. Many of the closed or inactive stations were beset with financial, political, or cultural encroachment problems.

Seven standing orders for WWSSN microfiches and one standing order for CSN monthly station reels were received this year. We also received 45 special orders, ranging from a few to several thousand filmed seismograms. Approximately 550,000 filmed seismograms were copied and distributed to fill the 53 orders.

Computer and Data Analysis Services

9920-04151

Madeleine Zirbes
Branch of Global Seismology and Geomagnetism
U.S. Geological Survey
Denver Federal Center
Box 25046, Mail Stop 967
Denver, Colorado 80225
(303) 236-1506

Investigations

1. NEIC Monthly Listing. Contribute waveform data for all events of magnitude 5.8 or greater when sufficient data exists.

2. Network Day Tape Support. Develop, distribute, and support FORTRAN programs to access network-day tapes and station tapes.

3. SEED Support. Develop, distribute, and support software for the Standard for the Exchange of Earthquake Data (SEED) format.

4. Event Tape Production and Distribution. Produce and distribute event tapes.

5. Event CD-ROM Production and Distribution. Produce and distribute event CD-ROM data.

Results

1. NEIC Monthly Listing. Since July 1982, digital waveform plots have been contributed to the Monthly Listings. USGS fault-plane and moment tensor solutions and broadband data have also been incorporated into the focal sphere plots.

2. Network Day Tape Support. FORTRAN software to read and extract digital data from station tapes (1976-1979) and network day tapes (1980-1987) has been developed and distributed to the research community worldwide. Users are supported on a variety of computers.

3. SEED Support. A new Standard for the Exchange of Earthquake Data (SEED) has been created and tapes are now being produced (1988 to present) and distributed by the Albuquerque Seismic Laboratory. FORTRAN software has been developed to read and extract the digital data from the SEED tapes and this software is being made available to the research community.

4. Event Tape Production and Distribution. Event tapes have been produced from network day tapes for data from 1980 through February 1987 for all events with magnitude 5.5 or greater. These tapes are distributed to 25 institutions worldwide, along with a waveform catalog that provides a visual display of the data available for each event.

5. Event CD-ROM Production and Distribution. Data from the event tapes are reformatted and sent to a CD-ROM mastering facility for replication. Six volumes have been produced, covering 1980 through May 1986. The CD-ROMs are being distributed to over 200 Universities across the United States and geophysical research institutes worldwide. Retrieval software, SONIC (C) and CDRETRV (FORTRAN), has been developed for the IBM/PC/AT/386 compatibles and distributed. It allows easy access to the digital data.

General Earthquake Observation System (GEOS)
General Analysis and Playback Systems (GAPS)

9910-03009

Roger D. Borcherdt
Branch of Engineering Seismology and Geology
U.S. Geological Survey
345 Middlefield Road, MS 977
Menlo Park, California 94025
(415) 329-5619

Investigations

1. Complete construction and development of 100 portable, broad band, high-resolution digital data acquisition systems for use in a wide variety of active and passive seismic experiments.

2. Develop PC-based capabilities for field retrieval, processing, and archival of large volumes of GEOS data.

3. Conduct Eurasian Seismic Studies Program.

Results

1. The following design modifications for new GEOS systems have been tested and are being implemented in construction of 55 new systems:

   a.) Expanded data buffer (1 M/sample) design by M. Kennedy.
   b.) Extended gain with improved noise for amp/filter board by J. van Schaack and G. Jensen.
   c.) New tape controller for new 16 Mbyte tape cartridges by Phoenix Data, Inc.
   d.) Software drivers for mag tape controller by G. Maxwell.
   e.) Software for RS 232 for use in satellite, radio, and telephone telemetry and data transfer to field computer by G. Maxwell.
   f.) Software for incorporating design modifications, teleseismic trigger, and field playback are being pursued by G. Maxwell.
   g.) Completion of the 55 new GEOS units is expected by February 1991.

2. GEOS maintenance laboratory under direction of J. Sena together with field support of G. Sembera and C. Dietel has facilitated the execution of several experiments within the last year, including experiments at Parkfield, Anza, Armenia, teleseismic receiver function experiments, and ground response investigations in Marina District, San Francisco. High fidelity dense seismic array has been installed.

   A portable, high-resolution, dense 3-dimensional array consisting of 12 sites with three-component, 1.0 hertz seismometers has been installed in and around a 2-dimensional tunnel with its longest dimension being 200 m at the Garni Observatory, Armenia. The sites are arranged in a nested tripartite configuration with expanding interstation spacings near 60, 120, 240, and 480 meters. Signals are routinely recorded at 200 sps on time synchronized GEOS recorders with maximum signal resolution of 96 dB. Simultaneous recording via pc-based data acquisition system is coupled to GEOS recorders and permits synchronized digitization and simultaneous tape playback and analysis capability. Data playback completed for the time period June 27-July 25, 1990 has yielded recordings of complete tunnel array for about 1-3 events per day, including teleseismic events, regional aftershocks of the Spitak earthquake, and high-frequency local events at a distance of 8-10 km from the tunnel. Data examples for a local and a regional event are shown in Figure 1.

Reports

Borcherdt, R.D., Celebi, M., Filson, J., Iyer, H.M., Johnston, M., Mooney, W., Rogers, A., 1989, A program for Large Array Seismic Observation (LASO): *U.S. Geological Survey Administrative Report*, 116 p.

Borcherdt, R.D., Langer, C., Filson, J.R., Simpson, D.W., Glassmoyer, G., Andrews, M., and Cranswick, E., 1990, On the rupture zone and effects of local geologic conditions on damages and ground motions for the Armenian earthquakes of December 7, 1988: National Conference on Earthquake Engineering, 4th, Palm Springs, Calif., 1990, Proceedings.

Filson, J. Borcherdt, R., Cranswick, E., Hakhverdian, L., Amirbekian, R., Aharonian, V., Safarian, K., Calagian, H., Hapoian, G., and Mori, J., 1990, Installation and first results of a dense 3-dimensional array at Garni, Armenia: *EOS*, in press.

(See projects Borcherdt *et al*., 9910-02089, 9910-02689;
Iyer; McGarr; Fletcher; Boatwright; Mueller; and Liu
for additional reports based on GEOS data sets.)

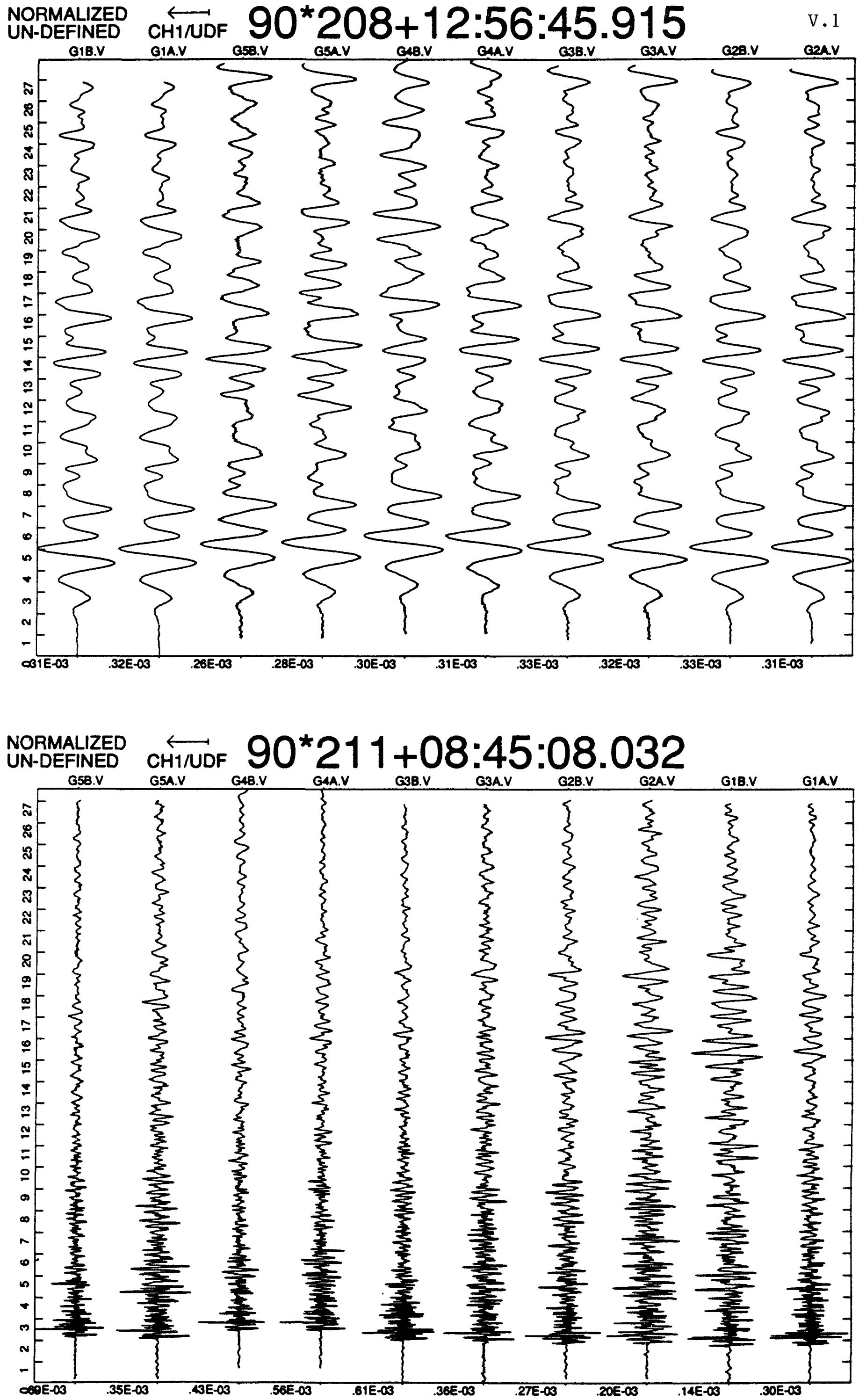
NORMALIZED
UN-DEFINED
CH1/UDF
90*208+12:56:45.915
V.1
G1B.V
G1A.V
G5B.V
G5A.V
G4B.V
G4A.V
G3B.V
G3A.V
G2B.V
G2A.V
0
1
2
3
4
5
6
7
8
9
10
11
12
13
14
15
16
17
18
19
20
21
22
23
24
25
26
27
.31E-03
.32E-03
.26E-03
.28E-03
.30E-03
.31E-03
.33E-03
.32E-03
.33E-03
.31E-03
NORMALIZED
UN-DEFINED
CH1/UDF
90*211+08:45:08.032
G5B.V
G5A.V
G4B.V
G4A.V
G3B.V
G3A.V
G2B.V
G2A.V
G1B.V
G1A.V
.69E-03
.35E-03
.43E-03
.56E-03
.61E-03
.36E-03
.27E-03
.20E-03
.14E-03
.30E-03

FIGURE 1

National Strong-Motion Network: Data Processing

9910-02757

A.G. Brady
Branch of Engineering Seismology and Geology
345 Middlefield Road, MS 977
Menlo Park, California 94025
(415) 329-5664

Investigations

1. Processing data from the Loma Prieta earthquake, including the determination of long-period limits.

2. Software improvements for PC network in various staff offices within the Branch, and for the processing program.

3. Cataloging all strong-motion records from the cooperative network operated by USGS for 1988.

Results

1. Digitizing and processing of the records from Loma Prieta continues. Digitization is complete on records from 38 stations, and the first volume of processed data, and two accompanying tapes, are available for distribution. Within the USGS, investigations have shown the contribution to damage of the Bay Bridge from ground resonances in the vicinity of the Oakland abutment.

2. Many subroutines in the accelerogram processing program have been streamlined and those parts dependent on current USGS hardware have been separated and treated for ability to transport. A limited PC version to be attached to a CDROM of strong motion uncorrected data is in preparation.

3. The annual report describing all strong-motion records recovered in a single year is called a "Catalog of U.S. Geological Survey Strong-Motion Records, 19--" and its Table 1 lists all important parameters obtainable from the original record: earthquake epicenter and magnitude, station name and location, trigger and S-T times, and component directions, peak acceleration and duration. The 1988 catalog is in preparation.

Reports/Tapes

Brady, A.G., and Mork, P.N., 1990, Loma Prieta, California, earthquake October 18 (GMT) 1989, processed strong-motion records, volume 2: a tape available from NGDC, NOAA, Boulder, Colorado.

10/90

National Strong-Motion Network: Engineering Data Analysis

9910-02760

A.G. Brady
Branch of Engineering Seismology and Geology
345 Middlefield Road, MS 977
Menlo Park, California 94025
(415) 329-5664

Investigations

Buildings and dams with extensive instrumentation triggered records from the M7.1 Loma Prieta earthquake of October 17, 1989. Anderson Dam is the closest USGS station to the epicenter, at 27 km, and is instrumented with 21 data channels of acceleration. Horizontal accelerations at the crest, downstream and left abutment from the recorders peaked at 0.39, 0.26, and 0.08 g, respectively. These records were studied for determination of the long-period content remaining relatively noise-free.

Records from the Loma Prieta earthquake are compared with records from earlier earthquakes affecting the dam.

Results

A comparison of the Fourier amplitude spectra of the left abutment, 243° component, with that of a reference trace from the same film, processed in the same way, shows that these spectra have barely merged at periods as long as 40 sec, a time interval equal to the digitized record length. At a period of 10 sec, equal approximately to the estimated rupture duration, there is at least an order of magnitude between these spectral ordinates.

Ten-second waves crossing the array of instruments associated with this dam remain remarkably coherent. Having displacement amplitudes of 12 cm, the errors remain less than 1 cm, in accordance with estimates of displacement accuracy made from digitization tests. There is a significant change in the natural frequencies from one event to the next, with magnitudes 5.8, 6.2, and 7.1.

Reports

Brady, A.G., and Fedock, J.J., 1990, Analysis of strong motion records from Leroy Anderson Dam, central California: *U.S. Geological Survey Open-File Report 90-480*, 74 p.

10/90

Branch of Engineering Seismology and Geology Computer Project

9910-02085

Howard Bundock
Branch of Engineering Seismology and Geology
U. S. Geological Survey 345 Middlefield Road, MS 977
Menlo Park, California 94025
(415) 329-5621, FTS 459-5621

INVESTIGATIONS

The objectives of the Branch of Engineering Seismology and Geology Computer Project are to:

Maintain a strong capability for the processing, analysis and dissemination of all strong motion data collected on the National Strong Motion Network and data collected on portable arrays;

Support research projects in the Branch of Engineering Seismology and Geology by providing programming and computer support including digitizing, graphics, processing and plotting capabilities as an aid to earthquake investigations;

Manage and maintain computer hardware and software so that it is ready to process data rapidly in the event of an earthquake.

The Branch facilities include a VAX 8250 running VMS version 5.02 and a VAX 11/750 computer operating under VMS Version 4.6, a PDP 11/70 running RSX-11M+ and a PDP 11/73 computer. The Branch computers are part of a local area network with other Branch, OEVE, Geologic Division, and ISD computers, and we have access to computers Survey-wide over Geonet. Project personnel join other office branches in the support of the OEVE VAX 11/785.

Investigations during the last six months of FY90 included resuming the installation of network hardware and software for linking Branch members' PCs and MacIntosh microcomputers to the VAXes. This work is being done for terminal emulation, file transfer and shared disk and plotter capabilities. Work was done in conjunction with Office scientists to collect and map seismic and other earth science instrumentation and marker stations in the Bay Area. Wide Area Network connection software was installed on Office computers for access to Internet for use of electronic mail and other functions. The project joined in planning the reorganization of Office computer facilities and joined in the reorganization and upgrade of computer systems within the Branch. As an ongoing policy, we have kept our hardware up to current revision levels, and operating system, network, and other software at the most recent versions possible.

RESULTS

As a result of these and previous investigations, the project has:

Connected all Branch members microcomputers to the Local Appletalk network for access to VAXes and shared resources,

Completed collecting a database of seismic and other stations in the Bay Area and California, and compiled maps of that data,

Installed network software on Office computers for use of scientists needing access to Internet and electronic mail, and access to VAX resources from Unix machines,

Completed plans for reorganization of Office computing, including transferring ownership of the Office VAX 11/785 to Seismology Branch, and insuring that all Office scientists will have access to computer resources,

Joined with ESG Branch members in the completion of plans and ordering of new equipment for replacement of old computer technology with the latest in minicomputer processing and storage systems.

The project managed and maintained the OEVE VAX 11/785, and

Managed, maintained, updated Branch and Office computer system hardware and software.

REPORTS

None

Structural Analysis

9910-02759

Erdal Şafak and Mehmet Çelebi
Branch of Engineering, Seismology, and Geology
U.S. Geological Survey
345 Middlefield Road, MS 977
Menlo Park, California 94025
(415)-329-5648, FTS 459-5648

Investigations

1. Analyses of seismic recordings obtained from instrumented structures during the October 17, 1989 Loma Prieta earthquake.

Results

1. Full set of records from six extensively instrumented structures (five buildings and one dam) have been obtained during the October 17, 1989 Loma Prieta earthquake. The analyses of data from two of the buildings, the pyramid-shaped 60-story Transamerica Building and the tree-winged (Y shaped) 30-story Pacific Park Plaza building have been completed. Analyses for the remaining structures are in progress.

Reports

Çelebi, M., and Şafak, E., 1990, Recorded response of Transamerica Building: Part I- Data and preliminary analysis, *Journal of Structural Engineering*, ASCE, submitted for publication.

Şafak , E., and Çelebi, M., 1990, Recorded response of Transamerica Building: Part II- System identification, *Journal of Structural Engineering*, ASCE, submitted for publication.

Çelebi, M., and Şafak, E., 1990, Recorded response of Pacific Park Plaza: Part I- Data and preliminary analysis, *Journal of Structural Engineering*, ASCE, submitted for publication.

Şafak , E., and Çelebi, M., 1990, Recorded response of Pacific Park Plaza: Part II- System identification, *Journal of Structural Engineering*, ASCE, submitted for publication.

Şafak , E., and Çelebi, M., 1990, Analyses of recorded responses of two high-rise buildings to Loma Prieta main shock, *Special Issue, Bull. Seis. Soc. Am.*, submitted for publication.

Çelebi, M., Şafak, E., 1990, Study of earthquake records from selected tall buildings (invited paper), *proceedings*, Tall Buildings Conference, Hong Kong, November 1990.

Physics of the Earthquake Process

9910-01915

D. J. Andrews
Branch of Engineering Seismology and Geology
U.S. Geological Survey
345 Middlefield Road, MS 977
Menlo Park, California 94025
(415) 329-5606

INVESTIGATIONS

Tectonic modeling of the San Francisco Bay Region.

RESULTS

A numerical iterative method has been developed to find quasistatic flow fields with a nonlinear creep law. No results have been found yet. Planned work is described below.

The long-term average state of stress in a region around a strike slip fault will be examined in a thermoplastic model. The stress fluctuation in an earthquake cycle will be ignored. A nonlinear temperature-dependent creep law with parameters appropriate to the material at different depths will be used throughout a two-dimensional cross secton through the fault. In addition, stress will be limited on the fault by a small constant coefficient of friction. Boundaries will move with plate velocities. The coupled problem of material flow and heat flow will be solved to find velocity, stress, and temperature throughout the 2-D cross section. The calculation will provide stress as a function of depth on the fault, reduction in shear stress approaching the fault due to basal traction, and heat flow as a function of position on the surface. A symmetric region around a strike slip fault will be modeled first, and then perhaps the evolution of the slabless window after the passage of the Mendocino triple junction will be modeled.

Ground Motion Prediction for Critical Structures

9910–01913

D. M. Boore
W. B. Joyner

Branch of Engineering Seismology and Geology
U. S. Geological Survey
345 Middlefield Road, MS 977
Menlo Park, California 94025

Investigations:

1. Develop equations for the ground motion at soil sites in ENA.

Results:

Equations giving ground motion as a function of magnitude and distance at rock sites in the central and eastern United States were recently published by Atkinson and Boore (1990). We have extended their work to a generic, deep soil site (soil thickness greater than 60 m). We first used a "quarter-wavelength" approximation first proposed by Joyner and Fumal to derive frequency-dependent amplification factors. We then computed theoretical ground motions for a suite of distances and magnitudes, using the stochastic model (e.g., Joyner and Boore, 1988). Finally, we used a two-stage regression to determine coefficients of the attenuation relation. We anticipate that these equations will find use in constructing probabilistic ground-shaking maps.

Reports:

Atkinson, G. M. and D. M. Boore (1990). Recent trends in ground motion and spectral response relations for North America, *Earthquake Spectra* **6**, 15–35.

26 September 1990

ANELASTIC WAVE PROPAGATION

9910-02689

Roger D. Borcherdt
Branch of Engineering Seismology and Geology
U.S. Geological Survey
345 Middlefield Road, MS 977
Menlo Park, California 94025
415/329-5619

Investigations

Interpretation of strong-motion and aftershock recordings of the Loma Prieta earthquake of October 17, 1989, with respect to influence of local geologic deposits and crustal structure on ground motions in the San Francisco Bay region.

Results

Damage and consequent loss of life in the San Francisco Bay region, from the Loma Prieta, California, earthquake of October 17, 1989, was concentrated in areas underlain by thick sections of fill, bay mud, and alluvium. Recordings of strong ground shaking generated by the earthquake show that in general the amplitude and duration of peak acceleration, velocity and displacement increase with decreasing firmness of the geologic deposits, with the increases for horizontal motion in general exceeding those for vertical motion. The largest amplifications with respect to the mean for sites on rocks of the Franciscan Complex consistently occur for the radial component of horizontal motion. Spectral ratios show the existence of predominant site periods with peak amplifications over narrow period bands of up to 15 for some sites on alluvium and bay mud. Short duration and coherent transverse motions on rock sites in the San Francisco-Oakland area are consistent with relatively simple short-duration source-time functions inferred from teleseismic data. Theoretical amplitude distributions calculated for a 10-layer anelastic model suggest that the dominant coherent transverse bedrock motion observed in the San Francisco-Oakland area exceeded previously derived empirical relations due to the wide-angle reflection of *SH* from the base of a relatively shallow (25 km) continental crust. Consistency between model results and observed dominant transverse motions suggest that the amplification effects of soft soil deposits and the efficient reflection of seismic energy from the base of the earth's crust were major contributors to levels of ground motion sufficient to cause damage to vulnerable structures and consequent loss of life in the cities of San Francisco and Oakland at distances near 100 km. Intensity increments ascribed for soft-soil sites with respect to sites on Franciscan rocks for the Loma Prieta earthquake are consistent with those predicted using 1906 California earthquake observations and low-strain amplification measurements.

Reports

Borcherdt, R.D., and Donovan, N.C., 1990, Geosciences overview, in Loma Prieta Earthquake Reconnaissance Report, *Earthquake Spectra*, suppl. v. 6, 448 p.

Glassmoyer, G., and Borcherdt, R.D., 1990, Source parameters and effects of bandwidth and local geology on high-frequency ground motions observed for aftershocks of northeastern Ohio earthquake of 31 January, 1986: *Bulletin of the Seismological Society of America*, v. 80, p. 889-912.

Borcherdt, R.D., 1990, Influence of local geology on ground motions generated by the Loma Prieta earthquake of October 17, 1989: International Symposium of Safety of Urban Life and Facilities, Proceedings, Tokyo Institute of Technology, Tokyo, Japan.

Borcherdt, R.D., and Glassmoyer, G., 1990, Local geology and its influence on strong motion: National Conference on The Loma Prieta Earthquake — One Year Later, Proceedings, Bay Area Regional Earthquake Preparedness Project, Oakland, CA.

Hough, S.E., Simpson, D., Lerner-Lan, A., Friberg, P.A., Busby, R., Shengold, L., Tuttle, M., Field, E.H., Jacob, K.H., Pacheco, J., Estabrook, C., Peterson, M., Johnson, D.H., Borcherdt, R.D., and Frankel, A., 1989, Observations of weak ground motion in the epicentral area and in west Oakland following the Loma Prieta earthquake of October 17, 1989, in Loma Prieta Earthquake Reconnaissance Report, *Earthquake Spectra*, suppl. v. 6, 448 p.

Hough, S.E., Friberg, P.A., Busby, R., Field, E.F., Jacob, K.H., and Borcherdt, R.D., 1990, Sediment induced amplification — A possible factor in the collapse of the Nimitz freeway during the October 17, 1989 Loma Prieta (CA) earthquake: accepted by *Nature*.

10/90

Prediction of Strong Ground Motion in Sedimentary Basins Using Numerical Simulations

9910-04482

A. Frankel

Branch of Engineering Seismology and Geology
U.S. Geological Survey
345 Middlefield Rd., MS 977
Menlo Park, CA 94025
(703) 648-4119

Investigations

1. Analyze recordings of Loma Prieta aftershocks from a dense array deployed in Sunnyvale (Santa Clara valley) shortly after the mainshock. Determine the characteristics of short-period surface waves produced by these aftershocks. Model the waveforms of the aftershocks and the mainshock for sites in the Santa Clara valley using 2-D and 3-D finite difference codes. Assess importance of short-period surface waves to seismic shaking in sedimentary basins.
2. Develop methods to discriminate anelastic from scattering attenuation. Apply these methods to recordings of earthquakes in New York State, South Africa and southern California.
3. Use a self-similar model of complex rupture to quantify the relationship between the high-frequency spectral fall-off of an earthquake and the scaling of strength on a fault.

Results

1. Slowness analysis of a M4.4 aftershock of the Loma Prieta earthquake using the Sunnyvale dense array indicates that surface waves dominate the seismograms for times greater than 7 sec after the S-wave. These surface waves produced the peak amplitude of the seismograms for periods of 2 sec and longer and account for the increased duration of shaking at the Sunnyvale site relative to stations at similar distances on rock. 2-D finite difference simulations for the Santa Clara valley demonstrate how these surface waves can be generated by conversion of S-waves incident on the edge of the valley. Strong motion records of the Loma Prieta mainshock indicate that surface waves produced the peak velocities and displacements for some sites in the Santa Clara valley.

2. Scattering attenuation in the crust is estimated by measuring the increase with distance of high-frequency energy in the coda relative to that in the direct wave. Anelastic attenuation is determined from the relative time decay of low and high-frequency energy in the coda. These procedures invoke the energy flux model of coda. Using these methods, the attenuation of 3-15 Hz L_g waves in New York State (Δ=100–350 km) is found to be caused equally by anelastic and scattering attenuation. The attenuation of local S-waves in South Africa (Δ=5–80 km) is found to be dominated by scattering. Anelastic attenuation is determined to be stronger for southern California than for New York and South Africa.
3. A model of complex rupture is developed that explains why ω^{-2} spectral fall-offs are typically observed for earthquake displacement spectra. This model assumes that the high-frequency energy of an earthquake is produced by sub-events with a self-similar distribution of source radii. These sub-events are themselves earthquakes, containing their own sub-events. Stress on the fault is assumed to be a self-similar function. I find that the exponent γ of the high-frequency fall-off $\omega^{-\gamma}$ equals $2+1.5\eta$, where η is the dependence of static stress drop $\Delta\sigma$ on source radius R, such that $\Delta\sigma \propto R^{\eta}$. Constant stress drop scaling (η=0) leads to ω^{-2} spectral fall-offs. I also show that constant stress drop scaling leads to b-values of one, for aftershocks occurring on a single fault.

Reports

Frankel, A., S. Hough, P. Friberg, and R. Busby, Analysis and modeling of waveforms of Loma Prieta aftershocks recorded on a dense array in Sunnyvale, California, *EOS Trans. Amer. Geophys. Union,* in press.

Frankel, A., A. McGarr, J. Bicknell, J. Mori, L. Seeber, and E. Cranswick, Attenuation of high-frequency shear waves in the crust: measurements from New York State, South Africa, and southern California, *J. Geophys. Res.,* in press.

Frankel, A., Mechanisms of seismic attenuation in the crust: scattering and anelasticity in New York State, South Africa, and southern California, submitted to *J. Geophys. Res.,* 1990.

Frankel, A., High-frequency spectral fall-off of earthquakes, fractal dimension of complex rupture, b-value, and the scaling of strength on faults, submitted to *J. Geophys. Res.,* 1990.

Precise Velocity and Attenuation Measurements in Engineering Seismology

9910-02413

Hsi-Ping Liu
Branch of Engineering Seismology and Geology
U. S. Geological Survey
345 Middlefield Road, MS 977
Menlo Park, California 94025
(415) 329-5643

Investigations

Installation of a vertical seismic array at Winfield Scott School in the Marina District of San Francisco: Amplification of earthquake ground motions occurs where sediment overlies bedrock. The consequence can be catastrophic as in the Loma Prieta earthquake of 1989 in the Marina District of San Francisco where water-saturated artificial-fill sand was liquefied by motions amplified by a thick section of estuarine deposits of sand and clay. Following the earthquake, the U.S. Geological Survey drilled a hole to 91 m depth at Winfield Scott School at Beach and Divisadero Streets. This site was chosen because of the locally heavy damage sustained to structures, pavement, and public works nearby. The soil stratigraphic and engineering properties have been determined from soil samples; *in situ* seismic velocities have been determined from a downhole velocity logging experiment (Kayen *et al.* 1990). A vertical seismic array consisting of three seismometers, one in bedrock (hydrothermally altered Franciscan serpentine) at 88 m depth, one in Pleistocene clay (Old Bay Mud) at 30 m depth, and one located at the surface, is being installed at the school site; local site amplification effects will be studied by analyzing earthquake seismograms recorded by the array.

Results

The 88-m depth seismometer has been emplaced in the borehole drilled for soil investigation; the surface seismometer has been installed at a distance of 2 m from the well head. A separate hole, 30 m deep, has been drilled and cased for the intermediate-depth seismometer, which as of September, 1990, has yet to be installed. Each seismometer consists of three orthogonally-oriented Mark Products L-22D geophones having a natural period of 0.5 s. Because the tilt angle cannot exceed 1.5 degrees for a reasonable coil movement, the horizontal geophones of the downhole units are mounted on a device that can be leveled to 0.1 degrees after emplacement. Local earthquakes (*e.g.,* Atherton Peak, east of Watsonville, $M = 3.0$, $\Delta = 117$ km; North of Fremont, $M = 2.8$, $\Delta = 46$ km; and Halls Valley $M = 3.6$, $\Delta = 89$ km) have been recorded at 200 samples/s on a GEOS digital recorder which triggers on a horizontal component of the seismometer located in bedrock. Compared to motions recorded in bedrock, the peak amplitude of the seismograms recorded at the surface are amplified by a factor of ~ 3.

References Cited

Kayen, R. E., Liu, H.-P., Fumal, T. E., Westerlund, R. E., Warrick, R. E., Gibbs, J. F., and Lee, H. J., 1990, Engineering and seismic properties of the soil column at Winfield Scott School, San Francisco, in *Effects of the Loma Prieta Earthquake on the Marina District, San Francisco, California*, *U. S. Geol. Surv. Prof. Pap. 90-253*, G-1–G-18.

Reports

Liu, H.-P., 1990, Calculation of zero-offset vertical seismic profiles generated by a horizontal point force acting on the surface of an anelastic half-space, *Bull. Seismol. Soc. Am.* , 80, 832–856.

Scaling of Seismic Sources
9910-04488

Art McGarr and John Bicknell
Branch of Engineering Seismology and Geology
345 Middlefield Road, MS 977
Menlo Park, California 94025
(415) 329-5645 or (415) 329-5625

Investigations

1. Seismic data recorded locally, both on the surface and underground, are analzed and modeled to gain insight into the seismic source process, especially with regard to source scaling.

2. Following the October 1989 Loma Prieta earthquake a four-station network of GEOS digital event recorders was operated at the San Francisco International Airport (SFO) to determine the response of various sites there to strong ground motion, especially that of the Loma Prieta mainshock.

Results

1. Fault slip during an earthquake entails a reduction in sheer stress acting on the fault from an initial value σ_1 to a final value σ_2. Denoting the average frictional stress resisting fault slip as σ_f , the overshoot is defined as $(\sigma_f-\sigma_2)/(\sigma_1-\sigma_f)$. An assumption common to many seismic analyses is an overshoot equal to zero; *i.e.*, $\sigma_2 = \sigma_f$. In contrast, a technique for can be used to show that $(\sigma_f-\sigma_2)/(\sigma_1-\sigma_f) \simeq 1/2$. Laboratory observations of strike-slip failure (Lockner and Okabo, 1983)support this conclusion, although the laboratory data show considerable scatter. With regard to source scaling, the extensive ground motion dataset for the 1987 Coalinguq earthquake sequence (McGarr *et al.*, 1990) was recently reanalyzed to highlight changes in scaling as a function of seismic moment. In esence, below the seismic moment M_o, corresponding to the scaling transition, the source radius scales as $M_o^{1/6}$, whereas, above this transition one finds the commonly assumed constant-stress-drop scaling for which the source radius scales as $M_o^{1/3}$.

2. During the first week of November 1989, the period of operation for the SFO network, three large aftershocks with magnitudes M of 4.2, 4.3, and 4.8 were recorded at all four stations, one of which is colocated with the CSMIP strong ground motion recorder of SFO. By comparing aftershock ground motion from site to site, we tentatively conclude that the

peak ground motion of the mainshock (29 cm/s on the east-west component) recorded at the CSMIP station was probably typical for SFO, most of which is situated on alluvium, partly natural and partly manmade. The thickness of the alluvium varies from nearly zero at one GEOS station up to about 150 m. The thickness and composition of the alluvial column beneath a station conditions its seismic response, of course. Compared to the "bedrock" site, the stations situated on alluvium show spectral ratios in the frequency based 0.5 to 3 Hz of as much as 6.

References

Lockner, D.A., and Okubo, P.G., 1983, Measurements of frictional heating in granite: *Journal of Geophysical Research*, v. 88, p. 4313-4320

McGarr, A., 1990, Observations constraining near-source ground motion estimated from locally-recorded seismograms: submitted for publication.

McGarr, A., Mueller, C., Fletcher, J.B., and Andrews, M., 1990, Ground motion and source parameters of the Coalinga earthquake sequence, in Rymer, M.J., and Ellsworth, W.L., eds., 1990, The Coalinga, California, earthquake of May 2, 1983: *U.S. Geological Survey, Professional Paper 1487*, p. 215-234.

Reports

McGarr, A., Bicknell, J., Churcher, J., and Spottiswoode, S., 1990, Comparisons of ground motion from tremors and explosions in deep gold mines: *Journal of Geophysical Research*, in press.

McGarr, A., 1990, Observations constraining near-source ground motion estimated from locally-recorded seismograms: submitted for publication.

Utilization of Electric Well-Log Data to Predict Long Term Slip Rates and Structure in the Loma Prieta Earthquake Zone

Contract 14-08-0001-G1827

R.E. Bischke and J. Suppe

Dept. of Geological and Geophysical Sciences
Princeton University
Princeton, NJ 08544
(609) 258-6769

Investigations

We have examined surface geologic and electric well log (E-log) data from the Loma Prieta area in an attempt to resolve the timing and nature of recent displacements on the San Andreas - Zayante fault system and possible interactions between the San Andreas and Zayante faults . In order to determine the age of the fault motions we studied *growth sediments* within the Purisima Formation that were deposited contemporaneous with fault movements.

Present Results

Evidence for recent deformation is present in the surface geology of the Loma Prieta area. Figure 1, which is generalized from Brabb (1989), shows that the Pliocene Purisima Formation is deformed into the Glenwood and Scotts Valley Synclines where the Purisima Formation enters bends in the San Andreas-Zayante fault system. This geometry is consistent with material moving through left handed (counterclockwise) bends in right lateral faults, and suggests that the San Andreas and Zayante faults were active during the Pliocene.

We have undertaken detailed stratigraphic correlation sedimentary sequences between the Pierce, Light and Blake wells (Section B-B', Figure 1) in order to study the vertical component of deformation within the Zayante fault zone. Correlating these data to water-well logs (Muir, 1972), and surface and subsurface geologic data (Clark and Rietman, 1973) suggests that the Purisima Formation, and perhaps the Santa Margarita Sandstone, are encountered in these wells (Figure 2). Using techniques presented below, cross section B-B' (Figure 2) can be interpreted to indicate that the Zayante fault was very active during the lower Pliocene to upper Miocene (?) and was reactivated in the upper Pliocene at about horizon 9 time (Figure 2, compare Light to Blake data). A close examination of the thickness changes in the sequences between the Pierce to Light wells indicates that differential or relative vertical motions associated with deformation on a fault between the two wells initiated at about horizons 5 to 6 time, or during the upper Pliocene (also see Figure 5). We have called this fault informally the Pleasant Valley branch of the Zayante fault system. As the Pleasant Valley fault was active while the Purisima Formation was being deposited it is a *growth* or *contemporaneous fault*, in direct analogy with expansion faults in the Gulf of Mexico (Thorsen, 1963; Tearpock and Bischke, 1991).

These relationships suggest a new method for studying the fine details of the growth or contemporaneous faulting. In a pre-growth or stable tectonic environment *change in vertical thicknesses* (Δd) of the sedimentary sequences between wells will be everywhere small (Figure 3). If the age of the strata are known, then a $(\Delta d/t)/t$ diagram can be constructed, which is acceleration. If age date or time information is lacking, then distance domain or $(\Delta d/d_1)$ diagrams can be constructed, where the depth (d_1) is taken relative to the structurally higher well. Therefore, in a pre-growth environment the accelerations in the sedimentation rate are everywhere small.

In an *unstable* or *growth environment* two wells, not on strike of each other, will exhibit larger changes in the thicknesses of the sedimentary sequences (Figure 4), and larger accelerations (or deaccelerations) in the sedimentation rates. In Figure 5 we plot the vertical changes (Δd) in the sedimentary sequences between the Pierce and Light wells relative to their corresponding correlative sequences in the structurally higher Pierce well, or on a $\Delta d/d$ diagram. This diagram shows that a pre-growth or stable environment existed between Pierce and Light prior to the deposition of horizon 6 (upper Pliocene). The younger vertical motions may have continued at nearly constant rates into the present, as shown by the change in topography across the fault (Figure 5). A similar diagram constructed for the Light and Blake wells (Figure 6) suggest the following growth history or vertical deformation path. Deformation paths are obtained by integrating the $\Delta d/d$ diagram and can be shown to be

$$\text{Deformation Path} = \ln(1 + \Delta d/d)$$

This approach indicates that the Zayante fault experienced large vertical displacements near the base of the Pliocene (horizons 17 to A, Figure 2) which deaccelerated during the middle Pliocene (at about horizon 9), and then grew more rapidly during the upper Pliocene and lower Pleistocene. Therefore, the Zayante fault appears to have experienced vertical displacements as well as strike-slip displacements, which is consistent with the Loma Prieta focal mechanisms solution and geodetic data (McNalley et al., 1989). Total relative uplift rates since the upper Pliocene are small however, and are on the order of $200\ \text{m}/2 \times 10^6\ \text{yrs} = 0.1$ mm/yr between the Pierce and Blake wells.

Our regional studies of the Zayante fault indicate that strike slip displacements along most portions of this fault are much larger than the dip slip displacements. However, even in the case of pure strike slip a regional slope (i.e. undulations) on the pre-growth or basement surface will create vertical displacements between the laterally displacing fault blocks. Well log data is able to resolve any vertical displacements resulting from lateral or dip slip motion and determine the onset and duration of structural deformation.

References

Brabb, E.E., 1989. Geologic map of Santa Cruz county, California, USGS Map I-1905.

Clark, I.C. and Rietman, J.D., 1973. Oligocene stratigraphy, tectonics and paleogeography southwest of the San Andreas Fault, Santa Cruz Mountains and Gabilan Range, California Coast Ranges, USGS Prof. Paper 783.

McNally, K.C., Lay, T., Protti-Quesada, M., Valensise, G., Orange, D. and Anderson, R.S., 1989. Santa Cruz Mountains (Loma Prieta) Earthquake, EOS, v. 70, no. 45, p. 1463 and 1467.

Muir, K.S. 1972. Geology and ground water of the Pajaro Valley area, Santa Cruz and Monterey counties, California, USGS Open File Report 73-199, p. 1-32.

Tearpock, D. and R. E. Bischke, 1991, Applied Subsurface Geological Mapping, Prentice Hall, N. J., 546p., in press.

Thorsen, C.E., 1963. Age of growth faulting in Southeast Louisiana: Trans. Gulf Coast Assoc. Geol. Soc., v. 13, p. 103-110.

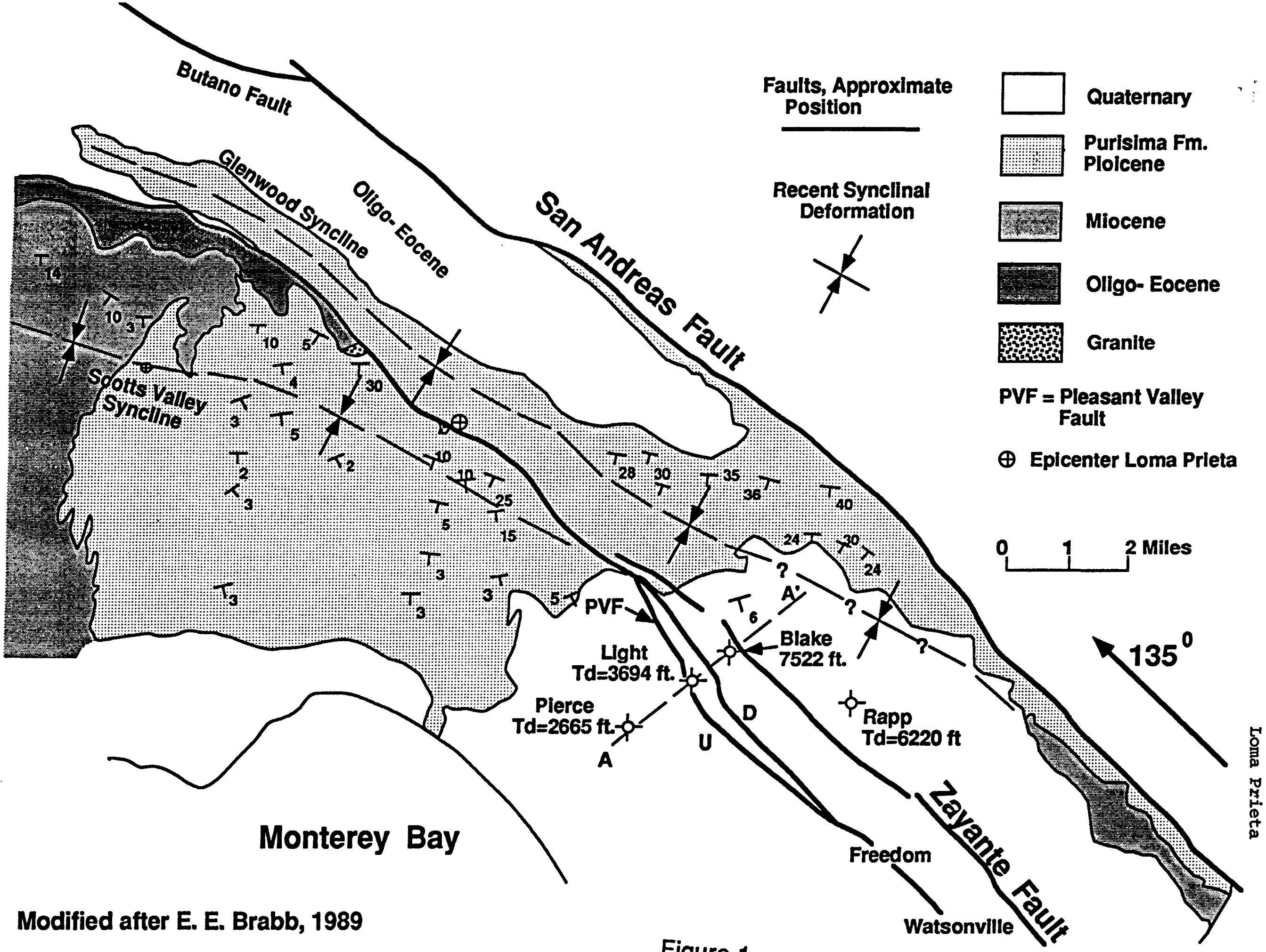

Modified after E. E. Brabb, 1989

Figure 1

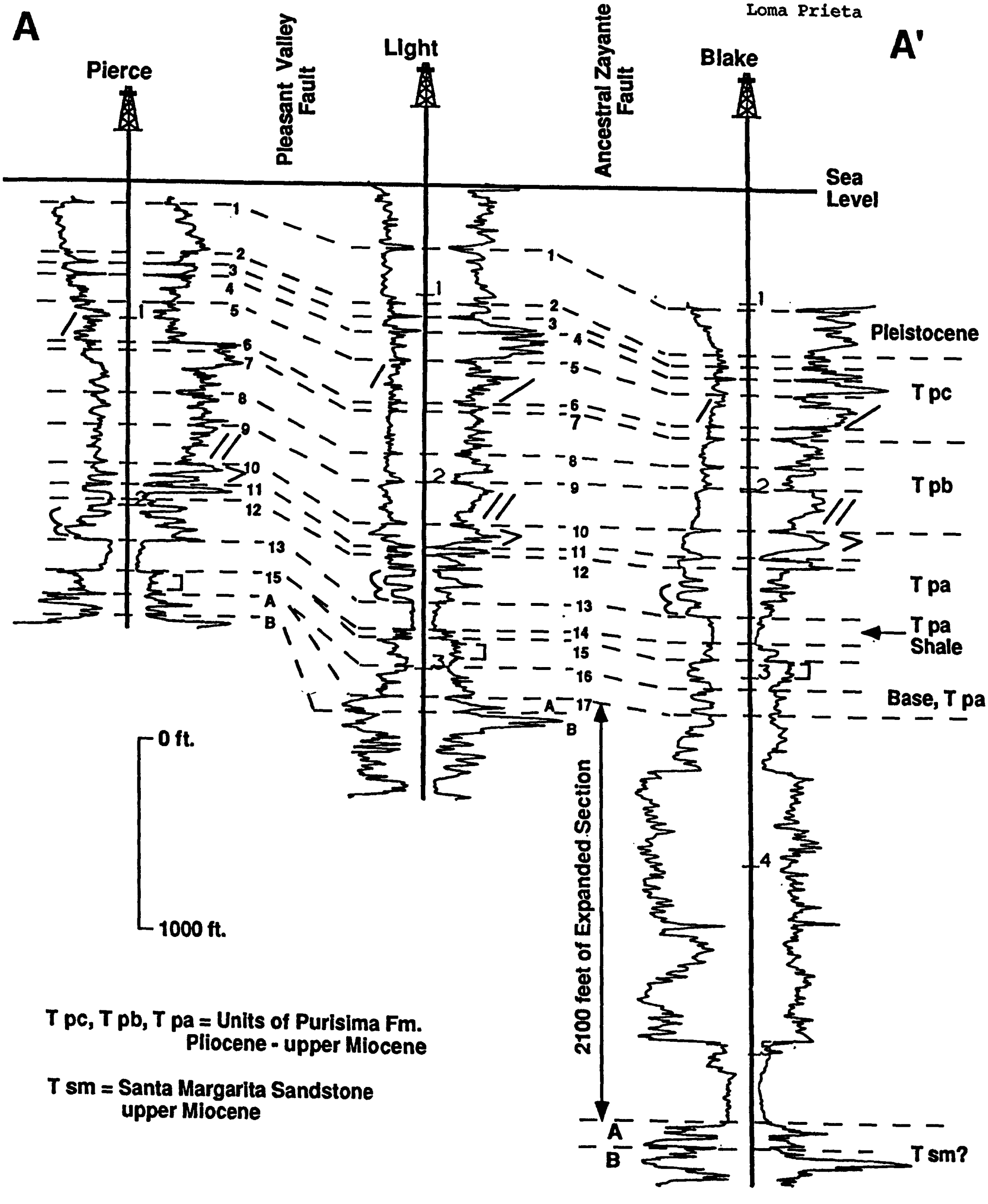
A
Pierce
Pleasant Valley Fault
Light
Ancestral Zayante Fault
Blake
A'
Sea Level
Pleistocene
T pc
T pb
T pa
T pa Shale
Base, T pa
T sm?
1
2
3
4
5
6
7
8
9
10
11
12
13
14
15
16
17
A
B
0 ft.
1000 ft.
2100 feet of Expanded Section
T pc, T pb, T pa = Units of Purisima Fm.
Pliocene - upper Miocene
T sm = Santa Margarita Sandstone
upper Miocene

Figure 2

Stable Tectonic Environment

(Pre-growth Sedimentation)

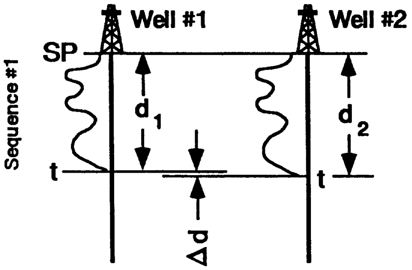

Δd is Small

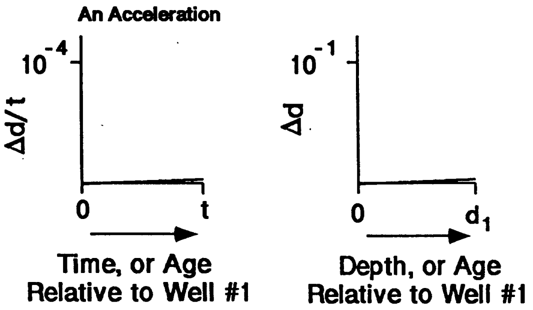

d = Distance or Depth
t = Time

Decreasing Information ⟶

Therefore, Accelerations in Sedimentation Rate or Change in Depth/ Depth Curves are Small

Figure 3

Unstable Tectonic Environment

(Growth Sedimentation)

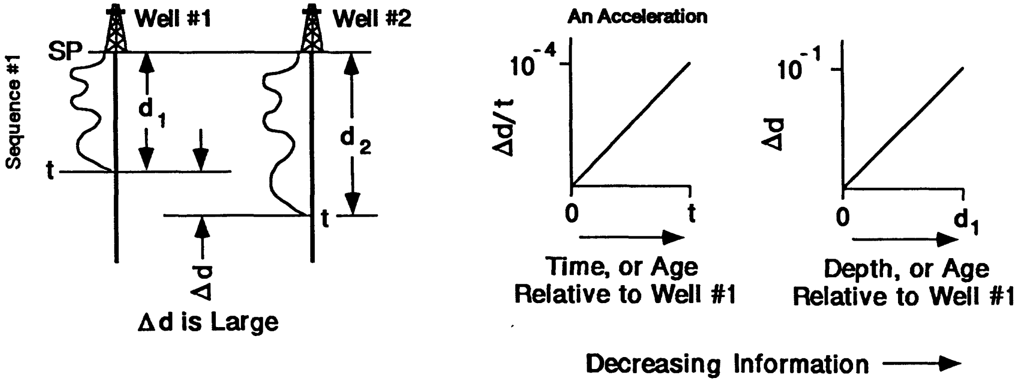

d = Distance or Depth
t = Time

Therefore, Accelerations in Sedimentation Rate or Change in Depth/ Depth Curves are Large

Figure 4

Relative Vertical Displacements between Pierce and Light Wells

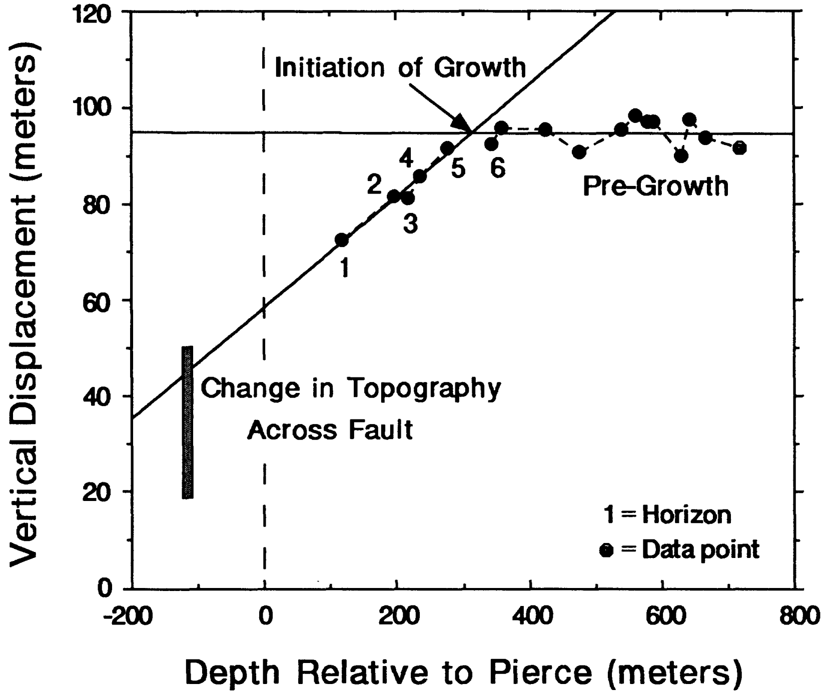

Figure 5

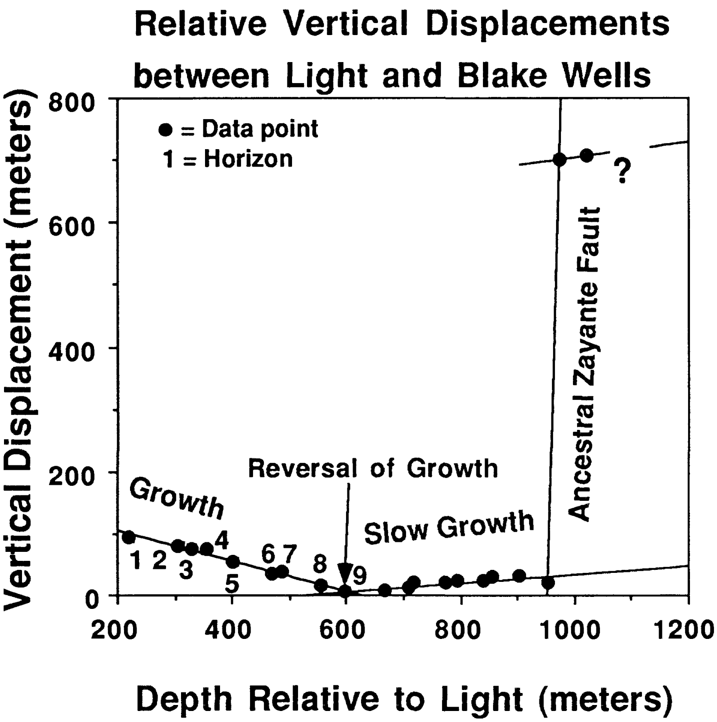
Relative Vertical Displacements
between Light and Blake Wells
Vertical Displacement (meters)
Depth Relative to Light (meters)
800
600
400
200
0
200
400
600
800
1000
1200
● = Data point
1 = Horizon
Growth
Reversal of Growth
Slow Growth
Ancestral Zayante Fault
?
1
2
3
4
5
6
7
8
9

Figure 6

Effects of the Loma Prieta Earthquake on Stream Channel Geometry North of Pajaro Gap

Project No. 14-08-0001-G1866

Deborah R. Harden
Department of Geology
San Jose State University
1 Washington Square
San Jose, CA 95192

(408)-924-5021

Detailed field surveys of two small basins crossing the San Andreas Fault north of Pajaro Gap were made in oreder to evaluate possible effects of the Loma Prieta Earthquake on stream channel geometry. Fern Canyon and Mill Canyon are small tributaries to the Pajaro River located approximately 8 km NE of Watsonville. Both flow across the active trace of the San Andreas Fault (Sarna-Wojcicki and others, 1976) Topographic maps at a 1:500 scale with 2' contour intervals, as well as longitudinal stream profiles with precision of 0.5', were made with a theodolite and EDM.during Feb.-April, 1990. Permanent reference monuments were established so that these channels can be resurveyed following significant runoff events, which are probably required in order to effect channel changes following subtle gradient changes caused by the earthquake.

Fern Canyon formerly flowed WSW directly across the Fault between two compressional ridges It was subsequently ponded in the linear valley east of the ridges and then diverted NW around the northern ridge. Following the 1989 earthquake, ponded water appeared at the head of the abandoned lower canyon of Fern Canyon. In addition, 2 zones of semilinear, subparallel cracks 20 m long with 1-2 cm of SE-side up relief, but with no discernable lateral displacement, were observed at the base of the ridges approximately 2 months after the earthquake.

Fern Canyon's overall gradient (.130) flattens to 0.030 for 200 meters upstream of the fault. A 0.8-m nick point marks the fault trace, followed by a short (18-m) flat reach (0.014 gradient). The canyon is then deeply incised into a headward-incising channel through the compressional ridge. The completed topographic maps are currently being used as base maps for a detailed map of low terraces and gravel bars present on the upstream side of the fault. Grain size analysis and relative dating techniques are being used to correlate and estimate the ages of these deposits, in order to determine possible earthquake-related deposition.

Mill Canyon also shows evidence of drainage disruption along the fault zone. A former channel of Mill Creek is preserved in a small alluviated flat N of the present incised channel. Because of capture by a headward-eroding tributary, the Mill Creek channel presently shows apparent left-lateral offset across the fault. Field observations indicate that the disruption of this drainage probably resulted from landslide activity; the former channel lies downslope of a large complex of landslide scarps. No changes in water level or cracks were observed in this drainage following the 1989 earthquake. Data reduction and map compilation for Mill Creek are still in progress.

Reference Cited

Sarna-Wojcicki, A.M., and other,1976, Map showing recently active breaks along the San Andreas Fault: U.S. Geological Survey, MF-650, scale 1:24,000.

Loma Prieta Aftershocks: Joint 3-D Structure and Hypocenter Inversion for Source Dynamics

14-08-0001-G1840

T.V. McEvilly, B. Foxall, and A. Michelini
Seismographic Station, University of California, Berkeley, CA 94720

INTRODUCTION

We seek an improved interpretation of the complex structure of the Loma Prieta source region, and an improved understanding of the complex dynamics of the source itself, by the application to the aftershock sequence of analysis techniques developed during the last three years in our research program at Parkfield. These techniques are based in part upon an efficient and highly accurate ray-tracing algorithm for fully three-dimensional media (*e.g.,* Cerveny *et*al., 1985), which is used in joint inversion for velocity structure and hypocenter parameters (Michelini and McEvilly, 1990). The velocity model is parameterized in terms of B-splines, which applies smoothness constraints directly on the model. The improved hypocenter locations allow study of the intricacies in the faulting geometry and mechanics of the aftershock sequence. Of particular importance is the fact that the 3-D location results provide the necessary source geometry and takeoff angle required for high-precision study of the source mechanisms of the aftershocks with either first motions or by moment-tensor inversion.

From October 18 (about 24 hours after the mainshock) to December 1, 1989, we operated an array of five temporary stations in the epicentral region. These stations each record six components of ground motion - three high-gain velocity channels and three components of acceleration from FBA instruments - all at 200 samples per second per channel. The network acquired on-scale data from both the large aftershocks and from small events, in order to study point- and extended-source mechanisms, using associated small events as empirical Green's functions to describe the propagation paths in studying rupture histories of the larger aftershocks. Subsequent to our deployment, the IRIS Instrument Center at Lamont, coordinating with our operations, deployed a number of PASSCAL recording instruments (also with high- and low-gain channels) at various sites.

INVESTIGATIONS

1) Modeling studies:
   - Development of fully 3-dimensional P- and S-velocity models for the aftershock region.
   - Relocation of the mainshock, aftershocks, and "background" seismicity through the models.
   - Determination of focal mechanism solutions of selected events.
   - Interpretation in terms of the complex crustal structure of the region.
2) Study of the source dynamics of the aftershock sequence using the 3-D structure and the wide dynamic-range data set.

RESULTS

We have completed processing and archiving the data collected by the small-aperture UCB Santa Cruz Mountains network. The accelerograms and seismograms for each aftershock are collected as 3-component event gathers in simple IEEE binary files. Time corrections for each remote station have been completed. The small dimensions (30x15 km) of the network probably precludes use of the S arrival times read from these seismograms to compute an S velocity model for the hypocentral zone. These data will be used to perform detailed investigations of the source dynamics of selected larger aftershocks. It is hoped that these data can be made available through IRIS.

We have completed the inversion of a set of selected CUSP aftershock data to obtain a 3-D P velocity model of the Santa Cruz Mountains hypocentral region (24 km wide by 64 km along SAF strike). The Loma Prieta mainshock and aftershocks that occurred in October and November, 1989 for which CUSP phase data are available have been relocated through the 3-D model. In addition, we have relocated the $M_L \geq 1.5$ earthquakes contained in the CUSP catalog for our model area for the period, 1984

- Oct 17, 1989. Focal mechanism solutions have been computed for selected events contained within spatially and temporally defined alignments and groups of earthquakes. We are presently in the final stages of a detailed integrated interpretation of the velocity structure, geology and seismicity distribution and mechanisms. This is providing a relatively detailed qualitative description of the mechanics of the 1989 sequence in terms of interaction among the components of the complex fault system within the hypocentral zone, the local stress field, and, in particular, juxtaposition of large-scale rock masses at hypocentral depths. It is this last, vitally important aspect of the description of the hypocentral zone that is uniquely afforded by the relatively well resolved 3-D velocity structure that has resulted from this investigation.

The reliability of the P velocity model (Figures 1 and 2) is indicated by the remarkably close correlation between the shallow velocities and surface geology (Figure 1); for example, thick (~4 km; see, *e.g.*, Aydin & Page, 1984, Fig.3) Eocene marine sediments that outcrop immediately to the SW of the San Andreas Fault correlate closely with a velocity "low" that is elongated along strike in the upper 4 km of the model (Figures 1 and 2). The velocity model also correlates closely with the regional gravity map.

The seismicity distributions before and after the Loma Prieta mainshock that result from relocation through the 3-D model (Figures 1 and 2) are similar to those previously described by Dietz and Ellsworth (1990) and Seeber and Armbruster (1990), although the significantly improved resolution of the 3-D locations allow more confident interpretation of these data in terms of faulting. The position of the seismic gap within which the Loma Prieta earthquake nucleated and of the restraining bend in the SAF, and the complex pattern of faulting within this zone - in particular the junction of the SAF with the Sargent fault - appear to be intimately related to large-scale, high-velocity rock masses on each side of the SAF that come into contact at hypocentral depths here. We are presently in the final stages of a detailed analysis of these relationships.

The focal mechanism of the mainshock computed using the 3-D locations and first motions recorded at close-in CALNET stations is shown in Figure 3. Note that all the data points are consistent with the solution. This pure thrust mechanism is in general agreement with that of the first of two mainshock sub-events tentatively proposed by Romanowicz and Lyon-Caen (1990), based upon modeling of very broadband teleseismic body wave data. This observation has lead us to examine the source dynamics of the Loma Prieta sequence in terms of slip partitioning. This work is continuing.

REFERENCES

Aydin, A. and B.M. Page (1984). Diverse Pliocene-Quaternary tectonics in a transform environment, San Francisco Bay region, California, *Geological Society of America Bulletin*, **95**, 1303-1317.

Cerveny, V. (1985). The application of ray tracing to the propagation of shear waves in complex media, in *Seismic Shear Waves, Part A: Theory*, Gerhard P. Dohr, editor, Geophysical Press, London and Amsterdam, 1-124.

Deitz, L.D., and W.L. Ellsworth (1990). The October 17, 1989, Loma Prieta, California, earthquake and its aftershocks: Geometry of the sequence from high-resolution locations, *Geophysical Research Letters*, **17**, 1417-1420.

Gajewski, Dirk and Ivan Psencik (1990). Vertical seismic profile synthetics by dynamic ray tracing in laterally varying anisotropic structures, *Jour. Geophys. Res.*, **95**, 11,301-11,315.

Michelini, A., and T.V.McEvilly, (1990). Seismological studies at Parkfield: Simultaneous inversion for velocity structure and hypocenters using cubic B-splines parameterization, in press, *Bull. Seis. Soc. Am.*

Romanowicz, B. and H. Lyon-Caen (1990). The Loma Prieta earthquake of October 18, 1989: Results of teleseismic mantle and body wave inversion, *Geophysical Research Letters*, **17**, 1191-1194.

Seeber, L. and J.G. Armbruster (1990). Fault kinematics in the 1989 Loma Prieta rupture area during 20 years before that event, *Geophysical Research Letters*, **17**, 1425-1428.

Papers in preparation

W. Foxall, A. Michelini, A. Lomax, T.V. McEvilly, and P. Williams,
The Loma Prieta earthquake: Structural heterogeneity and source complexity, to be submitted to *Bull. Seis. Soc. Am.*, 1990.

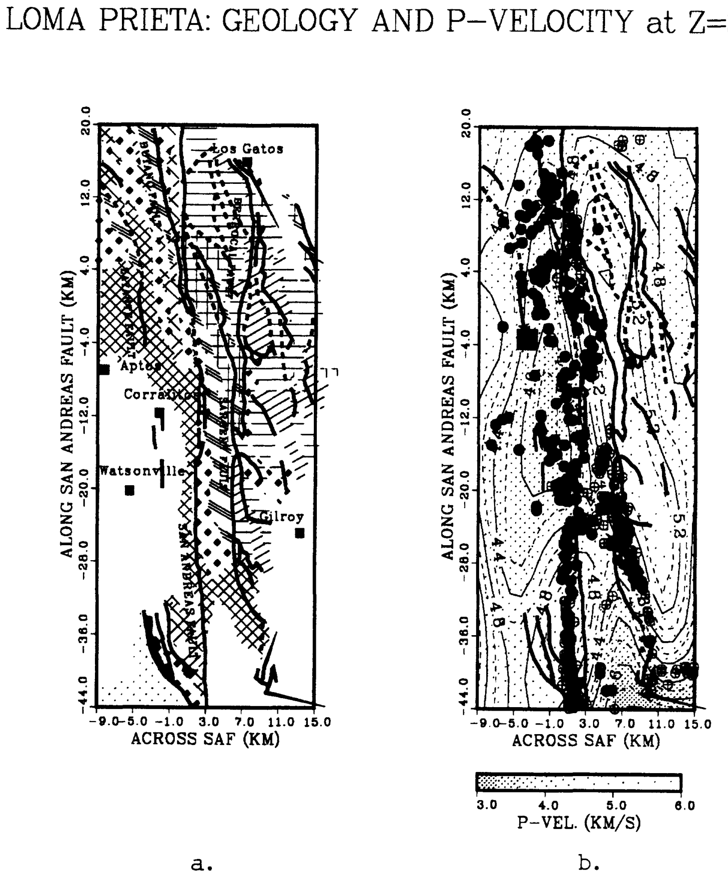

LOMA PRIETA: GEOLOGY AND P-VELOCITY at Z=2 KM

a. b.

Figure 1. Plan view plots of the epicentral area which was object of the 3-D joint velocity and hypocenters inversion: a) schematic geologic map; b) velocity section at 2 km depth with the relocated aftershocks that occurred in October and November 1989 (solid circles), the relocated background seismicity in the period 1984-Oct 17, 1989, (circles with inner cross) and the relocated main shock (solid square). For reference, the y-axis is along the San Andreas Fault.

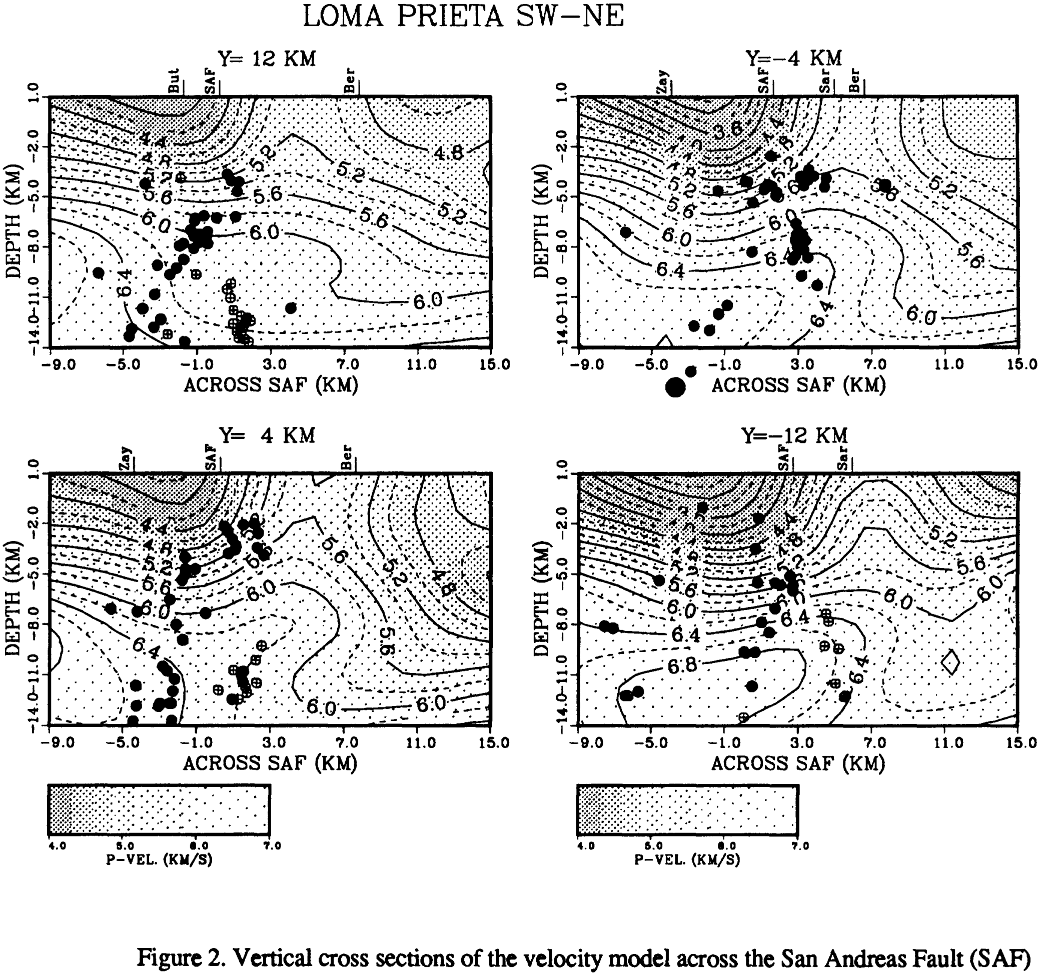

Figure 2. Vertical cross sections of the velocity model across the San Andreas Fault (SAF) with the relocated aftershocks (small solid circles), the background seismicity (circles with inner cross) and the main shock (large solid circle in the section y= -4 km). The y-axis is approximately along the SAF.

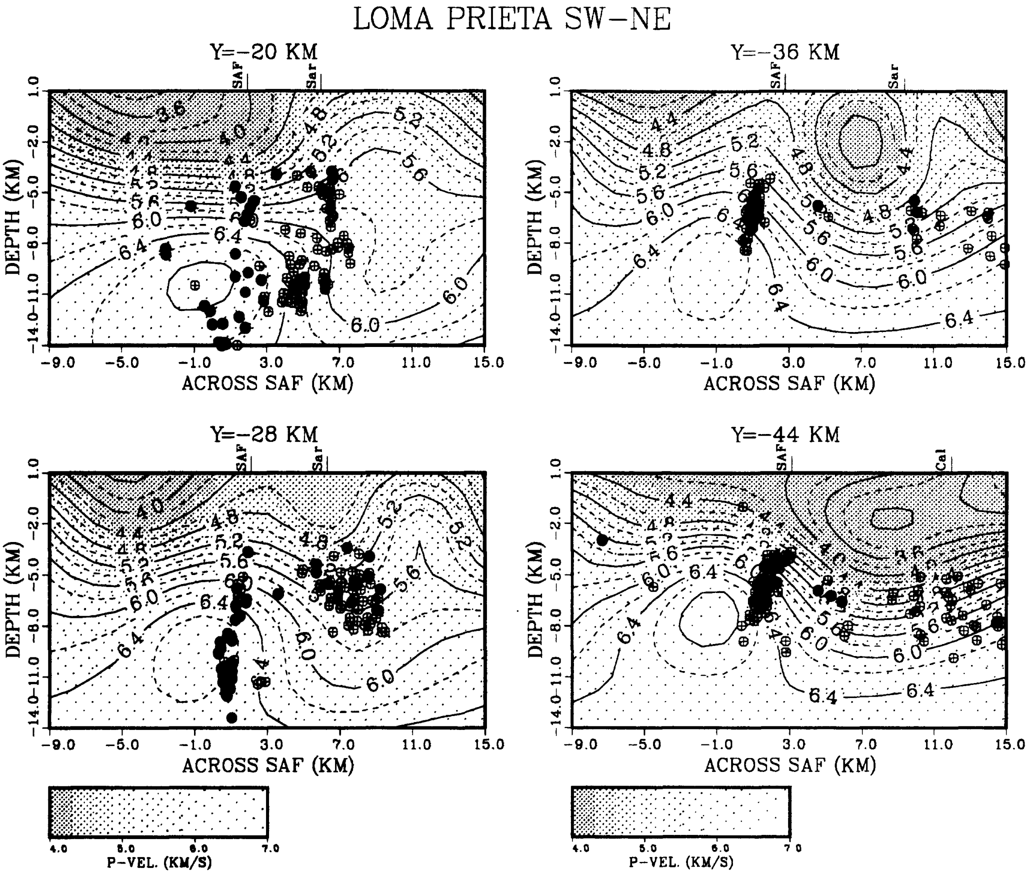

Figure 2 (continued)

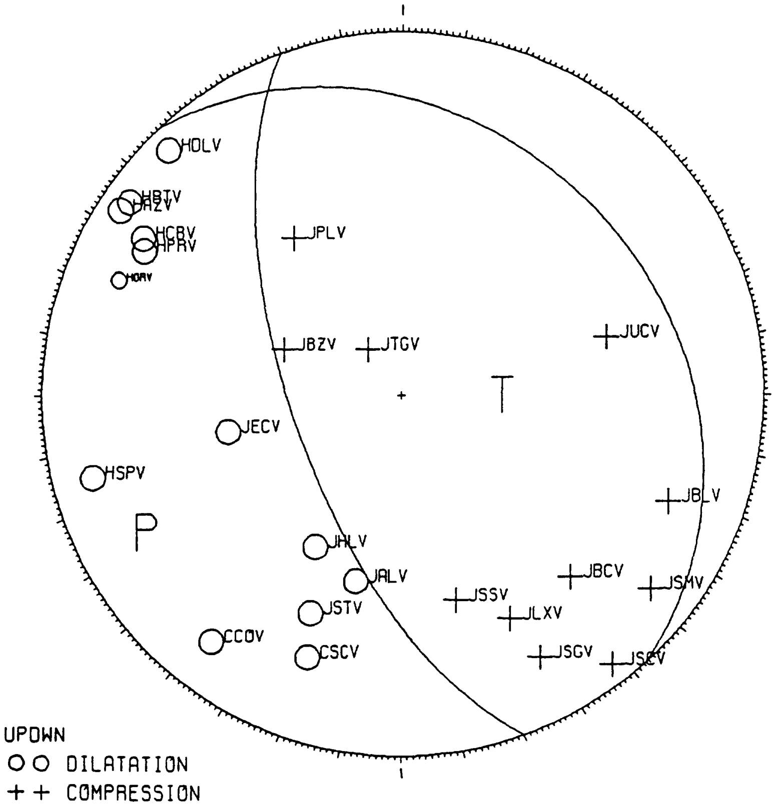

Figure 3. Fault plane solution of the main shock. The take-off angles at the focus are calculated using the 3-D model.

Post-Loma Prieta earthquake investigations: Geology and tectonic framework of southwestern San Francisco Bay Region

9910-04428

*R.J. McLaughlin, J.C. Clark, E.E. Brabb, E.J. Helley
Branch of Western Regional Geology
345 Middlefield Rd., MS 975
Menlo Park, CA 94025

FTS 459-4945 - McLaughlin
FTS 459-5140 - Brabb
FTS 459-4947 - Helley
(412) 357-5622 - Clark

Investigations Undertaken:

Geologic mapping for this project began 2 years prior to the Loma Prieta earthquake, as part of the San Jose 1:100,000 mapping project under the National Mapping program of the office of Regional Geology. At the time of the earthquake in October 1989, geologic mapping in Laurel 7 1/2' quadrangle had just been completed and was being prepared for open-filing. The geology of Loma Prieta 7 1/2 ' quadrangle had been already published in 1988. The Loma Prieta earthquake occurred in October, 1989, and its epicenter, along with most surface deformation fortuitously occurred in the Loma Prieta, Laurel, and Los Gatos quadrangles. In 1990, we have re-mapped the geology of most of the Los Gatos quadrangle, in cooperation with a number of topical post-earthquake investigations undertaken within the U.S.G.S., and through extramural U.S.G.S. and other outside funded projects. Mapping of the region northeast and southwest of the San Andreas and Sargent faults is essentially complete, and bedrock mapping in progress in the northern one-fourth of the quadrangle should be completed in 1991. Active faults such as the Berrocal and Shannon faults, across which shortening occurred during the October 1989 earthquake, will be examined in some detail.

Results of Investigations:

1. The bedrock trace of the main San Andreas fault-that is, the fault which juxtaposes Franciscan basement near or at the surface on the northeast, with an unexposed ($\geq$ 5km) deep, magnetic basement to the southwest, is consistently northeast of geomorphically youthful traces of the San Andreas fault zone. All of the 1906 surface faults in addition to almost all of the cracking and deformation associated with the Loma Prieta earthquake, occurred in the block southwest of the main bedrock trace of the fault, with the exception of deformation along the Sargent fault near Elsman Reservoir, and coseismic deformation along the Berrocal-Shannon fault zone in Los Gatos. This suggests that much of the upward-propagating deformation associated with the Loma Prieta event may have been deflected southwestward, away from the steep southwest-dipping Franciscan basement, into the thicker, softer Tertiary and Neogene sections on the hanging wall side of the San Andreas and Sargent faults.

*Investigation Coordinator

2. Much of the area immediately northeast of the San Andreas fault in the map area consists of a section of moderately thick, highly deformed late Mesozoic and early Tertiary rocks. The rocks in this section include middle and late Jurassic ophiolitic rocks, Late Jurassic to Early Cretaceous and Late Cretaceous deep water clastics, and marine Eocene to Miocene deep water strata. These rocks comprise a fault block bounded and imbricated by steep southwest-dipping faults with complex histories. All of the southwest-dipping faults are superposed on the low-angle Coast Range fault, which everywhere juxtaposes the Franciscan Complex with rocks of the Coast Range ophiolite and Great Valley sequence. Most movement on the Coast Range fault pre-dated the early Eocene and included compressional and extensional deformation. Later steep to moderately low-angle southwest-dipping faults include reverse or thrust faults with components of strike-slip (such as the Sargent, Berrocal, and Shannon faults) and low-angle normal faults. The normal faults are somewhat older, or cogenetic with the compressional faults. Across-fault differences in Miocene stratigraphy, and K-Ar dating of potassic hydrothermal alteration along the Sargent and Berrocal faults suggest that thrusting was initiated about 17-18 Ma, at about the time of passage of the Mendocino triple junction. Some of these faults have youthful geomorphic expression (the Sargent), or exhibit evidence of Quaternary and younger activity (the Shannon) and thus are active. More problematic are west-northwest-trending faults of the same system including the Hooker Gulch fault (which repeats and thickens the stratigraphic section in the same sense as the Sargent fault); the Sierra Azul-Soda Springs fault, which juxtaposes different Franciscan rocks and the Coast Range ophiolite; and the Limekiln Canyon fault, which juxtaposes different units of the Franciscan complex and has some geomorphic expression. All of these faults appear to have post-middle Miocene reverse- and strike-slip components. However, only the Sargent, Berrocal, and Shannon faults exhibit youthful geomorphology and (or) unequivocal evidence of Quaternary offsets.

3. The thick section of Jurassic ophiolite and Late Mesozoic, Eocene and Miocene rocks of the Sierra Azul structural block northeast of the San Andreas fault, is bounded on the northeast by the Soda Springs, Sierra Azul, and Berrocal faults. The rocks within the Sierra Azul block bear strong lithologic affinities and are similar in age to rocks in the Nacimiento structural block southwest of the Salinian block. The Sierra Azul rocks are largely dissimilar to rocks of equivalent age across the San Andreas-Calaveras fault system in the Diablo Range. The exceptions are a fault-bounded block of Eocene rocks along the east side of the San Andreas fault near Tres Pinos; an offset fault-bounded part of the Franciscan Permanente terrane near Chalome and Gold Hill; and another isolated area of distinctive Eocene marine strata near Devils Den and the Point of Rocks. Restoration of displaced Cenozoic volcanic rocks and hydrothermal systems along the San Andreas-Calaveras-Hayward fault system permits about 190 km of Miocene and younger (since 8-12 Ma) right-slip on the Calaveras-Hayward fault system. After Oligocene and younger slip on the San Andreas fault are restored, several hundred kilometers of additional Pre-San Andreas (probably dextral) strike-slip is required to align the Sierra Azul-Tres Pinos-Chalome-Devils Den sections with their apparent continuation in the Nacimiento block.

Reports:

McLaughlin, R.J., Sorg, D.H., Russell, P.C., and Lester, R., Uplift of the Coast Ranges along thrusts east of the San Andreas Fault, San Francisco Bay Region, California: Transform propagation structures?, in Branch Review, 10/5/90, 28 ms pages, 6 figures, 1 table; to be submitted to Tectonics (probably).

McLaughlin, R.J., 1990, Origin of active oblique reverse-slip faults in the region of the Loma Prieta earthquake and their relationship to the San Andreas fault system: Abstract submitted to Fall 1990 AGU meeting.

McLaughlin, R.J., Sliter, W.V., Elder, W.P., McDougall, K., Russell, P.C., Sorg, D.H., Sims J.D., and Blake, M.C., Jr., 1990, 190 km post-middle Miocene offset on the Tolay-Hayward-Calaveras fault system superposed on large-scale Late Cretaceous to Early Eocene translation: Abstracts with Programs, Geological Society of America, v. 22, no. 3, p. 67.

Jachens, R.C., Griscom, Andrew, Blake, M.C., McLaughlin, R.J., and Wentworth, C.M., 1990, Cross fault compression inferred from southwest dips of strike-slip faults in the south San Francisco Bay Region, California: Abstracts with programs, Geological Society of America, v. 22, no. 3, p. 31.

McLaughlin, R.J., 1990, Sargent fault zone of Loma Prieta, field trip stop #4, in: Field trip guide to Neotectonics of the San Andreas fault system, Santa Cruz Mountains, in light of the 1989 Loma Prieta Earthquake, prepared by U.S. Geological Survey staff for Seismological Society of America Annual Meeting, Santa Cruz, CA, U.S. Geological Survey open file Report 90-274, p. 19-21.

Stressing Processes Leading to and Following the Loma Prieta Earthquake

14-08-0001-G1844

J. R. Rice (PI) and R. Dmowska
Division of Applied Sciences and Department of Earth and Planetary Sciences
Harvard University, Cambridge, MA 02138
(617) 495-3445

Issues:

1. What constraints can we place on postseismic stress transfer onto the still locked San Francisco peninsula segment of the San Andreas fault and onto the Hayward and Calaveras faults? If there is measurable postseismic deformation with which to constrain relaxation properties in the lower fault zone and lower crust, where should that deformation be easiest to detect?

2. Are there plausible models for precursory deformation in the hypocentral regions of either the Lake Elsman earthquakes or the main Loma Prieta shock that produce deformation patterns at the earth's surface consistent with the reported geodetic and borehole strain anomalies?

3. Could the inferred locally deep locking depth, as delineated by the spatial distribution of pre-Loma Prieta micro-seismicity (Olson, 1990), and coincident with the Loma Prieta hypocenter, be resolved in the pre-earthquake geodetic data?

Approach:

We are using the finite element method to study 3D models of stressing and deformation associated with the Loma Prieta earthquake. Our primary computational tool is ABAQUS, a general purpose finite element code that allows incorporation of various material properties including elastic and Maxwell viscoelastic. Solution of such 3D problems generally requires use of a supercomputer, to which access is provided by the NSF on Cray XMP and Cray 2 computers at the National Center for Supercomputer Applications, University of Illinois at Urbana-Champaign.

In our preliminary work, we adopted a simplified model in which the Loma Prieta rupture surface was vertical and the focal mechanism was pure strike slip (Linker and Rice, 1990). Those assumptions allowed us to take advantage of symmetry and analyse only one quadrant of the fault model. In our present work, we include fault dip and oblique slip to more accurately represent the Loma Prieta rupture. This added complexity reduces the symmetry of the problem so that we must, in general, analyse all four quadrants of the model, thus increasing the computation time by at least a factor of four. However, in doing analyses with linear Maxwell material models, we make use of superposition and analyze only two quadrants, treating the strike slip and dip slip source components separately, and then add the two solutions to generate the solution to the oblique slip problem. This procedure reduces computation time and also cuts down on memory requirements and the size of output files.

Discussion and Preliminary Results:

Issue 1. In our model of postseismic stress transfer and deformation, the upper and middle crust are represented by an elastic layer, the hotter lower crust by a viscoelastic layer, and the mantle by a much more creep resistant viscoelastic layer. The San Andreas fault is represented by a thin layer in which the deep aseismic region is viscoelastic while the shallower region is either locked or slipped coseismically and then locked (Fig. 1). The coseismic slip is imposed via a transformation strain. In the present work all viscoelastic properties are taken as linear Maxwell. Coseismic slip produces stress throughout the body. With the passage of time, the viscoelastic lower fault and lower crust deform in response to those stresses. This relaxation results in time varying stresses and displacements. In all of the work discussed here, we have ignored the effects of the creeping zone along the San Andreas fault and consider only models that are symmetric along strike about the epicenter.

We have few *a priori* constraints on appropriate material relaxation times t_r (see Closing Discussion), and one aim of our work is to provide the background for constraining them from geodetic measurements. Thus far we have focused on two extreme models: #1) The relaxation time, t_r, for the material of the lower fault zone, down-dip from the now relocked seismic rupture zone, is much much less than for the adjacent material of the lower crust. #2) Lower fault zone t_r equals lower crust t_r.

In generating solutions of stressing and deformation over the entire earthquake cycle, one seeks solutions that are steady state in the sense that consecutive earthquakes yield identical stress and deformation histories. Generally, this "preconditioning" of the model is done by subjecting the model to repeated characteristic earthquakes until the solution becomes periodic. In the case of the Loma Prieta earthquake, this strategy may be difficult to attain with any confidence.

Several workers have argued that the Loma Prieta earthquake is not a characteristic event for this segment of the San Andreas fault (Anderson, 1990; Segall and Lisowski, 1990). Perhaps then, in the most general treatment of the postseismic effects of the Loma Prieta earthquake, one should first precondition the model with a sequence of 1906 earthquakes, if indeed the 1906 event is characteristic for the region.

In our work, we have avoided this complication, to the degree possible, by limiting our models to those with linear material properties. This restriction allows us to use superposition, so that our solution variables, stress and displacement, are those that should be added to the time histories that would have been present in the absence of the Loma Prieta earthquake. The effective t_r inferred by fitting geodetic data to such a linear model must, however, be understood to physically reflect the response of a nonlinear creep process to stress changes resulting from the Loma Prieta earthquake.

We present results from two simulations. In the first, to examine the stress field resulting from the Loma Prieta earthquake after substantial relaxation has occurred, we approximate relaxation of the lower crust and lower fault by assigning a low shear modulus to those regions. In the second, to examine the time history of the displacement field that develops during relaxation, linear viscoelastic material properties are assigned to the lower crust and lower fault.

In the elastic model, the low shear modulus assigned to the lower crust and lower fault is chosen to be 1% of the value that is assigned to the remainder of the crust and fault zone, 30,000 Mpa. Poisson's ratio is likewise chosen for the relaxing regions so that the bulk modulus is uniform. The faulting parameters are those determined to best fit the observed geodetic data with a single dislocation, dip = 64 degrees, strike slip = 1.7 m, reverse slip = 1.2 m, depth extent of rupture 5 to 17.5 km (Lisowski et al., 1990a). In an effort to smooth out the irregularity in the solution that results from the coarseness of the finite element mesh, we taper the imposed transformation strain to zero in the outermost elements of the rupture zone while adjusting the nominal transformation strain so that the net moment remains constant. In addition, the shear modulus in those outermost elements is set to the same 1% value of shear modulus that is assigned to the relaxing regions.

We summarize our observations from this first simulation in terms of changes in the strike slip component of shear traction on the San Andreas fault along the San Francisco peninsula, vertically averaged in the seismogenic layer.

- Both the coseismic and additional postseismic stress changes are largest close to the end of the rupture zone, 20 to 40 km from the epicenter. Here, postseismic deformation may result in additional stress transfer that is comparable to the coseismic stress change. However, the finite element mesh that we are currently using is too coarse to resolve details in the stress field within this region.
- The ratio of postseismic to coseismic stress change increases with distance from the end of the rupture. As noted by Rice and Gu (1983), this tendency occurs because dislocation-induced stresses in a plate with shear-free base fall off more slowly with distance than for a competent half space.

- Beyond about 30 km from the NW end of the rupture, about 50 km from the epicenter, the effect of the Loma Prieta rupture on the strike slip component of shear traction is less than 1 bar, even after substantial relaxation in the lower fault zone and lower crust has ocurred.

The predicted values of strike slip shear traction are listed in the following table.

Horizontal Shear Traction at 6 km Depth Induced by the Loma Prieta Earthquake on Vertical Plane Coincident with San Andreas Fault along the San Francisco Peninsula:

Distance along strike from epicenter	38 km	51 km	71 km
Coseismic	0.77 bars	0.23 bars	0.07 bars
Fully relaxed lower fault zone	1.09 bars	0.41 bars	0.12 bars
Fully relaxed lower crust	1.43 bars	0.67 bars	0.25 bars

The time scale to attain the fully relaxed limits is many times the presently unknown t_r and therefore, may be impractically long compared to recurrence intervals.

In our second simulation, which includes linear Maxwell viscoelastic material properties, only the lower fault is allowed to relax, i.e. model #1 at times before significant relaxation of the lower crust has occurred. As in the previous example, the fault dip is 64 degrees and the rupture extends over the depth interval from 5 to 17.5 km. The imposed transformation strain differs slightly from the previous example in that the equivalent slip vector corresponds to 1 m of strike slip and 1 m of reverse slip. Furthermore, the transformation strain and shear modulus are uniform in the rupture.

Since the coseismic rupture does not extend to the earth's surface, we have greater confidence in the computed surface displacement field near the rupture than we do in the computed shear tractions near the rupture that were discussed previously for the elastic model. We present computed displacement profiles at four positions along strike corresponding approximately to the middle of the Loma Prieta rupture (x3=0), its NW end (x3=L/2), one rupture length from mid-rupture (x3=L), and one rupture length from the NW end of the rupture (x3=3L/2). The first and third positions correspond, respectively, to the approximate locations of the USGS and Stanford GPS linear arrays, which extend a few tens of km either side of the San Andreas fault.

In Figure 2, we plot fault parallel displacement versus distance from the fault trace for two times following the earthquake. The coseismic displacement profiles are indicated by the solid curves and profiles at times equal to $5t_r$ and $20t_r$ are indicated by the dotted and dashed curves, respectively.

According to the example presented here, postseismic deformation will be greatest in the region within one rupture length of the San Andreas fault and within about 20 km of the NW end of the Loma Prieta rupture. Though not plotted on the figure, the displacement profiles for $1t_r$ esentially overlie the coseismic profiles. Therefore, we can safely conclude that postseismic deformation resulting from deep fault slip, as included in our model, will not yield detectable signals until at least $5t_r$.

Issue 2. Anomalous changes in deformation rate have been reported to precede the Loma Prieta earthquake (Lisowski et al., 1990b; Johnson et al., 1990). The timing of these changes coincides approximately with the first of two M 5 Lake Elsman foreshocks (June 1988, August 1989) whose hypocenters are about 10 km NW from the main shock hypocenter. We are testing the hypothesis that the observed anomalies were associated with deformation in the vicinity of either the Lake Elsman or Loma Prieta hypocenters.

The predicted coseismic strain at the earth's surface resulting from the Lake Elsman events, based on dislocation models, is less than any change that could been detected on the existing deformation instruments. Therefore, if the observed anomalies indeed resulted from slip at hypocentral depths, then that slip must have been in addition to the amount released coseimically in the foreshocks, and may have greatly exceeded it.

Our procedure involves imposing a transformation strain of specified orientation in the hypocentral regions and comparing the resulting deformation at the earth's surface to that observed as the anomalous signal. To date, we have no results to report.

Issue 3. The distribution of micro-earthquakes that occurred prior to the main shock as well as the depth of the main shock hypocenter and its aftershocks, indicates that the Loma Prieta rupture was the sight of a locally depressed locking depth (see for example Olson, 1990). Tse et al. (1985) have shown, theoretically, that a localized deepening of the base of the locked region, in a fault zone that otherwise slips freely, can cause an elevated stress concentration there. We are testing whether such variation in locking depth might have been detectable geodetically.

The deep fault, below the locked depth indicated by the pre-shock microearthquake distribution, was presumed to be vertical in a first analysis of this issue (Rice, 1990). The preliminary conclusion is that the signature at the earth's surface of the locally deepened locked patch would have been too subtle to detect. This conclusion, however, is sensitive to the degree of relaxation in the lower fault and lower crust, an issue that is addressed further in item 1 and again in the last section of this report.

Closing Remarks:

It is important to emphasize that our conclusions regarding Issues 1 and 3 will be strongly dependent on our choice of values for t_r. In the case of Issue 1, both the magnitude and time scale of postseismic stress transfer and deformation will depend directly on t_r. Similarly, in the case of Issue 3, the magnitude of any geodetic signature of nonuniform locking depth along strike will depend on the degree to which the lower crust is relaxed. Our primary route to constraints on t_r must come from fitting our model predictions to whatever postseismic deformation is recorded in the region. We also attempt to constrain t_r by considering laboratory derived constitutive parameters in conjunction with estimates of the geotherm. In addition, we consider earlier estimates of t_r based upon 2D models that are intended to represent the entire seismic cycle (Li and Rice, 1987; Fares and Rice, 1988).

References:

Anderson, R. S., Evolution of the northern Santa Cruz mountains by advection of crust past a San Andreas fault bend, *Science*, *249*, 397-401, 1990.

Fares, N. and J. R. Rice, Crustal deformation modeling for San Andreas fault earthquake cycles, abstract T32B-07, *AGU Fall Meeting Program*, p. 149, 1988.

Johnston, M. J. S., A. T. Linde and M. T. Gladwin, Near-field high resolution strain measurements prior to the October 18, 1989, Loma Prieta ML 7.1 earthquake, *Geophys. Res. Lett.*, *in press*, 1990.

Li, V. C. and J. R. Rice, Crustal deformation in great earthquake cycles, *J. Geophys. Res.*, *92*, 11,533-11,551, 1987.

Linker, M. F. and J. R. Rice, Constitutive parameters for crust and fault zone materials and their relationship to temporal patterns of deformation following plate rupturing earthquakes, presented as NSF-USGS Workshop on Crustal Deformation Measurement and Earthquake Mechanics, Morro Bay, 1990.

Lisowski, M., W. H. Prescott, M. J. Johnston and J. C. Savage, Geodetic estimate of coseismic slip during the 1989 Loma Prieta, California, earthquake, *Geophys. Res. Lett.*, *17*, in press, 1990a.

Lisowski, M., W. H. Prescott, J. C. Savage and J. L. Svarc, A possible geodetic anomaly observed prior to the Loma Prieta, California, earthquake, *Geophys. Res. Lett.*, *17*, 1211-1214, 1990b.

Olson, J., Seismicity in the twenty years preceding the 1989 Loma Prieta, California earthquake, *Geophys. Res. Lett.*, *17*, in press, 1990.

Rice, J. R., Interpretations of seismicity and geodetic data in terms of stressing along slipping faults, presented as NSF-USGS Workshop on Crustal Deformation Measurement and Earthquake Mechanics, Morro Bay, 1990.

Rice, J. R. and J. -. Gu, Earthquake aftereffects and triggered seismic phenomena, *Pure Appl. Geophys.*, *121*, 187-219, 1983.

Segall, P. and M. Lisowski, Comparison of surface displacements in the 1906 San Francisco and 1989 Loma Prieta earthquakes, *Science*, *in press*, 1990.

Tse, S. T., R. Dmowska and J. R. Rice, Stressing of locked patches along a creeping fault, *Bull. Seism. Soc. Am.*, *75*, 709-736, 1985.

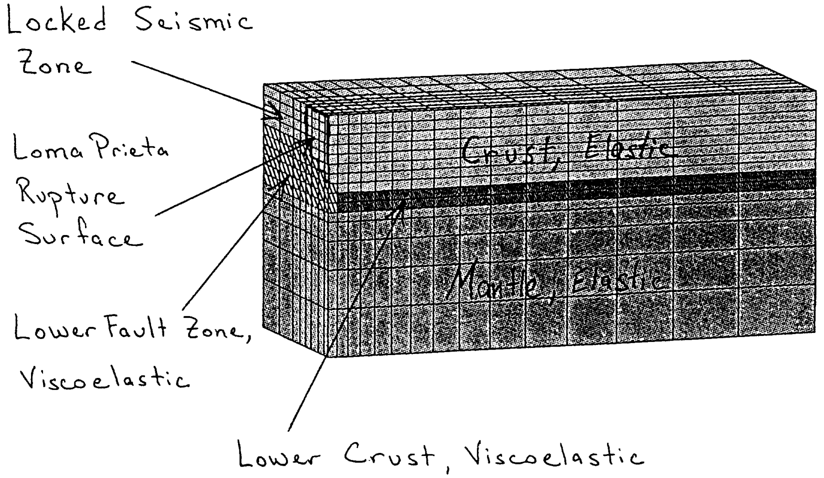

Figure 1. Schematic view of one quadrant of the finite element model for the region around Loma Prieta. The fault dip in this mesh is 90 degrees, but those discussed in the text employ a dip of 64 degrees. The fault is represented by a thin layer of elements. Coseismic slip is imposed via a transformation strain. The upper portion of the crust and the mantle are elastic. Both the lower region of the fault, above the Moho, and the lower portion of the crust are viscoelastic and so can relax the coseismic stress.

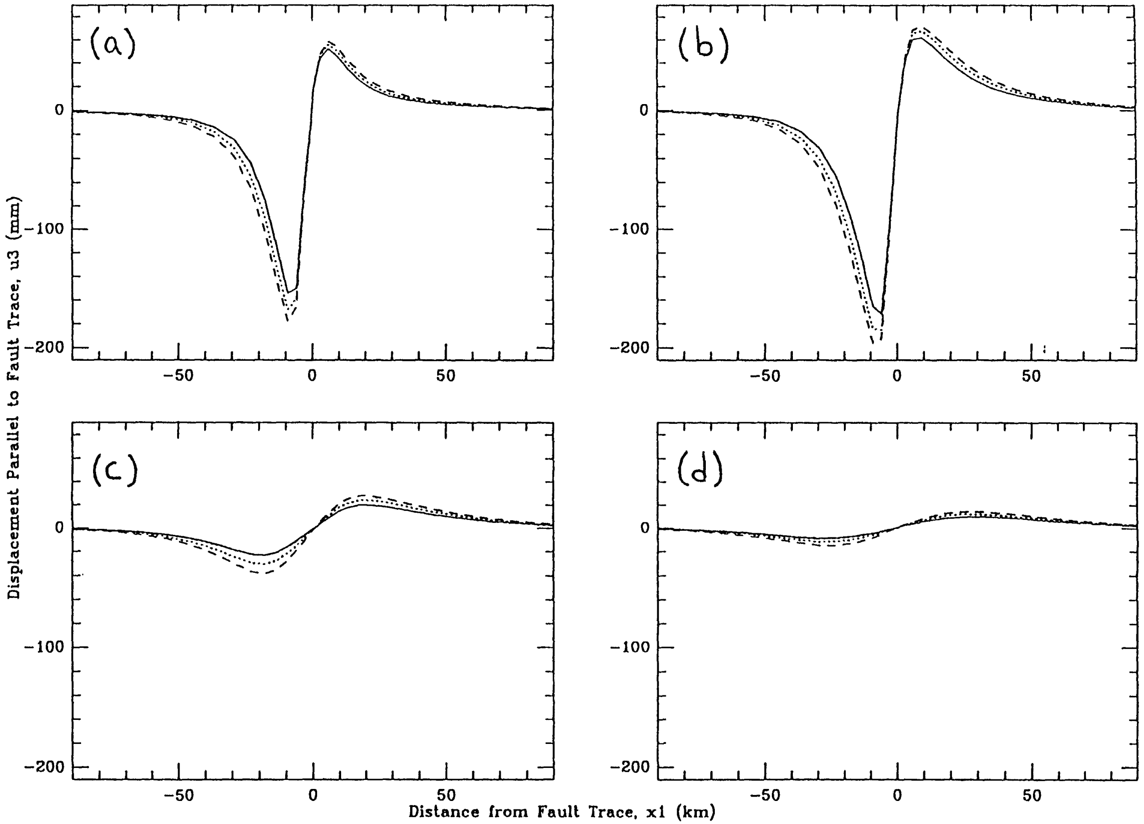

Figure 2. Fault parallel displacement on the earth's surface versus distance from the fault trace for a model in which the viscoelastic lower region of the fault is allowed to relax. For this simulation, the fault dip is 64 degrees, the imposed coseismic transformation strain corresponds to 1 m of strike slip plus 1 m of reverse slip, and the rupture extends from 17.5 to 5 km in depth. The solid curves represent the coseismic displacement field while the dotted and dashed curves represent the displacement field at times $5t_r$ and $20t_r$ after the earthquake. a) at the epicenter (x3=0), b) at the NW end of the rupture (x3=L/2), c) at one rupture length from the epicenter (x3=L), (d) at one rupture length from the NW end of the rupture (x3=3L/2). Figures (a) and (c) correspond, respectively, to the approximate locations of the USGS and Stanford GPS linear arrays, which extend a few tens of km either side of the San Andreas fault.

Use of Stress Drop Models to Interpret Geodetic Measurements at Loma Prieta

14-08-0001-G1847

J. W. Rudnicki, M. Wu and L. M. Keer
Department of Civil Engineering
Northwestern University
Evanston, IL 60208-3109
(708)-491-3411

(For period April 16, 1990 to Septemeber 30, 1990)

Objective

Surface deformation due to slip in the earth's crust is typically interpreted using the well-known dislocation method. Here, we employ an alternative approach in which slip regions are approximated by planar zones of prescribed stress drop (rather than relative displacement, i.e., dislocation). By applying this approach to the observed coseismic geodetic data associated with the 1989 Loma Prieta, California, earthquake, we are able to obtain estimates for the slip induced stress drop and moment, and the critical energy release rate at the termination of rupture.

Results

The Loma Prieta event is modeled as shear slip of an inclined elliptical crack embedded in an elastic half-space. The shear stress drop is assumed to be uniform with a component $\Delta\tau_s$ along the strike and a component $\Delta\tau_d$ along the dip direction of the fault. The resulting slip is calculated using the method of Lee et al. [1987]. Normal relative displacement over the fault plane, which tends to occur because of the free surface, is constrained to be zero. A fairly large set of forward searches was performed to find the model parameters that give a best fit to the observed coseismic geodetic data [Prescott, personal communication, 1990] subject to the constraint that the fault geometry agrees roughly with the aftershock locations [USGS staff, 1990].

Except for two lines lp1 - lp2 and lp1 - brush 2, most of the data are consistent with a right-lateral slip. In addition, a reverse dip slip is required. The fit of the preferred model to the geodetic data without these two lines is provided in Table 1. The mean misfit is 57 mm. The mean misfit to all data (including lp1 - lp2 and lp1 - brush 2) is 91 mm, 40% larger than for the case excluding these two lines. We suspect that these two lines are affected by local surface cracking and they are neglected in this study. The surface center of the best model is at $x = 121^\circ\ 48'\ 30''$ longitude and $y = 37^\circ\ 3'\ 10''$ latitude, about 5 km east of the main shock location. The inclination angle (downdip), the depth of the fault center, the fault length, and the fault width are about 72°, 11 km, 55 km, and 20 km, respectively. The shear stress drops determined by minimizing the difference between the observed and predicted surface deformation are $\Delta\tau_s =$

1.1 MPa and $\Delta\tau_d$ = 1.4 MPa. The calculated geodetic moment is 2.5 x 10^{19} Nm. The maximum energy release rate (energy released per unit area of fault advance) occurs near the top of the fault and is estimated to be 5.5 x 10^6 Jm^{-2}. If it is assumed that the slip propagated according to the criterion that the energy release rate is equal to a critical value, then the estimated value is the critical energy release rate corresponding to arrest of the earthquake. The slip over the fault surface is distributed approximately elliptically . The average slips in the strike and (reverse) dip directions are $[\bar{U}_s]$ = 1.0 m and $[\bar{U}_d]$ = 0.8 m, respectively.

The geodetic moment, the dipping angle, and the ratio between strike and dip slip are very close to those (3.5 x 10^{19} Nm, 70°, and 1.3) reported by Savage (cited by McNally et al. [1989]). The magnitudes of our strike and dip slip are smaller than Savage's (1.7 m and 1.3 m) because our best model prefers a fault geometry having a larger area. If we use the geometry suggested by Savage, the mean misfit to data is increased to be 84 mm. The mean misfit to all data for this geometry is 99 mm.

References

Lee, J. C., Farris, T. N. and L. M. Keer, Stress intensity factors for cracks of arbitrary shape near an interfacial boundary, Engn. Frac. Mech., 27, 27-41, 1987.

McNally, K. C., Lay, T., Protti-Quesada, M., Valensise, G., Orange, M., and R. S. Anderson, Santa Cruz mountains (Loma Prieta) earthquake, EOS, Trans. AGU, 70, 1463-1467, 1989.

USGS Staff, The Loma Prieta, California, earthquake: An anticipated event, Science, 247, 286-293, 1990.

Publication

Wu, M. and J. W. Rudnicki, Use of stress drop models to interpret geodetic measurments at Loma Prieta, California (Abstract), submitted for presentation at Fall AGU Meeting, 1990.

Table 1. Fit of Model to Geodetic Data

STATION - STATION		Observed (mm)	Calculated (mm)	Residual (mm)
Geodolite Line Length Changes				
american	hamilton	75.0 ± 9.4	47.4	27.6
american	loma use	-66.5 ± 7.8	8.6	-75.1
biel	eagle rk	101.5 ± 7.2	28.5	73.0
biel	loma use	235.4 ± 11.6	235.2	0.2
biel	mindego	-107.5 ± 8.8	-102.8	-4.7
bmt rf	loma use	176.2 ± 18.1	126.8	49.4
butano	eagle rk	-95.2 ± 5.5	-44.7	-50.5
llagas	sheeprm2	74.3 ± 11.9	11.6	62.7
loma use	mindego	175.0 ± 12.8	133.9	41.1
allison	lomancer	109.0 ± 8.0	106.6	2.4
eagle rk	lomancer	259.7 ± 5.8	171.5	88.2
lomadwr	pr6	-274.1 ± 20.1	-244.0	-30.1
lpl	lp4	-212.0 ± 7.9	-278.8	66.8
chamber	vargo	123.9 ± 7.2	146.9	-23.0
gilroy	juan	-63.4 ± 11.4	-28.6	-34.8
lpl	vargo	-204.0 ± 15.3	-270.4	66.4
canada	sargent	-86.3 ± 25.0	-2.6	-83.7
fairview	gilroy	-68.2 ± 13.7	-17.8	-50.4
gilroy	sargent	-89.9 ± 12.6	-14.8	-75.1
gilroy	sheeprm2	-69.8 ± 11.1	-19.0	-50.8
p3	p4	66.6 ± 14.0	3.9	62.7
p3	p5	66.6 ± 23.1	9.1	57.5
p5	p6	87.3 ± 13.7	-1.8	89.1
p7	p8	73.7 ± 10.6	7.5	66.2
GPS East				
lpl	allison	34.8 ± 5.9	84.6	-49.8
lpl	eagle un	225.2 ± 11.8	223.2	2.0
lpl	hamilton	65.6 ± 7.0	81.9	-16.3
lpl	brush 2	41.3 ± 15.6	95.4	-54.1
GPS North				
lpl	allison	-110.6 ± 3.8	-124.7	14.1
lpl	eagle un	-205.4 ± 5.6	-156.9	-48.5
lpl	hamilton	-106.6 ± 2.6	-115.2	8.5
lpl	brush 2	-229.2 ± 4.6	-204.8	-24.4
GPS Up				
lpl	allison	-105.5 ± 33.4	-124.2	18.7
lpl	eagle un	-211.8 ± 24.7	-162.8	-49.0
lpl	hamilton	-114.4 ± 25.5	-118.0	3.6
lpl	brush 2	-40.0 ± 27.8	-126.4	86.4

Total Mean Misfit ------- (rms) = 47.0 mm

Observed Changes are given with the conventions: Post-Seismic value - Preseismic value, and Station B - Station A.

GROUND MOTION PREDICTION AND INVERSION IN REALISTIC EARTH STRUCTURES

9910-03010

Paul Spudich
Branch of Engineering Seismology and Geology
U.S. Geological Survey
345 Middlefield Road, MS 977
Menlo Park, California 94025
415/329-5654

Investigations

1. Development of a new method for inverting earthquake ground motion data to infer rupture behavior.
2. Location of heterogeneities in the crust responsible for scattering of waves observed in recordings of aftershocks of the 1986 North Palm Springs earthquake.

Results

1. In collaboration with John Boatwright of the USGS, we are developing a new method for inverting earthquake ground motions. In order to achieve better resolution of the earthquake rupture process, investigators have introduced progressively more realistic constraints on the solution obtained from ground motion inversion. Solutions have been sought having propagating features (Mendez and others, 1990), for example. In our work we seek to introduce causality rigorously as a dynamic constraint. In particular, we wish to obtain earthquake rupture models parameterized in terms of stress distributions on the fault and fault constitutive laws, such that if these derived quantities are used in an initial-value simulation of dynamic rupture (using, for example, the method of Das, 1980), the initial-value simulation produces ground motions that agree with the observed motions from which the stress distribution and constitutive laws were derived. We accomplish this in the following manner. We use Das's algorithm, with a modification to allow slip-weakening of the fault material, as a time-stepping data modeling program. The usual procedure in such a simulation is, at a particular time step and point on the fault, to calculate the load on that point due to the waves radiated from all other points at all previous times. This load and the known fault compliance specify a linear relation between stress change and slip that must be satisfied at the point. Usually, a particular point on this linear curve is selected by specifying a slip-weakening relation, and solving for the single point in the stress-slip domain that satisfies both the unloading curve and the slip-weakening law. In our method, we do not impose a slip-weakening law; rather, we determine how far the point on the fault slips based on the requirement that the radiated motions fit the

observed ground motion data. From this requirement we can derive (rather than assume) a slip-weakening curve for the fault material.

2. In collaboration with Masahiro Iida of the University of Tokyo, we have extended the method of Spudich and Miller (1990) to attempt to identify heterogeneities in the crust responsible for scattering seismic waves. The extension of the method we are using is similar to that used by Lynnes and Lay (1989), except that we allow non-isotropic scattering as well as isotropic scattering, and we do not use semblance as our measure of scatterer amplitude. Our data set consisted of digital recordings of aftershocks of the 1986 North Palm Springs, California, earthquake, which occurred in a geologically complex zone of the San Andreas fault system where the fault zone consists of the Mission Creek and Banning faults (see Figure). Station SMC was emplaced near the Morongo Valley fault. The Figure shows a plot of the power (in arbitrary units) of waves scattered from the surface scatterers in the region near SMC. Also shown are the surface traces of the major faults of the region. The power peak lies near the junction of the Morongo Valley fault and the Mission Creek fault, and the peak is elongated parallel to the Mission Creek fault. This power distribution may suggest that the faults themselves are scattering considerable energy, although this interpretation is very preliminary because we are still trying to determine the significance of this (and similar) images.

References

Lynnes, C., and Lay, T., 1989, Analysis of near-source contributions to early P-coda for underground explosions III. Inversion for isotropic scatterers: Bulletin of the Seismological Society of America, v. 77, p. 1767-1783.

Mendez, A., Olson, A., and Anderson, J, 1990, A norm-minimization criterion for the inversion of earthquake ground motions: *Geophys. J. Internat.*, v. 109, p. 99-104.

Spudich, P., and Miller, D., 1990, Seismic site effects and the spatial interpolation of earthquake seismograms: results using aftershocks of the 1986 North Palm Springs, California, earthquake: *Bulletin of the Seismological Society of America*, in press (to appear December 1990).

Reports

Spudich, P., and Boatwright, J., 1990, Dynamically consistent inversion of ground motion data to infer fault constitutive laws, [abs.]: *EOS, Transactions of the American Geophysical Union*, in press.

Spudich, P., and Miller, D., 1990, Seismic site effects and the spatial interpolation of earthquake seismograms: results using aftershocks of the 1986 North Palm Springs, California, earthquake, *Bulletin of the Seismological Society of America*, in press (to appear December 1990).

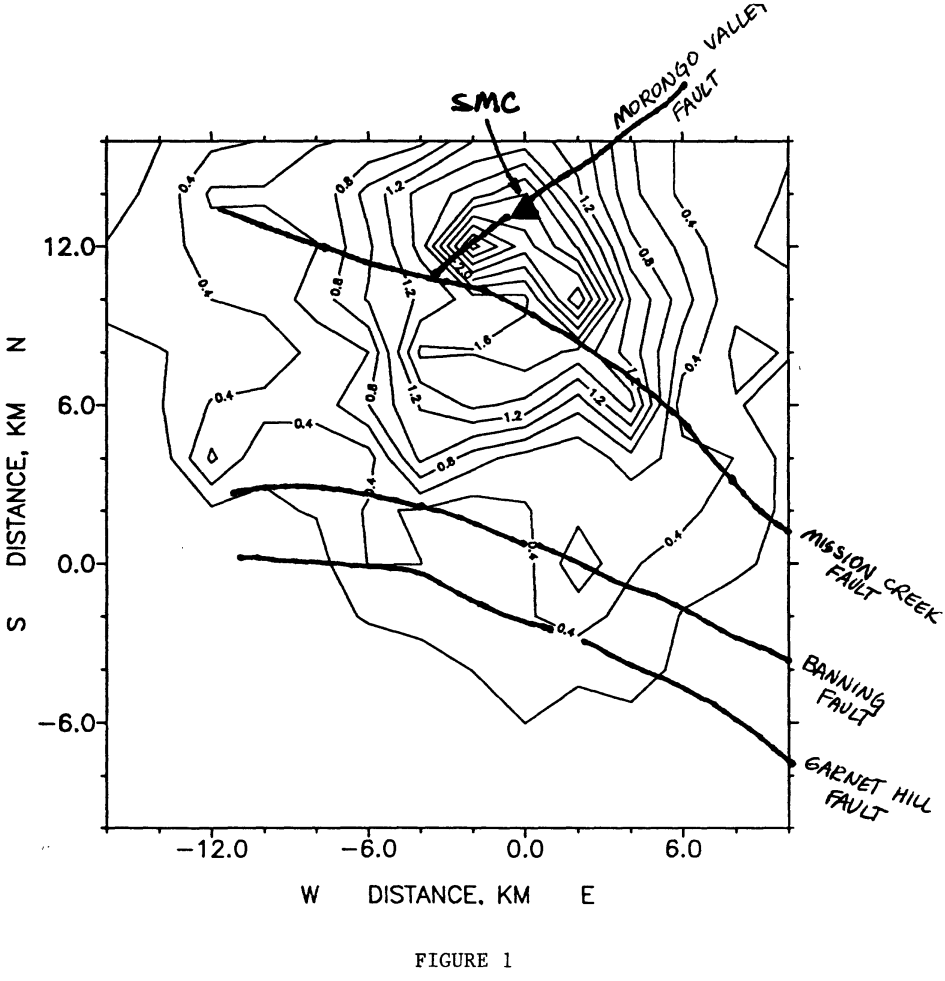
SMC
MORONGO VALLEY FAULT
MISSION CREEK FAULT
BANNING FAULT
GARNET HILL FAULT
12.0
6.0
0.0
-6.0
-12.0
-6.0
0.0
6.0
S DISTANCE, KM N
W DISTANCE, KM E
0.4
0.8
1.2
1.6
2.0

FIGURE 1

Liquefaction in the Monterey Bay Region (Emergency Earthquake Hazards)

0-9910-01629
0-9540-04530

John C. Tinsley
Branch of Western Regional Geology
345 Middlefield Road MS-975
Menlo Park, CA 94025
415-329-4928

Thomas L. Holzer and Michael J. Bennett
Branch of Engineering Geology and Seismology
345 Middlefield Road MS-977
Menlo Park, CA 94025
415-329-5637

William R. Dupre
Department of Geology
University of Houston
Houston, Texas 77004
713-749-3710

Investigations

1. A map at scale 1:62,500 scale, describing the distribution, location, and nature of liquefaction-related effects, including sand volcanos, lateral spreads, land settlements, and damage to works of man is in preparation. Ground failures were mapped in reconnaissance fashion using analyses of aerial photographs (scale 1:6000) and extensive in-field examination of most areas with a nearby free-face in the weeks following the Loma Prieta main shock.

2. Field study of 11 lateral spreading failures including detailed mapping, sampling of extruded sand, cone penetrometer and piezocone penetrometer studies (with John B. Berrill and Roger Vreugdenhil (University of Canterbury, Christchurch, New Zealand), standard penetrometer studies of key subsurface intervals, geologic facies associations and amount and distribution of lateral displacement was completed by mid-September, 1990. Samples are being processed in the sediment laboratory to enable proper classification and analysis of the data according to methods commonly used in engineering practice. These studies emphasize the facies of the alluvial plains of the Salinas and Pajaro Rivers, in Santa Cruz and Monterey Counties, California. Studies were taken in failed and in adjacent non-failed material, to facilitate comparisons among in-situ properties of the sediment subjected to

essentially identical levels of ground motion. These studies also include stratigraphic and geomorphic analyses of the facies associations of the ground failures; an evaluation of published USGS liquefaction potential map (Dupre and Tinsley, 1980) for the Monterey Bay region (scale 1:62,500), in light of the Loma Prieta earthquake effects; comparisons of 1989 liquefaction effects with published reports of permanent ground failures arising from the 1906 San Francisco earthquake.; cone penetrometer, standard penetrometer, and piezocone penetrometer studies of selected lateral spread ground failures to determine in-situ properties of failed and adjacent non-failed materials in relation to ground motion generated by the Loma Prieta earthquake; and comparisons among geotechnical properties of sediments involved in the failures of the natural deposits in relation to published curves for evaluating liquefaction susceptibility as used in standard engineering practice in the United States constitute the principal scientific thrusts of this investigation.

3. Several sites have been located which may afford good potential to evaluate 1906 and earlier earthquakes using paleoliquefaction evaluation techniques. Chronically high ground water tables in most areas affected by liquefaction limit trench exposures to shallow depths, unless dewatering measures can be implemented successfully.

Results

The initial compilation of ground failure effects using aerial photographic analysis coupled with field mapping and sampling of ejected sand is complete; particle size analysis of ejected sand samples is in progress in the soil laboratory at Menlo Park. From a stratigraphic perspective, there is a strong association between fluvial channel, levee, and point bar deposits and liquefaction effects observed following the 10/17/89 earthquake, especially among deposits which are less than a few hundred years old.

Liquefaction was widespread within late Holocene fluvial deposits of the Pajaro and Salinas rivers, especially in tidewater reaches where groundwater is within 1 to 2 meters of the ground surface year-round and the effects of prolonged drought on groundwater levels is minimal. In contrast to 1906, when wet soil moisture conditions contributed to widespread hillslope flow failures, in 1989, few if any slope failures related to liquefaction were reported. Intensity of liquefaction effects decreases upstream, as the fluvial deposits become more coarse, despite increasing proximity to the Loma Prieta earthquake seismic source zone. The proximity of a free-face within 50 to 150 m was commonly observed in lateral spread ground failures.

Components of displacements associated with ground failures measured in the field following the Loma Prieta earthquake range from a few millimeters to about 1 meter horizontally; settlements range from a few millimeters to less than 2 meters vertically.

The cone penetrometer studies facilitated rapid subsurface reconnaissance of lateral spread ground failures, and enabled us to identify key fluvial facies associations relative to the ground failures. Channel, levee, and point-bar deposits were most susceptible to failure;

vertically accreted floodplain deposits, especially those containing appreciable clayey silts and clays generally did not exhibit failure.

References Cited

Dupre, W. R. and Tinsley, J. C., 1980, Geology and liquefaction potential, northern Monterey and southern Santa Cruz Counties, California: U.S. Geological Survey Miscellaneous Field Studies Map MF-1199, 2 sheets, scale 1:62,500.

Publications

Dupre, W.R. and Tinsley, J.C., 1990, Geologic controls on liquefaction-induced ground failure in the Monterey Bay area, California, during the Loma Prieta earthquake, October 17, 1990: Geological Society of America, Abstracts with Programs, v. 22, no. 7, p. A188.

Bennett, Michael J., Bonilla, Manuel G., and Holzer, Thomas L., 1990, Liquefaction in the Marina District, San Francisco, California, during the Loma Prieta earthquake: Geological Society of America, Abstracts with Programs, v. 22, no. 7, p. A188.

10/90

Geologic Investigations of Surface Fractures
Loma Prieta, CA, earthquake

9540-04530

Ray E. Wells
Western Regional Geology
U.S. Geological Survey
345 Middlefield Rd., MS 975
Menlo Park, CA 94025
(415) 329-4933

Daniel J. Ponti
Engineering Seismology & Geology
U.S. Geological Survey
345 Middlefield Rd., MS 977
Menlo Park, CA 94025
(415) 329-5679

INVESTIGATIONS

1. Continued mapping of off-fault surface fractures that occurred above the northern end of the subsurface rupture zone during the Loma Prieta earthquake.
2. Comparison of crack geometry and sense of slip to underlying bedrock geology and regional topographic slope.
3. Analysis of displacement vector data to discriminate between tectonic and gravitational driving forces.

RESULTS

Many surface fractures in the Summit Road-Skyland Ridge area of the Santa Cruz Mountains apparently resulted from bedding-plane faulting within the folded Tertiary strata that underlie the area. Fractures commonly occur in laterally continuous NW-trending zones and have consistent displacement vectors, an observation suggesting that they are not related to near-surface slope failure. Most fractures are closely aligned to the strike of bedding, even in structural domains where bedding deviates from the overall trend. For some fracture sets, displacement vectors lie very close to bedding planes, and most of the fractures show downdip movement. Some fractures follow previously mapped bedrock faults, and one fracture set closely follows the axis of the Laurel Anticline for several kilometers.

Most cracks are extensional, with a subordinate component of vertical displacement. Nearly two-thirds of the fractures have a component of left slip, whereas most of the rest exhibit right-lateral displacement; only 5% of measured cracks show pure extension. Lateral motion (both left and right slip) of most fractures can be adequately explained by considering the individual fracture orientations with respect to local bedding and topography.

Two different models can describe the sense of lateral movement on the fractures. In the first, pure dip-slip faulting occurs on underlying bedding planes. Lateral motion results if a crack trend deviates somewhat from the strike of bedding as it propagates through the overlying colluvium. If the deviation is in a clockwise sense, left-lateral displacement occurs on the surface fracture; counterclockwise deviations result in right-lateral displacements. This model predicts the proper sense of displacement for more than 60% of the fractures studied. The other model assumes that displacements are controlled only by local slope direction; lateral components of motion occur where fractures are oblique to the local slope. This model explains most observed lateral displacements on fractures with downslope displacment vectors. A combination of dip-slip faulting on bedding planes and downslope motion could explain the orientation and sense of slip on most surface ruptures in the Summit Road-Skyland Ridge area. However, a small but significant portion of the fractures follow or parallel mapped structures and have displacements inconsistent with gravity-driven processes. These may be reflecting a tectonic component of deformation.

REPORTS

Ponti, D.J., and Wells, R.E., 1990, Origin of surface ruptures that formed in the Santa Cruz Mountains, California, during the Loma Prieta earthquake: Seismological Research Letters v. 61, p. 17.

Ponti, D.J., and Wells, R.E., 1990, Extent and origin of surface fractures in the Summit Road - Skyland Ridge area, in Schwartz, D.P. and Ponti, D.J., eds., Field guide to neotectonics of the San Andreas Fault System, Santa Cruz Mts., in light of the 1989 Loma Prieta earthquake: U.S. Geological Survey Open File Report 90-274, p. 27-30.

Ponti, D.J., Wells, R.E., Haugerud, R., Clark, M.M., and Hall, T., 1990, Surface rupture aspects, in Borcherdt, R.D. and Donovan, N.C., eds., Loma Prieta Earthquake Reconnaissance Report: Earthquake Spectra, v. 6 supplement, p. 13-23.

INDEX 1

INDEX ALPHABETIZED BY PRINCIPAL INVESTIGATOR

INDEX 2

INDEX ALPHABETIZED BY INSTITUTION

Nevada, University of, Reno	Peppin, W. A.	97
Nevada, University of, Reno	Wesnousky, S. G.	168
North Carolina, University of	Rial, J. A.	456
Northwestern University	Rudnicki, J. W.	229
Northwestern University	Rudnicki, J. W.	237
Northwestern University	Rudnicki, J. W.	585
Oregon State University	Kulm, L. D.	434
Oregon State University	Yeats, R. S.	171
Oregon State University	Yeats, R. S.	468
Queensland, University of	Gladwin, M. T.	269
Saint Louis, University of	Herrmann, R. B.	426
Saint Louis, University of	Stauder, W. V.	32
San Francisco State University	Galehouse, J. S.	260
Southern California, University of	Teng, T.	38
Southern California, University of	Teng, T.	111
Southern California, University of	Teng, T.	466
Stanford University	Beroza, G. C.	48
Texas A & M University	Fletcher, R. C.	350
Texas, University of, Austin	Stokoe, K. H.	452
U.S. Geological Survey	Algermissen, S. T.	404
U.S. Geological Survey	Allen, R. V.	174
U.S. Geological Survey	Andrews, D. J.	549
U.S. Geological Survey	Atwater, B. F.	406
U.S. Geological Survey	Boatwright, J.	52
U.S. Geological Survey	Bonilla, M. G.	115
U.S. Geological Survey	Boore, D. M.	550
U.S. Geological Survey	Borcherdt, R. D.	250
U.S. Geological Survey	Borcherdt, R. D.	541
U.S. Geological Survey	Borcherdt, R. D.	551
U.S. Geological Survey	Brady, A. G.	544
U.S. Geological Survey	Brady, A. G.	545
U.S. Geological Survey	Breckenridge, K. S.	187
U.S. Geological Survey	Brown, R. D.	116
U.S. Geological Survey	Buchanan-Banks, J.M	118
U.S. Geological Survey	Buchanan-Banks, J.M.	408
U.S. Geological Survey	Bucknam, R. C.	409
U.S. Geological Survey	Bundock, H.	546
U.S. Geological Survey	Campbell, R. H.	411
U.S. Geological Survey	Carlson, M. A.	508
U.S. Geological Survey	Celebi, M.	510
U.S. Geological Survey	Choy, G. L.	190
U.S. Geological Survey	Choy, G. L.	513
U.S. Geological Survey	Clark, M. M.	130
U.S. Geological Survey	Crone, A. J.	413
U.S. Geological Survey	Dewey, J. W.	515
U.S. Geological Survey	Ellsworth, W. L.	254

GPO 585-817/59059